

DEPOSITIONAL FACIES AND CALCITE CEMENTATION
IN THE AVALON FORMATION, HIBERNIA OIL FIELD,
JEANNE D'ARC BASIN, GRAND BANKS
OF NEWFOUNDLAND

CENTRE FOR NEWFOUNDLAND STUDIES

**TOTAL OF 10 PAGES ONLY
MAY BE XEROXED**

(Without Author's Permission)

OSAMA MAHMOUD SOLIMAN

DEPOSITIONAL FACIES AND CALCITE CEMENTATION
IN THE AVALON FORMATION, HIBERNIA OIL FIELD,
JEANNE D'ARC BASIN, GRAND BANKS OF NEWFOUNDLAND

BY

OSAMA MAHMOUD SOLIMAN

A thesis submitted to the
School of Graduate Studies
in partial fulfilment of the
requirements for the degree of
Doctor of Philosophy

DEPARTMENT OF EARTH SCIENCES
MEMORIAL UNIVERSITY OF NEWFOUNDLAND

July, 1995

St. John's

Newfoundland



National Library
of Canada

Acquisitions and
Bibliographic Services Branch

395, Avenue du Centre
Ottawa, Ontario
K1A 0N4

Bibliothèque nationale
du Canada

Direction des acquisitions et
des services bibliographiques

395, rue Wellington
Ottawa (Ontario)
K1A 0N4

The author has granted an irrevocable non-exclusive licence allowing the National Library of Canada to reproduce, loan, distribute or sell copies of his/her thesis by any means and in any form or format, making this thesis available to interested persons.

The author retains ownership of the copyright in his/her thesis. Neither the thesis nor substantial extracts from it may be printed or otherwise reproduced without his/her permission.

L'auteur a accordé une licence irrévocable et non exclusive permettant à la Bibliothèque nationale du Canada de reproduire, prêter, distribuer ou vendre des copies de sa thèse de quelque manière et sous quelque forme que ce soit pour mettre des exemplaires de cette thèse à la disposition des personnes intéressées.

L'auteur conserve la propriété du droit d'auteur qui protège sa thèse. Ni la thèse ni des extraits substantiels de celle-ci ne doivent être imprimés ou autrement reproduits sans son autorisation.

ISBN 0-612-17647-9

Canada

ABSTRACT

This study investigates the Aptian sedimentation and fluid flow patterns in the Avalon Formation, Hibernia field, Jeanne d'Arc basin. Such patterns are analyzed with respect to the tectonics and kinematics of the Hibernia rollover anticline.

Facies analysis of the cored intervals resulted in the recognition of fifteen facies. These facies were grouped into eight facies associations. Spatial distribution of the laterally equivalent associations was used to construct a series of paleogeographic maps for successively younger intervals. Such maps reveal the repetitive development of estuarine and transgressive barrier island depositional systems.

The estuarine system occupied a structurally-controlled river valley. The valley was incised into the rollover anticline during regional uplift of the area. The estuarine system was established in the valley consequent to subsidence along valley-bounding faults. This subsidence marks the initiation of extension during a rifting episode.

The barrier island system was developed during submergence of the rollover anticline. This submergence resulted from active displacement along the listric growth

fault. Such displacement reflects an advanced stage of extension during the rifting episode.

Decline of extension was followed by a regional uplift and re-emergence of the rollover anticline. Resumption of extension caused the revival of the estuarine system, subsequent redevelopment of the barrier island system and resubmergence of the rollover anticline.

Laterally extensive poikilotopic calcite-cemented beds in the Avalon Formation were used to explore fluid flow in the rollover anticline. Spatial variations in concentrations of trace elements in the calcite cement reflect different flow patterns of the calcite-precipitating fluids. In the barrier island sandstone bodies the fluids flowed preferentially along the depositional strike, from the NW towards the SE. The flow was supported by an apparent structural dip of about 0.066° towards the SE. In the fluvial channel-river mouth bar sandstone bodies, the fluids flowed favourably along the depositional dip, from NE towards SW.

A fresh water origin is interpreted for the calcite precipitating-fluids. These fluids infiltrated through the Avalon sediments during periods of emergence of the rollover anticline. The fluids flowed from the crest of the anticline towards the SE, S and SW.

ACKNOWLEDGEMENTS

I wish to thank Professor John D. Harper for his kind supervision, constructive criticism and untailing help during all steps of this work. His Devil's advocate role is greatly appreciated. I am also indebted to the members of the supervisory committee, Drs. T. Calon, H. Miller and M. Wadleigh, for their guidance and encouragement. Dr. T. Calon is particularly acknowledged for his critical review of the thesis and for his fruitful discussions. The critical evaluation of chapters 'V' and 'VI' by Dr. M. Wadleigh is much appreciated.

The writer is very grateful to the Hibernia Management and Development Company for financing this study. Financial support from the Graduate School in Memorial University of Newfoundland is also greatly appreciated.

Special gratitude is expressed to E. Albrechtsons and H. Klettli for their continuous support and illuminating discussions during all steps of this study. E. Albrechtsons is particularly acknowledged for drawing my attention to the possible occurrence of estuarine sediments.

I am particularly thankful to Dr. E. Burden for gaining access to his palynologic data and for the invaluable discussions of palynofacies in the Hibernia I-46 well. Deep

thanks are also extended to Dr. R. Hiscott for precious suggestions and fruitful discussions of many of the Hibernia cores.

Thanks are extended to the Canada Newfoundland Offshore Petroleum Board for their permission to gain access to the Hibernia cores. I am particularly thankful to E. Chippett and M. Walters for their patience and continuous help in the core storage facility.

Special thanks are extended to I. Sinclair, D. McAlpine and T. Jenkins for their thoughtful discussions and for providing a wealth of references.

I gratefully acknowledge the help given by the following people: M. Piranian and P. King for continuous guidance in the probe laboratory; I. Abid for help in sample impregnation; J. Taylor and R. Taylor for eliminating my computer illiteracy; A. Aksu for use of his copying machine.

At last but not least, I acknowledge the ever continued support and kindness of my parents. Recognition of their share is beyond expression in words. I gratefully dedicate this work to them.

TABLE OF CONTENTS

	Page
Abstract	ii
Acknowledgements	iv
List of tables	viii
List of figures	ix
I <u>Introduction</u>	1
I.1 Research problem	3
I.2 Contribution of the study	3
I.3 Approach	3
I.4 Organization	6
I.5 Geologic setting	8
I.6 Previous related work	11
II <u>Depositional facies & facies associations</u>	32
II.1 Depositional facies	33
II.2 Facies associations & successions	61
III <u>Depositional systems</u>	107
III.1 Stratigraphy of the B-27 well	110
III.2 Stratigraphy of the I-46 well	116
III.3 Facies and event correlation	122
III.4 Stratigraphic cross sections	128
III.5 Paleogeography	133
III.6 Diagnostic criteria	136

III.7	Stratigraphy of the J-34 well	143
III.8	Stratigraphic architecture	147
IV	<u>Sedimentation & tectonics</u>	173
IV.4	Sedimentary history	174
IV.4	The role of tectonics	178
IV.6	Controls on sedimentation	183
IV.3	Stratigraphic model	188
V	<u>Petrography of calcite cementation</u>	195
V.1	Petrography	196
V.2	Paragenetic sequence of diagenesis	203
VI	<u>Calcite cementation & fluid flow</u>	209
VI.1	Distribution of calcite cementation	210
VI.2	Carbonate analysis	214
VI.3	Geochemistry of the calcite cement	216
VI.4	Paleo-flow of the calcite-precipitating fluids	224
VI.5	Origin of the calcite-precipitating fluids.	223
VI.6	Tectonics & fluid flow	233
VI.7	Controls on calcite cementation	234
VII	<u>Summary & conclusions</u>	250
VIII	<u>References</u>	253
IX	<u>Appendix</u>	275
X	<u>Enclosures</u>	283

List Of Tables

Table	Page
I.1 Distribution of core, thin section and geochemical data in the studied Hibernia wells	6
II.1 Facies characteristics of the Avalon Formation, Hibernia field	34
II.2 Facies Associations in the Avalon Formation, Hibernia field	63
VI.1 Counting times and detection limits of trace elements	215
VI.2 Distribution coefficients of trace elements ...	230
VI.3 Molar concentration ratios of trace elements to calcium in the calcite-precipitating fluids and the sea and stream waters	231
VI.4 Extreme molar concentration ratios of trace elements to calcium in the calcite-precipitating fluids and the sea and stream waters	233
IX.1 Highest occurrences of various biostratigraphic events, recorded by different investigators ...	276
IX.2 Element percentages of Ca, Mg, Fe, Sr, Mn and Na in the poikilotopic calcite cement	277

List Of Figures

Figure	Page
I.1 Migrated time seismic section showing the Hibernia rollover anticline (Enachescu 1987) ...	24
I.2 Lithostratigraphic chart for the Jeanne d'Arc basin (Grant and McAlpine 1990)	25
I.3 North Atlantic Mesozoic rift basins (Welsink et al. 1989)	26
I.4 Diagrammatic structure and sediment thickness map for Jeanne d'Arc basin (Grant et al. 1986)	27
I.5 Depth map of the Avalon Sandstones in the Hibernia rollover anticline (CNOBP 1986)	28
I.6 Simplified structural map for the Hibernia rollover anticline	29
I.7 Difference in stratigraphic nomenclature of the Avalon Formation	30
I.8 Correlation of the Early Cretaceous sediments in 7 of the Hibernia wells (Davies 1990)	31
II.1 Legend for figures II, III & IV	100
II.2 Lake/Lagoonal Fill Facies Successions	101
II.3 Barrier-Backbarrier Facies Successions	102
II.4 Fluvial/Tidal Channel Fill Facies Succession ...	103
II.5 River Mouth Bar Facies Successions	104

II.6	Interdistributary Bay Fill Succession	105
II.7	Distal Delta Facies Succession	105
II.8	Two Stacked Shoreface Facies Successions	106
II.9	Shallow Marine Facies Succession, overlying Lower Shoreface Sandstones	106
III.1	Stratigraphy of the Hibernia B-27 well	149
III.2	Stratigraphy of the Hibernia I-46 well	150
III.3	Facies and event correlation showing correlatable transgressive surfaces, a conglomerate layer an erosional surface and laterally matching facies successions	151
III.4	Facies and event correlation of the Hibernia B-27, I-46 and K-14 wells	152
III.5	Facies and event correlation of the Hibernia I-46, B-27 and C-96 wells	153
III.6	Facies and event correlation of the Hibernia I-46, J-34, K-14 and C-96 wells	154
III.7	Stratigraphic cross section of the Hibernia B-27, I-46 and K-14 wells	155
III.8	Stratigraphic cross section of the Hibernia I-46, B-27 and C-96 wells	156
III.9	Schematic diagram illustrating landward migration of the barrier island shoreline	157
III.10	Stratigraphic cross section of the Hibernia I-46, J-34, K-14 and C-96 wells	158

III.11	Stratigraphic cross section of the Hibernia I-46, J-34 and K-14 wells	159
III.12	Paleogeography of the estuarine valley fill in the lowermost part of the Avalon Formation ..	160
III.13	Gamma-ray log correlation of the Hibernia B-27, I-46, O-35, J-34 and K-14 wells	161
III.14	Gamma-ray log correlation of the Hibernia K-14, P-15 and K-18 wells	162
III.15	Gamma-ray log correlation of the lower part of the Avalon Formation showing the occurrence of a barrier island sandstone body	163
III.16	Sand isolith map of the lower Avalon transgressive barrier island	164
III.17	Paleogeography during early stages of filling of the valley that is incised into the transgressive barrier island	165
III.18	Isopach map of the estuarine valley fill	166
III.19	Paleogeography of the estuarine valley fill that occurs below TS'V'	167
III.20	Stratigraphic offset between the valley trough and the valley flank increased gradually during deposition of the Avalon Fm.	168
III.21	An estuarine valley fill succession reflecting changes in the rate of subsidence relative to the rate of sediment supply	169

III.22	Stratigraphy of the Hibernia J-34 well	170
III.23	Gamma-ray log correlation of the Hibernia B-27, I-46, O-35, J-34 and K-14 wells	171
III.24	Gamma-ray log correlation of the Hibernia K-14, P-15 and K-18 wells	172
IV.1	Kinematic & sedimentation model for the Hibernia rollover anticline	192
IV.2	Stratigraphic facies model for the Avalon Formation in the Hibernia rollover anticline ...	193
IV.3	Ideal stratigraphic successions for the Avalon Formation in the Hibernia rollover anticline ...	194
VI.1	Distribution of calcite cementation in the Hibernia B-27 well	236
VI.2	Distribution of calcite cementation in the Hibernia I-46 well	237
VI.3	Sonic log correlation of the Hibernia J-34, K-14, B-27 and C-96 wells	238
VI.4	Sonic log correlation of the Hibernia J-34, I-46, B-27 and K-18 wells	239
VI.5	Facies influence on the composition of the poikilotopic calcite cement	240
VI.6	Siderite influence on the composition of the poikilotopic calcite cement	241

VI.7	Correlation of two vertical cycles of Fe concentration in the poikilotopic calcite in the B-27, K-14 and J-34 wells	242
VI.8	Fe% versus Mg% in poikilotopic calcite cement in the K-14 well	243
VI.9	Isoconcentration lines of Fe content in the poikilotopic calcite cement in two stacked barrier island sandstone bodies	244
VI.10	Isoconcentration lines of Mn content in the poikilotopic calcite cement in two stacked barrier island sandstone bodies	245
VI.11	Isoconcentration lines of Fe content in the poikilotopic calcite cement in the river mouth bar sandstone bodies	246
VI.12	Isoconcentration lines of Mn content in the poikilotopic calcite cement in the river mouth bar sandstone bodies	247
VI.13	Comparison of estimated composition of the calcite-precipitating fluids in the B-27 well and composition of stream and sea waters	248
VI.14	Recharge of fresh waters along an emergent rollover anticline	249

I- INTRODUCTION

Rollover anticlines, associated with extensional growth faults, are important sites for hydrocarbon accumulation (Evamy et al. 1978; Bally 1983; James 1984). Origin, geometry and kinematics of rollover anticlines have been the focus of much research (White et al. 1986; Groshong 1989; McClay 1989; Rowan and Kligfield 1989; Dula 1991; McClay et al. 1991; Xiao and Suppe 1992). On the other hand, patterns of sedimentation associated with the development of rollover anticlines have received little attention. Studies in several growth fault systems have related sedimentation to either mass flow deposits from nearby delta fronts or to progradational cycles of deltaic sediments (Evamy et al. 1978; Edwards 1981; Coleman et al. 1983; Winker and Edwards 1983; Jackson and Galloway 1984; Doust and Omatsola 1990). No studies, yet, have addressed the relationship between sedimentation and both the tectonics and kinematics of rollover anticlines.

Some rollover anticlines host multiple unconformities, e.g. the Slick Ranch rollover anticline of the Vicksburg glide plane in south Texas (Xiao and Suppe 1992). These unconformities reflect the recurrent emergence and submergence of the rollover anticlines. Such oscillatory movements certainly affect sedimentation, fluid flow, diagenesis, and thus the reservoir quality in the rollover anticlines. Valleys

can be incised and transgressive shorelines may be developed respectively during emergence and subsequent submergence of the rollover anticlines. Also fresh and marine waters may respectively infiltrate through reservoir facies during emergence and subsequent submergence of rollover anticlines. Consequent diagenetic alterations may result in either enhancement or deterioration of the reservoir quality.

Xiao and Suppe (1992) attributed the development of unconformities on rollover anticlines to the decrease of sedimentation rate, relative to the rate of subsidence. Rates of sedimentation and subsidence are in turn controlled by the tectonics. Therefore, understanding the impacts of tectonics and kinematics of rollover anticlines on both sedimentation and fluid flow will greatly enhance the capability to predict locations of hydrocarbon reservoir facies in these structures.

In the Jeanne d'Arc rift basin, Hibernia field is located on the rollover anticline of a growth fault, the Rankin fault (figure I.1). The sedimentary section that was associated with the development of the rollover anticline hosts several unconformities. The Avalon Formation is confined between two of such unconformities, namely the Barremian and Aptian unconformities (figure I.2). The Avalon Formation is a syn-rift rock unit (Sinclair 1993) that consists of fine to medium grained sandstones and mudstones. Laterally extensive calcite-cemented beds compartmentalize the sandstone bodies in the

Avalon Formation. These calcite-cemented beds attest to significant fluid flow in the Hibernia rollover anticline.

I.1- RESEARCH PROBLEM

This study explores the sedimentation and fluid flow patterns in a rollover anticline. These patterns are analyzed with respect to the tectonics and kinematics of such structure. The study investigates the depositional systems and tectono-sedimentary history of the Avalon Formation in the Hibernia rollover anticline. The study also addresses the origin and paleo-flow of the calcite-precipitating fluids in the Avalon Formation. The interaction of the kinematics of the Hibernia rollover anticline and both sedimentation and fluid flow is particularly highlighted.

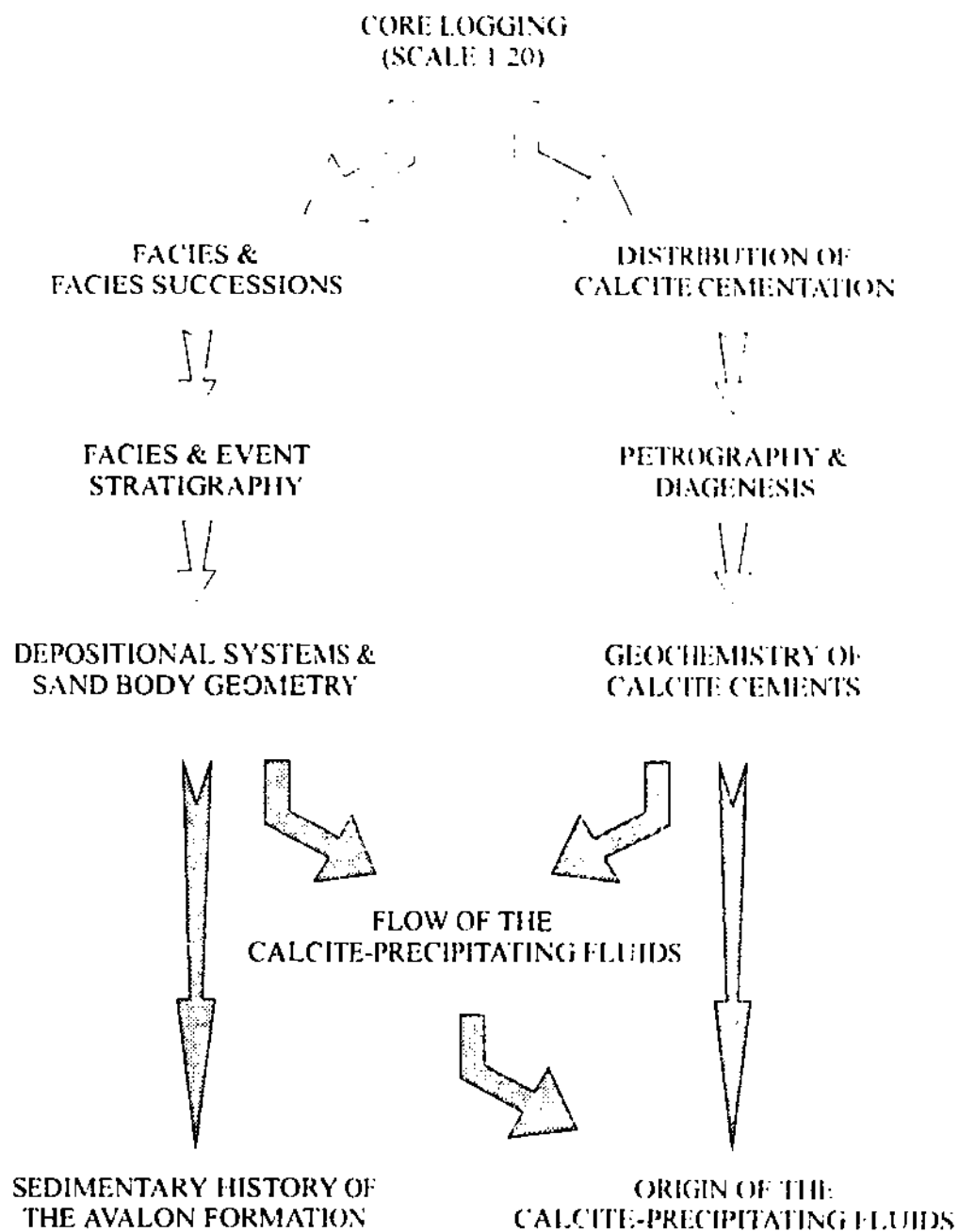
I.2- CONTRIBUTION OF THE STUDY

This study provides new insights into:-

- 1- Controls of tectonics and kinematics of a rollover anticline on sedimentation in this structure.
- 2- Stratigraphy of structurally-controlled valleys, and
- 3- Fluid flow in a rollover anticline.

I.3- APPROACH

The approach used in this study is illustrated in the following flow chart:



A total of 573 meters of cores were described in detail (Scale of 1:20, table I.1, enclosures). Facies, facies boundaries, grain size variations, sedimentary structures, trace fossils, oil staining, and calcite cementation were documented. Fifteen types of facies were recognized through this detailed core analysis. These facies types were grouped into eight facies associations. The associations and their bounding surfaces were correlated laterally between the wells using a facies and event correlation approach. Based on this correlation, stratigraphic cross sections were constructed and paleogeographic maps were synthesized for successively younger intervals of the Avalon Formation. Distribution and geometry of various sandstone bodies were particularly emphasized. Depositional history and controls on sedimentation were then contemplated. Finally, a stratigraphic model highlighting sedimentation of the Avalon Formation in the Hibernia rollover anticline is proposed.

Regarding calcite cementation, the distribution of cementation in various facies was investigated. Calcite-cemented intervals were systematically sampled according to their distribution (see chapter VI for details). Seventy two thin sections were prepared and were microscopically described (table I.1). Another set of 244 stained thin sections, provided by the Hibernia Management and Development Company (HMDC), were also described. Calcite cements in 42 of the

prepared thin sections were probed for calcium and five trace elements (Fe, Mn, Mg, Sr and Na). Lateral gradients in concentration of trace elements were used to explore flow of the calcite-precipitating fluids in various sandstone bodies. The fluid flow trends are highlighted on many stratigraphic cross sections in this study. The geochemical signature of calcite cements, in the closest location to the source of calcite-precipitating fluids, was used to deduce the type of these fluids. Finally, a model explaining the origin and flow of calcite-cementing fluids in the rollover anticline is advanced.

Table I.1- Distribution of core, thin section and geochemical data in the studied Hibernia wells.

Well	Core length (m.)	Stained thin sections*	New thin sections	Probed thin sections
I-46	187	96	20	10
J-34	160	77	11	6
K-14	94	34	16	13
B-27	64	34	12	7
C-96	26	18	10	6
K-18	17	12		
G-55	11			
O-35	14		3	
total	573	244	72	42

*provided by the Hibernia Management and Development Company

I.4- ORGANIZATION

This study is presented in five chapters, outlined below.

I.4.1- FACIES AND FACIES ASSOCIATIONS:

This chapter describes the different types of rocks and throws light on their depositional processes and environments. Fifteen types of facies and eight facies associations were

recognized. The facies associations and their bounding surfaces represent the primary tools for subsequent stratigraphic correlations.

I.4.2- DEPOSITIONAL SYSTEMS:

This chapter aims to reconstruct depositional environments and to discuss the depositional history. A facies and event correlation approach is used to correlate the lower part of the Avalon Formation in different wells. Paleogeographic maps are synthesized for successively younger intervals. Geometries of sandstone bodies that host extensive calcite cementation are delineated. Diagnostic criteria for recognizing different types of depositional systems are then discussed. Afterwards, depositional systems in the entire Avalon Formation and the lowermost part of the overlying Ben Nevis Formation are examined. Finally, the stratigraphic architecture of the entire Avalon Formation is highlighted.

I.4.3- SEDIMENTATION AND TECTONICS:

This chapter summarises the long term sedimentary history of the entire Avalon Formation. The role of tectonics in the kinematics of and sedimentation in the Hibernia rollover anticline is then discussed. Controls on sedimentation are subsequently contemplated. Finally, a stratigraphic model illuminating the main facies relationships and successions is proposed.

I.4.4- PETROGRAPHY OF CALCITE CEMENTATION:

This chapter describes the types of calcite cements and places them in chronologic order relative to the other diagenetic alterations in sandstones of the Avalon Formation.

I.4.5- CALCITE CEMENTATION AND FLUID FLOW:

This chapter explores the flow of the calcite-precipitating fluids in the Avalon Formation. The relationship between the tectonics and the flow of these fluids is also investigated. A model highlighting the origin and flow of such fluids in the Hibernia rollover anticline is advanced. Finally, controls on calcite cementation are discussed.

I.5- GEOLOGIC SETTING

The Jeanne d'Arc basin is one of the Mesozoic rift basins that were developed as a result of the opening of the Atlantic Ocean (figure I.3; Hubbard et al. 1985; Welsink and Tankard 1988; Tankard et al. 1989; Grant and McAlpine 1990). The basin is located about 315 kilometres E.S.E of Newfoundland. The sedimentary section in the deepest part of the basin is estimated to be more than 14.0 Km. thick (figure I.4; Grant et al 1986). This sedimentary section overlies a basement consisting of Precambrian metamorphic rocks and Paleozoic sedimentary, meta-sedimentary and igneous rocks (Enachescu 1987; Grant and McAlpine 1990).

The sedimentary succession in Jeanne d'Arc basin ranges in age from Triassic up to Recent and it records several stages of basin subsidence (figure I.2; Enachescu 1987; Hubbard 1988; Tankard et al. 1989; Grant and McAlpine 1990; Hiscott et al. 1990; Sinclair 1993). Enachescu (1987) subdivided this succession into extensional stage and thermal subsidence stage sediments (figure I.1). Enachescu stated *"Extensional stage sediments are represented by syn-rift Upper Triassic-Lower Jurassic deposits (red beds and evaporites), followed by Lower Jurassic-Lower Cretaceous failed rift or syn-rift deposits (Shallow marine limestones and paralic to marine clastics). Thermal subsidence stage sediments are represented by Upper Cretaceous-Tertiary marine beds (clastics and deep water carbonates)"*.

These two sedimentary successions are separated by a major Albian-Aptian unconformity that is described as 'Avalon Unconformity' (Swift and Williams 1980; Wade 1981; Powell 1985; Keen et al. 1987; Enachescu 1987; Grant and McAlpine 1990). The development of this unconformity coincides with separation of the Grand Banks and Iberian margins (Sullivan

"The extensional stage involves rapid stretching of continental lithosphere, which produces thinning and passive upwelling of hot asthenosphere. This stage is associated with block faulting and subsidence. The thermal subsidence stage includes thickening of the lithosphere, by heat conduction to the surface, and further slow subsidence which occurs without associated faulting" (McKenzie 1978).

1983; Masson and Miles 1984; Mauffret and Montadert 1987).

In contrast to the above interpretation, Hiscott et al. (1990) and Sinclair (1993) have suggested that the Aptian-Albian sediments above the Avalon unconformity are synrift rather than post-rift or thermal subsidence stage sediments. On the other hand, Tankard and Welsink (1988) reported that these Aptian-Albian sediments represent a transitional period to the post-rift thermal subsidence stage. In further contrast, the upper Cretaceous sediments overlying this unconformity are reported to represent transition to drift stage while the Tertiary sediments were deposited during the thermal subsidence stage (McAlpine 1990; Grant and McAlpine 1990).

The Hibernia field is located on the north-western side of a trans-basin fault zone (figure I.4). The Hibernia structure involves the rollover anticline of a growth fault, named the Rankin fault (figure I.1). The growth fault system is poorly documented and only the rollover anticline was mapped (e.g. Arthur et al. 1982; CNOPB 1986).

The rollover anticline is trending in a NW-SE direction and is bounded on the west and north, respectively, by the Murre fault and Nautilus fault (figure I.5). The anticline is highly dissected by faults and is plunging towards the SE. The main faults which have throws ≥ 200.0 meters define several grabens (figure I.6). One graben occurs in the hanging wall of

the Murre fault in the SW and hosts the G-55, I-46, O-35 and J-34 wells. This graben intersects the rollover anticline half the way between the G-55 and I-46 wells. Two other grabens run along the crest of the rollover anticline and are oriented in a NW-SE direction.

I.6- PREVIOUS WORK

I.6.1- STRATIGRAPHIC NOMENCLATURE:

McKenzie (1980) introduced the "Avalon sand zone" to designate the uppermost hydrocarbon reservoir in the Hibernia field. Arthur et al. (1982) called the same unit the "Avalon Member" of the Missisauga Formation, extending the stratigraphic nomenclature that was used by Jansa and Wade (1975) for the southern Grand Banks to the Jeanne d'Arc basin. Sinclair (1988 & 1993) and CNOPB (1990) proposed the "Avalon Formation" for the Hauterivian to Late Barremian or Early Aptian sediments in the Jeanne d'Arc basin. Tankard and Welsink (1987) and Tankard et al. (1989) called the same Hauterivian-Early Aptian sediments in the Hibernia field "the Avalon Sandstones". The top of the Avalon Formation is a basinwide unconformity surface named "mid-Aptian unconformity" (Sinclair 1988 & 1993; and CNOPB 1990). The hiatus associated with this unconformity represents late Barremian time (Tankard et al. 1989).

In contrast to Sinclair (1988 & 1993) and CNOPB (1990), Grant and McAlpine (1990) and McAlpine (1990) advanced the "Avalon Formation" for the Late Barremian to Late Aptian or Early Albian sediments in Jeanne d'Arc basin. The Avalon Formation is confined between two unconformities, namely the Barremian and Aptian unconformities (Grant and McAlpine 1990; and McAlpine 1990). It is important to note that the "mid-Aptian Unconformity" that is proposed by Sinclair (1988 & 1993) and CNOPB (1990) is named "Barremian unconformity" by Grant and McAlpine (1990) and McAlpine (1990; figure I.6).

In accordance with Grant and McAlpine (1990) and McAlpine (1990), the present study refers to the Late Barremian to Early Aptian rock unit, which is confined between the Barremian and Aptian unconformities as the Avalon Formation. The rock unit which overlies the Aptian unconformity is regarded here as the Ben Nevis Formation.

I.6.2- BIOSTRATIGRAPHY:

The depths of both the Barremian and Aptian unconformities have always been a matter of debate between geologists in different oil companies (see table IX.1 for the discrepancies in depths of both unconformities). These industry geologists conventionally used the highest occurrence of species belonging to what they called "Speeton Assemblage"

to mark top of the Barremian Stage . Gulf Canada geologists used the highest occurrence of an Ostracod subzone, *Hutsonia* sp. 3 subzone, to also mark top of the Barremian Stage. Similarly, the highest occurrences of what is termed "C. tabulata assemblage" and "C. Dampieri Assemblage" have traditionally been used in oil companies to designate the top of the Aptian Stage.

Jenkins (1984) recognized a substantial Aptian unconformity in nine of the Hibernia wells. The hiatus associated with the unconformity represents late Aptian time and in some wells possibly part or all of the Early Aptian and Albian time. An assessment of Jenkins' work indicated that he did not acknowledge the presence of the Barremian unconformity in his earlier 1984 study. Instead, he suggested either a significant facies change or a depositional hiatus at the contact between the Early Aptian-Late Barremian section and Early Barremian strata. In 1993, Jenkins updated his 1984 work and reviewed other biostratigraphic data generated in various oil companies. Jenkins (1993) reported that the hiatus, which is associated with the Barremian unconformity, represents Late Barremian time. In other words, much of the Barremian

The Speeton Assemblage includes a group of dinoflagellates species that occur abundantly throughout the Barremian Stage and disappear at its top. Although the different species in the assemblage vary in their stratigraphic ranges, they tend to disappear within a narrow interval (Jenkins, personal communication).

sedimentary record is missing. In contrast, Jenkins (1993) questioned the presence of the Aptian unconformity and stated *"Evidence for an unconformity at the Aptian-Albian contact is limited to sharp changes in both marine and non-marine palynological assemblages recorded across the contact. The changes do not indicate the period of time represented by this possible hiatus, however, because most of the biostratigraphic events concerned have not been dated at type sections"*.

Ascoli (1990) used foraminiferal-ostracod zonation to correlate Mesozoic rocks penetrated in 42 wells, including 6 of the Hibernia wells, in the North Atlantic margin of North America. Perhaps the most striking result that can be extracted out of Ascoli's correlation is that rocks of the Avalon Formation in the Hibernia field are of Hauterivian-Barremian age. The same intervals of the Avalon Formation in the 6 Hibernia wells, which were studied by Ascoli (1990), have been dated back to the Aptian or Late Barremian-Aptian time by Jenkins (1984 & 1993) and Davies (1990).

Davies (in Williams et al. 1990) divided the Kimmeridgian-Turonian section in Hibernia field into 14 biozones and 34 subzones. Davies subdivided the Late Barremian-Aptian section, that represents the Avalon Formation in this study, into three subzones, 10A - 10C, which have been correlated between 7 wells in the Hibernia field (figure I.6). It appears clearly that the magnitude of hiatuses, which are

associated with the Barremian and Aptian unconformities, varies significantly between the different wells.

I.6.3- PALEOECOLOGY:

Root (1983) used macrofossils, microfossils, trace fossils and sedimentary features to interpret the paleoenvironmental conditions for the cored section in the Hibernia I-46 well. He recognized five faunal associations:

- 1- The trace fossil-plant debris association reflects low energy soft-muddy substrate conditions that were seldom inhabited by benthic organisms with preservable hard parts.
- 2- The Corbula-Nucula-Turritella association indicates low energy, perhaps slightly restricted, lower shoreface environment.
- 3- The Cardiid-Trigonia association suggests stenohaline, firm substrate, middle shoreface environment.
- 4- The Oyster-Serpulid association represents shallow, high energy and periodically brackish environment. The small to moderate size oyster shell population with abundant serpulid tubes suggests a more marine origin. The large, thick-shelled oyster shell population points to a more restricted brackish environment.
- 5- The shell hash category reflects high energy, possibly storm-related, wash-over deposition.

Jenkins (1984) estimated the degree of marine influence on the environments of deposition of the Avalon sediments in

the Hibernia field. The estimate was based on a subjective assessment of the proportions of terrigenous and marine detrital organic matter in the sediments. Jenkins recognized four categories¹:

- 1- Non-marine, in which no in situ organic matter from a marine source was recognized.
- 2- Weak marine, in which a marine influence was detectible by the presence of minor, quantitatively insignificant (< 1%) amounts of marine organic matter.
- 3- Marine, where organic matter from marine sources constitutes a substantial proportion of the total organic matter, but does not predominate over terrigenous organic matter.
- 4- Strong marine, characterized by a predominance of marine over terrigenous organic matter.

Jenkins (1984) indicated that marine influence across the Hibernia area was progressively stronger towards the NE, in the Aptian-Late Barremian time.

Pemberton (1985) investigated the ichnofacies of the Avalon Formation in Hibernia Field. He distinguished ten different ichnofossil suites, based on the ichnogenera present

¹In this study, the type of organic matter that characterize Jenkins' categories 1 to 4 will be frequently referred to by the writer as terrigenous, essentially terrigenous, terrigenous & marine, and marine & terrigenous, respectively.

and their relative abundance. These ichnofossil suites reflect relatively shallow-water, fully marine to marginal marine environments. Pemberton used the Norton Sound on the eastern side of the Bering sea as a modern analogue for the depositional environment of the Avalon Formation. The Norton Sound model does not involve a physical barrier to restrict the sound and to account for changes in salinity. The salinity variations result from the excessive freshwater runoff from the Yukon river. Pemberton reported that the biogenic and possibly chemical characteristics of the Avalon Formation may mimic an estuarine environment."

Guilbault (1986) studied the foraminiferal and ostracod paleoecology in five of the Hibernia wells. Based on population diversity, dominance and species composition, Guilbault recognized seven biofacies:

Biofacies "G" represents an open marine rather quiet environment.

Biofacies "F" characterizes probably a quiet, strongly hyposaline¹ lagoon.

Biofacies "E" indicates a normal to near-normal marine

¹Salinity values used by Guilbault (1986):
"normal marine: > 33 part per thousand
near normal marine: 30 - 33
Slightly hyposaline: 25 - 30
Moderately hyposaline: 15 - 25
Strongly hyposaline: 2.5 - 15
Oligohaline: 0 - 2.5
Fresh water: 0 or nearly 0.

environment.

Biofacies "C" reflects slightly to moderately hyposaline conditions.

Biofacies "B" symbolizes an environment that was probably slightly to moderately hyposaline and rather quiet, but not a hyposaline lagoon as for biofacies 'F'. Guilbault and Vervloet (1983), however, interpreted this biofacies as typically estuarine.

Biofacies "A" reveals a normal marine to moderately hyposaline environment.

Biofacies "D" constitutes an environment similar to that of 'B' or 'C', except that the climate may have been warmer.

I.6.4- FACIES & DEPOSITIONAL ENVIRONMENTS:

No detailed facies study for the Avalon Formation in Hibernia field has yet been published. Regional stratigraphic studies were carried out by McAlpine (1990), Grant and McAlpine (1990) and Sinclair (1988b & 1993). Lee (1987) did a study that was centred on the diagenesis of the Avalon Formation in Hibernia field. Hurley et al. (1992) investigated the reservoir development of the Avalon and Hibernia Formations, in the Hibernia field. As a result of the diverse goals of all of these studies, significantly different interpretations were proposed for the facies and depositional environments of the Avalon Formation. These interpretations are summarised below.

Grant and McAlpine (1990) and McAlpine (1990) reported that sandstones of the Avalon Formation in Jeanne d'Arc basin were deposited in an estuarine environment, and the shales were laid down in lagoons and tidal flats. Neither data nor evidence for these interpretations were presented.

Lee (1987) identified four lithofacies in the Avalon Formation in Hibernia field: 1) shales, 2) bioturbated sandstones, 3) porous sandstones and 4) interbedded sandstones and shales. Based on mineralogy, grain size, sedimentary structures and trace fossils, depositional environments for the different lithofacies were interpreted. Lee (1987) reported that lithofacies 1 was deposited in basinal offshore or lagoonal environments. Lithofacies 2 was deposited in intertidal to supratidal environments. Lithofacies 3 represents deposition as a sand bar possibly in a foreshore to shoreface environment. Lithofacies 4 was laid down in an environment below fair weather wave base but one which is subject to episodic storms.

Sinclair (1988b & 1993) reported that the transgressive siliciclastic Ben-Nevis Formation (equivalent to the Avalon Formation in this study) in the Jeanne d'Arc basin comprises two separate but related facies associations. Sinclair (1993) stated "A locally preserved basal association represents interfingering backbarrier environments and is herein defined as the Gambo Member. An upper ubiquitous facies association

comprises tidal inlet channel, shoreface, and lower shoreface/offshore transition sandstones. This upper facies association overlapped marine ravinement diastems above the laterally equivalent backbarrier facies".

Hurley et al. (1992) reported that the lower part of the Avalon Formation in Hibernia field was deposited in a partially restricted, shallow bay environment that was subjected to episodic storms. "Subaerial exposure of the shallow bay sequence occurred during Barremian time and developed red shales. Gradual transgression gave way to deposition of shoreline sandstones and finer grained shelf shales over the mid-Barremian unconformity. Conglomerates that overlie coal and red mudstone in the most westerly G-55 well likely represent alluvial fan sedimentation adjacent to the basin margin" (Hurley et al. 1992).

1.6.5- Petrography & diagenesis:

Petrography and diagenesis of the Avalon Formation in Hibernia field have been extensively studied. Meloche (1985) and Hurley et al. (1992) have focused on the factors that affect porosity and permeability of the Avalon sandstones. Chaplin (1985) provided a good microscopic description of the calcite cements in the Avalon Sandstones. Hutcheon et al. (1985), Lee (1987) and Abid (1988) addressed the origin of calcite cementation and provided markedly different interpretations. The above-mentioned studies have neither

reported a sampling strategy nor attempted to delineate the paleo-flow of the calcite-precipitating fluids. The results of these studies are summarized below.

Chaplin (1985) recognized two generations of calcite cement in the Avalon Sandstones, in the Hibernia field. *"The two generations involve an early diagenetic rim cement and a later possibly mesodiagenetic pore-filling cement. The latter cement is largely responsible for the loss of porosity"*. Chaplin stated that there was no apparent textural controls on the carbonate cements. She mentioned that much of porosity is secondary in origin and developed due to dissolution of the carbonate cements.

Hutcheon et al. (1985) studied the geochemistry of calcite cements in the Avalon Sandstones. They reported that *"the trace element data indicate an influence of meteoric water on the composition of some, if not all of the diagenetic calcite (cements, veins, and recrystallized bioclasts). The comparison of the trace element and isotopic data suggests a possible effect of elevated temperature in the process of calcite precipitation and recrystallization. A major component of cementation, probably originating from the recrystallization of pre-existing carbonates, occurred during the time at which the mid-Cretaceous unconformity developed and allowed the influx of meteoric water into the Avalon sand. The influx of meteoric water, responsible for cementation,*

occurred when the Avalon Sandstones were buried at a depth of 400-600 meters".

Meloche (1985) reported that the calcite cementation in the Avalon Sandstones, in many Hibernia wells, ranges from early to relatively late diagenetic precipitate. There is no evidence to support a nodular or concretionary habit to the poikilotopic calcite cements. The cemented zones exhibit a facies control dictated by bioclast and/or conglomerate content, and should exhibit some lateral continuity.

Lee (1987) described sandstones of the Avalon Formation as mineralogically mature sublitharenites to quartz arenites or lithic wackes to quartz wackes. She reported that the paragenetic sequence of diagenesis in these sandstones involves: quartz, syntaxial calcite, siderite, pyrite, dolomite, poikilotopic calcite and void-filling matrix replacement calcite. The trace element and stable isotopic data suggest that calcite-precipitating fluids had a composition similar to sea water that has been slightly diluted by meteoric water. The source of the calcite cements was the dissolution of fossil fragments in the sandstones. The 'A' limestone marker below the Avalon Formation might also have been a source of calcite cements. Precipitation of calcite cements occurred at elevated temperatures ranging between 40 and 60°C and at a depth of 2.2 Km. It is interesting to note that Lee (1987) interpreted the Avalon

calcite cements as a product of late diagenetic processes, although she acknowledged the loose compaction of the calcite-cemented sandstones.

Abid (1988) recognized an early ferroan calcite cement, responsible for destroying primary porosity in the Avalon Sandstones, and also in other rock units, in the Hibernia field. Abid suggested an early stage of precipitation of this ferroan calcite cement because of the loose packing of detrital grains, high (>25%) minus-cement porosity and lack of other cements except minor siderite, silica and clay mineral coatings. Based on isotopic data from eight samples, none of which is collected from the Avalon Formation, Abid reported that the early ferroan calcite cement precipitated as a result of upward-moving hot shale waters mixed, at places, with meteoric waters. Abid argued that marine carbonate fragments are the main source of calcium and carbon for the early ferroan calcite cement.

Hurley et al. (1992) stated *"the most volumetrically significant porosity-reducing agent in the Avalon Sandstones is calcite cementation. There is no definite relationship between depositional facies and calcite cementation."* However, they acknowledged the fact that the dominant occurrence of cementation is within the basal transgressive deposits of the Avalon Formation.

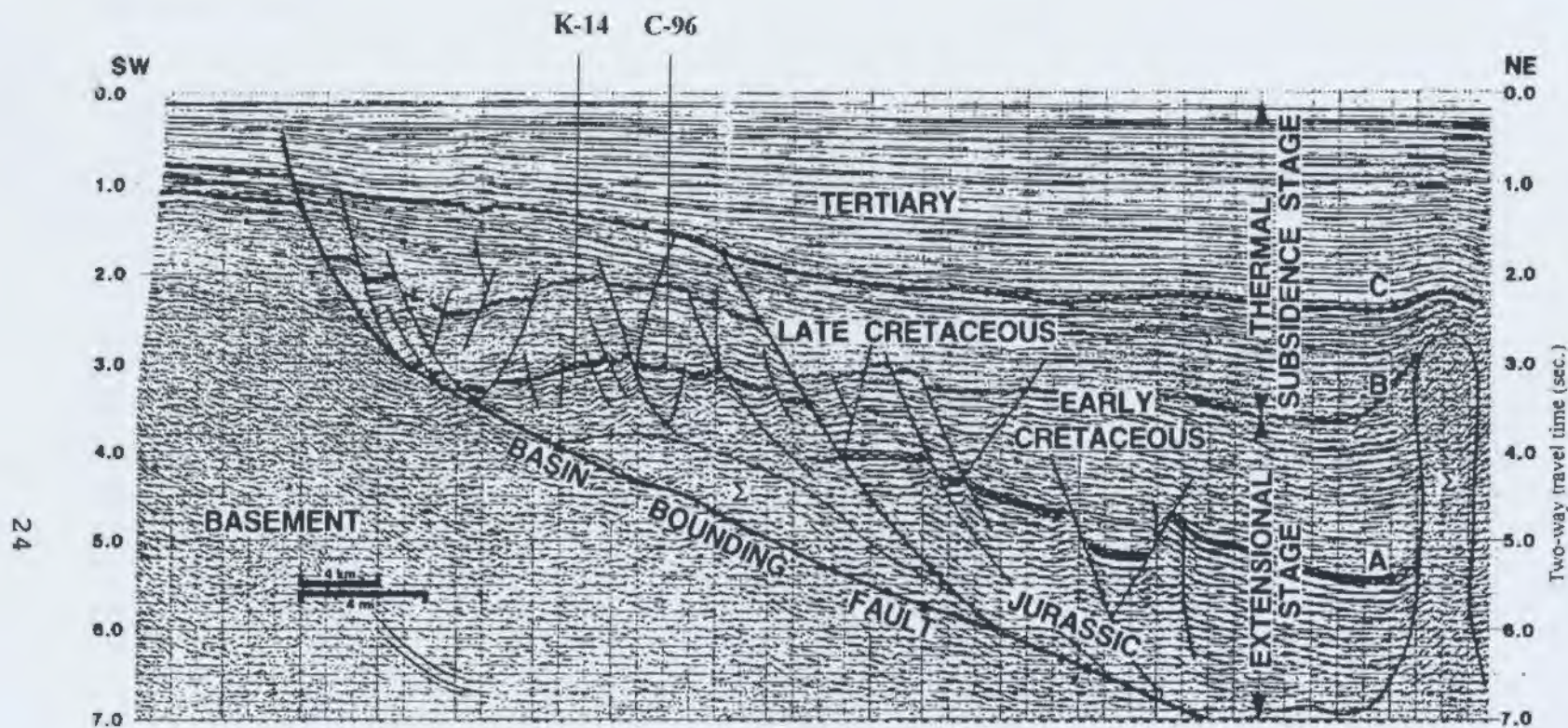


Figure I.1- Migrated time seismic section showing the Hibernia rollover anticline, extensional stage and thermal subsidence stage sediments, salt diapir and swell 'Σ', and major unconformities: 'A' top of Jurassic, 'B' Barremian, 'C' Sub-Tertiary. The basin bounding fault is the Rankin fault. Note the two grabens at the crest of the rollover anticline to the SW and NE of the Hibernia C-96 well. See these grabens in figure I.6. The orientation of the seismic line is shown in figure I.4 & 6. (Enachescu 1987).

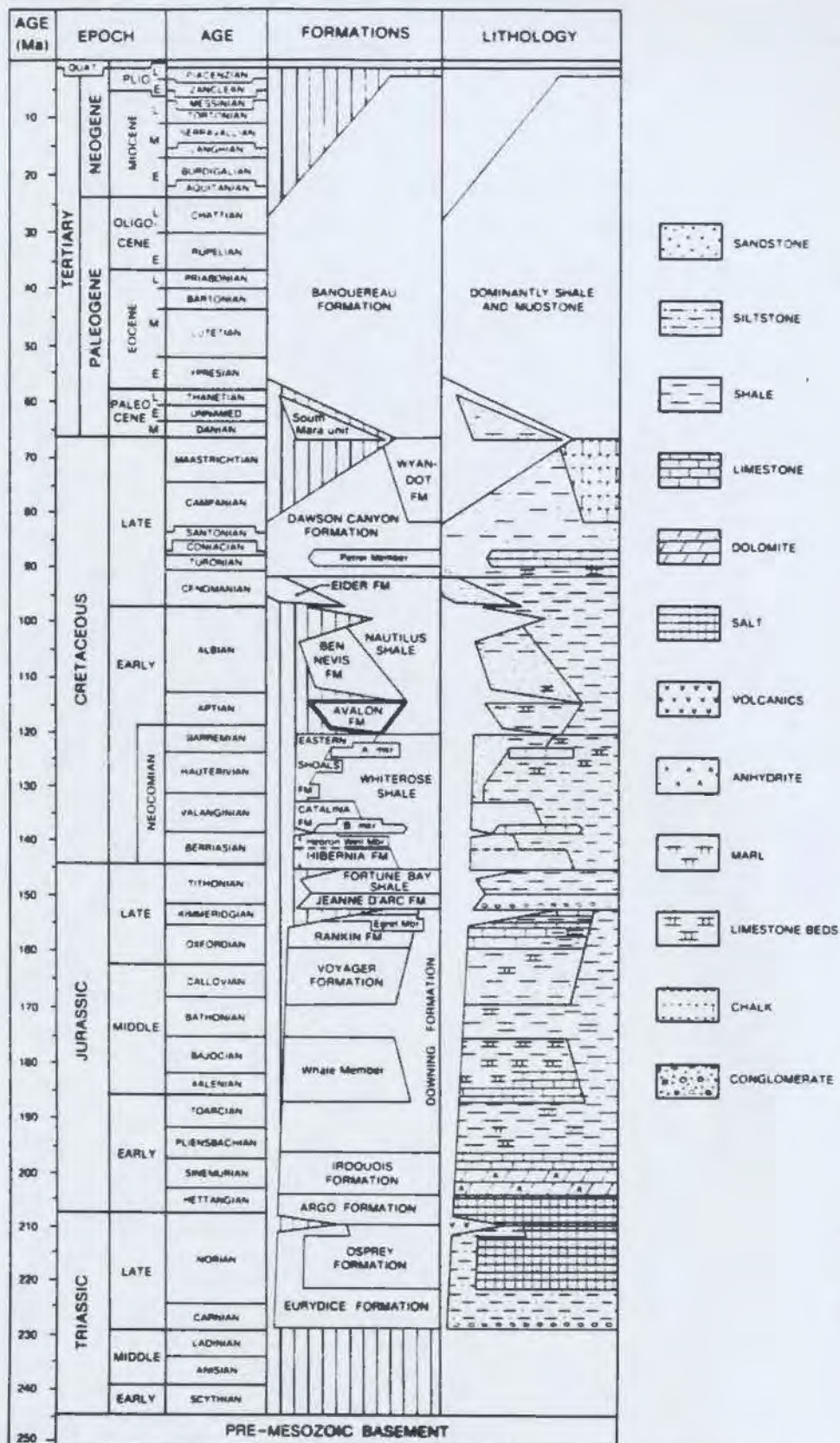


Figure I.2- Lithostratigraphic chart for the Jeanne d'Arc basin. Note the hiatuses at the top and bottom of the Avalon Formation (Grant and McAlpine 1990).

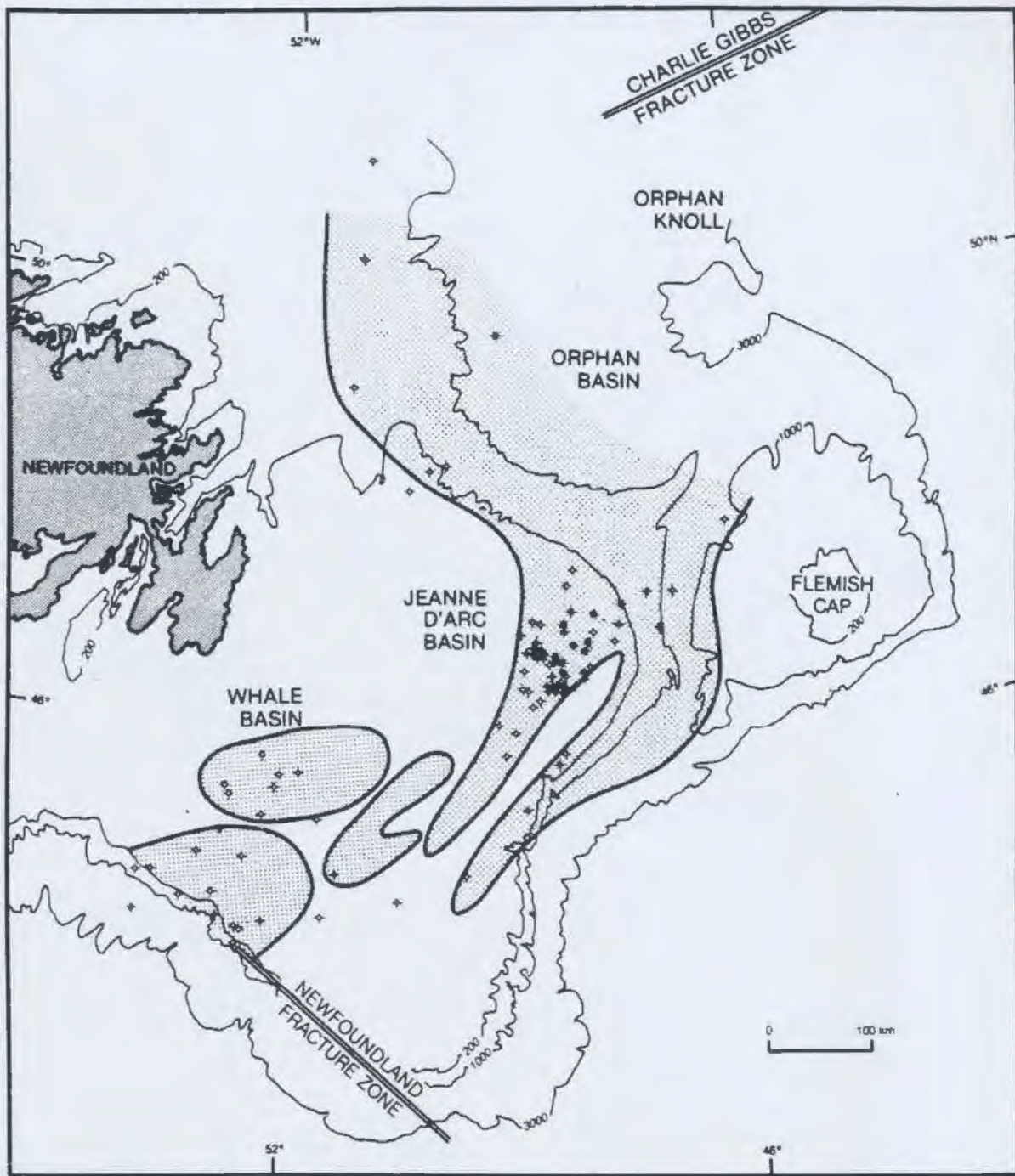


Figure 1.3- North Atlantic Mesozoic rift basins (Welsink et al. 1989).

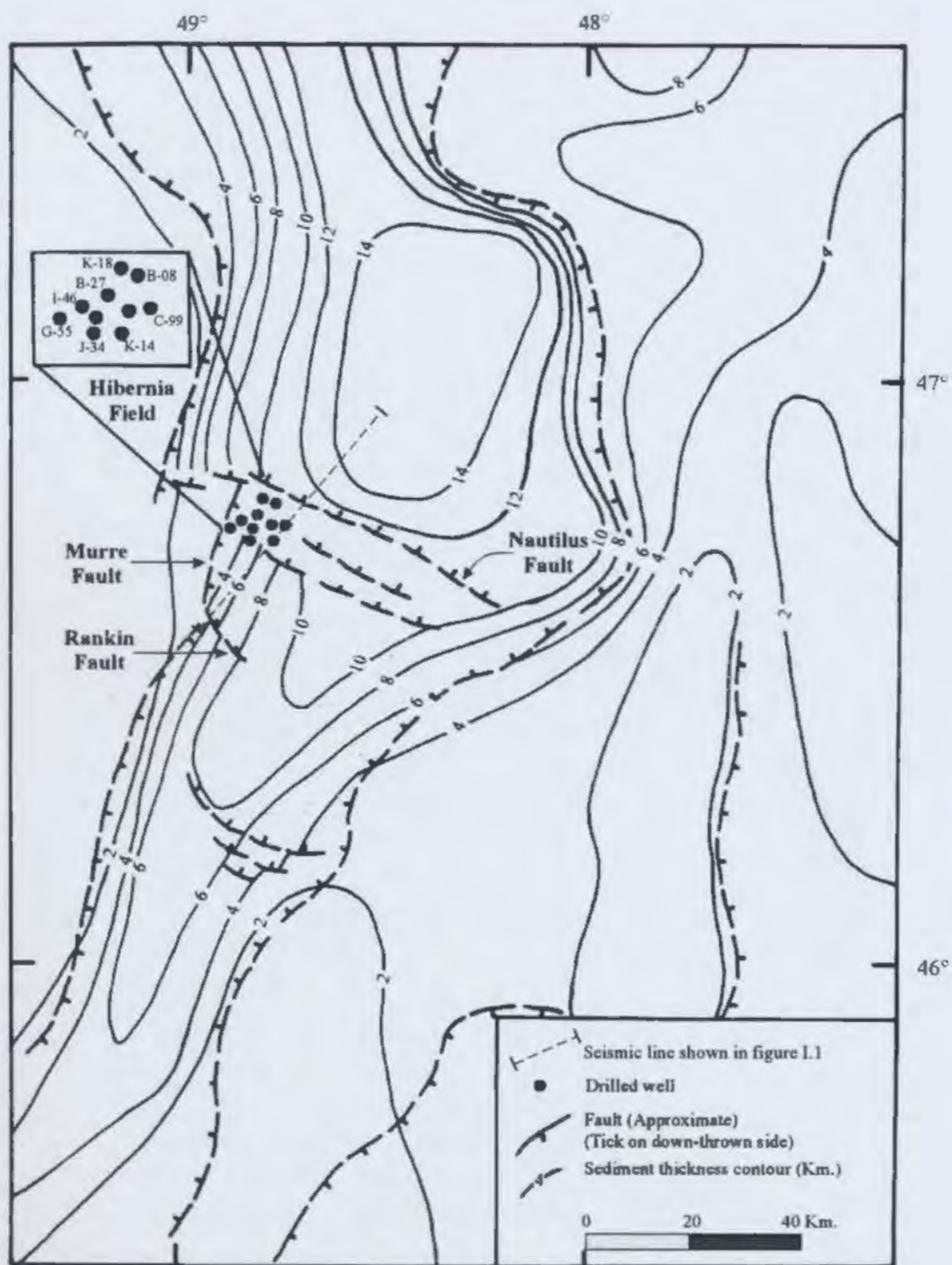


Figure I.4- Diagrammatic structure and sediment thickness map for the Jeanne d'Arc basin. The Hibernia field is located in the northwestern side of the trans-basin fault zone. (modified from Grant et al. 1986).

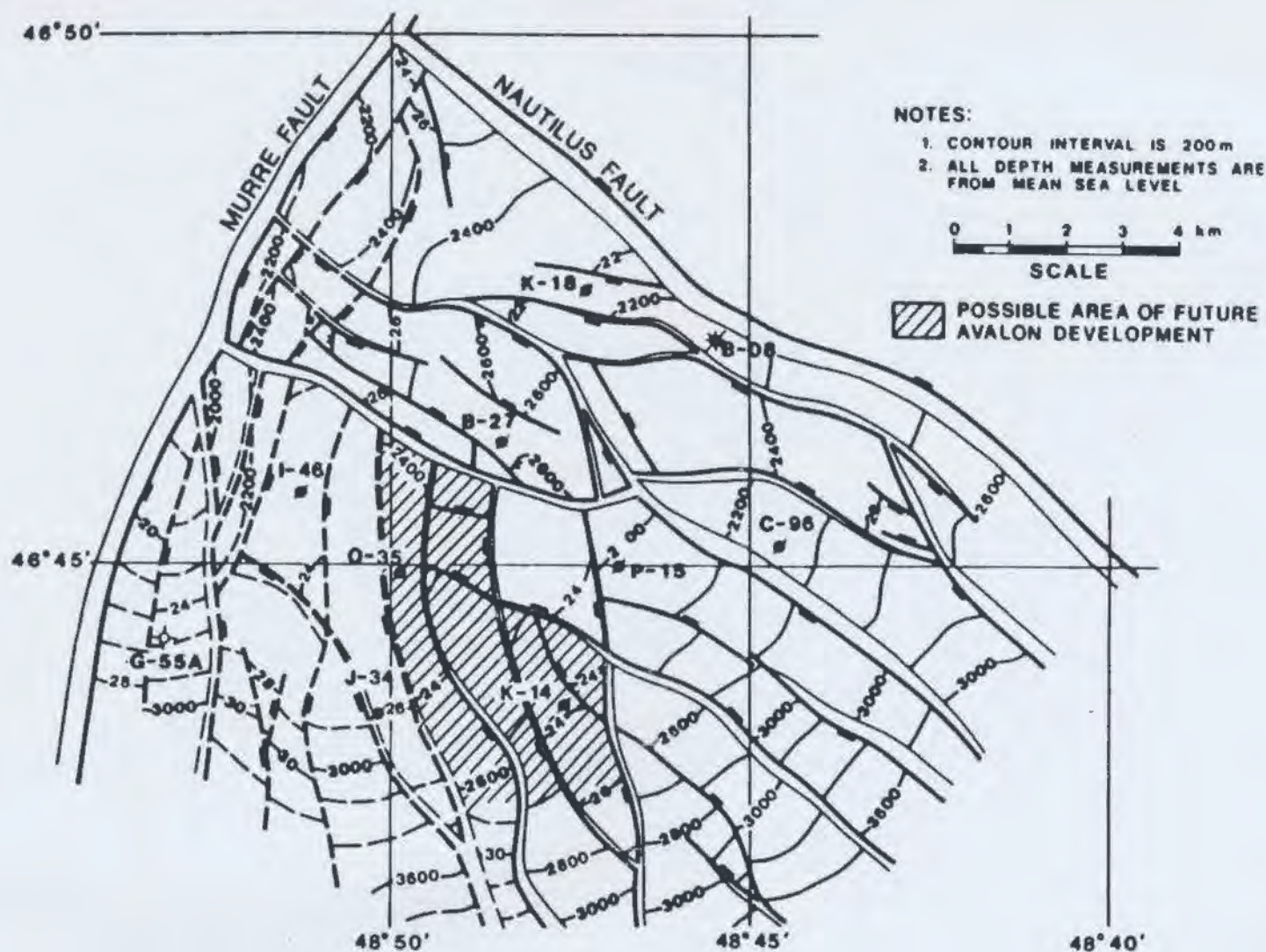


Figure 1.5- Depth map of the Avalon Sandstones in the Hibernia rollover anticline, base of the shale marker no. 2 (CNOBP 1986).

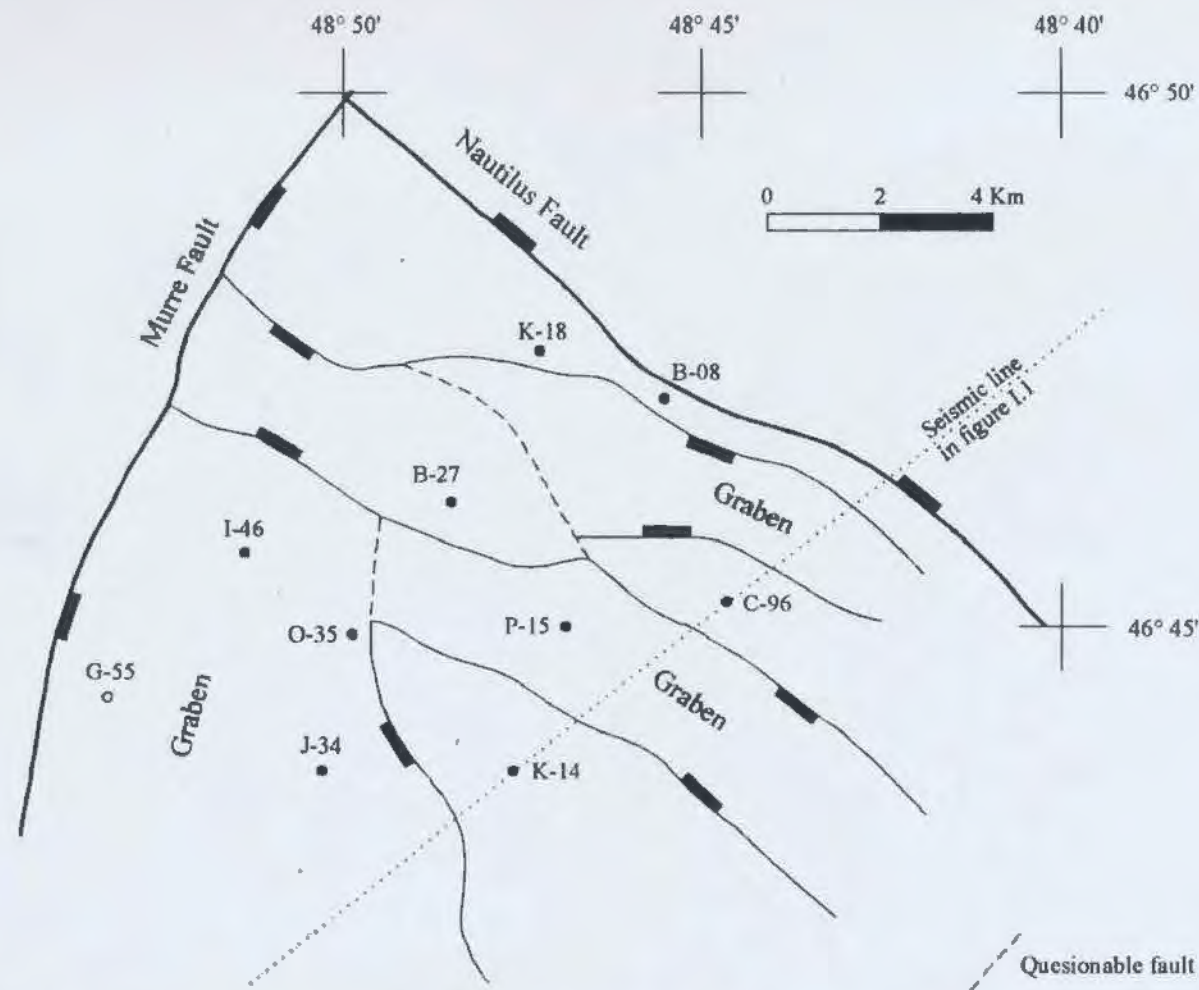


Figure I.6- Simplified structural map for the Hibernia rollover anticline showing the main faults which have throws ≥ 200 meters. Note the two NW-SE trending grabens that are parallel to the axis of the rollover anticline. These grabens are shown in the seismic line in figure I.1. Another graben occurs in the SW at the hanging wall of the Murre fault. (Modified from structural map shown in figure I.5).

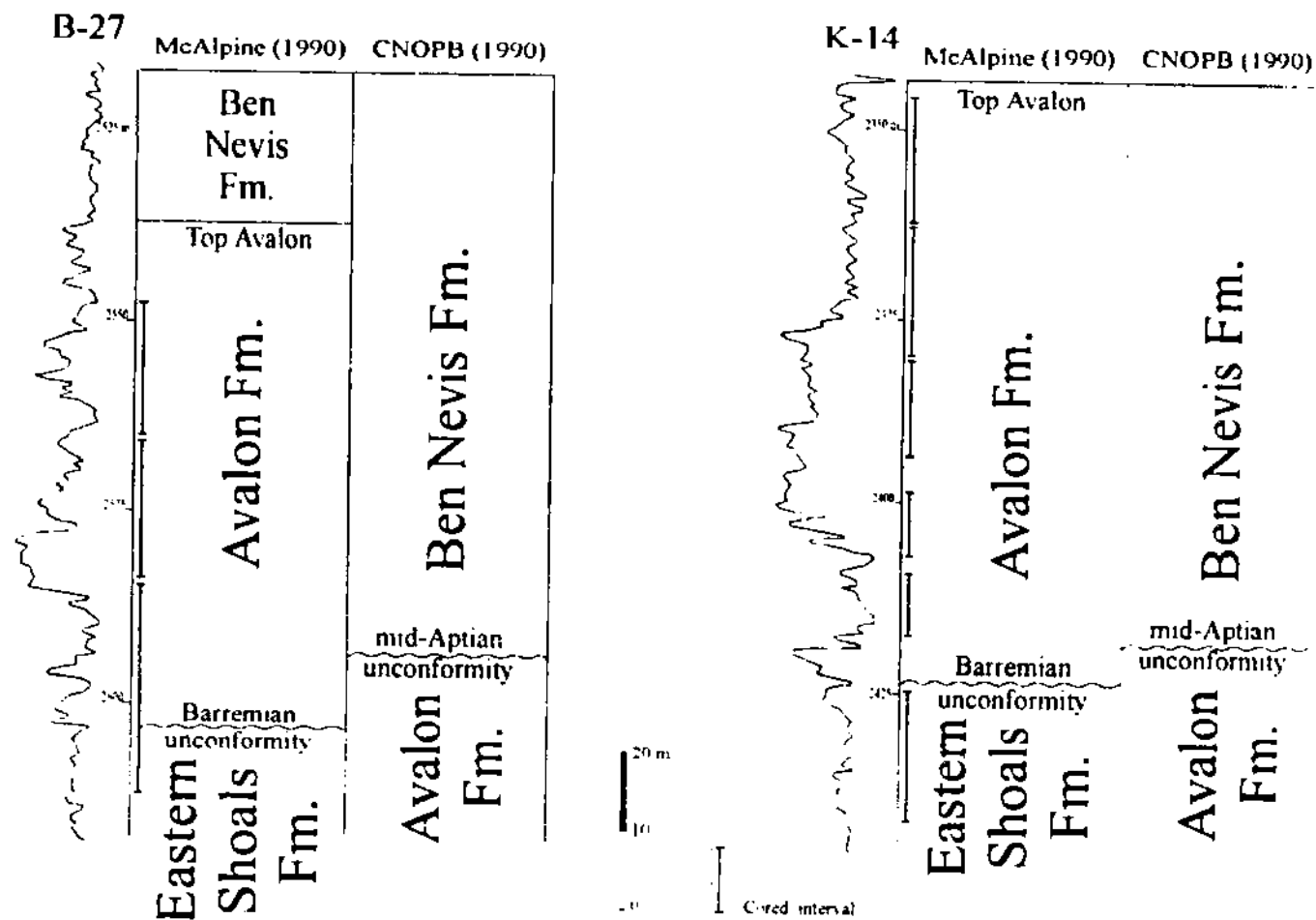


Figure 1.7- Difference in stratigraphic nomenclature of the Avalon Formation.

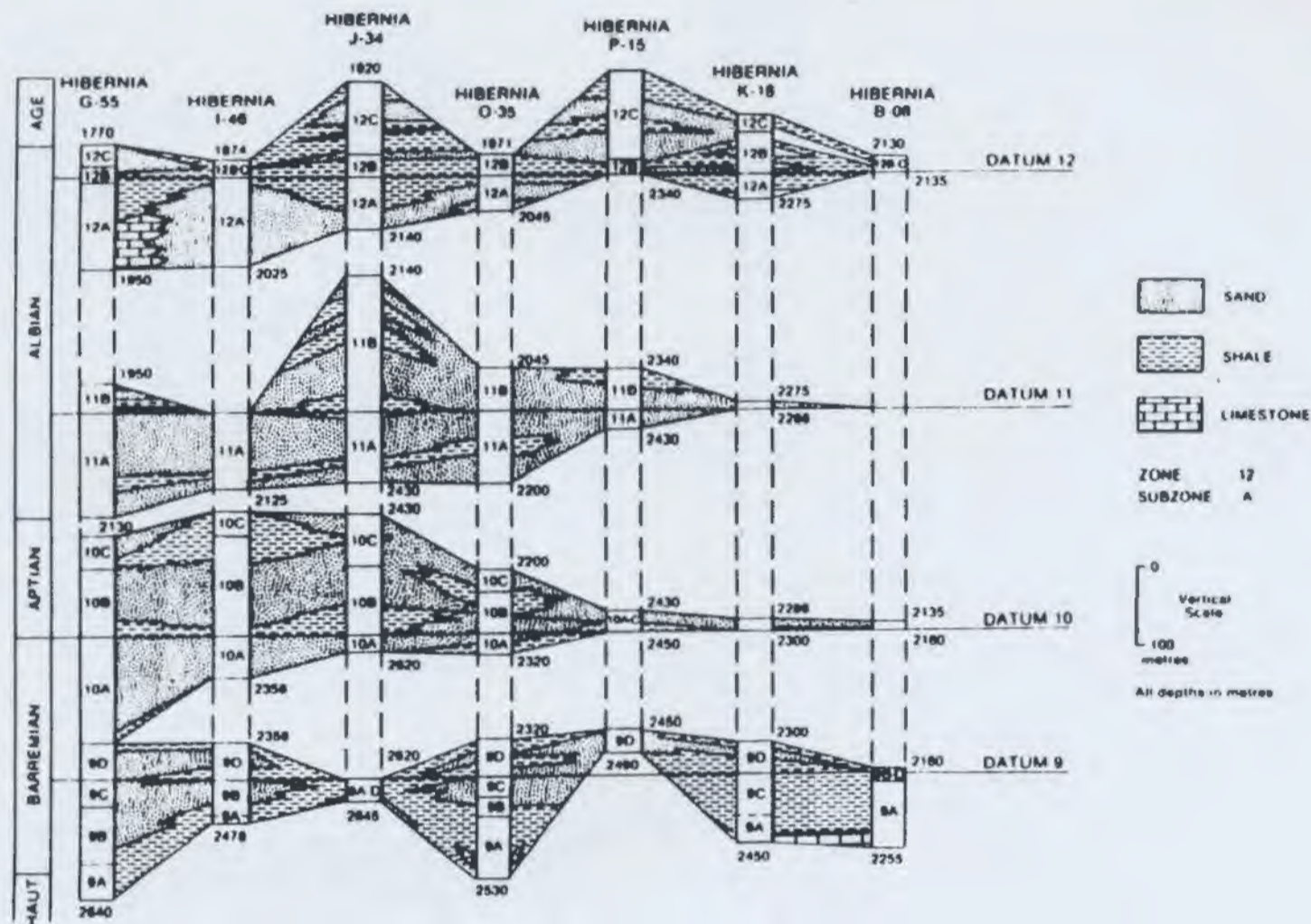


Figure I.8- Correlation of the Early Cretaceous sediments in 7 of the Hibernia wells. The Avalon Formation involves subzones 10A-10C. Note the variation in the magnitudes of the hiatuses at the top and bottom of the Avalon Formation (Davies 1990).

II- DEPOSITIONAL FACIES

&

FACIES ASSOCIATIONS

This chapter aims to describe the common types of rocks cored in the Hibernia field and to provide insight into their depositional processes and environments. Rocks are described here in terms of facies. A facies is defined as a body of rock characterized by a particular combination of lithology, physical and biological structures that bestow an aspect different from the surrounding rocks (Walker 1992). The term facies will be used in this study in a descriptive sense to infer depositional processes, paleoecologic conditions and occasionally post-depositional changes.

Applying Walther's Law of Facies, the vertical and spatial distribution of adjacent facies will be employed to interpret depositional environments. Walther (1894) stated that *"The various deposits of the same facies area and, similarly, the sum of the rocks of different facies areas were formed beside each other in space, but in a crustal profile we see them lying on top of each other"*. It follows that the vertical succession of conformable facies reflects the lateral juxtaposition of depositional environments (Reading 1986). These conformable facies comprise the facies association.

II.1- DEPOSITIONAL FACIES

Fifteen types of facies were recognized in the cored sections (table II.1). These facies are described below.

II.1.1- VARICOLOURED MUDSTONE FACIES (Plate II.1):

The Varicoloured Mudstone Facies ranges in thickness from few tens of centimetres up to five metres. It is composed mainly of mudstone and shale, with some sandy layers. These rocks commonly contain slickensided surfaces, and usually lack any distinct stratification. Small pelecypod and gastropod shells may be scattered throughout the rocks. The shells are occasionally concentrated in thin shell hash layers.

Colour banding is the most diagnostic feature of the facies. The rocks commonly change in colours upwards from dark grey, to orange, to reddish brown, to light greenish grey, to organic-rich darker grey. Contacts between the colour bands are diffuse. Greenish grey mottles are ordinarily present at the top of the reddish brown zone, and reddish brown mottles at the bottom of the greenish grey band.

The top dark grey zone is the thinnest, and hosts branching root traces. The greenish grey colour zone may be missing, and its mudstone is usually coarser grained and sandy. The reddish brown zone is usually the thickest colour band, particularly where the facies is thick. Occasionally, it may be overtaken by the orange zone. The reddish brown mudstone is usually dominated by greyish green grains and

Table II.1- Facies characteristics in the Avalon Formation, Hibernia field.

Facies (page no.)	Physical Structures	Biogenic Structures	Body Fossils	Trace Fossils	Dominant Processes
Varicoloured Mudstone (33)	Desiccation cracks	Root traces			Paedogenesis
Mudstone (36)	Laminated	Mi. burrowing & bioturbation	Oysters & Turritella	Ch, Pl, As, Th,Rh, Te & Zo	Biologic reworking
Shelly Sandstone (39)		Bioturbation	Oysters	Op, Th & Pl	Biologic reworking
Rippled Sand-Mud (40)	Flaser & lenticular bedding			Op	Bedload & suspension deposition
Sandy Siltstone (42)		Bioturbation		Th	Biologic reworking
Coquina (42)	Normal grading		Molluscan shells & Serpulid tubes		Storm deposition
Intraclastic Sandstone (43)	Cross stratification	Md. burrowing	Pelecypods	Op, Pa, Th, An & Pl	Dune migration & Biologic reworking
Heterolithic Mudstone (46)	Planar lamination & wave ripples	Md. burrowing			Storm deposition
Rhythmic Laminated Sandstone (47)	Planar lamination & wave ripples	Mi. burrowing			Storm deposition

Facies (page no.)	Physical Structures	Biogenic Structures	Body Fossils	Trace Fossils	Dominant Processes
Conglomerate- Sandstone (49)	Inclined lamination		Molluscan shells		Transgressive or channel lag
Bioturbated Muddy Sandstone (50)		Bioturbation	Pelecypod shells	Rh, Te, As, Ta, Pl, Pa, Di, Sk, Th, Ch, Zo & Op	Biologic reworking
Laminated Clean Sandstone (52)	Planar lamination & Cross stratification	Md. to in. burrowing		Op., Pa & Sk	Sheet flows & dune migration
Graded Laminated Sandstone (56)	Graded bedding & wave ripples	Mi. burrowing		Sk & Op	Storm deposition
Pebbly Sandstone (59)		Bioturbation		Op & Pa	Biologic reworking
Cross Bedded Sandstone (59)	Cross stratification	Bioturbation		Op & Pa	Biologic reworking & traction transport

An: Anchonichnus
As: Asterosoma
Ch: Chondrites
Di: Diplocraterion

In: Intense
Md: Medium
Mi: Minor
Op: Ophiomorpha

Pa: Palaeophycus
Pl: Planolites
Rh: Rhyzocorallium
Sk: Skolithos

Ta: Taenedium
Te: Teichichnus
Th: Thalassinoides
Zo: Zoophycus

veins. It frequently has desiccation cracks, and carbonate-rich globules.

The Varicoloured Mudstone Facies is intercalated with the Shelly Sandstone, and Mudstone 'A' Subfacies.

Interpretation: The Varicoloured Mudstone Facies represents ancient soils. Colour banding, colour mottling, lack of stratification, and presence of carbonate-rich globules are all diagnostic features of paleosols (Duchaufour 1982; Machette 1985; Retallack 1988; Wright 1989). The lowermost soils, in each of the wells B-27 and K-14, are dominantly brown in colour. Hence, they are the most mature soils and they reflect the longest subaerial exposures.

II.1.2- MUDSTONE FACIES (Plates II.2-5):

The Mudstone Facies includes four subfacies, that vary in the degree of burrowing, diversity of trace fossils, type of organic matter and shell content.

i- **Mudstone 'A' Subfacies** (Plate II.2): This subfacies consists of dark grey mudstone dominated by molluscan shells, particularly oyster and *Turritella* shells. Commonly, the shells are concentrated in shell hash layers. The mudstone varies

'Soil Maturity: is the relative length of time required to develop the soil, if all variables (e.g. parent material, moisture, temperature, and vegetation) remain relatively constant (Bown and Kraus 1987). The deeper the degree of reddening and the more distinct the soil horizons and colour banding, the more mature is the soil (Birkeland 1984; Bown and Kraus 1987).

from structureless to laminated, and frequently has siderite nodules and bands. Bituminous wood fragments and organic stringers are occasionally observed. Organic matter content in this subfacies varies from exclusively to essentially terrigenous (Jenkins 1984).

ii- Mudstone 'B' Subfacies (Plate II.3): This mudstone is dark grey to green coloured and structureless to bioturbated. Trace fossils present in any sample are not abundant and usually include one or two species. The trace fossils involve feeding structures (Chondrites, Planolites, Asterosoma and Thalassinoides) and grazing structures (Anchonicnus horizontalis). Rare dwelling structures (Terebellina and probable Paleophycus) may be observed. Disseminated plant material is occasionally present. Organic matter content of this subfacies is of essentially terrigenous origin (Jenkins 1984).

iii- Mudstone 'C' Subfacies (Plate II.4): This subfacies consists of highly burrowed to bioturbated mudstone with some sandy layers. Relict rhythmic sand-mud lamination, occasionally in discordant sets, is preserved in the sandy layers. About 5.0 degrees inclined stratification (depositional dip) is maintained throughout the rock. Organic matter content of this subfacies is of essentially terrigenous origin (Jenkins 1984). Trace fossils identified in this subfacies are deposit-feeders and include Rhyzocorallium and

Cylindrichnus.

iv- **Mudstone 'D' Subfacies** (Plate II.5): This mudstone is bioturbated and hosts relict layers of very fine grained laminated and graded sandstone. Trace fossils are abundant and include feeding (Teichichnus, Asterosoma, Planolites, Rhizocorallium, Chondrites and Cylindrichnus) and grazing (Zoophycus) structures. Organic matter content of this subfacies is of predominantly marine origin (Jenkins 1984).

Interpretation: The Mudstone Facies was deposited from suspension in a generally low energy environment. The occurrence of low diversity macrofossils and siderite nodules in subfacies 'A' indicates brackish water conditions and a highly stressed environment (Discussed in detail in p. 57). The Mudstone 'A' Subfacies is similar to the lagoonal silty shale and sandy siltstone which were described in the Upper Cretaceous sediments in SW Wyoming (Kirschbaum 1989).

The presence of mainly deposit feeders in subfacies 'B', 'C' and 'D' indicates nutrient-rich substrates. The essentially terrigenous organic matter and moderate to low diversity trace fossil assemblage in subfacies 'B' and 'C' may reflect low energy marginal marine environments. The Mudstone 'C' Subfacies is similar to the interlayered sand/mud bedding, described by Reineck and Wunderlich (1967 & 1969) in tidal environments of the North Sea. They suggested that sand layers are deposited during periods of current activity, both flood

and ebb currents. The mud is deposited during stand-still phases of high and low water tides.

The diverse trace fossil assemblage, relict storm sand layers and predominantly marine organic matter in subfacies 'D' suggest an offshore environment, that was subjected to episodic storms. The Mudstone 'D' Subfacies is analogous to the Pervasively Bioturbated Silty to Sandy Mudstone Facies, Upper Cretaceous in NW Alberta, which was deposited in an open marine environment (Bhattacharya and Walker 1991). The Subfacies 'D' is also similar to the Bioturbated Shelf Siltstone Facies, Upper Cretaceous in Wyoming, which was characterized by Tillman and Martinsen (1984).

II.1.3- SHELLY SANDSTONE FACIES (Plate II.6):

Beds of the Shelly Sandstone Facies can be up to 60 centimetres thick. The facies consists of fine to medium grained sandstone, which contains scattered molluscs, mainly oyster shells. The sandstone is usually bioturbated. Trace fossils include dwelling (Ophiomorpha) and feeding structures (Thalassinoides and Planolites).

Microscopically, the sandstone is composed of quartz grains, lithic and phosphatic fragments, biotite, and skeletal shell debris. Pyritized bituminous wood fragments are frequently present. Recycled quartz grains are commonly observed. These grains have shattered edges that cut across both quartz nuclei and their surrounding quartz overgrowth.

The shell debris are either non-ferroan fibrous calcitic, or ferroan neomorphosed varieties. The fibrous shells are characterized by abundant bores, and microbores. The bores are commonly filled with detrital quartz grains, or lined with siderite.

The Shelly Sandstone Facies is interbedded with the Mudstone 'A' Subfacies, and the Varicoloured Mudstone Facies. It usually has a sharp erosional basal boundary, that is overlain by shell lag.

Interpretation: The Shelly Sandstone Facies was deposited in a low energy environment dominated by biologic reworking. The low diversity of trace fossils and molluscan shells, almost restricted to oysters, reflects a stressed environment (discussed in detail in section II.2.1). The frequent occurrence of bored shells reflects long residence time, before burial, at the sea floor. The Shelly Sandstone Facies is similar to the Bay Margin Facies of the protected south shore of the Copano bay and the lagoonal deposits of the Laguna Madre, Texas coast (Morton and McGowen 1980).

II.1.4- RIPPLED SAND-MUD FACIES (Plates II.7 & 8):

The Rippled Sand-Mud Facies has a sharp basal boundary, and is about 40 centimetres thick. The facies consists of fine grained flaser rippled sandstone that changes abruptly upwards to heterolithic interlayered sand & mud. The layers decrease in thickness gradually upwards, from about 3.0 to 0.5

centimetres. They start at the base with a mud-rich layer, which drapes the underlying rippled sandstone. The mud-rich layers are lenticular bedded. They contain rippled sand lenses. The sand-rich layers consist of wavy bedded to flaser rippled very fine grained silty sandstone. Oppositely directed ripples were observed in successive sand-rich layers. Ophiomorpha burrows occur in the lower sandstone.

This Rippled Sand-Mud Facies is associated with the Shelly Sandstone Facies, the Coquina Facies, and the Mudstone 'A' Subfacies.

Interpretation: The rippled sandstone was deposited from bedload, under lower flow regime conditions. Mud flasers were deposited simultaneously from suspension. They were preserved only in ripple troughs where they were subsequently covered by new migrating ripples. The interlayering of mud and sand in the heterolithic interval reflects the alternation of slack water conditions and relatively active current activity, respectively. The upward decrease of layer thickness may indicate progressively weaker current activity. The presence of oppositely directed ripples reflects oscillatory currents.

The periodic alternation between bedload and suspension deposition, and the reversing nature of currents suggest deposition in a tidally-influenced environment. Reineck and Wunderlich (1969) and Wunderlich (1967) described similar tidally-influenced sediments in the German Bight, North Sea.

They stated that in a single tidal phase several layers, of rippled sands with mud flasers, are produced.

II.1.5- SANDY SILTSTONE FACIES (Plate II.9):

The Sandy Siltstone Facies is about 60 centimetres thick. The lower boundary of the facies is either sharp or gradational, while the upper boundary is sharp. The facies consists of very coarse grained sandy siltstone. The rock is bioturbated, and *Thalassinoides* represent the dominant burrow type. Vertical branching root-like traces are common. They are about one millimetre thick and are filled with dark muddy material.

The Sandy Siltstone Facies intercalates with Shelly Sandstone Facies, and Mudstone 'A' Subfacies.

Interpretation: The facies was deposited in a low energy environment, dominated by biologic reworking. Similar facies were reported in the marshes of the Delaware Atlantic coast (Kraft and John 1979).

II.1.6- COQUINA FACIES (Plates II.10 & 11):

The Coquina Facies varies in thickness from few tens of centimetres up to a metre. The lower boundary of the facies is sharp and erosional. The Coquina Facies consists of pelecypod and gastropod shells, with interstitial sand or mud matrix. Fragments of serpulid tubes occasionally represent an additional component. The shells and shell debris vary in abundance from about 50 to 90% of the whole rock. They can

show normal grading. The shell species and diversity vary according to the associated facies. For instance, oyster and *Turritella* shells represent the main species where the facies is intercalated with the Shelly Sandstone Facies, or the Intraclastic Sandstone 'B' Subfacies. A more diverse assemblage occurs where the facies is associated with the Bioturbated Muddy Sandstone Facies.

The Coquina Facies randomly intercalates with Mudstone, Shelly Sandstone, Bioturbated Muddy Sandstone and Intraclastic Sandstone Facies.

Interpretation: Fragmentation and the common normal grading of shells suggest that they were transported from their original habitats by strong storm currents. Similar transport and mixing of shells by storms has been described in modern shoreline environments (Kumar and Sanders 1976).

II.1.7- INTRACLASTIC SANDSTONE FACIES (Plates II.12-14):

The Intraclastic Sandstone Facies ranges in thickness from 2.5 to 9.5 metres. It consists of fine to medium grained sandstone. Pelecypod shells are occasionally scattered in the sandstone. The sandstone is moderately sorted.

'This diverse assemblage involves bivalve species belonging to the 'Shell Hash Category' and 'Cardiid - Trigonina Association', which were defined by Root (1983). The Cardiid -Trigonina Association includes several species of Cardiids, *Trigonina*, *Homomya*, *Pecten*, *Tapes*, *Tellina*, and *Barbatia*.

Microscopically, the sandstones consist of quartz grains, lithic fragments, carbonate skeletal debris, feldspars, chlorite, and mica (figure II.12). Rounded pyrite grains, phosphatic fragments, and organic chips are usually scattered in between framework grains. Concentric laminar oolites, with quartz or skeletal nuclei, are rarely dispersed among the framework grains. Lithic grains include carbonate micritic intraclasts, and basement fragments. Micritic intraclasts frequently have embedded quartz grains and skeletal fragments.

Skeletal debris involves mainly pelecypod and gastropod shells, echinoid and bryozoan fragments. Shells are either fibrous calcitic, or neomorphosed varieties. The former are consistently non-ferroan, while the latter are ferroan (this study). Shells in the lower part of the facies are commonly bored.

It is worth mentioning that micritic intraclasts and carbonate skeletal debris frequently constitute up to 30% of the total framework grains. Also, the micritic intraclasts are usually enveloped by bladed calcite cement, and the fibrous shells are associated with fibrous calcite cement (see V.1.I).

The Intraclastic Sandstone Facies overlies the Mudstone 'A' Subfacies, Conglomerate-Sandstone or Coquina Facies. The upper boundary of the Intraclastic Sandstone Facies is erosional, and is overlain by either the Conglomerate-Sandstone or Laminated Clean Sandstone Facies.

Two subfacies were recognized in the Intraclastic Sandstone Facies:

i- Intraclastic Sandstone 'A' Subfacies (Plate II.13):

Beds of this subfacies vary in thickness from 0.15 to 2.2 metres. They may have sharp basal boundaries, overlain by basal lags. The latter are composed of rounded basement pebbles, and bituminous wood fragments. A basal lag may range from one pebble up to about 20 centimetres thick and the overlying sandstone bed usually shows progressive upward change from dominant physical to dominant biologic reworking.

Faint parallel and inclined lamination as well as cross stratification are common physical structures. Relict ripples and bituminous organic stringers are occasionally observed. Burrowing can cause random scattering of wood fragments and basement pebbles within the beds. Physical structures may be totally eliminated in the uppermost beds, due to intense burrowing. Dominant burrows include *Ophiomorpha*, *Paleophycus*, *Planolites*, *Anchonichnus horizontalis*, *Thalassinoides*, and possibly *Taenidium*. Composite trace fossils, e.g. *Anchonichnus* penetrating *Planolites*, are also common.

ii- Intraclastic Sandstone 'B' Subfacies (Plate II.14):

This subfacies is usually overlain by subfacies 'A'. Subfacies 'B' has a maximum thickness of about 2.5 metres. It is bioturbated and it has a trace fossil assemblage similar to the one in subfacies 'A'. Microscopically, subfacies 'B' lacks

the bladed and fibrous calcite cements and it has fewer intraclasts and shell debris, than does subfacies 'A'.

Interpretation: In subfacies 'A', the physical structures were mainly developed by dune migration under lower flow regime conditions. Deposition of sands was commonly succeeded by active burrowing, which commonly eliminated the physical structures. The absence of physical structures in subfacies 'B' is due to deposition in a low energy environment.

II.1.8- HETEROLITHIC MUDSTONE FACIES (Plate II.15):

The Heterolithic Mudstone Facies has sharp boundaries. It varies in thickness from about 3.0 to 6.0 metres. The facies consists of grey mudstones with abundant siltstone lenses and discontinuous bands, which increase gradually upwards. The mudstones commonly contain siderite bands and nodules. Trace fossils and macrofossils are generally scarce (Root 1983), and organic matter content is of essentially terrigenous origin (Jenkins 1984).

The siltstone bands have a maximum thickness of about 2.5 centimetres. Their bases are always sharp, while their tops are commonly burrowed and disrupted. The siltstone bands are dominated by planar lamination, wave ripples, truncated wave ripples, and erosive wave ripples. An erosive wave ripple consists of a horizontally laminated siltstone layer. The top of which is eroded in the form of a wave ripple, and is draped by many laminae, resting parallel to the truncation surface.

The siltstone laminae range in thickness from 1 to 3 millimetres. Each lamina has a lighter coloured basal part changing gradually upwards to a darker coloured top.

The Heterolithic Mudstone Facies is associated with the Rhythmic Laminated Sandstone, Conglomerate-Sandstone, and the Bioturbated Muddy Sandstone Facies.

Interpretation: The Heterolithic Mudstones Facies was deposited from suspension, in a low energy environment. Root (1983) attributed the scarcity of fossils to anoxic conditions, soft substrate conditions, and low tidal flushing. The siltstones were deposited episodically during high wave activity. Their physical characteristics suggest that they represent a form of storm deposits. A storm origin has been suggested for similar laminated siltstones in Ordovician rocks in Iberia (Brenchly et al. 1986).

II.1.9- RHYTHMIC LAMINATED SANDSTONE FACIES

(Plates II.15 & 16):

Beds of the Rhythmic Laminated Sandstone Facies range in thickness from 5.0 up to about 60.0 centimetres. The beds always have sharp lower and upper boundaries. The beds are comprised of very fine grained silty sandstone. The sandstone is planar laminated. Few wave ripples are occasionally seen at the tops of sand beds. The thicker beds consist of smaller graded sets, 3 to 11 centimetres thick. The sets may have discordant boundaries. Internally, the sets are rhythmically

laminated and graded. The laminae decrease in thickness upwards from about 15.0 to 1.0 millimetres. Boundaries between the laminae are sharp. Each lamina is graded and changes gradually in colour from light grey at the base to dark grey upwards. Within any set, the darker coloured fractions of successive laminae increase progressively upwards, at the expense of the lighter ones. Tops of the sets are usually draped by thin films of organic chips. Burrowing disrupts lamination at top of one set in the middle of a thick bed as well as tops of many beds.

The Rhythmic Laminated Sandstone Facies is interbedded with the Heterolithic Mudstone Facies.

Interpretation: This facies was deposited from episodic high energy currents. The grain size and the normal grading suggest deposition from suspension. The planar lamination reflects high bottom shear stresses, and deposition in plane bed conditions. The occasional presence of wave ripples indicates oscillatory flows. Burrowing at tops of many beds mark recurrence of normal low energy conditions after deposition. The depositional processes and the oscillatory nature of currents suggest that this facies has a storm origin. A storm origin for quite similar rocks, the Graded Rhythmite Facies, was suggested Reineck and Singh (1972). Also, Schwartz (1982) described very similar storm washover sandstones in the Arnold Road Beach, California.

II.1.10- CONGLOMERATE-SANDSTONE FACIES

(Plates II.17 & 18):

The Conglomerate-Sandstone Facies ranges in thickness from about 5.0 to 35.0 centimetres. The facies consists of pebble and cobble conglomerate, that change gradually upwards to either sandstone or mudstone/muddy sandstone. The basal conglomerate is made up of well rounded basement, siderite, mudstone or sandstone clasts set in a sand matrix. The sandstone above the conglomerate varies in grain size from fine to medium grained. It commonly displays inclined lamination, and may host horizontal layers of crudely aligned small shells.

The mudstone/muddy sandstone, in contrast, is bioturbated and may be pebbly. Abundant large and small shell debris, articulated and disarticulated, from different habitats may also be scattered in the mudstone.

The Conglomerate-Sandstone Facies erosively overlies any of the Intraclastic Sandstone, the Heterolithic Mudstone, the Mudstone, the Pebbly Sandstone, or the Cross Bedded Sandstone Facies.

Interpretation: The variable character of the facies, below and above the conglomerate, reflects significant changes in depth and energy conditions of the depositional environment. When the basal conglomerate passes upwards to physically reworked sandstones, it may represent a basal channel lag.

This interpretation is confirmed only if an erosional channel boundary can be proven (e.g. figure III.4). In contrast, if the Conglomerate-Sandstone Facies cuts through barrier island sandstones, for instance, and changes upwards to bioturbated muddy sediments, it will mark a transition to a lower energy deeper environment (e.g. figure II.3). In this case the facies would constitute a transgressive lag deposited above a ravinement surface.

Similar transgressive lag deposits were described by Clifton (1981) and Ryer (1981). Clifton stated that "the conglomerate constitutes a surf-winnowed lag, that was left behind the landward-advancing sea. As the transgression proceeds, a water depth is reached such that fine sediment will begin to accumulate on the lag gravel, and waves will no longer be able to rework the deposit".

II.1.11- BIOTURBATED MUDDY SANDSTONE FACIES

(Plates II.19 & 20):

The Bioturbated Muddy Sandstone Facies is made up mainly of muddy fine to very fine grained sandstone. The facies is bioturbated in the lower part. The sandstone gets gradually cleaner and less burrowed upwards where relict lamination may be preserved. Trace fossils include *Anchonichnus horizontalis*, *Rhizocorallium*, *Teichichnus*, *Asterosoma*, *Taenidium*, *Planolites*, *Palaeophycus*, *Diplocraterion*, *Skolithos*, *Thalassinoides*, *Phoebichnus*, *Chondrites*, *Zoophycus*, and

Ophiomorpha. Serpulid worm tubes are frequently observed.

Two subfacies are recognized in this facies:

i- Bioturbated Muddy Sandstone 'A' Subfacies (Plate II.19):

This subfacies is characterized by abundant scattered Pelecypod shells and the aforementioned diverse trace fossil assemblage. The subfacies hosts a low diversity calcareous and arenaceous foraminiferal assemblage (Guilbault 1986).

ii- Bioturbated Muddy Sandstone 'B' Subfacies (Plate II.20):

This subfacies hosts mainly few large oyster shells and has a less diverse trace fossil assemblage. The latter includes mainly Asterosoma, Chondrites, Anchonichnus. The subfacies hosts essentially arenaceous foraminifera (Guilbault 1986).

The Bioturbated Muddy Sandstone Facies is associated with the Mudstone 'B' Subfacies.

Interpretation: The absence of physical structures and the dominance of bioturbation suggest a low energy environment. The marked changes in abundance and diversity of faunal content and trace fossils in the two subfacies reflect variable ecologic conditions. Subfacies 'A' hosted abundant suspension and deposit feeders, which indicate a well developed epibenthic and endobenthic community. The macro and microfaunal content of subfacies 'A' suggests salinity varying from open marine to brackish (Guilbault 1986; Root 1983). On the other hand, the presence of large Oyster shells, and absence of calcareous foraminefera and suspension feeders in

subfacies 'B' reflects a highly stressed brackish environment (Fallow 1973; Feldmann and Palubniak 1975; Root 1983).

II.1.12- LAMINATED CLEAN SANDSTONE FACIES

(Plates II.21-27):

The Laminated Clean Sandstone Facies is composed of very fine to fine grained clean-looking sandstone. The sandstone is fair to well sorted. It contains abundant organized basal lag deposits which consist of siderite and mud rip-up clasts and occasional shell debris. The rip-up clasts range in size from few millimetres up to 3.0 centimetres, and they are usually rounded to well rounded. The clasts are always supported in a sand matrix.

Microscopically, framework grains in this facies include quartz, lithic fragments, and occasional shell fragments. The shells comprise fibrous calcitic and neomorphosed varieties. Fibrous shells consist of nonferroan calcite, while the neomorphosed ones are made up of ferroan calcite. Lithic fragments are made up mainly of siderite grains, mud pelloids, and few basement clasts. Mud and siderite lithic grains range in size from 0.2 mm. up to several millimetres. They are commonly squeezed, due to compaction between other framework

³The organized basal lag deposits of the Laminated Clean Sandstone Facies contrast with the disorganized basal lag deposits of the Graded Laminated Sandstone Facies. The disorganized basal lag deposits are described in section II.1.13.

grains, forming local matrix-rich patches.

Frequently, rounded, subhedral and euhedral siderite crystals are randomly scattered between other framework grains (plate II.22). The siderite crystals show higher abundance immediately above the basal siderite rip-up clasts, and they are believed to be detrital in origin. Accessory minerals involve chlorite and mica. Wood fragments are commonly scattered in the sandstones. The clean sandstones may be visually classified as sublitharenites and quartz arenites.

The Laminated Clean Sandstone Facies is associated with the Bioturbated Muddy Sandstone Facies and the Mudstone 'B' Subfacies. It can also erosively overly the Intraclastic Sandstone Facies.

Two subfacies were recognized in the Laminated Clean Sandstone Facies:

1- Laminated Clean Sandstone Subfacies 'A':

This subfacies may reach thicknesses up to 4.0 metres. The sandstones in this subfacies are comprised of sets, that range in thickness from about 5 to 65 centimetres (Plate II.23). They are separated by erosional boundaries, that are blanketed by basal lag deposits.

The basal lag deposits are always organized and range from one pebble to few centimetres thick units. The thick basal lags may be made up of smaller layers, that vary in compositional and grain size sorting among one another (Plate

II.21). The clasts may show clast imbrication, normal distribution grading, or inverse grading. Commonly in thinner basal lags, the clasts are arranged such that their longest axes are horizontal and parallel to lamination in the overlying sandstone.

The sandstones are either structureless or planar laminated (Plates II.24 & 25). They rarely have wave or current ripples at the top few centimetres of the sets. Planar lamination is typically faint. The laminae range in thickness from 3 to 10 millimetres, and may have discordant relationships between adjacent sets. The sandstones may contain abundant organic chips that increase gradually towards tops of the sets. Commonly, isolated rip-up clasts are seen floating within the sandstone, with their long axes parallel to the lamination. Ophiomorpha, Palaeophycus and Skolithos are commonly observed, particularly close to the top of this subfacies.

ii- Laminated Clean Sandstone Subfacies 'B':

This subfacies has a lower erosional boundary, and is up to 2.75 metres thick. The subfacies is characterized by high angle inclined lamination and cross stratification (Plate II.26). The laminae occur in sets, that range in thickness from about 5 to 30 centimetres. The sets are separated by basal lags of siderite and mud clasts. The lag has a maximum thickness of about 5 centimetres. Ripples and rhythmic mud

drapes occur at the top part of this subfacies (Plate II.27). Occasional Ophiomorpha burrows are seen in this subfacies.

Interpretation: Sediments of the subfacies 'A' were deposited from high energy sediment-laden currents, under upper flow regime conditions. The currents flowed carrying rip up clasts, sand and mud. These three size fractions were partially segregated in the flow and they were transported by different mechanisms. The clasts dominantly rolled at the bottom of the flow. The sands were suspended, at least intermittently, because of their very fine to fine grain size. The mud was transported in suspension. When currents decelerated, deposition of rip up clasts occurred first, and was followed by rapid deposition of sands and farther away by mud.

Inversely graded lags mostly resulted from deposition of successive increments of clasts. Smaller and faster moving clasts reached the depositional site and deposited first. Then, they were blanketed by larger and slower moving clasts. Imbricated clasts formed by shearing induced by the overlying flowing current. Normally graded lags formed probably by direct settling of clasts, that were suspended along with sands. Isolated floating rip-up clasts, within the sands, were likely suspended and deposited along with the sands. Moss (1972) reported scattered pebbles in plane bedded sands, developed in the upper flow regime conditions.

The occasional presence of ripples, at the top of the facies, may reflect later reworking by either waves, or currents. Also, biologic reworking disrupted a great deal of the physical structures.

The Laminated Clean Sandstone 'A' Subfacies is similar to the Parallel-laminated to current rippled Sandstone and Structureless Sandstone Facies which have been described by Bhattacharya and Walker (1991), in the Upper Cretaceous sediments, NW Alberta. These sandstones facies have been interpreted as suspension deposits which were deposited rapidly from powerful and episodic waning flows of deltaic origin (Bhattacharya and Walker 1991).

Sandstones of subfacies 'B' were deposited by dune and ripple migration, under low flow regime conditions. The occurrence of rhythmic mud drapes at the top of the subfacies reflects some reworking by tidal currents.

II.1.13- GRADED LAMINATED SANDSTONE FACIES

(Plates II.28-30):

This facies usually ranges in thickness from about 5.0 to 50.0 centimetres. It consists of fine to very fine grained silty sandstone. It has a lower sharp erosional boundary, that is usually overlain by disorganized basal lag.

The sandstone is planar laminated, and normally graded. The lamination is always well developed. Each lamina is normally graded, and the upper part of which is commonly

darker in colour. The laminae range in thickness from 1 up to 6 millimetres. There are commonly many discordant sets of laminae. Truncation surfaces, between the sets, are commonly convex up, and are draped by laminae that thin gradually towards the crests (Plate II.29). The draping laminae become progressively more uniform, in thickness, and get almost horizontal upwards and away from the truncation surfaces. Occasionally, the horizontal laminae grade upwards to a thin wave rippled layer.

Slump fractures are frequently seen, particularly close to the top of the facies. Trace fossils may be present and involve mud-lined *Skolithos*, and *Ophiomorpha nodosa*. They are concentrated towards the top of the facies.

Two subfacies can be distinguished in this facies:

i- **Graded Laminated Sandstone 'A' Subfacies**, which is associated with the Mudstone, Bioturbated Muddy Sandstone, and Laminated Clean Sandstone Facies. It is characterized by well developed lamination, normal grading, a mud cap, and a disorganized basal lag. The lags and the mud cap have thicknesses of up to 20 centimetres. The lags consist of shell debris, and rounded mud pebble and cobble clasts, embedded in a sand matrix (Plate II.28). The mud cap is commonly laminated, and occasionally contains *Chondrites* and *Asterosoma* burrows (Plate II.30).

ii- Graded Laminated Sandstone 'B' Subfacies, which is randomly intercalated with the Mudstone Subfacies 'B'. The Graded Laminated Sandstone 'B' Subfacies lacks the mud cap and displays well developed planar lamination. Both the lower and upper boundaries are sharp. The basal lag occasionally occurs and it is made up of basement and siderite pebble clasts, set in a sand matrix.

Interpretation: The facies deposited episodically from high energy currents. The disorganized thick lag deposits reflect their rapid deposition. The fine grain size, and well developed normal grading indicate deposition from suspension. The distinct lamination reflects strong bottom shear stress. The presence of local truncation surfaces, within the laminated sands, refers to the concomitant erosion and deposition, during the same depositional events. The upward change from planar lamination to wave ripples is ascribed to the influence of waning oscillatory currents. The mud caps settled from suspension during progressively quieter conditions. Later, the sediment was biologically reworked.

The random occurrence, sequence of structures, depositional processes and the oscillatory nature of currents suggest a storm origin for this facies. Similar storm deposits were described by Brenchly et al. (1986) in Iberia and by Dott & Bourgeois (1982) in Oregon.

II.1.14- PEBBLY SANDSTONE FACIES (Plate II.31):

The facies consists of fine to medium grained muddy sandstone, with abundant randomly scattered basement pebbles and occasional shell debris. The pebbles are mainly rounded. The sandstone is bioturbated. Ophiomorpha and Palaeophycus can be distinguished among many other unidentified trace fossils. The rock is poorly sorted.

The pebbly Sandstone Facies occurs twice in the K-14 well. The facies ranges in thickness from 2.0 to 2.75 metres respectively. It is confined in between two erosional surfaces (K-14 well in figure III.1). Each surface is overlain by a Conglomerate-Sandstone Facies.

Interpretation: The facies was deposited in a low energy environment, dominated by biologic reworking. The organisms redistributed the pebbles randomly in the sandstone.

II.1.15- CROSS BEDDED SANDSTONE FACIES (Plate II.32):

The facies is composed of fine to medium grained sandstone. The sandstone is moderately to fairly well sorted. It is bioturbated and slightly muddy in the lower part. Physical structures dominate gradually upwards. They include cross bedding, and inclined lamination. The cross bedding is complex and involves discontinuity surfaces that separate between sets with variable characteristics. Some sets are highly burrowed. Others are ripple cross laminated. Some others involve foresets with variable dip directions.

Occasionally, burrows occur along the discontinuity surfaces that separate between successive sets. Ripple cross lamination becomes more pronounced in the uppermost part of the facies. The topmost 80 centimetres of the facies are totally churned. Ophiomorpha and Palaeophycus burrows were commonly observed in the upper part.

The Cross Bedded Sandstone Facies occurs once in the K-14 well. The facies attains a thickness of about 7.75 metres. The facies is usually bounded by transgressive erosional surfaces, that are overlain by a Conglomerate-Sandstone Facies.

Interpretation: The lower bioturbated part of the facies was deposited in a low energy environment, dominated by biologic reworking. Gradual shoaling accompanied deposition of the physically reworked sandstones. This deposition occurred under the lower flow regime conditions. The discontinuity surfaces in the complex cross bedded sandstones indicate short pauses between successive depositional pulses. This may reflect the discontinuous nature of sand transport and deposition. The increase of ripples in the uppermost part and the churning of the topmost 80 centimetres of the facies may indicate gradual drowning of the deposit before the ensuing transgression.

The Cross Bedded Sandstone Facies is similar to the Nearshore Facies in the Ventura-Port, Hueneme area of California (Howard and Reineck 1981). The characteristics of cross bedding in both facies are particularly alike. Similar

vertical sequence of biogenic and physical sedimentary structures was also described in the Shoreface Facies in Cape Lookout barrier islands, North Carolina (Heron et al. 1984).

II.2- FACIES ASSOCIATIONS & SUCCESSIONS

A **facies association** involves a group of facies which occur together. The component facies are considered to be genetically or environmentally related (Collinson 1969; Reading 1986). A vertical succession of the component facies forms a **facies succession**. The boundaries between the various facies in a facies succession are conformable. The boundaries between facies successions are erosional, transgressive or subaerial exposure surfaces.

A facies succession may be characterized by a progressive change in one or more parameters, e.g. abundance of sand, grain size, or sedimentary structures (Walker 1992). Consequently, the facies succession may show a coarsening or a fining upwards trend. This vertical change in grain size or any other parameter reflects a gradual change in the depositional environment. Interpretive terminologies will be applied here to designate various facies associations. In describing any facies succession, reference will always be made to the overlying and underlying facies successions. Stratigraphic logs showing the successive facies successions in different wells will be depicted in chapter III. Eight

types of facies associations are recognized in the Avalon Formation (table II.2, page 63). These associations are described below.

II.2.1- LAKE/LAGOONAL FILL FACIES ASSOCIATION

(Figure II.2):

This association occurs at many stratigraphic levels. It is usually terminated at its top by a transgressive surface. The thickness of the facies succession varies from about 5.5 to 9.0 metres.

The Lake/Lagoonal Fill Facies Association includes the Mudstone 'B' Subfacies and Shelly Sandstone, Bioturbated Muddy Sandstone, Coquina, Sandy Siltstone, Heterolithic Mudstone and Rhythmic Laminated Sandstone Facies. Soil sediments are commonly interbedded with the aforementioned facies. These facies form several types of facies successions. Three examples of such facies successions are described below.

Facies Succession 'A' has an overall sandier upwards pattern, reflected by a serrated gamma-ray log response (figure II.2A). The succession overlies soil horizons that pass upwards to marine facies. The latter involve Bioturbated Muddy Sandstone, Mudstone, Rippled Sand-Mud and Sandy Siltstone Facies. The Facies Succession 'A' is characterized by abundant oyster and Turritella shells, plentiful organic stringers and bituminous wood fragments, highly burrowed dirty sediments, and thixotropic soft sediment deformation.

Table II.2- Facies associations in the Avalon Formation, Hibernia field.

Facies Association (page no.)	Constituent Facies	Thickness (m.)	Accumulation Time [*] (Ma.)
Lake/Lagoonal Fill (62)	1, 2, 3, 5, 6, 8, 9 & 11	5.5-9.0	1000-10,000
Barrier/Backbarrier(67)	2, 6, 7 & 10	2.65-11.0	1000-10,000
Fluvial/Tidal Channel (71)	2, 8, 10 & 12	6.0	100-1000
River Mouth Bar (73)	2, 10, 11, 12 & 13	5.0-26.0	100-1000
Interdistributary Bay Fill (77)	2, 11 & 12	11.0-12.0	100-1000
Distal Delta (79)	2, 11 & 12	11.75-13.0	100-1000
Shoreface (81)	10, 14 & 15	8.0	1000-10,000
Shallow Marine (82)	2 & 13	2.0-50.0	10,000-100,000

1: Varicoloured Mudstone
2: Mudstone
3: Shelly Sandstone
4: Rippled Sand-Mud
5: Sandy Siltstone

6: Coquina
7: Intraclastic Sandstone
8: Heterolithic Mudstone
9: Rhythmic Laminated Sandstone
10: Conglomerate-Sandstone

11: Bioturbated Muddy Sandstone
12: Laminated Clean Sandstone
13: Graded Laminated Sandstone
14: Pebbly Sandstone
15: Cross Bedded Sandstone

^{*}The accumulation time is substantially shorter than the sedimentation time. The sedimentation is rarely continuous for more than a few weeks or months at most, at any one location, and typically is interrupted by long periods of erosion or nondeposition (Miall 1991).

Facies Succession 'B' displays an irregular vertical grain size pattern (figure II.2B). The succession consists of Mudstone and Sandy Siltstone Facies. Interbeds of soil sediments occur throughout the succession.

Facies Succession 'C' has an overall sandier upwards pattern (figure II.2C). It starts at base with dark coloured mudstones of the Heterolithic Mudstone Facies. The mudstones show a gradual upward increase of siltstone layers. Meanwhile, sharply based interbeds of the Rhythmic Laminated Sandstone Facies increase progressively upwards. The upper part of this succession consists mainly of sandstone beds, the tops of which are burrowed. The topmost beds are totally churned. Few opportunistic Corpulids are associated with these sands (Root 1983).

Interpretation: This facies association was deposited in a restricted lagoonal to coastal lake environment. This interpretation is based on the following criteria:

- i- Abundance of siderite nodules: Siderite commonly precipitates in environments ranging in salinity from brackish to brackish marine (Postma 1982; Boles 1987; Mozley 1989; Pye et al 1990).
- ii- Low diversity macrofossils: oysters and *Turritella* are dominant in the Facies Successions 'A' & 'B'. These species are adapted to tolerate fluctuating salinity conditions, ranging from brackish to open marine (Hudson 1963; Feldmann

and Palubniak 1975; Wu and Richards 1981; Allmon 1988). The Facies Succession 'C' has a greatly reduced macrofossil content, restricted to the opportunistic *Corpulids* (Root 1983). These *Corpulids* reflect an anoxic environment, soft substrate, and fluctuating energy and salinity conditions (Lewy and Samtleben 1979; Root 1983).

iii- Reduced content and diversity of forams and ostracods: Guilbault (1986) stated that "The forams are essentially arenaceous and involves species found in modern tidal marsh environments. The ostracods include the *Hutsonia* sp., a diagnostic brackish ostracod".

iv- Abundance of organic stringers and wood fragments, which are common in humid and temperate lagoons (Elliott 1986). Also, the occurrence of Charophyte oogonia, reproductive organs of algae, in Facies Successions 'A' & 'B' suggests fresh to brackish water conditions (Guilbault 1986).

v- Thixotropic soft sediment deformation, resulting from rapid deposition of sands over soft mud substrate. Masters (1965) described lagoonal sediments from the Mancos Formation, NW Colorado, having ball and pillow structures, that developed in a similar way.

The Facies Succession 'A' was deposited in a low energy protected area. Its sandier upwards nature reflects progressive filling of the lagoon/lake that terminated by deposition of the Sandy Siltstone Facies, which is mostly of

a marsh origin. The Facies Succession 'B' formed at the shoreline of the lagoon/lake, where recurrent subaerial exposure and inundation took place'. The Facies Succession 'C' was deposited in a lagoon dominated by wave and storm activity. Progressively increasing storm siltstones and washover sandstones accumulated therein. Brief marine incursions were associated with deposition of these storm sediments, which host the opportunistic Corpulids.

The Lake/Lagoonal Fill Facies association is postulated to have been formed over a period of 1000-10,000 years. Comparable Pleistocene paralic lithosomes accumulated over a time interval of 10,000 years or less (Demarest et al. 1981). Soil horizons require several thousand years to develop, and take up to 10,000 years to reach maturity (Leeder 1975; Retallack 1984).

'Subsequent to the completion of the thesis and following discussions with Dr. John C. Kraft, two of the soil horizons in the Facies Succession 'B' can alternatively be interpreted as marsh deposits fringing the landward shoreline of the lagoon/lake.

'Paralic: "All environment and associated deposits from the beach face landward to the limit of tidal influence" (Demarest et al. 1981).

'Lithosome: "A three-dimensional mass of essentially uniform (or uniformly heterogeneous) lithologic character, having intertonguing relationships in all directions with adjacent masses of different lithologic character." American Geological Institute Glossary of Geology 1972, p. 413.

II.2.2- BARRIER-BACKBARRIER FACIES ASSOCIATION

(Figure II.3):

This association erosively overlies the Lagoonal Facies Association. It is terminated at top by an erosional surface, which is usually overlain by a Conglomerate-Sandstone Facies. The association forms many types of facies successions. These successions vary in thickness from 2.65 to 11.0 metres. Two types of these facies successions are described below.

The Facies Succession 'A' is a sandier upwards succession (figure II.3A). The gamma-ray log response is serrated funnel shaped. The succession can be divided into a lower part and an upper part that are separated by an erosional surface. The lower part starts at base with the Mudstone 'A' Subfacies. The latter changes gradually upwards to the Intraclastic Sandstone Subfacies 'B', which is bioturbated and may host one or two bioturbated mudstone interbeds. The Coquina Facies may occur above the Intraclastic Sandstone 'B' Subfacies. The upper part of the facies succession (above the erosional surface) starts at base with rounded basement pebbles and/or molluscan shells. These pebbles and/or shells pass upwards to the Intraclastic Sandstone Subfacies 'A', which shows a progressive upward increase in inclined lamination and cross bedding.

Facies Succession 'B', displays a coarsening upward trend in the lowermost part and a crude fining upwards trend in the upper part (figure II.3B). The lowermost part consists of the

Mudstone 'B' Subfacies that changes upwards to the Intraclastic Sandstone 'B' Subfacies. The upper part of the succession comprises mainly the Intraclastic Sandstone 'A' Subfacies, which occurs above an erosional surface. The Intraclastic Sandstone 'A' Subfacies is cross bedded in the lower part and highly burrowed in the upper part. It has many internal erosional surfaces. Each erosional surface is overlain by a basal lag, which may be up to 20 centimetres thick. The basal lag consists of abundant bituminous wood fragments and/or basement pebbles. The succession is capped by a mudstone bed. The latter is bioturbated and contains plenty of wood stringers as well as oyster shells.

Interpretation: The Facies Succession 'A' represents a transgressive Barrier-Backbarrier complex. The lower part of the succession is made up of lagoonal and backbarrier sediments that change, across a ravinement surface into lower shoreface sandstones. The top boundary of the succession is another ravinement surface along which upper shoreface sandstones were stripped out. The Facies Succession 'B' constitutes a tidal inlet channel fill that is incised into the lower backbarrier sandstones.

¹Ravinement surface: A regional marine erosion surface produced during transgression by erosional retreat of the shoreface (Stamp 1921; Swift 1968). The ravinement surface is generally diachronous (Nummedal and Swift 1987).

Evidence for the aforementioned interpretations includes:

- i- The stratigraphic position of the association. Both Facies Succession 'A' and 'B' start with lagoonal and backbarrier sediments, at base, and pass upwards to shoreface/inlet channel fill and open marine deposits. Similar successions were described in Modern barrier islands and in ancient sediments (Kraft 1971; Kraft and John 1979; Demarest 1981; Demarest et al. 1981; Demarest and Kraft 1987; Donselaar 1989).
- ii- The progressive upwards change from bioturbated to physically reworked sediments in Facies Succession 'A'. Syndepositional marine cements, rimming bioclastic debris and micritic grains (see V.1.I) also increase upwards. The upward increase of physical structures and marine cements reflect the gradual shoaling of the environment, associated with growth of the barrier. Active flushing of the shoreface sands by marine waters helped cement nucleation around carbonate grains.
- iii- An elongate shoestring sand body geometry (figure III.11).
- iv- Fining upwards trend and multiple erosional surfaces, with basal lags in the tidal inlet channel fill of the Facies Succession 'B'. The progressive upward increase of burrowing resulted from the gradual abandonment of the channel. The erosional boundary of the channel and the incised backbarrier sediments, are depicted in figure III.9.

Similar lines of evidence were used in other areas, to identify various subenvironments in transgressive barrier islands. In a well exposed outcrop in Germany, Boersma (1991) relied heavily on the geometry of sandstone bodies and vertical and lateral facies relationships to identify flood tidal delta and washover deposits. Based on the stratigraphic relationships, sand body geometry, and sedimentary structures, Galloway (1986) suggested a complex of washover fans in a transgressive barrier island depositional environment, for similar sandstones in the Gulf of Mexico. In a similar approach, Horne et al. (1978) recognized flood tidal delta and washover sand bodies overlying lagoonal shales in Carboniferous exposures in the Appalachian region.

The Barrier-Backbarrier Facies Association is believed to have been developed over a period of 1000-10,000 years. The Pleistocene transgressive barrier island lithosomes in SE Delaware have been formed over a time span of 10,000 years or less (Demarest et al. 1981). The ravinement surfaces within these lithosomes represent hiatuses of the order of 1-100 years (Demarest et al. 1981). The hiatuses associated with the ravinement surfaces within and at the top of the Barrier-Backbarrier Succession are thought to record similar periods of time.

II.2.3- FLUVIAL/TIDAL CHANNEL FILL FACIES ASSOCIATION

(Figure II.4):

This facies association erosively overlies a Barrier-Backbarrier Complex and it passes upwards to the River Mouth Bar Facies Association. It is about 6.0 metres thick.

The association forms an overall fining upwards succession that is reflected by a serrated bell-shaped gamma-ray log response. It has a lower erosional boundary blanketed by a basal lag. The latter is about 20.0 centimetres thick and consists of rounded basement pebbles, randomly scattered in a sand matrix.

The basal lag is overlain by sharp-based cross bedded sandstones of the Laminated Clean Sandstone 'B' Subfacies. The sandstones comprise two fining upwards cycles, separated by an erosional boundary. In each cycle, sedimentary structures change upwards from cross bedding and inclined lamination to ripples and rhythmic lamination. The latter involves well developed rhythmic mud drapes and mud drape couplets in the top 10-20 centimetres.

The cross bedded sandstones are overlain by bioturbated sandy mudstones, with a sharp boundary in between. Relict rhythmic sand-mud lamination can be seen in the mudstones. An interbed of the cross bedded sandstone, with rhythmic mud drape couplets, recurs close to the top of the mudstones. The succession is capped by a 20.0 centimetres thick sandstone

bed. The latter is highly burrowed and it has a basal lag of molluscan shells and mud clasts. The succession is terminated at top by a transgressive surface, overlain by dark mudstones.

Interpretation: This facies association was deposited in a fluvial channel at the head of an estuary, where there was some tidal current influence. The cross bedded sandstones constitute the active channel fill. The overlying mudstones mark abandonment of the channel, during which tidal current and organisms actively reworked the sediments. The top transgressive sand cap reflects the ultimate transgression of the channel.

The following criteria support the above interpretation:

- i- The erosional channel boundary (figure III.11). The channel is incised into a Barrier-Backbarrier Complex, that is fully preserved outside the channel. Only the basal 20.0 centimetres of such barrier is preserved below the channel fill.
- ii- The fining upwards trend, when linked to the erosional channel boundary, points to a channel fill succession. Similar fining upward facies successions were cored in the fluvial channel of the Gironde estuary (Allen 1991; Allen and Posamentier 1994), and in abandoned distributary channels of Guadalupe delta (Donaldson et al. 1970). However, the influence of tidal currents is much more pronounced in the Gironde estuary. An ancient comparable example is represented by the meander belts (prism III) of the Jurassic Scalby

Formation in Cleveland basin, NE England (Eschard et al. 1991).

iii- Depositional processes suggest direct sand deposition from fluvial currents and subsequent minor reworking by tidal currents. The plentiful layers of mud and siderite clasts indicate a subordinate influence for tidal currents which would otherwise sort the clasts out. Only the top parts of sand dunes were reworked by tidal currents, as evidenced by the rhythmic mud drapes. Similar cross bedded sands with abundant clay clasts were recorded in the distributary channel of the Colorado delta (Kanes 1970).

The Fluvial/Tidal Channel Fill Facies Association is thought to have been accumulated over a period of 100-1000 years. Equivalent point bars have been reported to accumulate over time spans of 100-1000 years (Miall 1991).

II.2.4- RIVER MOUTH BAR FACIES ASSOCIATION

(Figure II.5):

This facies association is accompanied by the Distal Delta, Interdistributary Bay, and Shallow Marine Facies Associations. It ranges in thickness from 5 to 26 metres. The association forms either an overall coarsening or fining upwards facies successions.

The coarsening upwards succession commonly has a fining upwards interval at top (figure II.5A). The succession starts at base with the dark coloured Mudstone 'B' Subfacies. The

mudstone changes gradually upwards to the Bioturbated Muddy Sandstone Facies, which in turn changes to the Laminated Clean Sandstone Facies. Sharp-based storm interbeds of the Graded Laminated Sandstone facies occasionally intercalate with the previous facies. The top fining upwards interval consists of the Graded Laminated Sandstone Facies and/or the Bioturbated Muddy Sandstone Facies.

The fining upwards succession rests above an erosional surface, that is covered by a basal lag (figure II.5B). The latter may be up to several tens of centimetres thick and it consists of either rounded basement pebbles (Plate 11) or mudstone and siderite clasts, randomly scattered in a sand matrix. The basal lag passes upwards to the Laminated Clean Sandstone Facies. The latter changes, at top, to the Bioturbated Muddy Sandstone and/or the Graded Laminated Sandstone Facies. Many erosional surfaces, each with a basal lag, may occur within the succession.

The Laminated Clean Sandstone Facies always forms the bulk of both succession types. It has a sharp basal boundary and it is commonly composed of many sandstone packages. The latter may be separated by interbeds of Bioturbated Muddy Sandstone Facies and rarely by Graded Laminated Sandstone Facies. A sandstone package may be up to 4.0 metres thick, and is usually covered by a thin shale layer, crowded with horizontal burrows.

Interpretation: This facies association represents river mouth bar deposits of bay head deltas (these deltas are one element of an estuarine complex that will be discussed in chapter III). The coarsening upwards succession resulted from delta progradation. The storm and the bioturbated muddy sediments, of the fining upwards top interval, constitute the delta destructional facies. In contrast, the fining upwards succession was deposited during retrogradation of the delta. The basal erosional surface coincides with the basal boundary of the host estuary (figures III. 8 & 9).

This interpretation is based upon the following criteria:

- i- Depositional processes of the Clean Sandstone Facies suggest rapid deposition from sediment-laden currents, with minimum reworking by basinal processes. The consistent occurrence of abundant layers of siderite and mud clasts in the sandstone precludes any wave or tidal current reworking which would otherwise sort out the clasts. Similar layers of mudstones and siderite rip-up clasts in structureless and parallel laminated sandstones were interpreted to indicate rapid deposition from sediment-laden powerful currents at delta fronts, Upper Cretaceous sediments, NW Alberta (Bhattacharya and Walker 1991). The highly burrowed nature of the sediments reflects deposition in a low energy environment dominated by biologic reworking. Occasional storms stirred the mouth bar surface sediments, and deposited the Graded

Laminated Sandstone Facies.

ii- Abundant drifted organic chips in the Laminated Clean Sandstone Facies. Organic chips increase gradually upwards within many of the sand sets, comprising the Laminated Clean Sandstone Facies. Moreover, some of the sets are draped by thin films of organic chips. It is worth mentioning that Jenkins (1984) qualified the organic matter content, in sediments of this facies association, as of exclusively terrestrial origin to terrestrial with minor marine origin.

Martinsen (1990) reported an abundance of drifted plant and wood matter in similar parallel laminated, fine grained, delta front sandstones. He attributed this abundance to the near-proximity to a river mouth.

iii- Basal erosional boundary, reduced salinity conditions, and diminished faunal content and species diversity. Based on depressed foraminiferal and ostracod content, and species diversity, Guilbault (1986) suggested lowered salinity conditions for rocks of this facies association. The reduced salinity conditions and the basal erosional estuary boundary (discussed in chapter III) suggest a bay head deltaic setting.

The River Mouth Bar Facies Association is believed to have been developed over a period of 100-1000 years. River mouth bars of the Mississippi delta expand at a rate of 3 km/100 years (Gould 1970). Delta lobes of the Mississippi system are formed and abandoned in about 1000 years (Kolb and

Van Lopik 1966; Frazier 1967; Gould 1970).

II.2.5- INTERDISTRIBUTARY BAY FILL FACIES ASSOCIATION

(Figure II.6):

This facies association overlies either the River Mouth Bar or the Distal Delta Facies Associations. The association forms an overall sandier upward succession that varies in thickness from about 11.0 to 12.0 metres. The gamma-ray log pattern is serrated funnel-shaped.

The Interdistributary Bay Fill Succession consists of stacked coarsening upwards cycles^{*}, 0.3 - 3.0 m. thick, which are separated by highly burrowed boundaries. A cycle consists of dark-coloured Mudstone 'B' Subfacies, that changes gradually upwards to either Laminated Clean Sandstone 'A' Subfacies or Bioturbated Muddy Sandstone 'B' Subfacies. The uppermost muddy cycles may host shell hash layers and sandstones, with relict planar lamination. The cycles are characterized by: i- Presence of few large articulated Oyster shells, that are partially replaced by pyrite. ii- Restricted assemblage of trace fossils, including Chondrites, Asterosoma and Anchonichnus. iii- Abundant siderite nodules. iv- Plentiful disseminated organic chips that may locally

^{*}A cycle refers to the repetitive sequential transition from one facies to another. The cycle consists of two or more facies. The recurring change between the constituent facies usually results in coarsening or fining upwards cycles, and reflects a progressive alteration of one or more parameters in the depositional environment.

constitute up to 10% of the rock (visual estimate). The organic matter is of either exclusively terrigenous or essentially terrigenous with minor marine origins (Jenkins 1984).

Interpretation: This association was deposited in restricted interdistributary bay environment. Comparable bay-fill sediments are described by Elliott (1974) and Horn et al. (1978). The overall sandier upwards nature of the Interdistributary Bay Fill Succession reflects gradual filling of the bay.

The interpretation is based on the following criteria:

- i- low energy environment and abundance of terrestrial organic matter. These conditions induced active mining and churning of the nutrient-rich sediments by deposit feeders.
- ii- Reduced salinity conditions. The abundance of early diagenetic siderite and pyrite may reflect reduced oxygen content and lowered salinity conditions (Postma 1982; Boles 1987; Mozley 1989; Pye et al. 1990). The low diversity of trace fossils, and occurrence of large Oyster shells indicate a highly stressed, typically brackish bay environment (Puffer and Emerson 1953; Hopkins 1956; Fallow 1973; Feldman and Paluniok 1975; Root 1983).
- iii- The occurrence above the Distal Delta and River Mouth Bar Facies Associations. This stratigraphic relationship reflects an overall progradation or compaction-induced subsidence of

the delta.

The Interdistributary Bay Fill Facies Association is thought to have been developed over a time span of 100-1000 years. Gagliano and Van Beek (1970) reported that filling of an interdistributary bay in the Mississippi delta occurred by progradation from a single crevasse in about 100-150 years.

II.2.6- DISTAL DELTA FACIES ASSOCIATION (Figure II.7):

This facies association accompanies the River Mouth Bar, Interdistributary Bay Fill, and Shallow Marine Facies Associations. Its thickness varies from 11.75 to 13.0 metres.

The association is comprised of coarsening upwards cycles, that range in thickness from 0.25 to 3.5 metres. In a vertical succession, the stacked cycles may not reflect a regular pattern of grain size changes. The boundaries between the cycles are highly bioturbated.

A complete cycle starts at base with bioturbated dark Mudstone 'B' Subfacies, that changes gradually upwards to Bioturbated Muddy Sandstone Facies. A bed of the Laminated Clean Sandstone Facies, up to 1.0 metre thick, commonly caps the cycle. A thin storm interbed, up to 25 centimetres thick, of the Coquina or rarely Graded Laminated Sandstone Facies may also be present.

The rocks are characterized by plentiful molluscan shells and Serpulid tubes, abundant organic chips and coaly stringers and a diverse trace fossil assemblage (see page 17). Molluscan

shells are also diverse and include Trigonina, Cardiid, Oysters, Homomya, Pecten, Tellina, and Barbatia (Root 1983).

Interpretation: This association constitutes distal deposits of bay head deltas. Similar facies are described in riverine-influenced bay sediments adjacent to the Guadalupe delta (Donaldson et al. 1970).

The interpretation is supported by the following criteria:

i- The stratigraphic position above the River Mouth Bar Facies Association (figure III.2). This vertical change of facies reflects gradual lateral shift of the focus of active deposition of river mouth bar sands.

ii- Abundance of sediment supply and cyclic nature of sedimentation. The cyclicity, the lack of a regular pattern of vertical grain size changes, and the absence of significant overall shallowing or deepening reflect repetitive base level subsidence and active sediment supply. Each cycle is interpreted to represent an increment of distal deltaic sediments that deposited in the low energy bay environment.

iii- The abundance of organic chips and coaly stringers, which suggest a likely nearby riverine source. Also, Jenkins (1984) reported organic matter varying from exclusively terrigenous to predominantly terrigenous with minor marine component origin.

iv- The faunal and trace fossil content suggest salinity

conditions varying from slightly brackish to near normal marine (Guilbault 1986; Root 1983).

The Distal Delta Facies Association is believed to have been formed over a period of 100-1000 years. Delta lobes of the Mississippi system are formed and abandoned in about 1000 years (Kolb and Van Lopik 1966; Frazier 1967; Gould 1970).

II.2.7- SHOREFACE FACIES ASSOCIATION (Figure II.8):

The Shoreface Facies Association is found in the K-14 well. The association comprises the Pebbly Sandstone, Conglomerate-Sandstone and Cross Bedded Sandstone Facies. These facies form several stacked facies successions that are always bounded by ravinement surfaces. The facies successions can be up to 8.0 metres thick. The upper facies succession is erosively overlain by Shallow Marine Facies Association.

The lower succession in figure II.8, below the depth of 2375.0 m., is a coarsening upward succession. It starts at base with a Conglomerate-Sandstone Facies, which passes gradually upwards to bioturbated and then to cross bedded sandstones. Bioturbation recurs in the topmost 75.0 centimetres of the sandstone. The upper succession in figure II.8, above the depth of 2375.0 m., consists of bioturbated muddy sandstone that has abundant scattered pebbles.

Interpretation: This facies association was deposited in a shoreface environment. The lower succession in figure II.8, for example, represents a lower-middle shoreface deposit that

was partly eroded along the top-bounding ravinement surface.

This interpretation is based on:

i- The coarsening upward of the lower succession and the gradual transition from bioturbated to cross bedded sandstones. These features reflect progressive shoaling and transition from below to above the wave base. The absence of foreshore and upper shoreface sands is possible due to erosion along the top-bounding ravinement surface.

ii- The confinement between ravinement surfaces and the physically-reworked sandstones suggests a high energy coastal environment. The occurrence of the Shoreface Facies Successions below shallow marine mudstones, which host abundant storm beds indicates operation of waves and storms in a shoreface environment. Similar shoreface successions, bounded by ravinement surfaces, were recorded by Clifton (1981) and Duke et al. (1991).

The Shoreface Facies Association is thought to represent a period of 1000-10,000 years. Progradational shoreface sandstones of the Galveston barrier island in Texas represent about 3,500 years of accumulation (Bernard et al. 1962). The shoreface sandstones of the Sandy Neck spit in Massachusetts dates back to 3,300 years (Hays and Kana, 1976).

II.2.8- SHALLOW MARINE FACIES ASSOCIATION (Figure II.9):

The Shallow Marine Facies Association consists mainly of Bioturbated Muddy Sandstone Facies, Mudstone 'B' and 'D'

Subfacies and randomly intercalated storm beds of Graded Laminated Sandstone Facies. The vertical succession does not show any regular grain size pattern. The succession may be up to tens of metres thick. The Mudstone 'D' Subfacies contains a few scattered Pelecypod shells and a diverse trace fossil assemblage. Abundant and diverse open marine foraminifers were also recorded in it (Guilbault 1986). The Mudstone 'B' Subfacies, between 2550.5 - 2567.2 m. in the J-34 well, is darker coloured, less burrowed, and hosts less storm beds and frequent siderite nodules. It contains essentially arenaceous foraminifers (Guilbault 1986).

Interpretation: Low energy conditions interrupted by episodic storms prevailed during deposition of this facies association. Depositional rates were slow, allowing abundant bioturbation. The faunal content and trace fossils suggest deposition in offshore to nearshore, open embayment, environments. The Shallow Marine Facies Association is similar to the facies association '1' which was described and interpreted by Pattison and Walker (1994) to have been deposited in open marine waters below fair-weather wave base.

The Shallow Marine Facies Association is postulated to have been developed over a period of 10,000-100,000 years. Suter et al. (1987) reported 6 sequences that have formed on Louisiana continental shelf since 150 Ma, with an average duration of 25,000 years.



Plate II.1- Transition from reddish brown to greenish grey soil horizons. Note the red mottle in the green horizon. Green mottles and veinlets also occur in the red horizon. Varicoloured Mudstone Facies, B-27 well (2594.85 m).



Plate II.2- Dark grey shale with abundant siderite nodules and scattered Molluscan shells. Mudstone 'A' Subfacies, B-27 well (2588.8 m).



Plate II.3- Mudstone 'B' Subfacies with Chondrites burrows and other unidentified traces. I-46 well (2377.5 m).



Plate II.4- Bioturbated mudstone, with relict bands of interlaminated sand-mud. Note the two discordant bands in the upper left hand side. Mudstone 'C' Subfacies, J-34 well (2595.1 m).

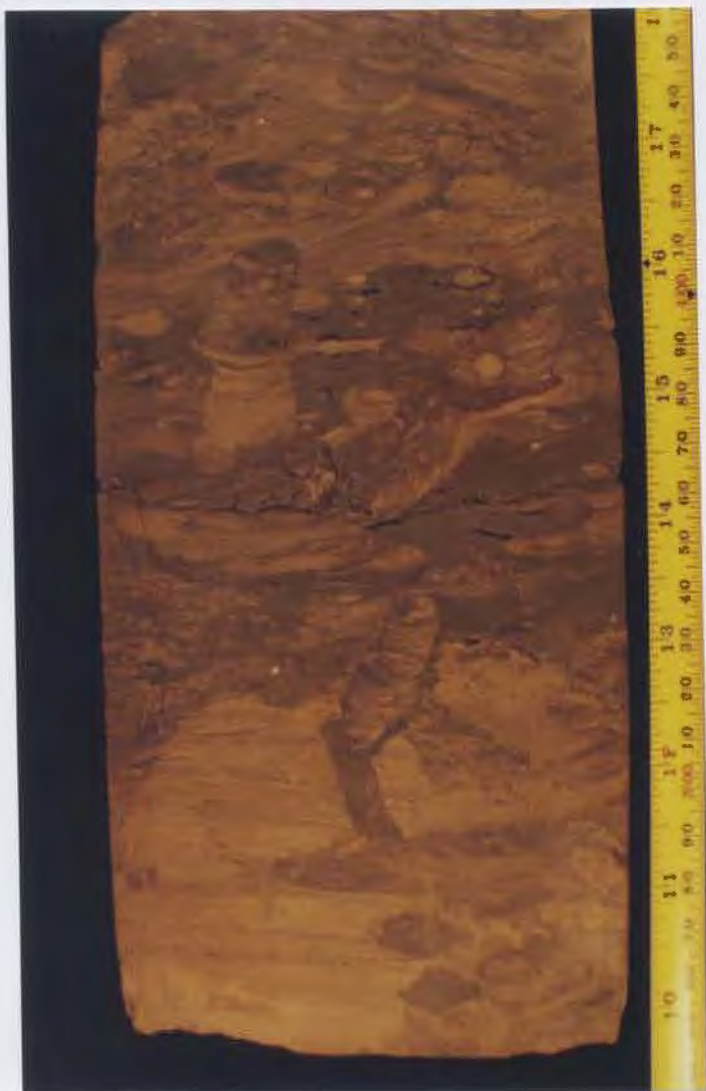


Plate II.5- Bioturbated mudstone with abundant trace fossils including *Teichichnus* and *Planolites*. Note the laminated and graded storm sandstone in the lower part. Mudstone 'D' Subfacies, K-14 well (2425.7 m).



Plate II.6- Bioturbated calcareous sandstone with composite burrows. Trace fossils include *Thalassinoides*, *Ophiomorpha* and *Planolites*. Note the scattered shells at the top. Shelly Sandstones Facies, J-34 well (2612.85 m).



Plate II.7- Ripple cross laminated sandstone with abundant mud flasers. Rippled Sand-Mud Facies, K-14 well (2403.65 m).



Plate II.8- Alternating flaser bedded sand-rich bands and lenticular bedded mud-rich bands. Note the oppositely dipping ripple cross laminations at the top left corner. Rippled Sand-Mud Facies, K-14 well (2403.05 m).



Plate II.9- Burrowed sandy siltstone with many vertical root-like traces. Sandy Siltstone Facies, K-14 well (2408.25 m).



Plate II.10- Abundant gastropod and few pelecypod shells in coquinooid sandstone. Abundant secondary pores occur in the upper part of the sample. Note the biomoldic pore to the right hand side of the coin. Coquina Facies, B-27 well (2582.0 m).



Plate II.11- Layered coquina bed, above the coin, composed of Serpulid tubes and pelecypod shell debris. Coquina Facies, I-46 well (2340.15 m).

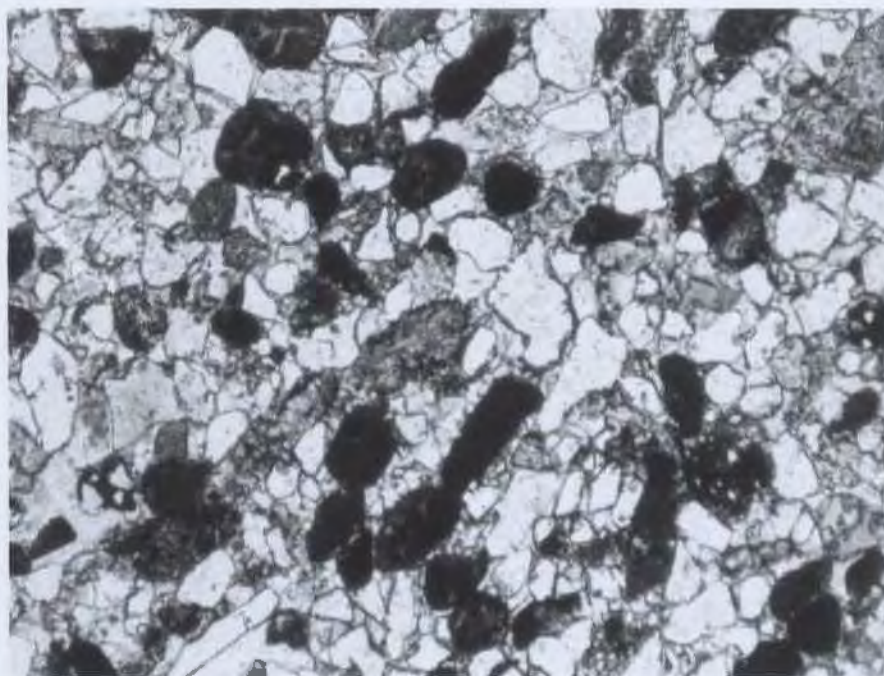


Plate II.12- Photomicrograph showing abundant micritic intraclasts (dark coloured), skeletal debris (grey coloured) and siliciclastic grains (white coloured). Note that many of the micritic intraclasts have embedded siliciclastic grains. Intraclastic Sandstone 'A' Subfacies, K-14 well (2389.2 m). Plane light 20X.



Plate II.13- Cross bedded calcareous sandstone. Note the Pelecypod shell in centre of the photograph. Intraclastic Sandstone 'A' Subfacies B-27 well (2577.0 m).



Plate II.14- Bioturbated calcareous sandstone with scattered shells. Intraclastic Sandstone 'B' Subfacies, J-34 well (2609.4 m).



Plate II.15- Mudstone overlain by laminated sandstone Facies. The mudstone hosts abundant disrupted laminated siltstone bands and lenses. The sandstone is comprised of several discordant sets. Note the siderite nodule in the lower left side. Heterolithic Mudstone & Rhythmic Laminated Sandstone Facies, I-46 well (2415.15 m).



Plate II.16- Rhythmic laminated and muddy sandstone, composed of several discordant sets. The laminae, in each set, get muddier. Note the set boundary below the coin, and the burrow at the set boundary in the upper left hand side. Rhythmic Laminated Sandstone Facies, I-46 well (2414.0 m).



Plate II.17- Layered conglomerate grading upwards to sandstone. The pebbles are rounded and are set in a sand matrix. Note the sharp erosional basal boundary. Conglomerate-Sandstone Facies, I-46 well (2482.7 m).



Plate II.18- Conglomerate grading upwards to bioturbated muddy sandstone. Note the relief of the erosional surface. Conglomerate- Sandstone Facies, B-27 well (2575.85 m).



Plate II.19- Bioturbated Muddy Sandstone 'A' Subfacies. Trace fossils include *Teichichnus*, *Asterosoma*, *Zoophycus*, and *Planolites*. Note the *Pelecypod* shells above and below the coin. J-34 well (2548.55 m).



Plate II.20- Bioturbated Muddy Sandstone 'B' Subfacies. Note the large oyster shell above the coin. J-34 well (2576.5 m).



Plate II.21- Layered basal lag overlain by laminated sandstone. The bottom layer consists of shell debris in a sand matrix. The top layer is composed of inverse graded conglomerate. The latter involves mud and siderite clasts, set in a sand matrix. Laminated Clean Sandstone Facies, I-46 well (2466.25 m).

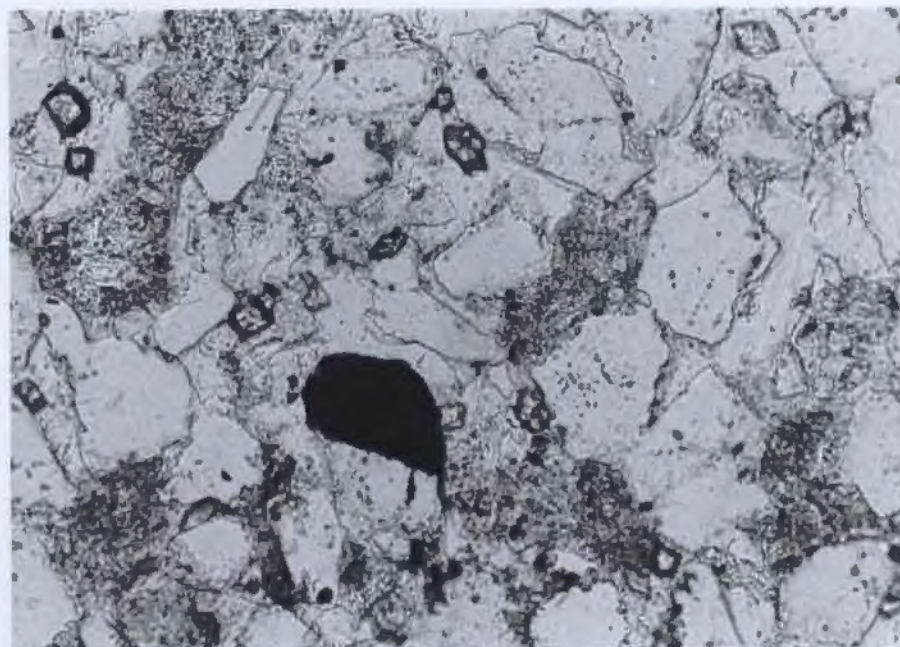


Plate II.22- Photomicrograph showing compacted mud lithic grains (grey) and siliciclastic grains (white). Note the scattered rhombic siderite grains and the black pyrite grain. Laminated Clean Sandstone Facies, B-27 well (2554.6 m).

Plate II.23- Oil-stained sandstone unit confined between bioturbated muddy sandstones. The base of the unit occurs below the pencil, and the top below the lens cap. The unit is composed of several sand sets. Each one has a basal lag of mud and siderite clasts. The top of the unit has a thin black shale cap, dominated by sand-filled *Thalassinoides* and *Planolites* burrows. Note the *Ophiomorpha* burrow to the right hand side of the coin. Laminated Clean Sandstone 'A' Subfacies, I-46 well (2458.45-2461.0 m).



Plate II.24- Faintly laminated calcareous sandstone. Note the scattered mud chips which are aligned parallel to the lamination. Laminated Clean Sandstone 'A' Subfacies, B-27 well (2559.6 m).



Plate II.25- Structureless sandstone, below the coin, overlain by layered sandstone with abundant siderite and mud clasts. Laminated Clean Sandstone 'A' Subfacies. J-34 well (2486.6 m).

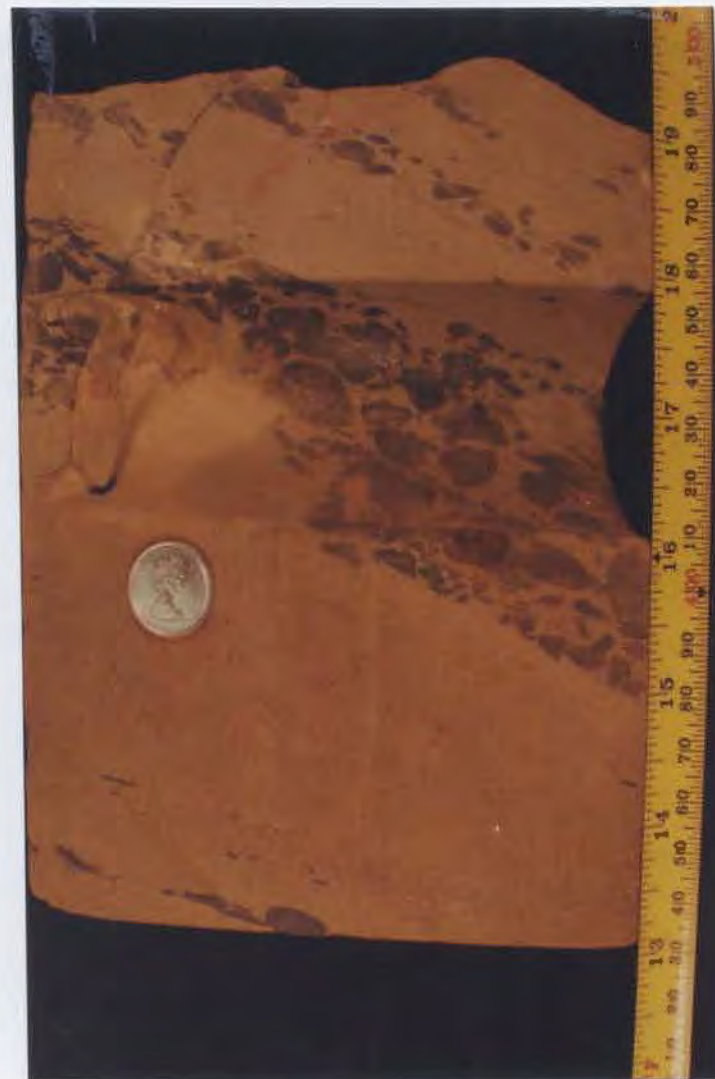


Plate II.26- Inclined stratified oil-stained sandstone, with layers of mud and siderite clasts. Laminated Clean Sandstone 'B' Subfacies, J-34 well (2596.65 m).



plate II.27- Inclined laminated sandstone, with rhythmic mud drapes. Note the Ophiomorpha burrows and the Mud drape couplet below the coin. Laminated Clean Sandstone 'B' Subfacies, J-34 well (2593.55 m).



Plate II.28- Disorganized basal lag overlain by Ophiomorpha-burrowed sandstone. Shell debris and mud clasts are randomly scattered in a sand matrix. Graded Laminated Sandstone 'A' Subfacies, B-27 well (2567.95 m).



Plate II.29- Two discordant sets of laminated sandstone. Laminae of the upper set decrease gradually in thickness to the left, towards the crest of the lower set. Graded Laminated Sandstone 'A' Subfacies, K-14 well (2365.2 m).

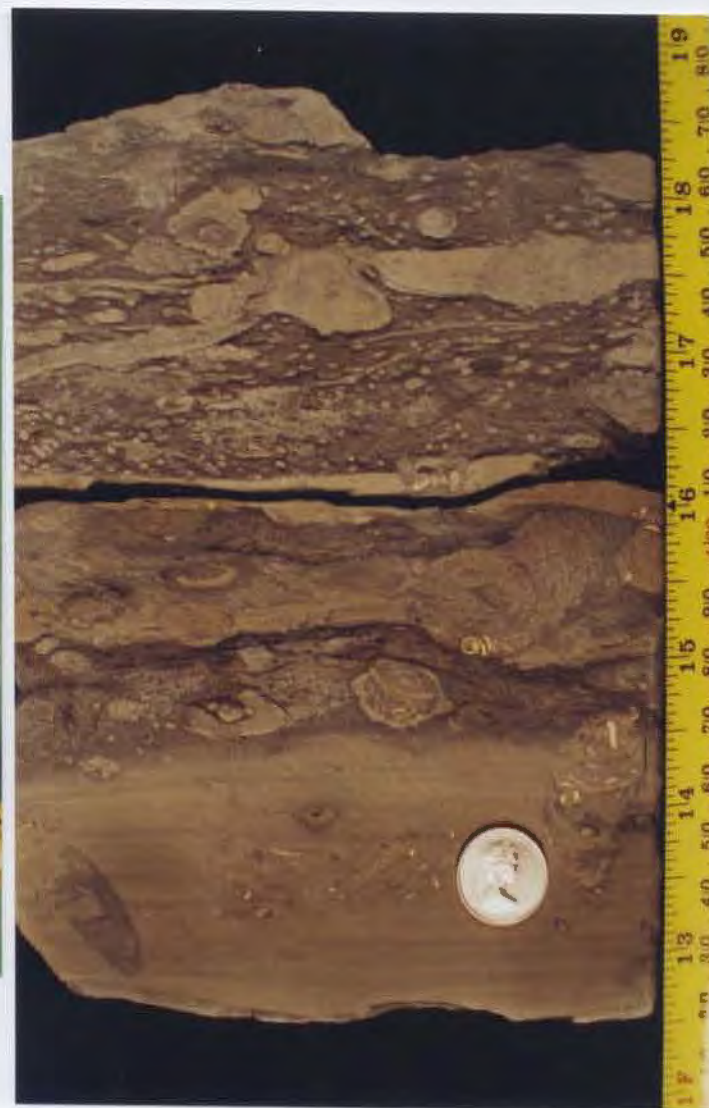


Plate II.30- Laminated silty sandstone grading upwards to highly burrowed mudstone. The burrows involve Chondrites and Asterosoma. Graded Laminated Sandstone 'A' Subfacies, K-14 well (2358.65 m).



Plate II.31- Abundant basement pebbles randomly scattered in highly burrowed sandstone. Pebbly Sandstone Facies, K-14 well (2383.9 m).



Plate II.32- Cross bedded sandstone. Note the burrow at the boundary between two sets, in the centre of the photo. The upper horizontally laminated set does not seem to cut through the underlying set. Cross Bedded Sandstone Facies, K-14 well (2376.8 m).

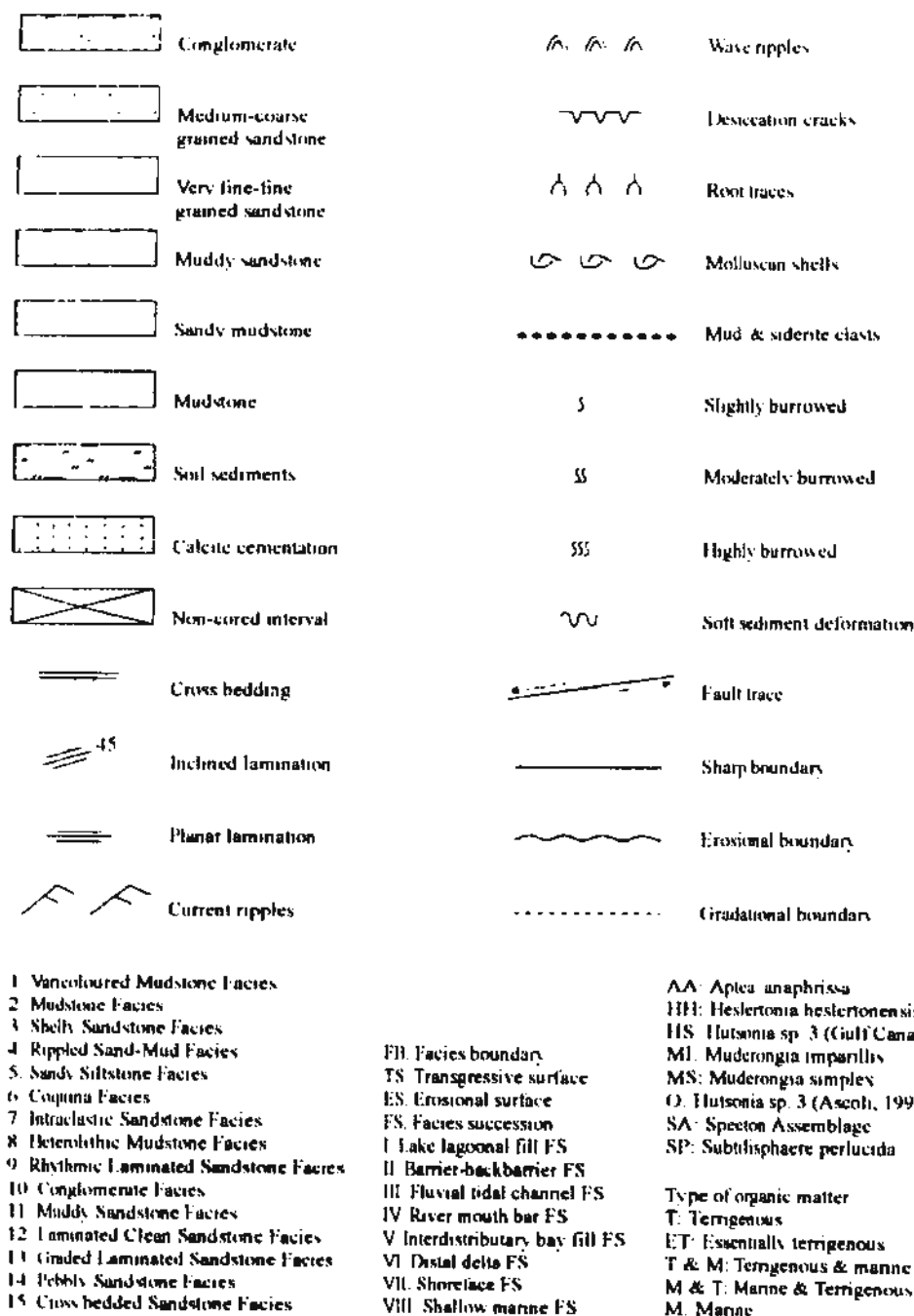


Figure II.1- LEGEND FOR FIGURES IN CHAPTERS II, III & IV.

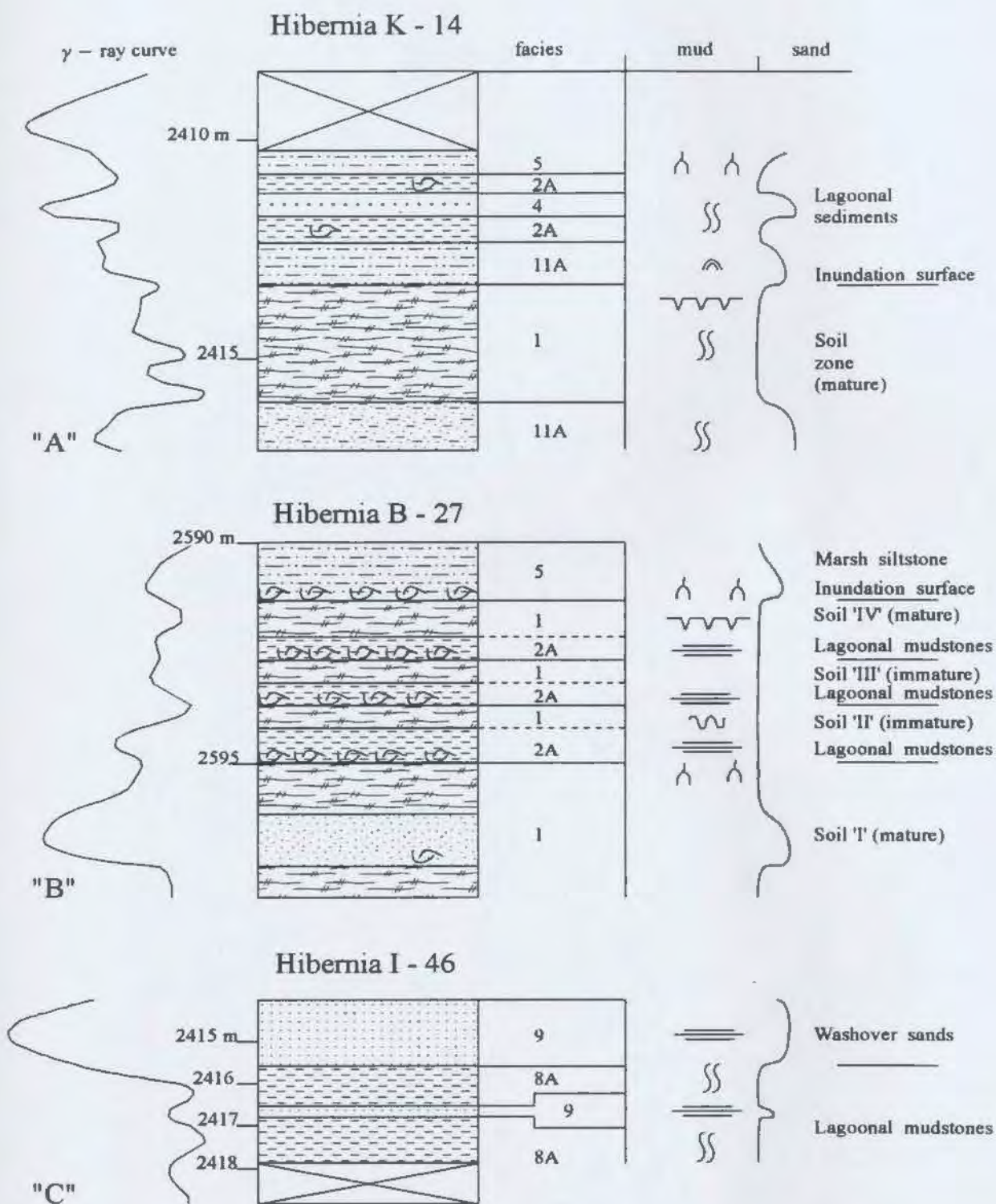


Figure II.2- LAKE / LAGOONAL FILL FACIES SUCCESSIONS.
(see legend in figure II.1)

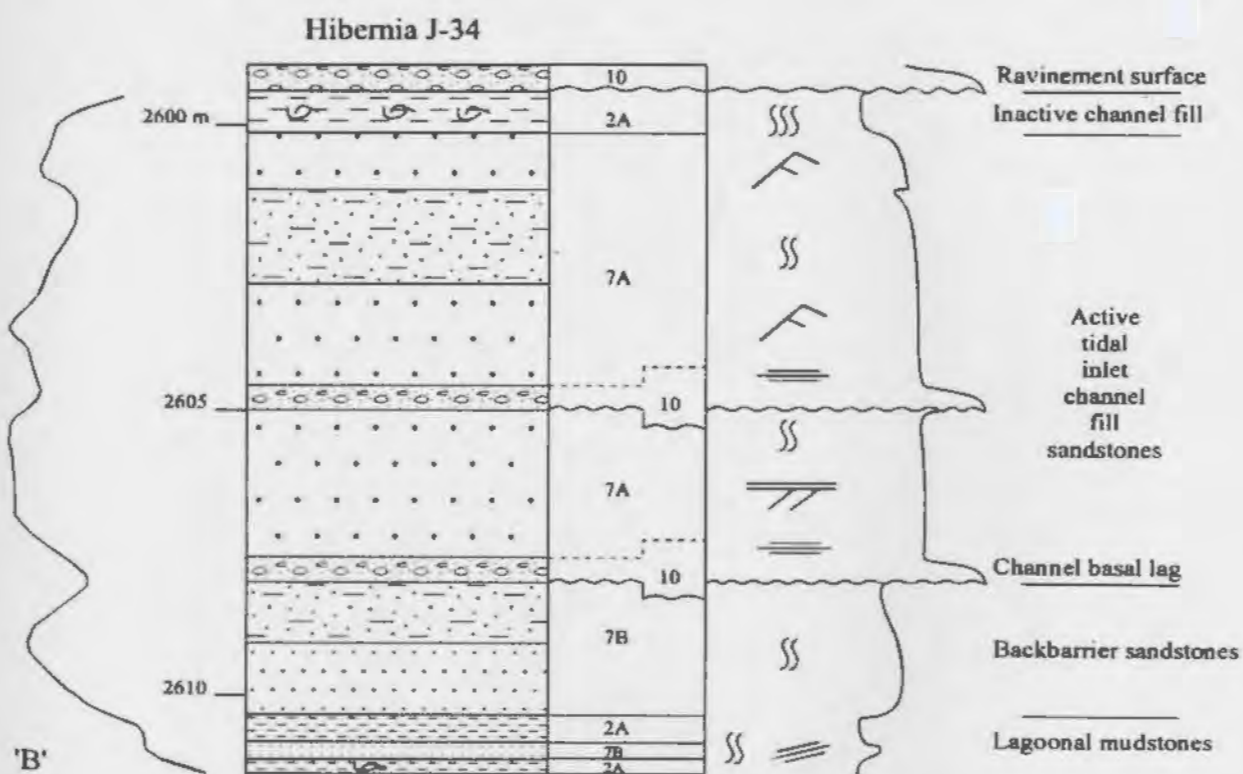
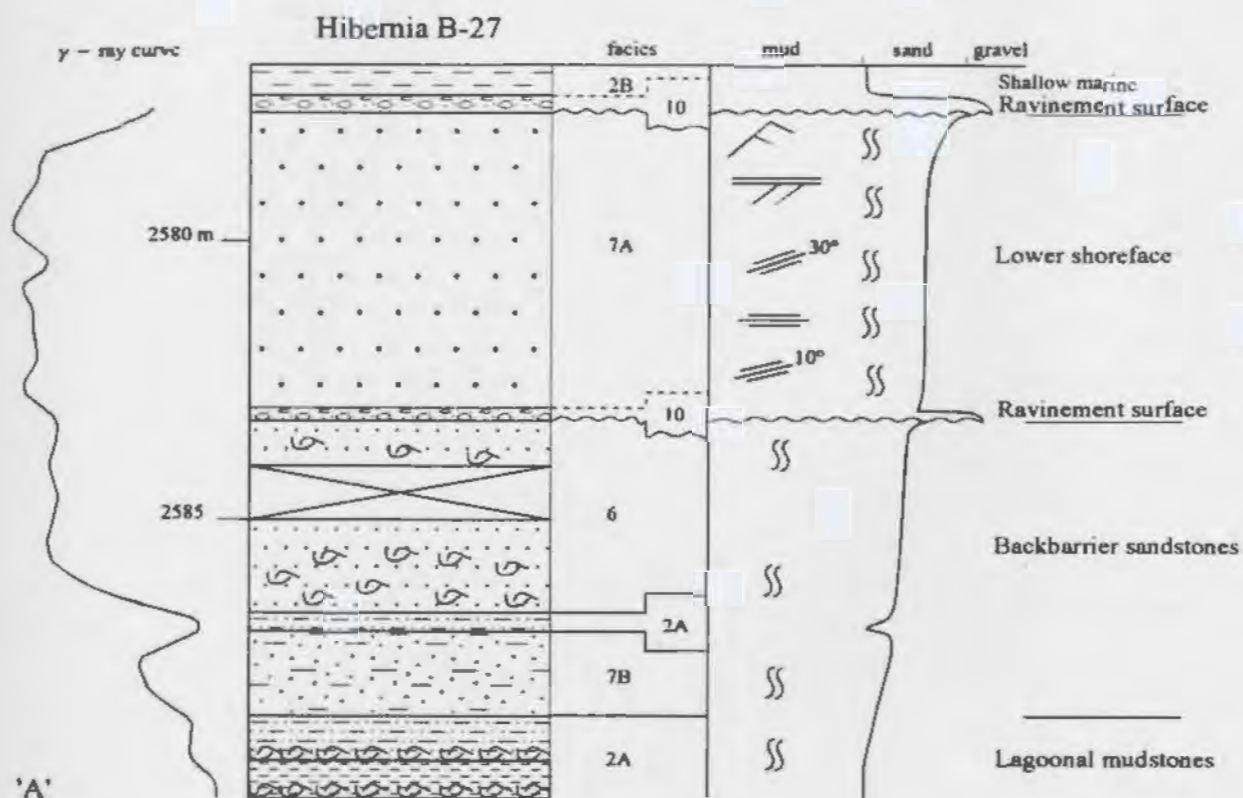


Figure II.3- BARRIER-BACKBARRIER FACIES SUCCESSIONS

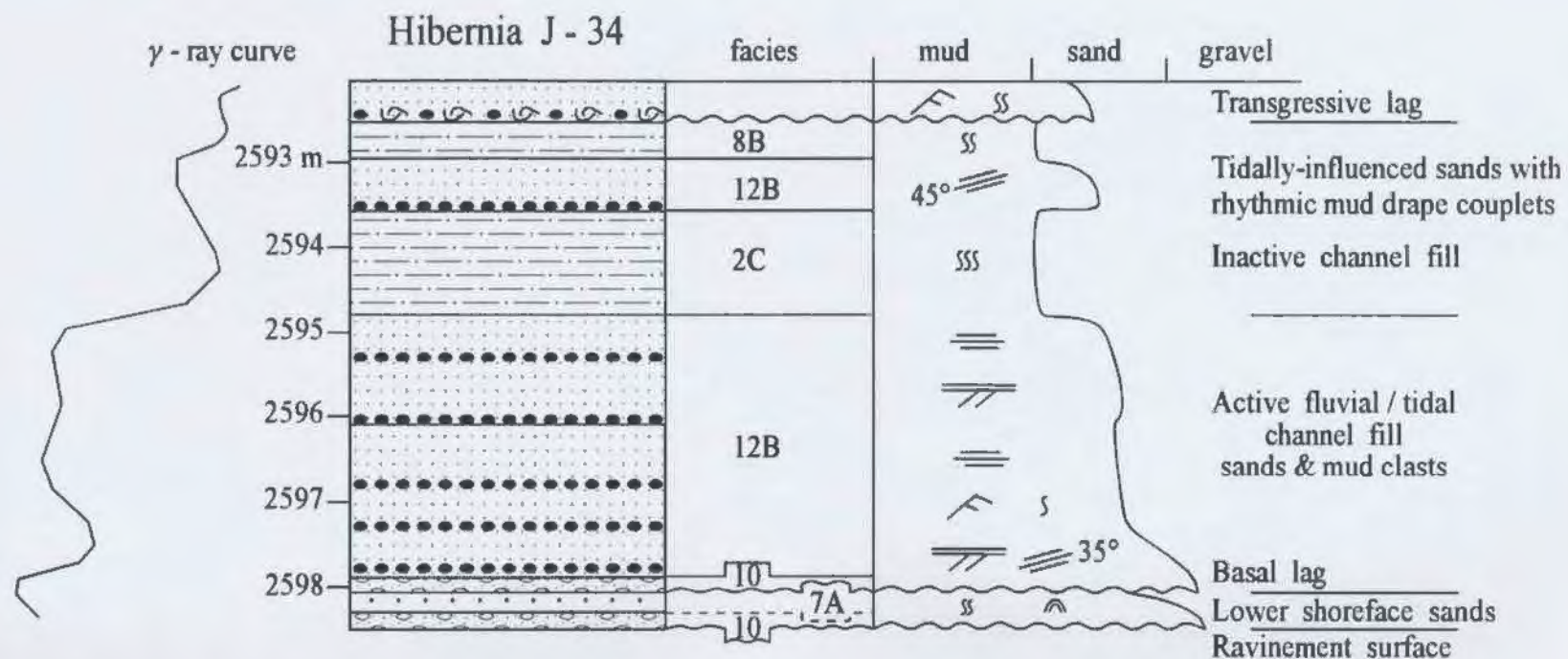


Figure II.4- FLUVIAL / TIDAL CHANNEL FILL FACIES SUCCESSION,
EROSIVELY OVERLYING LOWER SHOREFACE SANDS.

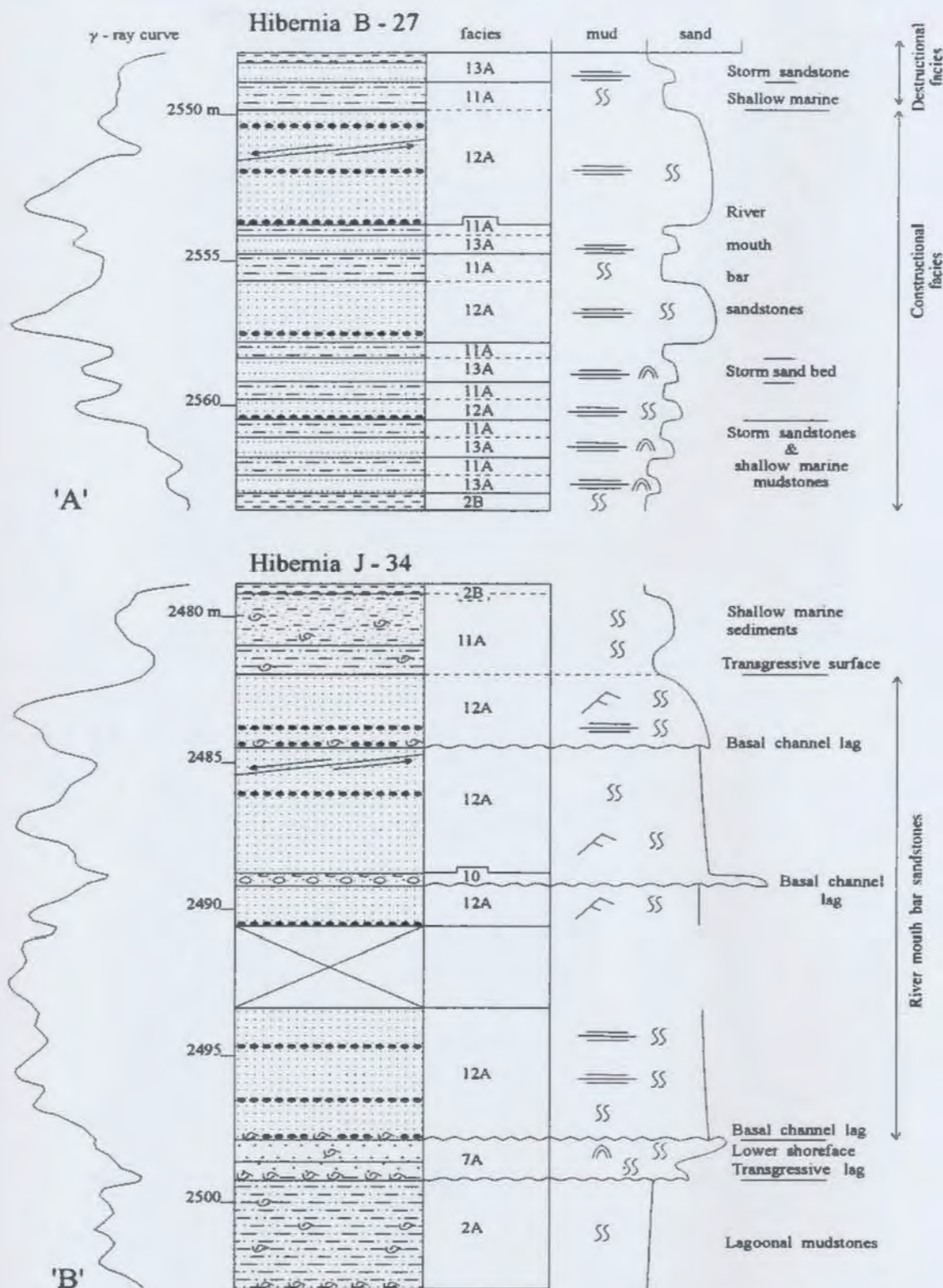


Figure II.5- RIVER MOUTH BAR FACIES SUCCESSIONS
 A: PROGRADATIONAL SUCCESSION
 B: RETROGRADATIONAL (ESTUARINE CHANNEL FILL).

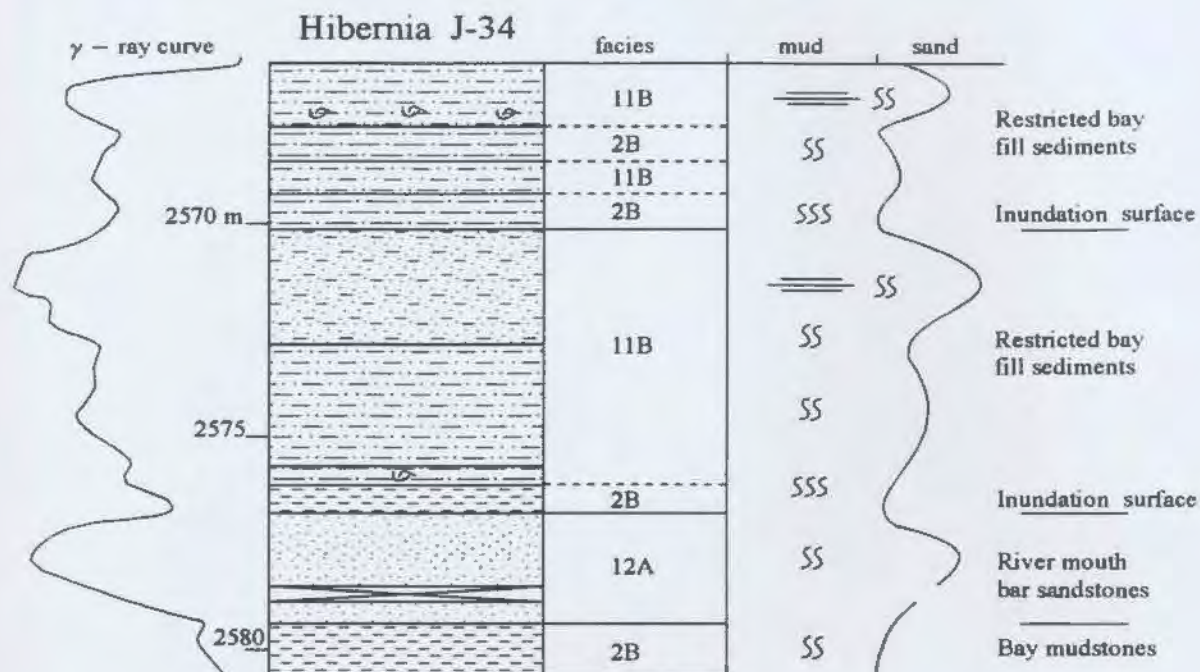


Figure II.6- INTERDISTRIBUTARY BAY FILL SUCCESSION.

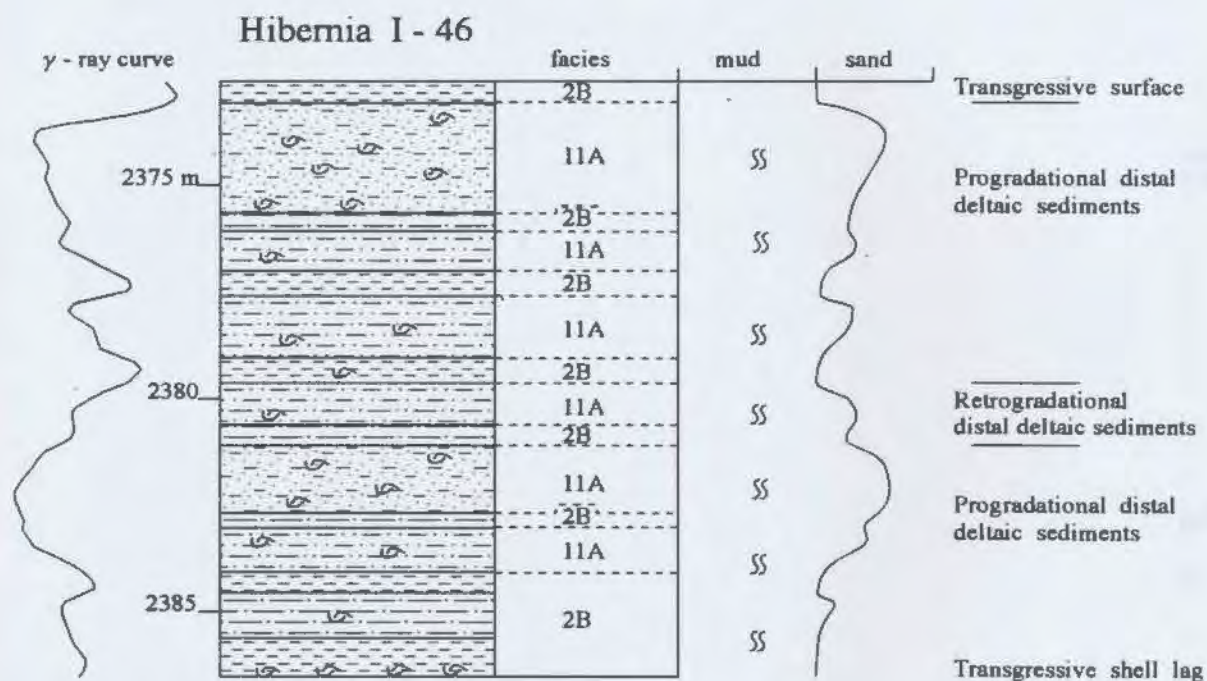


Figure II.7- DISTAL DELTA FACIES SUCCESSION.

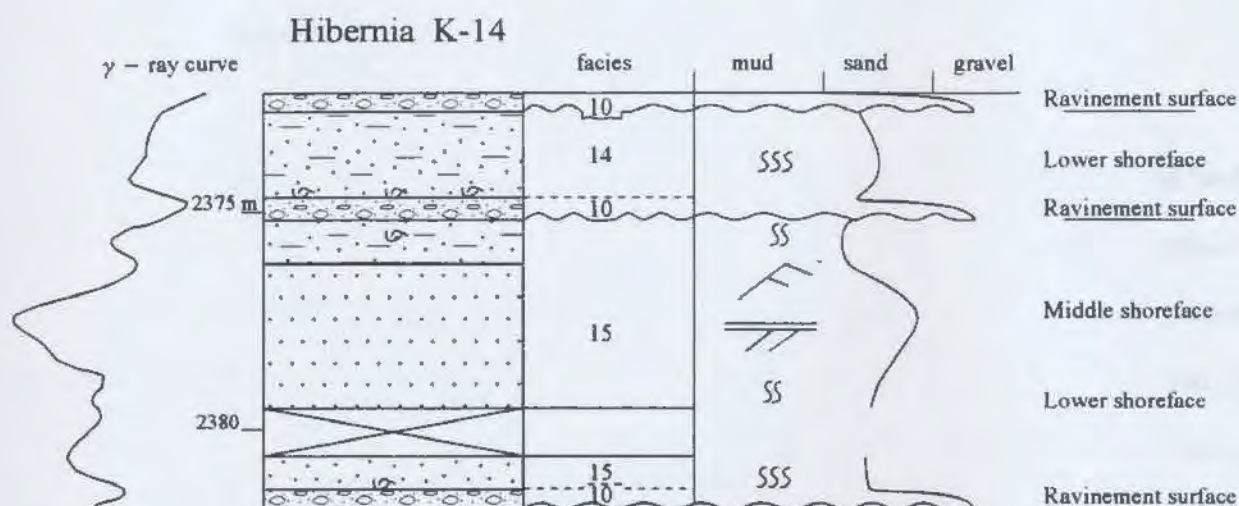


Figure II.8- TWO STACKED SHOREFACE FACIES SUCCESSIONS.

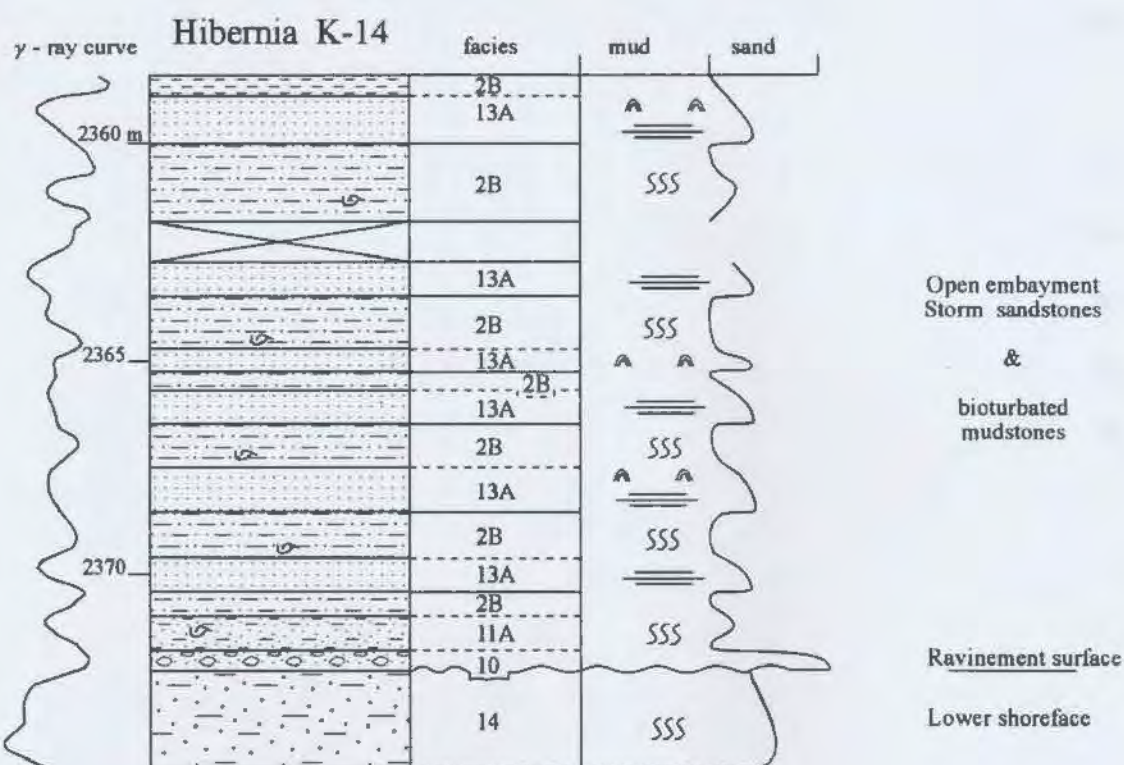


Figure II.9- SHALLOW MARINE FACIES SUCCESSION,
OVERLYING LOWER SHOREFACE SANDSTONES

III- DEPOSITIONAL SYSTEMS

"Depositional systems are assemblages of process-related sedimentary facies. As such they are the stratigraphic equivalents to geomorphic or physiographic units. Examples include fluvial, delta, strandplain and barrier island systems" (Scott and Fisher 1969). Depositional systems are bounded by unconformities or by facies transitions into adjacent, genetically unrelated systems, such as the passage of a deltaic coast into a clastic sediment-starved carbonate shelf (Miall 1990). The components of a depositional system, e.g. a deltaic system, would be smaller scale environments such as the river mouth bar or the distributary channel.

The concept of depositional systems was developed largely in the Gulf Coast region as a means of analyzing and interpreting the immense thicknesses of sediment that are so rich in oil and gas (Miall 1990). The depositional systems approach is essentially genetic stratigraphy that is based on an understanding of depositional environments and syn-depositional tectonics that control the deposition of sediment packages. The approach interprets rocks in terms of broad paleoenvironmental and paleogeographic reconstructions (Miall 1990) and it enables predictions to be made about geometry and orientation of reservoir sandstone bodies. The depositional systems approach can be applied on both local and regional

scales, respectively for reservoir geology and basin analysis purposes.

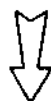
The depositional systems approach is applied in this chapter in order to:

- 1) decipher the depositional history of the abundantly cored lower part of the Avalon Formation,
- 2) reconstruct the paleogeography of the lower part of the Avalon Formation, and
- 3) to delineate various sandstones bodies in the lower part of the Avalon Formation.

Facies, facies associations and facies bounding surfaces, which were discussed in chapter II, are integrated with paleoecologic data¹ to construct stratigraphic cross sections and paleogeographic maps for thin sediment intervals in the lower part of the Avalon Formation. Diagnostic criteria for recognition of different types of depositional systems will then be contemplated. These diagnostic criteria will be applied to the poorly cored upper part of the Avalon Formation as well as the lowermost part of the Ben Nevis Formation. This is done in order to show the progression of depositional systems through time. Finally, the stratigraphic architecture of the entire Avalon Formation will be highlighted. The steps used to accomplish the above goals are illustrated below:

¹Sources of paleoecologic data include Root (1983), Jenkins (1984) and Guilbault (1986).

STRATIGRAPHY OF THE LOWER AVALON FORMATION
IN TWO KEY WELLS
(HIBERNIA B-27 & I-46)



FACIES AND EVENT CORRELATION



STRATIGRAPHIC CROSS SECTIONS



PALEOGEOGRAPHY



DIAGNOSTIC CRITERIA



STRATIGRAPHY OF THE AVALON & BEN NEVIS
FORMATIONS IN ONE KEY WELL (HIBERNIA J-34)



STRATIGRAPHIC ARCHITECTURE OF
THE AVALON FORMATION

III.1- STRATIGRAPHY OF THE B-27 WELL

III.1.1- FACIES & DEPOSITIONAL ENVIRONMENTS:

The cored interval in the Hibernia B-27 well is divided into eight facies successions (figure III.1). Boundaries between the successions are transgressive, erosional or subaerial exposure surfaces. Facies and depositional environments of the various successions, from oldest to youngest, are briefly discussed below:

2612.5-2603.0 m: Shallow Marine Facies Succession 'VIII'

This succession consists of offshore bioturbated mudstones, with some storm laminated sandstones. The mudstones are dominated by open marine microfossils (Guilbault 1986) and marine organic matter (Jenkins 1984).

2603.0-2598.5 m: Lake/Lagoonal Fill Facies Succession 'I'

This succession marks a drastic environmental change from the underlying offshore sediments to marginally marine deposits. The succession has a basal erosional boundary, that is covered by mud clasts. The succession consists of structureless muddy sandstones, 2.6 metres thick, that grade upwards to dark coloured mudstones. The latter are also structureless and host essentially terrigenous organic matter (Jenkins 1984). This facies succession was deposited in a restricted marginal marine environment.

2598.5-2590.0 m: Lake/Lagoonal Fill Facies Succession 'I'

This succession, 8.5 m. thick, records recurrent subaerial

exposure, and inundation by lake/lagoonal waters. It consists of four soil horizons, with thin intervening lagoonal sediments (figure II.2B). The bottom and top soils are mature and suggest lengthy subaerial exposures. The succession hosts essentially arenaceous forams and brackish water ostracods (Guilbault 1986). The organic matter content varies from exclusively to essentially terrigenous (Jenkins 1984). The succession is bounded at top by the transgressive surface 'I' that is covered by shell debris.

2590.0-2578.0 m: Barrier-Backbarrier Facies Succession 'II'

This succession, 12.0 m. thick, records the ultimate submergence of the underlying soils and recurrence of exclusively marine sedimentation. The succession starts at base with lagoonal mudstones, that change upwards to barrier-backbarrier sandstones (figure II.3A). The succession is bounded at top by the erosional transgressive surface 'II'.

2578.0-2576.5 m: Shallow Marine Facies Succession 'VIII'

This succession overlies the erosional transgressive surface 'II'. This surface is a ravinement surface that marks a significant lateral shift from shoreface to shallow marine environments, below and above it respectively. The ravinement surface is covered by well rounded basement gravels (Plate II.18). These gravels pass upwards to shallow marine mudstones and storm sandstones. The succession is terminated at top by an erosional surface.

2576.5-2570.0 m: River Mouth Bar Facies Succession 'IV'

This fining upwards succession, about 8.0 m. thick, records deposition of retrogradational river mouth bar sands. The succession has a basal erosional boundary. The latter is overlain by the Laminated Clean Sandstone Facies, which passes gradually upwards to shallow marine mudstones and storm sandstones. The succession hosts microfossils that indicate hyposaline water conditions (Guilbault 1986), and dominantly terrigenous and minor marine organic matter (Jenkins 1984).

2570.0-2563.5 m: River Mouth Bar Facies Succession 'IV'

This succession, about 6.5 m. thick, represents another phase of deposition of river mouth bar sands. It hosts fauna and flora similar to those in the underlying succession (Guilbault 1986; Jenkins 1984).

2563.5-2547.5 m: River Mouth Bar Facies Succession 'IV'

This coarsening upwards succession, 16.0 m. thick, records active progradation of the river mouth bars. The succession hosts marine and terrigenous organic matter (Jenkins 1984). The succession is terminated, at top, by a transgressive surface.

III.1.2- A BIOSTRATIGRAPHIC PROBLEM:

Biostratigraphic events shown in figure III.1, excluding the *Subtilisphaera perlucida* 'SP' event, have been recorded by

various parties to mark the top of the Barremian Stage, where the Barremian unconformity is located. Figure III.1 shows that the highest occurrence of the Speeton Assemblage¹, SA event, is recorded at three different depths by different investigators. The *Muderongia simplex* 'MS' event occurs at a shallower depth than the *Aptea anaphrissa* 'AA' event, although the MS becomes extinct in the Early Barremian while the AA disappears in the Middle Barremian (personal communication with Jenkins in 1993). Conceivably, there is a problem of fossil recycling. This problem poses great difficulties in drawing a time line at the top of the Barremian Stage (see III.3 for an alternative approach).

It is worth mentioning that the recycling problem has been acknowledged by Jenkins (1993) who reported a diverse Speeton Assemblage which has its highest occurrence at the depth of 2584.5 m. Jenkins questioned whether everything recorded to be Barremian above 2584.5 m is in fact recycled.

III.1.3- SYNOPSIS:

The basal offshore mudstones change upwards to restricted marine sandstones and soil mudstones. The transition occurs

²Jenkins (1993), Chevron, Gulf Canada, Petro Canada and Mobil.

³The Speeton Assemblage includes a group of dinoflagellates species that occur abundantly throughout the Barremian Stage, and disappears at its top (Jenkins, personal communication).

across an erosional boundary, at the depth of 2603.0 m (figure III.1). This transition reflects uplift and erosion of the offshore mudstones. A restricted marine environment was subsequently established. Subaerial exposure of the restricted marine deposits occurred shortly afterwards and resulted in the formation of soil sediments, at the depth of 2598.5 m.

Submergence of the soil sediments followed and was succeeded by deposition of lagoonal mudstones, transgressive barrier island sandstones and then shallow marine mudstones.

Shallow marine sedimentation was terminated by an important erosional event, at the depth of 2576.5 m. This erosional event was followed by active fluvial sediment supply and subsidence. These conditions resulted in river mouth bar deposition that was interrupted by several transgressions.

A problem of fossil recycling poses great difficulties in using biostratigraphic data to locate the top of the Barremian Stage, where the Barremian unconformity occurs. The facies data indicate three potential locations for the Barremian unconformity. The first location occurs at the depth of 2603.0 m. (figure III.1). where the offshore mudstones are erosively overlain by the restricted marine sediments. The second potential location for the Barremian unconformity coincides with the subaerial exposure surface at the depth of 2598.5 m. below which the mature soil sediments occur. However, the hiatus associated with this subaerial exposure surface is too

short, 10,000 years at best', to account for the missing time across the Barremian unconformity surface and therefore will not be considered further. The third and the most likely potential location for the Barremian unconformity is that erosional surface 'II' that occurs at the depth of 2576.5 m. This surface separates shallow marine from overlying river mouth bar sediments.

The four facies successions which occur between the erosional surfaces 'I' and 'II' at the depths of 2603.0 and 2576.5 m. (figure III.1) are postulated to have been accumulated over a period of 25,000-50,000 years (See sections II.2.1 & 2 & table II.2). This short period implies that the two erosional surfaces are closely spaced in terms of time and thickness of accumulated sediments. In such a narrow interval the resolution of the biostratigraphic data is too low to separate between the two erosional surfaces when attempting to determine which surface is the Barremian unconformity. In fact both erosional surfaces might have contributed to the Late Barremian hiatus which is reflected through the biostratigraphic data.

On the other hand, the approximately 30.0 m. thick interval of river mouth bar sediments above the upper

'Paleosols require several thousand years to develop, and take up to 10,000 thousand years to reach maturity (Leeder 1975; Retallack 1984).

erosional surface 'II' (2576.5 m. in figure III.1) represents a very short time span of 3000 years at best (See section II.2.4 & table II.2). A great deal of fossil recycling was associated with the deposition of these river mouth bar sediments. The spread of the various biostratigraphic tops within this thick interval of sediments has a significant impact on the physical placement of the Barremian unconformity. In contrast, such spread has only a trivial chronological meaning in terms of the short amount of time involved. Therefore, a careful integration of biostratigraphic and facies data is essential to locate the top Barremian time line in wells to be drilled in future in the Hibernia field.

III.2- STRATIGRAPHY OF THE I-46 WELL

III.2.1- FACIES & DEPOSITIONAL ENVIRONMENTS:

Nine facies successions were recognized in the cored interval of interest in the well I-46 (figure III.2). Boundaries between these facies associations are either erosional or transgressive surfaces. Facies and depositional environments of these successions are briefly outlined below:

2490.0-2457.0 m: River Mouth Bar Facies Succession 'IV'

This succession, 33.0 m thick, has a basal erosional boundary, which is overlain by many horizons of basal lag conglomerates (Plate II.17). The succession records aggradation of river mouth bar deposits. It consists of stacked cycles of the

Laminated Clean Sandstone Facies, separated by thin mudstone beds. The succession ends at top with a transgressive surface. The succession hosts microfossils which are indicative of hyposaline conditions (Guilbault 1986) and essentially terrigenous organic matter (Jenkins 1984).

2457.0-2444.0 m: Distal Delta Facies Succession 'VI'

This succession reflects progradation of the deltaic deposits in a marginal marine environment. It consists of bioturbated mudstones, storm sediments and a bed of the Laminated Clean Sandstone Facies, at top. It contains microfossils and organic matter similar to those in the underlying succession (Guilbault 1986; Jenkins 1984).

2444.0-2433.0 m: Interdistributary Bay Fill Succession 'V'

This facies succession records deposition of delta plain sediments in a shallow restricted marine environment. Brackish water conditions are suggested by the occurrence of siderite nodules, species and diversity of ostracod and foraminiferal content (Guilbault 1986) and exclusively terrigenous organic matter (Jenkins 1984). The succession has a basal erosional boundary and a top transgressive surface.

2433.0-2419.5 m: Restricted Marine Delta Facies Succession (?)

This sandier upwards succession, 13.5 m. thick, is not cored except in its basal part. This basal part consists of dark-coloured structureless to bioturbated mudstones. The succession hosts exclusively terrigenous organic matter

(Guilbault 1986). It is assumed here that it represents a continuation of deltaic sedimentation, which deposited the underlying successions. The facies and event correlation, discussed in the next section, indicates that this succession is laterally equivalent to lagoonal and soil facies (figures III.3 & 4).

2419.5-2407.5 m: Lagoonal Fill Facies Succession 'I'

This succession consists of lagoonal mudstones and washover sandstones. The mudstones host microfossils which are typical of brackish estuarine conditions (Guilbault and Vervloet 1983). However, brief marine incursions are suggested by the occurrence of opportunistic *Corpulids* (Root 1983), in the washover sands. The succession ends at top with the erosional transgressive surface 'II'.

2407.5-2405.5 m.: Barrier-Backbarrier Facies Succession 'II'

This succession has a basal ravinement surface that is overlain by the Conglomerate-Sandstone Subfacies 'B'. The latter passes upwards to the Intraclastic Sandstone Subfacies 'A' which host large oyster shells characteristic of a shoreface habitat (Root 1983). The basal ravinement surface of the succession records a dramatic lateral shift from brackish water lagoon to an open marine lower shoreface environment, respectively below and above the ravinement surface. This environmental shift reflects a transgression and landward translation of the shoreline.

2405.5-2398.0 m: River Mouth Bar Facies Succession 'IV'

This succession has a basal erosional boundary. The succession records the onset of another phase of deltaic sedimentation. It consists of river mouth bar sands and basal lag deposits, directly resting above the basal erosional surface. The succession ends at top with the transgressive surface 'III'.

2398.0-2386.5 m: Distal Delta Facies Successions 'VI'

This succession records gradual lateral shifting of locus of deposition of the river mouth bar, and deposition in more distal environments. The clean mouth bar sandstones, at the base, are overlain by successively increasing bioturbated muddy sediments. The latter host Molluscan shells, that increase in abundance and diversity upwards (Root 1983). This succession ends at top with the transgressive surface 'IV'.

2386.5-2373.0 m.: Distal Delta Facies Association 'VI'

This succession is more muddy and was deposited in a more distal position than the underlying succession. This succession hosts microfossils indicative of less hyposaline conditions (Guilbault 1986). The succession is bounded at top by a transgressive surface.

III.2.2- A BIOSTRATIGRAPHIC PROBLEM:

The problem of fossil recycling is far more pronounced in the I-46 well than in the B-27 well (figure III.2). For example, the highest occurrence of the Speeton Assemblage 'SA' has been recorded at four different depths. Depths of the

other biostratigraphic events used by different investigators to mark top of the Barremian Stage are also scattered throughout a depth range of about 160 metres. This large scatter of various biostratigraphic events makes it quite difficult to decide which event is most appropriate to locate the Barremian unconformity. Clearly, an alternative approach is needed to locate the Barremian unconformity (see III.3).

III.2.3- SYNOPSIS:

The basal erosional boundary of the cored section marks an important erosional event, at the depth of 2490.0 m (figure III.2). This event was followed by active fluvial sediment supply and contemporaneous subsidence. These conditions resulted in the deposition of stacked cycles of river mouth bar sandstones. Deposition of these cycles was ultimately terminated by a transgression, at the depth of 2457.0 m. This transgression was followed by delta progradation and shoaling of the environment. The shoaling was accompanied by the development of increasingly brackish water conditions.

Submergence and gradual diminution of brackish water conditions followed and accompanied deposition of the lagoonal mudstones, at the depth of 2419.5 m. Marine incursions occurred during deposition of the washover sandstones, at the depth of 2415.0 m. Optimum marine conditions accompanied deposition of the lower shoreface sandstones at the depth of 2407.5 m.

Another important erosional event occurred afterwards (at the depth of 2405.5 m., figure III.2). This erosional event was also followed by active fluvial sediment supply, subsidence and deposition of river mouth bar sandstones. These sandstones were subsequently transgressed (at the depth of 2398.0 m). Deposition of distal deltaic sediments followed.

A problem of fossil recycling poses great difficulties in using biostratigraphic data to locate the Barremian unconformity. The facies data indicate the occurrence of two significant erosional surfaces 'I' and 'II' at the depths of 2490.0 and 2405.5 m. These surfaces represent two potential locations for the Barremian unconformity. The two corresponding erosional events were followed by active fluvial sediment supply, subsidence and deposition of river mouth bar sandstones.

The sedimentary section which is confined between the two erosional surfaces is postulated to have been deposited over a period of 15,000 to 25,000 years (See table II.2). This short period suggests that the erosional surfaces are closely spaced in terms of time, in spite of their considerable physical separation (84.5 m. vertical distance). In such a short period the resolution of the biostratigraphic data is too low to separate between the two erosional events. In fact both erosional surfaces might have contributed to the Late Barremian hiatus which is reflected through the

biostratigraphic data.

On the other hand, the three facies successions which occur above the erosional surface 'II' at the depth 2405.5 m. (figure III.2) were developed over a very short time interval of 3000 years at best (See table II.2). The spread of various biostratigraphic tops within these successions significantly affects the physical placement of the Barremian unconformity. In contrast, such spread has a negligible chronological effect because of the very short amount of time involved. Therefore, careful integration of biostratigraphic and facies data is a must in order to locate the top Barremian time line in wells to be drilled in future in the Hibernia field⁵.

III.3- FACIES AND EVENT CORRELATION

A facies and event correlation approach is advanced here to establish several near isochronous surfaces in the lower Avalon Sandstones. These surfaces approximate time lines and are essential for the construction of small scale stratigraphic cross sections. The facies and event correlation approach is used as an alternative to the biostratigraphic approach because of the fossil recycling problem (discussed previously).

⁵The same conclusion has been reached in section III.1.3.

III.3.1- PRINCIPLES:

The facies and event correlation approach is based on matching of facies successions and correlation of events. For example, two different facies successions may be deposited in two adjacent locations as a result of one transgressive event. These facies successions, although different, are synchronous to each other and can provide good chronological markers. The principles of facies matching and event correlation, as applied in the Hibernia field, are discussed below:

1) Facies succession matching:

Facies successions can match between neighbouring wells if they are the same type or they are deposited adjacent to each other in modern depositional environments. In both cases the scale of the depositional system, which results from matching the facies successions should be comparable to the scale of the equivalent modern depositional environment. In figure III.3 the Barrier-backbarrier Facies Succession that occurs below TS'II' in the B-27 well can match up with the Lagoonal Fill Facies Succession in the I-46 well. The two facies successions are deposited adjacent to each other in modern barrier island shorelines. Also, the River Mouth Bar Facies Succession occurring above the erosional surface in both the B-27 and I-46 wells can represent equivalent sections in the same river mouth bar.

2) Conglomerate lag Facies:

A distinct conglomerate layer present in several wells in the Hibernia field provides a good chronostratigraphic marker (Plate II.18). The conglomerate layer consists of rounded basement pebbles that covers a ravinement surface. Figure III.3 shows the conglomerate layer extending between the B-27 and I-46 wells.

3) Transgressive or submergence events:

Submergence is recorded by the presence of shallow water facies below deeper water facies, e.g. Intraclastic Sandstone Facies below Mudstone 'D' Subfacies. The discontinuity surface separating the shallower facies from the deeper facies is near isochronous, if the surface can be delineated between the adjacent wells. All the facies which occur just above the discontinuity surface were deposited almost immediately after the submergence or transgressive event. These facies record the synchronous reestablishment of a new paleogeographic profile immediately following the transgressive event (Matthews 1984). Figure III.3 shows five transgressive surfaces that have been delineated between two closely spaced wells, 3.8 Km apart, in the Hibernia field.

4) Subaerial exposure and soil formation events:

Soil zones have been commonly used for local and regional correlations in terrestrial facies (Flores 1979; Retallack 1983; Fastovsky 1987). Soil zones in a small area like the

Hibernia field record important subaerial exposure events. These soil zones provide excellent chronostratigraphic markers that can be followed between the wells. Figure III.3 depicts a soil zone in the B-27 well that has a large potential to be a chronostratigraphic marker.

5) Erosional events:

Individual erosional surfaces on a local scale can record synchronous erosional events. On a regional scale these surfaces may in fact be diachronous. In both local and regional scales, erosional surfaces are important tools for event stratigraphy, although they can intersect time lines of the older rocks. Plint et al. (1986) recognized seven basin-wide erosional surfaces in the Cardium Formation in Alberta. Plint et al. suggested that these surfaces record erosional events that followed regressions. In fluvial deposits, some authors have suggested that individual channelling events may be widely synchronous between drainages as a result of rapid regional shifts in base level (Kauffman et al. 1991, page 804). Figure III.3 depicts an erosional surface that occurs shortly above a ravinement surface in both the B-27 and I-46 wells. This surface clearly represents a synchronous erosional event in both wells.

6) Marine cementation events:

Kauffman et al. (1991) reported that concretions produced by early diagenetic precipitation of carbonate cements in thin

stratigraphic intervals most commonly form regional stratigraphic marker beds. Waage (1964), Kantorowicz et al. (1987), Walderhaug et al. (1989), Gibbons et al (1993) correlated concretion beds, respectively for thousands of Km² in South Dakota, for several kilometres in Birdport Sands at England, for more than 6.0 Km in the Brage field at offshore Norway, and for more than 1000 metres in the Troll field at offshore Norway. In Hibernia field early marine fibrous and bladed calcite cements occur in the Intraclastic Sandstone 'A' Subfacies. The persistence of these marine cements and their host facies in most of the Hibernia wells provides good chronostratigraphic markers.

7) Sequential order of events:

The sequential order or the arrangement of events provides a powerful tool for correlation. For example, in the B-27 well there is a sequence of events involving soil formation, transgression 'I', transgression 'II', erosion, and transgressions 'III' up to 'V' (figure III.3). The same sequence of events, with the exception the soil formation event, occurs in the I-46 well.

III.3.2- APPLICATION:

Three facies and event correlations have been carried out (figures III.4-6). The chronostratigraphic markers which have been used and the main results of each of the three correlations are discussed below.

III.3.2.1- B-27, I-46 & K-14 correlation:

Important chronostratigraphic markers include the soil zone, transgressive surfaces 'I' to 'V', erosional surface 'II', Barrier-backbarrier Facies Successions 'I' & 'II' (below and above TS'II' in the K-14 well), marine calcite cementation and a conglomerate layer (figure III.4).

The sedimentary section can be subdivided into three genetically-related depositional packages. The lower depositional package 'A' is confined between the erosional surface 'I' and the transgressive surface 'I'. The middle depositional package 'B' is confined between the transgressive surface 'I' and the erosional surface 'II'. The upper depositional package 'C' occurs above the erosional surface 'II'. Using appropriate datums, stratigraphic cross sections have been constructed for each of the three depositional packages.

It is important to note that the offshore mudstones, which occur in the B-27 and K-14 wells below the ES'I', are absent in the I-46 well. Also, there are two fully preserved Barrier-backbarrier Facies Successions below the ES'II' in the K-14 well.

III.3.2.2- I-46, B-27 & C-26 correlation:

Important chronostratigraphic markers include the soil zone, transgressive surfaces 'I' to 'V', the erosional surface 'II', the Barrier-backbarrier Facies Successions (below and

above TS'II') and a conglomerate layer (figure III.5).

It is important to note that the shoreline sediments of depositional package 'B', confined between TS'I' and ES'II', decrease gradually in thickness towards the C-96 well. Also, the various types of deltaic sediments that occur above ES'II', decrease in thickness in the same direction.

III.3.2.3- I-46, J-34, K-14 and C-96 correlation:

Important chronostratigraphic markers include the soil zone, transgressive surfaces 'I' to 'V', the erosional surface 'II', the Barrier-backbarrier Facies Successions (below and above TS'II') and a conglomerate layer (figure III.6).

It is important to note that there are two Barrier-backbarrier Facies Successions fully preserved below ES'II' in the K-14 well. The upper Barrier-backbarrier Facies Succession is partially preserved and is erosively overlain by Fluvial/Tidal Channel fill and River Mouth Bar Facies Successions, respectively in the J-34 and I-46 wells.

III.4- STRATIGRAPHIC CROSS SECTIONS

Four stratigraphic cross sections are constructed for the three depositional packages, 'A' to 'C', that have been highlighted in figures III.4 & 5. The main stratigraphic relationships depicted in each cross section are discussed below:

III.4.1- B-27, I-46 & K-14 CROSS SECTION (Figure III.7):

The datum for the cross section is the transgressive surface 'I'. The surface is covered by shell hash that changes upwards into dark coloured mudstone in the B-27 and K-14 wells. The cross section illustrates a valley that is incised into offshore mudstones.

The valley floor is covered by many horizons of basal lag deposits (Plate II.17). The valley is filled with estuarine sediments. The estuarine sediments consist of stacked cycles of river mouth bar sandstones, bay mudstones, distal deltaic sediments and interdistributary bay fill sandstones.

Soil mudstones in the B-27 and K-14 wells resulted from subaerial exposure of the bay mudstones which occur in the immediate vicinity of the valley flanks. These soil mudstones increase in thickness away from the valley trough and they are expected to represent subaerially exposed offshore mudstones farther away on the valley flanks.

The interdistributary bay fill sandstones, at the upper part of the valley fill, have a basal erosional boundary. This erosional boundary may reflect a channelling event that occurred as a consequence of increased sediment supply following shoaling and filling of the valley. Similar channelling has been recorded in modern estuaries that receive abundant fluvial sediment supply. Cooper (1993) reported scouring of estuarine deposits during catastrophic flooding

events in the Mgeni river estuary, South Africa.

III.4.2- I-46, B-27 & C-96 CROSS SECTION (Figure III.8):

The datum is the transgressive surface 'I'. This datum marks the ultimate submergence of soil sediments in the B-27 and C-96 wells. These soil sediments were developed on the subaerially exposed valley flanks (figure III.7).

The soil sediments in the B-27 and C-96 wells change laterally into bay mudstones and deltaic sandstones in the I-46 well, which occurs in the valley trough.

The lower shoreface and backbarrier sandstones, that occur below TS'II' in the B-27 and C-96 wells, comprise a transgressive barrier island. The barrier island sandstones change laterally into lagoonal mudstones and washover sandstones, in the I-46. It is worth mentioning that the lower shoreface sandstones are separated from the backbarrier sandstones by a ravinement surface (figure II.3). This ravinement surface corresponds to a transgressive surface that occurs at the top of the washover sandstones in the I-46 well.

The thin interval that is confined between TS'II' and ES'II' involves lower shoreface sandstones in the I-46 well. These lower shoreface sandstones overlie lagoonal mudstones and change laterally into shallow marine mudstones towards the B-27 and C-96 wells. The lower shoreface sandstones in the I-46 well mark the position of a transgressive barrier island. This barrier island was subsequently eroded at the time of

ES'II'.

The shift in position of the lower shoreface sandstones across TS'II', from the B-27 to the I-46 well, reflects the landward translation of the shoreline. The process of landward migration of the shoreline is schematically illustrated in figure III.9.

The interval above ES'II' decreases gradually in thickness and gets more muddy towards the C-96 well. The interval consists of river mouth bar sandstones, bay mudstones and distal deltaic muddy sandstones. The presence of the transgressive surfaces 'III' to 'V' reflects active subsidence that accompanied abundant deltaic sediment supply.

III.4.3- I-46, J34, K-14 & C-96 CROSS SECTION (Figure III.10):

The datum is the transgressive surface 'I' which marks the ultimate submergence of soil sediments in the C-96 well.

The soil sediments in the C-96 and K-14 wells change laterally into bay mudstones and deltaic sandstones in the J-34 and I-46 wells.

The tidal inlet channel fill, lower shoreface and backbarrier sandstones, that occur below TS'II' in the J-34, K-14 and C-96 wells, comprise a transgressive barrier island. The barrier island sandstones change laterally into lagoonal mudstones and washover sandstones, in the I-46. In the K-14 well the lower shoreface sandstones are separated from the backbarrier sandstones by a ravinement surface. This

ravinement surface matches with a transgressive surface that occurs at the top of the washover sandstones in the I-46 well. In the J-34 well, the backbarrier sandstones are incised by tidal inlet channel fill sandstones (figure II.3B).

The interval that is confined between TS'II' and ES'II' consists of lower shoreface sandstones in the K-14, J-34 and I-46 wells. These lower shoreface sandstones change laterally into shallow marine mudstones in the C-96 well. In the K-14 well, the lower shoreface sandstones involve two cycles separated by a submergence surface at the depth of 2389.5 m. The lower cycle is fully preserved, while the upper cycle is highly eroded. In the J-34 and I-46 wells, the lower shoreface sandstones are highly eroded. The shift in position of the lower shoreface sandstones across TS'II' towards the I-46 well, reflects the landward translation of the shoreline.

The ES'II' surface is the basal boundary of a valley that was incised into the lower shoreface sandstones above TS'II'.

III.4.4- I-46, J-34 and K-14 CROSS SECTION (Figure III.11):

The cross section illustrates one side of a valley that is filled with various types of estuarine sediments. The top boundary of the valley fill is an erosional surface⁶. The datum is the transgressive surface 'V' which occurs within the

⁶This erosional surface marks the basal boundary of another valley fill that is discussed in III.8 (figure III.23).

valley fill. The valley is incised into older shoreface sandstones (figure III.10).

The valley fill records an overall upward deepening and increase of marine influence. In the I-46 well, the basal river mouth bar sandstones change upwards into distal deltaic sandstones and bay mudstones. In the J-34 well, the basal fluvial/tidal channel fill sandstones change upwards into interdistributary bay fill sediments. The latter are overlain by bay mudstones. In the K-14 well, the shoreface sandstones are overlain by bay mudstones. The bay mudstones in both the J-34 and K-14 wells host abundant storm sandstone beds, which suggest an open bay.

The transgressive surfaces 'IV' and 'V' are erosional and are covered by sandstone and basement pebbles in the K-14 well. In both the J-34 and I-46 wells, the TS 'IV' and 'V' are marked by dark mudstones overlying deltaic sandstones.

III.5- PALEOGEOGRAPHY

Three depositional systems developed during deposition of the three depositional packages, 'A' to 'C' (figures III.4 & 5). Paleogeography of each system is discussed below, starting with the oldest.

III.5.1- ESTUARINE DEPOSITIONAL SYSTEM "A":

This estuarine depositional system occupied a valley that was incised into offshore mudstones (figure III.4 & 7). The valley

is running through five of the Hibernia wells (figure III.12). A bay head delta provides sediments at the SW. The seaward side of the valley occurs in south east. The valley is structurally-controlled (see section IV.3.2.3). The SW part of the valley occupies a graben that occurs on the hanging wall of the Murre fault (figure I.6). The eastern part of the valley is hosted in another graben that is situated along the crestal area of the Hibernia rollover anticline (figure I.6).

In order to delineate the valley throughout the Hibernia field, paleoecologic data were integrated with well log correlations (figures III.13 & 14). Investigation of the paleoecologic data (Jenkins 1984 & 1986) indicated that sediments occurring outside the valley contain organic matter of mixed terrigenous and marine origin. In contrast, estuarine sediments that were deposited in the valley contain organic matter of exclusively to essentially terrigenous origin. In the P-15 well, which is close to estuary mouth, sediments containing essentially terrigenous organic matter alternate with sediments containing mixture of terrigenous and marine organic matter. Cored sections of sediments occurring outside the valley, in the K-14 and B-27 wells, were deposited in an offshore environment for these sediments. Cored sections of sediments filling the valley, in the I-46 well, were deposited mainly in a bay head deltaic environment.

III.5.2- BARRIER ISLAND DEPOSITIONAL SYSTEM "B":

This depositional system is represented by the depositional package 'B' that occurs between TS'I' and ES'II' (figures III.8 & 10). This depositional package experienced the development of mainly two transgressive barrier islands, below and above TS'II'. Well log correlation shows that the older barrier is well preserved throughout the Hibernia field (figure III.15) In contrast, the younger barrier is highly eroded, except in the K-14 well (figure III.10).

A sand isolith map for the well preserved older barrier island indicates a NW-SE trending barrier island (figure III.16). The open sea is towards the NE, while the lagoon lies to the SW. Transgression of this barrier island would result in landward translation of the shoreline and formation of a younger barrier island to the SW.

The younger barrier island that occurs above TS'II' (figure III.10) was developed following transgression of the older barrier. The younger barrier island was later incised by a valley. The paleogeographic map shown in figure III.17 depicts a barrier island cut by a valley. The barrier island is assumed to have been parallel to the older one. The northwestern extension of this new barrier is speculative. The valley is occupied by an estuary that includes a bay head delta in the SW and an open bay in the NE.

III.5.3- ESTUARINE DEPOSITIONAL SYSTEM "C":

This estuarine depositional system is represented by the depositional package 'C' which occurs above the ES'II' (figures III.8, 11 & 15). The estuarine system occupied a valley that was incised into older shoreface sandstones (figure III.10). An isopach map for the valley fill, confined between ES'II' and TS'V', shows a gradual decrease in thickness towards the east and north-east (figures III.15 & 18). In the B-08 well, most of the valley fill sediments were subsequently eroded (figure III.15).

The estuary involves a bay head delta in the SW and a set of barrier islands and a beach spit to the NE (figure III.19). The beach spit is suggested by the shoreface sandstones which are drilled only in the K-14 well (figure III.11). The trend of the beach spit is assumed to be perpendicular to the axis of the estuary. Future drilling data may verify this trend.

III.6- DIAGNOSTIC CRITERIA

III.6.1- THE BARRIER ISLAND DEPOSITIONAL SYSTEM:

The elongate shoestring geometry of the barrier island is the best criterion to recognize this depositional system. However, this geometry may occasionally be difficult to be proven because of subsequent erosion at the top of the system and/or due to the small number of wells. The types of facies successions are quite useful in recognizing this depositional

system. In case of poor preservation of facies successions, certain facies can be used to identify specific depositional environments in the barrier island depositional system. For instance, the Intraclastic Sandstones 'A' Subfacies can be used to recognize the shoreface environment. The following diagnostic criteria are arranged in a descending order of importance. Reference will also be made to other studies in which the same criteria have been applied elsewhere.

1- Elongate shoestring geometry of the barrier island:

The elongate shoestring geometry has been used to characterize shoreface sandstone bodies in Cretaceous Cardium 'B' Sandstone at Caroline, Alberta (Pattison 1988) and in the Tertiary Cornelius reservoir, Frio Formation at Texas (Tyler and Ambrose 1985).

2- Coarsening upwards facies succession:

This succession starts at base with lagoonal mudstones and changes upwards to shoreface sandstones (figure II.3A). The shoreface sandstones, which consist of the Intraclastic Sandstones Facies, may directly overlie lagoonal mudstones, with a ravinement surface in between, e.g. the shoreface sandstones above TS'II' in the I-46 well (figure III.10). Similar successions were reported by Kraft (1971), Demarest (1981), Demarest and Kraft (1987) and Donselaar (1989).

3- Fining upwards facies succession:

This succession characterizes the tidal inlet channel fill. The succession starts at base with the Intraclastic Sandstone facies and changes upwards to the Mudstone 'A' subfacies (figure II.3B). Multiple erosional surfaces occur in the succession. The tidal inlet channel is incised into lagoonal and backbarrier sediments (figure III.10). Comparable tidal inlet channel fill successions were described in the Upper Silurian Keyser Limestone in Virginia (Barwis and Makurath 1978) and in the Modern shoreline of North Carolina (Heron et al. 1984).

4- Composition and grain size:

The shoreface, tidal channel fill, and backbarrier sandstones consist mainly of the Intraclastic Sandstones Facies. This facies is coarser in grain size than all other facies in the Avalon Formation. The Intraclastic Sandstone Facies comprises fine to medium grain sands while the other sandstones consist of very fine to fine sands. In addition, the Intraclastic Sandstone Facies contains abundant skeletal debris and micritic intraclasts. The shoreface facies in particular hosts early marine fibrous and bladed calcite cements.

5- Ravinement surfaces and pebble lag layers:

Ravinement surfaces occur at many levels in the barrier island depositional system. These ravinement surfaces are covered by rounded basement pebbles (Plate II.18). Both the ravinement

surfaces and the pebble lag layers are very diagnostic to the barrier island depositional system and can be delineated between adjacent wells. Equivalent transgressive erosional surfaces covered with pebble lag layers was described in Miocene shoreline deposits, California (Clifton 1981).

6- Storm sandstones:

Storm sandstone beds are abundant in the shallow marine sediments which immediately overlie the shoreface sandstones. Abundant storm washover sandstones also occur in the lagoonal mudstones underlying the shoreface sandstones.

III.6.2- THE ESTUARINE DEPOSITIONAL SYSTEM:

Two lines of evidence are important to recognize the estuarine depositional system. The first line of evidence is related to identification of the valley which hosts the estuary. The second line of evidence is concerned with the facies and facies successions which were deposited in the estuary. Identification of the valley is essential, otherwise alternative interpretations can be made for the same facies and facies successions. Criteria for recognition of the estuarine depositional system are discussed below, in a descending order of importance.

1- Erosional boundaries of the incised valley:

Downcutting of older sediments by the valley creates a paleo-topographic relief between the valley flanks and the valley trough. Identifying this erosional relief is the most

important criterion to recognize the estuarine depositional system. This erosional relief is always accentuated due to subsequent subsidence of the valley (see IV.3.2.3). The erosional relief is the essential criterion that has been used to recognize other river valleys which were developed due to sea level changes (Reinson et al. 1988; Leckie and Singh 1991; Zaitlin et al. 1994).

2- Uplift and subaerial exposure of the valley flanks:

Incision of the valley occurs during a period of uplift and subaerial exposure (see IV.2.1 & 2). Evidence of subaerial exposure can be preserved in the valley flank sediments. The valley flank sediments of the depositional package 'A' show evidence of abrupt shoaling, erosion and/or subaerial exposure (figure III.7). Offshore facies that occur in the immediate vicinity of the valley flanks are erosively overlain by restricted marine sandstones and soil mudstones. The soil mudstones are expected to thicken and to occur directly above the offshore facies, farther away on the valley flanks. Soils and rooted horizons have been reported in the flanks of a Lower Cretaceous valley in Alberta (Leckie and Singh 1991).

3- Stratigraphic offset of chronostratigraphic markers:

Chronostratigraphic markers that occur in the valley trough are structurally-offset from their counterparts on the valley flanks. This stratigraphic offset repeatedly increases due to recurrent rejuvenation of the valley and renewed movements

along the valley-bounding faults (figure III.20; see section IV.3.2.3).

4- Abrupt facies change across the valley's basal boundary:

Initiation of the valley is always accompanied by abundant sediment supply. The constricted transport of this sediment supply results in erosion of older sediments in the valley trough. These older sediments vary significantly in character from the younger sediments deposited above which.

Facies below the basal erosional boundary of the valley may be Mudstone or Intraclastic Sandstones Facies. Facies above the basal erosional boundary are usually the Laminated Clean Sandstone Facies.

The abrupt facies change across the basal erosional boundary of the valley is also one of the criteria which are used to identify river valleys that were developed as result of sea level changes (MacEachern and Pemberton 1994; Zaitlin et al. 1994).

5- Multiple transgressive surfaces in the valley fill:

As the rate of subsidence of the valley trough increases, relative to the rate of sediment supply, the valley fill sediments are repeatedly submerged. Consequently, several transgressions take place and are recorded in the lower valley fill sediments. The resulting transgressive surfaces serve as good markers for correlation. The transgressive surface that occurs at the top of the lower deepening upward part of the

valley fill is particularly useful for correlation, e.g. TS'V' in figure III.11 (see section IV.3.2.4).

6- Deepening upward followed by shoaling upward facies:

Facies in the lower valley fill reflect progression of environments from fluvial/tidal channel, river mouth bar, interdistributary bay, distal delta to bay (figures III.11 & 21). This environmental deepening results from an increasing rate of subsidence relative to the rate of sediment supply. Facies in the upper valley fill indicate an upward change of distal deltaic to restricted interdistributary bay environments. The upper valley fill usually maintains a sandier upward trend and reflects an upward decrease in the rate of subsidence relative to the rate of sediment supply. These changes in the rates of subsidence and sediment supply are controlled by the tectonics (see section IV.3.2.4).

7- Brackish water conditions:

The trace fossils, faunal and floral content of different estuarine facies should reflect varying degrees of brackish water conditions. The most brackish water conditions are recorded in the uppermost part of the valley fill. The least brackish water conditions are associated with deposition of the bay mudstones which overlie the lower deepening upward facies. Laterally, less brackish water conditions are recorded by facies deposited in the outer estuary, e.g. the P-15 well (figure III.14).

It was found that the biofacies categories, which were proposed by Guilbault (1986), change in a systematic way upwards in the valley fill sequences. Biofacies 'C' always occurs in the lower valley fill. Biofacies 'C' changes upwards to biofacies 'A', 'E' and 'D'. Biofacies 'B' is recorded in the uppermost valley fill. Biofacies 'B' changes laterally to biofacies 'F' on the uplifted valley flanks.

The brackish water conditions, which are reflected by impoverished suites of trace fossils, dinoflagellates and agglutinated foraminifera, have also been used as one of the criteria of recognition of other estuarine valley fills (Brownridge and Moslow 1991; Leckie and Singh 1991; MacEachern and Pemberton 1994).

III.7- STRATIGRAPHY OF THE J-34 WELL

The cored interval in the J-34 well includes most of the Avalon Formation and the lowermost part of the Ben Nevis Formation (figure III.22). The stratigraphy of this reference well is briefly discussed below in order to show the progression of depositional systems through time.

III.7.1- DEPOSITIONAL SYSTEMS:

The cored interval in the J-34 well is subdivided into six depositional packages (figure III.22), each deposited in a distinct depositional system. The lower three depositional packages ('A', 'B', and 'C') belong to the lower part of the

Avalon Formation, which has already been discussed in detail. The depositional package 'D' represents the upper part of the Avalon Formation. The upper two depositional packages ('E' and 'F') belong to the Ben Nevis Formation. The depositional system of each package is briefly outlined below:

1) Depositional package 'A':

This package was deposited in an estuarine system (figure III.12). Such estuarine system occupied a valley that was incised into older offshore mudstones (figure III.13). The cored part of the depositional package 'A' consists of a Lake/Lagoonal Fill Facies Succession (4.0 m. thick).

2) Depositional package 'B':

This package was deposited in a transgressive barrier island system (figures III.10, 15 & 16). The package 'B' records gradual deepening of shoreline environments as a result of transgression. The package comprises two Barrier-Backbarrier Facies Successions. The upper succession is highly eroded below the erosional surface 'II'.

3) Depositional package 'C':

This depositional package was deposited in an estuarine depositional system (figure III.19). This estuarine system occupied a valley that was incised into the underlying lower shoreface sandstones (figure III.10 & 11). The valley fill has an overall fining upward trend and it consists of four facies successions. These successions reflect gradual deepening of

the estuary and progression of environments from a fluvial/tidal channel to a bay head delta to an open embayment.

4) Depositional package 'D':

This package was deposited in an estuarine system that occupied a valley (figure III.23). The valley was incised into older estuarine sediments. The depositional package has a basal erosional boundary covered by few rounded basement pebbles. The package comprises two Distal Delta Facies Successions overlain by an Interdistributary Bay Fill Facies Succession (figure III.22). The lower two facies successions record progressive deepening of the valley. The upper Interdistributary Bay Fill Facies Succession records gradual shoaling and filling of the valley.

The basal Distal Delta Facies Succession consists of Bioturbated Muddy Sandstones 'A' Subfacies that change upwards to Laminated Clean Sandstone Facies. This upward facies change reflects deltaic progradation that was terminated by a transgression, at the Transgressive Surface 'VI'. The succession above TS'VI' consists of Bioturbated Muddy Sandstones 'A' Subfacies that changes upwards to Mudstone 'B' Subfacies. This upward facies change suggests that the Distal Delta Facies Succession above TS'VI' was deposited in a slightly deeper environment than the underlying succession. Deposition of the interdistributary bay fill sediments above

TS'VII' was accompanied by gradual shoaling and increase of brackish water conditions. These brackish water conditions are well reflected by the appearance of large oyster shells.

5) Depositional package 'E':

This depositional package resembles the package 'B' and was similarly deposited in a transgressive barrier island depositional system. Depositional package 'E' records gradual deepening of shoreline environments, as a result of transgression. The package 'E' consists of a Lake/Lagoonal Fill Facies Succession overlain by a Shoreface Facies Succession. The Shoreface Facies Succession is highly eroded along the Erosional Surface 'IV'. This surface resembles the Erosional Surface 'II' which similarly cuts through shoreface sandstones (figure III.10).

6) Depositional package 'F':

This package resembles the package 'C' and was similarly deposited in an estuarine depositional system. The depositional package 'F' has an overall fining upwards trend. The package comprises a River Mouth Bar Facies Succession overlain by Distal Delta Facies Succession. This upward facies change reflects gradual deepening of the estuary.

III.7.2- SYNOPSIS:

The depositional packages cored in the J-34 well record a repetitive pattern of progression of depositional systems. The estuarine system (package 'A') was followed by the

development of a transgressive barrier island system. This barrier island system (package 'B') was succeeded by the formation of another estuarine depositional system (packages 'C' & 'D'). Such estuarine depositional system occupied a structurally-controlled valley (see IV.3.2.3). Filling of the valley by the estuarine sediments was followed by the redevelopment of a transgressive barrier island depositional system (package 'E'). Rejuvenation of the valley resulted in recurrence of the estuarine depositional system (package 'F').

III.9- STRATIGRAPHIC ARCHITECTURE

The depositional packages 'A' to 'D', which make up the Avalon Formation in the J-34 well (figure III.22), are correlated throughout the Hibernia field (figures III.23 & 24). Each of the depositional packages 'A', 'C' and 'D' has a basal erosional boundary and shows an axial thickening. The three depositional packages were deposited in estuarine depositional systems (figures III.7, 11 & 22). In contrast, the depositional package 'B' has a basal transgressive boundary and maintains almost a uniform thickness throughout the Hibernia field. The depositional package 'B' was deposited in a barrier island depositional system (figures III.8 & 10).

The estuarine depositional packages 'A', 'C' and 'D' were deposited in a valley. The valley is incised into offshore mudstones (figure III.7). The valley is structurally-

controlled (see IV.3.2.3) and was recurrently rejuvenated during deposition of the Avalon Formation (figure III.20). The upper part of the valley, where it intersects the Hibernia rollover anticline in the SW, was stable in position (figures III.12 & 19). In contrast, the lower part of the valley changed its course through time. The estuary mouth of the depositional package 'A' occurred in the SE where the valley occupied a graben that is parallel to the axis of Hibernia rollover anticline (parallel to the Nautilus fault, figures III.12 & I.6). The estuary mouth of the Depositional package 'C' was located in the NE and the valley crossed the Hibernia rollover anticline (across the Nautilus fault, figure III.19).

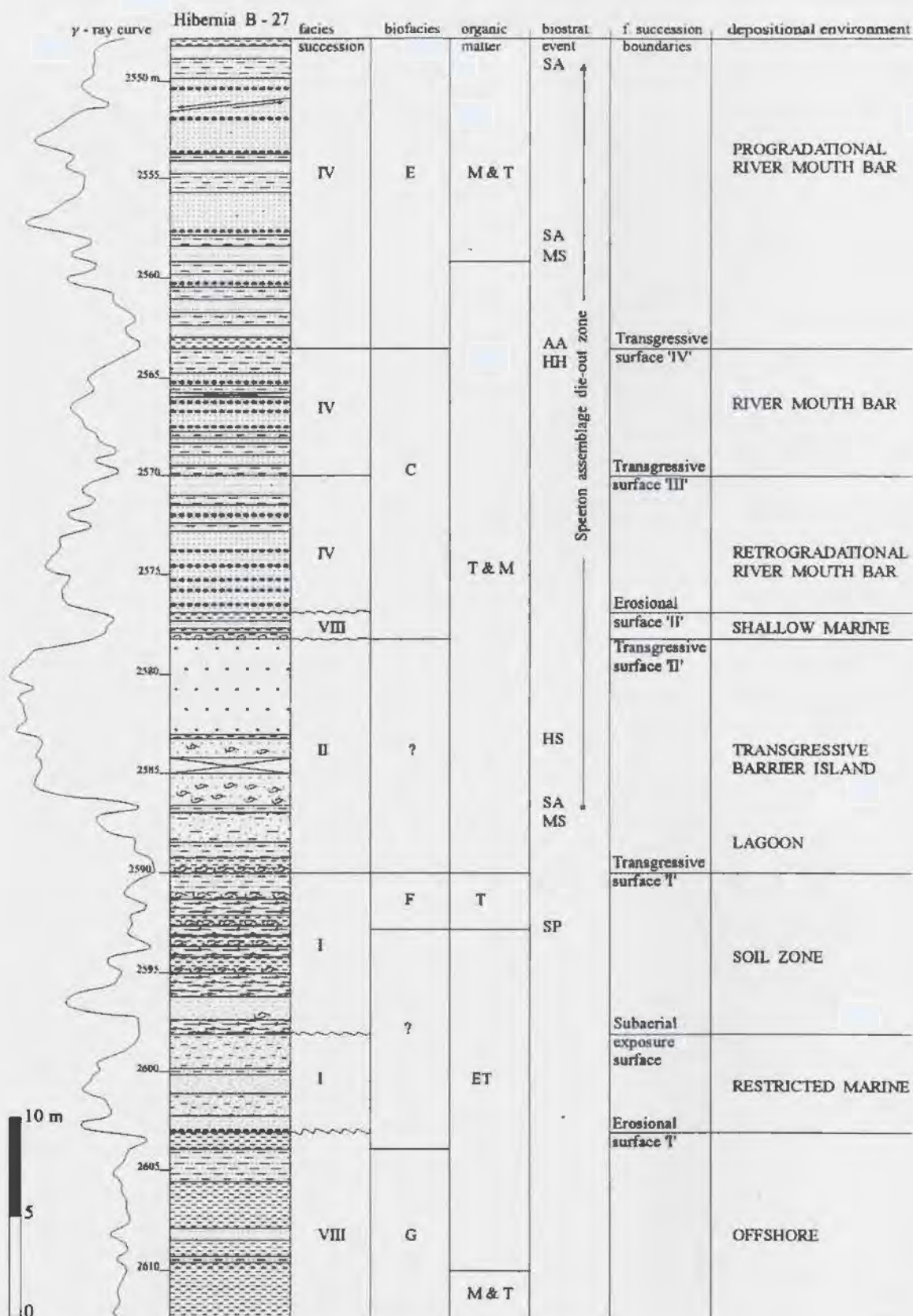


Figure III.1- STRATIGRAPHY OF THE HIBERNIA B - 27 WELL.
 (Biofacies and organic matter are modified after Guilbault 1986 and Jenkins 1984)
 (See legend in figure II.1)

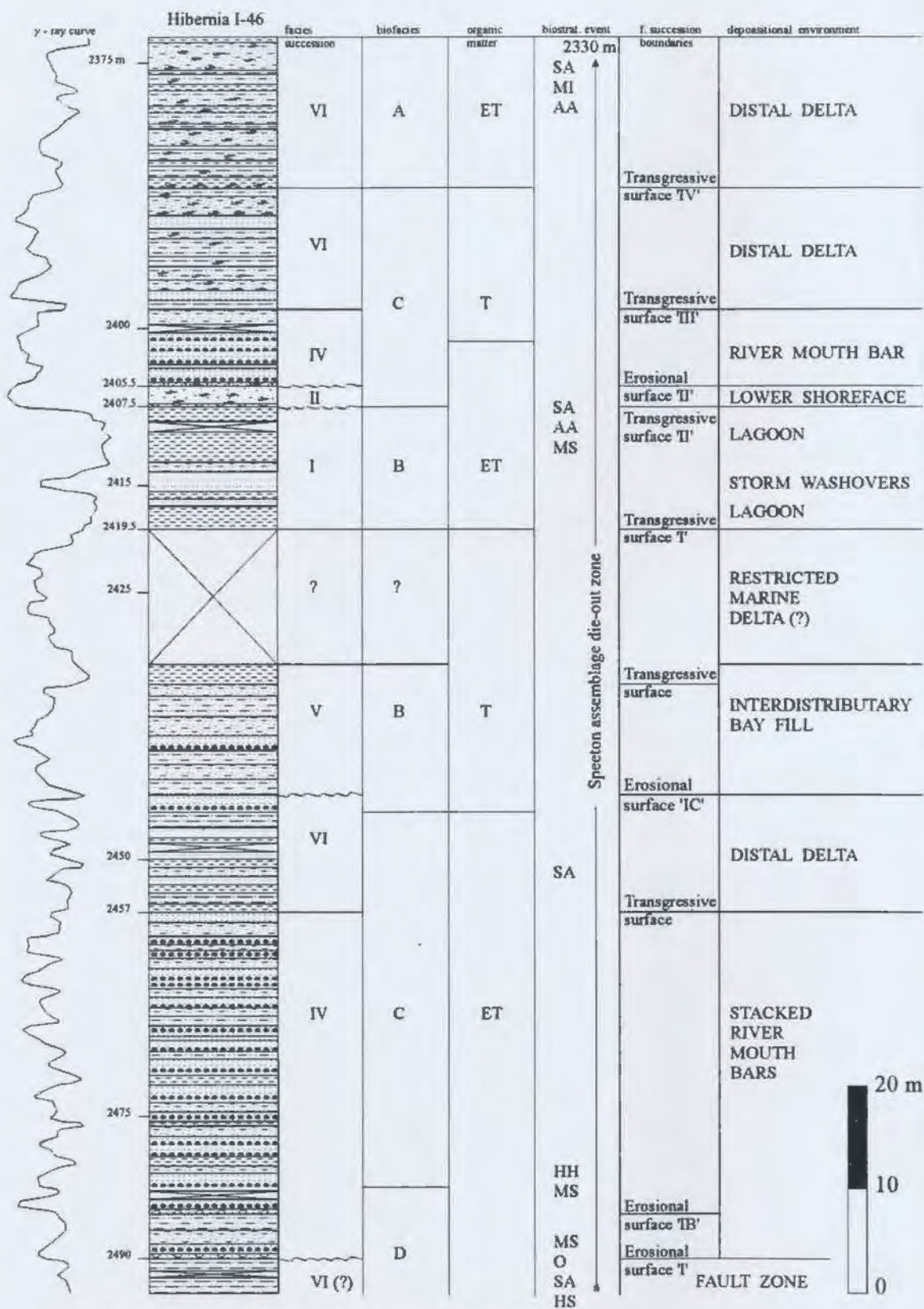


Figure III.2- STRATIGRAPHY OF THE HIBERNIA I-46 WELL.
(Biofacies and organic matter are modified after Guilbault 1986 and Jenkins 1984, respectively)

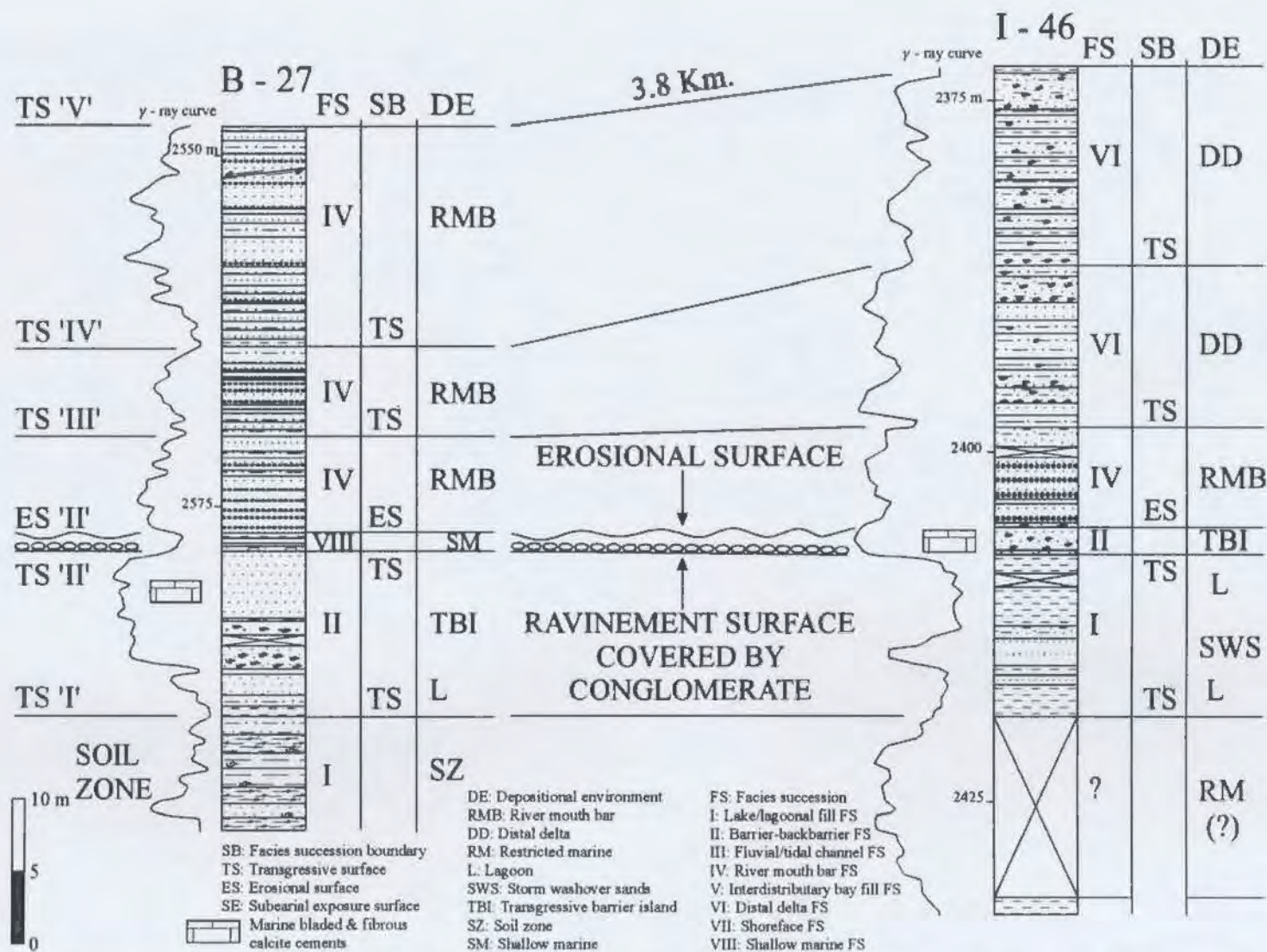
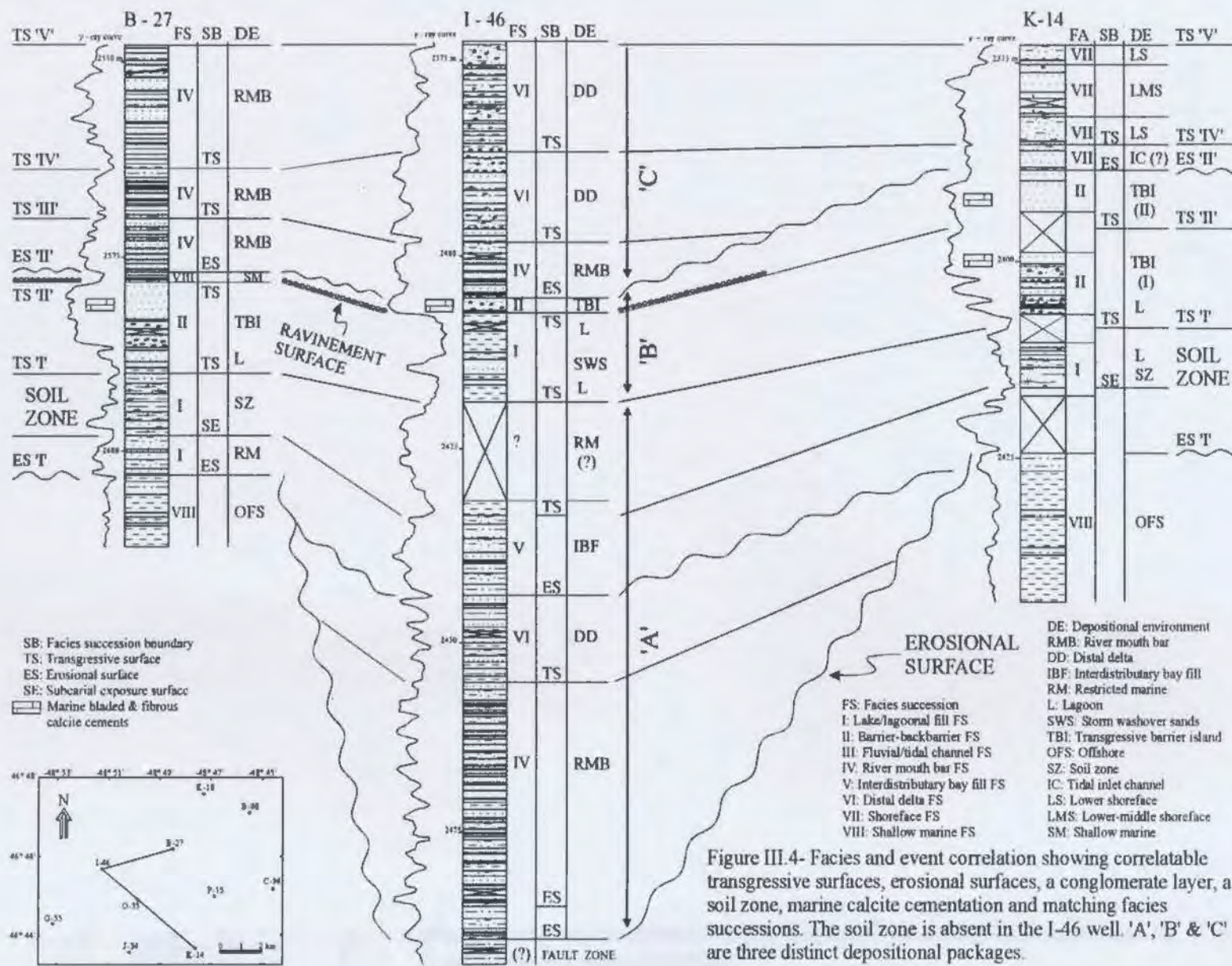
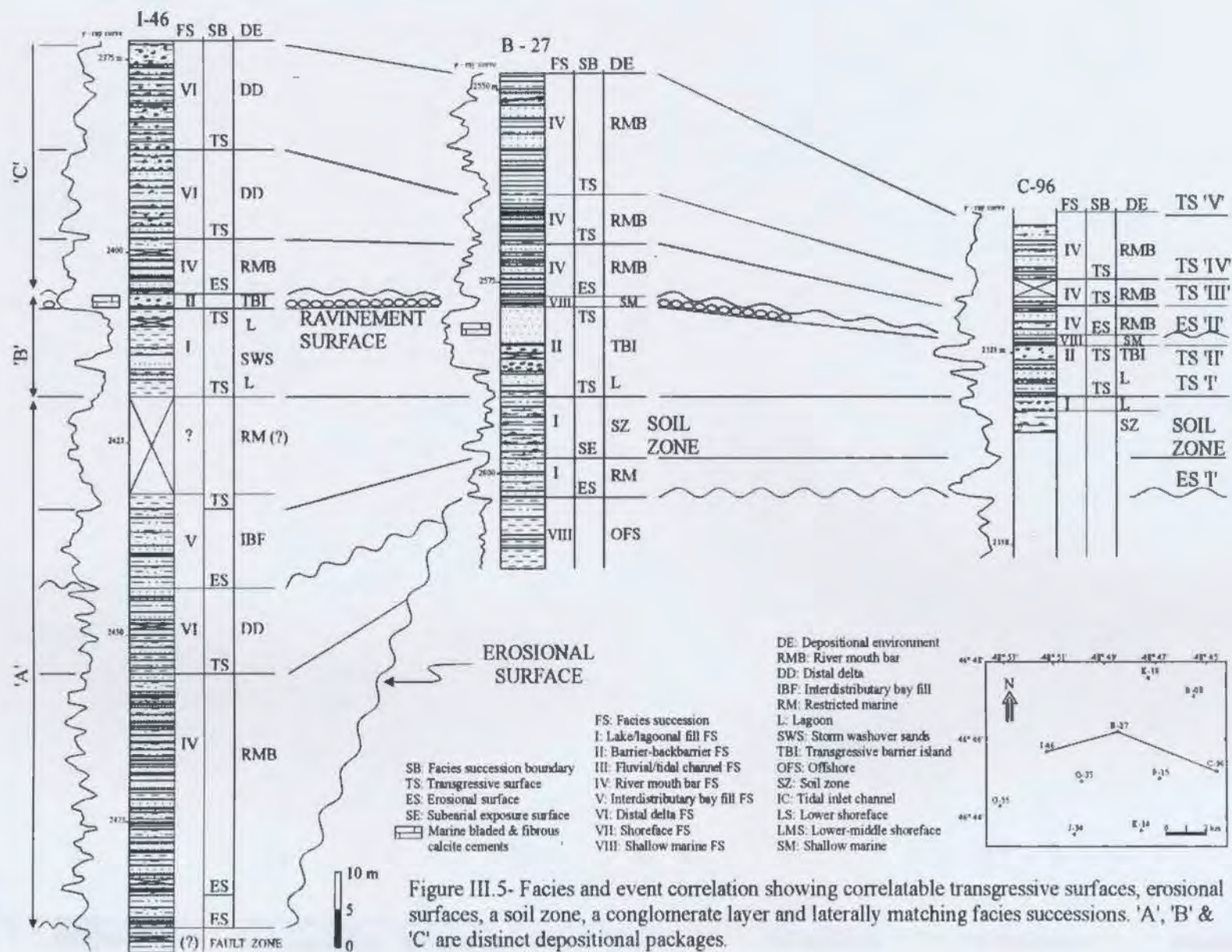


Figure III.3- Facies and event correlation showing correlatable transgressive surfaces, a conglomerate layer, an erosional surface and laterally matching facies successions.





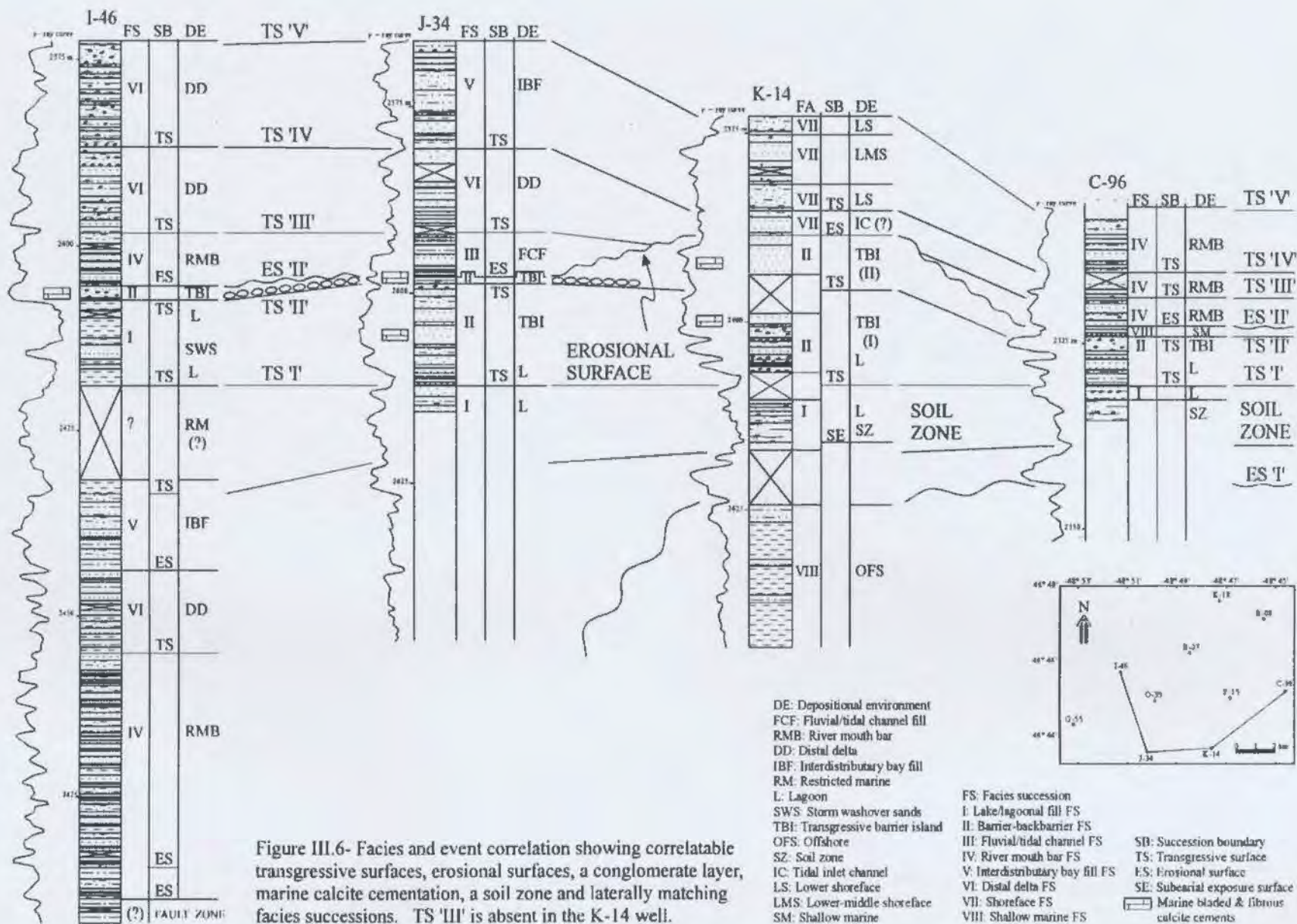


Figure III.6- Facies and event correlation showing correlatable transgressive surfaces, erosional surfaces, a conglomerate layer, marine calcite cementation, a soil zone and laterally matching facies successions. TS 'III' is absent in the K-14 well.

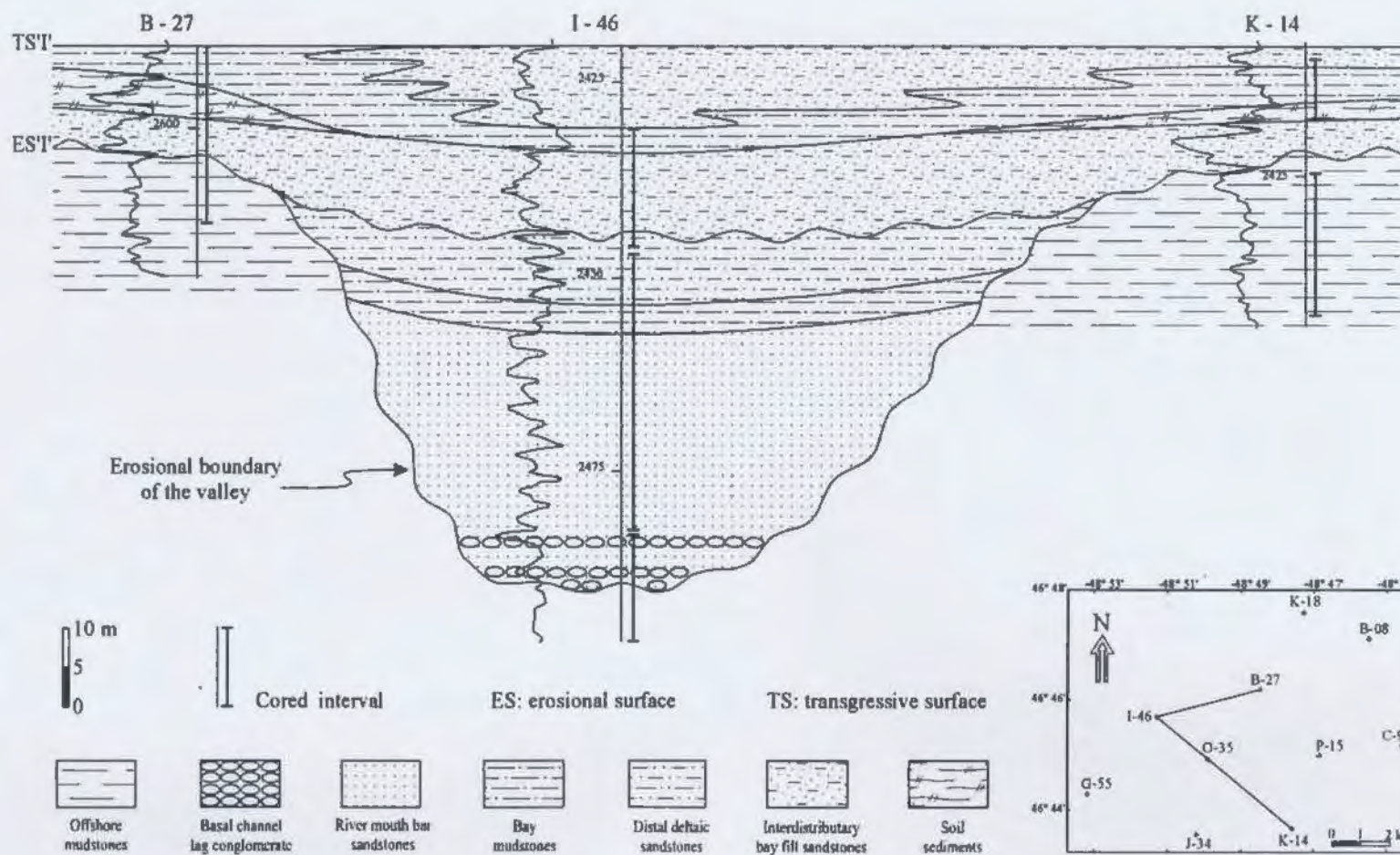


Figure III.7- Stratigraphic cross section depicting the estuarine valley fill in the lowermost part of the Avalon Formation. The valley is incised into offshore mudstones. Note that the soil sediments in the valley flanks change laterally into bay mudstones in the valley trough. The datum is TS 'T' which marks top of the valley fill.

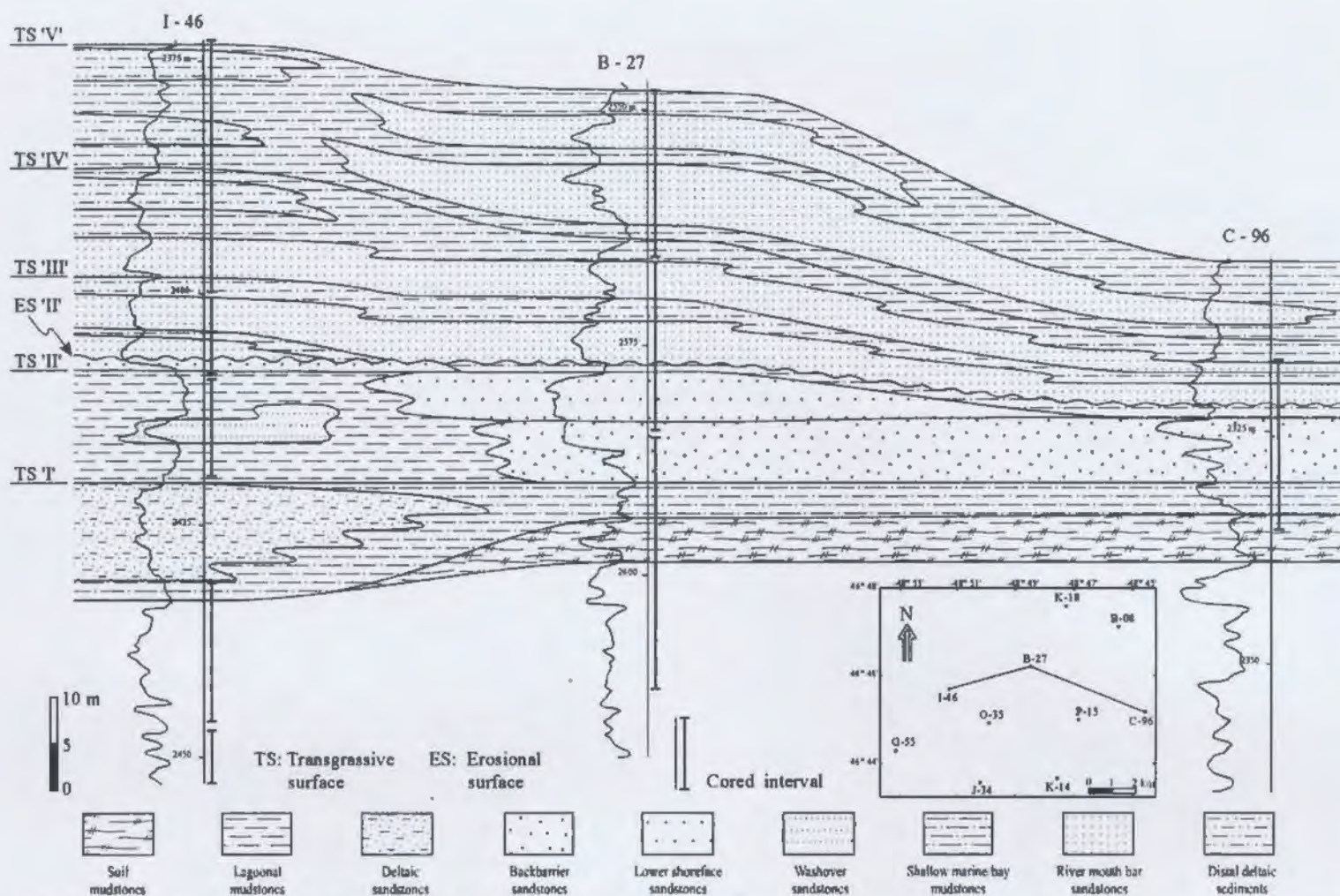


Figure III.8- Stratigraphic cross section portraying soil mudstones changing laterally into lagoonal mudstones and deltaic sandstones, below TS 'I'. A transgressive shoreline depositional package occurs between TS 'I' and ES 'II' and is erosively overlain by deltaic sandstones and bay mudstones. Below TS 'II', backbarrier and lower shoreface sandstones change laterally into lagoonal mudstones and washover sandstones. Above TS 'II', the shoreline position is shifted towards the I-46 well where the lower shoreface sandstones exist and change laterally into shallow marine mudstones in the B-27 and C-96 wells. The datum is TS 'I' which marks the top of an estuarine valley fill depositional package (see figure III.7).

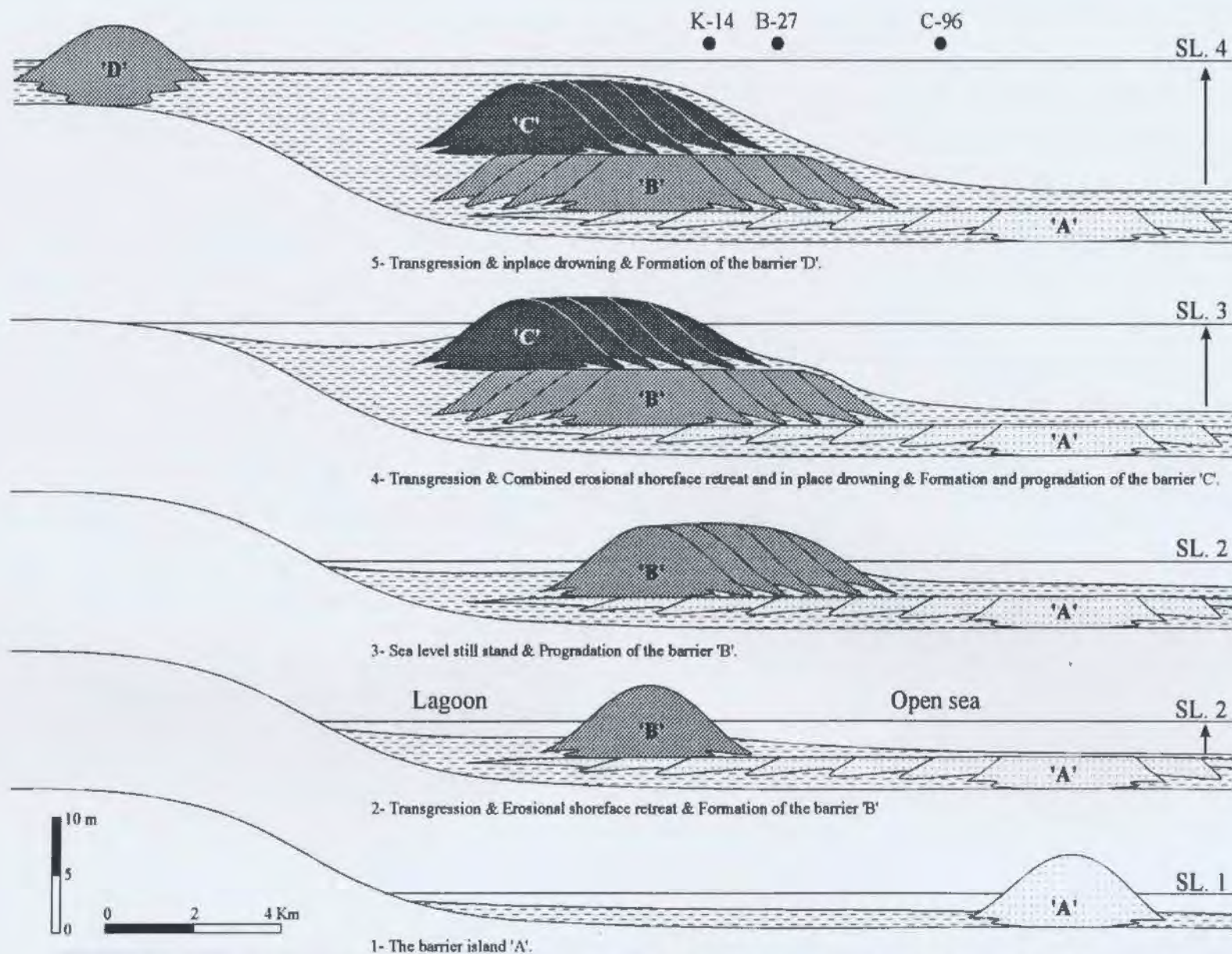


Figure III.9- Schematic diagram illustrating landward migration of the barrier island shoreline. Note the three well locations at the top.

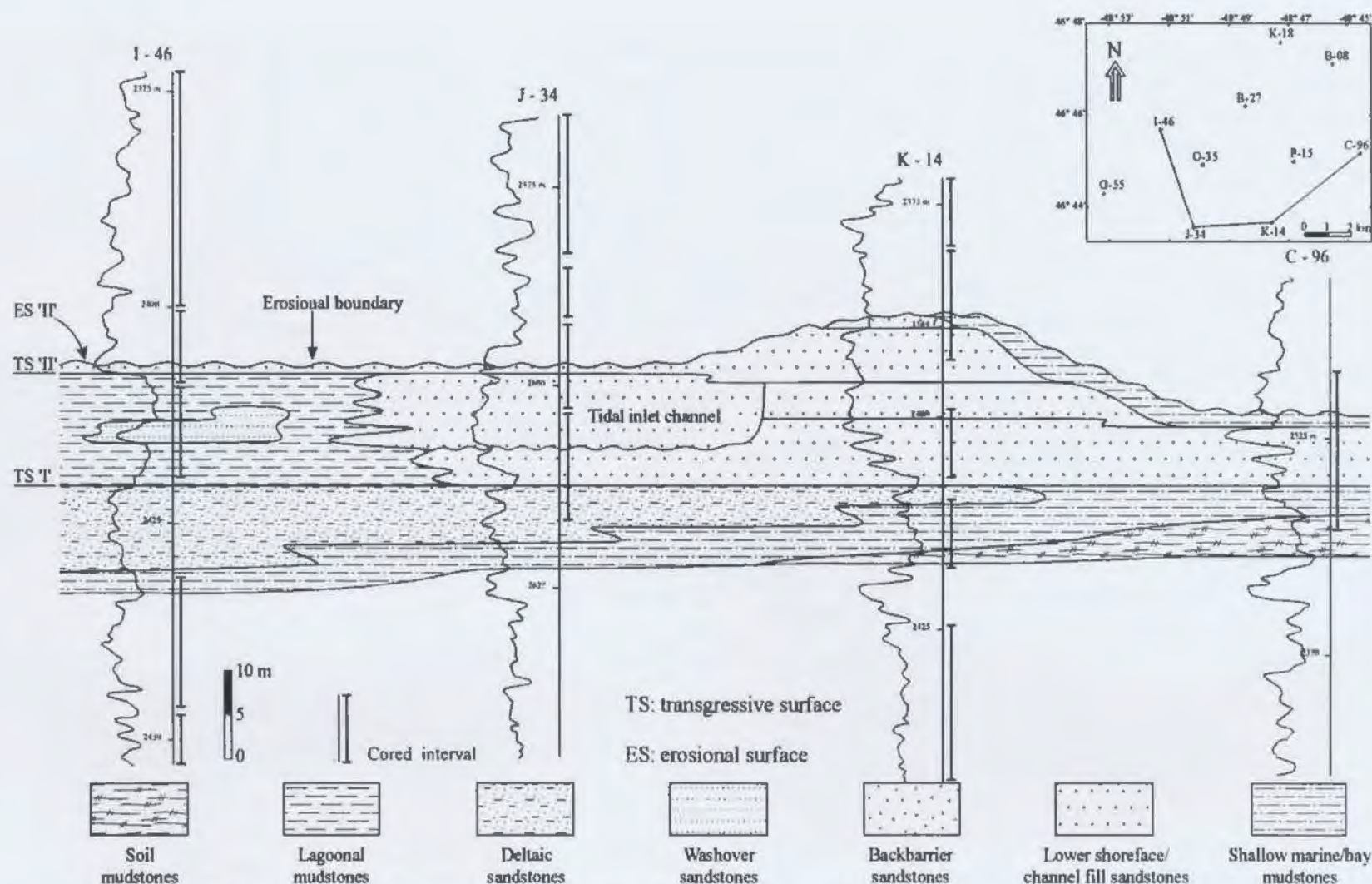


Figure III.10- Stratigraphic cross section showing soil mudstones changing laterally to lagoonal mudstones and deltaic sandstones, below TS 'I'. A shoreline depositional package occurs between TS 'I' and ES 'II'. Below TS 'II', the backbarrier and lower shoreface sandstones are incised by tidal inlet channel fill sandstones. The sandstones change laterally into lagoonal mudstones and washover sandstones. Above TS 'II', the shoreline position is shifted towards the I-46 well, where the lower shoreface sandstones overlie lagoonal mudstones. The datum is TS 'I', which marks the top of an estuarine valley fill depositional package. See figure III.11 for the depositional package occurring above ES 'II'.

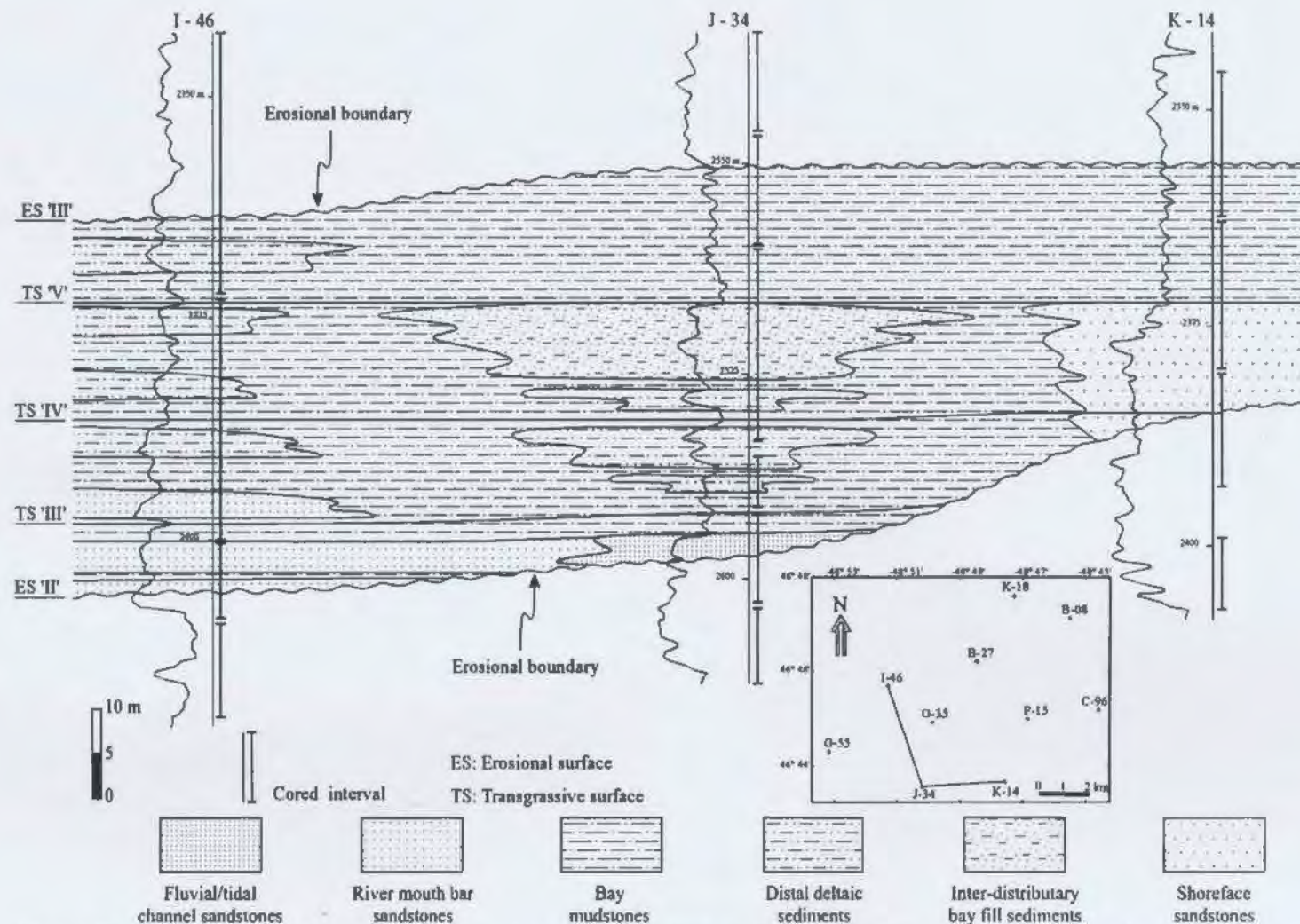


Figure III.11- Stratigraphic cross section showing estuarine valley fill sediments. The valley is incised into transgressive shoreline sediments (see figure III.10). The valley fill comprises fluvial/tidal and river mouth bar sandstones that change upwards into interdistributary bay fill and distal deltaic sediments. These sediments change laterally into bay mudstones and shoreface sandstones. The upper valley fill consists mainly of bay mudstones. The valley fill sediments are eroded at top. The datum is TS 'V'.

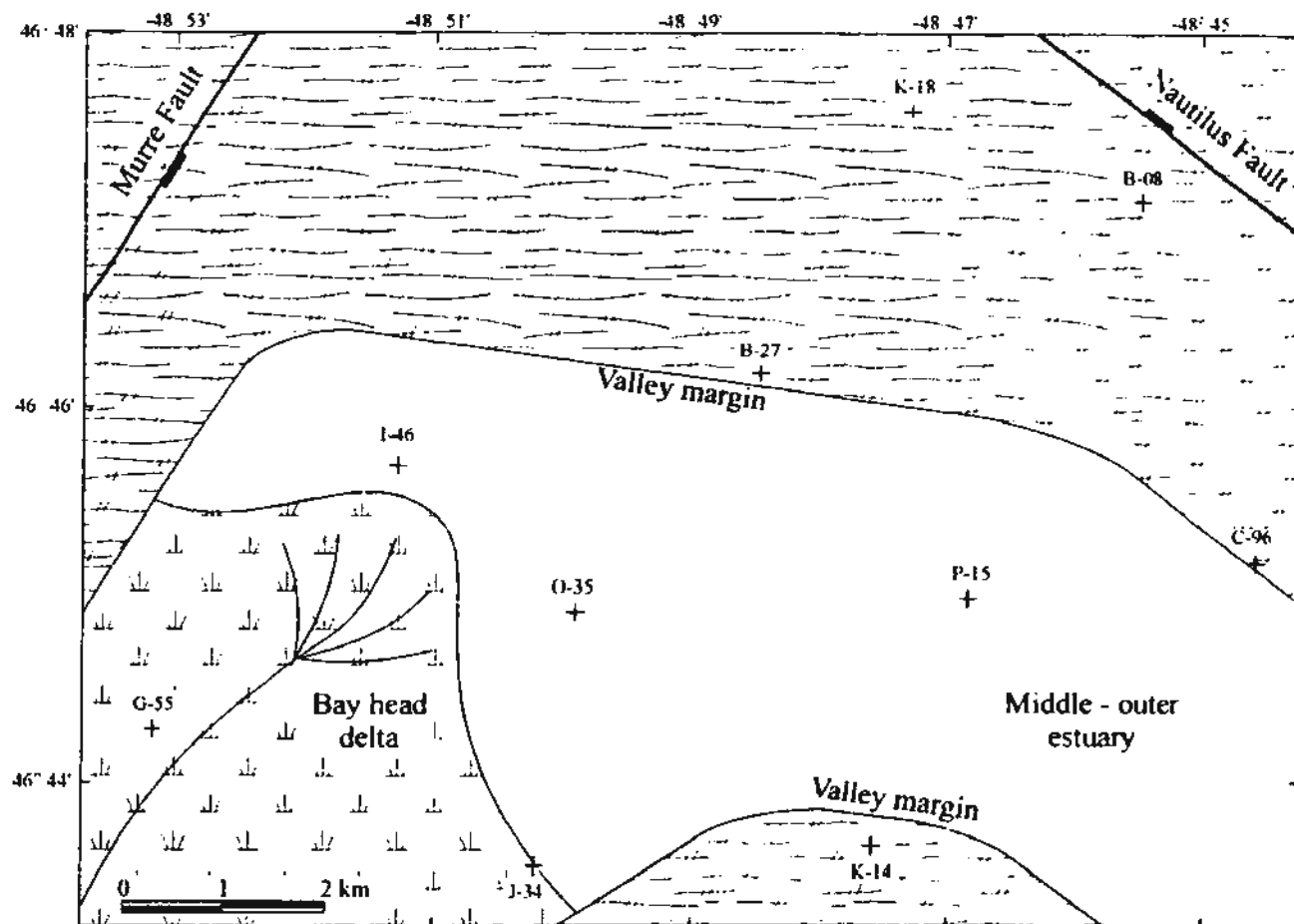


Figure III.12- Paleogeography of the estuarine valley fill in the lowermost part of the Avalon Formation. The boundaries of the valley are structurally-controlled (see the fault trends in figure I 6).

Figure III.13- Gamma-ray log correlation showing the valley fill in the lowermost part of the Avalon Formation. Note that the sediments that are incised by the valley contain terrigenous and marine organic matter. In contrast, the valley fill sediments host essentially to exclusively terrigenous organic matter. The upper valley fill in the O-35 well contains terrigenous and marine organic matter, as well. The datum is TS 'T' which marks the top of the valley fill. (Type of organic matter after Jenkins, 1984).

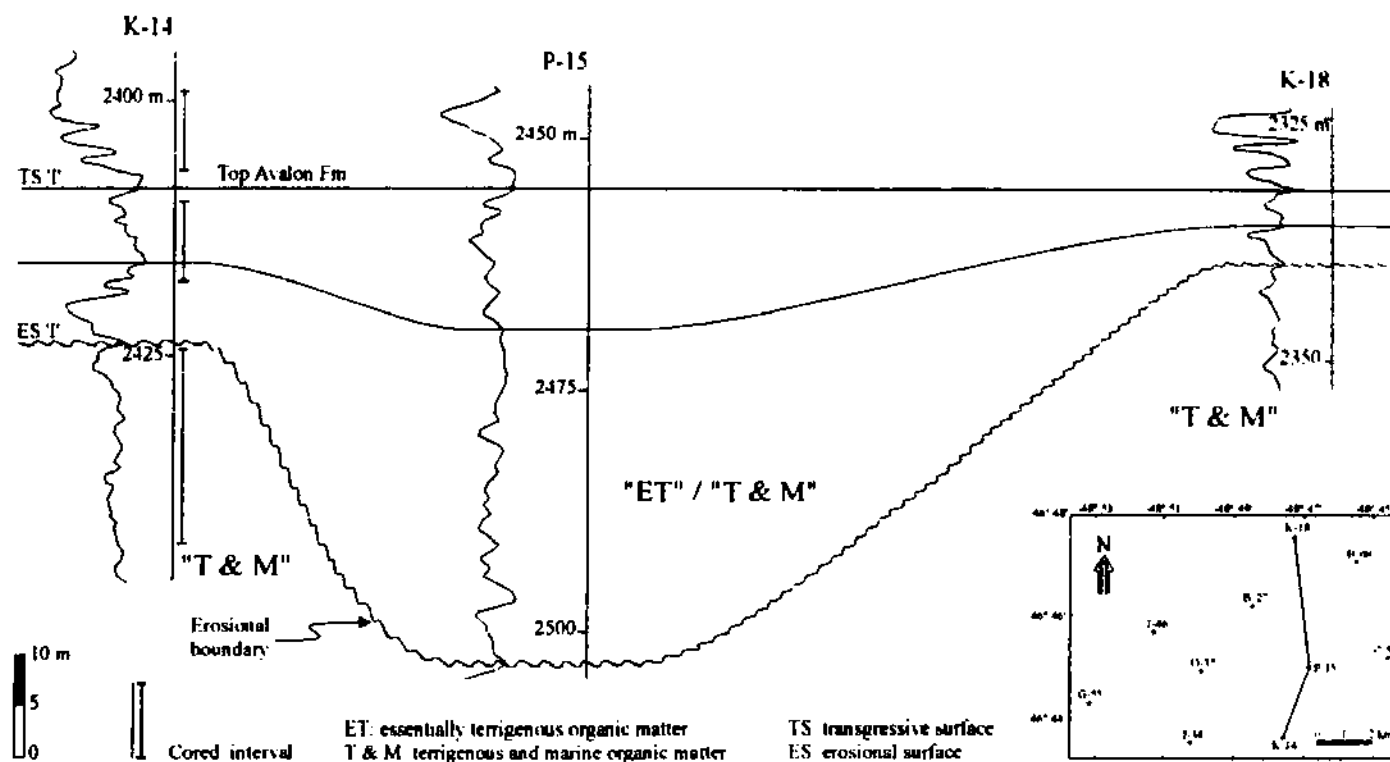


Figure III.14- Gamma-ray log correlation showing the valley fill in the lowermost part of the Avalon Formation. Note that the sediments that are incised by the valley contain terrigenous and marine organic matter. In contrast, the valley fill sediments host essentially terrigenous organic matter alternating with terrigenous and marine organic matter. The datum is TS 'I' which marks the top of the valley fill. (Type of organic matter after Jenkins, 1984).

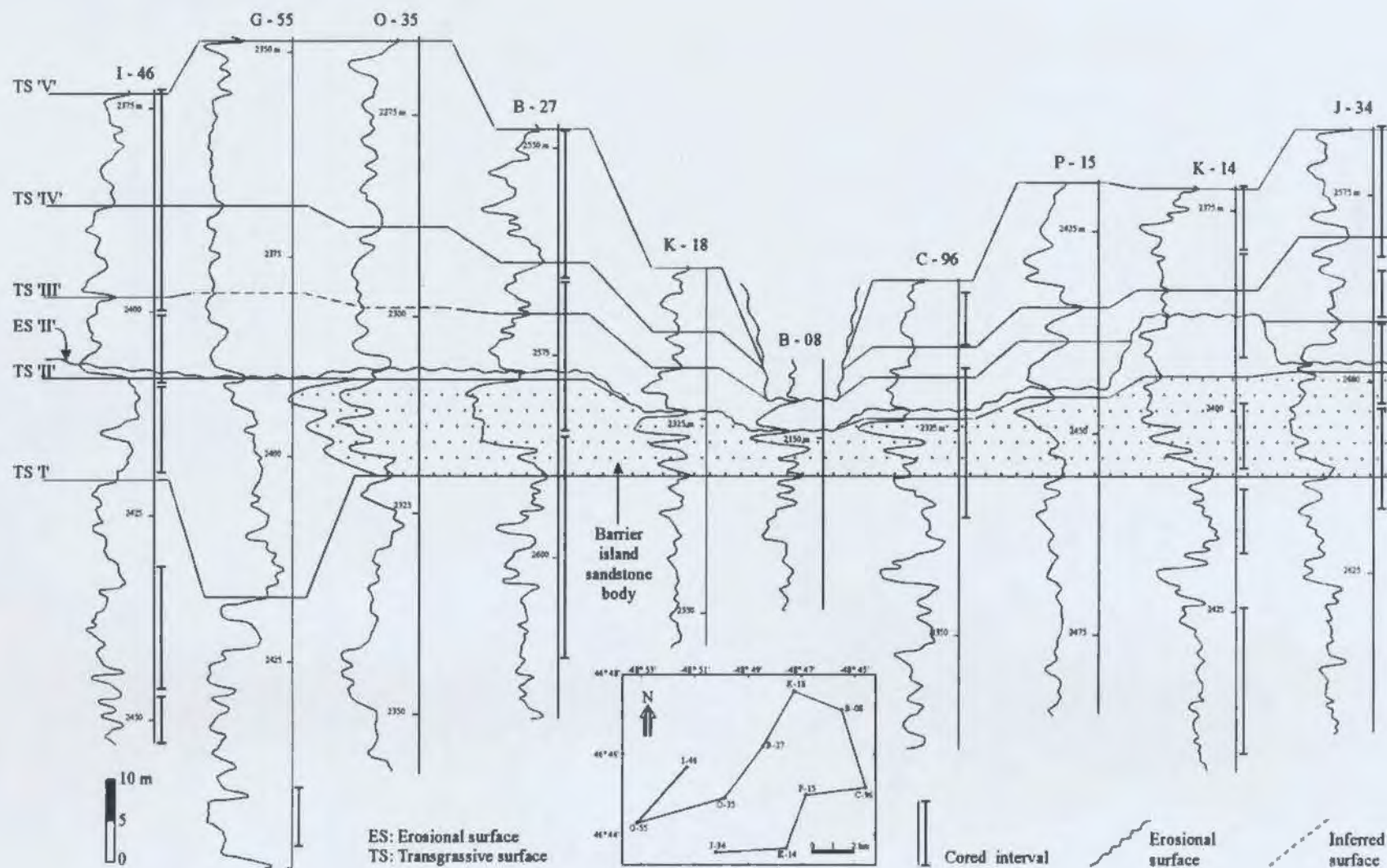


Figure III.15- γ -ray log correlation of the lower part of the Avalon Formation showing the occurrence of a barrier island sandstone body in eight wells in the Hibernia field. TS 'I' is the datum for these eight wells. TS 'II' is the datum for the I-46, G-55 and B-27 wells.

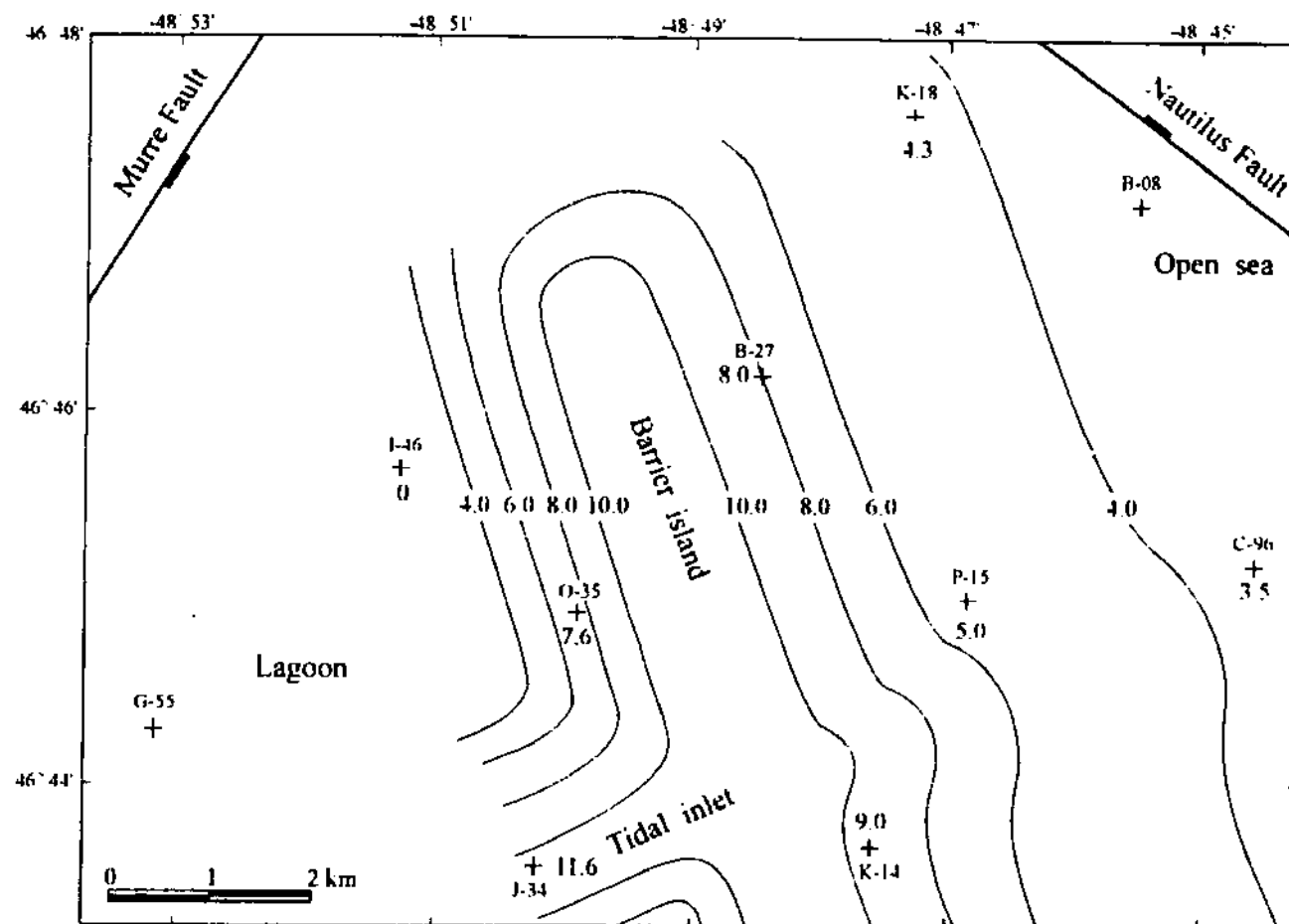


Figure III.16- Sand isolith map of the lower Avalon transgressive barrier island (see cross section in the barrier island in figure III.15).

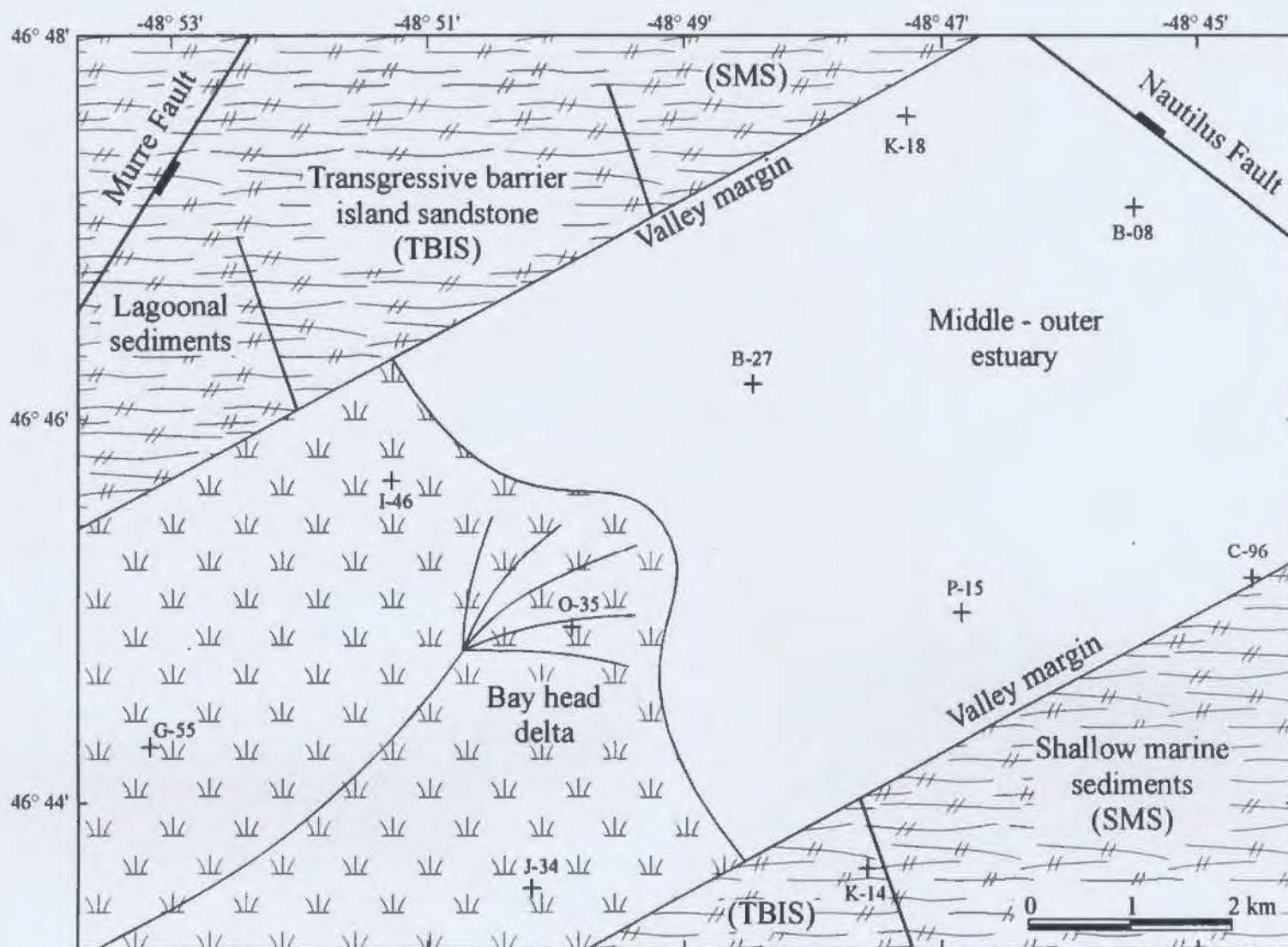


Figure III.17- Paleogeography during early stages of filling of the valley that is incised into the transgressive barrier island depositional system.

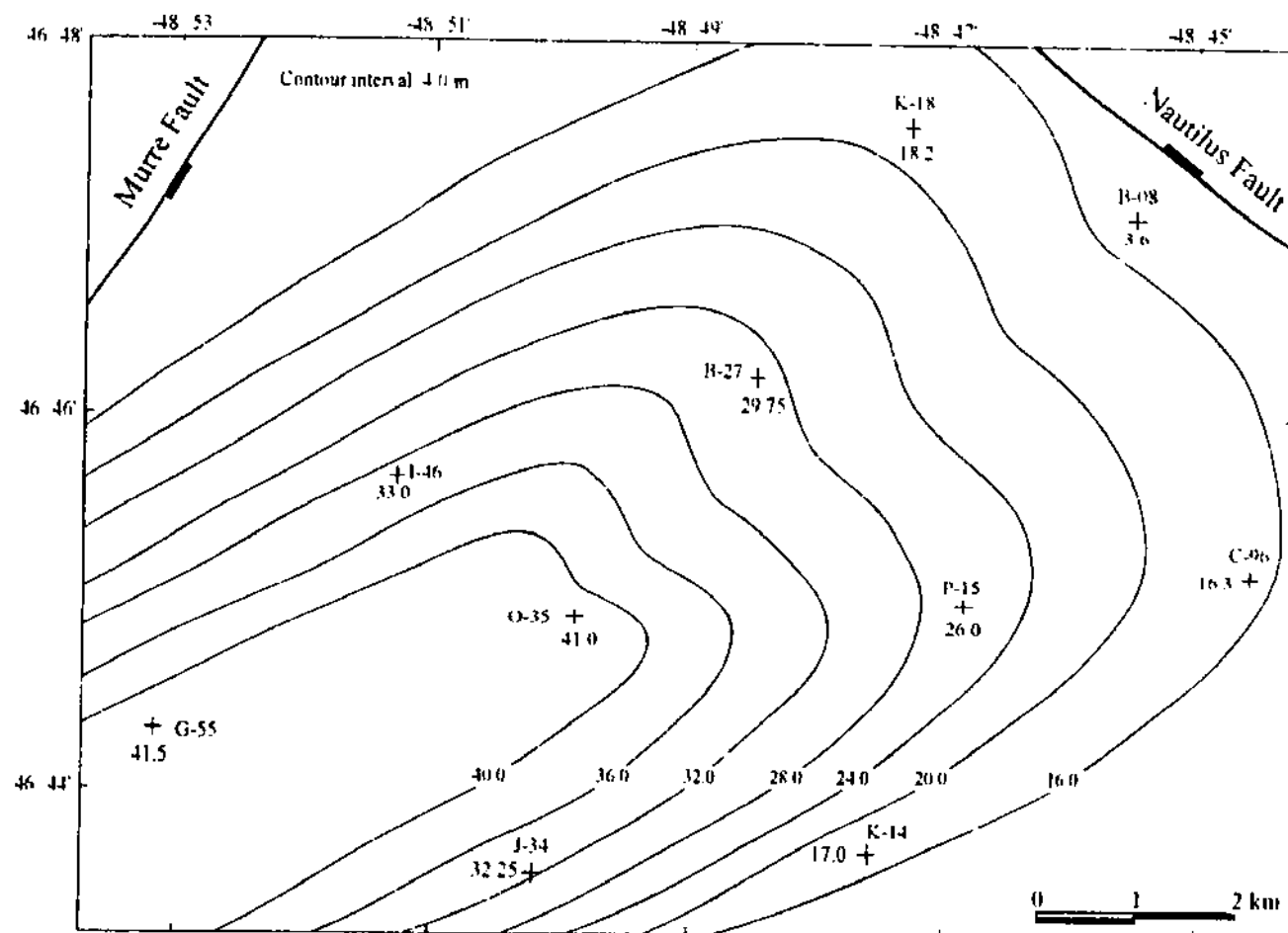


Figure III.18- Isopach map of the estuarine valley fill that is confined between ES 'II' and TS 'V' (see figure III.15). Most of valley fill is eroded in the B-08 well.

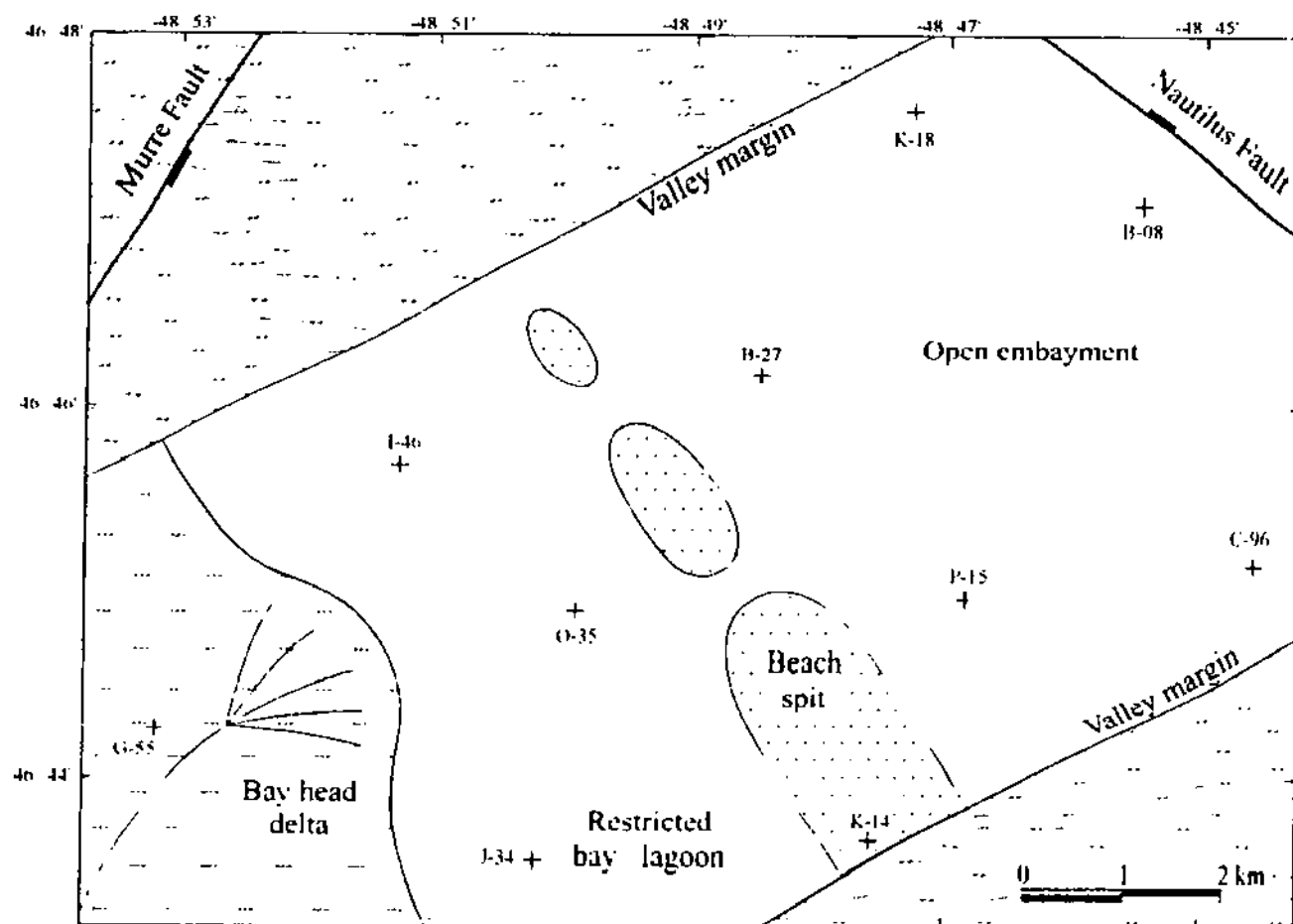


Figure III.19- Paleogeography of the estuarine valley fill that occurs below 7S 'V'
 (See figures III 11 & 15. Note change in position of the estuary mouth in figure III 12)

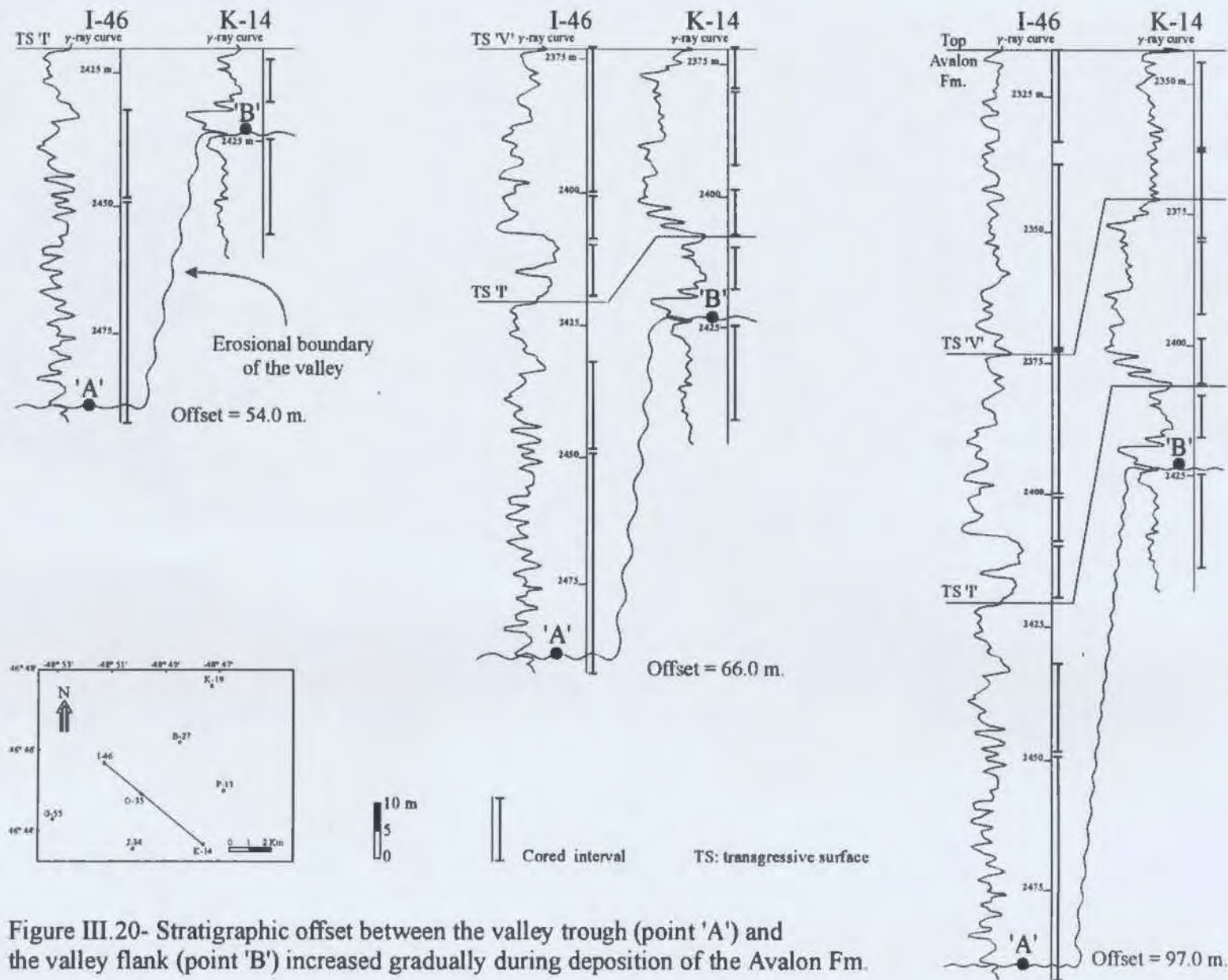


Figure III.20- Stratigraphic offset between the valley trough (point 'A') and the valley flank (point 'B') increased gradually during deposition of the Avalon Fm.

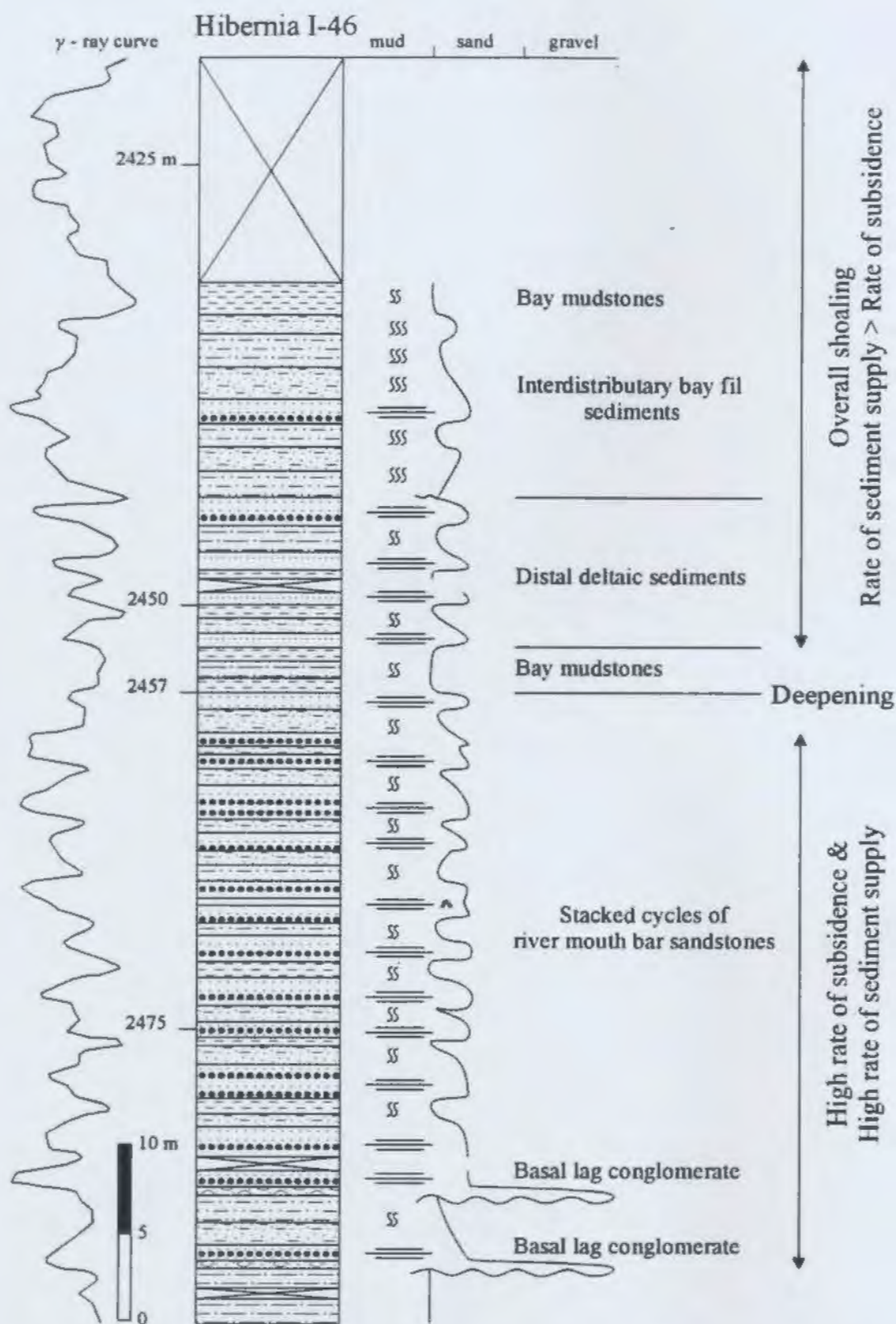


Figure III.21- An estuarine valley fill succession reflecting changes in the rate of subsidence relative to the rate of sediment supply.

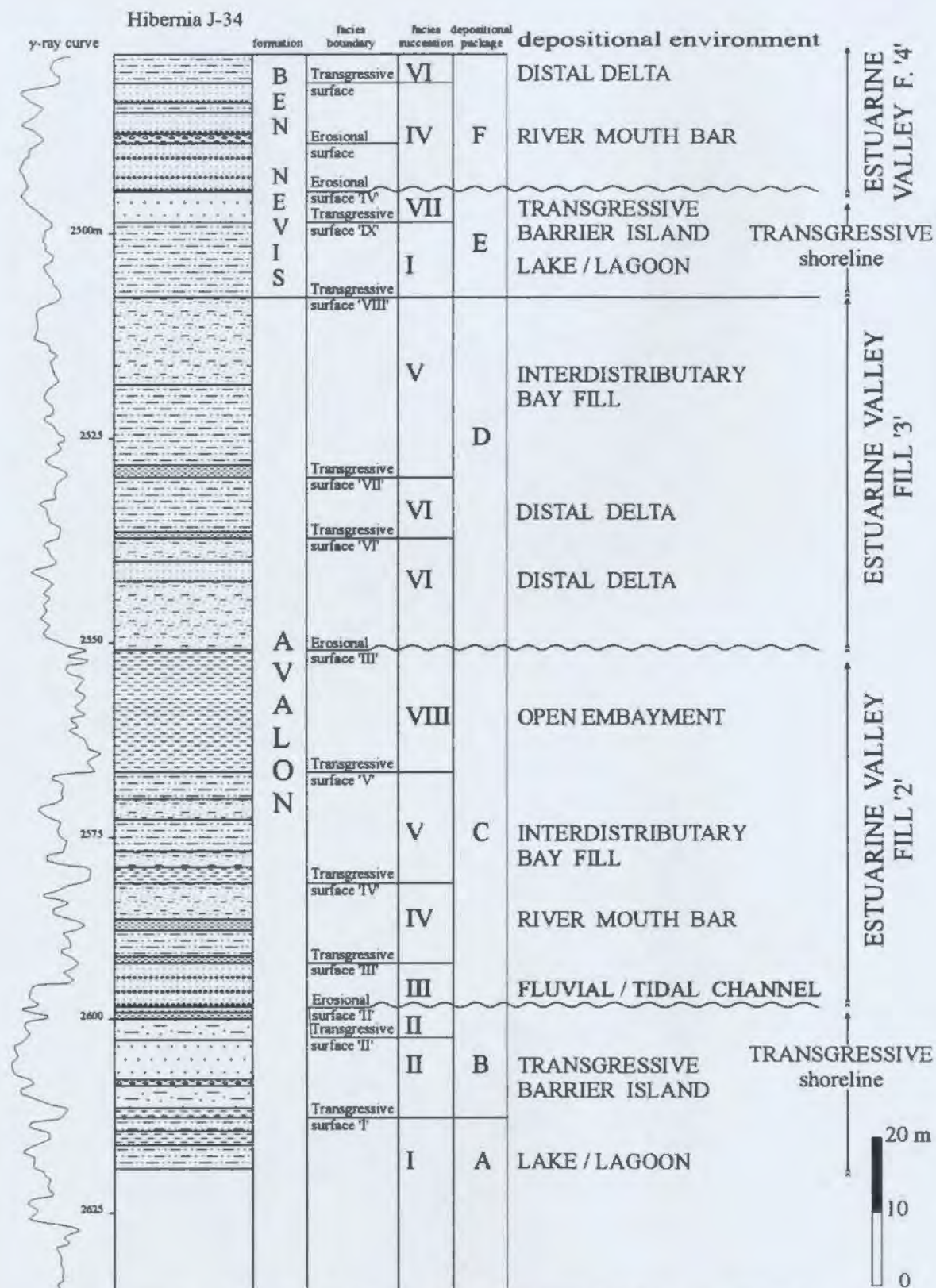


Figure III.22- STRATIGRAPHY OF THE HIBERNIA J-34 WELL.

Figure III.23- γ - ray log correlation of the Avalon Formation, showing successive valley fills (see figure III.13 for the valley fill '1').

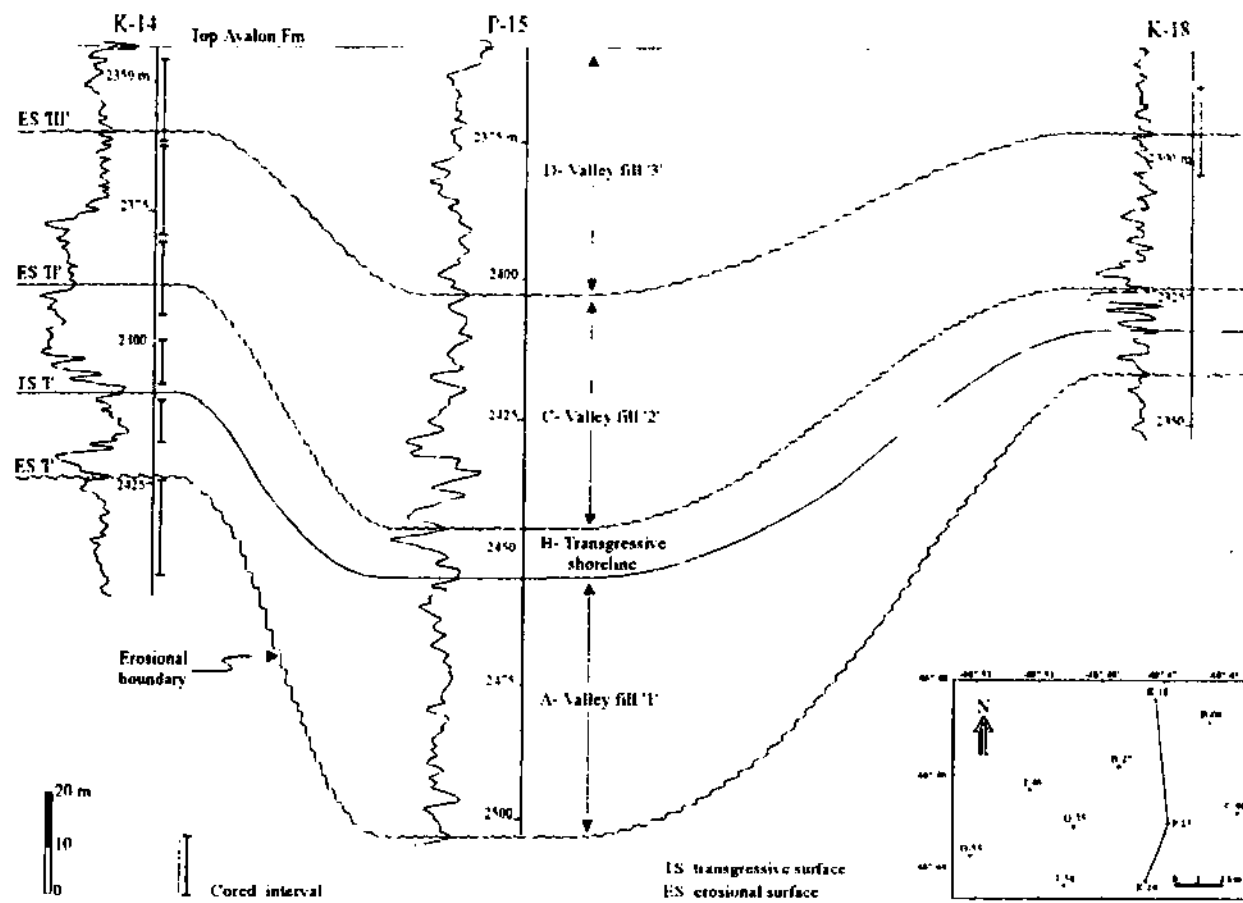


Figure III.24- γ -ray log correlation of the Avalon Formation, showing successive valley fills.

IV- SEDIMENTATION & TECTONICS

The results of the stratigraphic analysis presented in this study can be considered in the light of the geometric development and movement history of the Hibernia rollover anticline during deposition of the Avalon Formation. This history reflects the close inter-relationship between sedimentation and tectonics.

Tectonics was the main factor which controlled the development of the lower Cretaceous sedimentary sequences in Jeanne d'Arc basin (Hiscott et al. 1990; Sinclair 1993). The basin experienced active rifting that resulted in NE-SW extension during the Early Cretaceous time (Hubbard et al. 1985; Enachescu 1987; Hubbard 1988; Sinclair 1993). This extension coincided with the separation of the Grand Banks of Newfoundland and Iberian margins (Sullivan 1983; Masson and Miles 1984; Mauffret and Montadert 1987).

This chapter summarises the sedimentary history of that part of the Avalon Formation which occurs in the Hibernia rollover anticline. The role of tectonics in the kinematic development of and sedimentation in this rollover anticline is then discussed. Subsequently, controls on sedimentation are contemplated. Finally, a stratigraphic model highlighting the main facies relationships and successions is advanced.

IV.1- SEDIMENTARY HISTORY

The Avalon Formation in the Hibernia rollover anticline consists of four depositional packages (figures III.23 & 24). These packages record four stages of development. Each stage was characterized by distinct conditions of subsidence, sediment supply, facies and depositional environments. The main events that happened in each stage of development are summarised below, starting from the oldest to the youngest. Similar events which recurred in many stages will be discussed once in order to avoid redundancy.

1) Emergence, valley incision, submergence & filling:

Estuarine sediments of the depositional package 'A' in the lower part of the Avalon Formation (figures III.23 & 24) were deposited during this stage. These estuarine sediments are hosted in a river valley that was incised into offshore mudstones (figures III.7 & 12). The valley was developed subsequent to emergence of the Hibernia rollover anticline. This emergence coincided with a regional uplift of the Grand Banks and with the development of a widespread unconformity during the Late Barremian-Early Aptian (see section IV.2.2).

The constricted transport of fluvial sediments caused erosion of the older offshore mudstones in the valley floor. The fluvial sediments initially bypassed the valley and were transported and deposited at the valley mouth in the SE (figure III.12).

The valley was subsequently flooded with sea water and an estuary was established in the valley. The valley flanks were repeatedly submerged. Each submergence was followed by rapid deposition of lagoonal mudstones resulting in the re-exposure of the valley flanks. Interbedded lagoonal and soil sediments were consequently developed on the valley flanks. Flooding of the valley reflects the onset of fault activity and consequent subsidence of the valley trough. The recurrent submergence of the valley flanks indicates the commencement of submergence of the rollover anticline.

Continued subsidence of the valley trough associated with abundant sediment supply resulted in the deposition of about 70 metres of estuarine sediments in the valley (figure III.7). The stacking pattern of the estuarine facies reflects progressive environmental deepening followed by shoaling, respectively for the lower and upper parts of the valley fill (figure III.21). The initial progressive deepening suggests an acceleration of fault movement and increase of the rate of subsidence relative to the rate of sediment supply (see section IV.3.2.4). The later gradual shoaling is related to the deceleration of fault slip and decrease of the rate of subsidence relative to the rate of sediment supply. These conditions allowed deltaic progradation and gradual filling of the valley.

2) Accelerated submergence & transgressive barrier islands:

Transgressive shoreline sediments of the package 'B' (figure III.23 & 24) were deposited during this stage. These sediments reflect continued submergence and transgression of the Hibernia rollover anticline. The submergence was punctuated and its rate accelerated through time (see section IV.3.1.3). This acceleration resulted in repeated transgressions, gradual deepening of the early deposited shoreline sediments (figures III.8 & 10) and progression of transgression mechanisms from erosional shoreface retreat to in-place drowning (figure III.9).

The shoreline sediments consist of lagoonal mudstones that change upwards to barrier island sandstones and shallow marine mudstones (figures III.8 & 10). The barrier island sandstones contain considerable amounts of micritic carbonate intraclasts. These intraclasts were sourced from the open sea side. Deposition of these carbonates reflects siliciclastic sediment depletion in the open sea side. Such depletion and the contemporary submergence and deepening of the rollover anticline resulted from the entrapment of siliciclastic sediments close to the hinterland source in the SW.

3) Emergence, valley incision & submergence:

Valley fill sediments of the depositional package 'C' (figures III.23 & 24) were deposited during this stage. The river valley was incised subsequent to a second emergence of

the Hibernia rollover anticline with respect to the contemporary sea level (figure III.10).

Resumption of fault activity and consequent subsidence of the valley trough resulted in flooding of the fluvial sandstones and establishment of an estuary in the valley (figure III.19). At least 45.0 metres of estuarine sediments accumulated in the valley. These sediments reflect progressive environmental deepening (figure III.11) associated with the acceleration of fault movement (figure III.20) and submergence of the rollover anticline.

4) Emergence, valley incision, Submergence & filling:

Valley fill sediments of the depositional package 'D' (figures III.23 & 24) were deposited during this stage. The river valley was incised subsequent to a third emergence of the Hibernia rollover anticline with respect to the contemporary sea level.

Renewed fault activity and subsidence of the valley trough caused the establishment of an estuary and the gradual filling of the valley with estuarine sediments.

Filling of the valley was followed by more uniform submergence of the Hibernia rollover anticline. This submergence resulted in the deposition of transgressive shoreline deposits of the depositional package 'E' which occurs at the base of the Ben Nevis Formation (figure III.22). These shoreline deposits are erosively overlain by estuarine

deposits of the depositional package 'F' (figures III.22). This reflects recurrence of the emergence and redevelopment of a river valley.

IV.2- THE ROLE OF TECTONICS

The depositional history of the Avalon Formation in the study area establishes the recurrent emergence and submergence of the Hibernia rollover anticline. Emergence of the anticline occurred during periods of cessation of fault activity and was caused by factors which were regional in their extent (see section IV.2.2). In contrast, submergence of the anticline occurred consequent to periods of active slip along the Rankin growth fault as well as activity on the synthetic and antithetic faults running along the rollover anticline (figure I.1). Each period of fault activity corresponds to an episode of NE-SW extension of the Jeanne d'Arc rift basin. The effects of this extension on the kinematics of and sedimentation in the rollover anticline are further elaborated in the following model:

IV.2.1- KINEMATIC AND SEDIMENTATION MODEL:

The model involves a listric growth fault and rollover anticline in its hanging wall (figure IV.1A). Deltaic sediments are deposited on the portion of the hanging wall that is immediately adjacent to the growth fault. Meanwhile, offshore mudstones accumulate on the crestal area of the

rollover anticline. The anticline is dissected by synthetic and antithetic faults that bound a crestal collapse graben .

Cessation of the fault activity and a regional relative uplift of the area with respect to sea level result in (figure IV.1B):

- 1- Subaerial exposure of the rollover anticline and the footwall of the growth fault, as well as other high areas.
- 2- Filling of the half graben on the hanging wall adjacent to the growth fault and progradation of the delta towards the NE.
- 3- Incision of a river valley through the rollover anticline and erosion of the valley floor sediments.

Resumption of fault activity, in response to initiation of NE-SW extension during a rifting episode, results in activation of slip along the growth fault and synchronous movements along the synthetic and antithetic faults. These movements cause subsidence of the valley trough, flooding with sea water and establishment of an estuary in the valley (figure IV.1C). A bay head delta develops in the estuary and retrogrades gradually in response to the fault-induced deepening. Deceleration of fault activity induces subsequent

"Crestal Collapse Grabens" were described in experimental models of growth fault geometry by McClay (1989) and McClay et al. (1991). Similar grabens were also mapped along the Cottonwood rollover anticline in the Death Valley region at California (Snow and White 1990). Synorogenic Tertiary sediments overly the Cottonwood rollover and the Racetrack Valley runs along one of these grabens (Snow and White 1990).

deltaic progradation and gradual filling of the valley.

Renewed fault activity, in response to advanced NE-SW extension during the rifting episode, results in accelerated slip along the growth fault and consequent submergence of the rollover anticline (figure IV.10). The delta steps back towards the SW and siliciclastic sediments are trapped in the rapidly-growing half graben on the hanging wall of the growth fault. Meanwhile, a transgressive barrier island is developed on the rollover anticline. The trend of this barrier island is diagonal to the axis of the rollover anticline, due to movements along the growth fault and the NE-SW oriented basin-bounding fault (Murre fault). Continued submergence of the rollover anticline leads to drowning of the barrier island and deposition of offshore mudstones above it. Fault activity and sedimentation in this stage corresponds to the "Rift Climax Phase" described by Prosser (1993) and the "Mid Syn-Rift Phase" proposed by Sinclair et al. (1994).

IV.2.2- EMERGENCE OF THE HIBERNIA ROLLOVER ANTICLINE:

The repeated emergence of the Hibernia rollover anticline can not be explained by virtue of local factors related to the kinematics of the Rankin and Murre fault systems. It is therefore proposed here that the recurrent emergence of the anticline and the resulting unconformities coincided with regional relative uplifts of at least the SE part of the Jeanne d'Arc basin. Potential causes for these relative

uplifts are sea level drops and/or regional rifting tectonics.

Haq et al. (1988) proposed two major sea level drops approximately at the base and top of the Aptian (112 Ma & 107.5 Ma) and another minor drop within the Aptian (109.5 Ma). Accurate dating of the unconformities, which are associated with the four emergences of the Hibernia rollover anticline, is not possible with the available biostratigraphic data set. However, one can assume that the sea level drops at 112 Ma and 107.5 Ma may correspond respectively to the Barremian and Aptian unconformities at the base and top of the Avalon Formation. The sea level drop at 109.5 Ma conceivably cannot account for the two remaining unconformities.

The data presented in this study suggest that the emergence of the Hibernia rollover anticline precedes a period of fault activity. The valley fills overlying three of the four unconformities reflect progressive deepening followed by shoaling (figure III.21). The initial environmental deepening was clearly caused by active fault movement (figure III.20) that is attributed to an episode of extension of the Jeanne d'Arc basin (figure IV.1C; see section IV.3.2.4). However, one may not eliminate the possibility of an eustatic sea level rise synchronous with this fault activity.

It is probable that during the Aptian the basin was subjected to continuous uplifting forces which were periodically released by rupture and extension. The resultant

uplift and the periodic extension coincided with the separation of the Grand Banks of Newfoundland and Iberia. This separation occurred during the Aptian (Sullivan 1983; Masson and Miles 1984; Mauffret and Montadert 1987; Driscoll et al. 1995) and must have followed sufficient thinning of the lithosphere. Such thinning could have induced heating and doming of the crust.

It has been suggested that thinning of the lithosphere and extension of rift basins result in a thermal anomaly and consequent uplift and doming (Blundell 1978; deCharpal et al. 1978; King 1978; Ramberg and Larsen 1978; Chaplin 1979; Fallor and Soper 1979; Rosendahl 1987). Doming of the warm crust probably induced continuous uplift of the Jeanne d'Arc basin and recurrent development of unconformities during the Aptian. It is worth mentioning in this context that several unconformities developed at different times during the Aptian in many north Atlantic basins (Hiscott et al. 1990).

In conclusion, the repeated emergences of the Hibernia rollover anticline are likely induced by tectonic processes related to the mechanics of rifting rather than by eustatic sea level changes. A tectonic origin for the Barremian unconformity, which corresponds to one of the emergences of the rollover anticline, has also been favoured in many other studies (Hubbard 1988; Tankard and Welsink 1988; Hiscott et al. 1990; Sinclair 1993; Driscoll et al. 1995).

IV.3- CONTROLS ON SEDIMENTATION

IV.3.1- CONTROLS ON THE BARRIER ISLAND DEPOSITIONAL SYSTEM:

1) Wave-dominated shoreline:

In the lagoonal side of the barrier, in the I-46 well, wave-domination is well reflected by the abundance of storm washover sandstones and siltstones. On the seaward side of the barrier, in B-27 and C-96 wells, the shallow marine mudstones immediately overlying TS'II' (figure III.8) also contain storm sandstone beds. As well, ravinement surfaces in the barrier island sandstones attest to the wave-induced erosion that was associated with shoreface retreat.

2) Carbonate sediment contribution:

The barrier island sand bodies consist mainly of the Intraclastic Sandstone Facies. Framework grains of this facies include up to 30.0 % micritic intraclasts and bioclastic shell debris (visual estimate). The transgressive nature of the barrier islands suggests that the micritic intraclasts were sourced from the seaward side, to the E and NE (figure III.16), where carbonate deposition occurred due to deficiency of siliciclastic sediment supply. It is worth mentioning that the Intraclastic Sandstone Facies is coarser in grain size than all the other sandstones in the overlying and underlying estuarine depositional systems. The Intraclastic Sandstone Facies range in grain size from fine to medium sands while the other sandstones consist of very fine to fine sands.

3) Accelerating rate of submergence of the rollover anticline:

The barrier island sandstones record three transgressions corresponding to three relative sea level rises associated with submergence of the Hibernia rollover anticline (figure III.9). The first transgression occurred by erosional shoreface retreat of the shoreline. The second transgression took place by a combination of erosional shoreface retreat and in-place drowning. The third transgression happened by in-place drowning. The progression of the transgression mechanism, from erosional shoreface retreat to in-place drowning, reflects the accelerating rate of submergence of the Hibernia rollover anticline. This acceleration is a direct response to the increasing rate of slip along the Rankin fault (figure IV.1D).

The presence of ravinement surfaces at the tops of barriers 'A' and 'B' (figure III.9) manifests the erosion that accompanied the first and second transgressions. The preservation of a significant thickness of the barrier 'B' (4.7 m. thick section of lower shoreface sandstones below TS'II' in the B-27 well, figure III.8) suggests a combination of erosional shoreface retreat and in-place drowning. In contrast, barrier 'C' is fully preserved in the K-14 well (figure III.9). Barrier 'C' is abruptly overlain by mud-rich layers and a 2.0 m. thick section of lower shoreface sandstones (immediately below ES'II' in figure III.10).

IV.3.2- CONTROLS ON THE ESTUARINE DEPOSITIONAL SYSTEM:

1) Sediment character:

The bay head deltaic sediments include mudstones and very fine to fine grained sandstones. These fine-grained deltaic sediments were transported to the system via a fairly stable distributary channel. Orton and Reading (1993) reported that the fine grain size of deltaic sediments suggests a relatively stable point source and partially controls the physical processes operating at the river mouth.

2) Fluvial-dominated to wave-dominated system:

In the inner part of the estuary the bay head delta was fluvial-dominated. Deltaic sediments were reworked only by organisms. Limited tidal reworking was recorded in the fluvial/tidal channel fill sandstones. The outer part of the estuary was wave-dominated. Wave and storm reworking developed shoreface sandstones in the K-14 well (figure III.11). These shoreface sandstones have many ravinement surfaces that also attest to the wave-induced erosion associated with shoreface retreat. As well, the shoreface sandstones are overlain by mudstones that host abundant storm sandstone beds.

3) Structurally-controlled estuaries:

The estuarine sediments were deposited in a structurally-controlled valley. This valley was recurrently rejuvenated during deposition of the Avalon Formation. The stratigraphic offset, or the relief, between the valley trough and the

valley flanks increased through time, from 54.0 m. to 97.0 m. due to renewed movements along the valley-bounding faults (figure III.20). During structural rejuvenation the upper part of the valley remained in the same position, while the lower part changed its position (figures I.6, III.12 & 19). The older estuary mouth was located in the SE, whereas the younger estuary mouth occurred in the NE.

4) Tectonics:

Establishment of an estuary and filling of the valley with estuarine sediments resulted from the initiation of extension during a rifting episode (figure IV.1C). This extension affected the rate of slip along the valley-bounding faults. The slip rate changed systematically relative to rate of sediment supply and affected the stacking pattern of estuarine facies in the valley (Figure III.21).

The slip rate along the valley-bounding faults gradually accelerated and outpaced the sediment supply resulting in transgression of the estuarine sediments. Slip rate subsequently decelerated and the valley was gradually filled with sediments. The acceleration of slip rate is attributed to the initial waxing of extension. Subsequent deceleration of subsidence rate is related to the gradual waning of extension.

The stacked cycles of river mouth bar sandstones in the older estuarine sediments reflect an initial high rate of fault slip associated with ample sediment supply (figures

III.7 & 21). The transgressive surface at the depth of 2457.0 m. in the I-46 well suggests that the rate of fault slip outpaced the rate of sediment supply. The slip rate subsequently decreased relative to the rate of sediment supply causing:

- 1) progradation, shoaling of the estuary and development of increasingly restricted brackish water conditions, and
- 2) filling of the valley and gradual diminishment of its topographic relief.

Waterson (1986) suggested that displacement rate along individual growth faults may increase through time. Assuming a constant rate of sediment supply, the initial deepening of the estuary would coincide with the increase of displacement rate and waxing of extension. In contrast, subsequent shoaling of the estuary and filling of the valley would be associated with the deceleration of fault displacement and waning of extension. Surlyk (1978 & 1984) attributed the upward deepening trend in fan delta and submarine fan facies in Greenland to the effect of syn-depositional faulting. Rigsby (1994) also pointed out that the deepening upwards fluvial to fan delta successions in California were developed due to regional tectonic subsidence and synchronous sea level rise. Cartwright (1991) reported that during rifting the rate of displacement along the Coffee Soil Fault in the North Sea rapidly increased relative to the rate of sediment supply.

Bilodeau and Blair (1986) and Blair (1987 & 1988) suggested that the drainage basin expands and incises into new areas only when fault movement ceases at the end of rifting. Expansion of the drainage basin results in the increase of rates of erosion and sediment supply (Blair 1987, 1988). Accordingly, shoaling of the estuary and filling of the valley would occur due to deceleration of fault movement and increase of sediment supply consequent to waning of extension.

IV.4- STRATIGRAPHIC MODEL

The data obtained in this study permit the development of a stratigraphic model for the Avalon Formation in the Hibernia rollover anticline. The model highlights the stratigraphic organization of the different facies deposited in the rollover anticline (figure IV.2). The model particularly describes those facies which accumulated in the inner to middle parts of the valley which runs along the rollover anticline. The writer acknowledges that the model requires refinement as additional drilling data become available. However, the model can serve as a predictor of facies relationships and architecture in the Hibernia field as well as other similar rollover anticlines. The model consists of four stratigraphic units:

1) Basal offshore mudstones:

These mudstones represent the typical sedimentation in the Hibernia rollover anticline (figure IV.1A).

2) An older estuarine valley fill:

The estuarine sediments occupy a valley that is incised into the offshore mudstones. The valley was incised subsequent to emergence of Hibernia rollover anticline (figure IV.1B).

The estuarine valley fill ranges in thickness from 30.0 up to 70.0 metres. The estuarine sediments in the inner part of the valley typically consist of fluvial and river mouth bar sandstones, bay mudstones, distal deltaic sediments and interdistributary bay fill sandstones (figure IV.2).

In a vertical succession, the estuarine valley fill can be subdivided into two intervals, a lower retrogradational interval and an upper progradational interval, separated by a significant transgressive surface³ (figure IV.3B). This surface can be used as a good correlation marker. The lower interval maintains an overall fining upward trend. This interval consists of the fluvial and river mouth bar

³This thickness is significantly larger than the thicknesses of estuarine valley fills, which are developed as a result of eustatic sea level changes. The thicknesses of those eustatically-controlled estuarine valley fills vary from 20 to 40 metres (Reinson et al. 1988; Leckie and Singh 1991; Belknap et al. 1994; Thomas and Anderson 1994; Wood 1994).

³Estuarine valley fills that are developed due to changes in eustatic sea level maintain an overall upward transgressive succession (Zaitlin and Shultz 1990; Leckie and Singh 1991; Pattison and Walker 1994; Wood 1994). This succession is terminated at top by a significant transgressive surface that signifies the maximum flooding. Such surface can be delineated inside and outside the valley and is usually overlain by offshore mudstones followed by progradational sands.

sandstones overlain by bay mudstones. Where fluvial sediments are absent, the river mouth bar sandstones would then overly directly the basal erosional boundary of the valley. The lower interval marks the initial waxing of extension and consequent gradual increase of fault slip rate relative to the rate of sediment supply. The upper interval has an overall coarsening upward trend. This interval comprises distal delta and interdistributary bay fill sediments. Fauna and flora in this interval reflect the most brackish water conditions in the valley fill. The upper interval reflects the progressive waning of extension and the resulting gradual decrease of the rate of fault slip relative to the rate of sediment supply.

The fluvial and river mouth bar sandstones pinch out gradually towards the outer part of the valley where they change into distal deltaic sediments and bay mudstones. The interdistributary bay fill sediments of the upper interval change laterally into distal deltaic sediments, bay mudstones and estuary mouth sandstones in the outer part of the valley.

Soil sediments occur on the valley flanks. They can overly a thin interval of estuarine sediments (figure IV.3A) or occur directly above the offshore mudstones.

3) Transgressive shoreline-offshore sediments:

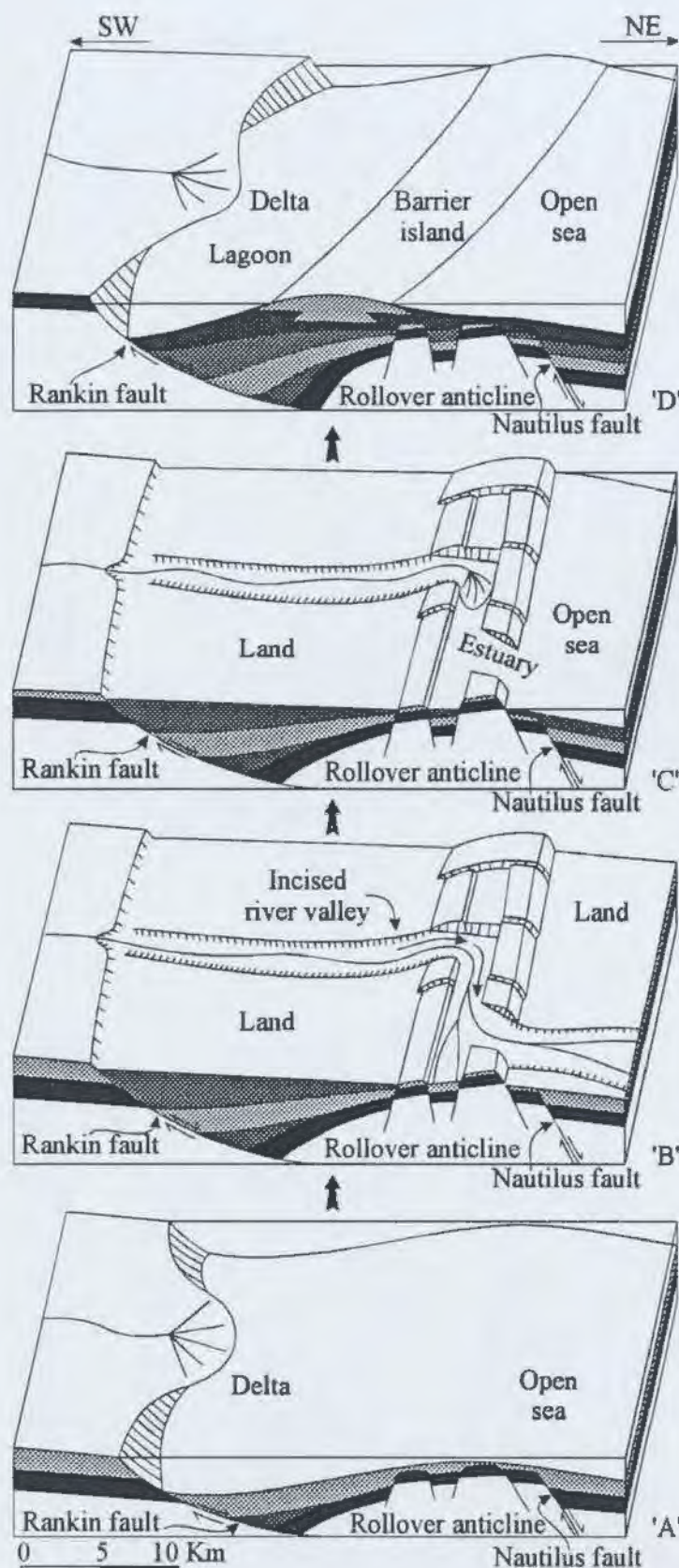
The transgressive shoreline and offshore sediments are deposited respectively during and subsequent to submergence of the Hibernia rollover anticline. The submergence is a

consequence of an advanced phase of extension and active displacement along the Rankin growth fault (figure IV.1D & A). They overly both the valley fill and valley flank deposits, with a transgressive surface in between. This surface is usually covered with shell hash layers.

The transgressive shoreline deposits show a coarsening upward trend (figure IV.3). The deposits consist of lagoonal mudstones that change upwards into barrier island sandstones and offshore mudstones. Several barrier island sandstone bodies may occur instead of a single body. Ravinement surfaces usually separate successive bodies and also occur between the barrier sandstones and the overlying offshore mudstones. The barrier sandstones contain considerable amounts of diagnostic carbonate micritic intraclasts sourced from the open sea side. The barrier island sandstone bodies extend continuously above both the valley fill and valley flank sediments.

4) A younger estuarine valley fill:

This valley fill cuts into the offshore mudstones and barrier island sandstones. It can also cut down to the older valley fill. Facies in both the younger and older valley fills are quite similar to each other. Incision of the younger valley fill reflects re-emergence of the Hibernia rollover anticline. Filling of the valley with estuarine sediments marks resumption of extension and renewal of fault activity.



ADVANCED EXTENSION

- * Acceleration of fault slip
- * Submergence of the rollover anticline,
- * Delta retrogradation &
- * Development of a transgressive barrier island.

INITIATION OF EXTENSION

- * Initiation of fault slip,
- * Relative sea level rise &
- * Development of an estuary.

REGIONAL UPLIFT

- * Cessation of fault slip,
- * Relative sea level drop
- * Emergence of the rollover anticline,
- * Delta progradation,
- * Incision of a river valley.

SUBMERGED ROLLOVER ANTICLINE

- * Active fault slip
- * Deposition of offshore mudstones on the rollover anticline

Figure IV.1- Kinematic & sedimentation model of the Hibernia rollover anticline.

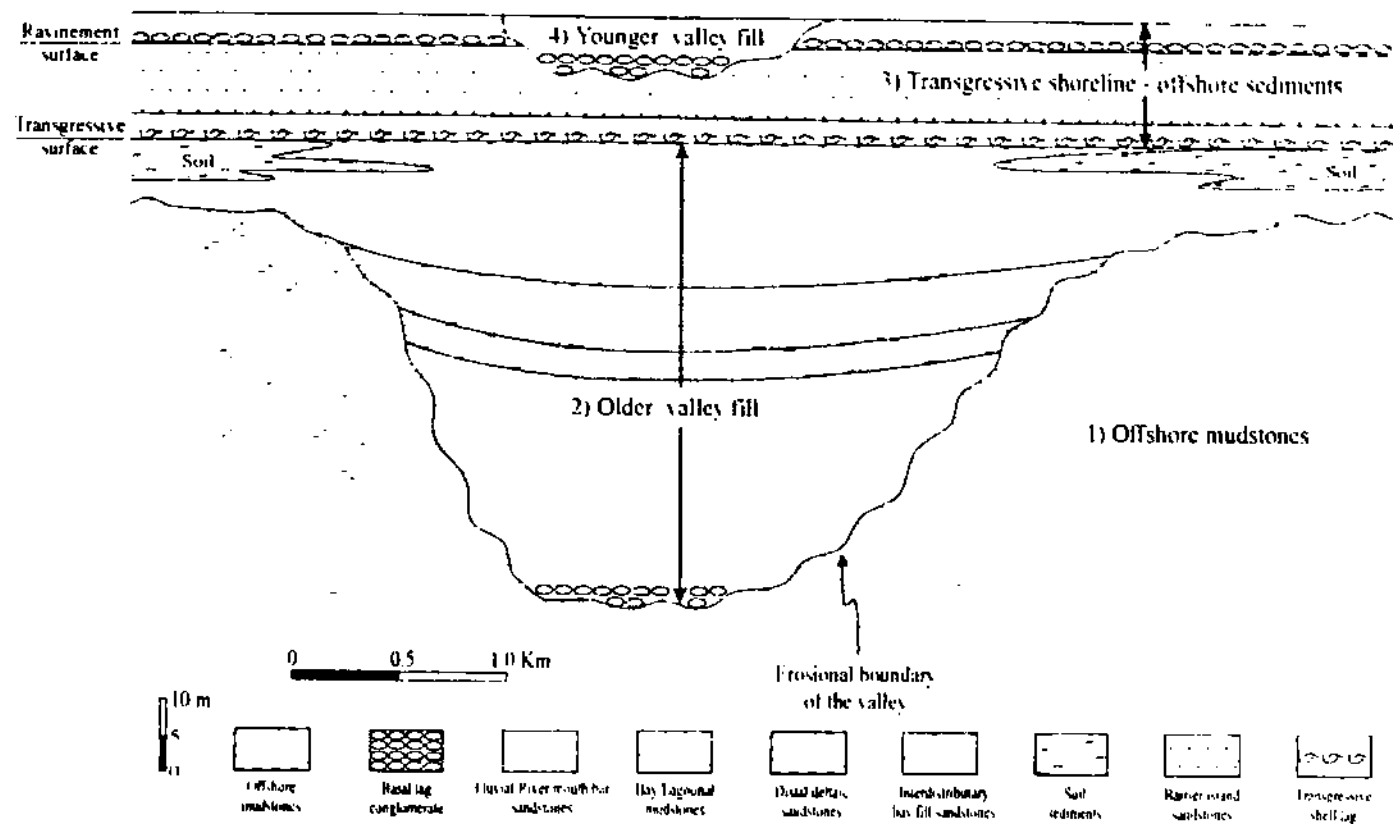


Figure IV2- Stratigraphic model for the Avalon Formation in the Hibernia rollover anticline

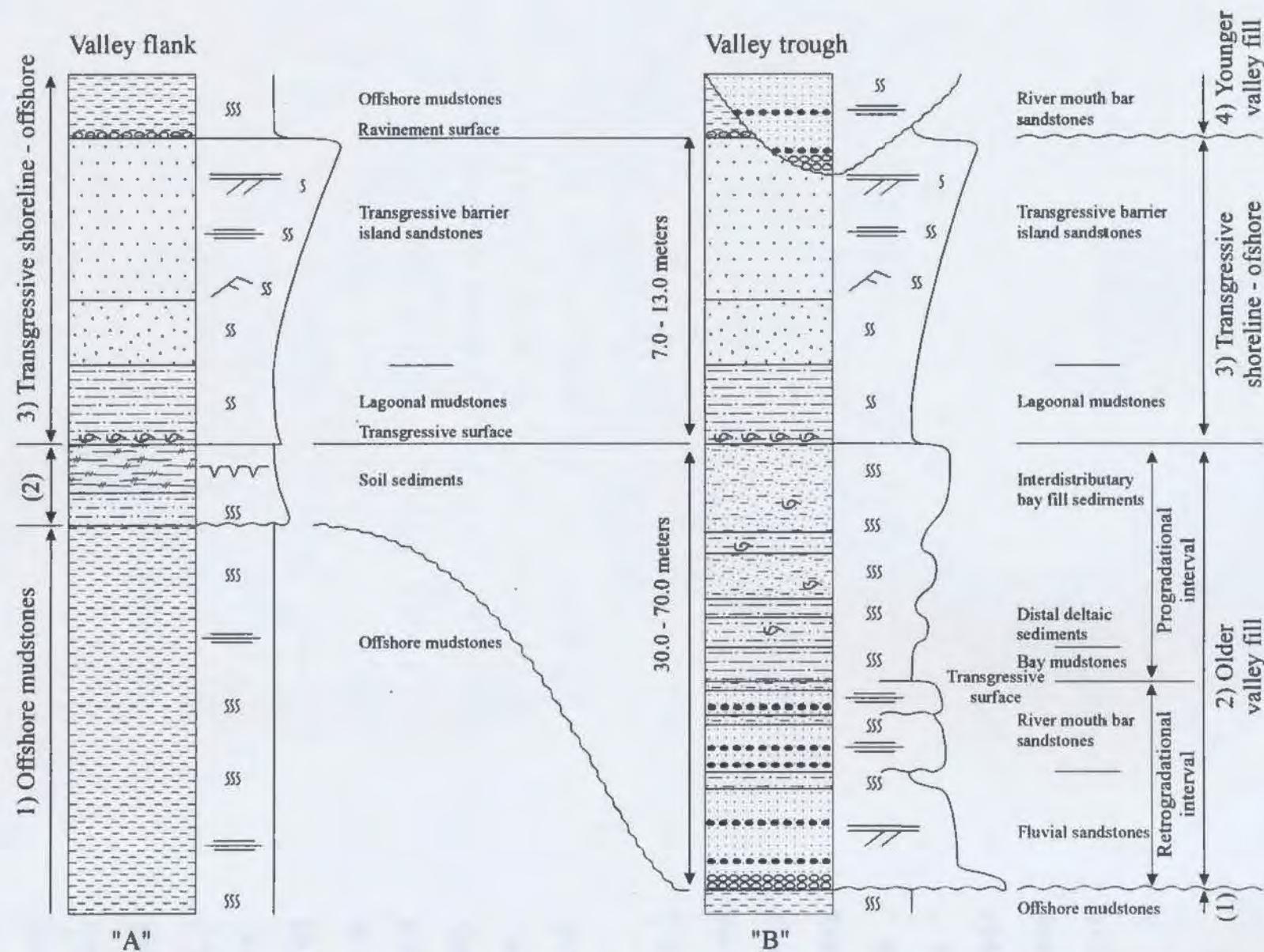


Figure IV.3- Ideal stratigraphic successions for the Avalon Formation in the Hibernia rollover anticline.

V- PETROGRAPHY OF CALCITE CEMENTATION

Laterally extensive calcite cementation occurs in sandstones of the Avalon Formation. This calcite cementation attests to the vast fluid flow in the Hibernia rollover anticline. Such fluid flow will be investigated, in chapter VI, by studying the geochemistry of the calcite cements. The geochemical approach necessitates a good knowledge of the petrography of these cements. This chapter describes the types of such calcite cements and places them in a chronologic order relative to the other diagenetic alterations in sandstones of the Avalon Formation. These other diagenetic alterations are thus briefly characterized, as well.

A total of 316 thin sections were used to investigate various diagenetic alterations (table I.1). Two hundred and forty four thin sections were provided by Hibernia Management and Development Company. These samples are stained with Alizarine red S and potassium ferri-cyanide. Another set of 72 thin sections was prepared, by the writer, for petrographic investigation and subsequent microprobe analysis. This set involves calcite-cemented sandstone samples belonging to following facies; the Intraclastic Sandstone, Coquina, Laminated Clean Sandstone, Shelly Sandstone, Sandy Siltstone and Bioturbated Muddy Sandstones Facies. Authigenic minerals, cements and paragenetic sequence of diagenetic alterations

were routinely described for each thin section. The type of calcite, ferroan versus non-ferroan calcite, was characterized in the stained thin sections (applying the method proposed by Dickson 1966).

V.1- PETROGRAPHY

Six types of diagenetic alterations were recognized.

These alterations include:

- I) Bladed and fibrous calcite cements,
- II) Siderite,
- III) Pyrite,
- IV) Compaction and quartz overgrowth,
- V) Poikilotopic calcite cement, and
- VI) Secondary porosity.

The above diagenetic alterations are not found altogether in any single facies. Some diagenetic alterations are associated with certain facies. For example, the bladed and fibrous calcite cements occur only in the Intraclastic Sandstone Facies. Siderite is common in the Shelly Sandstone Facies and does not exist in the Intraclastic Sandstone Facies. Other diagenetic alterations, e.g. the poikilotopic calcite cement, occur in most of the facies. Each of the above diagenetic alterations is described briefly, below:

1) Bladed & fibrous calcite (Plates V.1 & 2):

Circumgranular bladed calcite cement selectively envelopes micritic intraclasts in the Intraclastic Sandstone 'A' subfacies. Rarely, quartz grains are surrounded by bladed calcite. A bladed calcite cement rim varies in thickness around the same nucleus grain. The calcite crystals in the bladed calcite cement rim range in length from about 5.0 to 20.0 μm . The crystals commonly show a gradual increase in width, along their length, away from the nucleus grain. This cement is believed to be of a syndepositional marine origin. Similar circumgranular bladed calcite cements have been described in modern beach rock of St. Croix, U.S. Virgin Islands (Moore 1939).

Fibrous calcite cement is preferentially associated with fibrous calcitic shells and rare oolites. This cement forms palisade fringes (all crystal axes parallel) around and frequently beneath the shells. Two types of fibrous cement, associated with fibrous shells, have been recognized. These are radiaxial fibrous and fascicular-optic fibrous calcite¹.

¹In both the radiaxial fibrous and fascicular-optic fibrous calcite, each crystal has undulose extinction, as a result of convergent fast-vibration directions (optic axes) in the first case and divergent in the second (Kendall 1985). In the RFC crystals, the direction of extinction-swing in each crystal is the same as the direction of turning the microscope stage. In the FOFC the direction of extinction swing in each crystal is opposite to the direction of turning the microscope stage (Tucker 1990).

In contrast, the oolites are surrounded by only the radiaxial-fibrous variety. It has been recently argued that fibrous calcites are primary marine cements (Kendall 1985; Sandberg 1985; Saller 1986).

The bladed and fibrous calcite cements are restricted to the Intraclastic Sandstone 'A' Subfacies. They are usually superposed by poikilotopic calcite cement.

II) Siderite (Plate V.3):

Siderite occurs both as a cement and as a replacement mineral. Siderite cement rhombs bind the detrital framework grains and can reach up to about 20% in abundance. Siderite occasionally replaces fibrous shells. It can also line borings in these shells. The siderite rhombs are generally euhedral to anhedral. They range in size from 5-30 μm . Siderite is usually superposed by poikilotopic calcite cement.

Siderite occurs in the Shelly Sandstone and the Sandy Siltstone Facies, both of which were deposited in a brackish lagoonal environment (See II.2.1). Modern brackish water environments are widely reported to host early diagenetic siderite (Curtis et al. 1975; Gautier 1982; Mozley 1989; Pye et al. 1990; Mozley and Carothers 1992). Similarly, an early diagenetic origin in the sulfate reducing zone is postulated for the siderite in the Avalon Sandstones.

III) Pyrite (Plates V.4 & 5):

Pyrite occurs as a replacement mineral, as a patchy cement, and as a secondary pore filling. It also exists as euhedral to subhedral crystals that fill central cavities in calcite veins.

Replacement pyrite occurs as randomly disseminated rounded grains, that range in diameter from about 0.03 to 0.2 millimetres. The pyrite replaces, partially to completely, wood fragments and other organic chips. Cellular structure is usually retained in the wood fragments. Poikilotopic calcite cement usually fills the cellular voids and surrounds the replacement pyrite grains. Therefore, the replacement pyrite predates the poikilotopic calcite cementation. Replacement pyrite is frequently found in the Shelly Sandstone and the Laminated Clean Sandstone Facies.

Patchy pyrite cement coexists with poikilotopic calcite cement (plate V.5). The boundary between both cements is gradational and their relative chronology is ambiguous. In the calcite-cemented side of the boundary, there are some pyrite crystals and small spots, 0.02-0.2 mm, of pyrite cemented sands.

Pyrite that fills secondary pores and central cavities in calcite veins postdates calcite cementation and secondary porosity development. This void filling pyrite and the patchy pyrite cement are rarely encountered in the Intraclastic

Sandstone and the Laminated Clean Sandstone Facies.

IV) Compaction & quartz overgrowth (Plates V.6 & 7):

In general, sandstones of the Avalon Formation are moderately packed. Detrital framework grains have point and plane contacts. Adjacent detrital grains rarely show concavo-convex boundaries. Mica plates are slightly deformed and bent between other framework grains. Mud clasts are commonly distorted and squeezed in between framework grains. In the calcite-cemented sandstones, framework grains are less compacted than in the non-cemented sandstones. This phenomenon indicates that compaction was arrested by calcite cementation in an early stage of diagenesis.

Quartz overgrowth is common in all sandstone facies. The overgrowth ranges in thickness from about 5 to 20 μm . and frequently show marked thickening in adjacent open pores. This thickening suggests that it developed due to compaction and pressure solution along grain contacts. Quartz overgrowth is commonly superposed by poikilotopic calcite cement.

V) Poikilotopic calcite (Plates V.6-8):

Poikilotopic calcite cement consists of ferroan calcite crystals that range in diameter from about 0.05 up to few millimetres. The more abundant the carbonate skeletal debris and micritic intraclasts, the smaller are the poikilotopic calcite cement crystals. Large poikilotopic calcite crystals usually encompass large number of detrital grains. These

detrital grains commonly include randomly scattered detrital siderite (plate II.22). Small poikilotopic calcite crystals, described here as blocky, fill one or more intergranular pores. Where there are many blocky calcite crystals in one pore, they do not show any grain size increase towards the pore's centre.

Poikilotopic calcite occasionally fills biomoldic pores, developed after dissolution of former aragonitic shells. Spalled and collapsed parts of micritic walls of former shells are commonly incorporated in the poikilotopic calcite crystals. There is always optical continuity between the poikilotopic calcite crystals inside and outside the shells. There is little compaction and rare collapse of the biomoldic pores. Therefore, it is possible that the shells were dissolved and refilled shortly afterwards by the same calcite-precipitating fluids.

Calcite veins occasionally cut through the poikilotopic calcite-cemented sandstone beds. The veins are composed of ferroan calcite crystals that increase in grain size towards the veins' centres. Therein, the calcite crystals commonly have a rhombic shape. It is conceivable that the vein-filling calcite postdates the poikilotopic calcite cementation. However, it is not obvious whether the vein-filling calcite precipitated directly subsequent to the poikilotopic calcite cementation, or the former is a considerably later phenomenon.

Poikilotopic calcite cement occurs in the Intraclastic Sandstone, the Shelly Sandstone, the Laminated Clean Sandstone, the Sandy Siltstone and the Bioturbated Muddy Sandstone Facies.

VI) Secondary porosity (Plates II.10 & V.10):

Secondary porosity rarely occurs in sandstones of the Avalon Formation. In the poikilotopic calcite-cemented sandstone beds, biomoldic pores occasionally occur. The poikilotopic calcite cement itself is partially dissolved adjacent to the biomoldic pores. The poikilotopic calcite cement is also preferentially dissolved at the contacts with the non-cemented beds, and around mud-rich patches. Conceivably, these contacts and the mud-rich patches provided routes for migration of the calcite-dissolving fluids. The secondary pores are frequently lined or partially filled with euhedral to subhedral pyrite, and/or bitumen.

In the non-cemented sandstones, evidence of secondary porosity involves rare honeycomb and enlarged pores. The honeycomb pores are associated with partially dissolved feldspar grains.

In general, secondary porosity is rarely observed in the Intraclastic Sandstone and the Laminated Clean Sandstone Facies. However, Meloche (1982) suggested that the porosity of sandstones of the Avalon Formation is mainly of secondary origin. This study suggests, on the contrary, that secondary

porosity is a minor diagenetic phenomenon and does not contribute significantly to the overall primary porosity of sandstones of the Avalon Formation.

V.2- PARAGENETIC SEQUENCE OF DIAGENESIS:

The textural relationships between the previously described diagenetic alterations suggest the following paragenetic sequence of diagenesis:

Bladed & fibrous	I --	
calcite	I	
Siderite & pyrite	I -----	
	I	
Compaction	I -----	
	I	
Quartz overgrowth	I -----	
	I	
Poikilotopic calcite	I -----	
	I	
Secondary porosity	I -----	
	I	
Late pyrite	I -----	

The early pyrite includes the replacement type. The late pyrite involves the vein cavity-filling and secondary pore filling varieties. The terms early and late are used here to describe the chronological order, not the depth.

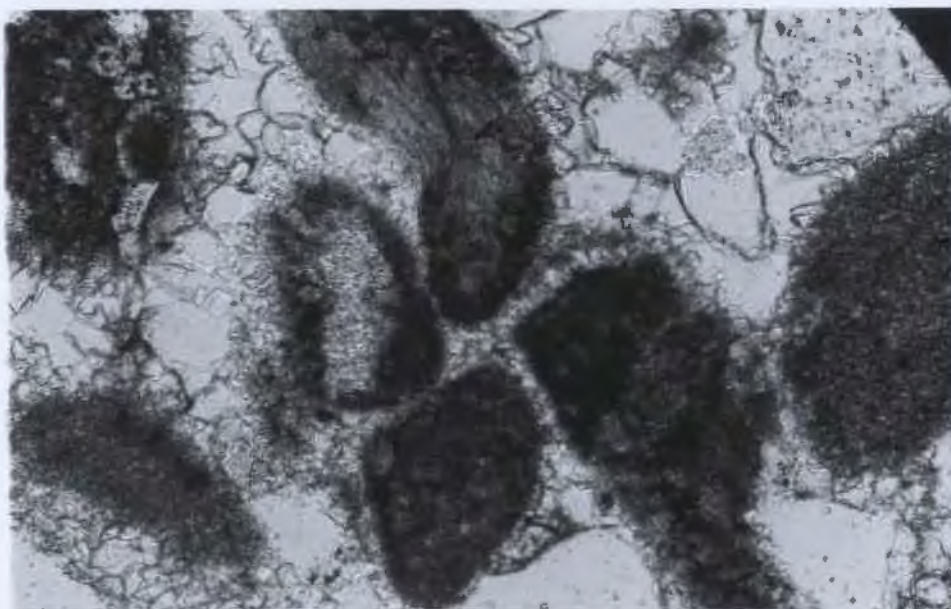


Plate V.1- Bladed calcite cement surrounding micritic intraclasts. Note the change in width of the bladed calcite cement rims around the intraclasts. The Intraclastic Sandstone Facies in the K-14 well (2398.0 m). Plane light 10X.



Plate V.2- A palisade fringe of fibrous calcite cement at the lower side of a fibrous shell. The Intraclastic Sandstone Facies in the B-27 well (2580.35 m). Crossed polars 10X.

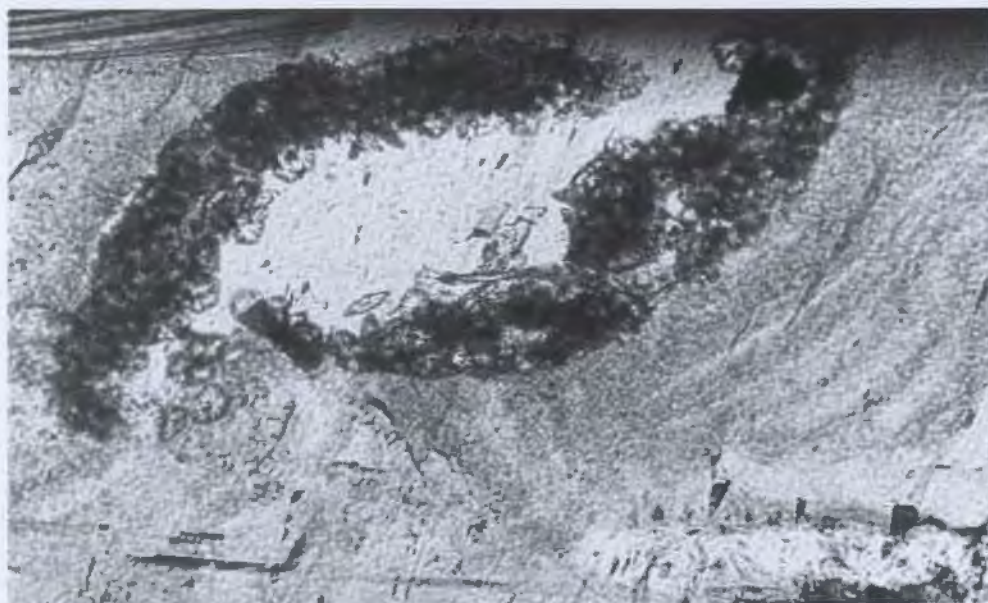


Plate V.3- A shell boring lined with authigenic siderite crystals and filled with poikilotopic calcite cement. Compaction resulted in collapse of the shell bore before precipitation of the poikilotopic calcite cement. The Sandy Siltstone Facies in the B-27 well (2585.2 m). Plane light 100X.

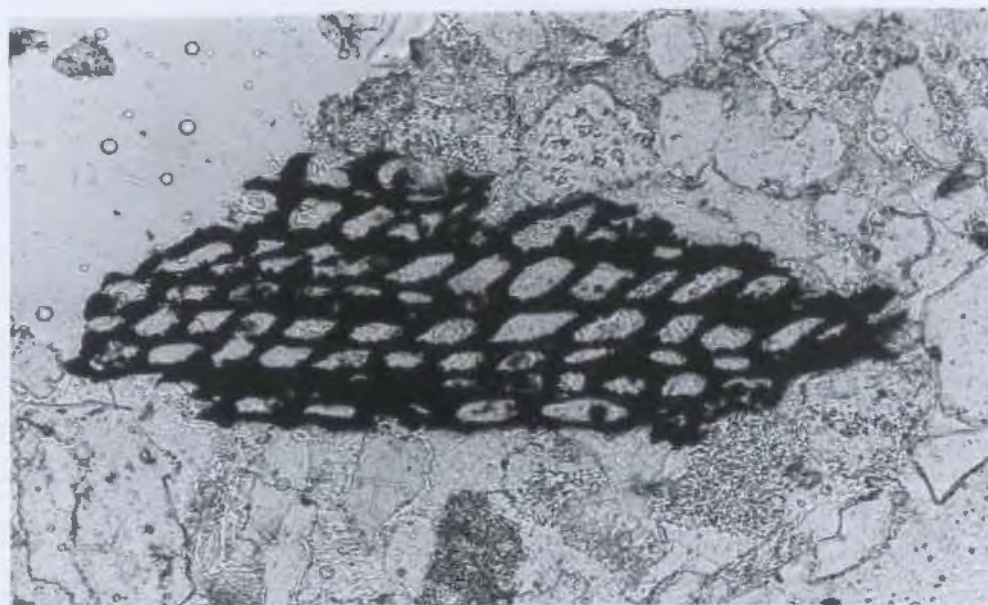


Plate V.4- A well preserved cellular structure in a pyrite-replaced wood fragment. The Laminated Clean Sandstone Facies in the I-46 well (2399.25 m). Plane light 100X.

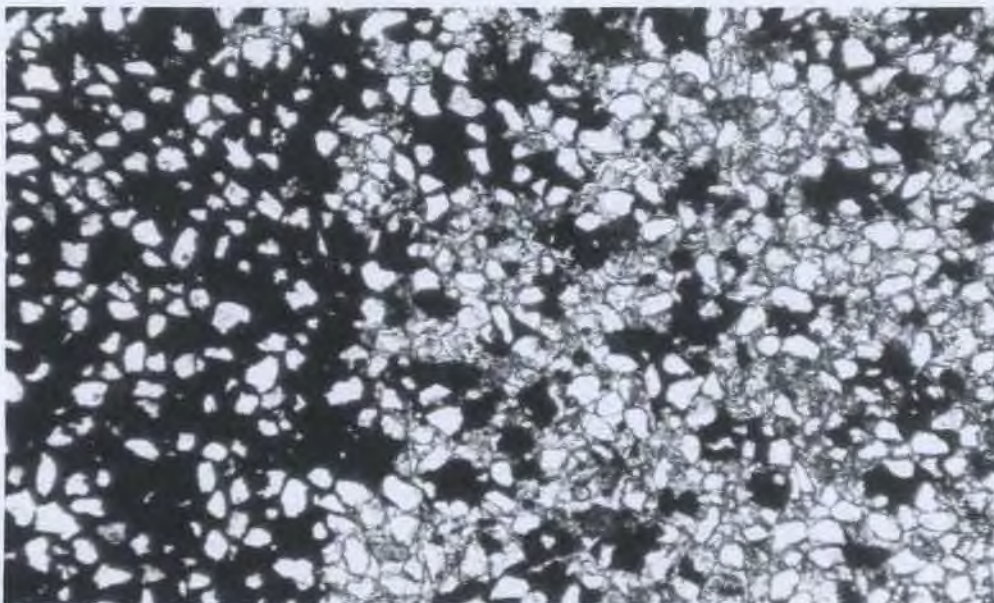


Plate V.5- Gradational boundary between the poikilotopic calcite and pyrite cements, respectively at the right and left hand sides. Note the pyrite cement patches in the right hand side. The Laminated Clean Sandstone Facies in the I-46 well (2464.15 m). Plane light 20X.

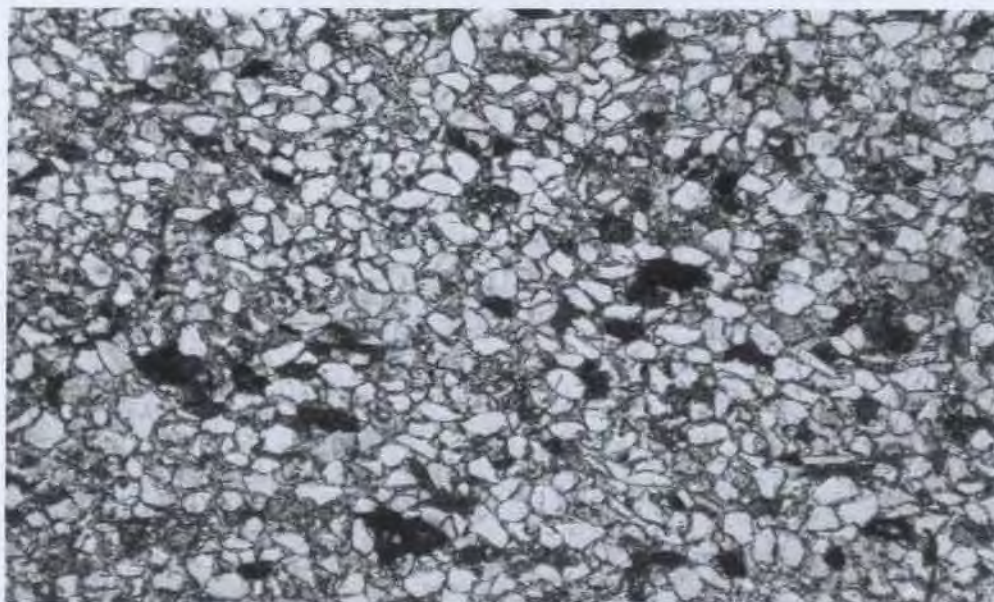


Plate V.6- Moderately packed sandstone with abundant concavo-convex grain boundaries. Note the scattered mud grains and mud-rich patches. The Laminated Clean Sandstone Facies in the B-27 well (2552.11 m). Plane light 20X.

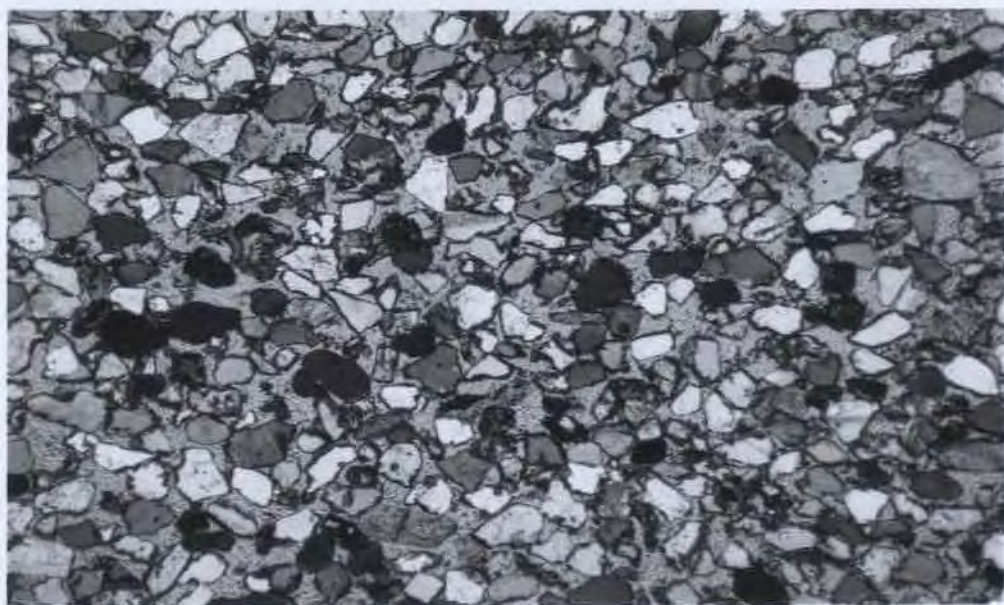


Plate V.7- Moderately to loosely packed sandstone that is cemented with one large poikilotopic calcite crystal. Note the thin quartz overgrowth rim that surrounds a quartz grain at the centre of the photomicrograph. The Intraclastic Sandstone Facies in the K-14 well (2398.75 m). Crossed polars 20X.

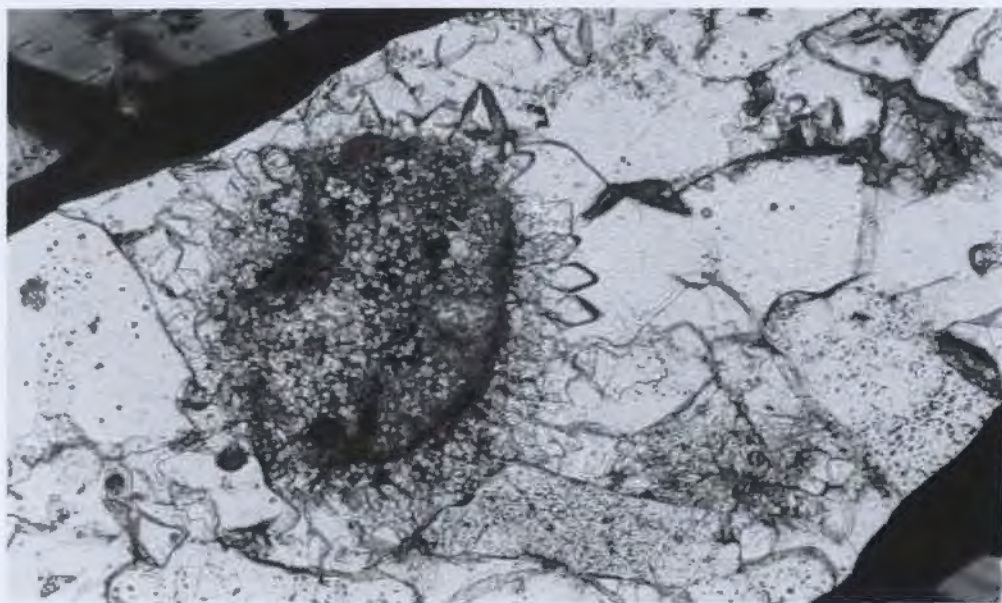


Plate V.8- Blocky calcite crystals superposed on bladed calcite cement crystals. The blocky calcite crystal in the upper right hand corner occupies several adjacent intergranular pores. The Intraclastic Sandstone Facies in the K-14 well (2398.0 m). Plane light 10X.

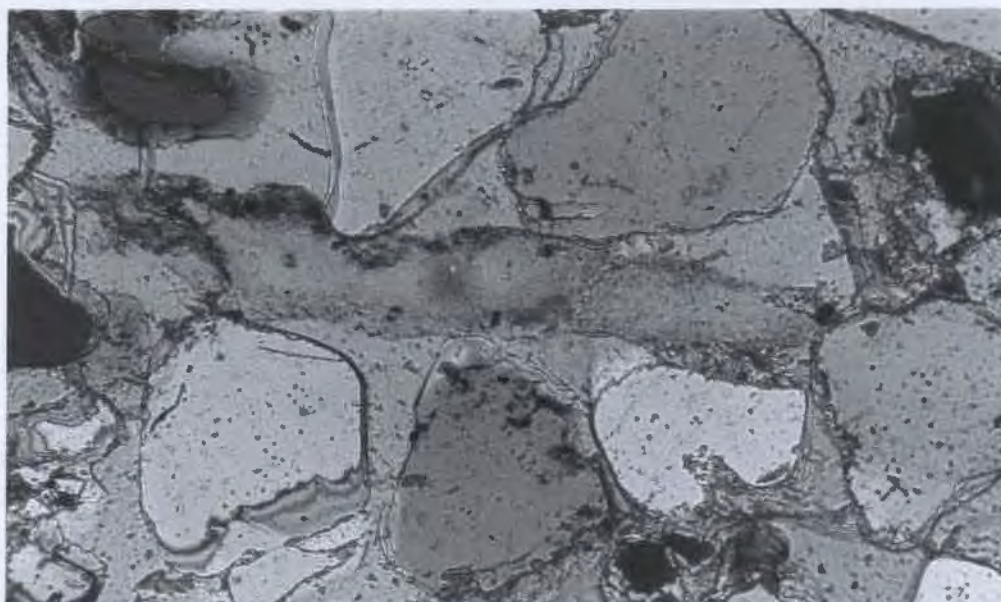


Plate V.9- Partially collapsed biomoldic pore filled with poikilotopic calcite cement. Note the optical continuity between the poikilotopic calcite inside and outside the biomoldic pore. The Complex Cross Bedded Sandstone Facies in the K-14 well (2373.35 m). Crossed polars 100X.

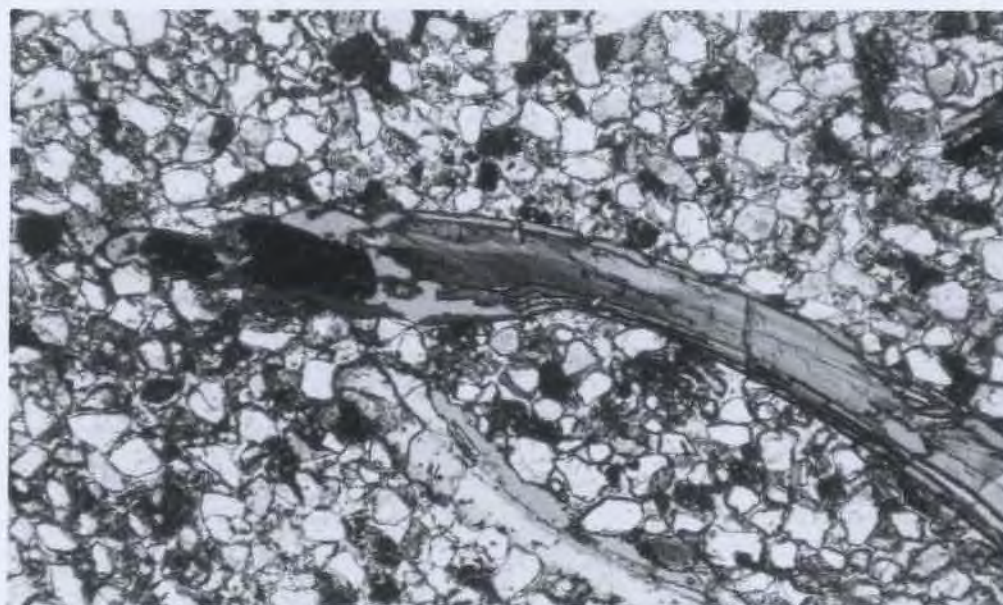


Plate V.10- Bitumen-filled secondary pore in a large pelecypod shell fragment. Another secondary pore occurs just above the shell fragment at the central lower part of the photomicrograph. The Laminated Clean Sandstone Facies in the I-46 well (2401.6 m). Plane light 20X.

VI- CALCITE CEMENTATION & FLUID FLOW

Laterally extensive beds of poikilotopic calcite-cemented sandstone are common in the Avalon Formation. These beds attest to a significant flow of the poikilotopic calcite-precipitating fluids in the Hibernia rollover anticline. This chapter explores the flow of these fluids in the rollover anticline. As well, the relationship between the tectonics and the flow of such fluids is investigated. The approach used to tackle these questions involves:

Distribution of the calcite cementation



Geochemistry of the poikilotopic calcite cement



Flow of the calcite-precipitating fluids



Origin of the calcite-precipitating fluids



Tectonics & Fluid flow
in the Hibernia rollover anticline

Vertical and lateral distributions of the poikilotopic calcite-cemented intervals are investigated in order to evaluate any facies and stratigraphic controls on calcite cementation. Sampling for subsequent geochemical analysis of calcite cements is also based on the distribution of these calcite-cemented intervals. Geochemical signatures of the calcite cements are used to reveal the nature of the calcite-precipitating fluids and to follow the paleomigration trends of these fluids. Finally, the relationship between the paleomigration trends and tectonics of the rollover anticline is explored.

VI.1- DISTRIBUTION OF CALCITE CEMENTATION

VI.1.1- VERTICAL DISTRIBUTION (Figures VI.1 & 2):

Sonic logs are used to illustrate the distribution of poikilotopic calcite-cemented intervals in the B-27 and I-46 wells. A sonic log simply measures the interval transit time, during which a sound wave traverses one foot of the rock. The more porous the rock, the longer is the transit time. Conceivably, the poikilotopic calcite-cemented beds record shorter transit times than do the non-cemented beds. These shorter transit times are reflected by deflection of the sonic curve to the right hand side.

In the B-27 well, poikilotopic calcite-cemented beds are concentrated immediately above a soil zone, at the depth of

2590.0 meters, in transgressive shoreline sediments. These calcite-cemented shoreline sediments include the Coquina and Intraclastic Sandstone Facies. Two separate occurrences of calcite-cemented beds exist at the depths of 2575.0 and 2557.0 meters. Both occurrences are associated with the Laminated Clean Sandstone Facies.

In the I-46 well, poikilotopic calcite-cemented beds are concentrated immediately above lagoonal mudstones, at the depth of 2408.0 meters. They are associated with the Intraclastic Sandstone, Laminated Clean Sandstone and Bioturbated Muddy Sandstone Facies. Scattered occurrences of calcite-cemented beds also exist above the basal erosional boundary of the estuarine sediments, at the depth of 2490.0 meters. They are associated with the Laminated Clean Sandstone Facies.

VI.1.2- LATERAL DISTRIBUTION (Figures VI.3 & 4):

Sonic log correlation is used to examine the lateral distribution and extension of the poikilotopic calcite-cemented beds. Figure VI.3 illustrates that calcite cementation is most abundant and laterally extensive in the barrier island sand body, which is confined between Transgressive Surfaces 'I' and 'II'. This barrier island sand body consists mainly of Intraclastic Sandstone, Coquina and Shelly Sandstone Facies. The sand body hosts three to five calcite-cemented beds. These beds occur in both the cored and

non-cored wells. The persistence of these beds in cored and non-cored wells suggests a high chance of inter-connection between them.

Scattered occurrences of poikilotopic calcite-cemented beds occur above the transgressive surface 'II'. These beds consist of the Intraclastic Sandstone, the Laminated Clean Sandstone or the Complex Cross-Bedded Sandstone Facies. Several calcite-cemented beds of the Laminated Clean Sandstone Facies are mostly continuous between adjacent wells (figure VI.4).

Many other dispersed occurrences of poikilotopic calcite cemented-beds exist immediately below the transgressive surface 'I'. These beds consist of the Shelly Sandstone or Sandy Siltstone Facies (figure VI.3).

VI.1.3- SYNOPSIS:

Distribution of the poikilotopic calcite-cemented intervals is controlled by facies and stratigraphic position. On the other hand, lateral extension of the calcite-cemented beds is a function of continuity and depositional geometry of the host sandstone bodies (figures VI.3 & 4).

Calcite cementation occurs preferentially in facies which have abundant carbonate grains, around which the poikilotopic calcite cement nucleated. The Intraclastic Sandstone and Coquina Facies are the most favourable hosts of poikilotopic calcite cement, since they contain much skeletal debris. The

Intraclastic Sandstone Facies has micritic intraclasts as well as early marine fibrous and bladed calcite cements, in addition to the poikilotopic calcite cement. The Shelly Sandstone Facies, the Laminated Clean Sandstone Facies, and the Bioturbated Muddy Sandstone Facies contain fewer carbonate constituents and less poikilotopic calcite cement than the Intraclastic Sandstone and Coquina Facies.

The Intraclastic Sandstone Facies makes up the upper coarsest sediment of a barrier island sand body (figure VI.3). Persistence of this barrier island and its favourable lithology throughout most of the Hibernia field resulted in the formation of several laterally extensive calcite-cemented beds. Also, the stratigraphic position of this permeable barrier island sand body above an impermeable zone of lagoonal and soil mudstones enhanced its chance for calcite cementation. Conceivably, the calcite-cementing fluids were perched above the mudstone zone and flowed preferentially in the barrier island sands.

Calcite-cemented beds of the Shelly Sandstone Facies are not expected to be laterally extensive because of limited continuity of the facies. This facies was deposited in a lagoonal environment. In contrast, calcite-cemented beds of the Laminated Clean Sandstone Facies, which forms larger river mouth bar sand bodies, are laterally extensive. However, calcite cementation is relatively scarce in the Laminated

Clean Sandstone Facies because of the scarcity of pre-existing carbonate constituents.

VI.2- CARBONATE ANALYSIS

VI.2.1- Sampling & analytical technique:

Forty-two calcite-cemented sandstone samples were collected for microprobe analysis of calcite cements. Almost all the cored calcite-cemented beds in the lower Avalon Formation were sampled (figures VI.3 & 4). Calcite-cemented beds of the Bioturbated Muddy Sandstone Facies, in the I-46 well were not sampled. These were eliminated in order to avoid the influence of high clay content in this facies on the chemistry of the poikilotopic calcite cement.

The samples were selected to assess:

- A- Influence of specific facies on the chemistry of calcite cements.
- B- Vertical changes with depth in the chemistry of calcite cements throughout the lower part of the Avalon Formation.
- C- Continuity and flow trends of calcite-precipitating fluids within discrete sand bodies. This fluid flow question, in particular, necessitated the sampling of every available cemented bed in the interval of interest.

Polished thin sections, one for each of the 42 samples, were prepared for electron microprobe analysis of the calcite cements. Four to eleven points were probed in each thin

section. A total of 305 points of poikilotopic calcite cement were probed.

Five trace elements in addition to calcium were quantitatively analyzed in every probed point. Calcium was analyzed using the energy dispersive system (EDS). The five trace elements were analyzed using the wavelength-dispersive system (WDS). Counting times and detection limits for each trace element are listed in table VI.1.

Table VI.1- Counting times and detection limits of the trace elements.

Element	Counting time (sec)	Detection limit (ppm)
Mn	360	214
Fe	360	214
Mg	60	135
Sr	200	312
Na	60	147

VI.2.2- INSTRUMENT & OPERATING CONDITIONS:

A Cameca SX50 machine was used. It was adjusted under the following operating conditions:

Accelerating voltage: 15.00 KV

Beam current: 10.00 nA

Probe diameter: 20 μm

The beam current was measured every one minute and reset every five minutes to maintain constant analytical conditions. The large beam diameter was used to preclude thermal decomposition of the poikilotopic calcite cement.

VI.2.3- SELECTION OF PROBED POINTS:

Examination of the poikilotopic calcite cement in the backscattered mode showed no zoning. Therefore, probed points in the poikilotopic calcite were located in randomly distributed pores which have minimum impurities. One and less commonly two points were probed per pore. The probed points were selected so as to be separate from any adjacent skeletal debris or other carbonate grains.

VI.3- GEOCHEMISTRY OF THE POIKILOTOPIC CALCITE CEMENT

This section discusses the factors which affect the composition of the poikilotopic calcite cement and alter the original chemical signature of the calcite-precipitating fluids. The composition of the poikilotopic calcite cement was found to change according to the type of the host facies. It also changes with depth in any well location. In addition, the composition varies in any one facies laterally from one location to another. This lateral compositional variation is highlighted here in one example and will be discussed in

detail in section VI.4.

VI.3.1- FACIES INFLUENCE:

Three constituents in the host facies affect the composition of the poikilotopic calcite cement. These constituents are bioclastic debris, early marine calcite cements and siderite. In addition to these three constituents, pre-cementation porosity and permeability were found to control residence time of the calcite-precipitating fluids in the host facies. This residence time has had an important additional facies-related influence on chemistry of the poikilotopic calcite. The effects of the above-mentioned facies constituents and residence time are elaborated below:

VI.3.1.1- Bioclastic debris & marine cements (Figure VI.5):

Recrystallization of skeletal debris and early marine calcite cements releases Na, Mg and Sr while it exhausts Fe and Mn from the pore filling fluids (Brand and Veiser 1980; Veiser 1983; James and Choquette 1984; Dickson 1990). Accordingly, the pore-filling fluids/cements would be gradually enriched in Na, Mg and Sr, and depleted in Fe and Mn. The poikilotopic calcite cement in the Intraclastic Sandstone Facies, which contains the most abundant skeletal debris and marine calcite cements, is depleted in Fe and Mn relative to the other facies (figure VI.5). However, this cement has fairly low concentrations of Sr, Na and Mg comparable to their concentrations in the other facies. One

would normally expect that the depletion in Fe and Mn would be accompanied by enrichment in Sr, Na and Mg.

The calcite-cemented beds in the Laminated Clean Sandstone Facies contain abundant skeletal debris. The poikilotopic calcite cement in this facies is fairly depleted in Fe and Mn and enriched Sr, relative to the other facies in the B-27 well. Yet, this cement has low concentrations of Na and its Mg content is comparable with the Mg content in the poikilotopic calcite of the other facies.

The low concentrations of Sr, Na and Mg in the poikilotopic calcite cement of the Intraclastic Sandstone Facies is attributed to their flushing by the calcite-cementing fluids. These calcite-cementing fluids were depleted in Sr, Na and Mg. The fluids were actively replenished because of the initial high permeability and hence low residence time in the Intraclastic Sandstone Facies¹. This active replenishment caused significant consumption of Sr, Na and Mg which were released from the recrystallizing pre-existing carbonates. However, considerable amounts of Mg were retained in the pore-filling fluids and later in the precipitated calcite. In other words, the calcite-cementing fluids were

¹It is worth mentioning that non-cemented beds of the Intraclastic Sandstone Facies have the highest permeability, relative to other facies. Therefore, residence time of the calcite-precipitating fluids would be shortest in the Intraclastic Sandstone Facies.

buffered by the released Mg. The amount of this released Mg is much more than the amounts of released Sr and Na. Equilibrium concentrations of Mg, Sr and Na in marine calcites are 16300-75400, 1000, and 200-300 ppm, respectively (Veiser 1983).

The Laminated Clean Sandstone Facies contains less skeletal debris, has lower permeability and hence longer residence time than the Intraclastic Sandstone Facies. Accordingly, more Sr and Mg is retained in the pore-filling fluids and later in the precipitated calcite cement.

VI.3.1.2- Siderite (Figure VI.6):

Poikilotopic calcite cement becomes slightly depleted in Fe and Mg, while fairly enriched in Mn in the siderite-rich samples. Regarding Sr and Na, their concentrations become highly fluctuating between different probed points in any siderite-bearing sample. The Na content may show an overall increase in the siderite-rich samples.

The effect of detrital siderite on the composition of the poikilotopic calcite cement can be observed on samples collected from the same facies (figure VI.6). Sample 25 is collected from the base of a calcite-cemented bed, which contains abundant siderite clasts and detrital siderite grains. Sample 26 occurs at the top of the same bed. The top of the bed hosts no clasts and much fewer detrital siderite grains. Poikilotopic calcite in sample 25 is slightly depleted in Fe and Mg while enriched in Mn relative to sample 26. Sr

and Na contents in sample 25 become highly fluctuating and may indicate an overall depletion of Sr and enrichment of Na.

On a microscopic scale, the same influence of siderite can also be observed. Points which are adjacent to siderite contain slightly less Fe and Mg but more Mn than points which are farther away from the siderite. Sample 1 in the B-27 well contains abundant diagenetic siderite and large shell borings (figure VI.6 & Plate V.3). The shell borings are filled with poikilotopic calcite. Probed points in the shell bore-filling calcite contain the highest concentrations of Fe, Mg, and Sr and lowest concentrations of Na and Mn. Probed points which are adjacent to the siderite are slightly depleted in Fe and Mg while enriched in Mn. Na concentration becomes highly fluctuating, although showing an overall increase. Sr gets highly depleted (all the analyses are negative, i.e. below detection limit).

VI.3.1.3- Synopsis:

The poikilotopic calcite cement in the Intraclastic Sandstone and the Laminated Clean Sandstone Facies has low contents of Fe and Mn relative to the other facies. These two elements were depleted due to their consumption through recrystallization of the pre-existing carbonates. However, this depletion in Fe and Mn is not accompanied by enrichment in Na and Mg. Sr is enriched only in the Laminated Clean Sandstone Facies.

The calcite-precipitating fluids were depleted in Na, Sr, and Mg. The co-precipitation of Na with the poikilotopic calcite occurred under open diagenetic system conditions in both the Intraclastic Sandstone and the Laminated Clean Sandstone Facies. The co-precipitation of Mg with the calcite took place under less open system conditions in both facies. The co-precipitation of Sr with the calcite happened under open system conditions in the Intraclastic Sandstone Facies and closed system conditions in the Laminated Clean Sandstone Facies. These variable diagenetic conditions were controlled by the amount of pre-existing carbonates and the pre-cementation permeability in each facies as well as the original composition of the calcite-precipitating fluids.

In the Laminated Clean Sandstone and Sandy Siltstone Facies, poikilotopic calcite is depleted in Fe and Mg while enriched in Mn and Na in points adjacent to siderite.

²An open diagenetic system characterizes situations where the volume of diagenetic waters was so large that the dissolving CaCO_3 phase did not cause significant alteration of the bulk water chemistry. In contrast, a closed system signifies conditions where the composition of diagenetic water is buffered by the dissolving CaCO_3 (Veiser 1983). Under physically identical conditions, the same configuration may yield variable water/rock ratios for each trace element or isotope (Pangitore, 1982).

VI.3.2- VARIATIONS WITH DEPTH (Figures VI.7 & 8):

The concentration of iron is indirectly plotted against depth in three wells penetrating a laterally continuous Barrier-Backbarrier Facies Succession (figure VI.7). In each well, samples are arranged sequentially according to their depths. For each sample, Fe concentrations measured in the different probed points are arranged from base upwards in a descending order of magnitude.

Figure VI.7 indicates that there is a break in iron concentration that can be correlated between the three wells. This break crudely defines two cycles of changing Fe concentrations with depth. The lower cycle maintains a steady upward decrease of Fe concentration. The upper cycle does not show a consistent trend of change of Fe concentration due to facies changes between the wells (figure VI.7). In the upper cycle in the K-14 well, the average concentration of iron in the Complex Cross Bedded Sandstone Facies (1.298 Fe%) is higher than the average in the Intraclastic Sandstones Facies (0.638 Fe%). The former facies contains no marine cements and much less bioclastic debris than in the latter facies.

Iron is chosen to investigate the above questions because; A) It is the most abundant trace element, B) It is sourced from the parent calcite-precipitating fluids and not from within the rocks, and C) It is always exhausted in all facies types.

Figure IV.8 illustrates four populations of the poikilotopic calcite cement in the K-14 well. The differentiation of the four populations is controlled by both facies and depth. For instance, the differentiation between populations 'C' and 'D' is facies-controlled. This differentiation resulted from the uptake of Fe and release of Mg by the skeletal debris and marine calcite cements in the Intraclastic Sandstone Facies of population 'C'. In contrast, the separation of populations 'A & B' from populations 'C & D' is controlled by depth. Populations 'A' and 'B' belong to the lower cycle, while populations 'C' and 'D' are related to the upper cycle (figure IV.7). The iron concentration decreases gradually upwards in the lower cycle (populations 'A' and 'B'). A sudden increase in the iron concentration marks the transition to the upper cycle (populations 'C' and 'D').

The break between the two cycles of Fe occurs in the Intraclastic Sandstone Facies, in each of the three wells (figure IV.7). This position precludes any facies control on the presence of this break. Since this break is persistent in laterally equivalent rocks and the cycle '1' occupies a laterally continuous barrier island sand body (figure VI.3), it is therefore concluded that the calcite cementation was synchronous in the three wells. The poikilotopic calcite cement precipitated from the same fluids which passed through the three well locations. The origin of the break between the

two cycles is, however, not understood.

VI.3.3- LATERAL VARIATIONS:

The composition of the poikilotopic calcite in the Intraclastic Sandstone Facies changes laterally from the B-27 to the K-14 well (Figure IV.5). This facies forms a sandstone body that is continuous between the two wells. The lateral variation in composition can be attributed to multiple source points of the calcite-cementing fluids. Alternatively, it can be ascribed to the length of the flow path of the calcite-precipitating fluids within the rock. As these fluids move, they react with the rock constituents. Therefore, the fluids continuously change in composition as they move away from their source (see section VI.4).

VI.4- PALEO-FLOW OF THE CALCITE-PRECIPITATING FLUIDS

This section attempts to follow the paleomigration trends and favourable flow routes of the calcite-precipitating fluids. The approach relies on using gradients in trace element concentrations as indicators of paleoflow directions in various sand bodies. Similar attempts were made for dolostone sequences (Land et al. 1975; Land 1980; Buelter and Guilmette 1988) and for limestones (Meyers 1978; Meyers and Lohmann 1978).

Iron and Manganese are trace elements that are sourced from the calcite-precipitating fluids. Consumption of these

trace elements through recrystallization of pre-existing carbonates results in their depletion in pore water in the downflow direction (Veiser 1983; Machel 1988). In the Laminated Clean Sandstone Facies Fe is consumed through precipitation of siderite, as well.

Figures VI.9-12 illustrate gradients of Fe and Mn concentrations in poikilotopic calcite in the lower Avalon Sandstones. Highest concentrations of Fe and Mn occur dominantly around the B-27 well, which is thus closest to the source of calcite-precipitating fluids. As these fluids flowed towards other well locations, they were gradually depleted in Mn and Fe. The fluids moved preferentially in the most permeable rocks, such as the lower shoreface, the river mouth bar and fluvial/tidal channel sandstones. Fluid flow within these sandstone bodies was constrained by their geometries and internal depositional heterogeneities, permeability anisotropy as well as their structural dip at the time of flow.

VI.4.1- Fluid FLOW IN THE BARRIER ISLAND SAND BODY

(Figures VI.9 &10):

In the lower shoreface sandstones, fluids flowed favourably along strike of the barrier island sand body. The latter was dipping, about 0.066° , towards the K-14 well (apparent dip). This structural dip is suggested by the thicker water column in the K-14 well than in the B-27 well. The thicker water column is reflected by the slope and wider

spacing of contour lines as well as the greater number of calcite-cemented beds in the K-14 well (figure VI.3).

Thin water columns existed in the C-96 and J-34 wells, relative to the B-27 and K-14 wells. Since the C-96 and J-34 wells are respectively in down-dip and up-dip positions relative to both the B-27 and K-14 wells, it can be concluded that the cross barrier fluid flow was less favourable than fluid flow along the barrier.

VI.4.2- FLUID FLOW IN THE FLUVIAL-RIVER MOUTH BAR

SAND BODIES (Figures VI.11 & 12):

In the fluvial and river mouth bar sandstone bodies, the gradients of Fe concentration in poikilotopic calcite cements in different locations reflect neither a clear trend nor a conclusive direction of flow of the calcite-precipitating fluids. On the other hand, gradients in Mn concentrations in the poikilotopic calcite, in the fluvial-river mouth bar sand body below transgressive surface 'III', suggest that fluid flow occurred along its depositional dip. Continuous fluid flow took place from around the B-27 well to the I-46 and J-34 wells for a distance of about 5.5 kilometres. The flow was supported by a structural dip towards the J-34 well.

VI.4.3- SYNOPSIS:

Gradients in concentrations of Fe and Mn in the poikilotopic calcite illustrate that the B-27 well was closest to the source of calcite-precipitating fluids. The fluids

moved towards other well locations preferentially in the permeable barrier island and fluvial-river mouth bar sandstone bodies. Different flow patterns occurred in these sandstone bodies.

In the barrier island sandstone body fluids flowed preferentially along its depositional strike. The barrier was dipping, about 0.066° towards the K-14 well location (apparent dip). Hence, the flow increased in thickness from the B-27 to the K-14 well. This thickness increase induced greater calcite-cementation around the K-14 well. In other words, the larger number of calcite cemented beds around the K-14 well would merge along the barrier strike towards the B-27 well to a smaller number (figure VI.3).

In the fluvial and river mouth bar sandstone bodies, fluid flow occurred along their depositional dip. Fluids flowed from around the B-27 well towards the I-46 and J-34 wells, for distances of at least 5.5 kilometres. The flow was supported by structural dip towards the J-34 well. A calcite-cemented bed of that length extends between the three wells and continues farther up to the K-18 well (figure VI.4).

The facies factors which influenced flow of the calcite-precipitating fluids include the sand body geometry, internal heterogeneities and permeability anisotropy. These facies factors are expected to equally affect the movement and production of hydrocarbons from the Avalon reservoir. Present

day structural dip and permeability barriers, which are imposed by the calcite-cemented beds, represent additional factors that influence flow of the hydrocarbons.

V.5- ORIGIN OF THE CALCITE-PRECIPITATING FLUIDS

This section attempts to determine the type of fluids which precipitated the poikilotopic calcite cement. Since this cement is a bulk solution equilibrium precipitate from the calcite-cementing fluids, it is theoretically possible to calculate an approximate composition of such parent fluids (Veiser 1983). The composition of the parent fluids can then be compared with to compositions of other natural fluids, e.g. fresh or marine waters.

VI.5.1- THEORETICAL BACKGROUND:

Veiser (1983) stated that "The incorporation of a trace element into a CaCO_3 lattice is governed by the so-called distribution coefficient 'D' in the following manner (McIntire 1963; Kinsman 1969).

$$^m\text{Me}/^m\text{Ca}_s = D \ ^m\text{Me}/^m\text{Ca}_w$$

where the superscript 'm' indicates molar concentrations, 'Me' stands for trace element, and the subscripts 'S' and 'W' signify the solid phase (in this case CaCO_3) and the water respectively. This relationship is valid only when the system

is at complete equilibrium, and the water and solid phase do not show any concentration gradients in Me during precipitation."

The molar concentration ratio of a trace element to Calcium in the poikilotopic calcite is a measured quantity and the distribution coefficient is a constant. Using the above equation, the molar concentration ratio of that trace element to Calcium in the calcite-precipitating fluids can be calculated. The type of fluids can then be determined by comparison of the calculated values with the measured compositions of different types of waters.

The distribution coefficients are selected from experimentally determined and published values (table VI.2). The following factors were considered in the selection of distribution coefficients:

- 1- The rate of precipitation of poikilotopic calcite cements is very low (Tucker 1990).
- 2- Poikilotopic calcite, in the Avalon Sandstones, is ferroan in composition.
- 3- Poikilotopic calcite is an abiotic precipitate.
- 4- Precipitation of poikilotopic calcite was a shallow burial phenomenon, i.e. it occurred at near surface temperatures. The shallow burial is suggested by the low compaction of calcite-cemented beds.

The distribution coefficient of Mn was determined

experimentally at 40°C (Bodine et al. 1965) and was recommended for direct calcite precipitates (Veiser 1983). Distribution coefficients for Fe and Mg were determined experimentally, at 25°C, for isometric ferroan calcite cement (Richter and Fuchtbauer 1978).

Table VI.2- Distribution coefficients of trace elements.

Trace element	Distribution coefficient 'D'	Source of data
Fe	1.0	Richter & Fuchtbauer 1978
Mn	6.0	Bodine et al. 1965; Veiser 1983
Mg	0.03	Richter & Fuchtbauer 1978

VI.5.2- TYPE OF FLUIDS (Figure VI.13):

The composition of the calcite-precipitating fluids was least altered in the B-27 well location, since the latter is closest to source of the fluids. Accordingly, the composition of poikilotopic calcite cement in this well is used to deduce the type of calcite-precipitating fluids. The calculated molar ratios of trace elements to calcium in the parent fluids as well as in sea and stream waters are listed in table VI.3.

The data suggest a fresh water origin for the calcite precipitating fluids (figure VI.13). The high iron content of

the calcite-precipitating fluids is attributed to the presence of iron oxides, mostly in soil horizons, in the catchment area.

Table VI.3- Molar concentration ratios of trace elements to calcium in the calcite-precipitating fluids (calculated in this study) and the sea and stream waters (Drever 1982).

	$^{56}\text{Fe}/^{40}\text{Ca}$	$^{55}\text{Mn}/^{40}\text{Ca}$	$^{24}\text{Mg}/^{40}\text{Ca}$
Parent fluids (max)	0.066813	0.001796	1.025253
Parent fluids (avg)	0.034377	0.00042	0.397272
Parent fluids (min)	0.0148	0.000059	0.116681
Sea water	3.49 E^{-04}	3.55 E^{-07}	5.1748
Stream water	0.00197	0.0003997	0.429

A point worth mentioning, is that a fresh water origin is also suggested even if extreme values of distribution coefficients are used. The molar concentration ratios of trace elements to calcium, which are calculated by using $D_{\text{Fe}} = 20$, $D_{\text{Mn}} = 30$ and $D_{\text{Mg}} = 0.013$, are listed in table VI.4.

The fresh water origin proposed in this study supports the interpretation of Hutcheon et al. (1985) who acknowledged the strong influence of fresh waters on the composition of the poikilotopic calcite cement in the Avalon Formation, Hibernia

field (see section I.6.5). Hutcheon et al. (1985) suggested an influx of meteoric water, via the mid-Cretaceous unconformity, into sandstones of the Avalon Formation, Hibernia field. Hutcheon et al. added that this influx occurred when the sandstones were buried at a depth of 400-600 meters. On the other hand, Lee (1987) pointed out that the calcite-precipitating fluids had a composition similar to the sea water that has been slightly diluted by meteoric water. Lee reported low values of $\delta^{18}\text{O}$ {-3 to -8‰ (PDB)} for the poikilotopic calcite cement¹ and therefore suggested that the precipitation of calcite occurred at elevated temperatures (40-60 °C) and at a depth of 2.2 kilometres.

The loose packing of the calcite-cemented beds in the Avalon Formation⁵, on the contrary, suggests much shallower depths of calcite cementation. The present study highlights several unconformities, associated with relative sea level falls and valley incisions, within the Avalon Formation (See section IV.2.2). The development of each of these

¹The low values of $\delta^{18}\text{O}$ can be attributed to the influence of fresh waters rather than high temperatures. A negative correlation between $\delta^{18}\text{O}$ and $\text{Fe}^{2+}/\text{Ca}^{2+}$ is presented by Lee (1987; figure 19; page 105). This negative correlation suggests on the contrary a fresh water origin for the calcite-precipitating fluids.

⁵Abid (1988) reported high (>25%) minus cement porosity in the poikilotopic calcite-cemented sandstones of the Avalon Formation, Hibernia field. Abid therefore suggested an early stage of precipitation of the poikilotopic calcite cement.

unconformities might have contributed to the total influx of fresh waters into the Avalon Formation. The sandstones were then buried at depths in the order of tens of meters. These shallow burial depths accounts for the loose packing of the calcite-cemented beds.

Table VI.4- Extreme molar concentration ratios of trace elements to calcium in the calcite-precipitating fluids (calculated in this study) and the sea and stream waters (Drever 1982).

	"Fe/"Ca	"Mn/"Ca	"Mg/"Ca
Parent fluids (max)	0.003340	0.000359	2.365969
Parent fluids (avg)	0.001718	0.000084	0.916784
Parent fluids (min)	0.00074	0.000011	0.269264

VI.6- TECTONICS & FLUID FLOW

Poikilotopic calcite cements were precipitated from fresh waters. The latter were recharged into the Avalon Sandstones during periods of cessation of fault activity, regional uplift (see section IV.2.2) and emergence of the Hibernia rollover anticline (Figure VI.14).

During these periods of emergence, fresh waters infiltrated through the Avalon Sandstones and flowed towards

the S and SW resulting in extensive calcite cementation in the lower Sandstones. These flow trends are suggested by the gradients in trace element concentrations in the poikilotopic calcite (figures VI.9, 10 & 12). A structural dip of about 0.066° (see section VI.4.1) supported the fresh water flow towards S and SW.

VI.7- CONTROLS ON CALCITE CEMENTATION

VI.7.1- FACIES CONTROL:

Calcite cementation is associated with facies that contain carbonate bioclastic debris and/or early marine calcite cements. The Intraclastic Sandstone Facies represents the most favourable host for calcite cementation, because of the highest abundance of pre-existing carbonate grains.

VI.7.2- STRATIGRAPHIC CONTROL:

Laterally extensive calcite cementation occurs in transgressive barrier island sandstones, shortly above the Barremian unconformity (figure VI.3). These barrier island sandstones offer a laterally continuous permeability conduit. They overlie impervious lagoonal and soil mudstones and underlie impervious shallow marine mudstones, for the most part. Therefore, the barrier island sandstones provide a favourable confined aquifer for accumulation and flow of the calcite-precipitating fluids.

VI.7.3- STRUCTURAL & TECTONIC CONTROLS:

The calcite-cementing fluids infiltrated through the Avalon Sandstones during uplift or emergence of the rollover anticline. Furthermore, the catchment area was closest to the crest of the rollover anticline in the NE. The fluids flowed downdip towards the S and SW (figures VI.9, 10 & 12).

VI.7.4- FRACTURE CONTROL:

Any fractures along the main permeability conduits are expected to provide secondary routes for flow of the calcite-cementing fluids. The potential role of fractures in fluid flow is still to be investigated.

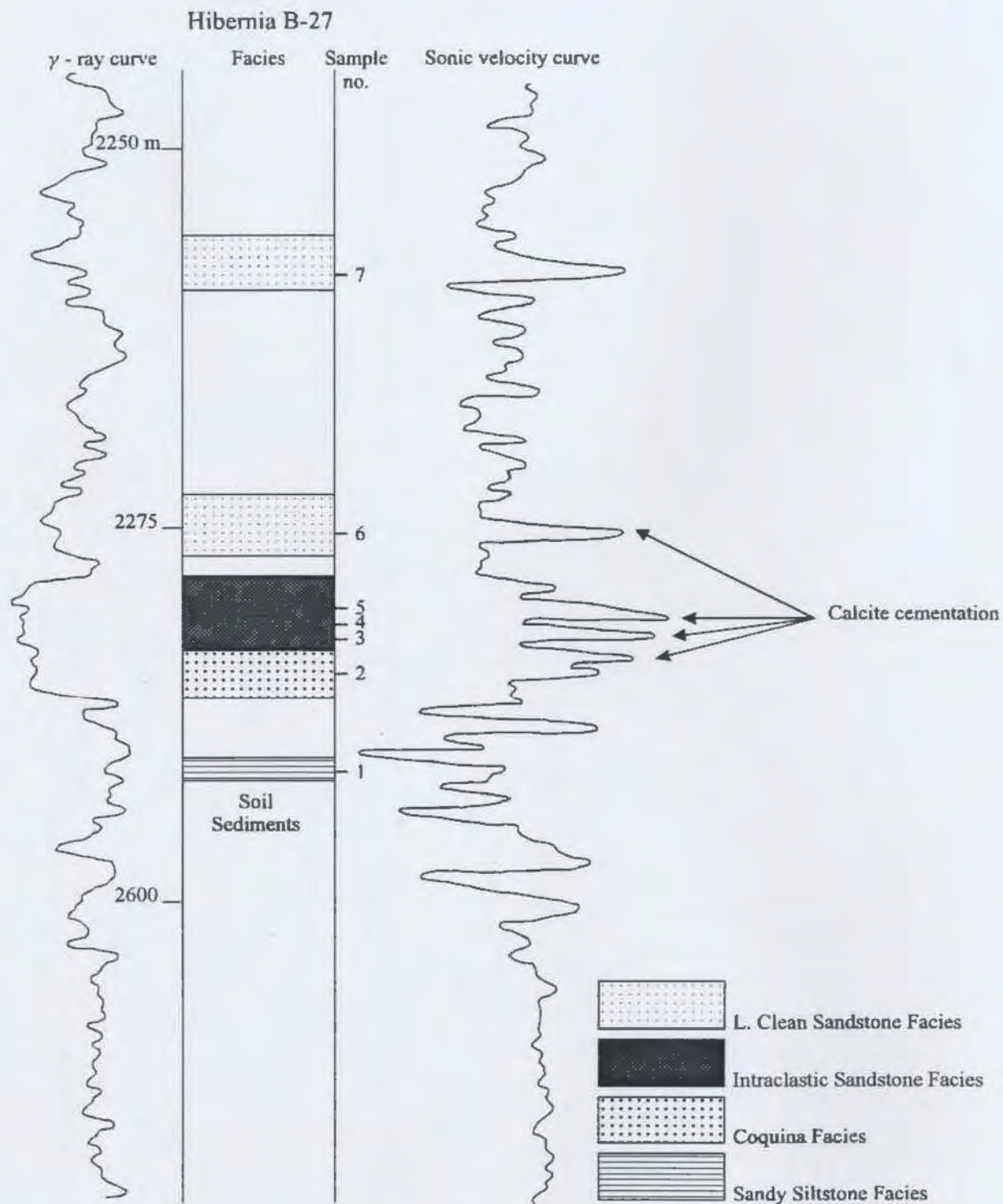


Figure VI.1- Distribution of calcite cementation in the Hibernia B-27 well.

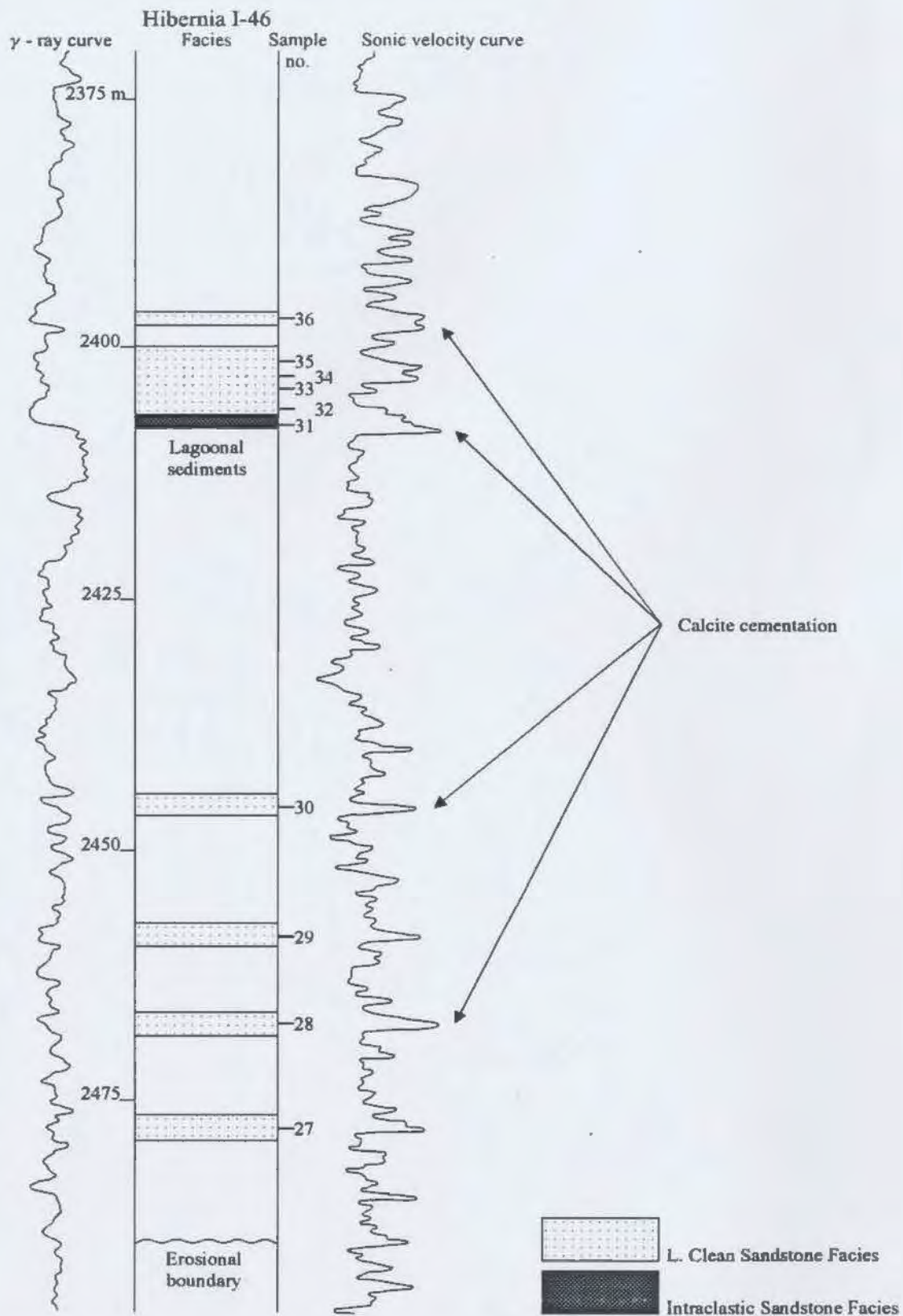


Figure VI.2- Distribution of calcite cementation in the Hibernia I-46 well.

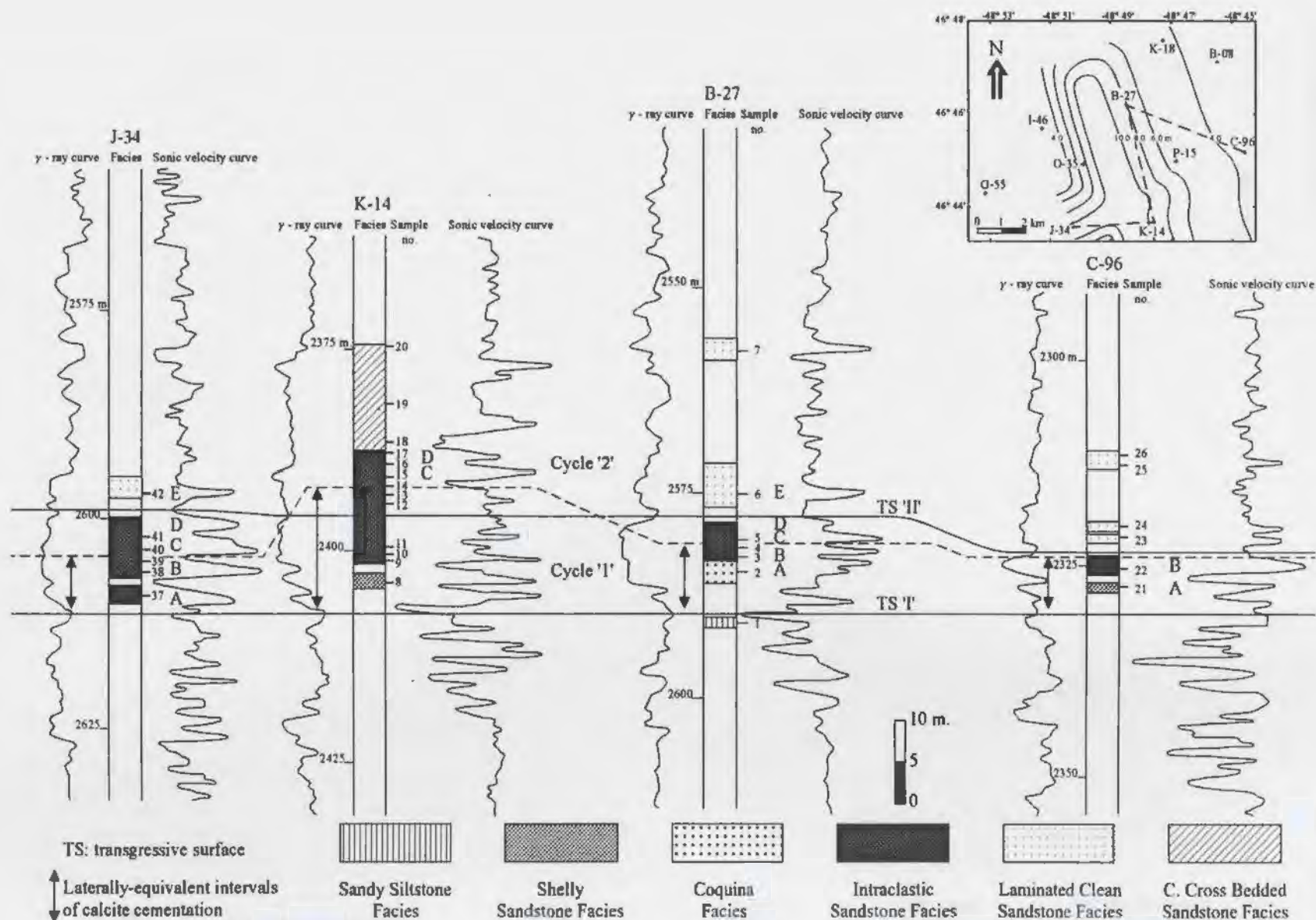


Figure VI.3- Sonic log correlation showing laterally-extensive calcite-cemented beds occurring in the barrier island sandstone body, which is confined between the transgressive surfaces 'I' and 'II'. A sand isolith map of this barrier island sandstone body is depicted in the upper right-hand side. Note that the calcite-cemented beds 'A' and 'B' diverge to a larger number of beds in the K-14 well.

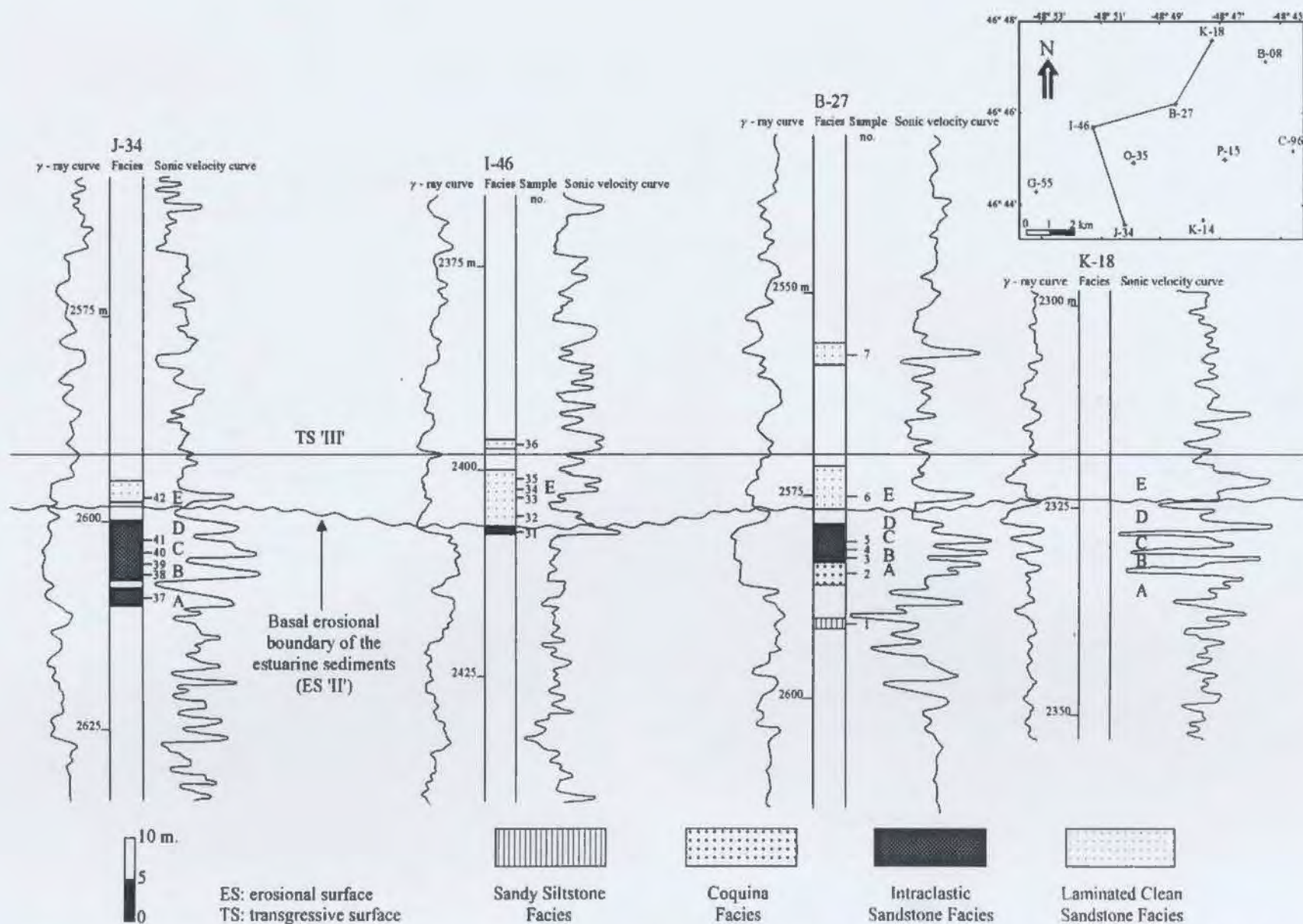


Figure VI.4- Sonic log correlation showing a laterally-extensive calcite-cemented bed 'E' occurring in the Laminated Clean Sandstone Facies.

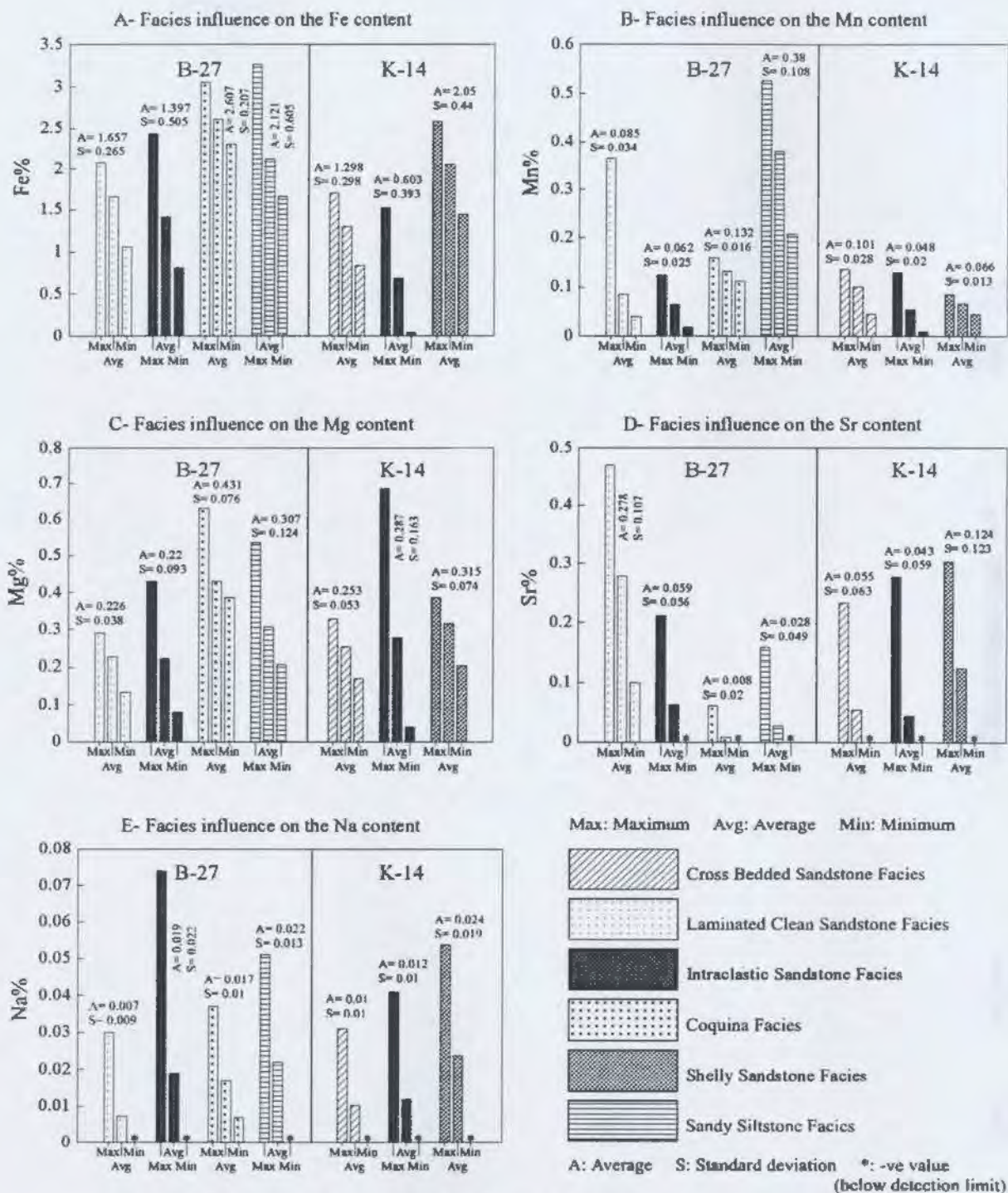


Figure VI.5- Facies influence on composition of the poikilotopic calcite cement, Avalon Formation, Hibernia B-27 and K-14 wells. The Intralastic Sandstone Facies changes in composition between the two wells. Note the negative values of Sr and Na (negative values, i.e. below detection limits, are plotted as zero).

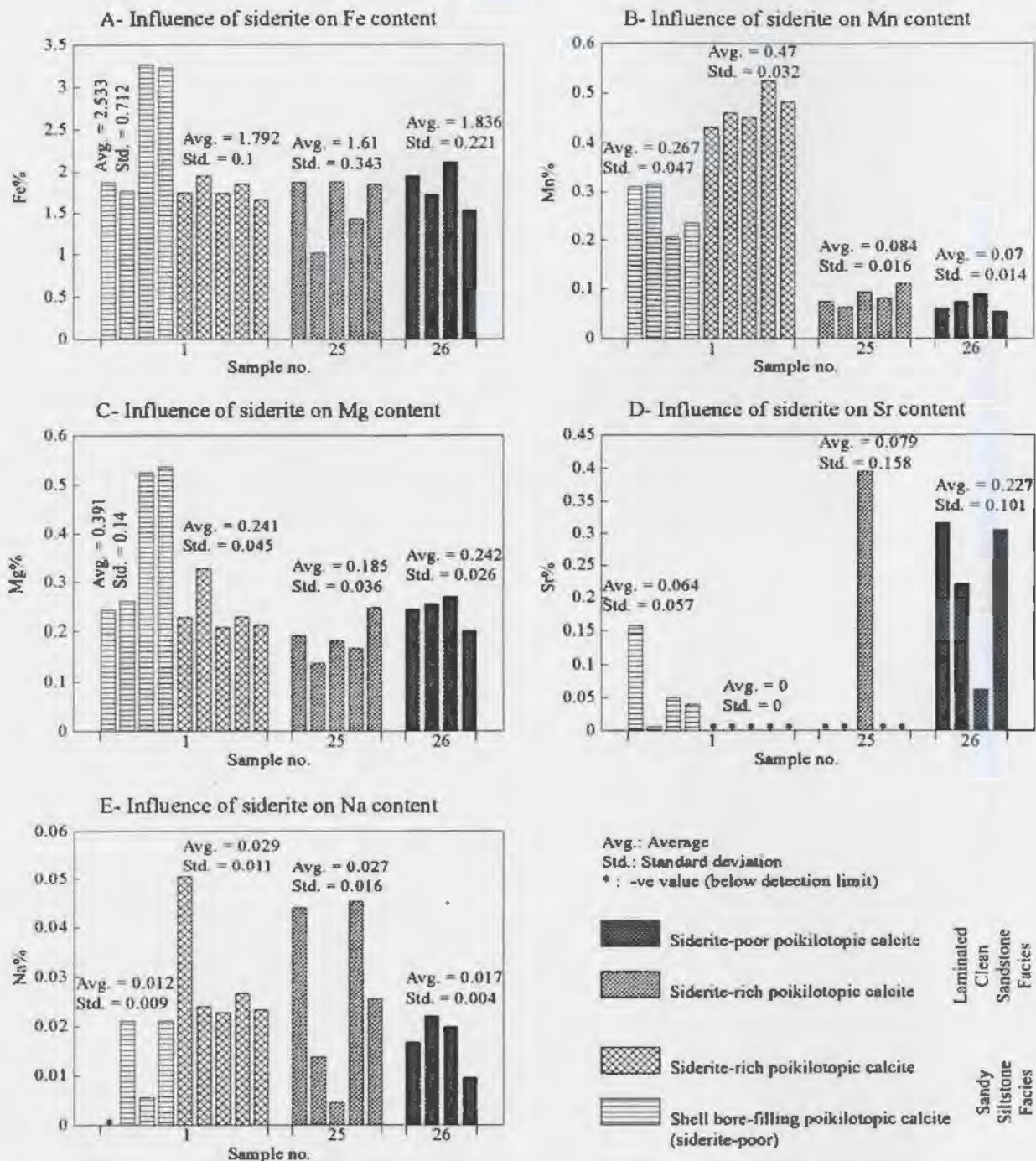


Figure VI.6- Siderite influence on composition of the poikilotopic calcite cement in the Sandy Siltstone and Laminated Clean Sandstone Facies, Avalon Formation, Hibernia field. Note the negative values, i.e. below detection limits, of the Sr and Na (plotted as zero).

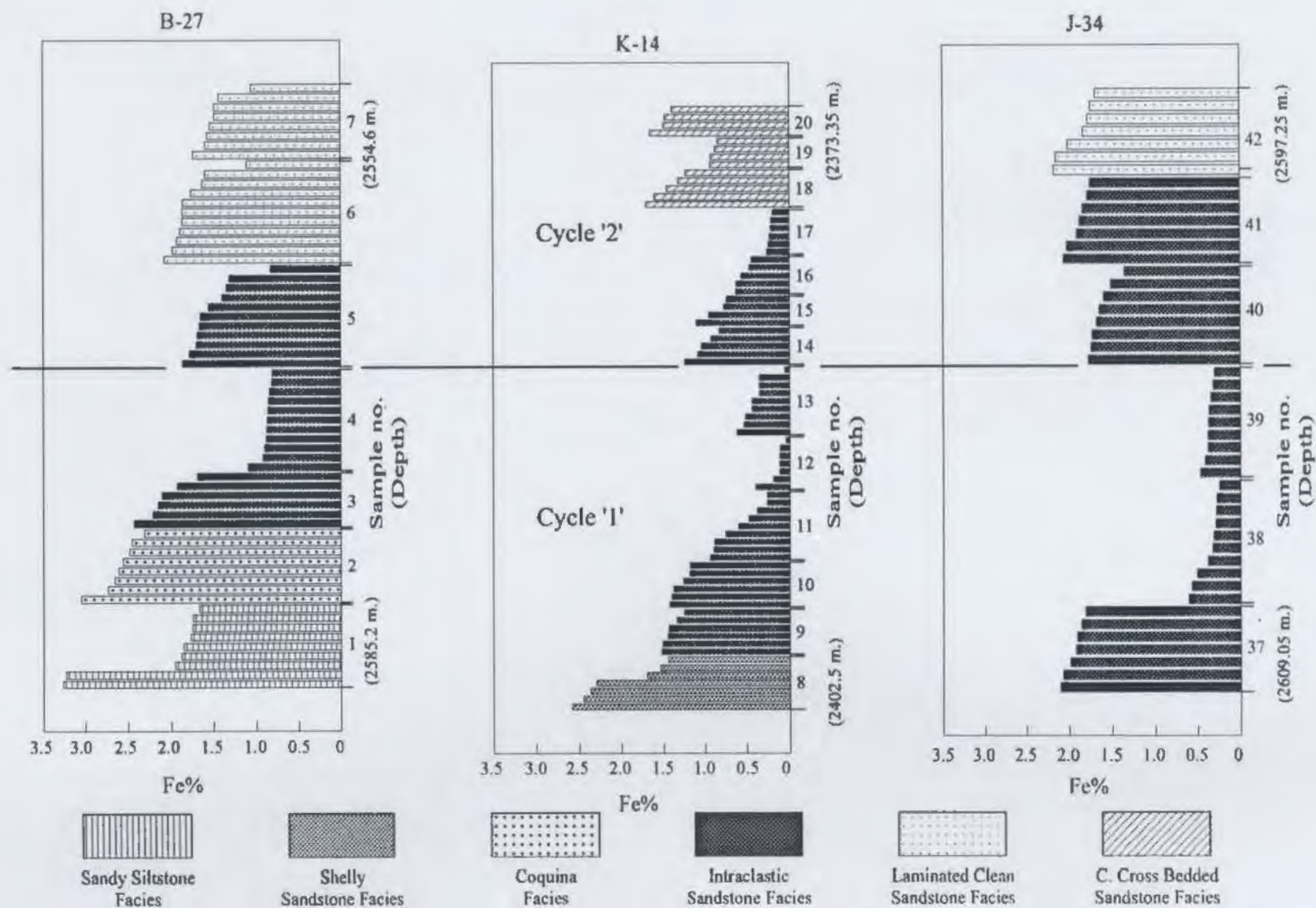


Figure VI.7- Correlation of two vertical cycles of Fe concentration in the poikilotopic calcite cement in the B-27, K-14 and J-34 wells. Note that the boundary between the two cycles occurs in the Intralastic Sandstone Facies. See the sample distribution in figure VI.3.

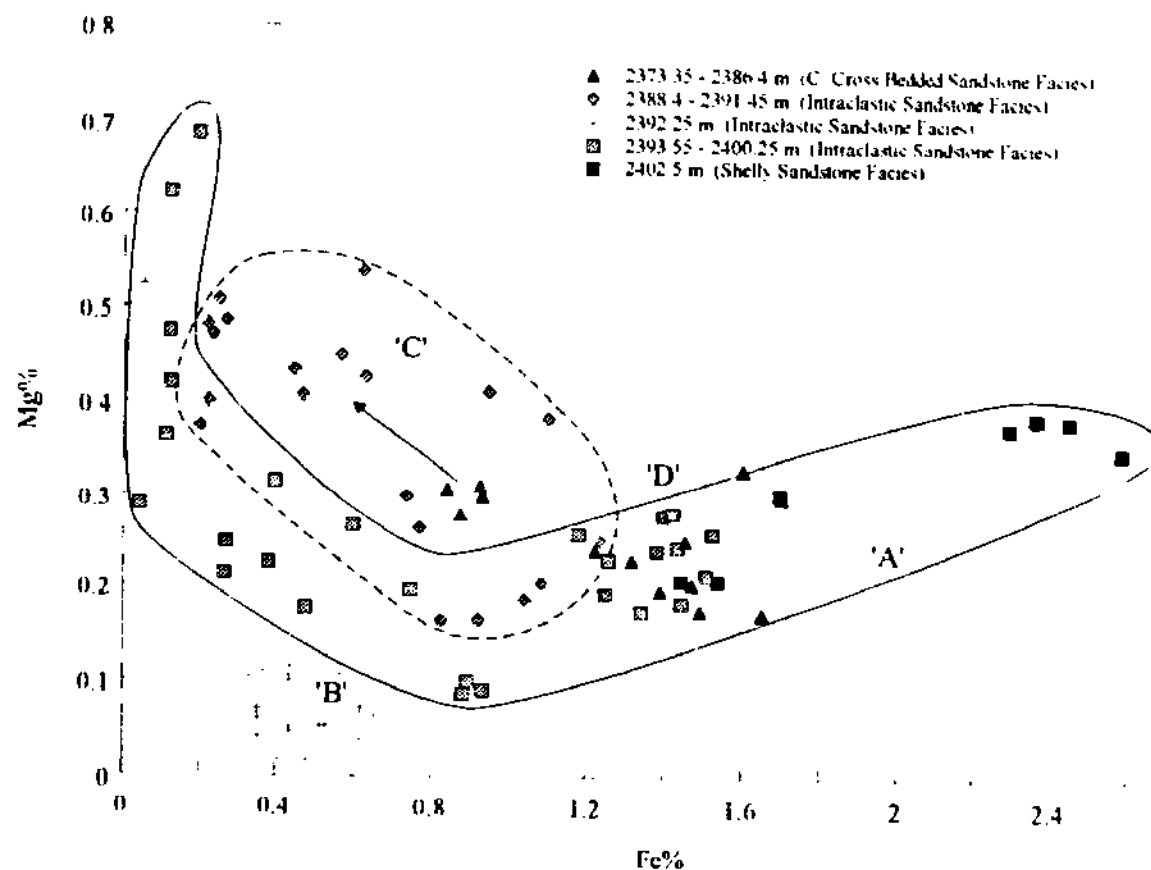


Figure VI 8- Fe% versus Mg% in poikilotopic calcite cement in the K-14 well. Four populations (A-D) exist at different depths. Differentiation between populations 'C' and 'D' is controlled by facies. Population 'C' occurs in the Intraclastic Sandstone Facies, which hosts abundant bioclastic debris and early marine calcite cements. The arrow indicates the direction of differentiation due to increasing abundance of the pre-existing carbonates.

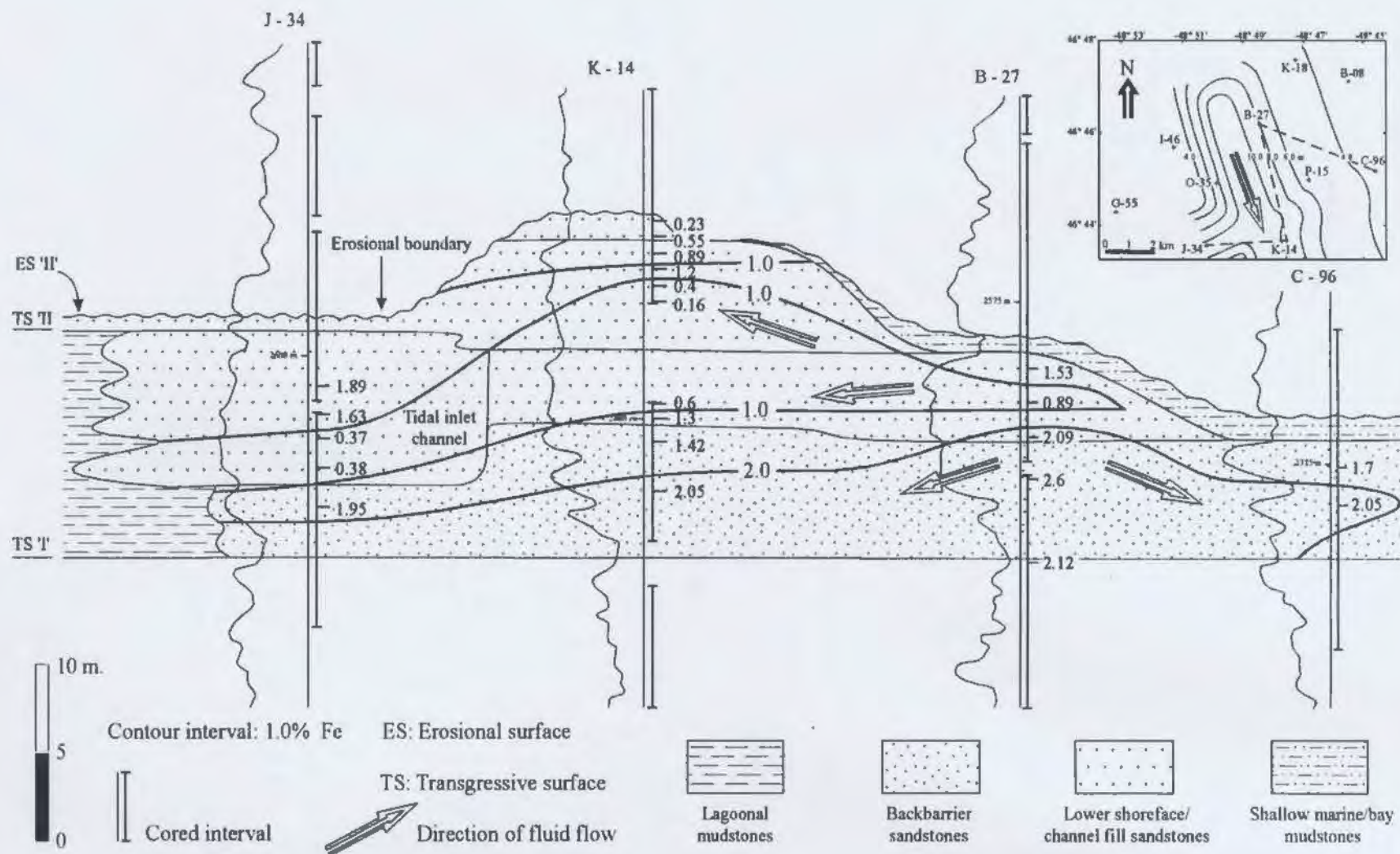


Figure VI.9- Isoconcentration lines of Fe content in the poikilotopic calcite cement in two stacked barrier island sandstone bodies. A sand isolith map of the lower barrier, below TS'II', is depicted in the upper right hand side. The highest concentrations of Fe occur in the B-27 well, which is closest to the source of calcite-precipitating fluids. The arrows illustrate the flow trends of these fluids. Note the diversion of the isoconcentration lines towards the K-14 well.

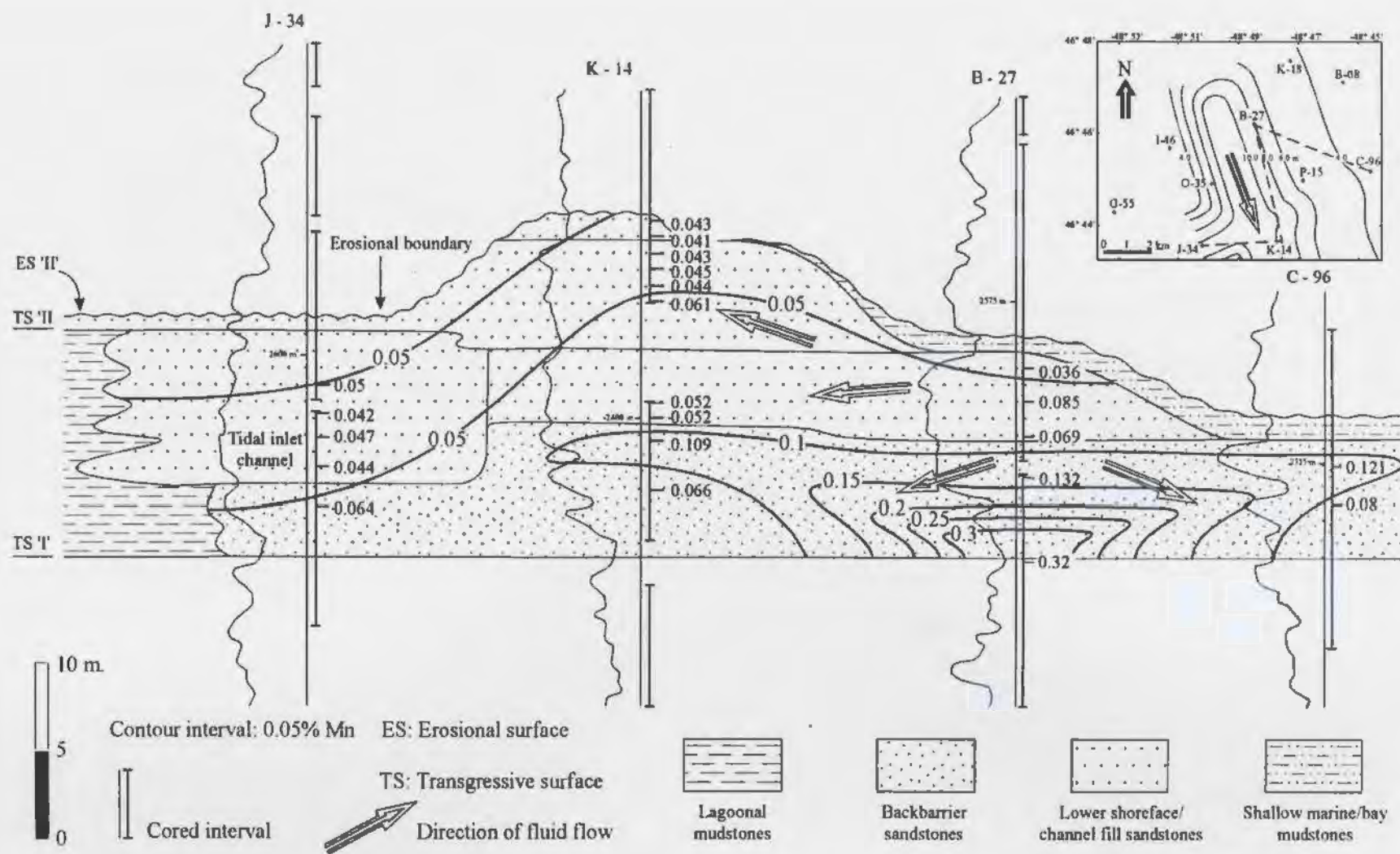


Figure VI.10- Isoconcentration lines of Mn content in the poikilotopic calcite cement in two stacked barrier island sandstone bodies. A sand isolith map of the lower barrier, below TS'II', is depicted in the upper right hand side. The highest concentrations of Mn occur in the B-27 well, which is closest to the source of calcite-precipitating fluids. The arrows illustrate the flow trends of these fluids. Note the diversion of the isoconcentration lines towards the K-14 well.

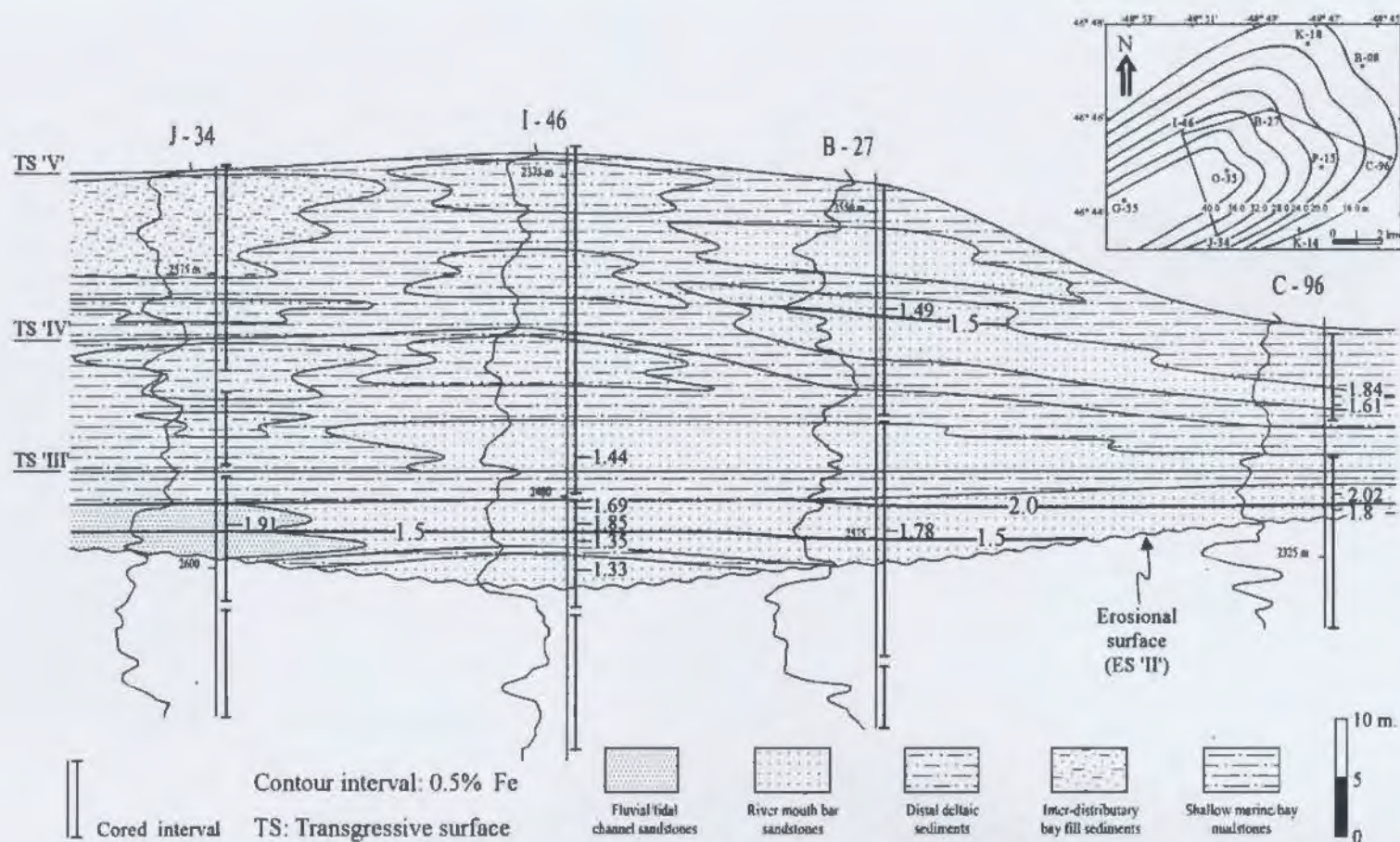


Figure VI.11- Isoconcentration lines of Fe content in the poikilotopic calcite cement in river mouth bar sandstone bodies. The lines reflect neither a clear trend of changing Fe concentration nor a conclusive direction of flow of the calcite-precipitating fluids. The continuity of calcite cementation between the B-27 and C-96 wells, in the upper river mouth bar sandstone body above TS 'IV', is questionable. An isopach map of the whole sediment package, between the basal erosional surface and TS 'V', is depicted in the upper right hand side.

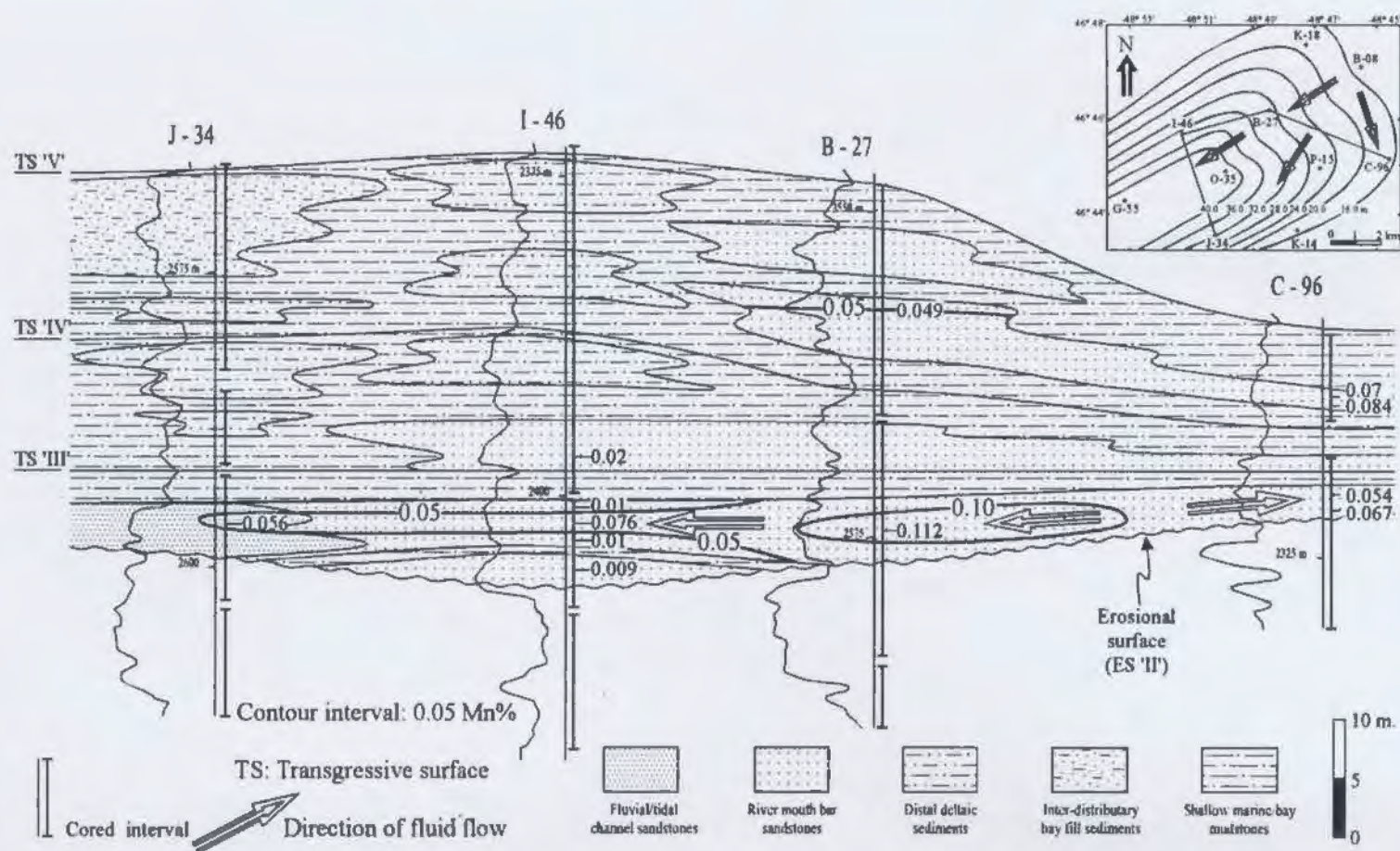


Figure VI.12- Isoconcentration lines of Mn content in the poikilotopic calcite cement in river mouth bar sandstone bodies. Highest concentrations of Mn in the lower sandstone body occur in the B-27 well, which is closest to the source of calcite-precipitating fluids. The continuity of calcite cementation between the B-27 and C-96 wells, in the upper sandstone body above TS 'IV', is questionable. An isopach map of the whole estuarine sediment package, between the basal erosional surface and TS 'V', is depicted in the upper right hand side. The arrows on the map illustrate inferred flow trends of the calcite-cementing fluids through the Hibernia field area.

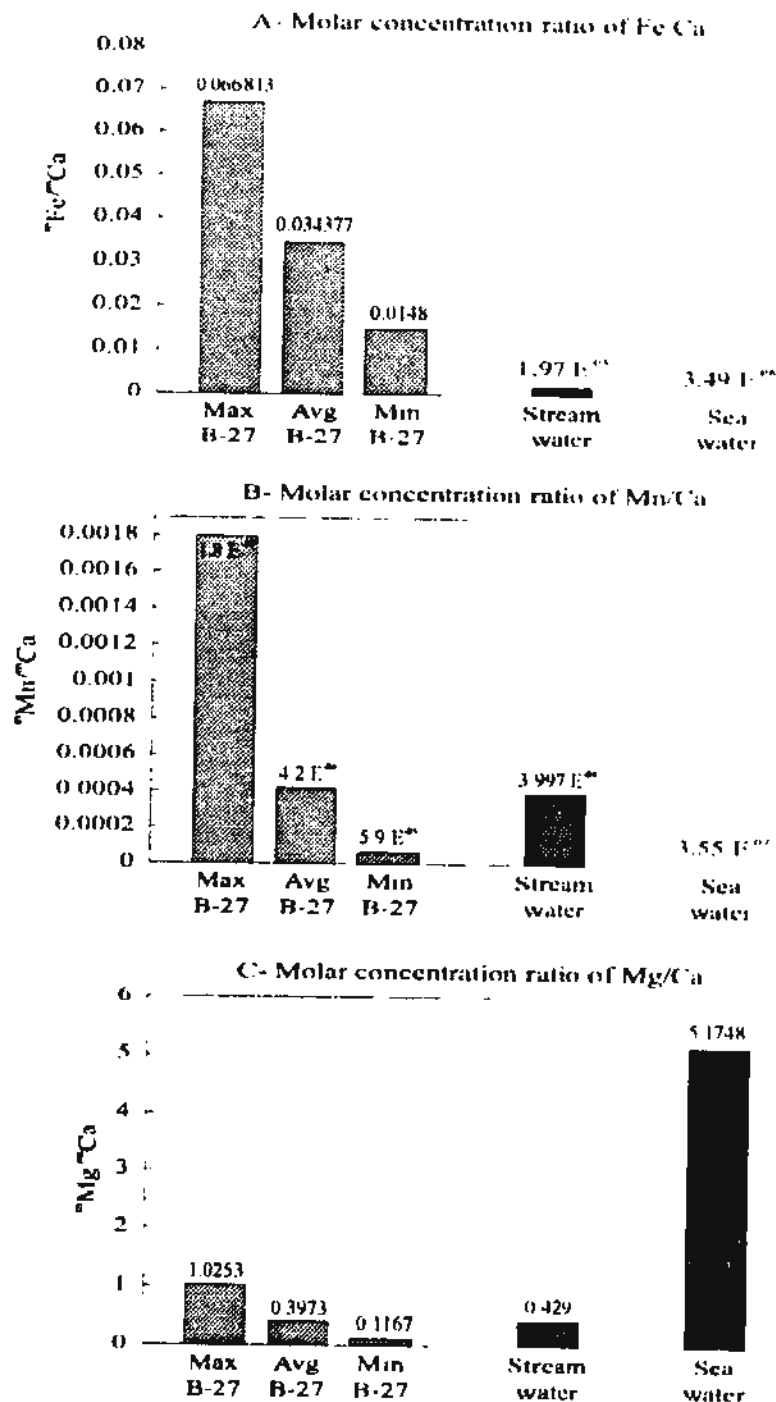


Figure VI.13- Comparison of estimated composition of the calcite-precipitating fluids in the B-27 well and compositions of stream and sea waters.

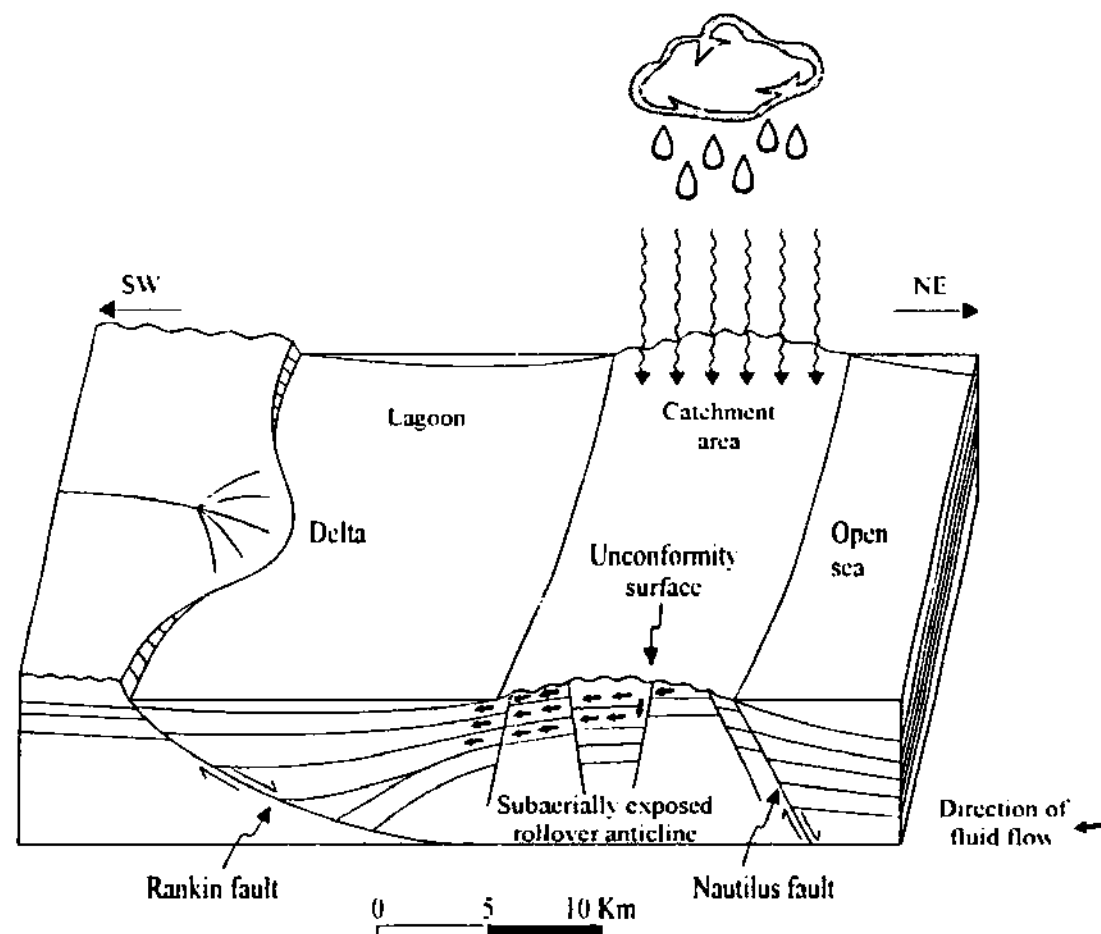


Figure VI.14- Recharge of fresh waters during emergence of the rollover anticline.
The underground water flowed dominantly towards the SW and S.

VII- SUMMARY & CONCLUSIONS

This study investigates the sedimentation and fluid flow patterns in the Avalon Formation, Hibernia field, Jeanne d'Arc rift basin. Such patterns are analyzed with respect to the tectonics and kinematics of the Hibernia rollover anticline.

Facies analysis of the cored intervals resulted in the recognition of fifteen facies. These facies were grouped into eight facies associations. Such associations were deposited in distinct environments including: lagoon/lake, transgressive barrier island, fluvial/tidal channel, river mouth bar, interdistributary bay, distal delta, shoreface and shallow shelf/open embayment. The facies associations are bounded by transgressive, erosional or subaerial exposure surfaces.

A facies and event correlation approach was used to match the facies associations and their bounding discontinuities. The correlation allowed the construction of stratigraphic cross sections and paleogeographic maps for successively younger intervals. These cross sections and maps as well as well log correlations reflect the repetitive development of estuarine and barrier island depositional systems.

The estuarine system occupied a structurally-controlled river valley. The valley was incised into the rollover anticline during regional uplift of the area. The estuarine system was established in the valley consequent to subsidence

induced by slip along the valley-bounding faults and flooding with sea water. The gradual acceleration of slip along these faults resulted in progressive deepening and deposition of retrogradational estuarine successions in the valley. Subsequent deceleration of fault slip caused deposition of progradational successions, gradual shoaling and filling of the valley. The fault activity that is associated with the development of the estuarine system marks the initiation of extension during a rifting episode.

The barrier island system was developed during submergence of the rollover anticline. This submergence resulted from active displacement along the Rankin growth fault. The barrier islands were oriented in a NW-SE direction diagonal to the axis of the rollover anticline. This orientation reflects a NE depositional slope and suggests some displacement along the Murre fault, as well. Displacements along the Rankin and the Murre faults caused environmental deepening and entrapment of the siliciclastic sediments close to the hinterland in the SW. Such displacements reflect an advanced stage of extension during the rifting episode.

Decline of extension was followed by a regional uplift and re-emergence of the rollover anticline. Resumption of extension caused the revival of the estuarine system, subsequent re-development of the barrier island system, and re-submergence of the rollover anticline.

Abundant marine and poikilotopic calcite cements occur in sandstones of the Avalon Formation. The poikilotopic calcite cement is a shallow burial diagenetic alteration. This alteration produced laterally extensive calcite-cemented beds in the barrier island and fluvial-river mouth bar sandstone bodies. These calcite-cemented beds are used to explore the fluid flow in the Hibernia rollover anticline.

Spatial variations in concentrations of trace elements in the poikilotopic calcite cement reflect different flow patterns of the calcite-precipitating fluids. In the barrier island sandstone bodies, the fluids flowed preferentially along the depositional strike, from the NW towards the SE. The flow was supported by an apparent structural dip of about 0.066° towards the SE. In the fluvial channel-river mouth bar sandstone bodies, the fluids flowed favourably along the depositional dip, from the NE towards the SW.

The concentrations of trace elements in the poikilotopic calcite cement suggest a fresh water origin for the calcite precipitating-fluids. These fluids infiltrated through the Avalon sediments during periods of emergence of the rollover anticline. The fluids flowed from the crest of the rollover anticline towards the SE, S and SW.

The facies factors that influenced flow of the calcite-precipitating fluids are expected to equally affect hydrocarbon movement and production from the Avalon reservoir.

VIII- REFERENCES

- Abid, I.A., 1988, Mineral diagenesis and porosity evolution in the Hibernia oil field, Jurassic-Cretaceous Jeanne D'Arc graben, eastern Grand Banks of Newfoundland, Canada (unpublished M.Sc. thesis): McGill University, Quebec, Canada, 280 p.
- Allen, G.P., 1991, Sedimentary processes and facies in the Gironde estuary: a recent model for macrotidal estuarine systems, in Smith, D.G., Reinson, G.E., Zaitlin, B.A., and Rahmani, R.A., eds., *Clastic tidal sedimentology: Canadian Society of Petroleum Geologists, Memoir no. 16*, p. 29-39.
- Allen, G.P., and Posamentier, H., 1994, Transgressive facies and sequence architecture in mixed tide- and wave-dominated incised valleys: examples from the Gironde estuary, France, in Dalrymple, R.W., Boyd, R., and Zaitlin, B.A., eds., *Incised valley systems: origin and sedimentary sequences: Society for Sedimentary Geology, Special Publication no. 51*, p. 225-240.
- Allmon, W.D., 1988, Ecology of Recent Turritelline Gastropods (prosobranchia, Turritellidae): current knowledge and paleontological implications: *Palaos*, v. 3, p. 259-284.
- Arthur, K.R., Cole, D.R., Henderson, G.G.L., and Kushnir, D.W., 1982, Geology of the Hibernia discovery, in Halbouty, M.T., ed., *The deliberate search for the subtle trap: American Association of Petroleum Geologists, Memoir no 32*, p. 181-195.
- Ascoli, P., 1990, Foraminiferal, ostracode and calpionellid zonation and correlation of 42 selected wells from the north Atlantic margin of North America: *Bulletin of Canadian Petroleum Geology*, v. 38, no. 4, p. 485-492.
- Bally, A.W., ed., 1983, Seismic expression of structural styles: *American Association of Petroleum Geologists, Studies in Geology no. 15*, v. 2.
- Barwis, J.H., and Makurath, J.H., 1978, Recognition of ancient tidal inlet sequences: an example from the Upper Silurian Keyser Limestone in Virginia: *Sedimentology*, v. 25, p. 61-82.

- Belknap, D.F., Kraft, J.C., and Dunn, R.K., 1994, Transgressive valley fill lithosomes: Delaware and Maine, in Dalrymple, R.W., Boyd, R., and Zaitlin, B.A., eds., Incised-valley systems: origin and sedimentary sequences: Society for Sedimentary Geology, Special publication no. 51, p. 303-320.
- Bernard, H.A., Le Blanc, R.J., Sr., and Major, C.F., 1962, Recent and Pleistocene geology of southeast Texas, field excursion no. 3, in Geology of the Gulf Coast and Guidebook of excursions: Geological Society of America, p. 174-224.
- Bhattacharya, J., and Walker, R.G., 1991, River and wave-dominated depositional systems of the Upper Cretaceous Dunvegan Formation, northwestern Alberta: Bulletin of Canadian Petroleum Geology, v. 39, no. 2, p. 165-191.
- Bilodeau, W.L., and Blair, T.C., 1986, Tectonics and sedimentation: timing of tectonic events using sedimentary rocks and facies: Geological Society of America Abstract Programs, no 18, p. 542.
- Birkeland, P.W., 1984, Soils and geomorphology: Oxford University Press, New York.
- Blair, T.C., 1987, Tectonic and hydrologic controls on cyclic alluvial fan, fluvial and lacustrine rift basin sedimentation, Jurassic-Lowermost Cretaceous Todos Santos Formation, Chiapas, Mexico: Journal of Sedimentary Petrology, v. 57, p. 845-862.
- Blair, T.C., 1988, Development of tectonic cyclothems in rift, pull-apart and foreland basins: sedimentary response to episodic tectonism: Geology, v. 16, p. 517-520.
- Blundell, D.J., 1978, A gravity survey across the Gardar igneous province, southwest Greenland: Journal of the Geological Society of London, v. 135, p. 545-554.
- Bodine, M.W., Holland, H.D., and Borcsik, M., 1965, Co-precipitation of manganese and strontium with calcite, in Symposium on problems of postmagmatic ore deposition, II: Prague, p. 401-406.

- Boersma, J.R., 1991, A large flood tidal delta and its successive spillover apron: detailed proximal-distal facies relationships (Miocene Lignite Suite, lower Rhine Embayment, Germany), in Smith, D.G., Reinson, G.E., Zaitlin, B.A., and Rahmani, eds., *Clastic tidal sedimentology: Canadian Society of Petroleum Geologists, Memoir no. 16*, p. 227-253.
- Boles, J.R., 1987, Six million year diagenetic history, North Coles Levee, San Joaquin basin, California, in Marshal, J.D., ed., *Diagenesis of sedimentary sequences: Geological Society Special Publication no. 36*, p. 191-200.
- Bown, T.M., and Kraus, M.J., 1987, Integration of channel and floodplain suites in aggrading alluvial systems, I. Developmental sequence and lateral relations of lower Eocene alluvial paleosols, Willwood Formation, Bighorn Basin, Wyoming: *Journal of Sedimentary Petrology*, v. 57, p. 587-601.
- Brand, U., and Veiser, J., 1980, Chemical diagenesis of a multicomponent carbonate system, I: trace elements: *Journal of sedimentary petrology*, v. 50, p. 1219-1236.
- Brenchley, P.J., Romano, M., and Marco, J.C.G., 1986, Proximal and distal Hummocky cross-stratified facies on a wide Ordovician shelf in Iberia, in Knight, R.J., and McLean, J.R., eds., *Shelf sands and sandstones: Canadian Society of Petroleum Geologists, Memoir II*, p. 241-255.
- Brownridge, S., and Moslow, T.F., 1991, Tidal estuary and marine facies of the Glauconitic Member, Drayton Valley, central Alberta, in Smith, D.G., Reinson, G.E., Zaitlin, B.A., and Rahmani, R.A., eds., *Clastic tidal sedimentology: Canadian Society of Petroleum Geologists, Memoir no. 16*, p. 107-122.
- Buelter, D.P., and Guillemette, R.N., 1988, Geochemistry of epigenetic dolomite associated with lead-zinc mineralization of the Viburnum Trend, southeast Missouri: A reconnaissance study, in Shukla, V., and Baker, P.A., eds., *Sedimentology and geochemistry of dolostones: Society of Economic Paleontologists and Mineralogists, Special Publication no. 43*, p. 85- 93.
- Cartwright, J., 1991, The kinematic evolution of the Coffee Soil fault, in Roberts, A.M., Yielding, A.M., and Freeman, B., eds., *The geometry of normal faults: Geological Society Special Publication n. 56*, p. 29-40.

- Chaplin, C.E., 1979, Evolution of the Rio Grand rift, a summary, in Reicher, R.E., ed., Tectonics and magmatism: American Geophysical Union, Washington, D.C., p. 1-5.
- Chaplin, C.E., 1985, Cements of the Avalon Zone, Hibernia field, petrographic study: Mobil internal report, 15 p.
- Clifton, H.E., 1981, Progradational sequences in Miocene Shoreline deposits, southeastern Caliente range, California: Journal of Sedimentary Petrology, v. 51, p. 165-184.
- CNOBP (Canada Newfoundland Offshore Petroleum Board), 1986, Decision 86.01, Application for approval, Hibernia, Canada-Newfoundland Benefits plan, Hibernia development plan.
- CNOBP, 1990, Schedule of wells, Newfoundland offshore area.
- Coleman, J.M., Prior, D., and Lindsay, J.F., 1983, Deltaic influences on shelf edge instability processes, in Stanley, D.J., and Moore, G.T., eds., The shelf break: critical interface on continental margins: Society of Economic Paleontologists and Mineralogists, Special Publication no. 33, p. 121-137.
- Collinson, J.D., 1969, The sedimentology of the Grindslow Shales and the Kinderscout Grit: a deltaic complex in the Namurian of northern England: Journal of Sedimentary Petrology, v. 39, p. 194-221.
- Cooper, J.A.G., 1993, Sedimentation in a river-dominated estuary: Sedimentology, v. 40, p. 979-1017.
- Curtis, C.D., Pearson, M.J., and Somogy, V.A., 1975, Mineralogy, chemistry, and origin of concretionary siderite sheet (clay-ironstone band) in the Westphalian of Yorkshire: Mineralogical Magazine, v. 40, p. 385-393.
- de Charpal, O., Guennoc, P., Motadert, L., and Roberts, D.G., 1978, Rifting, crustal attenuation and subsidence in the Bay of Biscay: Nature, v. 275, p. 706-711.
- Demarest, J.M., 1981, Genesis and preservation of Quaternary paralic deposits on Delmarva Peninsula: unpublished Ph.D. Dissertation, Department of Geology, University of Delaware, Newark, 240 p.

- Demarest, J.M., Biggs, R.B., Kraft, J.C., 1981, Time stratigraphic aspects of a formation: interpretation of surficial Pleistocene deposits by analogy with Holocene paralic deposits, southeastern Delaware: *Geology*, v. 9., p. 360-365.
- Demarest, J.M., and Kraft, J.C., 1987, Stratigraphic record of Quaternary sea levels: implications for more ancient strata, in Nummedal, D., Pilkey, O.H., and Howard, J.D., eds., *Sea level fluctuation and coastal evolution: Society of Economic Paleontologists and Mineralogists, Special Publication no. 41*, p. 223-239.
- Dickson, J.A.D., 1966, Carbonate identification and genesis as revealed by staining: *Journal of Sedimentary Petrology*, v. 36, p. 491-505.
- Dickson, J.A.D., 1990, Carbonate mineralogy and chemistry, in Tucker, M.E., and Wright, V.P., *Carbonate sedimentology: Blackwell Scientific Publication*, p. 284-313.
- Donaldson, A.C., Martin, R.H., and Kanes, W.H., 1970, Holocene Guadalupe delta of Texas Gulf Coast, in Morgan, J., and Shaver, R.H., eds., *Deltaic Sedimentation, modern and ancient: Society of Economic Paleontologists and Mineralogists, Special Publication no. 15*, p. 107-137.
- Donselaar, M.E., 1989, The Cliff House Sandstone, San Juan Basin, New Mexico: model for the stacking of transgressive barrier complexes: *Journal of Sedimentary Petrology*, v. 59, no.1, p. 13-27.
- Dott, R.H. Jr., and Bourgeois, J., 1982, Hummocky stratification: significance of its variable bedding sequences: *Geological Society of America, Bulletin* v. 93, p. 663-80.
- Doust, H., and Omatsola, E., 1990, Niger Delta, in Edwards, J.D., and Santogrossi, P.A., *Divergent/passive margin basins: American Association of Petroleum Geologists, Memoir no. 48*, p. 201-238.
- Drever, J.I., 1982, *The geochemistry of natural waters: Prentice Hall, Englewood Cliffs, N.J.*, 388 p.

- Driscoll, N.W., Hogg, J.R., Christie-Blick, N., and Karner, G.D., 1995, Extensional tectonics in the Jeanne d'Arc basin, offshore Newfoundland: implications for the timing of break-up between Grand Banks and Iberia, in Scrutton, R.A., Stoker, M.S., Shimmield, G.B., and Tudhope, A.W., eds., The tectonics, sedimentation and palaeoceanography of the north Atlantic region: Geological Society Special Publication no. 900, p. 1-28.
- Duchaufour, P., 1982, *Pedology*: Allen & Unwin, London.
- Duke, W.L., Fawcett, P.J., and Brusse, W.C., 1991, Prograding shoreline deposits in the lower Silurian Medina Group, Ontario and New York: Storm and tide-influenced sedimentation in a shallow epicontinental sea, and the origin of enigmatic shore-normal channels encapsulated by open shallow marine deposits, in Swift, D.J.P., Oertel, G.F., Tillman, R.W., and Thorn, J.A., eds., Shelf sands and sandstone bodies; geometry, facies and sequence stratigraphy: International Association of Sedimentologists, Special Publication no 14, p. 339-375.
- Dula, W.F., Jr., 1991, Geometric models of listric normal faults and rollover folds: American Association of Petroleum Geologists Bulletin, v. 62, p. 1-39.
- Edwards, M.B., 1981, Upper Wilcox Rosita Delta system of south Texas: growth-faulted shelf edge deltas: American Association of Petroleum Geologists Bulletin, v. 65, p. 45-73.
- Elliott, T., 1974, Interdistributary bay sequences and their genesis: Sedimentology, v. 21, p. 611-622.
- Elliott, T., 1986, Siliciclastic shorelines, in Reading, H.G., Sedimentary environments and facies: Blackwell Scientific Publications, p. 155-188.
- Enachescu, M.E., 1987, Tectonic and structural framework of the northeast Newfoundland continental margin, in Beaumont, C., and Tankard, A.J., eds., Sedimentary basins and basin-forming mechanisms: Canadian Petroleum Geology, Memoir no. 12, p. 117-147.

- Eschard, R., Ravenne, C., Houel, P., and Knox, R., 1991, Three dimensional reservoir architecture of a valley fill sequence and a deltaic aggradational sequence: influence of minor relative sea level variations (Scalby Formation, England), in Miall, A.D., and Tyler, N., eds., Three-dimensional facies architecture of the terrigenous clastic sediments and its implications for hydrocarbon discovery and recovery: Society for Sedimentary Geology, Concepts in Sedimentology and Paleontology, v. 3, p. 133-147.
- Evamy, B.D., Haremboure, J., Kamerling, P., Knaap, W.A., Molloy, A. and Rowlands, P.H., 1978, Hydrocarbon habitat of Tertiary Niger delta: American Association of Petroleum Geology Bulletin, v. 62, p. 1-39.
- Faller, A.M., Soper, N.J., 1979, Paleomagnetic evidence for the origin of the coastal flexure and dyke swarm in central east Greenland: Journal of the Geological Society of London, v. 135, p. 737-744.
- Fallow, W.C., 1973, Depositional environments of marine Pleistocene deposits in southeastern North Carolina: Geological Society of America, Bulletin v. 84, p. 257-268.
- Fastovsky, D.E., 1987, Paleoenvironments of vertebrate-bearing strata during the Cretaceous-Paleogene transition, eastern Montana and western Dakota: Palaios, v. 2, p. 282-295.
- Feldman, R.M., Palubnoik, D.S., 1975, Paleoecology of Maestrichtian oyster assemblage in the Fox Hills Formation: Geological Association of Canada, Special Paper, v. 6, p. 44-58.
- Flores, R.M., 1979, Restored stratigraphic cross sections and coal correlation in the Tongue River Member of the Fort Union Formation, Poeder River area, Montana: US Geological Survey Map, MF-1127.
- Frazier, D.E., 1967, Recent deltaic deposits of the Mississippi river: their development and chronology: Transactions of the Gulf Coast Association of the Geological Societies, v. 17, p. 287-315.
- Gagliano, S.M., and Van Beek, J.L., 1970, Geologic and geomorphic aspects of deltaic processes, Mississippi delta system, in hydrologic and geologic studies of coastal Louisiana: Centre for Wetland Resources, Louisiana State University, report no. 1, 140 p.

- Galloway, W.E., 1986, Reservoir facies architecture of microtidal barrier systems: American Association of Petroleum Geologists Bulletin, v. 70, p. 787-808.
- Gautier, D.L., 1982, Siderite concretions: indicators of early diagenesis in the Gammon Shale (Cretaceous): Journal of Sedimentary Petrology, v. 52, p. 859-871.
- Gibbons, K., Hellem, T., Kjemperud, A., Nio, S.D., and Veberstad, 1993, Sequence architecture, facies development and carbonate-cemented horizons in the troll field reservoir, offshore Norway, in Ashton, M., ed., Advances in reservoir geology: Geological Society Special Publication no. 69, p. 1-31.
- Gould, H.R., 1970, The Mississippi delta complex, in Morgan, J.P., ed., Deltaic sedimentation: modern and ancient: Society of Economic Paleontologists and Mineralogists, Special Publication no 15, p. 3-30.
- Grant, A.C., McAlpine, K.D., and Wade, J.A., 1986, The continental margin of eastern Canada: Geological framework and petroleum potential, in Halbouty, M.T., ed., Future petroleum provinces of the world: American Association of Petroleum Geologists, Memoir no. 40, p. 177- 205.
- Grant, A.C., and McAlpine, K.D., 1990, The continental margin around Newfoundland, in Keen, M.J., and Williams, G.L., eds., Geology of the continental margin of Eastern Canada: Geological Survey of Canada, Geology of Canada, no 2, p. 239-292.
- Groshong, R.H. Jr., 1989, Half graben structures: balanced models of extensional fault-bend folds: Geological Society of America Bulletin, v. 101, p. 96-105.
- Guilbault, J.P., and Vervloet, C.C., 1983, Microfossil paleoecology in the Hibernia I-46 cores: File note, Gulf Canada Resources, Geological research and services.
- Guilbault, J.P., 1986, Foraminiferal and ostracodal paleoecology of 5 cores from the Avalon Sand, Hibernia Field, Grand Banks: Mobil report G-19.55, 37 p.

- Haq, B.U., Hardenbol, J., and Vail, P.R., 1988, Mesozoic and Cenozoic chronostratigraphy and eustatic cycles, in Wilgus, C.K., Posamentier, H., Ross, C.A., and Kendall, C.G.St.C., eds., Sea level changes: an integrated approach: Society of Economic Paleontologists and Mineralogists, Special Publication no. 42, p. 71-108.
- Hayes, M.O., and Kana, T.W., 1976, Terrigenous clastic depositional environments: University of South Carolina, Department of Geology, Coastal Research Division, technical report no. 11-CRD, 302 p.
- Heron Jr., S.D., Moslow, T.F., Berelson, W.M., Herbert, J.R., Steele III, G.A., and Susman, K.R., 1984, Holocene sedimentation of a wave-dominated barrier-island shoreline: Cape Lookout, North Carolina: Marine Geology, v. 60, p. 413-434.
- Hiscott, R.N., Wilson, R.C.L., Gradstein, F.M., Pujalte, V., Garcia-Mondejar, J., Boudreau, R.R., and Wishart, H.A., 1990, Comparative stratigraphy and subsidence history of Mesozoic rift basins of North Atlantic: American Association of Petroleum Geologists Bulletin, v. 74, p. 60-76.
- Hopkins, S.H., 1956, Notes on the boring sponges in Gulf Coast estuaries and their relation to salinity: Bulletin of Marine Science, Gulf and Caribbean, v. 6, p. 44-58.
- Horne, J.C., Ferm, J.C., Caruccio, F.T., and Baganz, B.P., 1978, Depositional models in coal exploration and mine planning in the Appalachian region: American Association of Petroleum Geologists Bulletin, v. 62, p. 2379-2411.
- Howard, J.D., and Reineck, H-E., 1981, Depositional Facies of High energy beach-to-offshore sequence: composition with low-energy sequence: American Association of Petroleum Geologists Bulletin, v. 65, no. 5, p. 807-830.
- Hubbard, R.J., Pape, J., and Roberts, D.J., 1985, Depositional sequence mapping to illustrate the evolution of a passive continental margin, in Berg, O.R., and Woolverton, D., eds., Seismic stratigraphy II: American Association of Petroleum Geologists, Memoir no. 39, p. 93-115.
- Hubbard, R.J., 1988, Age and significance of sequence boundaries on Jurassic and Early Cretaceous rifted continental margins: American Association of Petroleum Geologists Bulletin, v. 72, p. 49-72.

- Hudson, J.D., 1963, The recognition of salinity-controlled mollusc assemblages in the Great Estuarine Series (Middle Jurassic) of the inner Hebrides: *Palaeontology*, v. 6, p. 327-348.
- Hurley, T.J., Kreisa, R.D., Taylor, G.G., and Yates, W.R.L., 1992, The reservoir geology and geophysics of the Hibernia field, Offshore Newfoundland, in Halbouty, M.T., ed., *Giant oil and gas fields of the decade 1977-88*: American Association of Petroleum Geologists, Memoir 54, p. 35-54.
- Hutcheon, I., Nahnybida, C., and Krouse, H.R., 1985, The geochemistry of carbonate cements in the Avalon sand, Grand Banks of Newfoundland: *Mineralogical Magazine*, v. 49, p. 457-467.
- Jackson, M.P.A., and Galloway, W.E., 1984, Structural and depositional styles of the Gulf coast Tertiary Continental Margins: Application to hydrocarbon exploration: American Association of Petroleum Geologists, Continuing Education Course Note Series no. 25, 226 p.
- James, D.M.D., ed., 1984, The geology and hydrocarbon resources of Negara Brunei Darussalam: Muzium Brunei, Bander Seri Begawan, 164 p.
- James, N.P., and Choquette, P.W., 1984, Diagenesis 9-limestones-the meteoric diagenetic environment: *Geoscience Canada*, v. 161-194.
- Jansa, L.F., and Wade, J.A., 1975, Geology of the continental margin off Nova Scotia and Newfoundland: Van Der Linden, and Wade, J.A., eds., *Offshore geology of Eastern Canada*, paper 74-30, p. 51-106.
- Jenkins, A., 1984, Palynology and stratigraphy of the Avalon reservoir rocks, Hibernia structure, Grand Banks of Newfoundland: Mobil internal report, 57 p.
- Jenkins, A., 1984, Palynology and stratigraphic correlation of the Avalon reservoir rocks in the Hibernia C-96 well, Grand Banks of Newfoundland: Mobil internal report, 9 p.
- Jenkins, A., 1986, Palynology of the Avalon Succession at Hibernia I-46 and its correlation with Hibernia O-35 and Hibernia K-14, Grand Banks of Newfoundland: Mobil internal report, 8 p.

- Jenkins, A., 1993, Age interpretation and biostratigraphic correlation of the Avalon and Ben Nevis Formations at Hibernia, Grand Banks of Newfoundland: Hibernia Management and Development Company, internal report.
- Kanes, W.H., 1970, Facies and development of the Colorado river delta in Texas, in Morgan, J.P., ed., Deltaic sedimentation, modern and ancient: Society of Economic Paleontologists and Mineralogists, Special Publication no. 15, p. 78-106.
- Kantorowicz, J.D., Bryant, I.D., and Dawans, J.M., 1987, Controls on the geometry and distribution of carbonate cements in Jurassic Sandstones: Birdport Sands, southern England and Viking Group, Troll Field, Norway, in Marshal, J.D., ed., Diagenesis of sedimentary sequences: Geological Society Special Publication no. 36, p. 103-118.
- Kauffman, E.G., Elder, W.P., and Sageman, B.B., 1991, High resolution correlation, a new tool in chronostratigraphy, in Einsele, G., Ricken, W. and Seilacher, A., eds., Cycles and events in stratigraphy: Springer-Verlag, p. 795-819.
- Keen, C.E., Boutilier, R., De Voogd, B., Mudford, B., and Enachescu, M.E., 1987, Crustal geometry and extensional models for the Grand Banks, eastern Canada, constraints from deep seismic reflection data, in Beaumont, C., and Tankard, A., eds., Sedimentary basins and basin-forming mechanisms: Canadian Society of Petroleum Geologists, Memoir no. 12, p. 101-115.
- Kendall, A.C., 1985, Radial fibrous calcite: a reappraisal, in Schneidermann, N., and Harris, P.M., eds., Carbonate Cements: Society of Economic Paleontologists and Mineralogists, Special Publication no. 36, p. 59-77.
- King, B.C., 1978, A comparison between the older (Karoo) rifts and the younger (Cenozoic) rifts of eastern Africa, in Ramberg I.B., and Neumann, E.R., eds., Tectonics and geophysics of continental rifts: Dordrecht, Reidel, p. 347-350.
- Kinsman, D.J.J., 1969, Interpretation of Sr^{2+} concentrations in carbonate minerals and rocks: Journal of Sedimentary Petrology, v. 39, p. 486-508.
- Kirschbaum, M.A., 1989, Lagoonal deposits in the Upper Cretaceous Rock Springs Formation (Mesaverde Group), southwest Wyoming: Marine Geology, v. 88, p. 349-364.

- Kolb, C.R., and Van Lopik, J.R., 1966, Depositional environment of the Mississippi river deltaic plain - southeast Louisiana, in Shirley, M.L., ed., Deltas in their geologic framework: Houston Geological Society, p. 17-61.
- Kraft, J.C., 1971, Sedimentary facies patterns and geologic history of a Holocene transgression: Geological Society of America Bulletin, v. 82, p. 2131-2158.
- Kraft, J.C., and John, C.J., 1979, Lateral and vertical facies relations of transgressive barrier: American Association of Petroleum Geologists Bulletin, v. 63, no. 12, p. 2145-2163.
- Kumar, N., Sanders, J.E., 1975, Characteristics of shoreface storm deposits: modern and ancient examples: Journal of Sedimentary Petrology, v. 46, p. 145-162.
- Land, L.S., 1980, The isotopic and trace element geochemistry of dolomite: the state of the art: Society of Economic Paleontologists and Mineralogists, Special Publication no. 28, p. 87-110.
- Land, L.S., Salem, M.R.I., and Morrow, D.W., 1975, Paleohydrology of ancient dolomites: geochemical evidence: American Association of Petroleum Geologists Bulletin, v. 59, p. 1602-1625.
- Leckie, D.A., and Singh, C., 1991, Estuarine deposits of the Albian Paddy Member (Peace River Formation) and lowermost Shaftesbury Formation, Alberta, Canada: Journal of Sedimentary Petrology, v. 61, no. 5, p. 825-849.
- Lee, J.M., 1987, Sedimentology and diagenesis of the Avalon Member of the Mississauga Formation, Hibernia Field, Grand Banks of Newfoundland (unpublished M.Sc. thesis): University of Calgary, Calgary, Alberta, Canada, 132 p.
- Leeder, M.R., 1975, Pedogenic carbonates and flood sediment accumulation rates: a quantitative model for arid zone lithofacies: Geological Magazine, v. 112, p. 257-270.
- Lewy, Z., and Samtleben, C., 1979, Functional morphology and paleontological significance of the conhiolin layers in corbulid pelecypods: Lethaia, v. 12, p. 341-351.

- MacEachern, J.A., and Pemberton, S.G., 1994, Ichnological aspects of incised valley fill systems from the Viking Formation of the Western Canada Sedimentary basin, Alberta, Canada, in Dalrymple, R.W., Boyd, R., Zaitlin, B.A., eds., Incised-valley systems: origin and sedimentary sequences: Society for Sedimentary Geology, Special Publication no. 51, p. 129-157.
- Machel, H.G., 1988, Fluid flow direction during dolomite formation as deduced from trace-element trends, in Shukla, V., and Baker, P.A., eds., Sedimentology and geochemistry of dolomites: Society of Economic Paleontologists and Mineralogists, Special publication no. 43, p. 115-125.
- Machette, M.N., 1985, Calcic soils of the southwestern United States, in Weide, D.L., ed., Soils and Quaternary Geology of the southwestern United States: Geological Society of America, Special Publication no. 203, p. 1-21.
- Martinsen, O.J., 1990, Fluvial, inertia-dominated deltaic deposition in the Namurian (Carboniferous) of northern England: Sedimentology, v. 37, p. 1099-1113.
- Masson, D.G., and Miles, P.R., 1984, Mesozoic seafloor spreading between Iberia, Europe and North America: Marine Geology, v. 56, p. 279-287.
- Masters, C.D., 1965, Sedimentology of the Mesaverde Group and of the upper part of the Mancos Formation, northwestern Colorado: Dissertation, Yale University, United States of America, 88 p.
- Matthews, R.K., 1984, Time stratigraphic correlation based on physical events of short duration, in Matthews, R.K., Dynamic stratigraphy, an introduction to sedimentation and stratigraphy: Prentice-Hall, Englewood Cliffs, New Jersey, p. 81-93.
- Mauffret, A., and Montadert, L., 1987, Rift tectonics on the passive continental margin off Galicia (Spain): Marine and Petroleum Geology, v. 4, p. 49-70.
- McAlpine, K.D., 1990, Mesozoic stratigraphy, sedimentary evolution and petroleum potential of the Jeanne d'Arc basin, Grand Banks of Newfoundland: Geological Survey of Canada, paper no. 89-17. 50 p.

- McClay, K.R., 1989, Physical models of structural styles during extension, in Tankard, A.J., and Balkwill, H.R., eds., Extensional tectonics and stratigraphy of the North Atlantic margins: American Association of Petroleum Geologists, Memoir 46, p. 95-110.
- McClay, K.R., Waltham, D.A., Scott, A.D., and Abousetta, A., 1991, Physical and seismic modelling of listric normal fault geometries, in Roberts, A.M., Yielding, G., and Freeman, B., eds., The geometry of normal faults: Geological Society Special Publication no. 56, p. 231- 239.
- McIntire, W.L., 1963, Trace element partition coefficients- a review of theory and application to geology: *Geochemica et Cosmochemica Acta*, v. 27, p. 1209-1264.
- McKenzie, D., 1978, Some remarks on the development of sedimentary basins: *Earth and Planetary Science Letters*, v. 40, p. 25-32.
- McKenzie, R.M., 1980, The Hibernia structure: Oilweek, December 15, p. 59.
- Meyers, W.J., 1978, Carbonate cements: their regional distribution and interpretation in Mississippian limestones, New Mexico: *Sedimentology*, v. 25, p. 371-400.
- Meyers, W.J., and Lohmann, K.C., 1978, Microdolomite-rich syntaxial cements: proposed meteoric marine mixing zone phreatic cements from Mississippian limestones, New Mexico: *Journal of Sedimentary Petrology*, v. 48, 475-488.
- Meloche, J.D, 1985, Fracture-controlled dissolution porosity within the Avalon of the Hibernia field: Petro-Canada, internal report, 19 p.
- Meloche, J.D., 1982, Petrographic analysis of sandstones from the Avalon intervals of the O-35, K-18, G-55A, P-15, and J-34 wells: Geological Research and Service, Petro-Canada, internal report P/S-109, 51 p.
- Miall, A.D., 1990, Principles of sedimentary basin analysis: Springer-Verlag, 668 p.

- Miall, A.D., 1991, Hierarchies of architectural units in terrigenous clastic rocks, and their relationship to sedimentation rate, in Miall, A.D., and Tyler, N., eds., the three-dimensional facies architecture of terrigenous clastic sediments and its implications for hydrocarbon discovery and recovery: Society for Sedimentary Geology, concepts in sedimentology and paleontology, v. 3, p. 6-12.
- Moore, C.H., 1989, Carbonate diagenesis and porosity: Elsevier Publishing Company, 338 p.
- Morton, R.A., and McGowen, J.H., 1980, Modern depositional environments of the Texas coast: Bureau of Economic Geology, the University of Texas at Austin, Austin, Texas 78712, 167 p.
- Moss, A.J., 1972, Bed-load sediments: Sedimentology, v. 18, p. 159- 219.
- Mozley, P.S., 1989, Relation between depositional environment and the elemental composition of early diagenetic siderite: Geology, v. 17, p. 704-706.
- Mozley, P.S., and Carothers, W.W., 1992, Elemental and isotopic composition of siderite in the Kuparuk Formation, Alaska: effect of microbial activity and water/sediment interaction on early pore-water chemistry: Journal of Sedimentary Petrology, v. 62, p. 681- 692.
- Nummedal, D., and Swift, D.J.P., 1987, Transgressive stratigraphy at sequence-bounding unconformities: some principles derived from Holocene and Cretaceous examples, in Nummedal, D., Pilkey, O.H., and Howard, J.D., eds., Sea level fluctuation and coastal evolution: Society of Economic Paleontologists and Mineralogists, Special Publication no. 41, p. 241-260.
- Orton, G.J., and Reading, H.G., 1993, Variability of deltaic processes in terms of sediment supply, with particular emphasis on grain size: Sedimentology, v. 40, p. 475-512.
- Pattison, S.A.J., 1988, Transgressive, incised shoreface deposits of the Burnstick Member (Cardium 'B' Sandstone) at Caroline, Crossfield, Garrington and Lochend; Cretaceous western interior seaway, Alberta, Canada, in James, D.P., and Leckie, D.A., eds., Sequences, stratigraphy, sedimentology: surface and subsurface: Canadian Society of Petroleum Geologists, Memoir no. 15, p. 155-165.

- Pattison, S.A.J., and Walker, R.G., 1994, Incision and filling of a lowstand valley: Late Albian Viking Formation at Crystal, Alberta, Canada: *Journal of Sedimentary Research*, v. B64, no. 5, 365-379.
- Pemberton, G. S., 1984, Ichnology of the Avalon cores, offshore Newfoundland: Mobil internal report, 82 p.
- Pemberton, G.S., 1985, Synthesis of ichnology, Hibernia-related core: Mobil internal report, 41 p.
- Plint, A.G., Walker, R.G., and Bergman, K.M., 1986, Cardium Formation 6, stratigraphic framework of the Cardium in subsurface: *Bulletin of Canadian Petroleum Geology*, v. 34, p. 213-225.
- Pingitore, N.E., 1982, The role of diffusion during carbonate diagenesis: *Journal of Sedimentary Petrology*, v. 52, p. 27-39.
- Postma, D., 1982, Pyrite and siderite formation in brackish and freshwater swamp sediments: *American Journal of Science*, v. 282, p. 1151-1183.
- Powell, T.G., 1985, Paleogeographic implications for the distribution of Upper Jurassic source beds: offshore eastern Canada: *Bulletin of Canadian Petroleum Geology*, v. 33, p. 116-119.
- Prosser, S., 1993, Rift-related linked depositional systems and their seismic expression, in Williams, G.D., and Dobb, A., eds., *Tectonics and seismic sequence stratigraphy: Geological Society Special Publication no. 71*, p. 35-66.
- Puffer, E.L., and Emerson, W.K., 1953, The Molluscan Community of the Oyster-Reef Biotope on the central Texas Coast: *Journal of Paleontology*, v. 27, p. 537-544.
- Pye, K., Dickson, J.A.D., Schiavon, N., Coleman, M.L., and Cox, M., 1990, Formation of siderite-Mg-calcite-iron sulphide concretions in intertidal marsh and sandflat sediments, north Norfolk, England: *Sedimentology*, v. 37, p. 325-343.
- Ramberg, I.B., and Larsen, B.T., 1978, Tectomagnetic evolution, in Dons, B.T., ed., *The Oslo paleorift: Norges Geology Bulletin*, v. 335, p. 55-73.

- Reading, H.G., 1986, Facies, in Reading, H.G., ed., Sedimentary environments and facies: Blackwell Scientific Publications, p. 4-19.
- Reineck, H.E., and Wunderlich, F., 1967, Zeitmessungen an Gezeitschichten: *Nature Mus.*, v. 97, p. 193-197.
- Reineck, H.E., and Wunderlich, F., 1969, Die Entstehung von Schichten und Schichtbanken im Watt: *Senckenbergiana marit.*, v. 1, p. 85-106.
- Retallack, G.J., 1983, Late Eocene and Oligocene paleosols from Badlands National Park, South Dakota: *Geological Society of America Bulletin*, v. 94, p. 823-840.
- Retallack, G.T., 1984, Completeness of the rock and fossil record: some estimates using fossil soils: *Paleobiology*, v. 10, p. 59-78.
- Retallack, G.J., 1988, Field recognition of paleosols, in Reinhardt, J., and Sigels, W.R., eds., *Paleosols and weathering through geologic time: principles and applications*: Geological Society of America, Special Publication no. 216, p. 1-20.
- Reineck, H.E., and Singh, I.B., 1972, Genesis of laminated sand and graded rhythmites in storm-sand layers of shelf mud: *Sedimentology*, v. 18, p. 123-128.
- Reinson, G.E., Clark, J.E., and Foscolos, A.E., 1988, Reservoir geology of the Crystal Viking field, Lower Cretaceous tidal channel-bay complex, south-central Alberta: *American Association of Petroleum Geologists Bulletin*, v. 72, no. 10, p. 1270-1294.
- Richter, D.K., and Fuchtbauer, H., 1978, Ferroan calcite replacement indicates former magnesian calcite skeletons: *Sedimentology*, v. 25, p. 843-860.
- Rigsby, C.A., 1994, Deepening upward sequences in Oligocene and Lower Miocene fan-delta deposits, western Santa Ynez mountains, California: *Journal of Sedimentary Research*, v. B64, no. 3, p. 380-391.
- Root, S.A., 1983, Macrofossil paleoenvironmental interpretation of 8 cores from the Mobil Hibernia I-46 well, Grand Banks, Canada: Mobil internal report, 34 p.

- Root, S.A., 1983, Macrofossil paleoenvironmental interpretation of 20 cores from the Mobil Hibernia 1-46 well, Grand Banks, Canada: Mobil internal report, 64 p.
- Rosendahl, B.R., 1987, Architecture of continental rifts with special reference to east Africa: Annual Review of Earth and Planetary Sciences, v. 15, p. 445-503.
- Rowan, H.G., and Kligfield, R., 1989, Cross section restoration and balancing as aid to seismic interpretation in extensional terrains: American Association of Petroleum Geologists Bulletin, v. 73,, p. 955-966.
- Ryer, T.A., 1981, Deltaic coals of Ferroan Sandstone Member of Mancos Shale: predictive model for Cretaceous coal-bearing strata of Western Interior: American Association of Petroleum Geologists Bulletin, v. 65, no. 12, p. 2323-2340.
- Saller, A.H., 1986, Radial calcite in Lower Miocene strata, subsurface Enewetak Atoll: Journal of Sedimentary Petrology, v. 56, p. 743-762.
- Sandberg, P.A., 1985, Aragonite cements and their occurrence in ancient limestones, in Schneidermann, N., Harris, P.M., Carbonate Cements: Society of Economic Paleontologists and Mineralogists, Special Publication no. 36, p. 33-57.
- Scott, A.J., and Fisher, W.L., 1969, Delta systems and deltaic deposition, in Fisher, W.L., Brown, L.F., Scott, A.J., and McGowen, J.H., eds., Delta systems in exploration for oil and gas: Bureau of Economic Geology, the University of Texas at Austin, Austin, Texas, p.10-29.
- Schwartz, R.K., 1982, Bedform and stratification characteristics of some modern small-scale washover sand bodies: Sedimentology, v. 29, p. 835-849.
- Sinclair, I.K., 1988, Evolution of Mesozoic-Cenozoic sedimentary basins in the Grand Banks area of Newfoundland and comparison with Falvey's (1974): Canadian Petroleum Geology Bulletin, v. 36, no. 3, p. 255-273.
- Sinclair, I.K., 1988b, Avalon, Ben Nevis and Nautilus Formations of the Jeanne d'Arc basin, Canada Newfoundland Offshore Petroleum Board, report no. GL-88-2, 58 p.
- Sinclair, I.K., 1993, Tectonism: the dominant factor in mid-Cretaceous deposition in the Jeanne d'Arc basin, Grand Banks: Marine and Petroleum Geology, v. 10, p. 530-549.

- Sinclair, I.K., Shannon, P.M., Williams, B.P.J., Harker, S.D., and Moore, J.G., 1994, Tectonic control on sedimentary evolution of three North Atlantic borderland Mesozoic basins: *Basin Research*, no. 6, p. 193-217.
- Snow, J.K., and White, C., 1990, Listric normal faulting and synorogenic sedimentation, northern Cottonwood Mountains, Death Valley region, California, in Wernicke, B., ed., *Basin and Range extensional tectonics near the latitude of Las Vegas*: Geological Society of America, Memoir no. 176, p. 413-445.
- Stamp, L.D., 1921, On cycles of sedimentation in the Eocene strata of the Anglo-Franco-Belgium Basin: *Geological magazine*, v. 58, p. 108-114.
- Sullivan, K.D., 1983, The Newfoundland basin: ocean-continent boundary and Mesozoic sea-floor spreading history: *Earth and Planetary Science letters*, v. 62, p. 321-339.
- Surlyk, F., 1978, Submarine fan sedimentation along fault scarps on tilted fault blocks (Jurassic-Cretaceous boundary, east Greenland): *Gronlands Geologiske Undersogelse Bulletin* no. 128, 108 p.
- Surlyk, F., 1984, Fan-Delta to submarine fan conglomerates of the Volgian-Valanginian Wollaston Forland Group, east Greenland, in Koster, E.H., and Steel, R.J., eds., *Sedimentology of gravels and conglomerates*: Canadian Society of Petroleum Geologists, Memoir no 10, p. 359-382.
- Suter, J.R., Berryhili, H.L., and Penland, S., 1987, Late Quaternary sea level fluctuations and depositional sequences, southwest Louisiana continental shelf, in Nummedal, D., Pilkey, O.H., and Howard, J.D., eds., *Sea-level fluctuation and coastal evolution*: Society of Economic Paleontologists and Mineralogists, Special Publication no. 41, p. 199-219.
- Swift, D.J.P., 1968, Coastal erosion and transgressive stratigraphy: *Journal of Geology*, v. 76, p. 444-456.
- Swift, J.H., and Williams, J.A., 1980, Petroleum source rocks, Grand Banks area, in Miall, A.D., ed., *Facts and principles of world petroleum occurrences*: Canadian Society of Petroleum Geologists, Memoir no. 6, p. 567-588.

- Tankard A.J., and Welsink, H.J., 1988, Extensional tectonics, structural styles and stratigraphy of the Mesozoic Grand Banks of Newfoundland, in Manspeizer, W., ed., Triassic-Jurassic rifting, Continental breakup and the origin of the Atlantic Ocean and passive margins, part "A", Elsevier, p. 129-165.
- Tankard, A.J., Welsink, H.J., and Jenkins, W.A.M., 1989, Structural styles and stratigraphy of the Jeanne d'Arc basin, Grand Banks of Newfoundland, in Tankard, A.J., and Balkwill, H.R., eds., Extensional tectonics and stratigraphy of the North Atlantic margins: American Association of Petroleum Geologists, memoir no. 46, p.265-282.
- Thomas, M.A., and Anderson, J.B., 1994, Sea level controls on the facies architecture of the Trinity/Sabine incised valley system, Texas continental shelf, in Dalrymple, R.W., Boyd, R., and Zaitlin, B.A., eds., Incised-valley systems: origin and sedimentary sequences: Society for Sedimentary Geology, Special publication no. 51, p. 63-82.
- Tillman, R.W., and Matinsen, R.S., 1984, The Shannon Shelf-Ridge Sandstone Complex, Salt Creek Anticline, Powder River Basin, Wyoming, in Tillman, R.W., and Siemers, C.T., eds., Siliciclastic shelf sediments: Society of Economic Paleontologists and Mineralogists, Special Publication no. 34, p. 85-142.
- Tucker, M.E., 1990, Diagenetic processes, products and environments, in Tucker, M.E., and Wright, V.P., Carbonate sedimentology: Blackwell Scientific Publications, p. 314-364.
- Tyler, N., and Ambrose, W.A., 1985, Facies architecture and production characteristics of strandplain reservoirs in the Frio Formation, Texas: Bureau of Economic Geology, report of investigation no. 146, 42 p.
- Veiser, J., 1983, Chemical diagenesis of carbonates: theory and application of trace element technique, in Arthur, M.A., Anderson, T.F., Kaplan, I.R., Veiser, J, and Land, L.S., eds., Stable isotopes in sedimentary geology: Society of Economic Paleontologists and Mineralogists, Short Course no. 10, p. 3.1-100.
- Waage, K.M., 1964, Origin of repeated fossiliferous concretion layers in the Fox Hill Formation: Bulletin of the Geological Survey of Kansas: v. 169 (2), p. 541-563.

- Wade, J.A., 1981, Geology of the Canadian Atlantic margin from Georges Bank to the Grand Banks, in Kerr, J.W., Ferguson, A.J., eds., Geology of the north Atlantic borderlands: Canadian Society of Petroleum Geologists, Memoir no. 7., p. 447-460.
- Walderhaug, O., Bjorkum, P.A., and Bolas, H.M.N., 1989, Correlation of calcite-cemented layers in shallow-marine sandstones of the Fensfjord Formation in the Brage Field, in Collinson, J.D., ed., Correlation in hydrocarbon exploration: Norwegian Petroleum Society, Graham & Tortman, London, p. 367-375.
- Walker, R.G., 1992, Facies, facies models and modern stratigraphic concepts, in Walker, R.G., and James, N.P., eds., Facies models, response to sea level change: Geological Association of Canada, p. 1-14.
- Walther, J., 1894, Einleitung in die Geologie als historische Wissenschaft, Bd. 3, Lithogenesis der Gevenwart: Fischer Verlag, Jena, p. 535-1055.
- Waterson, J., 1986, Fault dimensions, displacement and growth: PAGEOPH, v. 124, p. 365-373.
- Welsink, H.J., and Tankard, A.J., 1988, Structural and stratigraphic framework of the Jeanne d'Arc basin, Grand Banks, in Bally, A.W., ed., Atlas of seismic stratigraphy, v.2: American Association of Petroleum Geologists, Studies in Geology no. 27, p. 14-21.
- White, N.J., Jackson, J.A., and McKenzie D.P., 1986, The relationship between the geometry of normal faults and that of sedimentary layers in their hanging walls: Journal of Structural Geology, v. 8, p. 897-909.
- Williams, G.L, Ascoli, P., Barss, M.S., Bujak, J.P., Davies, E.H., Fensome, R.A., and Williamson, M.A., 1990, Biostratigraphy and related studies, in Keen, M.J., and Williams, G.L., eds., Geology of the continental margin of eastern Canada, p. 87-137.
- Winker, C.D., and Edwards, M.B, 1983, Unstable progradational clastic shelf margins, in Stanley, D.J., and Moore, G.T., eds., The shelf break: critical interface on continental margins: Society of Economic Paleontologists and Mineralogists, Special Publication no. 33, p. 139-157.

- Wood, J.M., 1994, Sequence stratigraphic and sedimentological model for estuarine reservoirs in the lower Cretaceous Glauconitic Member, southern Alberta; Bulletin of Canadian Petroleum Geology, v. 42, no. 3, p. 332-351.
- Wright, V.P., 1989, Paleosol recognition, in Wright, V.P., ed., Paleosols in siliciclastic sequences: Postgraduate Research Institute for sedimentology, Reading University, Short Course Notes no. 001, p. 1-25.
- Wu, R.S.S, and Richards, J., 1981, Variations in benthic community structure in a subtrophic estuary: Marine Biology, v. 64, p. 191-198.
- Wunderlich, F., 1967, Feinblattrige Wechselichtung und Gezeitenschichtung: Senckenbergiana Lethaea, v. 48, p. 337-343.
- Xiao, H., and Suppe, J., 1992, Origin of rollover: American Association of Petroleum Geologists Bulletin, v. 62, no. 4, p. 509-529.
- Zaitlin, B.A., and Shultz, B.C., 1990, Wave-influenced estuarine sand body, Senlac heavy oil pool, Saskatchewan, Canada, in Barwis, J.H., McPherson, JG, and Studlick, J.R.J., eds., Sandstone petroleum reservoirs: Springer-Verlag, p. 363- 387.
- Zaitlin, B.A., Dalrymple R.W., and Boyd, R., 1994, The stratigraphic organization of incised-valley systems associated with relative sea-level changes, in Dalrymple, R.W., Boyd, R., and Zaitlin, B.A., eds., Incised-valley systems: origin and sedimentary sequences: Society for Sedimentary Geology, Special Publication no. 51, p. 45-60.

IX- APPENDIX

Table IX.1 - Highest occurrences of various biostratigraphic events, recorded by different investigators.

marker fossil (age)	O-35	K-14	B-27	P-15	C-96	K-18	B-08	J-34	I-46	G-55
C. Dampieri Assemblage (Jenkins, 1984) (top Aptian)	2205	2353	2545	2330	2260	2270	2165	2355	2299	2070
C. Dampieri Assemblage (Jenkins, 1993) (top Aptian)	2196.7	2353.2	2500	2375	2246.5	2270	2150	2490	2315	
C. tabulata (Chevron) (Aptian)	2150			2310		2286	2150.2	2460	2285	
C. tabulata (Jenkins 1984) (Aptian)	2195	2300	2535	2335	2260	2286.2	2150.3	2235	2165	1900
C. tabulata (Jenkins 1993) (Aptian)	2186.7	2345	2535	2360	2246.5	2286	2150	2500	2328.1	
C. tabulata (Mobil) (Aptian)	2200	2345.1	2545	2350	2250.1			2450		
C. tabulata (Sinclair) (Aptian)			2501					2455		
Hutsonia sp.3 (Gulf) (Upper Barremian)	2340	2405	2580	2450	2340	2335.1	2155.2	2620	2496	
Hutsonia sp.3 (Ascoli, 1990) (top Barremian)						2293		2230	2312	
Hutsonia sp.3* (Ascoli, 1990) (base Barremian)	2350			2440		2310	2145	2635	2488	
Speeton Assemblage (Chevron) (Barremian)	2270	2365	2547.5	2450.1		2300	2155	2545	2408	2445
Speeton Assemblage (Mobil) (Barremian)	2320	2365.2	2555.1	2440	2323			2550	2450	
Speeton Assemblage (Sinclair) (Barremian)					2327					
Speeton Assemblage (P. Canada) (Barremian)	2240	2380						2557		
Speeton Assemblage (Jenkins, 1983) (Barremian)	2325	2406.2	2555.5	2435	2317	2335	2155.1	2549.8	2406.5	2443
Speeton Assemblage (Bedford Institute) (Barremian)	2350								2330.3	2549.8
Aptea anaphrissa (Bedford Institute) (top Barremian)	2385								2382.7	2579.5
Aptea anaphrissa (Jenkins, 1984) (top Barremian)	2240	2335	2562		2307.4	2325	2175	2557	2411	
Aptea anaphrissa (Jenkins, 1993) (top Barremian)			2561	2435	2317	2335			2408.4	2830
Muderongia simplex (Jenkins, 1984) (top Barremian)	2250	2406.2	2557.5	2450	2307.4			2557	2479	2240
Muderongia simplex (Jenkins, 1993) (top Barremian)	2335	2406.2	2557.5		2323.6	2355			2412	2857
H. heslertonensis (Jenkins, 1984) (top Barremian)	2305	2400	2562	2530	2390	2355	2180	2625	2479	
Muderongia imparilis (Davies, 1990) (top Barremian)	2320			2460		2300	2150	2620	2358.4	2414

*base of the Hutsonia sp.3 subzone

Table IX.2— Element percentages of Ca, Mg, Fe, Mn, Sr and Na in the poikilotopic calcite cement.

Sample no.	Depth (m.)	Ca %	Mg %	Fe %	Mn %	Sr %	Na %
1	2585.2	36.0549	0.2423	1.8737	0.3109	0.1576	0
1	2585.2	36.1815	0.2805	1.7705	0.3151	0.0061	0.021
1	2585.2	35.0452	0.5252	3.2628	0.208	0.0505	0.0056
1	2585.2	35.3353	0.5363	3.2256	0.2353	0.0408	0.0211
1	2585.2	32.3751	0.228	1.7482	0.432	0	0.0505
1	2585.2	31.6236	0.3279	1.9529	0.46	0	0.024
1	2585.2	32.9758	0.2069	1.7417	0.4529	0	0.0227
1	2585.2	35.5842	0.2285	1.8515	0.5255	0	0.0267
1	2585.2	34.7774	0.2113	1.6659	0.484	0	0.0233
2	2582.15	34.189	0.4274	2.5587	0.1346	0	0.0084
2	2582.15	34.9647	0.4107	2.6101	0.1438	0	0.0366
2	2582.15	35.675	0.3869	2.7329	0.1157	0.0615	0.0104
2	2582.15	35.5113	0.3972	2.4802	0.1354	0	0.0073
2	2582.15	34.2874	0.3917	2.4583	0.1123	0	0.0125
2	2582.15	33.7807	0.6302	3.049	0.1408	0	0.0287
2	2582.15	32.224	0.4042	2.3096	0.1132	0	0.0152
2	2582.15	35.602	0.3979	2.6562	0.1594	0	0.0153
3	2580.35	37.9189	0.2991	2.2122	0.0658	0.0082	0.005
3	2580.35	38.1761	0.1954	1.6916	0.0626	0.0458	0.0694
3	2580.35	37.0661	0.339	1.9257	0.0649	0.0286	0.0567
3	2580.35	37.1071	0.3589	2.1053	0.057	0.0168	0.0597
3	2580.35	36.6796	0.3156	2.1489	0.0648	0.0041	0.0742
3	2580.35	36.3663	0.2951	2.4336	0.1006	0.0089	0.0375
4	2578.6	38.9031	0.1036	0.8561	0.1041	0.0921	0.0162
4	2578.6	39.0686	0.1758	0.9215	0.0792	0.0152	0.0064
4	2578.6	37.5594	0.1215	1.0931	0.0641	0.0704	0.0081
4	2578.6	37.616	0.134	0.873	0.077	0.133	0
4	2578.6	37.773	0.134	0.886	0.103	0.12	0.004
4	2578.6	37.671	0.116	0.864	0.085	0.152	0.033
4	2578.6	41.021	0.177	0.846	0.076	0.116	0
4	2578.6	38.299	0.084	0.903	0.095	0.126	0.01
4	2578.6	37.68	0.08	0.813	0.096	0.15	0.02
4	2578.6	37.846	0.102	0.823	0.065	0.146	0.015
4	2578.6	38.154	0.11	0.877	0.087	0.147	0.011
5	2576.9	36.479	0.316	1.317	0.045	0.051	0.015
5	2576.9	36.779	0.229	1.352	0.018	0.103	0.039
5	2576.9	36.547	0.264	1.56	0.042	0.05	0.012
5	2576.9	37.0221	0.2736	1.6541	0.0394	0	0.0129
5	2576.9	36.5142	0.2641	1.7066	0.0285	0.0096	0.0124
5	2576.9	37.06	0.2364	1.7816	0.0479	0	0
5	2576.9	37.3537	0.2692	1.6923	0.0348	0.0583	0
5	2576.9	39.5934	0.2952	1.8668	0.0448	0	0.0028
5	2576.9	37.0875	0.2412	1.6676	0.0246	0	0
5	2576.9	37.4389	0.212	1.3986	0.0346	0	0
5	2576.9	37.9139	0.4311	0.8334	0.0354	0	0.0221
6	2572.1	35.5	0.25	1.89	0.11	0.3	0
6	2572.1	36.2	0.2	1.63	0.1	0.32	0
6	2572.1	36.1	0.23	1.76	0.11	0.37	0
6	2572.1	36.4	0.2	1.6	0.1	0.35	0.01
6	2572.1	36.411	0.132	1.108	0.07	0.303	0.016

Table IX.2— Element percentages of Ca, Mg, Fe, Mn, Sr and Na in the poikilotopic calcite cement

6	2572.1	35.708	0.244	1.864	0.118	0.27	0
6	2572.1	36.217	0.253	1.978	0.131	0.187	0.019
6	2572.1	36.551	0.238	1.926	0.113	0.209	0
6	2572.1	38.918	0.222	1.859	0.129	0.393	0
6	2572.1	35.228	0.247	2.073	0.126	0.267	0.002
6	2572.1	36.592	0.232	1.864	0.125	0.212	0
7	2554.6	37.3	0.14	1.06	0.04	0.41	0.02
7	2554.6	37.2	0.25	1.49	0.05	0.15	0.02
7	2554.6	37.4	0.2	1.54	0.05	0.47	0.01
7	2554.6	36.6	0.29	1.74	0.06	0.12	0
7	2554.6	36.7	0.26	1.57	0.06	0.1	0
7	2554.6	37.1	0.22	1.44	0.04	0.4	0.01
7	2554.6	36.5	0.23	1.49	0.04	0.33	0
7	2554.6	36.6	0.25	1.6	0.05	0.12	0.03
8	2402.5	39.041	0.2059	1.4438	0.0591	0.3028	0.0538
8	2402.5	38.4238	0.2051	1.539	0.0697	0.2388	0.0375
8	2402.5	37.7585	0.3832	2.4487	0.0781	0.0846	0.0054
8	2402.5	35.5088	0.3752	2.2949	0.0453	0	0.0068
8	2402.5	36.5914	0.3867	2.3647	0.0539	0	0
8	2402.5	38.2596	0.303	1.6973	0.0719	0.2389	0.0379
8	2402.5	36.7849	0.3493	2.5841	0.0865	0	0.0245
9	2400.25	37.5173	0.2438	1.4345	0.1155	0.0169	0.0197
9	2400.25	38.2847	0.1915	1.2506	0.1118	0	0.0152
9	2400.25	38.0699	0.2121	1.5093	0.1075	0	0.0183
9	2400.25	35.6259	0.2588	1.5248	0.13	0	0.023
9	2400.25	37.3819	0.1815	1.4467	0.093	0.2776	0
9	2400.25	37.4967	0.1719	1.3432	0.0975	0	0.0072
10	2398.75	38.9955	0.2582	1.1752	0.0521	0.0649	0.0019
10	2398.75	39.2254	0.2287	1.2582	0.04	0.1515	0.0129
10	2398.75	38.8734	0.278	1.401	0.0529	0.0719	0
10	2398.75	39.5921	0.2389	1.3821	0.0718	0.1473	0.0128
10	2398.75	39.1534	0.2814	1.4225	0.0471	0.1422	0.0097
10	2398.75	39.0112	0.2577	1.1806	0.0452	0.1288	0.0076
11	2398	40.6694	0.2133	0.2632	0.0785	0	0.0284
11	2398	39.776	0.2253	0.3791	0.064	0	0.0209
11	2398	39.8205	0.2485	0.2673	0.0816	0	0.0093
11	2398	39.0761	0.2675	0.5976	0.0597	0	0.0043
11	2398	37.96	0.1956	0.7456	0.0379	0	0.0032
11	2398	36.5206	0.0989	0.8918	0.0402	0.045	0
11	2398	38.5079	0.0902	0.9304	0.0401	0	0.0049
11	2398	38.8593	0.0857	0.8803	0.0225	0	0.0054
11	2398	39.0392	0.1755	0.4764	0.0409	0	0.0196
12	2393.55	40.0185	0.3637	0.1104	0.0598	0.0174	0.012
12	2393.55	38.6385	0.6867	0.1912	0.1072	0	0.0133
12	2393.55	39.5251	0.4739	0.1192	0.0923	0.0165	0.0081
12	2393.55	38.6583	0.3152	0.3963	0.0138	0.0688	0.0411
12	2393.55	39.6611	0.2898	0.0418	0.0092	0.0209	0.0223
12	2393.55	38.4133	0.4188	0.1214	0.0813	0.0767	0
12	2393.55	33.5326	0.6232	0.1209	0.0612	0.0367	0.006
13	2392.25	40.008	0.1002	0.4367	0.0226	0	0
13	2392.25	39.8912	0.0694	0.3521	0.0377	0.0638	0.0084

Table IX.2- Element percentages of Ca, Mg, Fe, Mn, Sr and Na in the poikilotopic calcite cement.

13	2392.25	38.7836	0.0507	0.5153	0.0224	0.2	0.0063
13	2392.25	39.7112	0.5222	0.0533	0.0443	0.0798	0
13	2392.25	38.4219	0.0706	0.6171	0.0175	0.1668	0.0104
13	2392.25	39.2965	0.0455	0.4352	0.0654	0.167	0
13	2392.25	39.0488	0.0594	0.3545	0.0741	0	0
13	2392.25	39.497	0.0404	0.3539	0.0423	0.1768	0.0114
13	2392.25	38.8693	0.051	0.5303	0.0697	0.1479	0.0016
14	2391.45	38.9009	0.163	0.9192	0.0279	0.0104	0.0127
14	2391.45	39.6565	0.203	1.083	0.0321	0.0404	0.0184
14	2391.45	38.479	0.25	1.237	0.052	0.024	0
14	2391.45	38.4228	0.1845	1.0383	0.0691	0.0265	0.0075
14	2391.45	38.6714	0.1623	0.8232	0.0444	0	0.0162
15	2390.95	38.942	0.3841	1.0978	0.0425	0	0.0118
15	2390.95	38.4817	0.2646	0.7672	0.0393	0.0324	0
15	2390.95	38.2346	0.411	0.9452	0.0544	0.0069	0
15	2390.95	39.3054	0.2999	0.7341	0.0345	0.0524	0.0136
16	2389.2	37.6845	0.5377	0.6207	0.0541	0	0.0164
16	2389.2	38.0485	0.4259	0.6294	0.0449	0	0.024
16	2389.2	37.8316	0.4072	0.4695	0.0291	0	0.0249
16	2389.2	38.451	0.433	0.4471	0.0267	0	0.018
16	2389.2	37.6144	0.4492	0.567	0.0498	0	0.0169
17	2388.4	38.4698	0.3743	0.1984	0.0518	0	0.0281
17	2388.4	36.9437	0.4006	0.2205	0.04	0	0.0282
17	2388.4	38.0588	0.4712	0.2313	0.0391	0	0.0208
17	2388.4	35.4545	0.507	0.2474	0.041	0	0.0325
17	2388.4	36.0837	0.4856	0.2666	0.0458	0	0.0145
17	2388.4	38.713	0.4819	0.2176	0.042	0.0158	0.0124
18	2386.4	37.6352	0.298	1.7005	0.1366	0.072	0.0084
18	2386.4	37.6581	0.3294	1.602	0.1337	0.0049	0.001
18	2386.4	38.2303	0.2293	1.3169	0.1151	0.2327	0
18	2386.4	37.8495	0.2507	1.4558	0.1274	0.0279	0.0003
18	2386.4	39.0063	0.2394	1.2225	0.0922	0.0968	0.0045
19	2381.5	37.5821	0.3112	0.9237	0.0749	0.0179	0.0125
19	2381.5	38.2007	0.2798	0.8723	0.0729	0.0469	0.0275
19	2381.5	36.9611	0.3077	0.8391	0.0454	0	0.0312
19	2381.5	38.197	0.2996	0.9284	0.0607	0.1252	0.0139
20	2373.35	37.4077	0.173	1.4934	0.1215	0.005	0.0096
20	2373.35	37.6245	0.1952	1.3907	0.106	0.0315	0.0116
20	2373.35	37.3753	0.2021	1.4729	0.1122	0	0
20	2373.35	38.4218	0.1702	1.6516	0.1162	0.05	0.0135
21	2324.8	35.6533	0.3539	2.26	0.1025	0.1583	0.0195
21	2324.8	34.5724	0.2962	2.0642	0.1064	0	0.0233
21	2324.8	38.6407	0.1759	1.3266	0.067	0.2464	0.05
21	2324.8	36.4555	0.2876	2.1747	0.0955	0.2051	0.0009
21	2324.8	35.5373	0.309	2.2646	0.0998	0.0863	0.0366
21	2324.8	35.7085	0.2969	2.1975	0.0697	0.1018	0
22	2322.55	36.6422	0.2162	1.8285	0.1481	0	0.0106
22	2322.55	36.1783	0.2469	1.9104	0.1238	0.1227	0.0048
22	2322.55	37.4172	0.1841	1.6411	0.1403	0	0
22	2322.55	36.927	0.1894	1.4637	0.1033	0.0518	0.0067
22	2322.55	37.3991	0.174	1.5316	0.088	0.0747	0.0271

Table IX.2- Element percentages of Ca, Mg, Fe, Mn, Sr and Na in the poikilotopic calcite cement.

22	2322.55	37.1977	0.2123	1.8034	0.1244	0	0.0183
23	2319.5	36.3521	0.2597	1.7677	0.0688	0.1723	0.0203
23	2319.5	36.4168	0.2449	1.7714	0.051	0.3476	0.1698
23	2319.5	36.0082	0.3026	1.9342	0.0824	0.0121	0.0174
23	2319.5	36.0761	0.2958	1.922	0.0595	0.0377	0.0103
23	2319.5	36.3383	0.2839	1.9309	0.0692	0.0171	0.0067
23	2319.5	37.0694	0.2006	1.4841	0.0732	0.4064	0.0253
24	2318	36.7651	0.3562	2.0909	0.0436	0.2627	0
24	2318	37.1814	0.3475	2.0838	0.0599	0.0434	0.0162
24	2318	36.1513	0.3091	1.878	0.0509	0	0.0394
24	2318	36.5131	0.3451	1.9848	0.071	0.028	0.0135
24	2318	35.8658	0.3476	1.9496	0.043	0.2061	0.0122
25	2308	35.8465	0.1932	1.8714	0.0741	0	0.044
25	2308	36.3297	0.1373	1.0141	0.0629	0	0.0138
25	2308	37.3794	0.1823	1.8794	0.0933	0.3953	0.0045
25	2308	35.0548	0.1664	1.4327	0.0816	0	0.0453
25	2308	37.0357	0.247	1.8531	0.1101	0	0.0256
26	2307.65	35.9503	0.2439	1.9521	0.0606	0.3157	0.0168
26	2307.65	36.4417	0.2547	1.7315	0.0742	0.2214	0.0221
26	2307.65	36.8327	0.2696	2.1226	0.0903	0.0636	0.0199
26	2307.65	37.0934	0.2004	1.5366	0.0543	0.3061	0.0097
27	2475.1	38.1367	0.1794	1.421	0.0456	0.2151	0
27	2475.1	37.4979	0.2231	1.5478	0.047	0.0069	0.0266
27	2475.1	36.7196	0.2503	1.7174	0.0528	0.1791	0.0238
27	2475.1	38.0262	0.1398	1.1493	0.0565	0.2006	0.001
27	2475.1	38.036	0.2043	1.4013	0.0435	0.1273	0.005
27	2475.1	37.3026	0.2393	1.6053	0.0617	0	0.0198
28	2464.45	36.5521	0.3424	2.2092	0.0946	0.1242	0.0414
28	2464.45	36.7659	0.2523	1.8204	0.0444	0.1023	0.0191
28	2464.45	36.8547	0.3346	2.0672	0.084	0.144	0.0153
28	2464.45	36.9176	0.3141	1.9535	0.0896	0.046	0.0211
29	2456.15	36.6855	0.1409	1.145	0.0667	0.241	0
29	2456.15	36.5631	0.1387	1.1206	0.0816	0.2102	0.0178
29	2456.15	36.3565	0.1378	1.1131	0.0625	0.1554	0.0319
29	2456.15	36.143	0.1641	1.4765	0.0848	0.2173	0.0148
30	2442.45	35.4515	0.3077	2.0877	0.0735	0.1217	0.0235
30	2442.45	36.3467	0.1889	1.396	0.0363	0.0706	0.0211
30	2442.45	35.7632	0.2662	1.7896	0.0654	0.0252	0.0264
30	2442.45	35.9753	0.2848	1.7763	0.0655	0	0.0413
30	2442.45	35.9505	0.2567	1.8115	0.069	0	0.0755
31	2405.15	37.4803	0.4527	1.7696	0.0091	0.0262	0.0407
31	2405.15	37.1743	0.4347	1.7763	0.0231	0.0471	0.0209
31	2405.15	37.7522	0.323	1.3456	0.0171	0.0118	0.0156
31	2405.15	36.8706	0.42	1.6022	0.0256	0	0
31	2405.15	37.5905	0.3926	1.584	0.0089	0.0215	0.0099
31	2405.15	36.7135	0.423	1.6987	0.0241	0.0349	0.0316
31	2405.15	36.6794	0.4222	1.7285	0.0243	0	0.0294
32	2403.25	37.4239	0.4484	1.205	0.025	0.1122	0.0227
32	2403.25	37.5904	0.3309	1.0554	0	0.2475	0.0265
32	2403.25	37.37	0.56	1.5585	0	0.1014	0.0348
32	2403.25	37.604	0.519	1.5073	0.0226	0.0675	0.0356

Table IX.2— Element percentages of Ca, Mg, Fe, Mn, Sr and Na in the poikilotopic calcite cement.

33	2401.6	38.496	0.2257	0.9097	0.0138	0.2032	0.0241
33	2401.6	37.3506	0.442	1.2905	0.006	0.12	0.0228
33	2401.6	37.2805	0.5257	1.5368	0.0112	0.0816	0.0417
33	2401.6	37.4823	0.4409	1.2245	0.0162	0.1442	0.0252
33	2401.6	36.4713	0.5777	1.5607	0.0033	0.0167	0.0137
33	2401.6	37.493	0.5838	1.6286	0.0114	0.1075	0.0059
34	2400.15	38.1723	0.2804	1.7405	0.0682	0	0.0242
34	2400.15	37.3482	0.3212	2.1995	0.1382	0	0.0322
34	2400.15	36.9877	0.3042	1.9151	0.0352	0.0127	0.0129
34	2400.15	37.6011	0.2506	1.6714	0.0345	0.0116	0.0395
34	2400.15	37.4514	0.2976	1.6712	0.0642	0	0.027
34	2400.15	37.8337	0.2597	1.7936	0.1232	0	0.0332
34	2400.15	37.131	0.2759	1.8475	0.094	0	0.0716
34	2400.15	36.5023	0.33	2.0102	0.0497	0	0.0159
35	2399.25	37.8976	0.3993	1.5718	0.0256	0.0655	0
35	2399.25	37.3577	0.5344	1.8817	0	0.0195	0.0181
35	2399.25	38.2822	0.4422	1.6293	0.0175	0.0846	0.0504
35	2399.25	36.6333	0.4208	1.5405	0.0079	0.0667	0.037
35	2399.25	36.3022	0.4964	1.8439	0.0035	0.0453	0.0259
36	2395	37.8478	0.1573	1.5496	0.0317	0.2206	0.0075
36	2395	36.8176	0.1545	1.2737	0.0198	0.2167	0.0131
36	2395	36.1397	0.2025	1.4114	0.015	0	0.0303
36	2395	36.5622	0.1638	1.4842	0.0186	0.2019	0.0017
36	2395	36.662	0.2011	1.48	0.016	0.1037	0.0208
37	2609.05	36.8114	0.4116	1.9877	0.0657	0	0.0102
37	2609.05	36.1395	0.4194	2.1026	0.0679	0	0.0204
37	2609.05	36.0839	0.3722	1.8627	0.056	0	0.0138
37	2609.05	37.3295	0.3562	1.8139	0.0665	0	0.0106
37	2609.05	36.3938	0.3993	1.9169	0.0543	0	0.0201
37	2609.05	36.0489	0.3907	1.9281	0.0737	0	0.0478
37	2609.05	36.2453	0.4345	2.0718	0.0649	0	0.0282
38	2606.15	37.6859	0.3254	0.2504	0.0331	0	0.0292
38	2606.15	38.9045	0.2751	0.5068	0.0399	0	0.0394
38	2606.15	38.7723	0.0684	0.6128	0.055	0	0
38	2606.15	38.9609	0.0498	0.5727	0.0046	0	0.0116
38	2606.15	38.1571	0.4173	0.2934	0.0434	0	0
38	2606.15	37.7725	0.3583	0.2811	0.062	0	0.0062
38	2606.15	38.8693	0.4168	0.319	0.0589	0	0
38	2606.15	38.2271	0.5024	0.3828	0.046	0	0.0098
38	2606.15	38.4433	0.2553	0.2868	0.0512	0	0.0033
38	2606.15	37.9709	0.2184	0.3304	0.0467	0	0.0041
39	2605.2	38.4022	0.3816	0.3536	0.0485	0	0.0049
39	2605.2	39.0693	0.3494	0.3228	0.0523	0	0.0259
39	2605.2	38.188	0.4776	0.4118	0.0598	0	0.0327
39	2605.2	39.1226	0.4451	0.3771	0.0303	0	0.0137
39	2605.2	39.2869	0.381	0.3071	0.0427	0	0.0234
39	2605.2	38.3808	0.5242	0.472	0.0511	0	0.0056
39	2605.2	38.787	0.4484	0.38	0.0447	0	0.0245
39	2605.2	38.453	0.3708	0.3803	0.0547	0	0.0215
39	2605.2	38.7442	0.4405	0.3699	0.0367	0	0.0092
40	2603.6	36.1267	0.3255	1.742	0.047	0	0.0115

Table IX.2— Element percentages of Ca, Mg, Fe, Mn, Sr and Na in the poikilotopic calcite cement.

40	2603.6	36.2071	0.3016	1.7312	0.0345	0	0.008
40	2603.6	35.5188	0.2822	1.6784	0.0257	0	0
40	2603.6	36.5887	0.2635	1.5158	0.0466	0.0653	0.0061
40	2603.6	37.469	0.2172	1.3535	0.0295	0.0516	0.0096
40	2603.6	36.2048	0.3103	1.7758	0.0532	0	0
40	2603.6	36.0991	0.278	1.5997	0.0451	0	0.0086
40	2603.6	36.5133	0.3211	1.6447	0.0579	0.031	0
41	2602	36.7279	0.2749	1.8774	0.0524	0.0542	0.006
41	2602	36.6446	0.2665	1.7555	0.051	0	0.0151
41	2602	36.7666	0.306	2.0224	0.0279	0.0783	0.0125
41	2602	36.4954	0.2833	2.0617	0.0601	0	0.0166
41	2602	36.6149	0.2636	1.7893	0.0449	0.0472	0.0156
41	2602	37.4169	0.2447	1.9065	0.07	0	0.0388
41	2602	37.7044	0.286	1.8386	0.045	0	0.0386
42	2597.25	36.5912	0.3053	1.7786	0.0496	0.1065	0.0203
42	2597.25	36.9036	0.3663	2.1769	0.0634	0.1357	0.0055
42	2597.25	37.299	0.2576	1.6934	0.0663	0.1712	0.0219
42	2597.25	36.4602	0.3016	1.8304	0.0584	0.1192	0.0108
42	2597.25	37.6017	0.2668	2.153	0.0634	0.0345	0.0483
42	2597.25	36.7528	0.2809	1.7468	0.0389	0.1141	0.0112
42	2597.25	37.2926	0.3036	2.0075	0.0519	0.0219	0.0348

Well Name: Hibernia C-96

Location: 46° 45' 10.0" N Lat. 48° 46' 35.77" W. Long. Logged by: Osamu M. Soliman
 K.B.: 33.2 m. G.L.: -81.1 m. R.T.: Date: February 8th, 1994 1/2, 1, 2

Core no./	Box no.	P. Prints	S. Slides	Sample no.	Fractures	Cements	Lithology	Sed Structures	Fossils	Remarks	Facies	Environment
2303	2/1			3		01		mud				
				4		02						
				4A		03						
				5								
				5A								
	2/2			6		C3						
				7		C3						
2304				CS10								
	2/3											
				SP8		03						
				P1								
				9								
2305	2/4			10								
				11		02						
				11A		03						
	2/5											

Shallow marine

Storm sands

Shallow marine

Distal No

2308	2/8	18 CS9 19	C2 C3 C3+ P4 O3		Ophiomorpha	Laminated sandstone with abundant suble burrows - lag composed of mud clasts. Reddish grey bioturbated calcareous sandstone - pyrite dissemination. Laminated sandstone with abundant subtle burrows	12A
2309	2/9	19/19 15/19 20A 21A 21			Ophiomorpha	Bioturbated mudstone grading upwards to muddy sandstone - wood fragments. Graded sandstone with abundant basal mud clasts.	11A
2310	2/10	22 22A				Black shale with few burrows	2B
2311	2/11						11A
2312							

2313

2314

2315

23A

23

24

24A

25

26

P7

27A

27

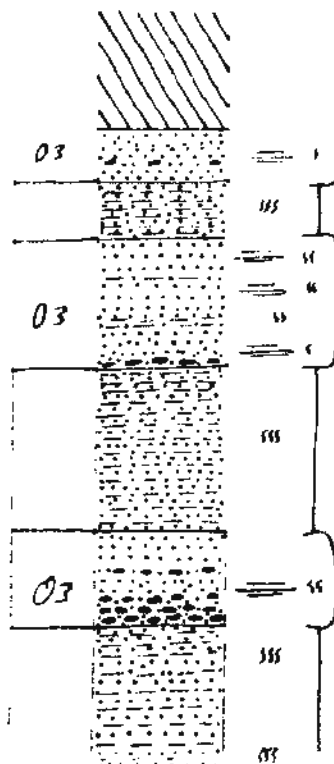
28

3/1

2316

3/2

3/3



Ophiomorpha

Laminated sandstone with abundant subtle burrows.

12A

Bioturbated muddy sandstone

11A

Laminated sandstone with abundant subtle burrows

12A

Bioturbated muddy sandstone

11A

Fine grained sandstone with abundant subtle burrows and relict lamination.

12A

Bioturbated muddy sandstone.

11A

2313

2314

2315



3/1

2316

3/2

2317

3/3

3/4

P4/8
5/16
17

23 A

23

24

24 A

25

26

P?

27 A

27

28

29

29 A

30

03

03

03

03

03

03

SS

SS

SS

SS

SSS

SS

SSS

SSS

SS

SS

SS

SS

Ophiomorpha

Ophiomorpha

Laminated sandstone with abundant subtle burrows.

Bioturbated muddy sandstone

Laminated sandstone with abundant subtle burrows

Bioturbated muddy sandstone

Fine grained sandstone with abundant subtle burrows and relict lamination.

Bioturbated muddy sandstone.

Faintly planar laminated fine

12 A

11 A

12 A

11 A

12 A

11 A

m/s

Distal Mouth Bar sediments

Erosional surface II

Shallow marine

10 Ravinement surface

Family planar laminated fine grained sandstone with abundant subtle burrows

The sandstone is composed of smaller sets with basal erosional boundaries overlain by lags of rounded mud clasts. Few shells are scattered. The sets range in thickness from few cm. up to 20 cm.

Planolites
Rhizocorallium
Ophiomorpha

biolurbated muddy sandstone

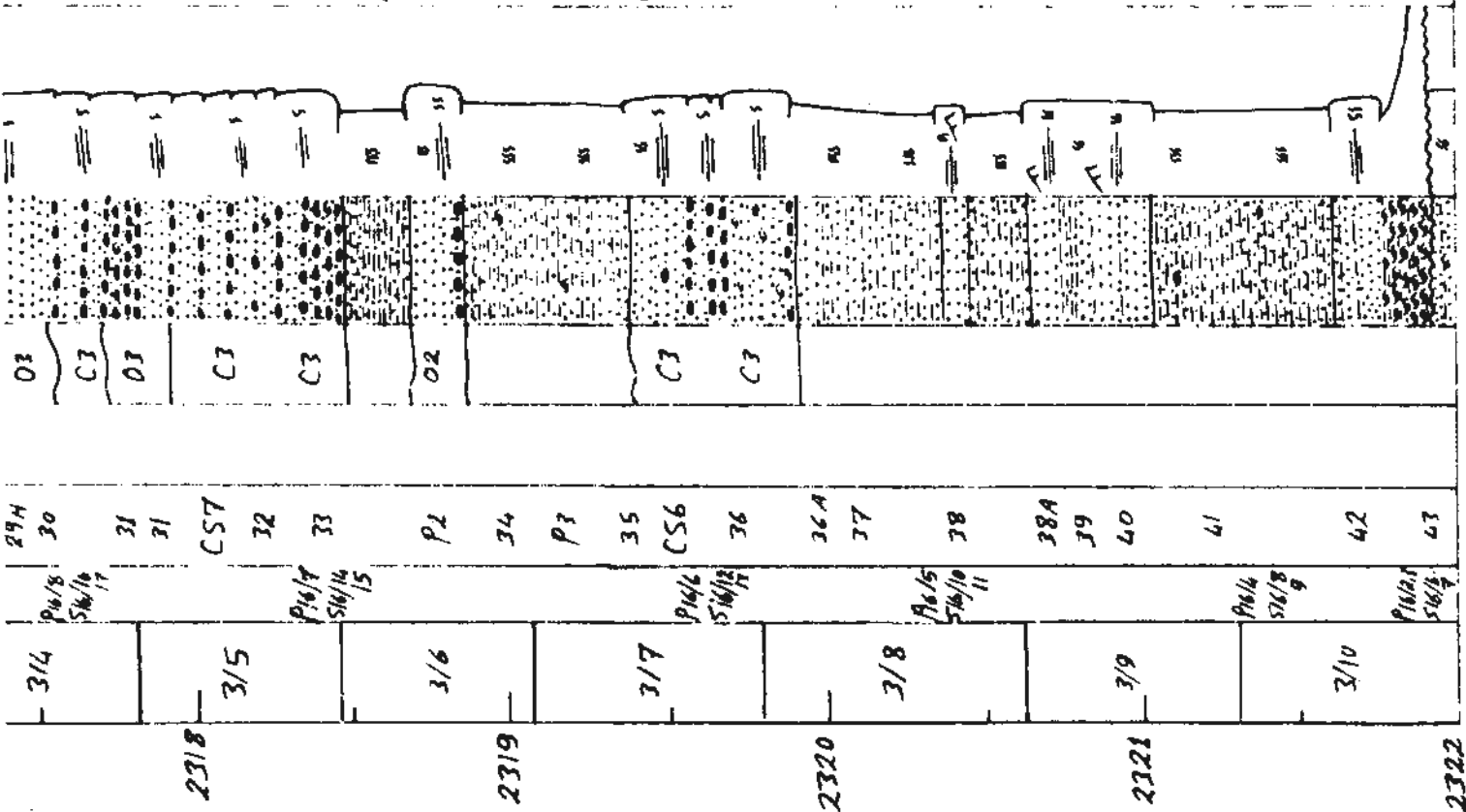
Fine grained laminated sandstone composed of few cm. thick sets with lower erosive boundaries and basal lags made up of mud clasts.

Ophiomorpha

rippled and faintly laminated sand

Fine to very fine grained laminated and rippled muddy sandstone with rhythmic mud laminae in the middle part. Biolurbated sandy mudstone to muddy sandstone with few scattered teleost fish debris.

Faintly laminated sand with relict rhythmic mud laminae at top. Lag deposit composed of teleost fish debris in a muddy sand matrix that becomes dominantly mud at top.



Well Name: Hibernia C-96

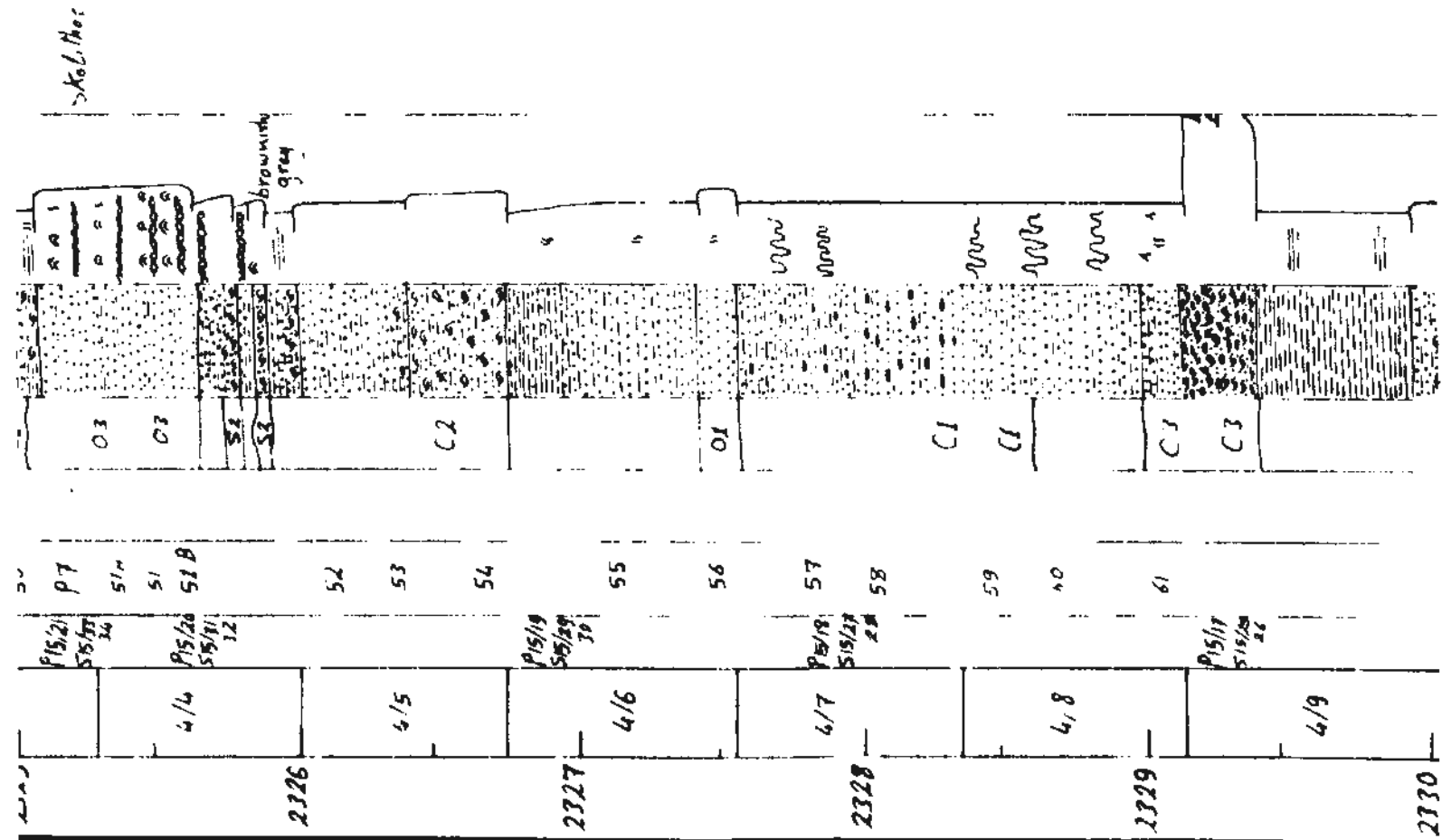
Location 46° 45' 10.01" N Lat. 48° 44' 35.37" W Long.

K.B.: 33.2 m G.L.: -81.1 m R.T.

Logged by: Osama M. Soliman
Depth from K.B. → 2/2
Date: February 8th, 1996

Core no./Box no.	Prints = Slides	Sample no.	Fractures	Cements oil stain	Lithology	Sed. Structures	Fossils	Remarks	Facies	Environment
3/10	9/10/1 5/16/4	CS5		C4	mud					
	9/15/20 5/15/17 5/16/2	44 CS4		C3			Ophiomorpha	Calcareous, muddy sandstone with abundant articulated and disarticulated shells. Organic chips and disseminated pyrite	7B	
3/11	9/15/20 5/15/17 5/16/1	CS3 45		C3			Ophiomorpha Ophiomorpha	Fine to medium grained, relatively clean calcareous sandstone with some scattered open marine (?) Pelecypod shells - Lower gradational boundary - disseminated pyrite		
	9/15/20 5/15/17 5/16/2	46 CS2		C1			Planolites	Dark grey shale, with abundant o. leopod shells and many shell hash layers. The shale grades upwards to sandy mudstone to muddy sandstone. Few bituminous wood fragments	2A	
4/2	9/15/20 5/15/17 5/16/2	48		C1 C2				Dark grey shale grading upwards to highly burrowed calcareous sandstone	3	
4/3	9/15/20 5/15/17 5/16/2	49 CS1 50		C1 C3 C1				Fine grained sandstone with abundant wave ripples and mud flasers - Many mid. landward upward moving Skolithos burrows at top	4	Lagoonal tidal sands
4/4	9/15/20 5/15/17 5/16/2	51 51B		C3 C3			Skolithos			

Barrier - Backbarrier Complex
Transgressive



→ Kol. Tho:

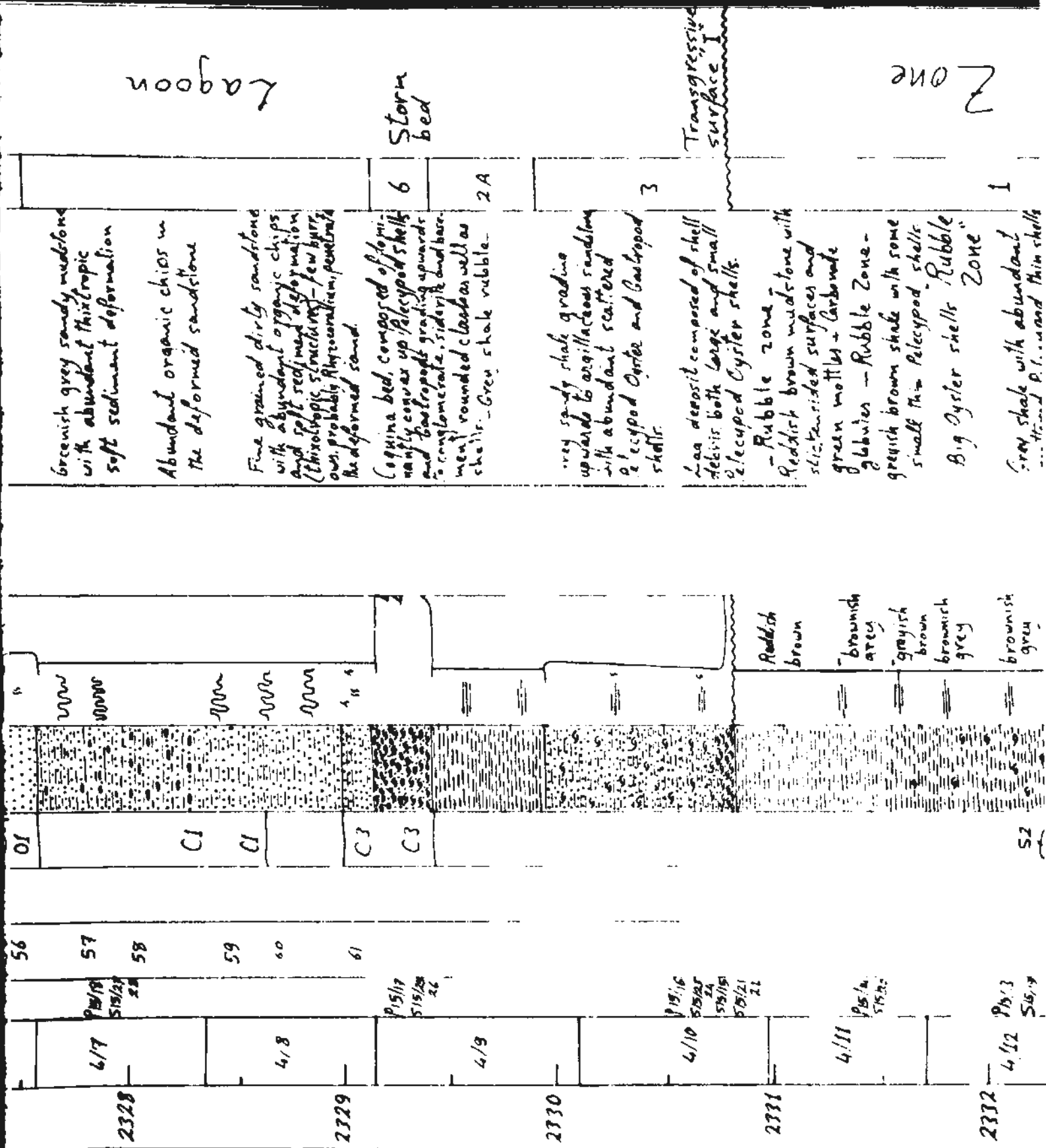
gray
brownish

Lagoon
tidal
sands

Лаборатория

Storm
bed

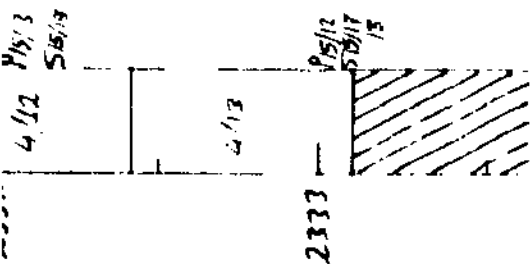
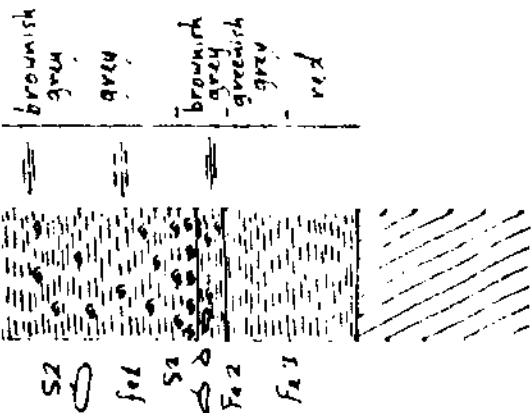
2A



7105

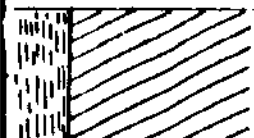
1

Grey shale with abundant scattered Pelecypod thin shells and large Oyster shells
 Rubble, Cong
 brownish grey shale with abundant Pelecypod shells and many siderite nodules.
 greenish grey and reddish brown mudstone with slickensided surfaces and green veinlets.



brown mudstone with
slickensided surfaces and
green veins.

red



P5/12
50/17
18



2333

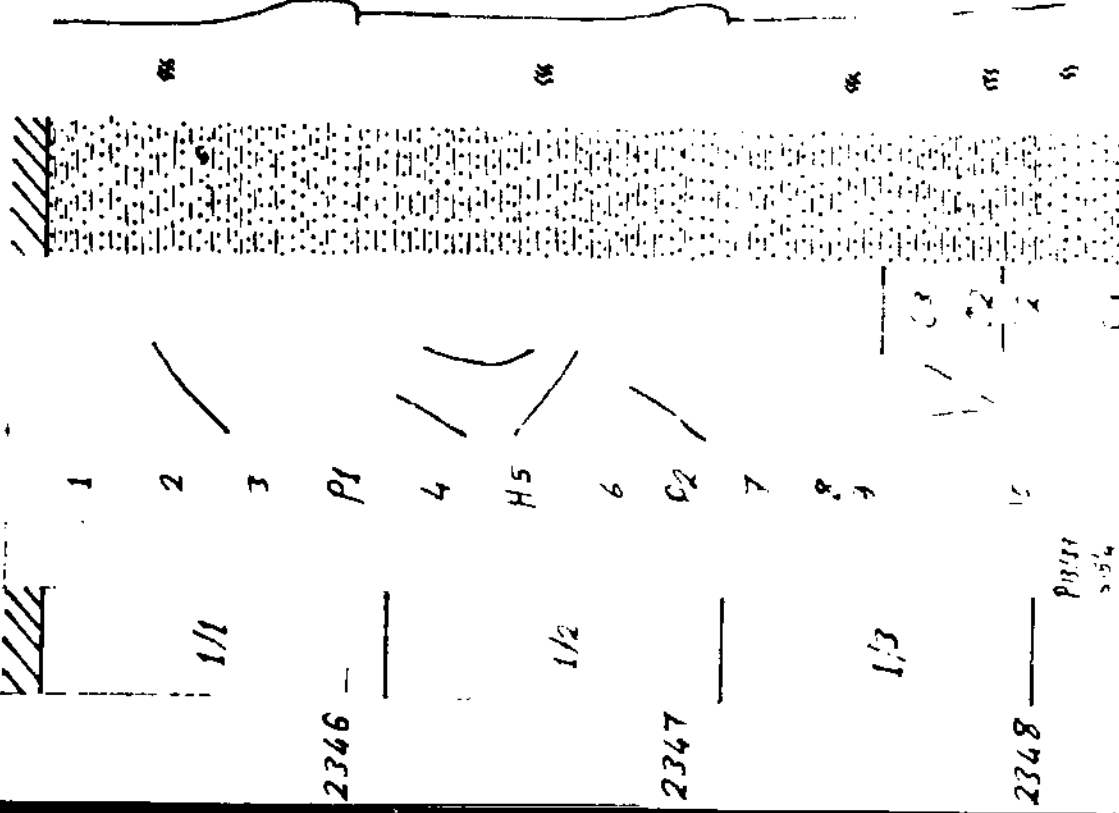
1. The first part of the document is a list of the names of the persons who were present at the meeting.

Well N12m Hibernia K-16

Location 46° 43' 39.8" N Lat. 48° 47' 35.9" W Long.
K.B. 33.2m. - 79.8m.

Osama H. Soliman
K.B.
September 15th. 1992 1/5

Core
1
2
3
4
5
6
7
8
9
10
11
12
13
14
15
16
17
18
19
20
21
22
23
24
25
26
27
28
29
30
31
32
33
34
35
36
37
38
39
40
41
42
43
44
45
46
47
48
49
50
51
52
53
54
55
56
57
58
59
60
61
62
63
64
65
66
67
68
69
70
71
72
73
74
75
76
77
78
79
80
81
82
83
84
85
86
87
88
89
90
91
92
93
94
95
96
97
98
99
100



Slacken sided fracture

11A

Slump fracture

11A

Planolites
Teichichnus
Palaeophycus

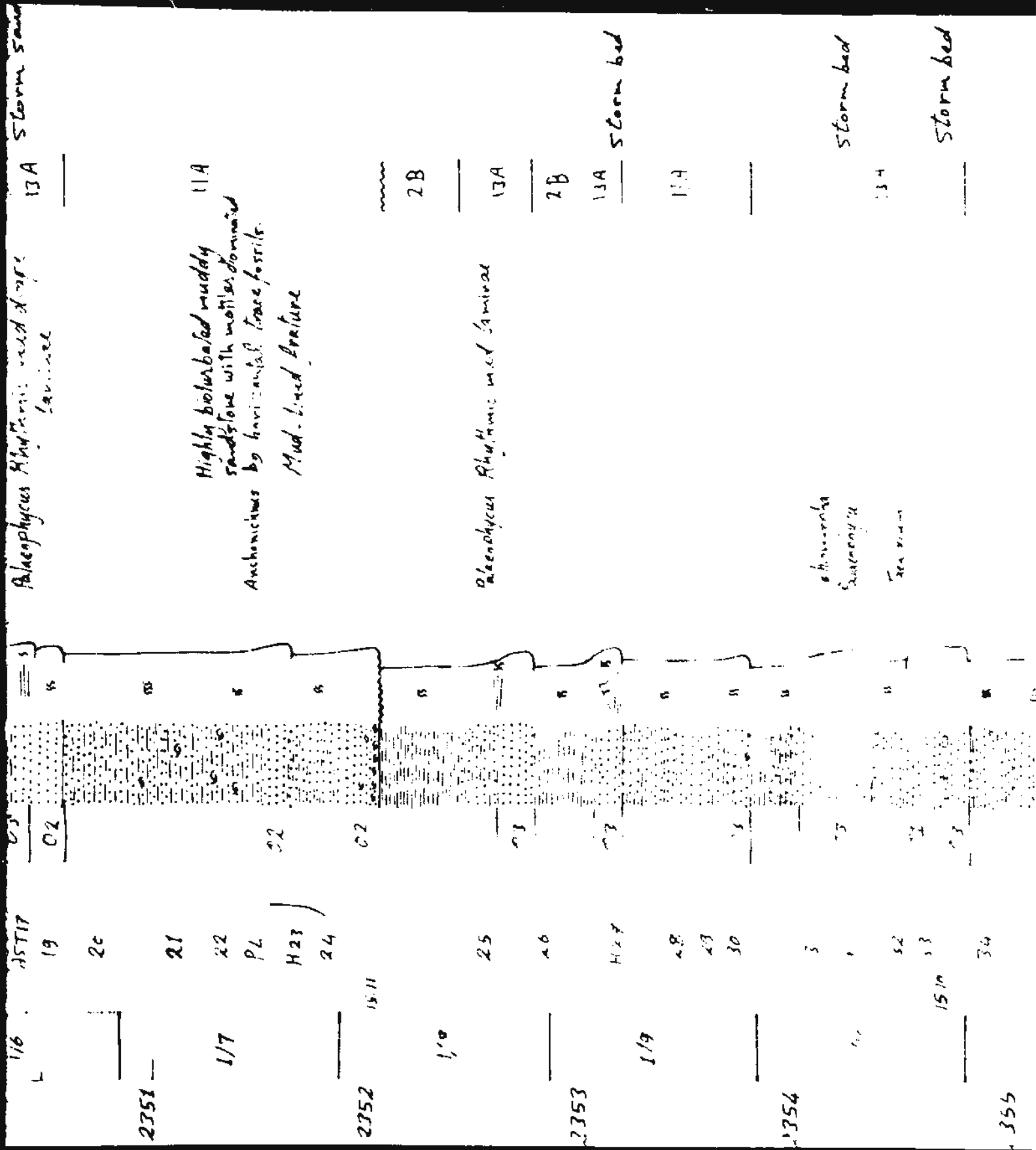
Palaeophycus

Ind. 1 of fractures
between boundaries between the
caliche cementation and 1/2
1/2 5/1000 3

Relative orientation of the bore

Restricted Marine

2346 —
2347 —
2348 —
P8114
5.56



2355

1/11

35

36

37

38

2356

1/12

39

40

41

2357

1/13

42 42.5

43 43.5

44

2358

1/14 44.5 45.5

45

46

47 47.5 48.5

2359

1/15

49 49.5

50

51

Shallow marine

1/12

1/12 1/12 1/12

1/12 1/12 1/12

1/12

1/12 1/12 1/12

1/12

1/12 1/12 1/12

1/12 1/12 1/12

1/12 1/12 1/12

1/12 1/12 1/12

1/12 1/12 1/12

1/12 1/12 1/12

112

62

96

40

2357

113

13

三

٥٤

574

45763

P. 325

١٠

2

2
1
I

5/10

4

658

51

15

2

2

6952

10

2

2

20

119

Phaeophanus *Articulatus* *lanceolatus* *lanceolatus*

Veridiana

2000-01-01

1. 2. 3. 4. 5. 6. 7. 8. 9. 10. 11. 12. 13. 14. 15. 16. 17. 18. 19. 20. 21. 22. 23. 24. 25. 26. 27. 28. 29. 30. 31. 32. 33. 34. 35. 36. 37. 38. 39. 40. 41. 42. 43. 44. 45. 46. 47. 48. 49. 50. 51. 52. 53. 54. 55. 56. 57. 58. 59. 60. 61. 62. 63. 64. 65. 66. 67. 68. 69. 70. 71. 72. 73. 74. 75. 76. 77. 78. 79. 80. 81. 82. 83. 84. 85. 86. 87. 88. 89. 90. 91. 92. 93. 94. 95. 96. 97. 98. 99. 100. 101. 102. 103. 104. 105. 106. 107. 108. 109. 110. 111. 112. 113. 114. 115. 116. 117. 118. 119. 120. 121. 122. 123. 124. 125. 126. 127. 128. 129. 130. 131. 132. 133. 134. 135. 136. 137. 138. 139. 140. 141. 142. 143. 144. 145. 146. 147. 148. 149. 150. 151. 152. 153. 154. 155. 156. 157. 158. 159. 160. 161. 162. 163. 164. 165. 166. 167. 168. 169. 170. 171. 172. 173. 174. 175. 176. 177. 178. 179. 180. 181. 182. 183. 184. 185. 186. 187. 188. 189. 190. 191. 192. 193. 194. 195. 196. 197. 198. 199. 200. 201. 202. 203. 204. 205. 206. 207. 208. 209. 210. 211. 212. 213. 214. 215. 216. 217. 218. 219. 220. 221. 222. 223. 224. 225. 226. 227. 228. 229. 230. 231. 232. 233. 234. 235. 236. 237. 238. 239. 240. 241. 242. 243. 244. 245. 246. 247. 248. 249. 250. 251. 252. 253. 254. 255. 256. 257. 258. 259. 260. 261. 262. 263. 264. 265. 266. 267. 268. 269. 270. 271. 272. 273. 274. 275. 276. 277. 278. 279. 280. 281. 282. 283. 284. 285. 286. 287. 288. 289. 290. 291. 292. 293. 294. 295. 296. 297. 298. 299. 300. 301. 302. 303. 304. 305. 306. 307. 308. 309. 310. 311. 312. 313. 314. 315. 316. 317. 318. 319. 320. 321. 322. 323. 324. 325. 326. 327. 328. 329. 330. 331. 332. 333. 334. 335. 336. 337. 338. 339. 340. 341. 342. 343. 344. 345. 346. 347. 348. 349. 350. 351. 352. 353. 354. 355. 356. 357. 358. 359. 360. 361. 362. 363. 364. 365. 366. 367. 368. 369. 370. 371. 372. 373. 374. 375. 376. 377. 378. 379. 380. 381. 382. 383. 384. 385. 386. 387. 388. 389. 390. 391. 392. 393. 394. 395. 396. 397. 398. 399. 400. 401. 402. 403. 404. 405. 406. 407. 408. 409. 410. 411. 412. 413. 414. 415. 416. 417. 418. 419. 420. 421. 422. 423. 424. 425. 426. 427. 428. 429. 430. 431. 432. 433. 434. 435. 436. 437. 438. 439. 440. 441. 442. 443. 444. 445. 446. 447. 448. 449. 450. 451. 452. 453. 454. 455. 456. 457. 458. 459. 460. 461. 462. 463. 464. 465. 466. 467. 468. 469. 470. 471. 472. 473. 474. 475. 476. 477. 478. 479. 480. 481. 482. 483. 484. 485. 486. 487. 488. 489. 490. 491. 492. 493. 494. 495. 496. 497. 498. 499. 500. 501. 502. 503. 504. 505. 506. 507. 508. 509. 510. 511. 512. 513. 514. 515. 516. 517. 518. 519. 520. 521. 522. 523. 524. 525. 526. 527. 528. 529. 530. 531. 532. 533. 534. 535. 536. 537. 538. 539. 540. 541. 542. 543. 544. 545. 546. 547. 548. 549. 550. 551. 552. 553. 554. 555. 556. 557. 558. 559. 560. 561. 562. 563. 564. 565. 566. 567. 568. 569. 570. 571. 572. 573. 574. 575. 576. 577. 578. 579. 580. 581. 582. 583. 584. 585. 586. 587. 588. 589. 590. 591. 592. 593. 594. 595. 596. 597. 598. 599. 600. 601. 602. 603. 604. 605. 606. 607. 608. 609. 610. 611. 612. 613. 614. 615. 616. 617. 618. 619. 620. 621. 622. 623. 624. 625. 626. 627. 628. 629. 630. 631. 632. 633. 634. 635. 636. 637. 638. 639. 640. 641. 642. 643. 644. 645. 646. 647. 648. 649. 650. 651. 652. 653. 654. 655. 656. 657. 658. 659. 660. 661. 662. 663. 664. 665. 666. 667. 668. 669. 670. 671. 672. 673. 674. 675. 676. 677. 678. 679. 680. 681. 682. 683. 684. 685. 686. 687. 688. 689. 690. 691. 692. 693. 694. 695. 696. 697. 698. 699. 700. 701. 702. 703. 704. 705. 706. 707. 708. 709. 710. 711. 712. 713. 714. 715. 716. 717. 718. 719. 720. 721. 722. 723. 724. 725. 726. 727. 728. 729. 730. 731. 732. 733. 734. 735. 736. 737. 738. 739. 740. 741. 742. 743. 744. 745. 746. 747. 748. 749. 750. 751. 752. 753. 754. 755. 756. 757. 758. 759. 760. 761. 762. 763. 764. 765. 766. 767. 768. 769. 770. 771. 772. 773. 774. 775. 776. 777. 778. 779. 780. 781. 782. 783. 784. 785. 786. 787. 788. 789. 790. 791. 792. 793. 794. 795. 796. 797. 798. 799. 800. 801. 802. 803. 804. 805. 806. 807. 808. 809. 810. 811. 812. 813. 814. 815. 816. 817. 818. 819. 820. 821. 822. 823. 824. 825. 826. 827. 828. 829. 830. 831. 832. 833. 834. 835. 836. 837. 838. 839. 840. 84

www.ck12.org

indicates

[illegible]

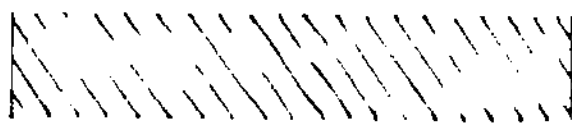
En: 34000000

storm
bed

Shallow marine

2361

1.1



2362

2363

45TSS

P7A

H55

56

57

59

4.1

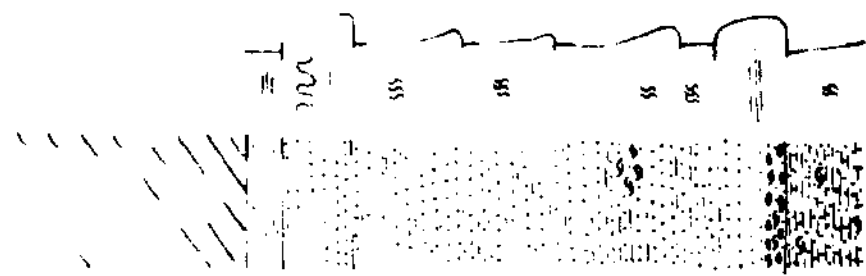
2364

2/2

59

P15th
S14.14

2365



Burrows in silty shale
and sand

Dark grey laminated shale

Clump burrows lined

with mud and shell debris

Storm bed

Thickened, defined burrows

Some burrows are filled

with sand and shell debris

Clumps of shell debris

Mud clasts and pelecypod

shell debris as lag

deposits.

13A

2B

Well Name Hibernia K-14

Location 46° 43' 39" N Lat. 48° 47' 39" W Long
KB-33.2m GL-79.8m R1

Logged by: Orana M. Saliman
Dep'n. K.B.

Date September 15th 1992 2/5

| Core no/
Box no | Prints
5: slides | Sample
no | Fractures | Cements
oil stain | Lithology | Sed Structures
mud & sand | Fossils | Remarks | Notes | Environment |
|--------------------|---------------------------|--------------|-----------|----------------------|-----------|------------------------------|--|---|-------|--------------|
| 2/2 | P13/20
S14/26
15/16 | H60 | | 04 | | | Ophiomorpha
Ophiomorpha
Salicophycus
Palaophycus
Ophiomorpha | Surrounding are filled with sand
and shell debris.
Rhythmic mud drapes
- lump faulting | 13A | Storm bed |
| 2/3 | 15/15
15/16 | 62 | | 04 | | | | Thin-walled small shell
debris on lag deposits | | Storm
bed |
| 2/4 | 15/18 | 64 | | | | | Palaophycus | Thin-walled mud. sea
debris on lag deposits | 1/4 | |
| 2/5 | P13/20
S14/26
15/16 | 66 | | | | | | | | |
| 2/6 | P13/20
S14/26
15/16 | 68 | | | | | | | | |
| 2/7 | P13/20
S14/26
15/16 | 70 | | | | | | | | |
| 2/8 | P13/20
S14/26
15/16 | 72 | | | | | | | | |
| 2/9 | P13/20
S14/26
15/16 | 74 | | | | | | | | |
| 2/10 | P13/20
S14/26
15/16 | 76 | | | | | | | | |
| 2/11 | P13/20
S14/26
15/16 | 78 | | | | | | | | |
| 2/12 | P13/20
S14/26
15/16 | 80 | | | | | | | | |
| 2/13 | P13/20
S14/26
15/16 | 82 | | | | | | | | |
| 2/14 | P13/20
S14/26
15/16 | 84 | | | | | | | | |
| 2/15 | P13/20
S14/26
15/16 | 86 | | | | | | | | |
| 2/16 | P13/20
S14/26
15/16 | 88 | | | | | | | | |
| 2/17 | P13/20
S14/26
15/16 | 90 | | | | | | | | |
| 2/18 | P13/20
S14/26
15/16 | 92 | | | | | | | | |
| 2/19 | P13/20
S14/26
15/16 | 94 | | | | | | | | |
| 2/20 | P13/20
S14/26
15/16 | 96 | | | | | | | | |
| 2/21 | P13/20
S14/26
15/16 | 98 | | | | | | | | |
| 2/22 | P13/20
S14/26
15/16 | 100 | | | | | | | | |
| 2/23 | P13/20
S14/26
15/16 | 102 | | | | | | | | |
| 2/24 | P13/20
S14/26
15/16 | 104 | | | | | | | | |
| 2/25 | P13/20
S14/26
15/16 | 106 | | | | | | | | |
| 2/26 | P13/20
S14/26
15/16 | 108 | | | | | | | | |
| 2/27 | P13/20
S14/26
15/16 | 110 | | | | | | | | |
| 2/28 | P13/20
S14/26
15/16 | 112 | | | | | | | | |
| 2/29 | P13/20
S14/26
15/16 | 114 | | | | | | | | |
| 2/30 | P13/20
S14/26
15/16 | 116 | | | | | | | | |
| 2/31 | P13/20
S14/26
15/16 | 118 | | | | | | | | |
| 2/32 | P13/20
S14/26
15/16 | 120 | | | | | | | | |
| 2/33 | P13/20
S14/26
15/16 | 122 | | | | | | | | |
| 2/34 | P13/20
S14/26
15/16 | 124 | | | | | | | | |
| 2/35 | P13/20
S14/26
15/16 | 126 | | | | | | | | |
| 2/36 | P13/20
S14/26
15/16 | 128 | | | | | | | | |
| 2/37 | P13/20
S14/26
15/16 | 130 | | | | | | | | |
| 2/38 | P13/20
S14/26
15/16 | 132 | | | | | | | | |
| 2/39 | P13/20
S14/26
15/16 | 134 | | | | | | | | |
| 2/40 | P13/20
S14/26
15/16 | 136 | | | | | | | | |
| 2/41 | P13/20
S14/26
15/16 | 138 | | | | | | | | |
| 2/42 | P13/20
S14/26
15/16 | 140 | | | | | | | | |
| 2/43 | P13/20
S14/26
15/16 | 142 | | | | | | | | |
| 2/44 | P13/20
S14/26
15/16 | 144 | | | | | | | | |
| 2/45 | P13/20
S14/26
15/16 | 146 | | | | | | | | |
| 2/46 | P13/20
S14/26
15/16 | 148 | | | | | | | | |
| 2/47 | P13/20
S14/26
15/16 | 150 | | | | | | | | |
| 2/48 | P13/20
S14/26
15/16 | 152 | | | | | | | | |
| 2/49 | P13/20
S14/26
15/16 | 154 | | | | | | | | |
| 2/50 | P13/20
S14/26
15/16 | 156 | | | | | | | | |
| 2/51 | P13/20
S14/26
15/16 | 158 | | | | | | | | |
| 2/52 | P13/20
S14/26
15/16 | 160 | | | | | | | | |
| 2/53 | P13/20
S14/26
15/16 | 162 | | | | | | | | |
| 2/54 | P13/20
S14/26
15/16 | 164 | | | | | | | | |
| 2/55 | P13/20
S14/26
15/16 | 166 | | | | | | | | |
| 2/56 | P13/20
S14/26
15/16 | 168 | | | | | | | | |
| 2/57 | P13/20
S14/26
15/16 | 170 | | | | | | | | |
| 2/58 | P13/20
S14/26
15/16 | 172 | | | | | | | | |
| 2/59 | P13/20
S14/26
15/16 | 174 | | | | | | | | |
| 2/60 | P13/20
S14/26
15/16 | 176 | | | | | | | | |
| 2/61 | P13/20
S14/26
15/16 | 178 | | | | | | | | |
| 2/62 | P13/20
S14/26
15/16 | 180 | | | | | | | | |
| 2/63 | P13/20
S14/26
15/16 | 182 | | | | | | | | |
| 2/64 | P13/20
S14/26
15/16 | 184 | | | | | | | | |
| 2/65 | P13/20
S14/26
15/16 | 186 | | | | | | | | |
| 2/66 | P13/20
S14/26
15/16 | 188 | | | | | | | | |
| 2/67 | P13/20
S14/26
15/16 | 190 | | | | | | | | |
| 2/68 | P13/20
S14/26
15/16 | 192 | | | | | | | | |
| 2/69 | P13/20
S14/26
15/16 | 194 | | | | | | | | |
| 2/70 | P13/20
S14/26
15/16 | 196 | | | | | | | | |
| 2/71 | P13/20
S14/26
15/16 | 198 | | | | | | | | |
| 2/72 | P13/20
S14/26
15/16 | 200 | | | | | | | | |
| 2/73 | P13/20
S14/26
15/16 | 202 | | | | | | | | |
| 2/74 | P13/20
S14/26
15/16 | 204 | | | | | | | | |
| 2/75 | P13/20
S14/26
15/16 | 206 | | | | | | | | |
| 2/76 | P13/20
S14/26
15/16 | 208 | | | | | | | | |
| 2/77 | P13/20
S14/26
15/16 | 210 | | | | | | | | |
| 2/78 | P13/20
S14/26
15/16 | 212 | | | | | | | | |
| 2/79 | P13/20
S14/26
15/16 | 214 | | | | | | | | |
| 2/80 | P13/20
S14/26
15/16 | 216 | | | | | | | | |
| 2/81 | P13/20
S14/26
15/16 | 218 | | | | | | | | |
| 2/82 | P13/20
S14/26
15/16 | 220 | | | | | | | | |
| 2/83 | P13/20
S14/26
15/16 | 222 | | | | | | | | |
| 2/84 | P13/20
S14/26
15/16 | 224 | | | | | | | | |
| 2/85 | P13/20
S14/26
15/16 | 226 | | | | | | | | |
| 2/86 | P13/20
S14/26
15/16 | 228 | | | | | | | | |
| 2/87 | P13/20
S14/26
15/16 | 230 | | | | | | | | |
| 2/88 | P13/20
S14/26
15/16 | 232 | | | | | | | | |
| 2/89 | P13/20
S14/26
15/16 | 234 | | | | | | | | |
| 2/90 | P13/20
S14/26
15/16 | 236 | | | | | | | | |
| 2/91 | P13/20
S14/26
15/16 | 238 | | | | | | | | |
| 2/92 | P13/20
S14/26
15/16 | 240 | | | | | | | | |
| 2/93 | P13/20
S14/26
15/16 | 242 | | | | | | | | |
| 2/94 | P13/20
S14/26
15/16 | 244 | | | | | | | | |
| 2/95 | P13/20
S14/26
15/16 | 246 | | | | | | | | |
| 2/96 | P13/20
S14/26
15/16 | 248 | | | | | | | | |
| 2/97 | P13/20
S14/26
15/16 | 250 | | | | | | | | |
| 2/98 | P13/20
S14/26
15/16 | 252 | | | | | | | | |
| 2/99 | P13/20
S14/26
15/16 | 254 | | | | | | | | |
| 2/100 | P13/20
S14/26
15/16 | 256 | | | | | | | | |
| 2/101 | P13/20
S14/26
15/16 | 258 | | | | | | | | |
| 2/102 | P13/20
S14/26
15/16 | 260 | | | | | | | | |
| 2/103 | P13/20
S14/26
15/16 | 262 | | | | | | | | |
| 2/104 | P13/20
S14/26
15/16 | 264 | | | | | | | | |
| 2/105 | P13/20
S14/26
15/16 | 266 | | | | | | | | |
| 2/106 | P13/20
S14/26
15/16 | 268 | | | | | | | | |
| 2/107 | P13/20
S14/26
15/16 | 270 | | | | | | | | |
| 2/108 | P13/20
S14/26
15/16 | 272 | | | | | | | | |
| 2/109 | P13/20
S14/26
15/16 | 274 | | | | | | | | |
| 2/110 | P13/20
S14/26
15/16 | 276 | | | | | | | | |
| 2/111 | P13/20
S14/26
15/16 | 278 | | | | | | | | |
| 2/112 | P13/20
S14/26
15/16 | 280 | | | | | | | | |
| 2/113 | P13/20
S14/26
15/16 | 282 | | | | | | | | |
| 2/114 | P13/20
S14/26
15/16 | 284 | | | | | | | | |
| 2/115 | P13/20
S14/26
15/16 | 286 | | | | | | | | |
| 2/116 | P13/20
S14/26
15/16 | 288 | | | | | | | | |
| 2/117 | P13/20
S14/26
15/16 | 290 | | | | | | | | |
| 2/118 | P13/20
S14/26
15/16 | 292 | | | | | | | | |
| 2/119 | P13/20
S14/26
15/16 | 294 | | | | | | | | |
| 2/120 | P13/20
S14/26
15/16 | 296 | | | | | | | | |
| 2/121 | P13/20
S14/26
15/16 | 298 | | | | | | | | |
| 2/122 | P13/20
S14/26
15/16 | 300 | | | | | | | | |
| 2/123 | P13/20
S14/26
15/16 | 302 | | | | | | | | |
| 2/124 | P13/20
S14/26
15/16 | 304 | | | | | | | | |
| 2/125 | P13/20
S14/26
15/16 | 306 | | | | | | | | |
| 2/126 | P13/20
S14/26
15/16 | 308 | | | | | | | | |
| 2/127 | P13/20
S14/26
15/16 | 310 | | | | | | | | |
| 2/128 | P13/20
S14/26
15/16 | 312 | | | | | | | | |
| 2/129 | P13/20
S14/26
15/16 | 314 | | | | | | | | |
| 2/130 | P13/20
S14/26
15/16 | 316 | | | | | | | | |
| 2/131 | P13/20
S14/26
15/16 | 318 | | | | | | | | |
| 2/132 | P13/20
S14/26
15/16 | 320 | | | | | | | | |
| 2/133 | P13/20
S14/26
15/16 | 322 | | | | | | | | |
| 2/134 | P13/20
S14/26
15/16 | 324 | | | | | | | | |
| 2/135 | P13/20
S14/26
15/16 | 326 | | | | | | | | |
| 2/136 | P13/20
S14/26
15/16 | 328 | | | | | | | | |
| 2/137 | P13/20
S14/26
15/16 | 330 | | | | | | | | |
| 2/138 | P13/20
S14/26
15/16 | 332 | | | | | | | | |
| 2/139 | P13/20
S14/26
15/16 | 334 | | | | | | | | |
| 2/140 | P13/20
S14/26
15/16 | 336 | | | | | | | | |
| 2/141 | P13/20
S14/26
15/16 | 338 | | | | | | | | |
| 2/142 | P13/20
S14/26
15/16 | 340 | | | | | | | | |
| 2/143 | P13/20
S14/26
15/16 | 342 | | | | | | | | |
| 2/144 | P13/20
S14/26
15/16 | 344 | | | | | | | | |
| 2/145 | P13/20
S14/26
15/16 | 346 | | | | | | | | |
| 2/146 | P13/20
S14/26
15/16 | 348 | | | | | | | | |
| 2/147 | P13/20
S14/26
15/16 | 350 | | | | | | | | |
| 2/148 | P13/20
S14/26
15/16 | 352 | | | | | | | | |
| 2/149 | P13/20
S14/26
15/16 | 354 | | | | | | | | |
| 2/150 | P13/20
S14/26
15/16 | 356 | | | | | </ | | | |

Shallow Marine

P1380
S14124
27

2369

71
72
73
61

27

2370

74

28

2371

75

76

157

29

2372

77

78

P1380

S14124

25

15.6

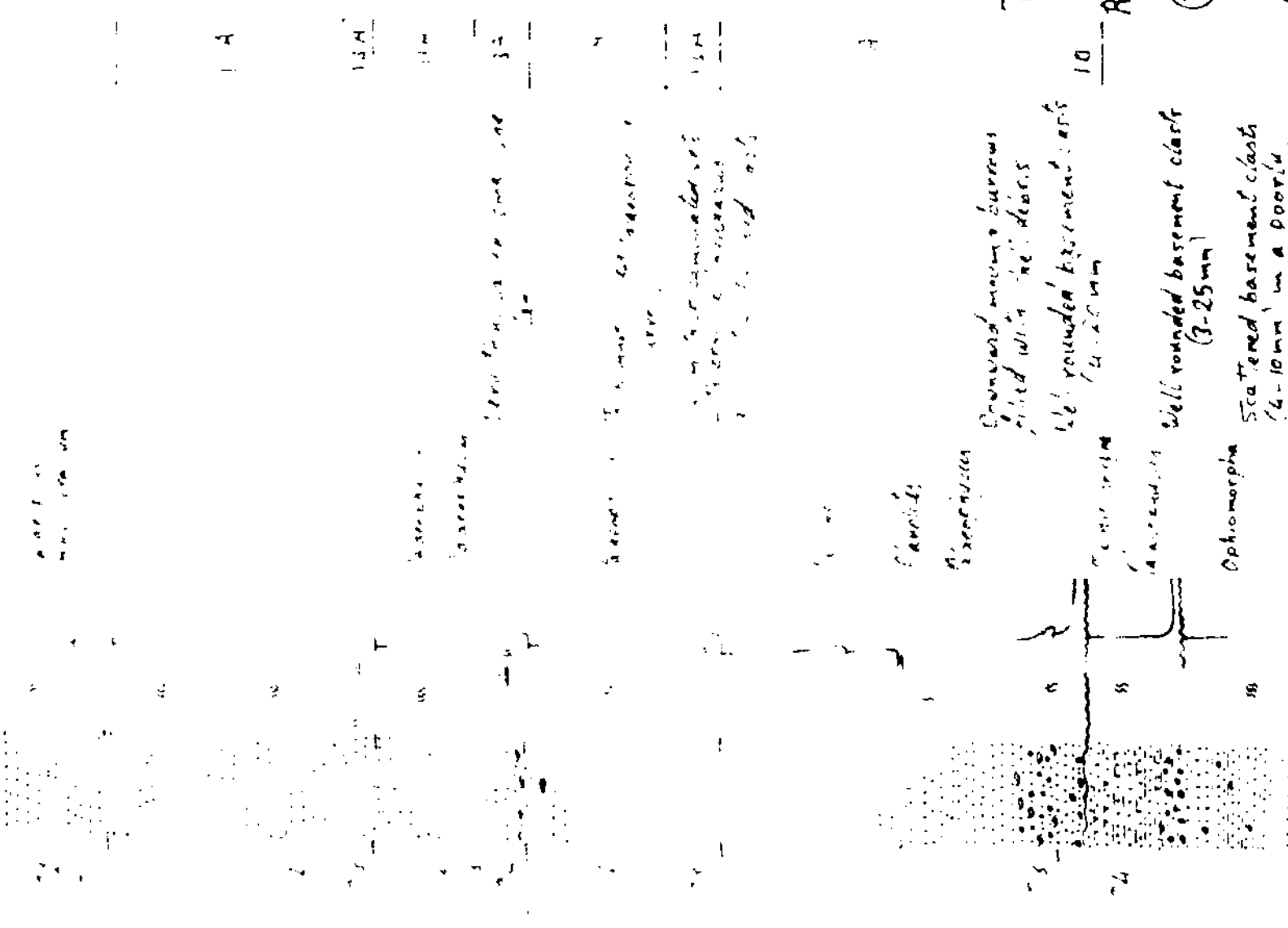
81

2/10

2373

82

P11



Transgressive
Lag

Ravinement
Surface
(TSI)

Groundward moving burrows
filled with "cl" debris
Well rounded fragment clasts
(4-25mm)

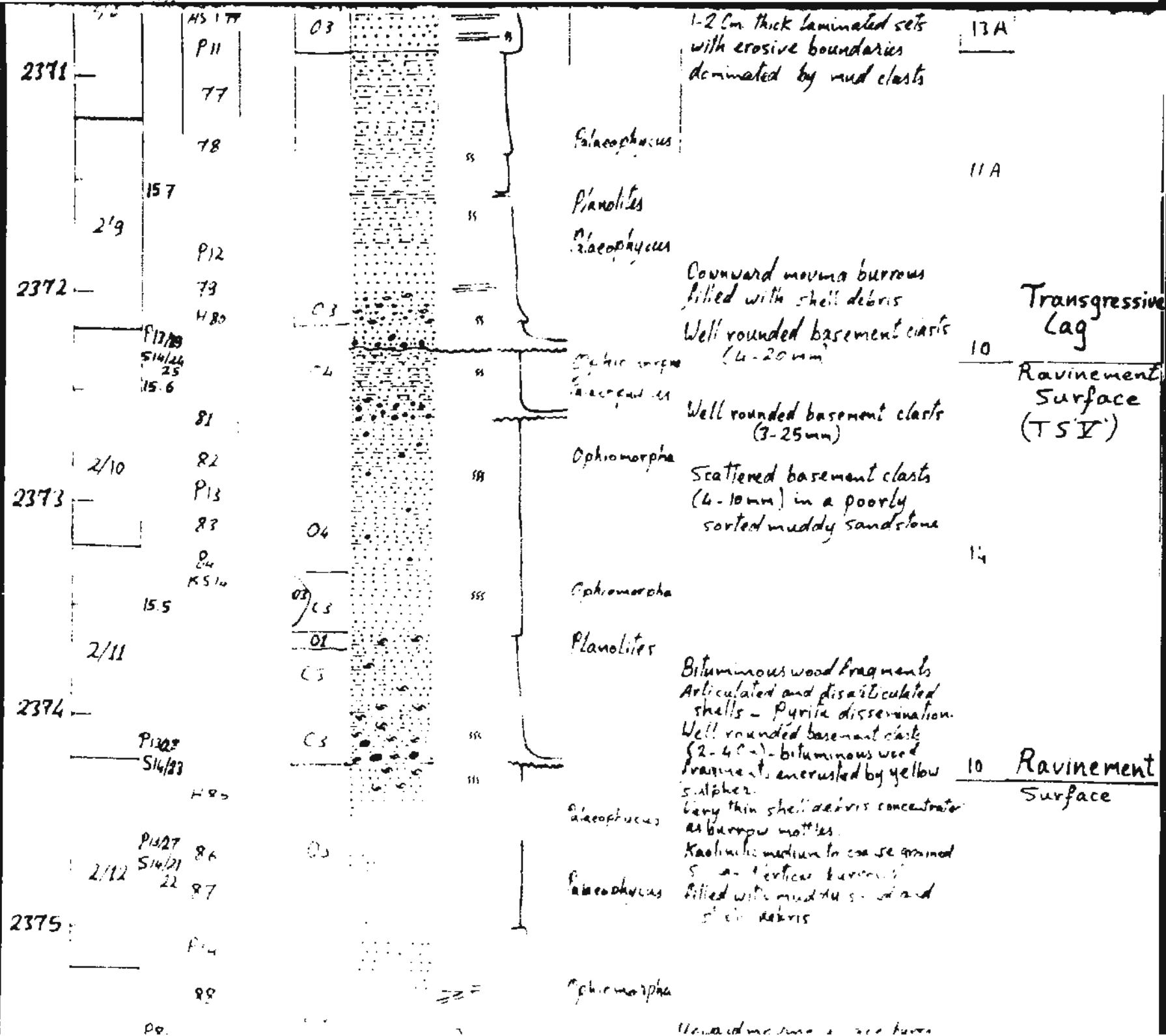
Well rounded basement clasts
(3-25mm)

Scattered basement clasts
(4-10mm) in a poorly

Clavids
M. xanthopora

Clavids
M. xanthopora

Ophiomorpha



Shoreface Sands

11 paces in diameter as are tubes

15

15

6 tubes in sand fragments

medium to coarse
grained sandstone
uninterrupted in the lower
part and in the lower
part of the section
the upper part is
interrupted by
lenses of
limestone between
the sandstone layers

1. 10 paces in diameter

89

99/26
54/8
2113 99/25 93
P15
54/1 92
5

2376

P16
2114 P1326 91
54/116 92

2377

93
2115 94

2378

95
2116 P1325 96
54/15

2379

97
P17
2117 45777

2380



|||||

2381

98
99
F18
H100

3/1

K515

101
102

2382

P8/24
S4/1

3/2

103
104
105
P19
106
107
108

2383

3/3

109
H110
P20
111
P8/23

2384

P8/24
S4/1

3/4

112
113
114
H115
116
P21

2385

3/5 P8/23
S4/10

117
118

thin-bedded
sandstone

thin-bedded sandstone
basement last 5 cm

thin-bedded
sandstone

thin-bedded
sandstone

thin-bedded sandstone
thin-bedded sandstone
thin-bedded sandstone
thin-bedded sandstone

thin-bedded sandstone
thin-bedded sandstone
thin-bedded sandstone
thin-bedded sandstone

Ravinement
Surface

Lower shoreface

10 Ravinement
14 Surface (TS IV)

Well Name: Hibernia K-14

Location 46° 43' 39.8" N Lat 48° 47' 35.9" W Long.
K.B.: 33.2 m G.L. - 79.8 m. RT

Logged by Osama H. Soliman
K.B.
Date September 15th, 1992 3/5

| Core no/
Box no | P-Prints
S=slides | Sample
no | Fractures | Cements | Lithology | Sed Structures | Fossils | Environment |
|--------------------|---|---------------------------|-----------|---------|-----------|----------------|---------|-------------|
| 3/5 | | 119
H120
121
P22 | | | | ms | | |
| | | | | 04 | | ms | | |
| 2386 | P14/22
S14/9
122
KS23
123
KS13
KS12
KS12A
125 | | | C4 | | ms | | |
| | | | | | | ms | | |
| 2387 | P14/20
21
S14/5
127
P23
128 | 126
127 | | | | ms | | |
| | | | | | | ms | | |
| 2388 | P14/18
19
S14/6
130
F14/17
131
S14/5
K20 | 124
KS11
130
131 | | | | ms | | |

Tidal inlet channel (?)

Ophiomorpha Irregularly scattered pebbles
clasts in sandstone

Ophiomorpha Relict inclined lamination

6" rounded basement clasts -
(3-30 mm) - thin-walled
Pelecypod shell debris

5" rounded basement
clasts

very coarse poorly sorted fine grained
sandstone with small and large
clasts (3-20 mm) - thin-walled
Pelecypod shell debris and laminae
- poorly sorted very coarse sand
with abundant well rounded
shell debris, with large
clasts

Erosional
Surface II

Complex Transpress Surface

Transf. Surface

1

coarse to very coarse grained
 sandstone with well rounded
 basement clasts 3-8 mm
 Brownish pores
 highly indurated

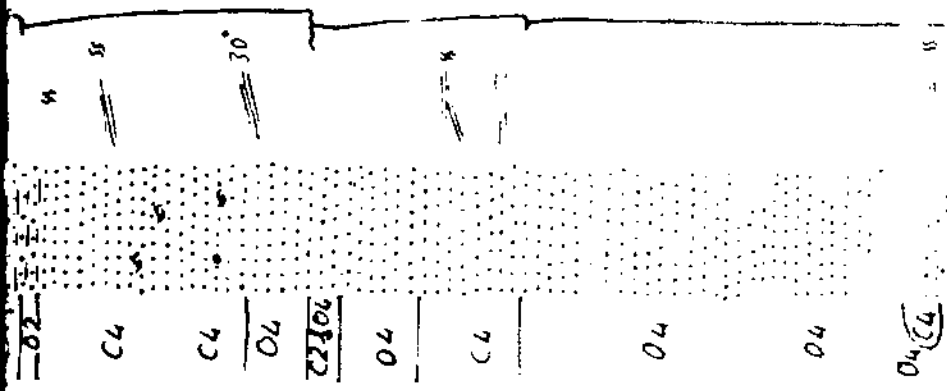
9/13/15
544/1, K59
2 143 144

854 2/15
5914 7/15

671
12-54
148

151
150
D28

152
KS222
25T
027
KSY



Pistia - wisp. laminae

Ophiomorpho Relict inclined lamination

Ophiomorphic
sandstone with well rounded
basement clasts (3-8 mm)
Biomoldic pores

Wispypy bituminous laminae

City of Chicago

Bavaria

3A

Transverse
Surface

Barrier-Backbarrier Complex

Some basement
beds are base-
ment rocks, others are
unindurated, some are
laminated, some are
thinly bedded, some
are massive, some are
interbedded.

Lagoon

Lagoon

Lagoon

5045

2604

2605

2604

2601

Aug
51429

Aug
51428

Aug
51427

Well Name Hibernia K-14

Location 46° 43' 39.8" N Lat. 48° 47' 35.9" W Long

KB 332 m GL - 79.8 m RI

Logged by: Osama M. Soliman

KB

Date September 15th, 1991 4/5

| Core no.
Box no. | Prints
Slides | Sample no. | Features | Remarks | Environment |
|---------------------|------------------|------------|----------|--|----------------------------|
| 4/8 | | | | | |
| 4/9 | 913/8
518/26 | | | Dark grey Coquina with a sandstone matrix | 2A Reef talus |
| | 913/7
518/25 | | | Dark grey shale | 2A Transgressive surface I |
| | | | | Dark grey coquina with a shell hash layer | I Subaerial exposure |
| | | | | Brownish dark grey shale with many shell hash layers | |
| | | | | Scattered Felcepodonta | |
| | | | | Isolated shells | |

IV

Pond (?)

Marsh

5

Marsh

P126

518/26

- 51

P125

Plus

5/5/54

三

2

5/2/5

875

2.4

5.

5/15/92
F. J. A. M.

P1312

P1313

1411

54

5/2

1. The first part of the document is a list of names and titles, including "The Hon. Mr. Justice" and "The Hon. Mr. Justice".

4

[Faint handwritten notes at the bottom of the page, possibly "Lars" and "N"]

$\frac{1}{\sqrt{2}}$

Very good and
very interesting

20150508 11:11:11 20150508 11:11:11 20150508 11:11:11

[illegible]

7

III

040

27

5016

$\frac{d}{dt} \left(\frac{1}{r^2} \right) = -\frac{2}{r^3} \frac{dr}{dt}$

in quick succession, as if to say, "I am now, I am here, I am now, I am here."

irradiated sandstone irradiation
induced by ultraviolet

$$2\pi i \int_{\partial D} \frac{1}{z} dz = 2\pi i \cdot 1 = 2\pi i$$
[illegible]

27

11. 11. 1956, 15

600-5m. 980-4. 57m. e. 1011/2

and organic-rich laminae
few bleached shells

hundreds of trees are

the previous paragraph is
to satisfy other

100

| Core No. | Interval | Depth (m) | Lithology | Description | Notes | Zone |
|----------|----------|------------------------------------|--|---|---------|--------------------|
| 2410 | 5/3 | | Brown
Greyish green
Reddish brown
Greenish grey | abundant green veins.
Greyish green mudstone rubble
Reddish brown mudstone with abundant green grains.
Greenish grey mudstone with abundant brown grains and mottles | 1
2A | Inundation |
| 2411 | 5/4 | P13/4
S13/28
P13/3
S13/21 | C2
Greenish grey
Light grey
Greyish brown | Greenish grey sandy mudstone
Light grey argillaceous ss.
2-10 cm. thick sets of rippled to laminated sandstone grading upward to bioturbated mudstone - disseminate pyrite | 1
4 | Subaerial exposure |
| 2412 | 5/5 | | Reddish brown
Greenish grey
greyish brown | Reddish brown shale with many greenish grey veils and some laminated to rippled sand layers that grade upwards to shale
Pelecypod shells
Greenish grey shale with many organic-rich laminae few pelecypod shells
Abundant greenish green grains in the brown mudstone.
Slickensided surfaces
Hubble zone | 1 | "II" Soil zone |
| 2413 | 5/6 | P13/2
S13/19
20 | Reddish brown | Reddish brown shale that has some bioturbated intervals and many greyish green sand layers and veins.
Slickensided surfaces. | 1 | I' Soil Zone |
| 2414 | 5/7 | P13/1
S13/17
18 | brownish-grey
Dark grey
brownish grey | Brownish grey mudstone with scattered pelecypod and | 2A | |

Brownish grey mudstone with scattered "Elocypod and Gastropod shell" debris

Rubble zone

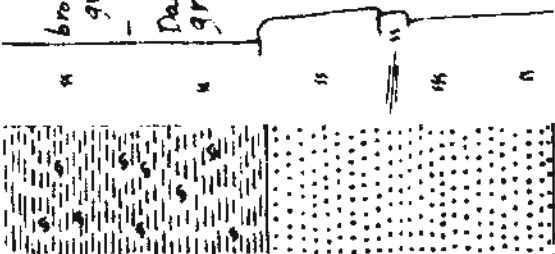
Dark grey mudstone with abundant scattered small "Elocypod and Gastropod shell" debris and "lenses of shell hash" with muddy matrix - few bituminous organic chips.

2A

11A

brownish grey

Dark grey



2415

5/8

2416

5/9

2411

2418

2419

2417

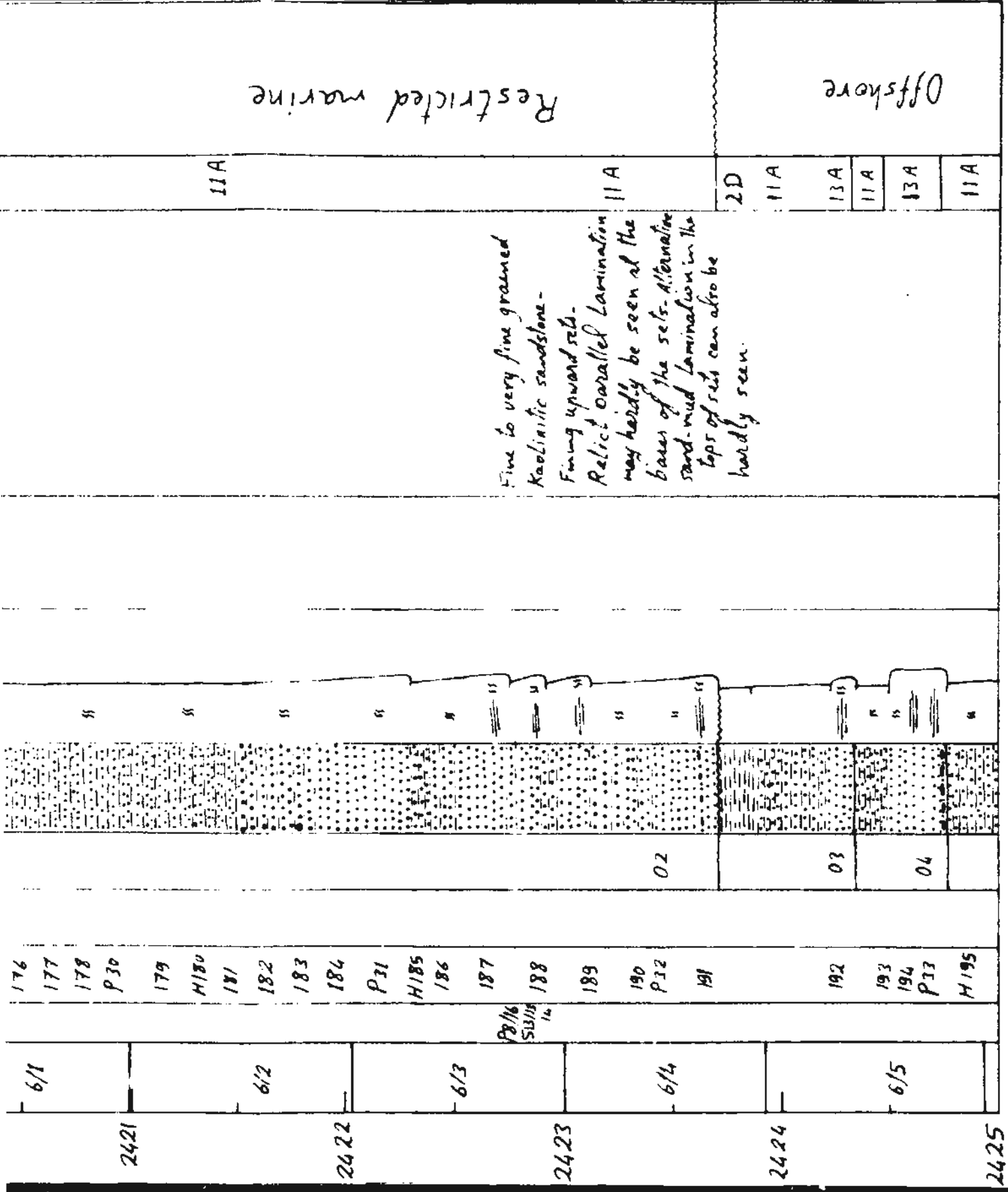
2418

2419

2420

174
175
176
177
178

6/1



Well Name: Hibernia K-14

Location: 46° 43' 39.8" N Lat. 48° 47' 35.9" W Long

K.B.: 33.2 m GL - 97.8 m RT.

Logged by: Osama M. Soliman

Depth from K.B.

Date: September 15th 1992 5/5

| Core no/
Box no | P=Prints
S=slides | Sample
no | Fractures | cements
oil stain | Lithology | Sed Structures
mud $\frac{VF}{VF} \frac{EU}{EU} \frac{X}{X} \frac{S}{S}$ | Fossils | Remarks | Facies | Environment |
|--------------------|-----------------------|--------------------|-----------|----------------------|-----------|---|---------------|---|--------|-------------|
| 6/6 | P8/15
S13/11
12 | 195 | | | | $\frac{S}{S}$
$\frac{H}{H}$
$\frac{S}{S}$ | Palaeophycus | Upward increase of frequency of mud laminae | 2D | |
| | | 196 | | 03
04 | | | | | 13A | |
| | | P34 | | | | | Sphionomorpha | Rhythmic mud laminae that increase in frequency upwards | 2D | |
| | | AST 195
AST 196 | | 02 | | | | | 13A | |
| 6/7 | | | | | | $\frac{S}{S}$ | Palaeophycus | | | |
| | | | | | | | | | | |
| | | | | | | | | | | |
| 2427 | | | | | | $\frac{S}{S}$ | | | 2D | |
| | | | | | | | | | | |
| 6.8 | | | | | | $\frac{S}{S}$ | | | | |
| | | | | | | | | | | |
| 2428 | | | | | | $\frac{S}{S}$ | | | | |

K. M. Soliman

7/5/92

Offshore

2429

2430

2431

2432

2433

6/9

6/10

6/12

6/13

100

100

100

100

52

52

52

52

Offshore

21

Amphioxus
fluorescent biluminous opaque matter

Ten. in

6/11

2431

6/12

2432

6/13

2433

6/14

2434

6/15

2435

6/16

4205

2435

6.16

4205

2436 6'17

9810
5114
0

6.18

4224

2437

6.19

2438

6/10 9810
5114
0

438 51

Huber zone

Trichinus
in the meat

Disseminated virus

in fragments, water, etc.
in the meat
in the
in the
in the

in the
in the
in the
in the
in the

| | | | | | | |
|--------|------|------|--|--|--|----|
| 2437 | 6/18 | 205H | | | Disseminated pyrite | 2D |
| | | | | | Small fragments and scattered
mineralized Pelosypod
shells | |
| | | | | | Rhyzocrinus
Tetradium
Chondrites | |
| | | | | | Small Chondrites | |
| | | | | | Recess | |
| 2438 | 6/20 | 48H | | | Disseminated pyrite | |
| 438 51 | | 54H | | | Disseminated pyrite | |



Well Name: Hibernia K-18
 Location: 46° 47' 34.8" Lat. 48° 47' 17.3" Long.
 K.B.: 29.7 m GL - 78.3 m RT
 Logged by: Osana M. Soliman
 Date: December 1992

| Core no./Box no. | Prints
= slides | Sample no. | Fractures | Cements
oil stain | Lithology | Sed Structures
mud shale | Fossils | Remarks | Environment |
|------------------|--------------------|------------|-----------|----------------------|-----------|-----------------------------|---------|---------|-------------|
| 2286 | | | | | | | | | |
| 2287 | | | | | | | | | |

2B

is present in
mudstone - 2 m
sandstone

2288

2288

medium - fine
sandy ss

2B

2289

medium sand
tuffaceous

2B

2290

medium to muddy
sandy siltstone and
fine grained sandstone
with small pebbles

13A

2B

2291

medium sandstone in
large laminae
medium to coarse sandstone

13A

Storm
sands

2B

medium to coarse sandstone

11A

medium to coarse sandstone
with some siltstone
and mudstone

2292

medium to coarse
sandstone

2B

11A

medium to coarse sandstone

2B

medium to coarse
sandstone

11A

Shallow marine

Shale

Storm
Sands

Basal layer of mud clasts
and small Pelecypod shells

Bioturbated mudstone

Ophiomorphic Relict rhythmic mud
drapage laminae

Bioturbated sandy mudstone

beds rich in Pelecypod shells

Bioturbated muddy sandstone
with some scattered
Pelecypod shells

Bioturbated sandy
mudstone

Bioturbated mud SS

Bioturbated sandy
mudstone

lentic and mudstone

greenish gray shale

Bioturbated sandy mudstone

interbedded mudstone SS
and sandy mudstone

2291

1/4

01/12
02/25
26

01

02

2292

15

2293

03

03

03

2294

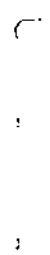
10

2295

interbedded mudstone and sandstone

20

2295



Dist. mouth

12A

light colored mudstone or sandstone

2296



1/4
500
20

Lower laminated to coarse grained sandstone in mud flat's rich bands and some suble sheets

12A

2297



1/4
500
20

interbedded mudstone and sandstone

23

Erosional Surface "III"

1/4

2298



1/4
500
20

laminated mudstone with vertical burrows interbedded with sandstone

1/4
500
20

fine grained silt with abundant organic matter arranged parallel to the bedding

1/4

2299



32 Storm sands

interbedded very fine grained silt with thin mudstone lenses and laminated fine

interbedded mudstone

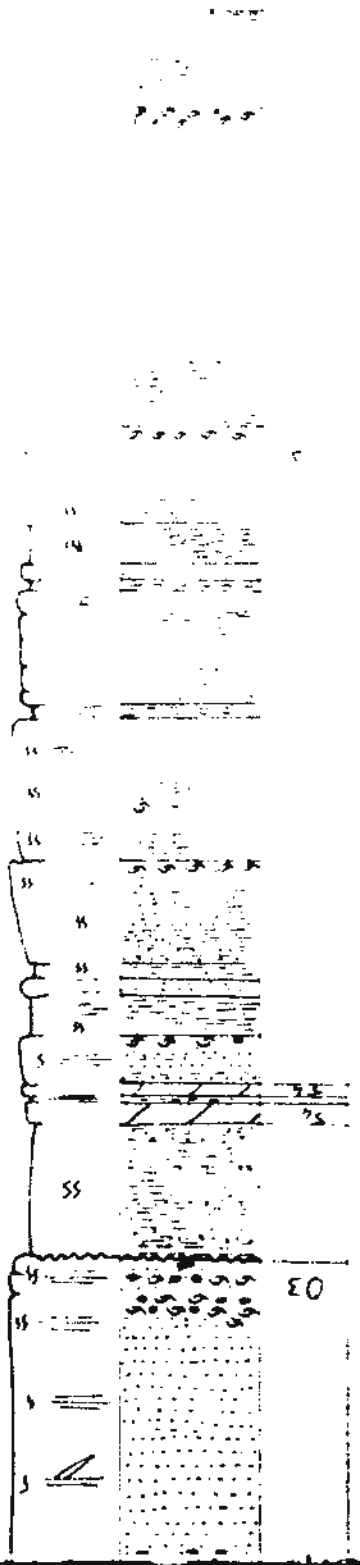
1300

2299

2298

2297

1/8
P11/5
K10/21
22
1/8
P11/5
K10/21
20
5K/19
P11/5
510-7
19



stratified sandstone with mud
clasts-rich bands and
some subH shells
burrows

12A

Erosional
Surface "III"

Distal

28

28

3A

25

28

Storm
Sands

Storm
Sands

marine

2301—

Shallow
Storm
Sands
13A
T.A.

2302

Storm
Sands
13A
Storm
Sands
13A
Storm
Sands
13A

2303

2304

Well Name *Hibernia G-55*

Location *46° 44' 17.8" Lat. 48° 53' 10.9" Long.*

K.B.: *29.72 m. GL*

RT

Logged by *Osama M. Soliman*
K.B.

Date

| Core no/
Box no | P-Prints
S-slides | Sample
no | Tracings | Cements
oil stain | Logging | Sed Structures | Fossils | Remarks | Facies | Environment |
|--------------------|----------------------|--------------|----------|----------------------|---------|----------------|---------|---------|--------|-------------|
| 2445 | | | | | | | | | | |
| 2446 | | | | | | | | | | |
| 2447 | | | | | | | | | | |

*Bioturbated muddy SS
 with abundant coal chips
 and red oxidized
 burrow linings at the
 top 50 cm.*

11A

12B

*Highly dirty bioturbated
 sandstone*

11A

*bioturbated sandy mudstone
 with wavy rhythmic
 lamination*

2C

2448

216

2449 —

3.

5

3

1572

2452

915

100

no. 1 very fine grained
fine grained sandstone
very fine grained sandstone
fine grained sandstone
fine grained sandstone
fine grained sandstone

2

[illegible]

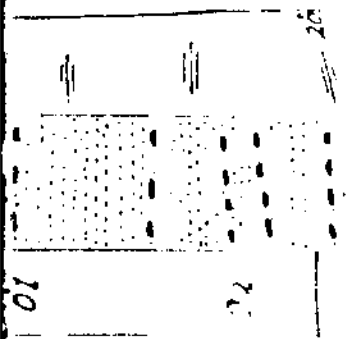
1

1894

Fluor

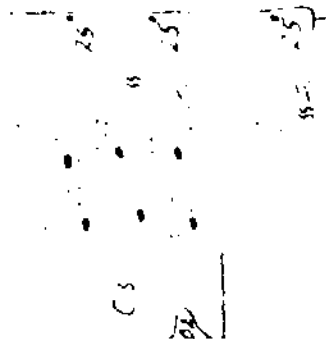
12B

very fine to fine
grained -
inc. w/pt. cemented
siliceous mud and
s. det. to 255



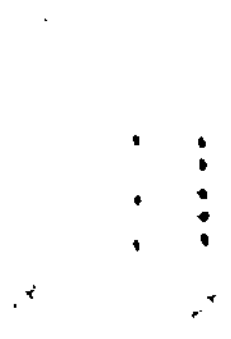
2451

4/6



2452

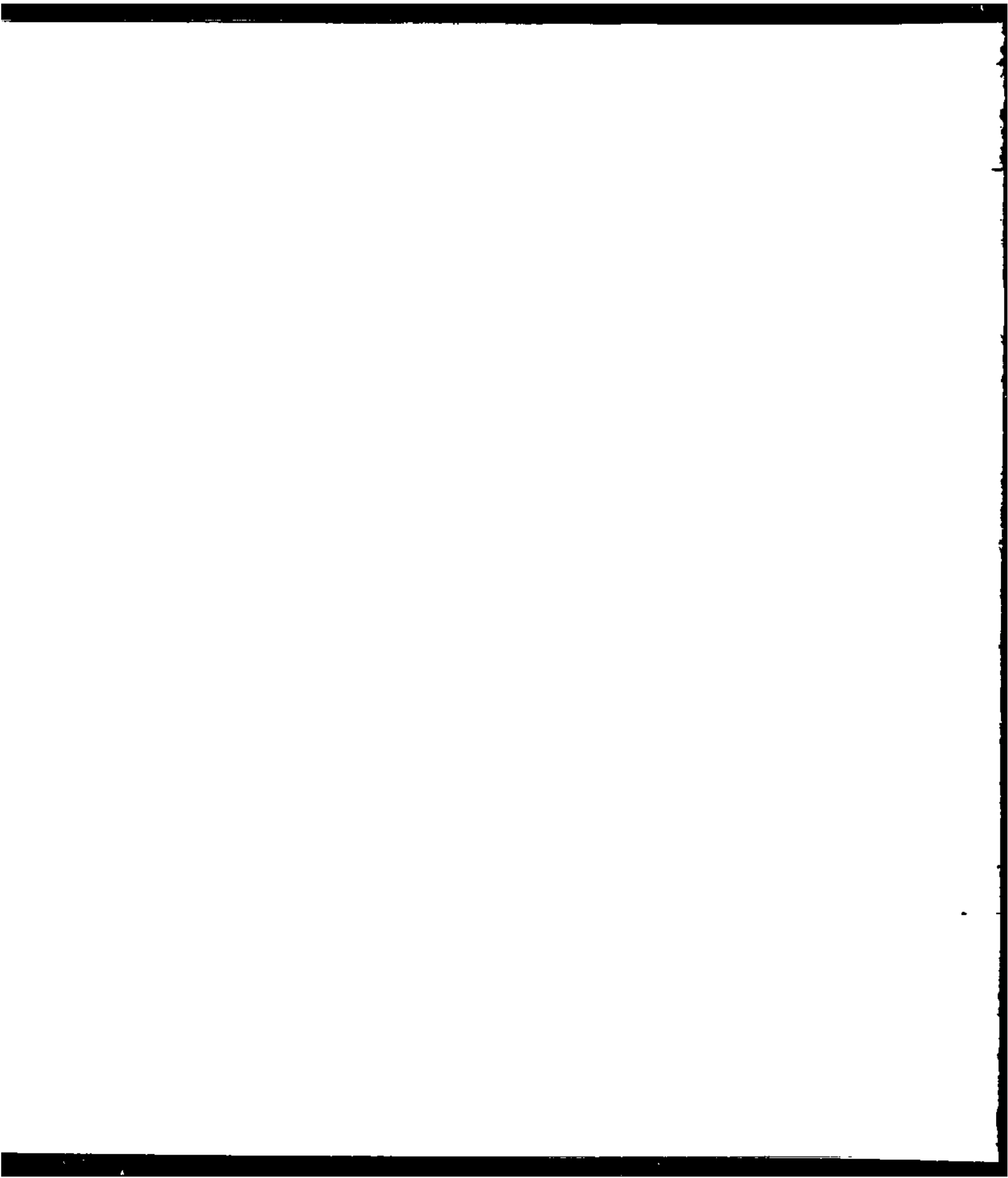
5/6

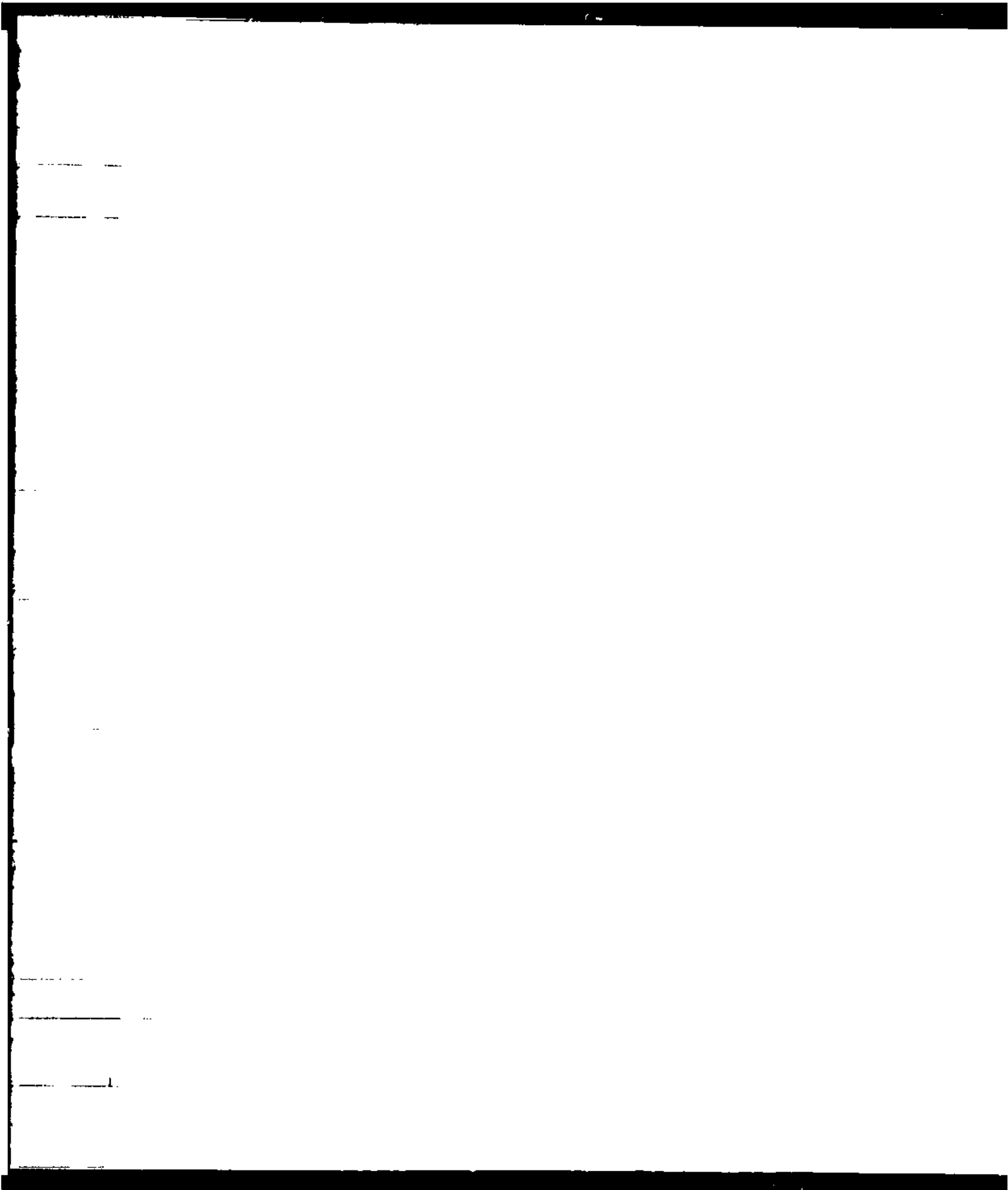


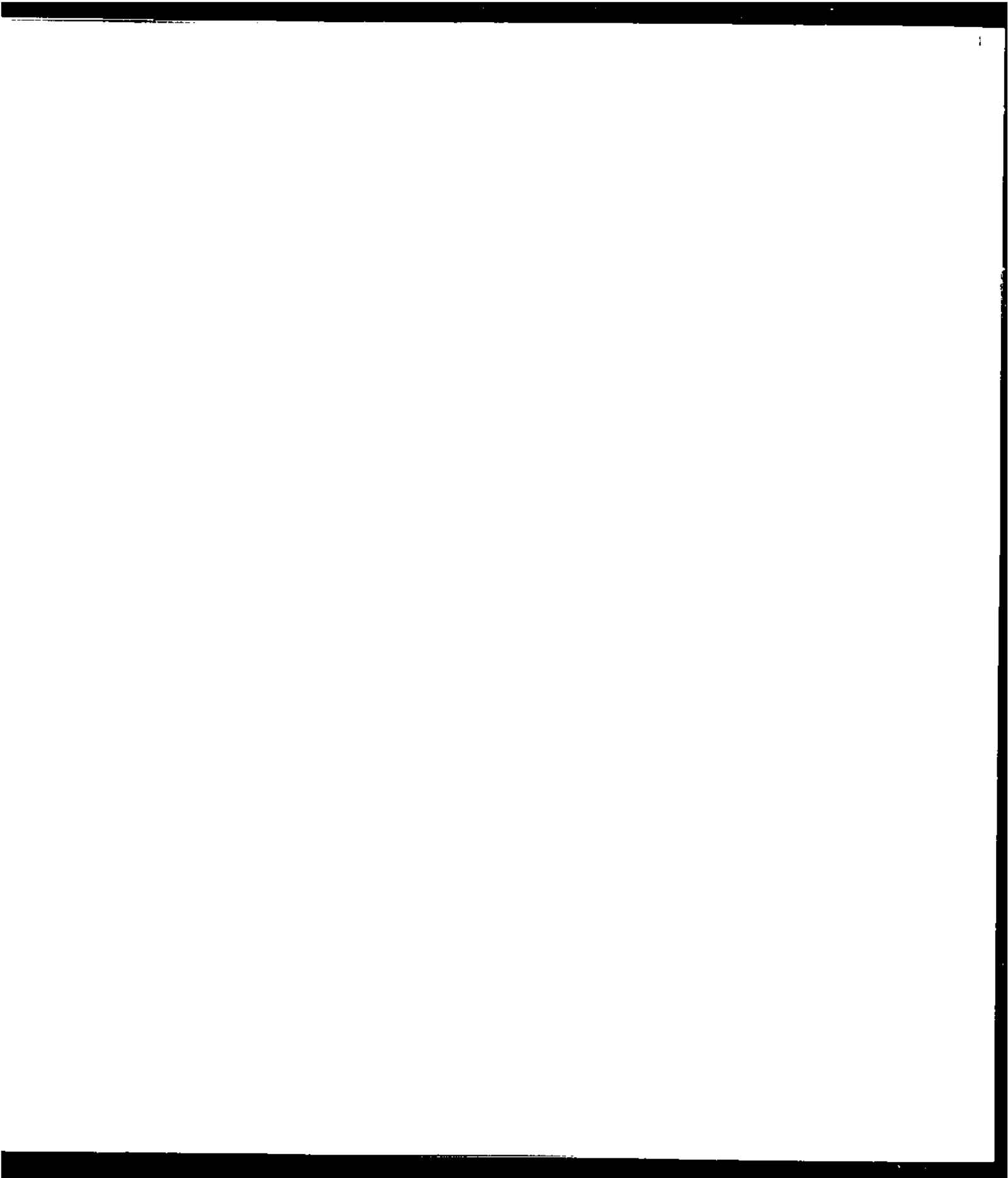
2453



2454







Well Name: Hibernia B-27

Location 46° 46' 16.24" N Lat. 48° 48' 27.94" W Long

KB 2705m GL - 76.81 KT 26.92m

Logged by Osama M. Soliman

Deposited R.T

Date February 8th, 1994

| Core no/
Box no | P. Prints
S-slides | Sample
no | Structures | Cements
oil stain | Lithology | Sed Structures
mud & E. etc. | Fossils | Remarks | Env. | Environment |
|--------------------|-----------------------|--------------|------------|----------------------|-----------|---------------------------------|---------|---------------|------|-------------|
| 1/1 | P1/26
S1/26
26 | 1 | | | | | | 13A Storm bed | | |
| 1/2 | P1/26
S1/26
27 | 2 | | | | | | 13A Storm bed | | |
| | | 3 | | | | | | 11H | | |
| | | 4 | | | | | | 13A Storm bed | | |
| | | 5 | | | | | | 13A Storm bed | | |
| | | 6 | | | | | | 13A Storm bed | | |
| | | 7 | | | | | | 13A Storm bed | | |
| | | 8 | | | | | | 13A Storm bed | | |
| | | 9 | | | | | | 13A Storm bed | | |
| | | 10 | | | | | | 13A Storm bed | | |
| | | 11 | | | | | | 13A Storm bed | | |
| | | 12 | | | | | | 13A Storm bed | | |
| | | 13 | | | | | | 13A Storm bed | | |
| | | 14 | | | | | | 13A Storm bed | | |
| | | 15 | | | | | | 13A Storm bed | | |
| | | 16 | | | | | | 13A Storm bed | | |
| | | 17 | | | | | | 13A Storm bed | | |
| | | 18 | | | | | | 13A Storm bed | | |
| | | 19 | | | | | | 13A Storm bed | | |
| | | 20 | | | | | | 13A Storm bed | | |
| | | 21 | | | | | | 13A Storm bed | | |
| | | 22 | | | | | | 13A Storm bed | | |
| | | 23 | | | | | | 13A Storm bed | | |
| | | 24 | | | | | | 13A Storm bed | | |
| | | 25 | | | | | | 13A Storm bed | | |
| | | 26 | | | | | | 13A Storm bed | | |
| | | 27 | | | | | | 13A Storm bed | | |
| | | 28 | | | | | | 13A Storm bed | | |
| | | 29 | | | | | | 13A Storm bed | | |
| | | 30 | | | | | | 13A Storm bed | | |

Abandonment facies

Distal Mouth bar sandstones

III

1/4

543

8731

8917

1/5

550

2351

1/4

2552

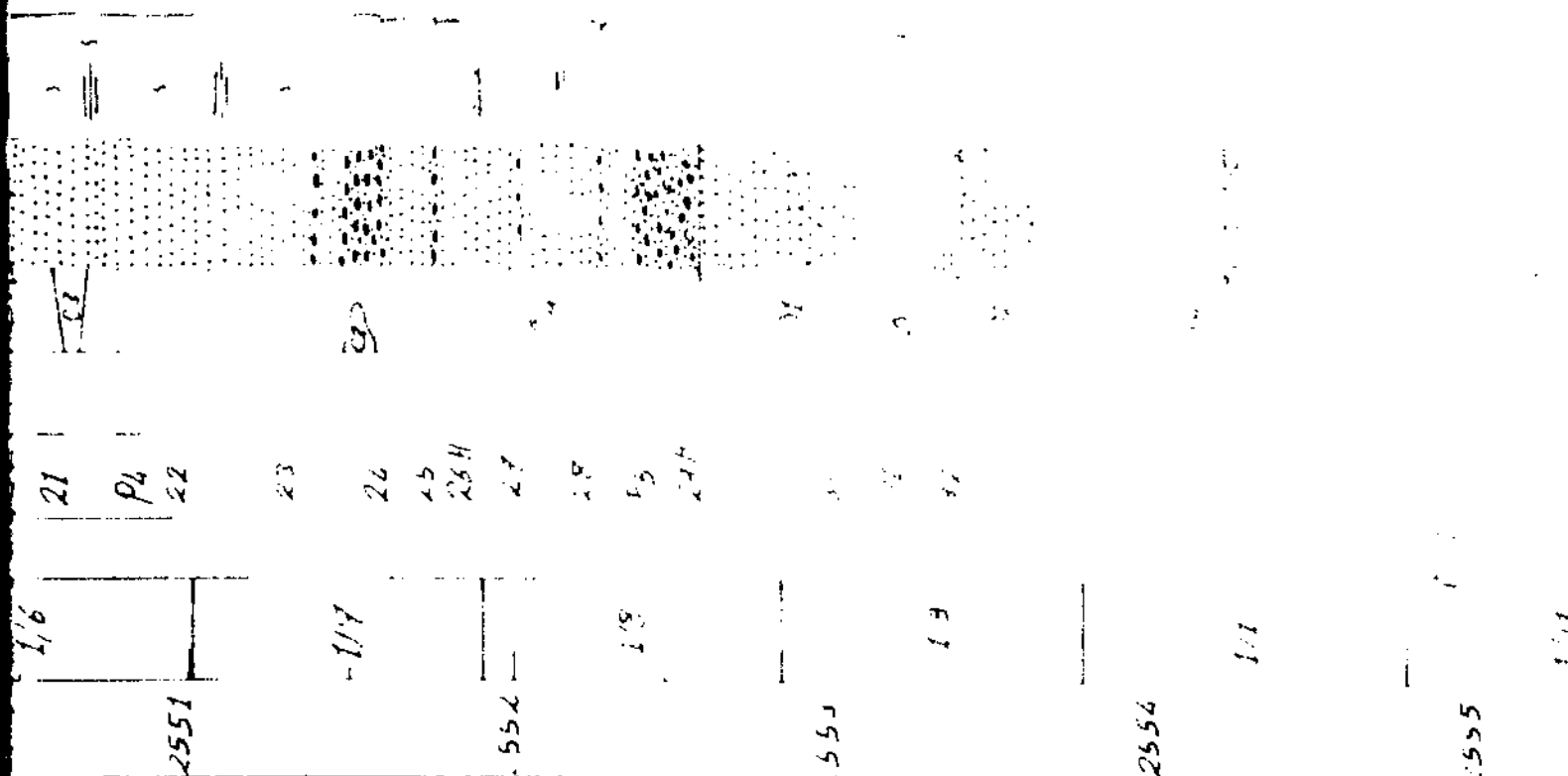
1/8

81

47

Distal Mouth bar sands

12A
 12B
 12C
 12D
 12E
 12F
 12G
 12H
 12I
 12J
 12K
 12L
 12M
 12N
 12O
 12P
 12Q
 12R
 12S
 12T
 12U
 12V
 12W
 12X
 12Y
 12Z



555

1/11

556

1/12

557

558

559

511

514

un-bed

un-bed

un-bed

un-bed

un-bed

13A Storm bed

Shallow marine

2B

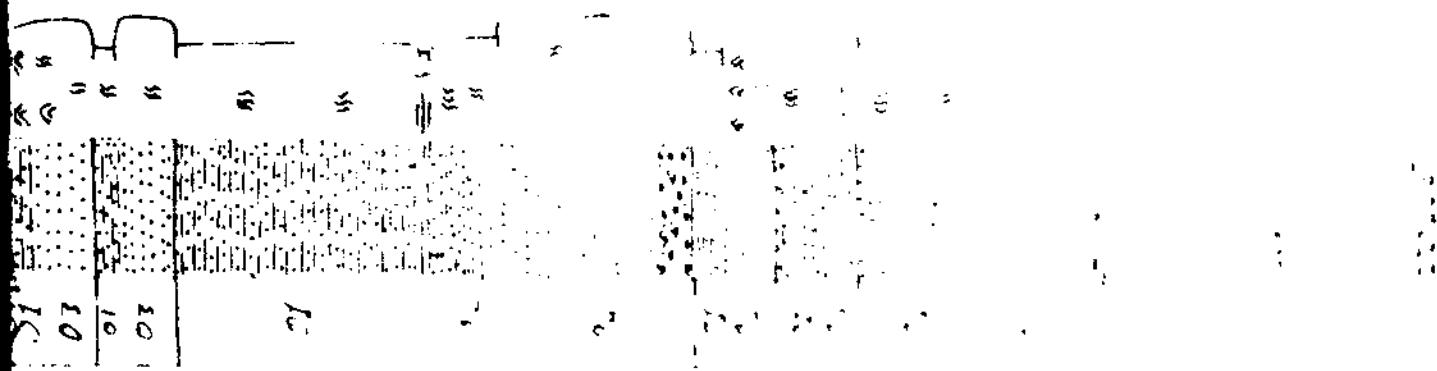
Shale with fine to medium grained

Thinly bedded

Storm bed

Storm bed

Storm bed



2557

2558

2559

2560

Distal N. 1/4.
bar sandstone

bar sandstone

bar sandstone

501

111

2562 1/8

1/13

2563



2564

2/1

2/1

2565

89 584

Location $41^{\circ} 41' 16.22''$ N. Lat $48^{\circ} 48' 27.34''$ W. Long.
K.B.: 27.05 m G.L. - 76.81 m R.T. 26.82 m

Logged by: Osama M. Soliman
Depth - in RT 2/4
Date February 8th. 1994

| Core no/
Box no | P Prints
S Slides | Sample
no | Structures | cements
oil stain | Lithology | Sed Structures
mud vs. silt | Fossils | Remarks | Index | Environment |
|--------------------|----------------------|--------------|------------|----------------------|-----------|--------------------------------|------------|---|-------|-------------|
| 2/2 | | 59 | | | | m | | Subtle parallel lamination due to distortion by burrowing | 12A | |
| | | 60 | | | | k | | 5-30 cm thick sets with mud clasts and Pelecypod shell debris as lag deposits | | |
| | | 61 | | | | m | | | | |
| | | 62 | | | | m | | Thin silty coal chip | 11A | |
| | | 63A | | 01 | | m | | Highly burrowed boundary | | |
| 2/3 | | 64 | | Ju | | m | Trilobites | Mud drupe couplets | 13A | Storm bed |
| | | | | | | m | | Applied sand lenses and relicts of sedimentary rhythmical laminae in sand rich layers | 11A | |
| | | 65 | | | | m | | | | |
| | | 66 | | Qu | | m | Trilobites | Thin silty clay partings | 12A | |
| 2/4 | | 67 | | | | m | | | | |

Shallow marine

Shallow marine

Storm beds

Sandstones

Abandonment

2569

2.7

2.7

2570

2.8

2571

2.7

2572

2.7
4.08
6.15
8.1

2573

[illegible]

5105

Expenditure

14

2571

257

4657

2579

2577

2578

2579

258

1501 1502 1503 1504 1505 1506 1507 1508 1509 1510 1511 1512 1513 1514 1515 1516 1517 1518 1519 1520 1521 1522 1523 1524 1525 1526 1527 1528 1529 1530 1531 1532 1533 1534 1535 1536 1537 1538 1539 1540 1541 1542 1543 1544 1545 1546 1547 1548 1549 1550 1551 1552 1553 1554 1555 1556 1557 1558 1559 1560 1561 1562 1563 1564 1565 1566 1567 1568 1569 1570 1571 1572 1573 1574 1575 1576 1577 1578 1579 1580 1581 1582 1583 1584 1585 1586 1587 1588 1589 1590 1591 1592 1593 1594 1595 1596 1597 1598 1599 1600

row
row

10

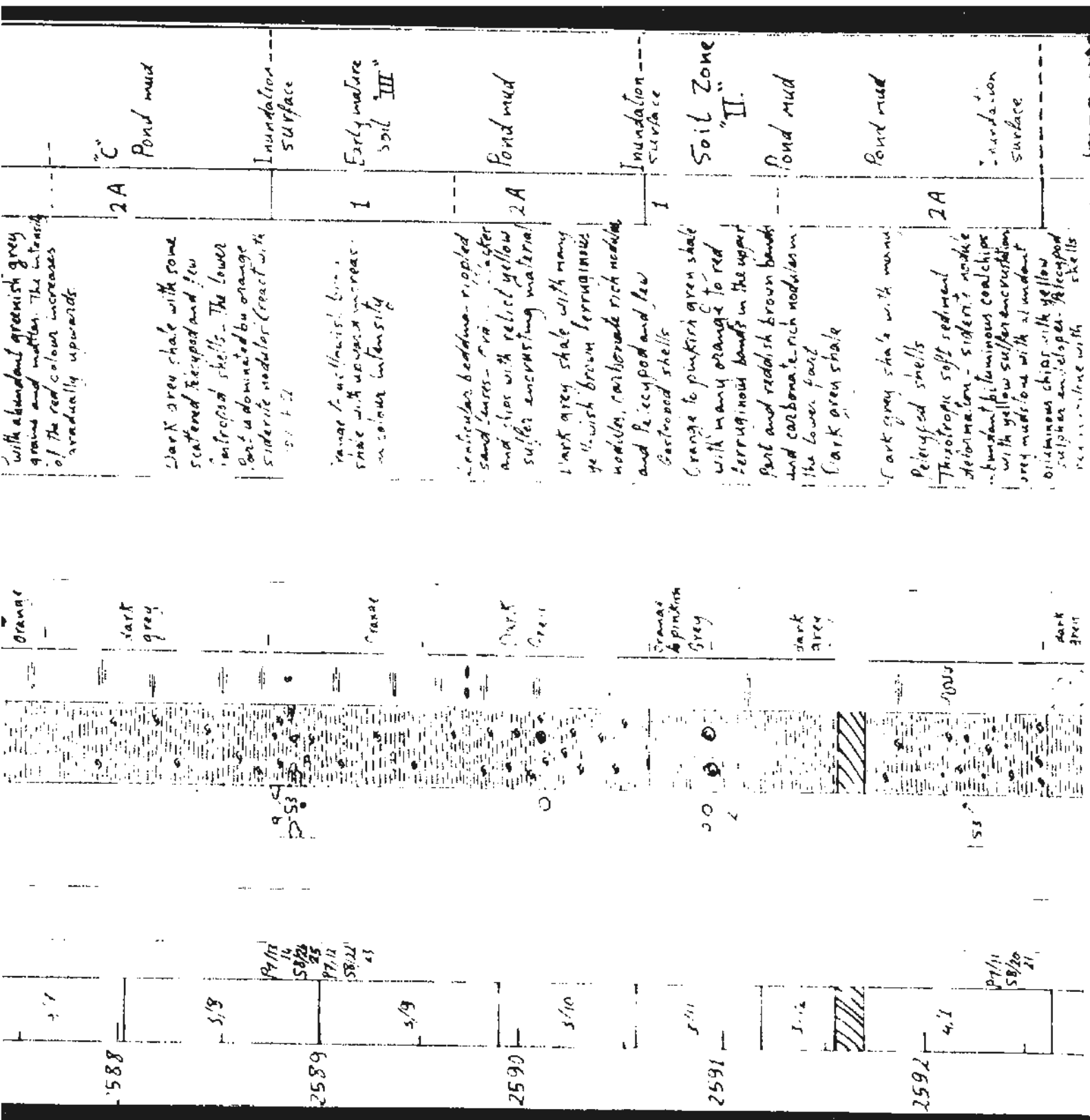
258.

Well Name: Hibernia B-27

Location 46° 46' 16.24" N. Lat. 48° 48' 27.94" W. Long.
K.B.: 27.05 m. G.L.: -76.81 m. R.T.: 26.82 m.

Logged by: Osama M. Soliman
Depth from R.T. 3/4
Date: February 8th, 1994

| Core no/
Box no | P. Prints
S. slides | Sample
no | Fractures | cements
oil stain | Lithology | Sed Structures
mud | Fossils | Remarks | Facies | Environment |
|--------------------|------------------------|----------------------|-----------|----------------------|-----------|------------------------------------|----------------|---|--------|-----------------------|
| 2586 | 3/4 | P7/16
S8/28
29 | | | | " A
" A
" " | | Light grey calcareous muddy
s.s. with abundant long, clay-
filled, burrows (root traces??) | 5 | Marsh |
| | | | | | | | Thalassinoides | Thalassinoides burrows filled
with calcareous sandstone | | Transgressive |
| | | B5? | | | | | | Greenish grey muddy S.S. -
Lower erosive boundary with
Pelecypod shells - disseminated | 5 | Surface "I" |
| | 3/5 | | | | | greenish
grey | | Greenish grey sandy mudstone
Greenish grey calcareous sandy
mudstone with abundant
reddish brown argillaceous
mottles. | | Inundation
surface |
| | | | | | | reddish
brown | | Reddish brown shale with some
greenish dotted mud. racted
(?) sandy layers - Fossils in
lost gradually upwards and the
rock changes to reddish brown
mudstone in the upper part. | 1 | "B" |
| 2587 | 3/6 | P7/15
S8/26
27 | | | | yellowish
brown
to
orange | | A Gastropod shell is well
preserved close to the top.
Yellowish brown to orange shale
with abundant greenish grey
grains and mottles. The intensity
of the red colour increases
gradually upwards | | Soil zone "IV" |
| | | | | | | dark
grey | | Dark grey shale with some
scattered Pelecypod and few | 2A | "C"
Pond mud |



with abundant greenish grey grains and matter. The intensity of the red colour increases gradually upwards.

Dark grey shale with some scattered pelecypod and few invertebrate shells. The lower part is dominated by orange siderite nodules (react with HCl).

Orange to yellowish brown shale with upward increase in colour intensity.

lenticular bedded - rippled sand lenses - with pelecypod and chips with red yellow sulfur encrusting material.

Dark grey shale with many yellowish brown ferruginous nodules, carbonate rich nodules and pelecypod and few Gastroiod shells.

Orange to pinkish green shale with many orange to red ferruginous bands in the upper part and reddish brown bands and carbonate rich nodules in the lower part.

Dark green shale.

Dark grey shale with many pelecypod shells.

Thixotropic soft sedimentation - siderite nodules abundant p. luminous coal chips with yellow sulfur encrustation grey mudstone with abundant siliceous chips with yellow sulfur envelopes - pelecypod remains - line with shells.

2A Pond mud

Inundation surface

Early mature soil "III"

2A Pond mud

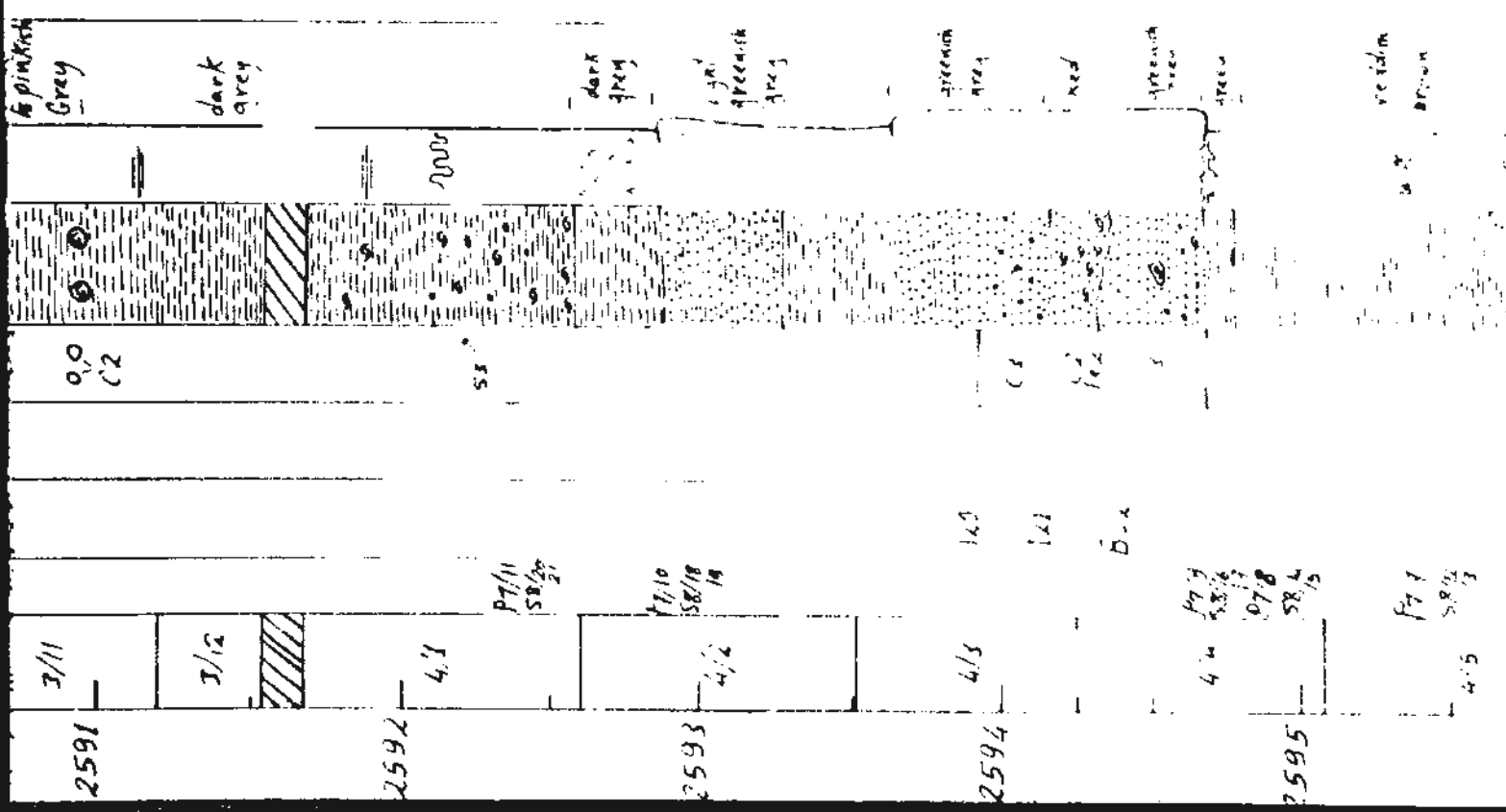
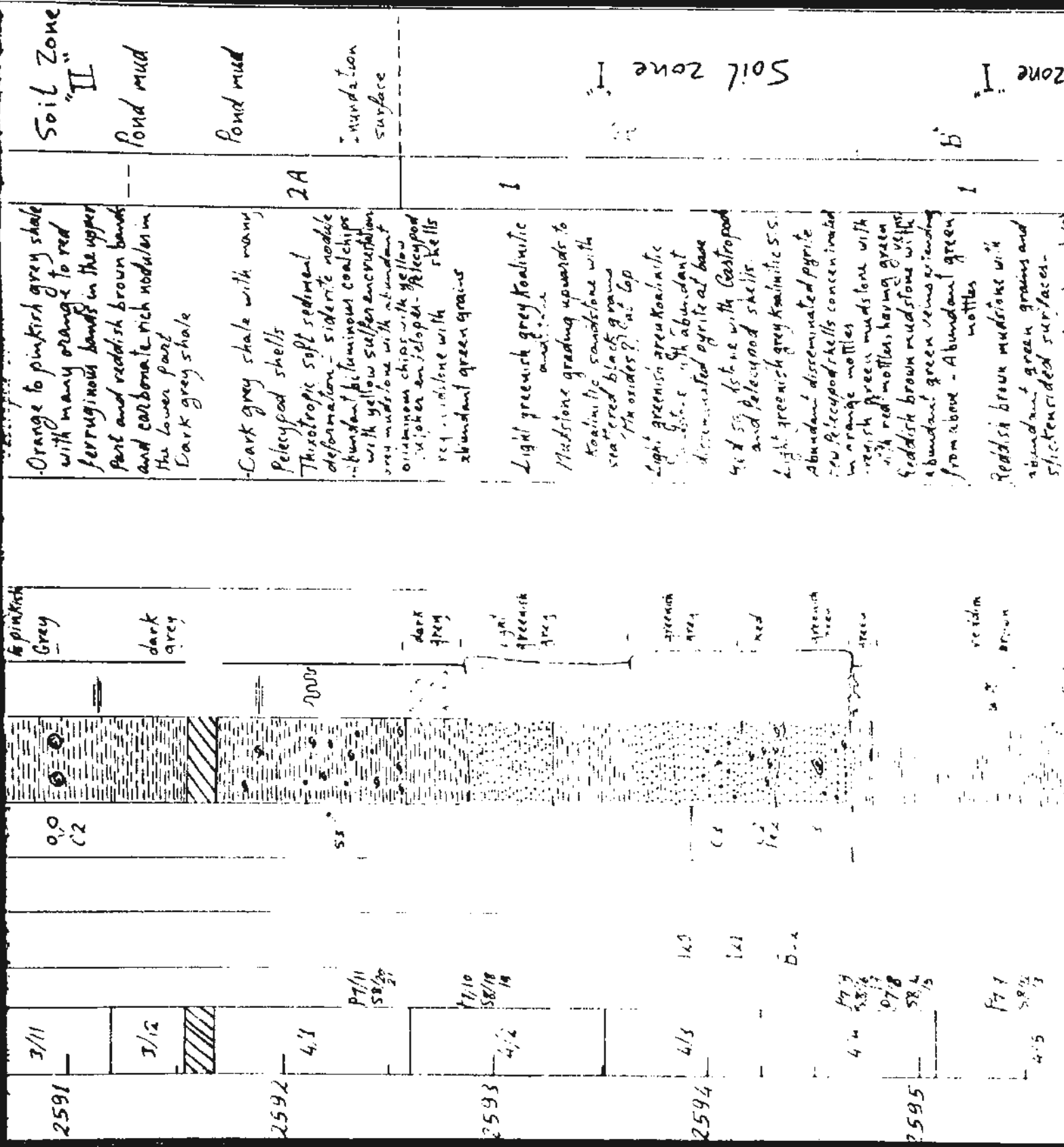
Inundation surface

Soil Zone "II"

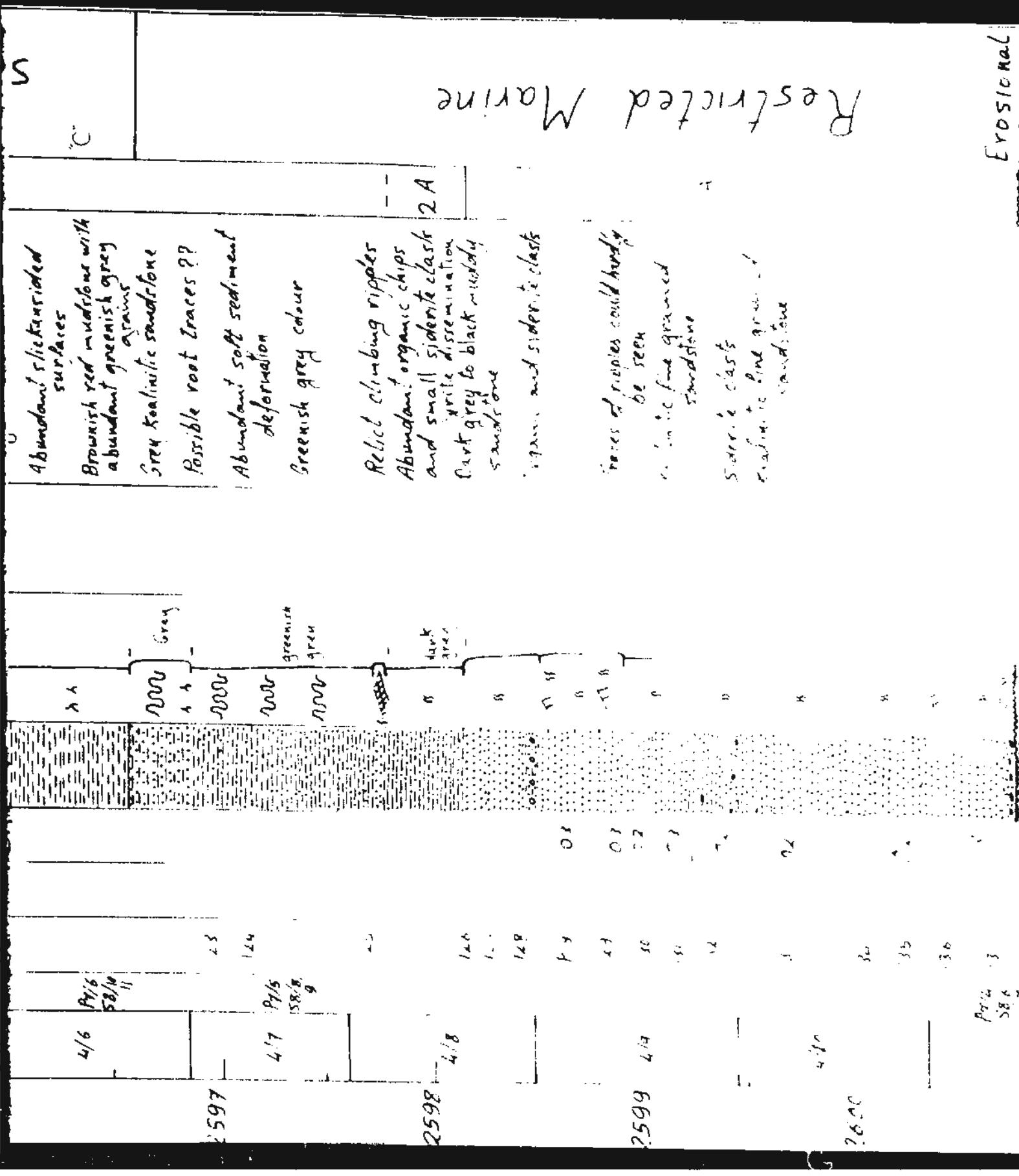
Pond mud

Pond mud

Inundation surface



Restricted Marine



1

more rich carcasses
associated with many extinct plants
and an entire zone composed
of sediments with many large
fossils.

dark grey mudstone

inner red band with a thin
layer of thin life-wood shells

Differential ventilation of
the burrow pits

Th. = sa'ed Aleypod shell
Lobers

men. rich carcasses

muscle with many extrinsic veins
and an outer zone composed
of adipose with many large
blood vessels.

various products

[illegible]

LaTeX: The LaTeX system

571-2017

10

...

三、

15

55

55

45

Well Name: *Hibernia B-27*

Location: $46^{\circ}46'16.24''$ N Lat. $48^{\circ}48'27.94''$ W Long.

K.B.: 27.05 m

G.L.: 76.81

R.T.: 26.82 m

Logged by: *Osama M. Soliman*

Depth from R.T.

Date: February 8th, 1996

4/6

| Core no/
Box no | P=Prints
S=slides | Sample
no | Fractures | cements
oil stain | Lithology | Sed. Structures
mud
VF
FE
CY
G | Fossils | Remarks | Facies | Environment |
|--------------------|----------------------|--------------|-----------|----------------------|-----------|---|----------------------|--|--------|-------------|
| 2606 | | 142 | | | | | <i>Rhynchonellum</i> | Thin small <i>Pelecypod</i> shells | 2.D | OFFSHORE |
| | | 143 | | | | | <i>Planolites</i> | Basal Lag of mud clasts | 13.A | |
| | | 144 | | | | | <i>Rhynchonellum</i> | Grey argillaceous siltstone | | |
| | | | | | | | <i>Planolites</i> | | | |
| 2607 | | 851 | | | | | | Organic-rich nodules enveloped
yellowish green layers | | |
| | | | | | | | <i>Palaephiacus</i> | Siderite and organic-rich
nodules
Siderite nodule | | |
| 2608 | | | | | | | | | 2.D | |

OFFSHORE

Disturbed sand siltstone
scattered thin
laminated shells within

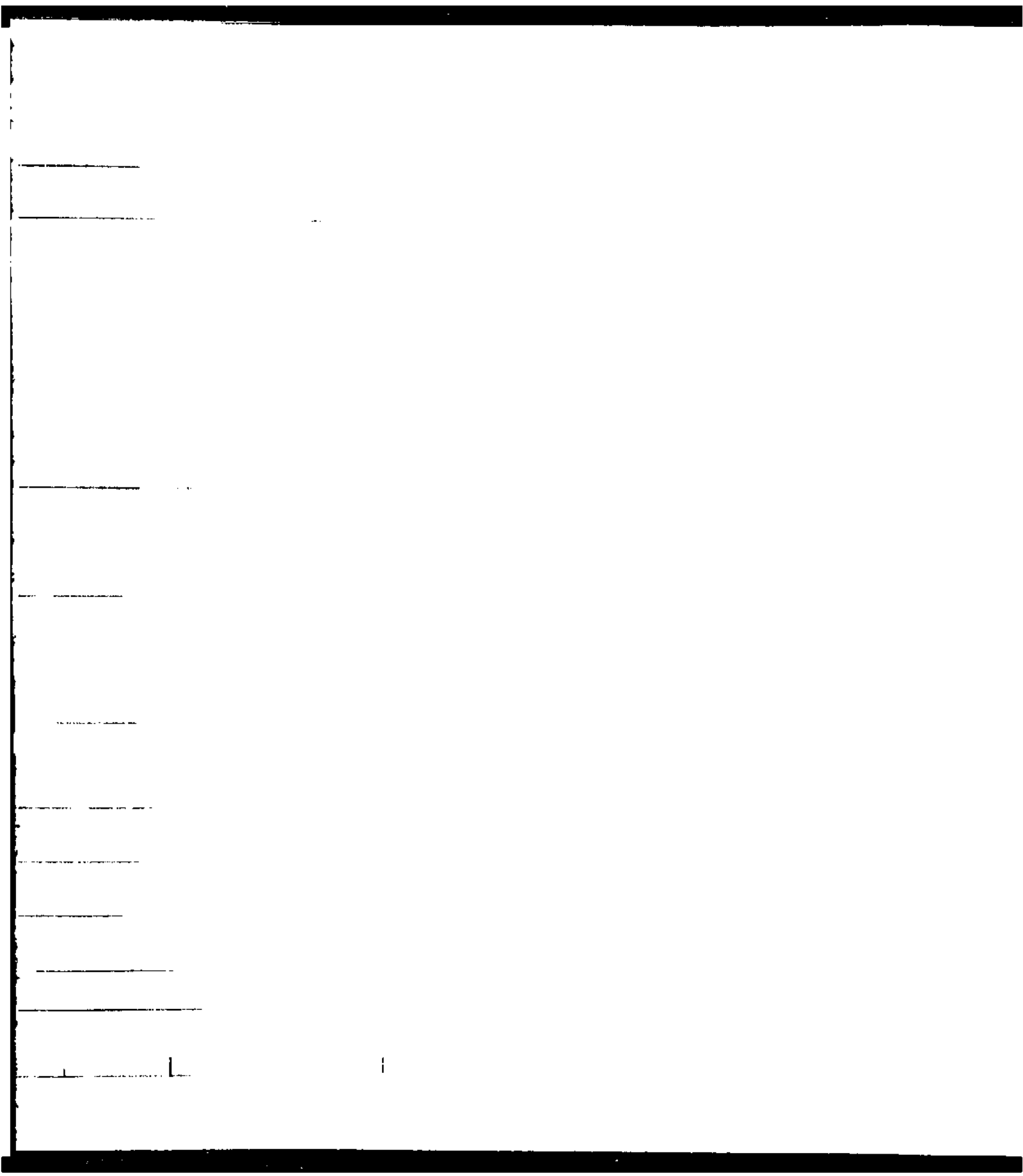
2609.

4/2

147
148
149

150
151
152

Ground soil is whitish
green nodules rich in organic
matter. Soil is somewhat
inferior to soil in comen-
ta in of the sandy burrow
fills
rows with men scale
147





Well Name: Hibernia 1-46

Location: 46°45'40.24" Lat 49°51'12.19" W Long

K.B.: 32.2 m G.L.: -89.4 m R.T.:

Logged by: Osama M. Soliman

Depth from: K.B.

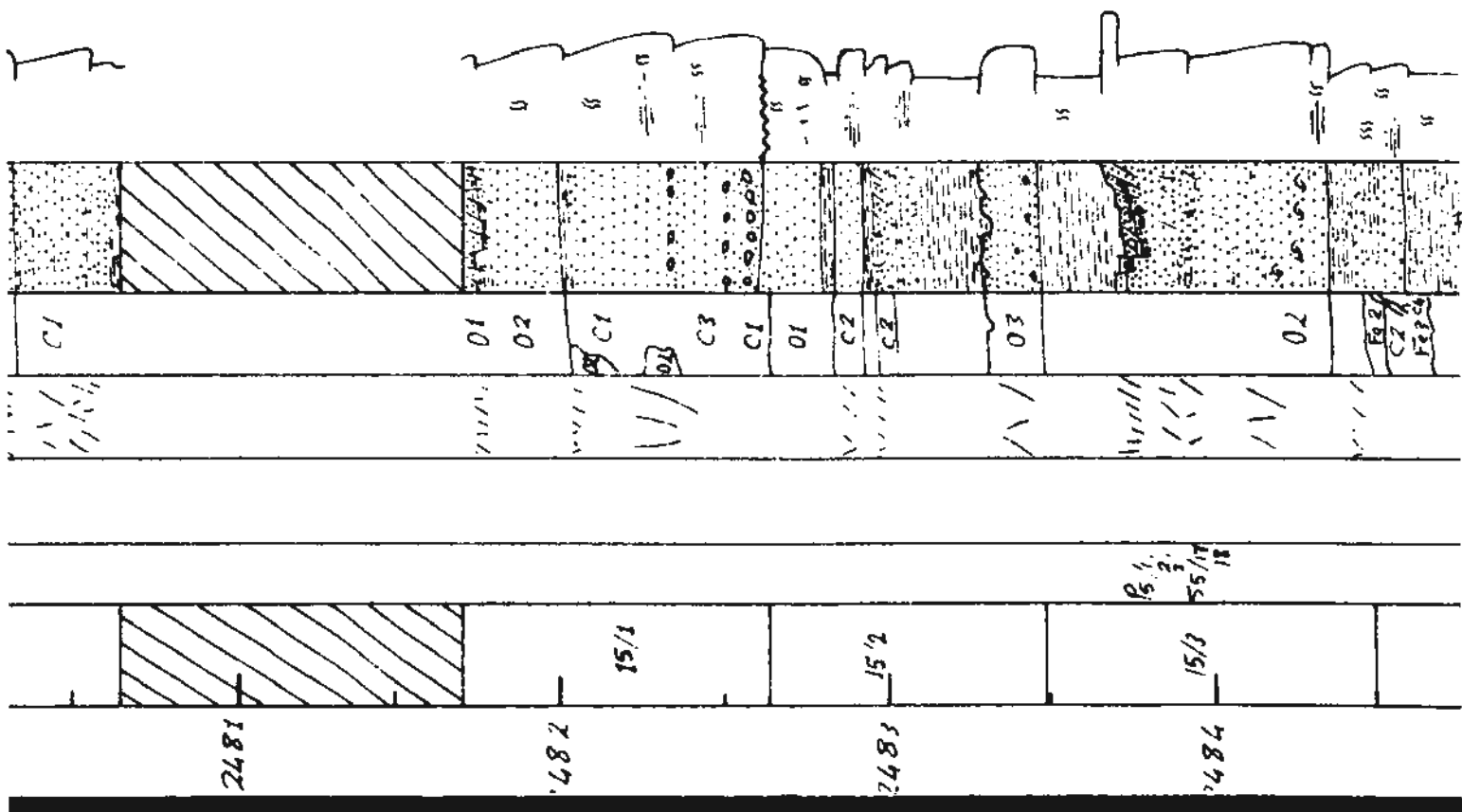
Date: 19.06.92

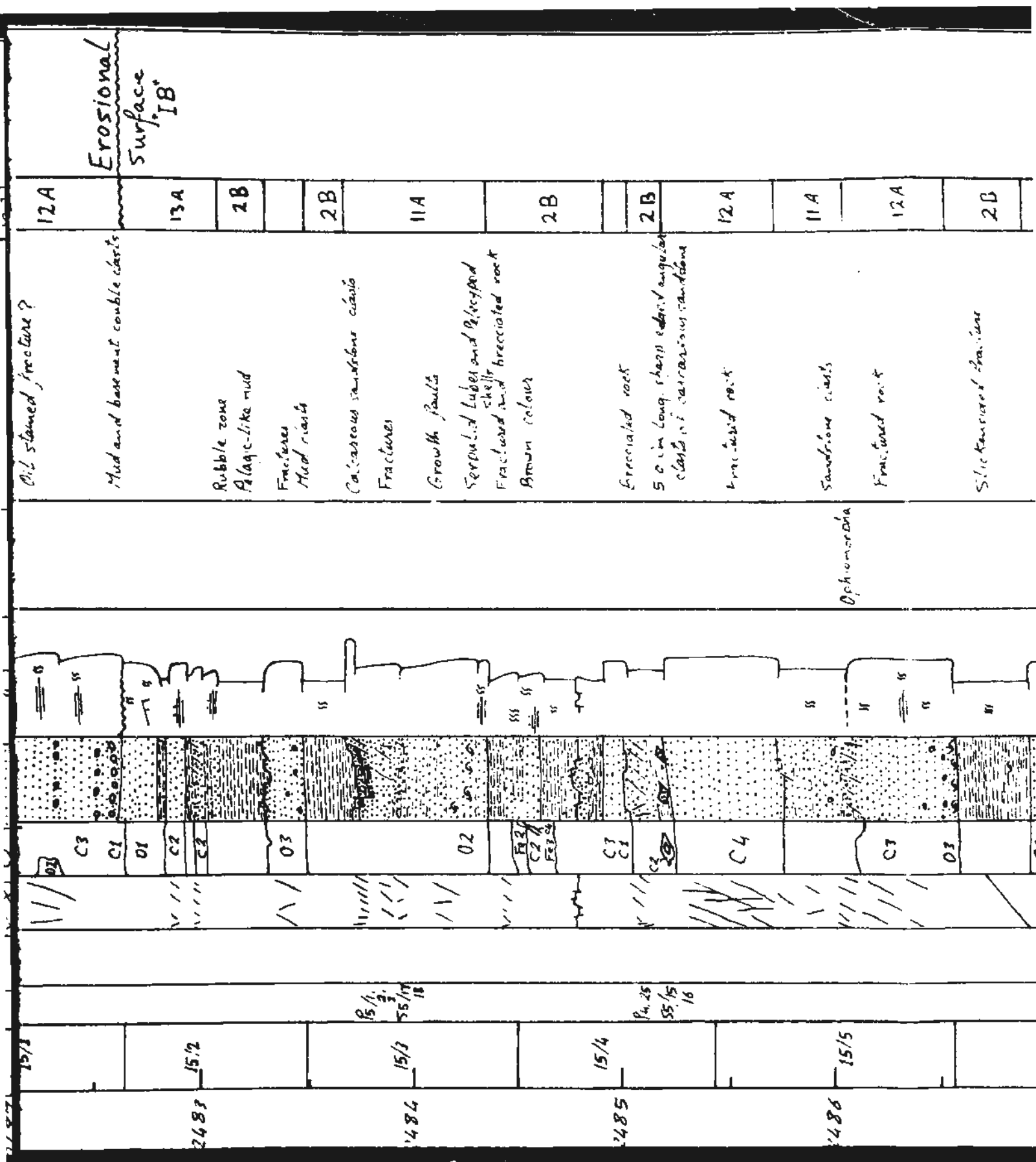
1/9

| Core no/
Box no. | P-Prints | S=slides | Sample
no | Fractures | ce-
ments | Lithology | Sed Structures | Fossils | Remarks | Facies | Environment |
|---------------------|----------|----------|--------------|-----------|--------------|-----------|----------------|---------|--|--------|-------------|
| 2478 | 14/18 | | P740 | | 02 | | mud. & lign. | | | 2B | |
| | | | | | 01 | | | | | 11A | |
| | | | | | 03 | | | | | 12A | |
| 2479 | 14/15 | | | | 04 | | | | Fractures | 2B | |
| | | | | | 01 | | | | | 12A | |
| 2480 | 14/16 | | | | 06 | | | | horizontal and almost vertical fractures | 12A | mouth bar |
| | | | | | 07 | | | | | | |

River

| | | | | | | |
|--|-----|-------------------------------|----|----|-----|----|
| 11A | 12A | 13A | 2B | 2B | 11A | 2B |
| <p>11A: fine to medium sand</p> <p>12A: sand and gravel, medium to coarse, silty sandstone</p> <p>13A: sandstone, medium to coarse, silty sandstone</p> <p>2B: sandstone, medium to coarse, silty sandstone</p> <p>2B: sandstone, medium to coarse, silty sandstone</p> <p>11A: sandstone, medium to coarse, silty sandstone</p> <p>2B: sandstone, medium to coarse, silty sandstone</p> | | <p>Erosional Surface 1.8'</p> | | | | |





Erosional
Surface
18"

Ophiomorpha

15/1
15/2
15/3
15/4
15/5

15/1
15/2
15/3
15/4
15/5

15/1
15/2
15/3
15/4
15/5

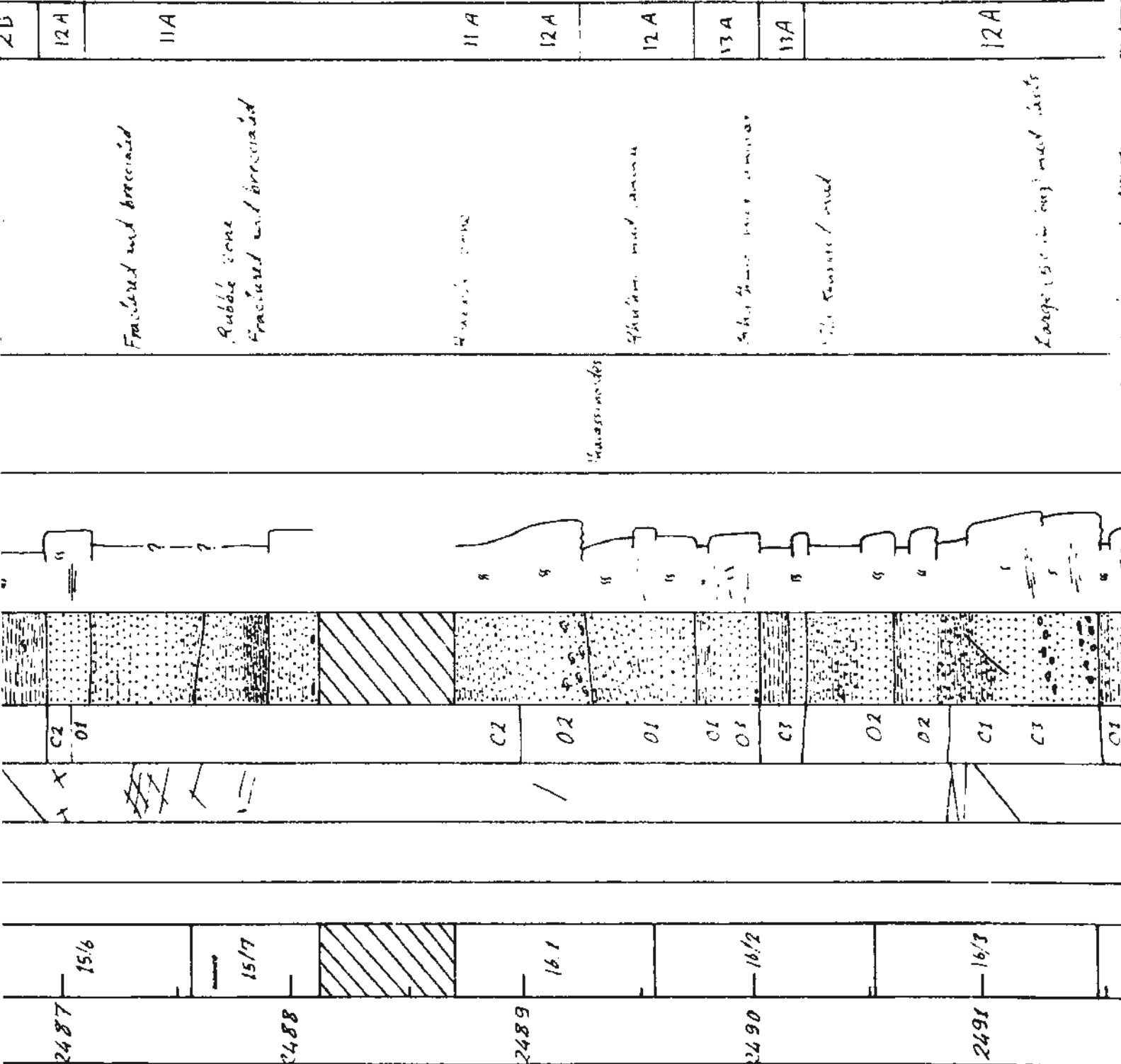
2483

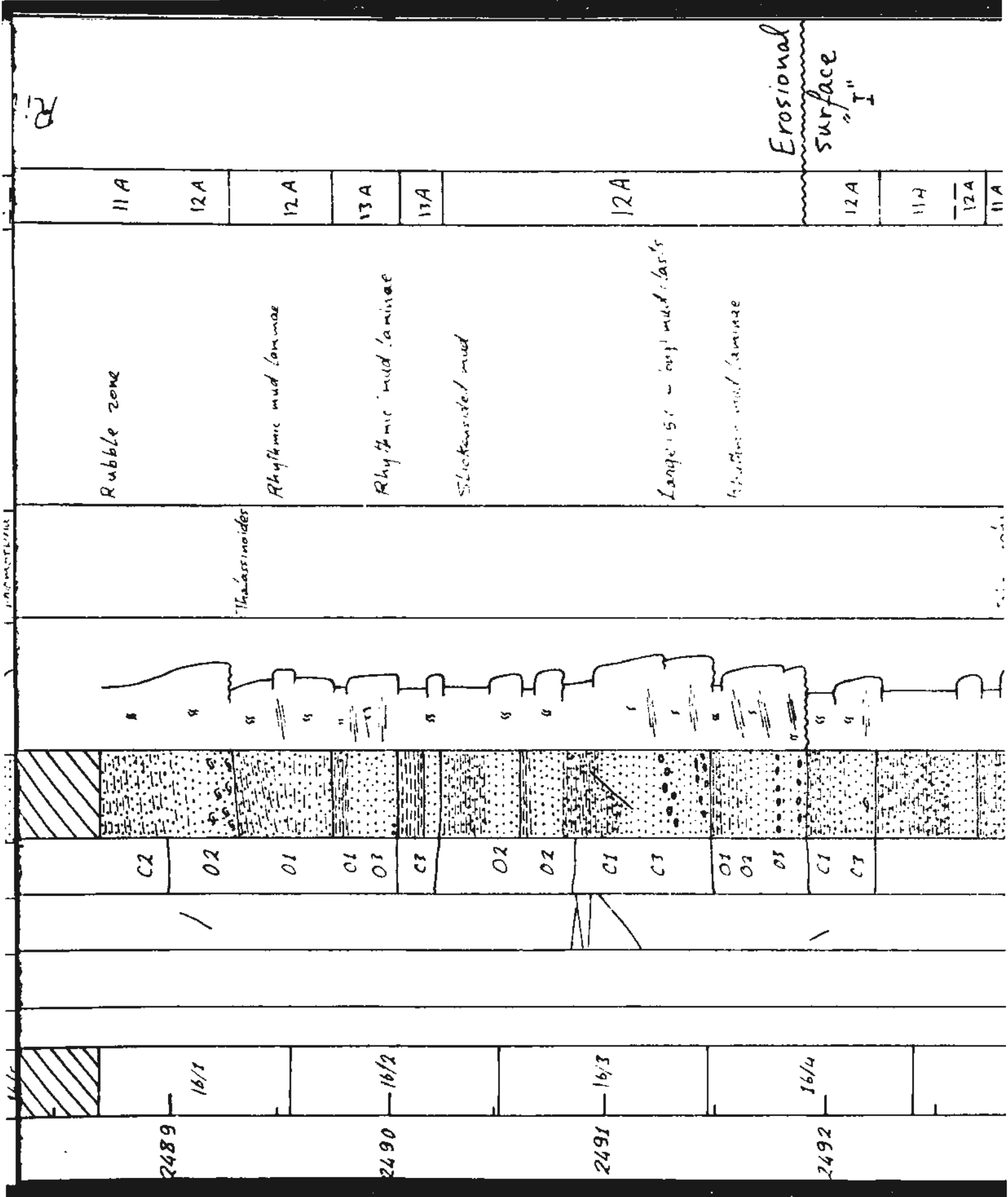
2484

2485

2486

River mouth bar



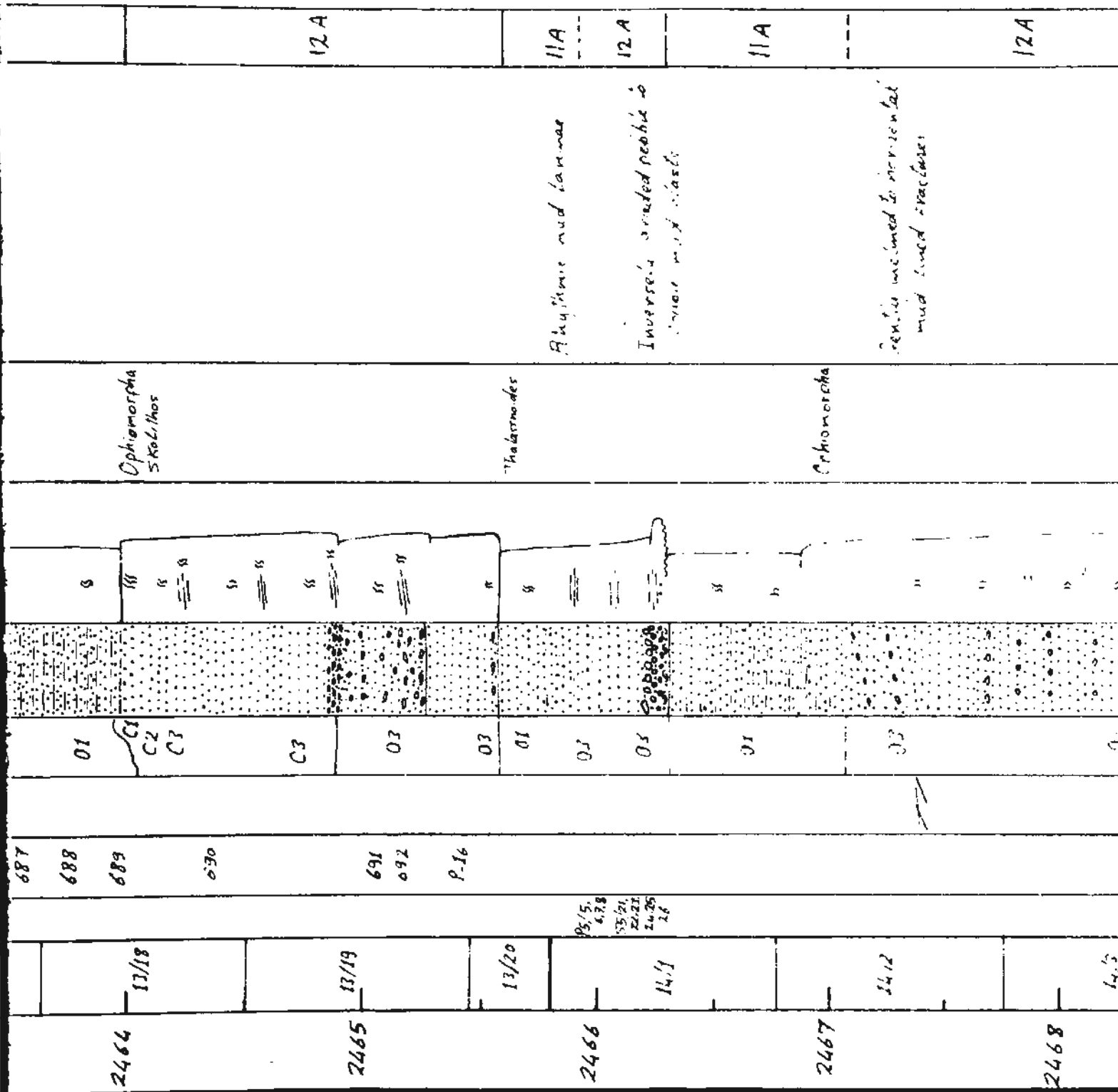


[illegible]

2/9

2460

Stacked river mouth bars



687
688
689
690
691
692
P.16
13/18
13/19
13/20
14/1
14/2
14/3

2464
2465
2466
2467
2468

| | | | | | | | |
|-----|----|-----|----|-----|-----|-----|----|
| 11A | 2B | 12A | 2B | 12A | 11A | 12A | 2B |
|-----|----|-----|----|-----|-----|-----|----|

Grubbe

Hyphomys phaeocephalus no. 10
Hyphomys mud. same
 1st. 1234

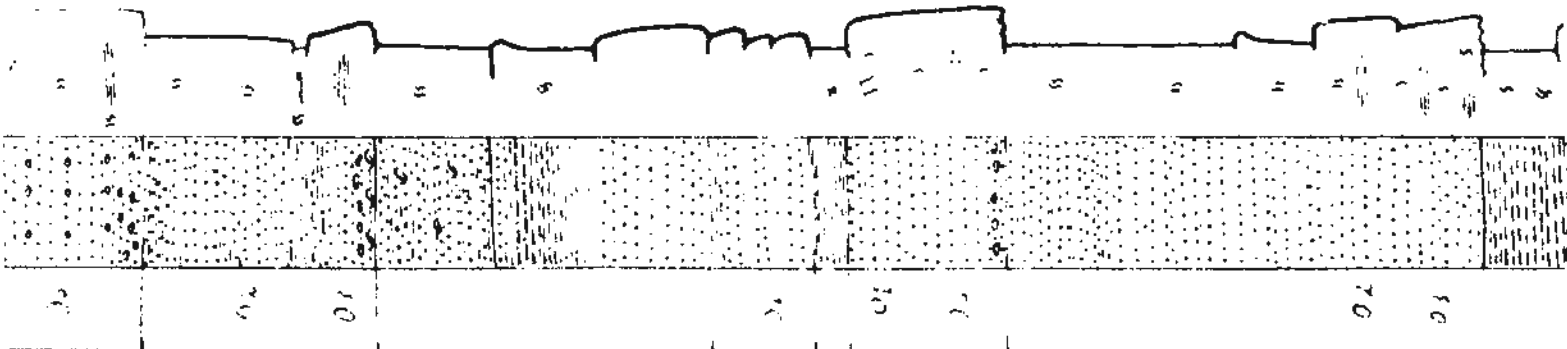
Hyphomys phaeocephalus

Pianalis

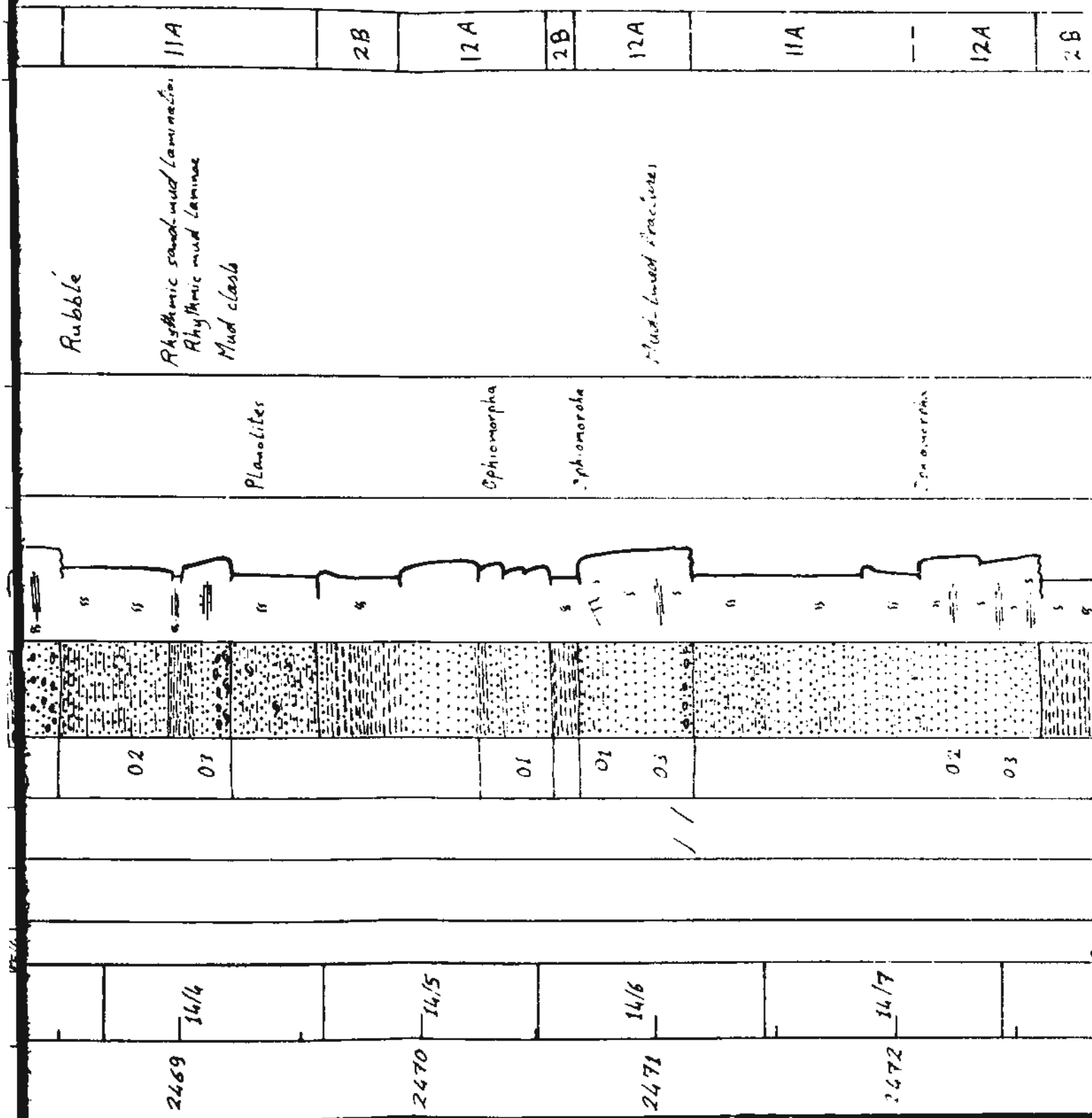
Hyphomys

Hyphomys

Hyphomys



| | | | | |
|------|------|------|------|------|
| 14/3 | 14/4 | 14/5 | 14/6 | 14/7 |
| 2469 | 2470 | 2471 | 2472 | |



| | 2B | 12A | 11A | 12A | 11A | 12A | 11A |
|------|--------------------|-----|-----|-----|-----|-----|-----|
| 2473 | 14/S
88/4
20 | | | | | | |
| 2474 | 14/9 | | | | | | |
| 2475 | 14/10 | | | | | | |
| 2476 | 14/11 | | | | | | |
| 2477 | 14/12 | | | | | | |

Well Name: Hibernia I-46

Location: 46°45'40.24" Lat 49°51'17.19" W Long

K.B.: 32.2 m

G.L.: -89.4 m

R.T.:

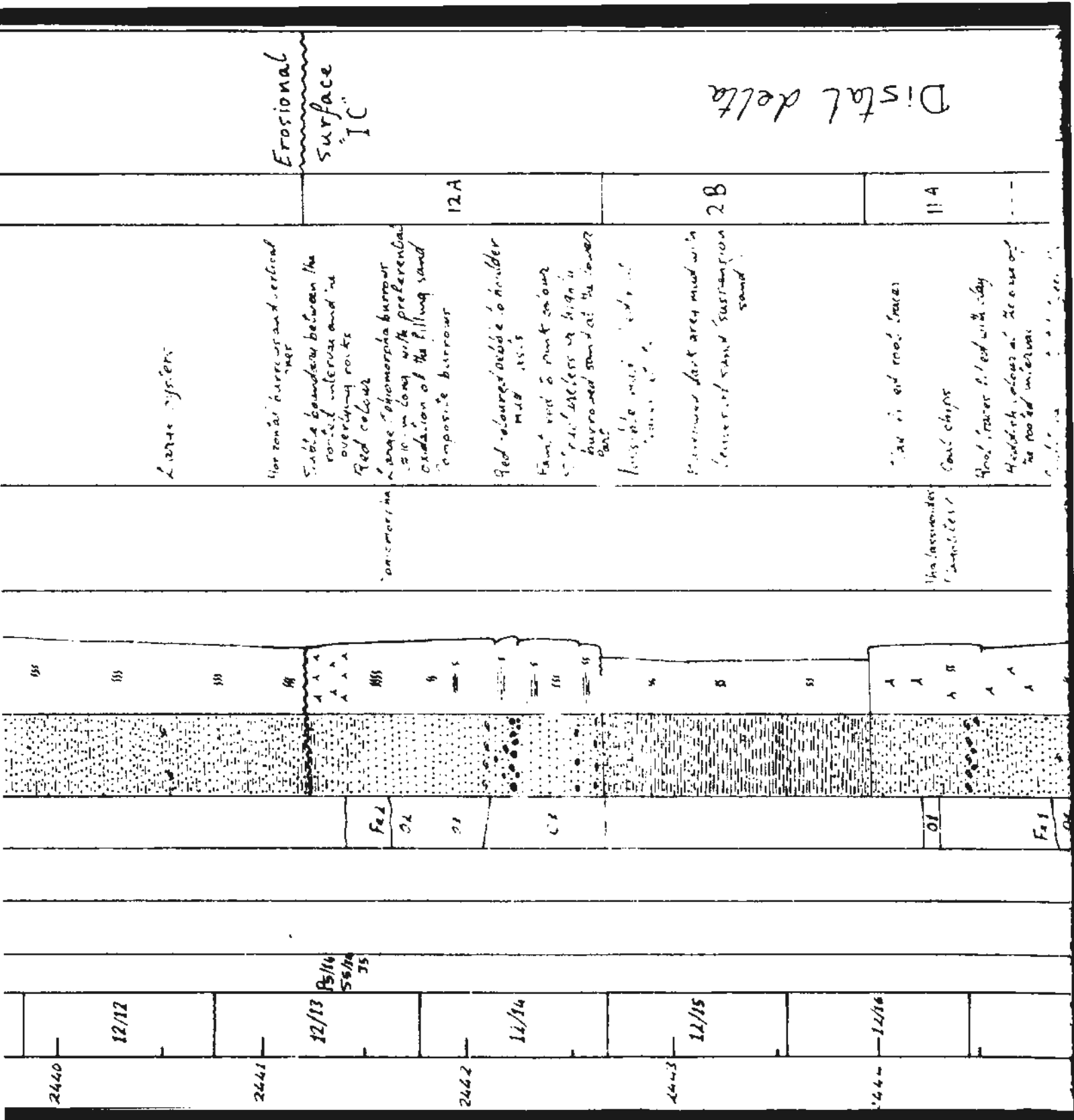
Logged by: Osama M. Soliman
Depth from: K.B.

Date: 19.06.92

3/9

| Core no/
Box no | P=prints
S=slides | Sample
no | Fractures | Cements
oil stain | Lithology | Sed Structures
mud $\frac{1}{2}$ $\frac{1}{4}$ $\frac{1}{8}$ $\frac{1}{16}$ $\frac{1}{32}$ $\frac{1}{64}$ | Fossils | Remarks | Facies | Environment |
|--------------------|----------------------|--------------|-----------|----------------------|-----------|--|----------------|--|--------|-------------|
| 2438 | | | | 03 | | " | | | 12A | |
| 12/9 | | | | ?02 | | " | | | | |
| | | | | | | " | Optiomorpha | | | |
| | | | | | | " | | | 11A | |
| 2439 | | | | | | AAAAA | Thalassinoides | Clay filled root traces | | |
| 12/10 | | | | | | AAAAA | | Fine to very fine grained laminated
to rippled sandstone with mud
drapes | | |
| | P5/15
S6/1
2 | | | 01 | | AAAAA | | Very thin shell hash | | |
| | | | | 01 | | AAAAA | | Clay filled root traces | | |
| | | | | (2-12) | | SS | | Reddish colour | | |
| 12/11 | | | | | | " | Optiomorpha | | 11A | |
| | | | | | | " | | | | |
| 2440 | | | | | | SS | | | | |
| 12/12 | | | | | | SS | | | | |
| | | | | | | " | | Large oysters | | |

Bay fill sediments



Distal delta

Erosional surface "IC"

Large system

Horizontal burrows and vertical

Stable banding between the

Red colour

Large Ophiomorphia burrow
10-15 cm long with preferential
oxidation of the filling sand
Composite burrows

12A

Red coloured debris to boulder
M.B. 185.5

Faint red to pink colour

Small burrows up to 10 cm
burrowed sand at the lower
part

Horizontal burrows

2B

Intermediate dark grey mud with
lenses of sand suspension
sand

11A

Dark red mud (mud)

Coarse chips

Good, rather filled with clay

Hardish, colour at the base of
the mud interval

The mass under
the chips

2440

12/12

2441

12/13

BS/14
SS/14
75

2442

11/14

2443

12/15

2444

12/16

Fe2

OL

CL

OL

Fe1

Distal delta

Faint red to pink colour
Structureless or highly
burrowed sand at the lower
part.

Possible mud-filled root
traces at top

Arrowed dark grey mud with
lenses of sand (suspension
sand).

Clay-filled root traces

Coal chips

Root traces filled with clay

Reddish colour at the base of
the rooted interval

Gradational contact between the
red stained sand and the above
rooted interval. Very thin shells
about 1 cm thick laminae with shells
and ashite basal lag
Slump

Quartzite

Thalassiozoides
Planolites?

C3

O1

F+1

O1

O3

2443

12/15

2444

12/16

2445

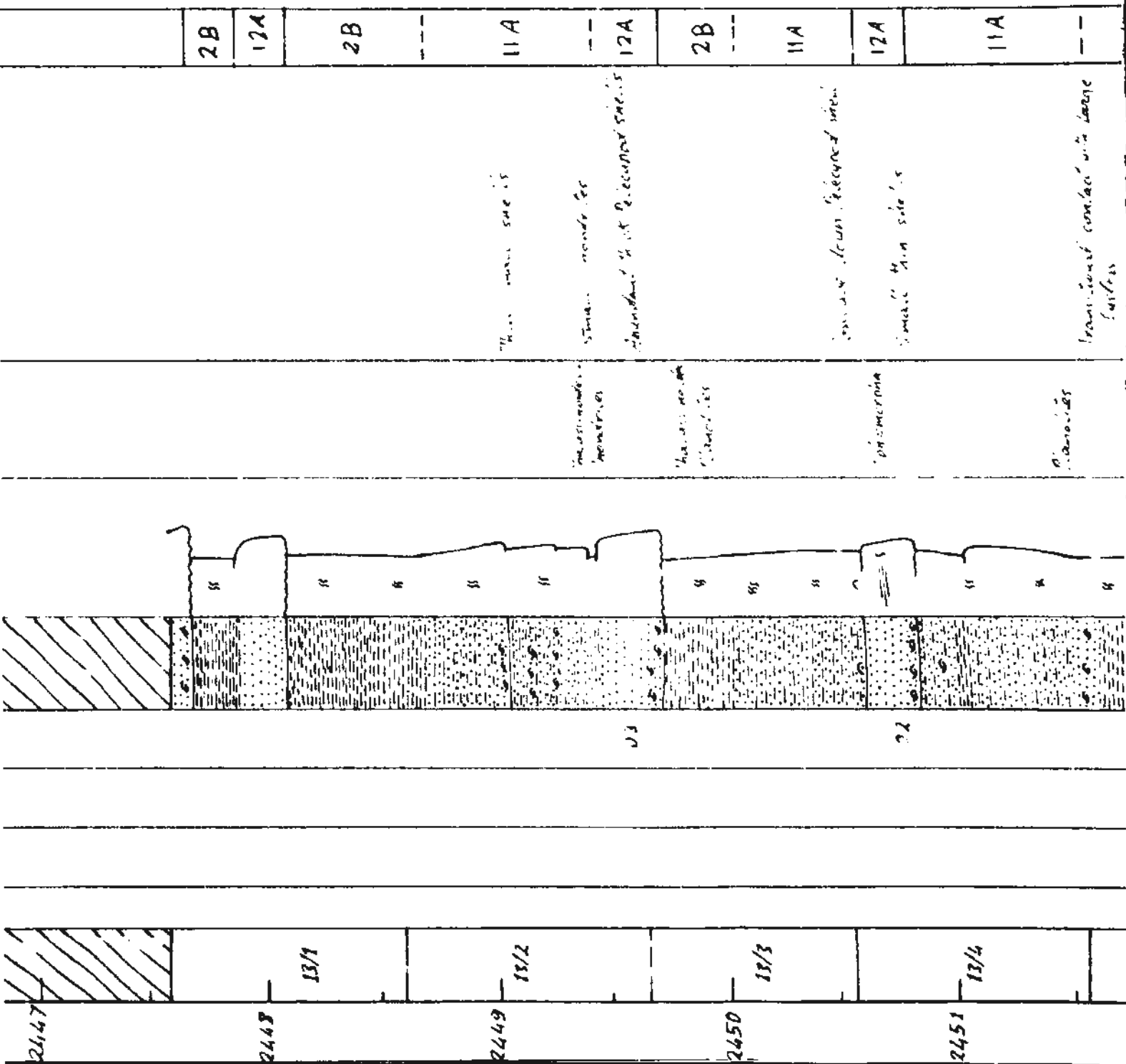
12/17

2446

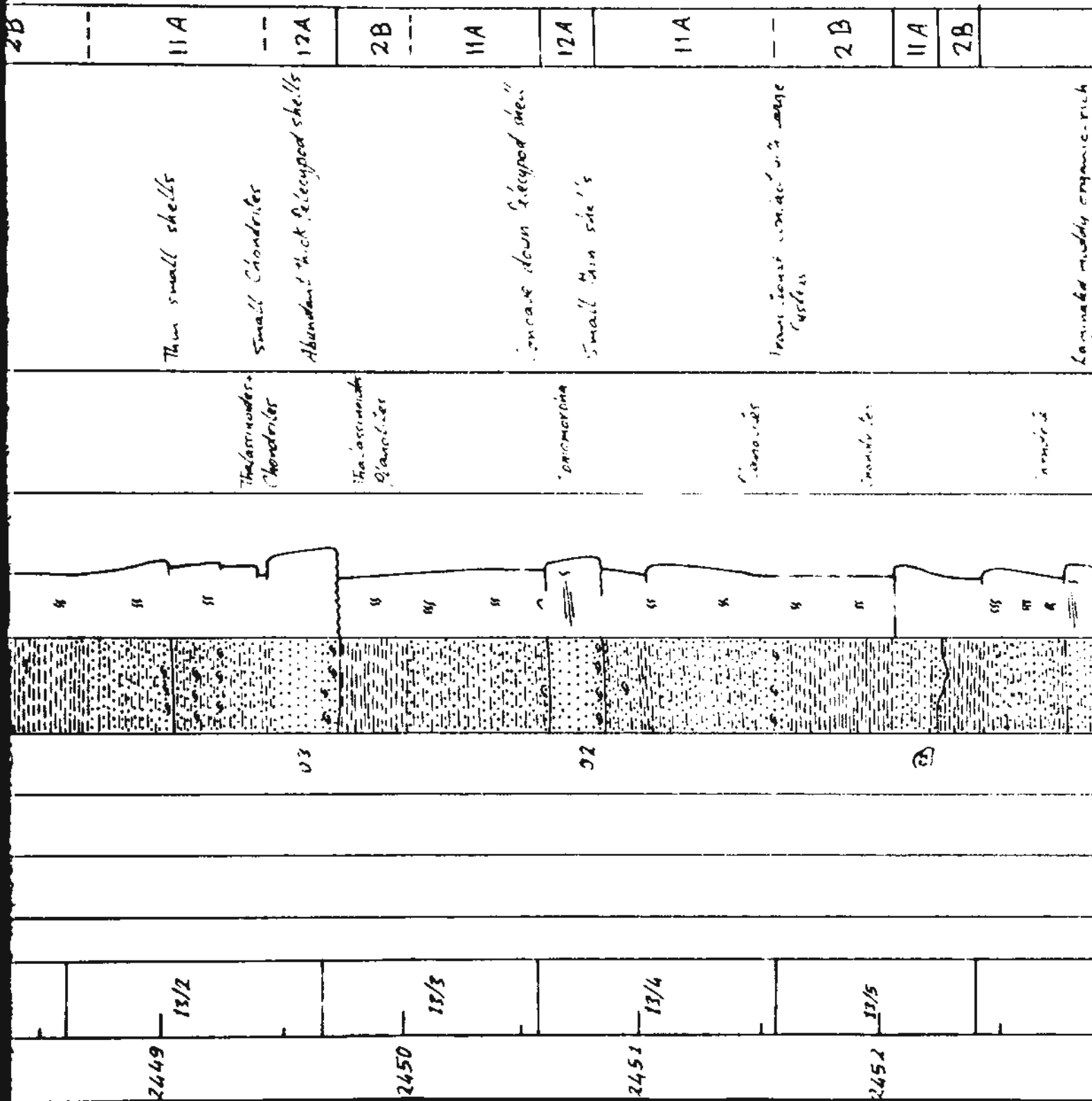
12/18

2447

Distal delta



Distal delta



| Core Number | Depth (m) | Interval (m) | Core Description | Notes | Remarks |
|-------------|-----------|--------------|------------------|-------|---------|
| 2453 | 13/6 | | | | |
| 2454 | 13/7 | | | | |
| 2455 | 13/8 | | | | |
| 2456 | 13/9 | | | | |
| 2457 | 13/10 | | | | |

Well Name: Hibernia I-46
Location: $46^{\circ}45'40.24''$ Lat. $48^{\circ}51'13.19''$ W Long
K.B.: 32.2 m G.L.: -39.4 m R.T.:

K.B.: 32.2 m G.L.: - 39.4 m R.T.:

Logged by: Osama M. Soliman
Depth from: K.B.
Date: 19.06.92 4/9

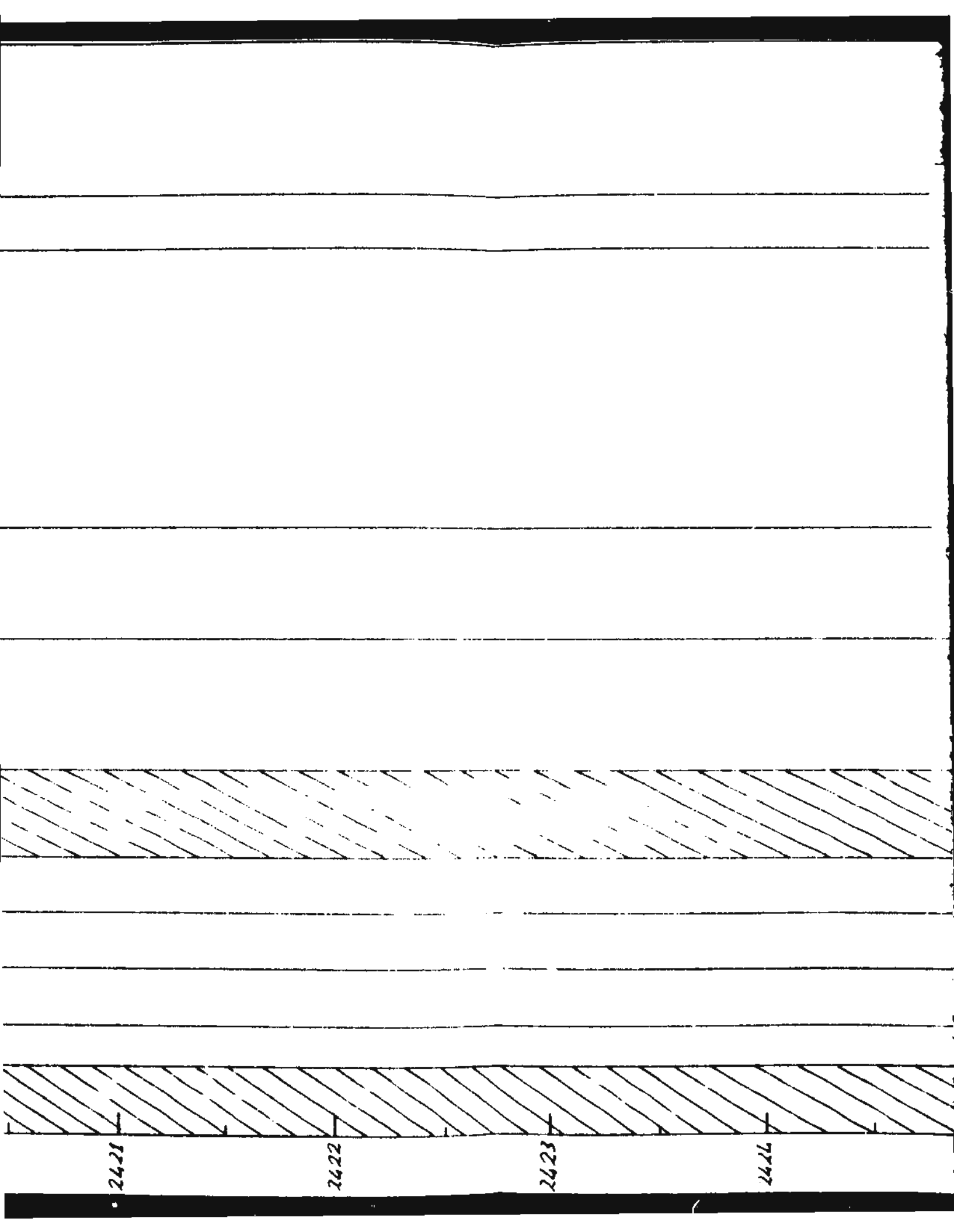
Date: 14.06.92

1

2418

2419

2420



2421

2422

2423

2424

2422

2423

2424

2425

2426

2B

Dark grey mudstone with some
reddish brown ferruginous
bands
Slump?

Dark grey mudstone with some
reddish brown ferruginous
bands

nm

2427

2428

2429

2430

11/1

2431

Bay fill sediments

Transgress surface

2B

11A

12A

11A

12A

11A

12A

Mud lined slump fractures

braiding mud-lined fractures

Time associated soft sediment deformation

Irregular sand lenses and bands (suspension sand)

Clay filled root traces ???

Carbonate nodules

Coar chips

Reddish clay filled root traces

radational contact

in the sand cells (2-3 cm)

mud beds

Patches filled with

sil. mass

Clay lined enclosures ???

Chondrites

Chondrites

Chondrites

Chondrites

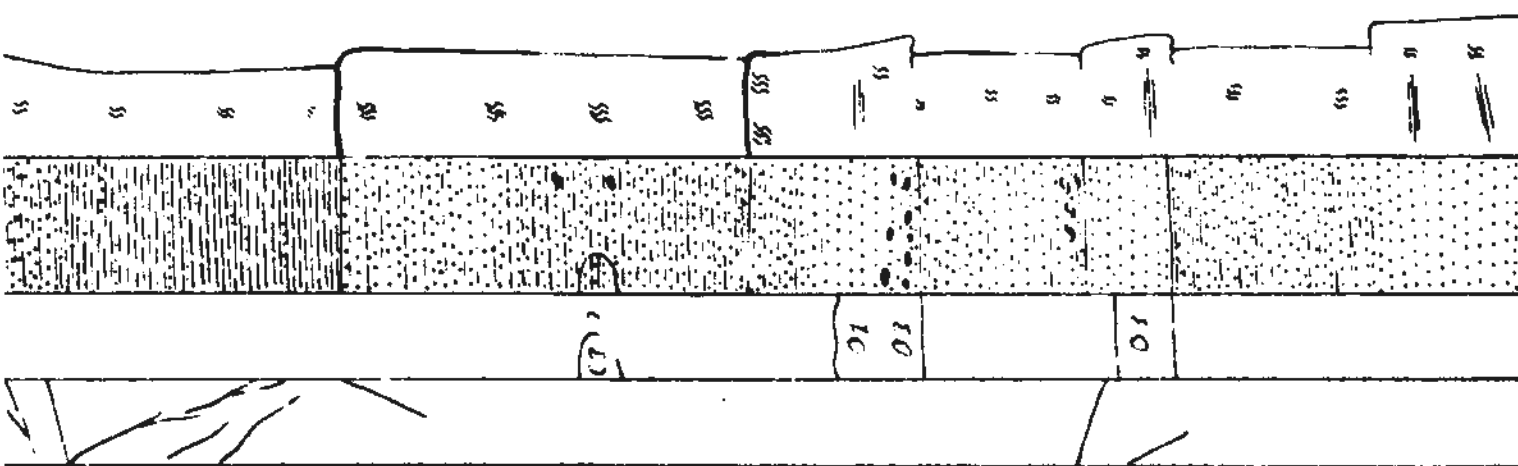
Chondrites

Chondrites

Chondrites

Chondrites

Chondrites



| | | | | | | | | | | | | | | | | | | | | | |
|------|------|-----|-----|-----|------|-----|-----|-----|------|------|-----|-----|-----|------|------|-----|-----|-----|------|-----|------|
| 589 | 590 | 591 | 592 | 593 | P.2 | 594 | 595 | 596 | 597 | P.3 | 598 | 599 | 600 | P.4 | 601 | 602 | P.5 | 603 | 604 | 605 | 606 |
| 2433 | 12/4 | | | | 12/5 | | | | 12/6 | | | | | 12/7 | | | | | 12/8 | | |
| 2434 | | | | | | | | | | 2435 | | | | | 2436 | | | | | | 2437 |

Well Name: Hibernia- I-46

Location: 46°45'40.24" Lat. 48°51'13.19W Long

K.B.: 92.2 m

G.L.: -89.4 m

R.T.:

Logged by: Osama M. Soliman

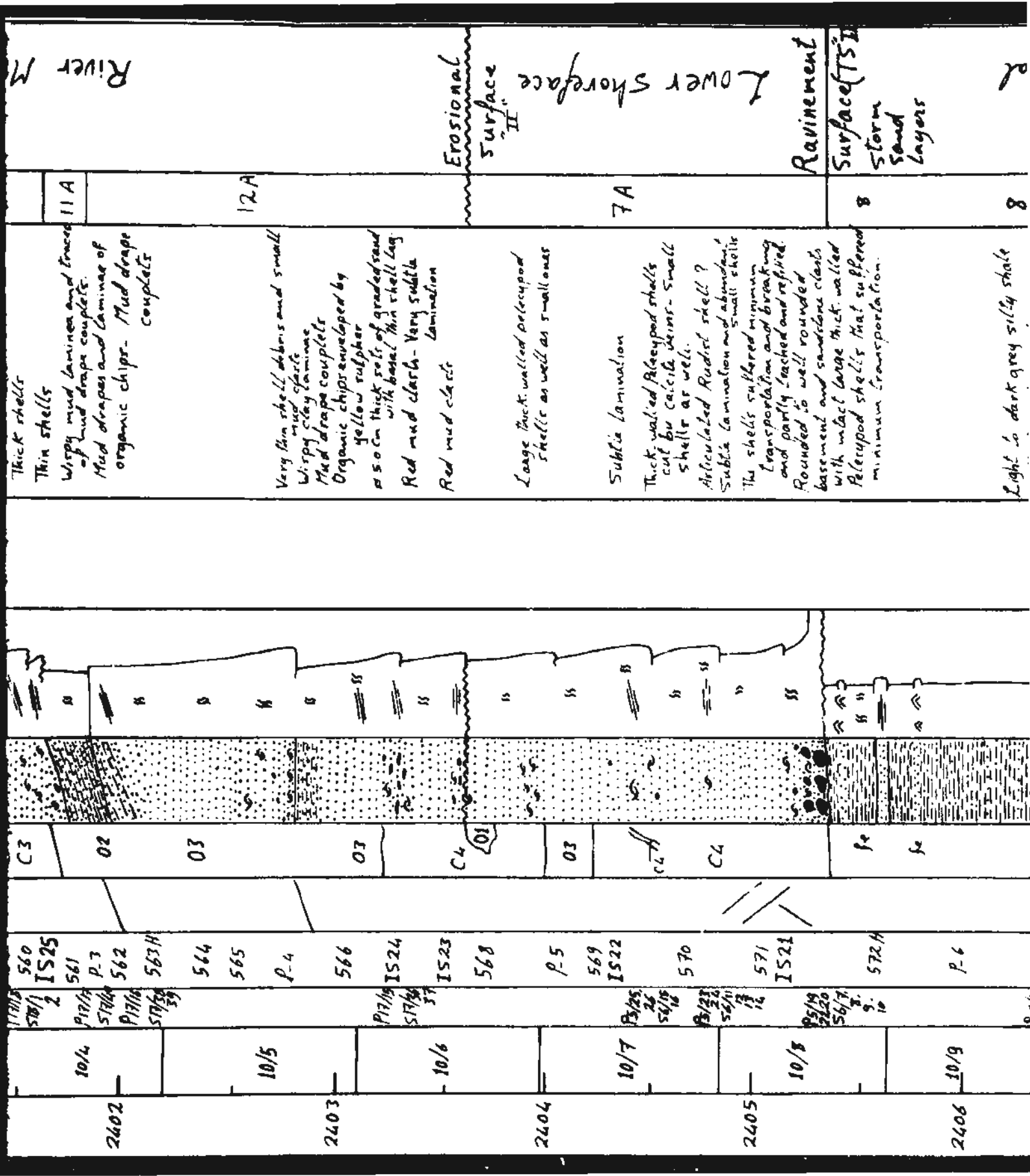
Depth from: K.B.

Date: 19.06.92

5/9

| Core no/
Box no. | P=Prints
S=slides | Sample
no | Fractures | Cements
oil stain | Lithology | Sed Structures
mud. $\frac{L}{K} \frac{E}{U} \frac{G}{S}$ | Fossils | Remarks | Facies | Environment |
|---------------------|--|--------------|-----------|----------------------|-----------|--|--|--|--------|-------------|
| 9/28 | P6/62
56/21,
22 | 552H | | 02 | | " | | | | |
| 9/29 | | P.12
553 | | | | " | | Waxy clay laminae
Remains of ripples and
inclined lamination | 11A | |
| 2398 | | | | | | | | | | |
| 2399 | | | | | | | | | | |
| 10/1 | P5/28
56/19
20
P5/27
56/17
18 | 554
IS27 | | C2
C3
C3 | | | Ophiomorpha
"phiomorpha
"phiomorpha
"phiomorpha | Millimeter to centimeter thick
sets of graded sand that are
draped by mud and organic
chips
0.5-50cm thick sets of graded sand
with erosive bases- General fining
upward. Sand, mud clasts and
thick walled shells as inq | 12A | |
| 2400 | | P.1
555 | | 02 | | " | Ophiomorpha | Very thin shells | | |
| 10/2 | P17/4
518/3
4 | IS26
556 | 1 | C4
C3 | | | | | | |

ds



River M

2

Lagoon

Lagoon

8

Light to dark grey silty shale with discontinuous laminae and lenses of rippled sand

Calcareous nodule
Mudstone with platy fabric and abundant sandstone bands and disrupted lenses. The s.s. is laminated and wave rippled (form concordant and form discordant ripples & truncated wave ripples, the tops of which are burrowed and disrupted). The laminae are graded light dark couplets with sharp upper and lower boundaries. The laminae are 1-3 mm thick

Dark mudstone with many sideritic bands and upwards increasing sand laminae and bands

P 17/14
S 17/14
35

10/10

2407

2408

P 11/2
S 11/2
22

11/1

2409

11/2

2410

11/3

Cl⁺O

Fe

Fe

Fe

Fe

Fe

Fe

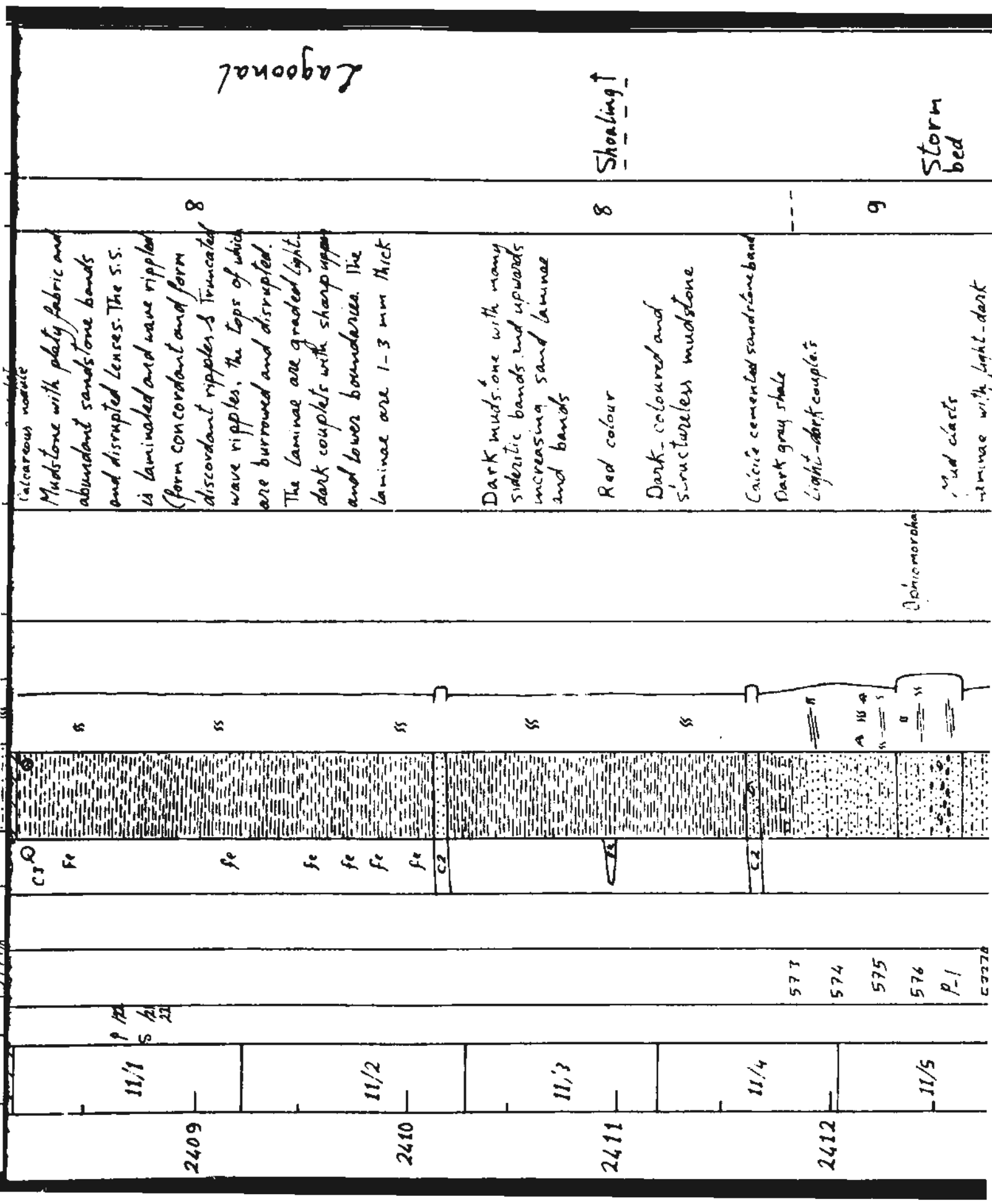
Cl⁺

"

"

"

"



11/1

2409

11/2

2410

11/3

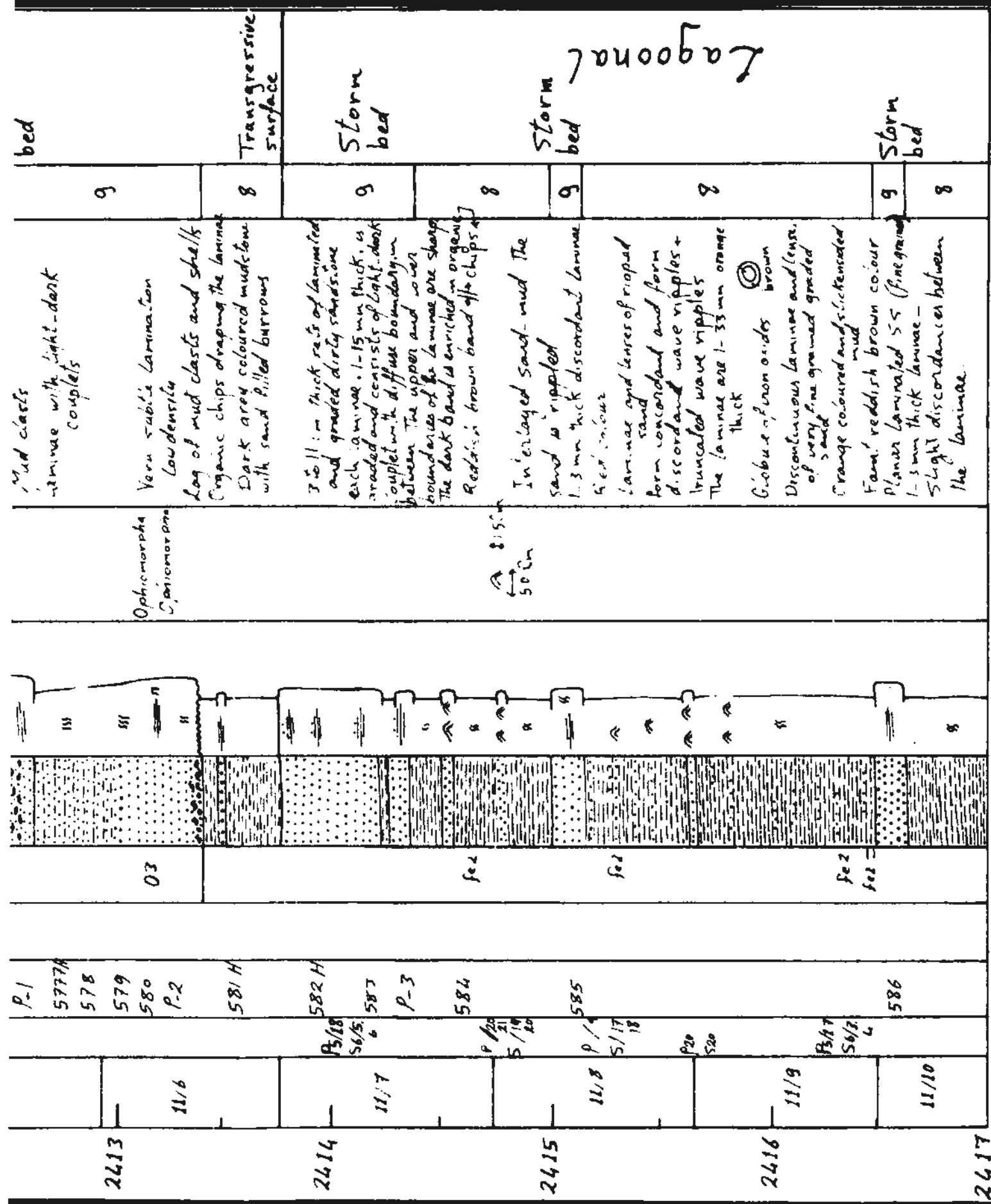
2411

11/4

2412

11/5

573
574
575
576
P-1
577



Lagoon

8.5 cm
50 cm

Well Name: Hibernia I-46

Location: 46° 45' 40.24" Lat. 48° 51' 17.19" W. Long. Depth from: K.B.

K.B.: 33.2 m. G.L.: - 89.4 m.

R.T.:

Logged by: Osama M. Soliman
Date: 6/9

| Core no/
Box no. | P=Prints
S=Slides | Sample
no. | Fractures | cements
oil stain | Lithology | Sed. Structures
mud. vs. Eux. | Fossils | Remarks | Facies | Environment |
|---------------------|----------------------|---------------|-----------|----------------------|-----------|----------------------------------|---------|---|--------|-------------|
| 2378 | | 9/7 | | | | | | | 11A | |
| | | 9/8 | | | | | | Coal chips with traces of sulphur
Few Serpulid tubes
Serpulid tubes | 2B | |
| 2379 | | 9/9 | | | | | | Serpulid tubes
Transitional boundary | | |
| 2380 | | 9/10 | | | | | | Serpulid tubes
Pyrite | 11A | |

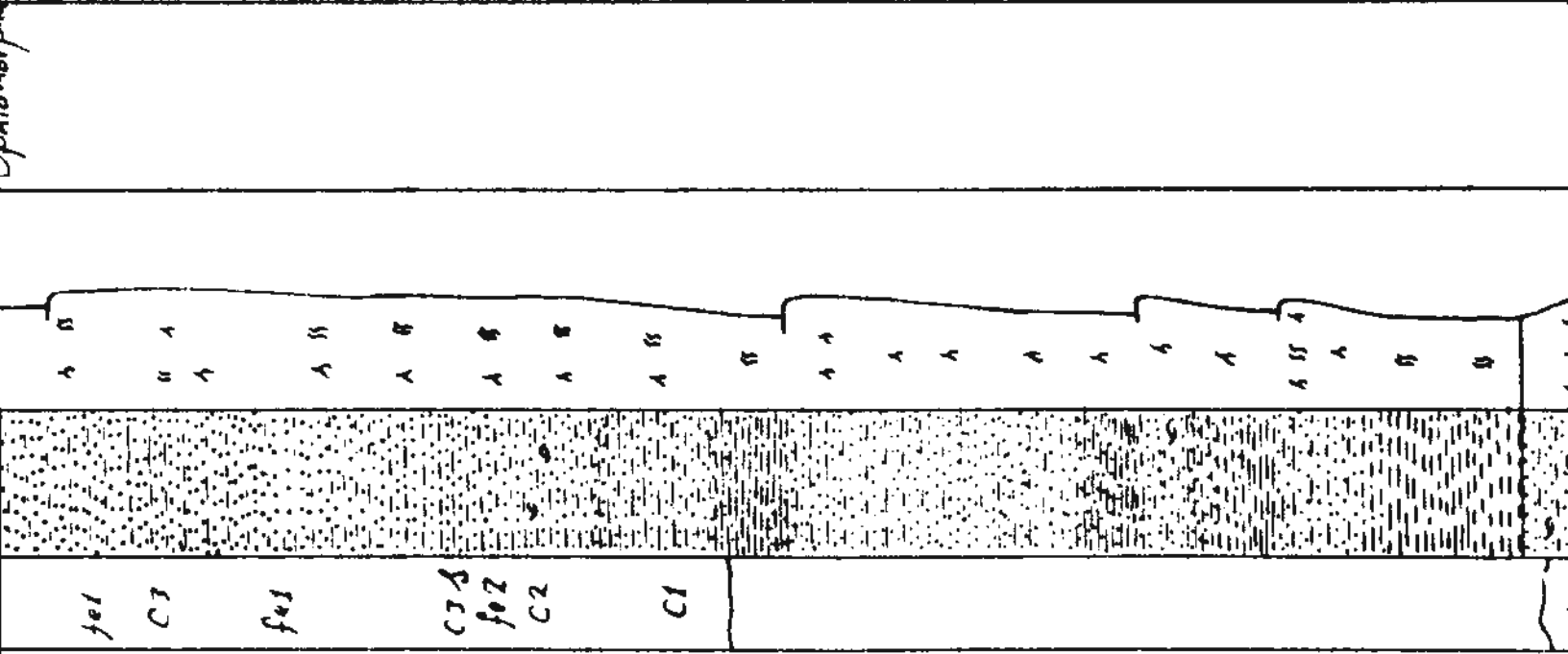
Distal delta

| | | | | | | |
|-----|----|-----|-------|-----------|-----------|---------------------------|
| 11A | 2B | 11A | -- 2B | 11A -- 2B | 11A -- 2B | Transgressive surface IR. |
|-----|----|-----|-------|-----------|-----------|---------------------------|

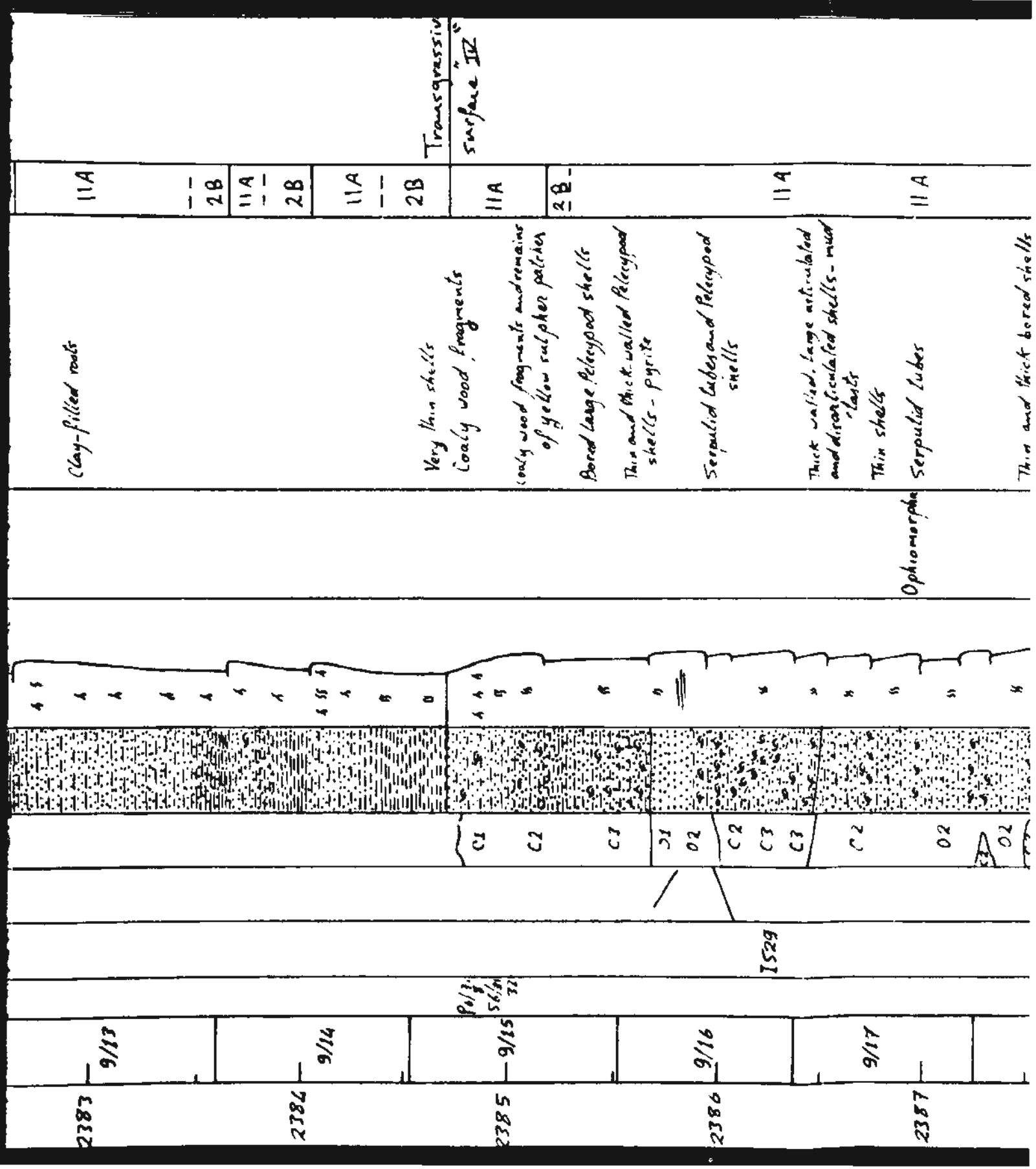
Thin bedded shales

gray - mottled shales

Very thin shales
coarse wood fragments



| | | | | | | | | |
|------|------|------|------|------|------|------|------|------|
| 2381 | 9/11 | 2382 | 9/12 | 2383 | 9/13 | 2384 | 9/14 | 9/15 |
|------|------|------|------|------|------|------|------|------|



2383

9/13

2384

9/14

2385

9/15

9/13
56/24
32

2386

9/16

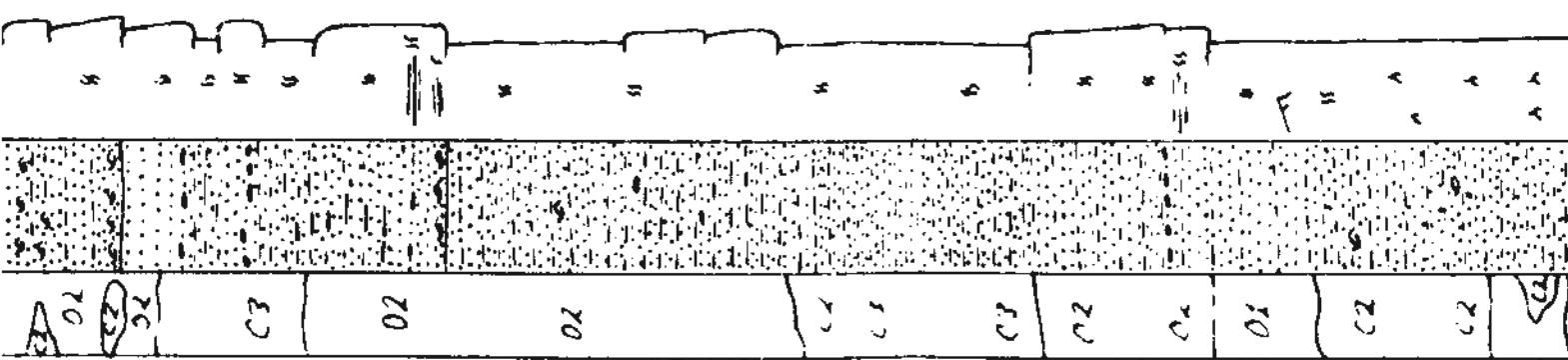
IS29

2387

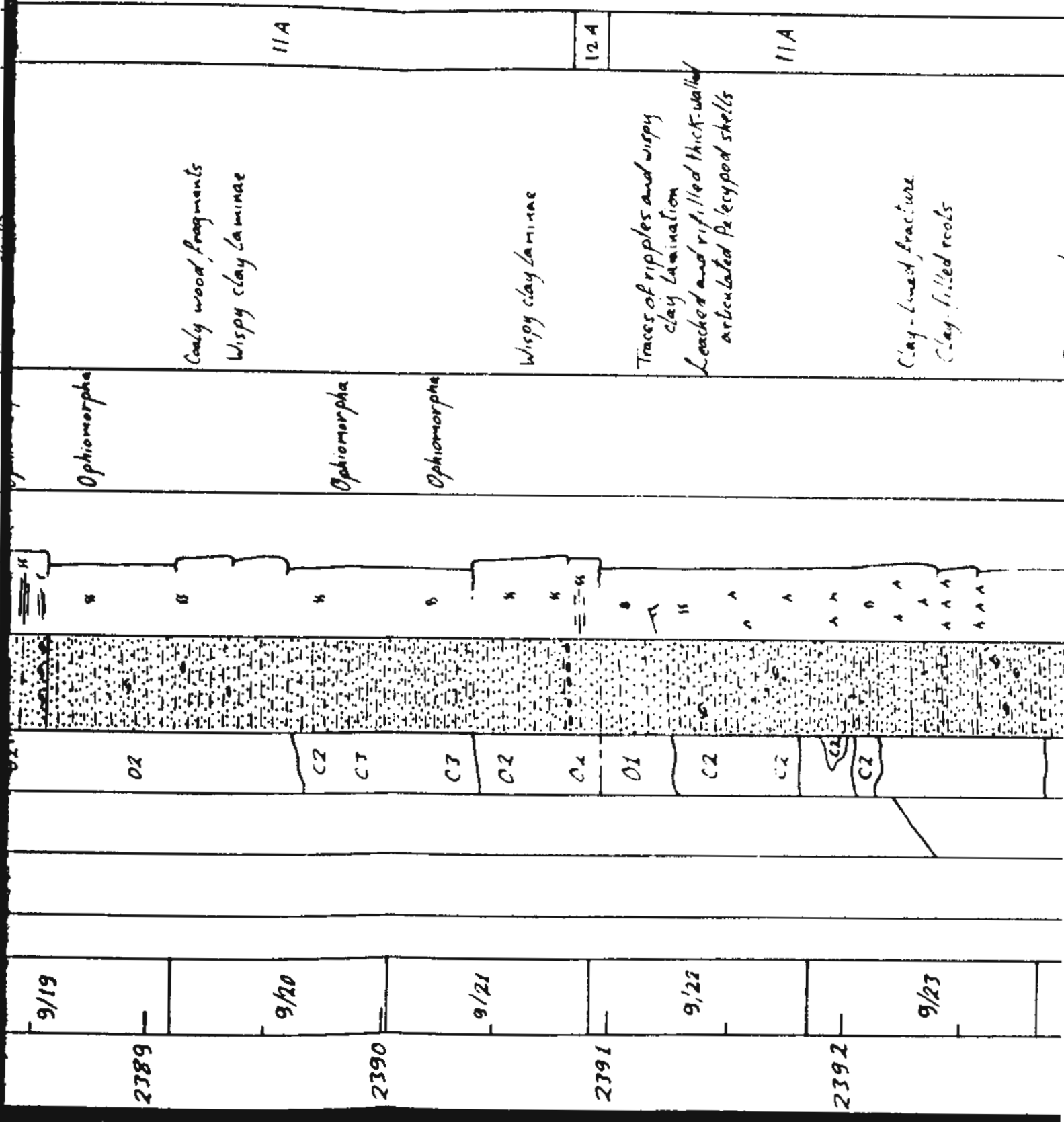
9/17

delta

| | | | | | |
|------|------|----|-------------|---|-----|
| 2388 | 9/18 | 02 | Ophiomorpha | Thin and thick banded shells | 11A |
| | | 02 | Ophiomorpha | Reddish mud clasts | |
| | | 03 | Ophiomorpha | | |
| | | 02 | Ophiomorpha | | |
| 2389 | 9/19 | 02 | Ophiomorpha | Caly wood fragments
Wisp clay laminae | 11A |
| | | 02 | Ophiomorpha | | |
| | | 03 | Ophiomorpha | | |
| 2390 | 9/20 | 02 | Ophiomorpha | Wisp clay laminae | 12A |
| | | 02 | Ophiomorpha | | |
| | | 02 | Ophiomorpha | Traces of ripples and wisp
clay lamination
Leached and vitified thick walled
articulated pteropod shells | 11A |
| 2391 | 9/21 | 02 | | | |
| | | 02 | | | |
| 2392 | 9/22 | 02 | | | |



Distal delta



| | | | | | | | | | |
|------|------|--|--|--|--|-------------|--|-----|--------------------------------|
| 2393 | 9/20 | | | | | Ophiomorpha | organic chips
Serpulid tubes | 11A | |
| 2394 | 9/25 | | | | | | articulated large shells
thick walled large P. lewyi shells
Serpulid tubes +
olimus wood fragment
Small lewyi shells
Thick and thin-walled P. lewyi
shells | 11A | |
| 2395 | 9/26 | | | | | Ophiomorpha | Thick walled large P. lewyi shells
with abundant bore and
teaching features - P. lewyi
5 to 10 cm thick laminated sets
with lower erosive contact
Serpulid tubes and thin shells
Serpulid tubes at the bottom
coal chips and organic chips
very thin roots
Serpulid tubes | 12A | |
| 2396 | 9/27 | | | | | Ophiomorpha | Thin articulated and disarticulated
lewyi shells - Very thin small
shell debris - Organic chips
Wispily clay laminae | 2B | Transgressive
surface "III" |
| 2397 | 9/28 | | | | | Ophiomorpha | Thin chips of organics
Few scattered thin small shells
Wispily clay laminae | 11A | |
| | | | | | | Ophiomorpha | Remains of horizontal
lamination | | |

Well Name: *Hibernia I-66*

Location: *46° 45' 40" N Lat 48° 51' 17.19" W Long* Depth from: *K.B.*

K.B.: *33.2 m* G.L.: *- 89.4 m* R.T.: *7/9*

Logged by: *Osama M Soliman*

Date:

| Core no/
Box no | P-Prints
S-slides | Sample
no | Fracture | Cements
oil stain | Lithology | Sed. Structures | Fossils | Remarks | Facies | Environment |
|--------------------|-----------------------|--------------|----------|----------------------|-----------|-----------------|---------|---|--------|--------------|
| 8/14 | | | | | | mud | | | | |
| 8/15 | 8/14
57/4
5 | | | | | | | Small organic chips
Few Serpulid tubes
Very large articulated Pelycopod shells
Few scattered Serpulid tubes and Pelycopod shells | 2B | Bay mudstone |
| 8/16 | 8/15
57/2
1 | | | | | | | Pyrite
Slit-kensided fracture
Organic chips
Large shells
Serpulid tubes and shalical top (Ferruginous 25 cm thick sat) | 11A | |
| 8/17 | 8/16
56/39
57/1 | IS 12 | | | | | | Organic chips
Slit-kensided fracture
Granular with nodules | 11A | Distal delta |
| 8/18 | 8/17 | IS 11 | | | | | | | | |

2358

2359

2360

sediments

119

Dominantly non-zen'at root
faces

Serpulid tubes and Piddlers

113

good price for his manuscript

811

Ver. angez. u. kalkuliert & exportiert
S. 161

82

Erosional
surface "III"

42

- Serpentine talus and shales at top (Ferruginous 25cm thick ref.)
- organic chips
- Slickensided fracture
- Crane-rich nodules

24. 10. 1940

Одобрено

24.05.08-2017

98/12/1532

56.79
5711

5715

7551

96/11
44/95
38

46/95

2

95
56/95
06/96

92
5/95

42

817

8/18

3

8-20

8171

26

2360

2361

2362

2363

2364

8

Bay fill sediments

11B

Dominantly horizontal root traces

Serpulid tubes and Pelecypod shells

Scattered pyrite

Serpulid tubes

Optiomorpha

11A

Serpulid tubes and Pelecypod shells

Pyrite - Red colour

Optiomorpha

11A

Some scattered Serpulid tubes and Pelecypod shells

Optiomorpha

11A

Fine to very fine grained muddy sandstone - bioturbated - possible clay-filled root traces

Few Serpulid tubes

8/21

2364

8/22

2365

8/23

2366

8/24

2367

8/25

2368

IS 30

9/19
5/17
34

C1
C2
C1

C3
F2
C3

C3

| Core Number | Date | Core Description | Notes |
|-------------|------|--------------------------|--|
| 2368 | 8/26 | 11A | Few Serpulid tubes
Coal fragments |
| 2369 | 8/27 | 2B | Dark grey to black mudstone |
| 2370 | 8/28 | 2B | Possible roots
Transitional boundary |
| 2371 | 9/1 | Transgressive surface IV | Coaly organic fragments enriched in yellow sulphur
Reddish color - pyrite |
| 2372 | | | Disseminated pyrite |

Distal delta

| | | | | | | |
|------|-----|----|----|----|-----|--|
| 2373 | 9/2 | C1 | C3 | C1 | 11A | isomorphous pyrite |
| 2374 | 9/2 | C1 | C1 | C2 | 2B | Serpulid tubes & small
Olecyropod shells |
| 2375 | 9/4 | C1 | C1 | C2 | 11A | Serpulid tubes |
| 2376 | 9/5 | C1 | C1 | C2 | 2B | Serpulid tubes |
| 2377 | 9/6 | C1 | C1 | C2 | 11A | Transitional contact |
| | 9/1 | C1 | C1 | C2 | 11A | Stemmed wood fragments
Thin Olecyropod shells
and few Serpulid tubes |

Well Name: Hibernia I-46

Location: $46^{\circ} 45' 40.42''$ N. Lat. $48^{\circ} 51' 17.19''$ W. Long. Depth from: K.B.

Logged by: Osama M. Soliman

K.B.: 33.2 m.

G.L.: - 89.4 m.

R.T.:

Date:

8/9

| Core no/
Box no. | P=Prints
S=slides | Sample
no | Fractures | cements
oil stain | Lithology | Sed. Structures | Fossils | Remarks | Facies | Environment |
|---------------------|----------------------|--------------|-----------|----------------------|-----------|--------------------------------------|--------------|---|--------|-------------|
| | | | | | | mud. $\frac{VF}{EF}$ $\frac{EU}{UG}$ | | | | |
| 2338 | 7/22 | | | | | ? }
? | | -

Rubble zone

Coquinaoid shell hash

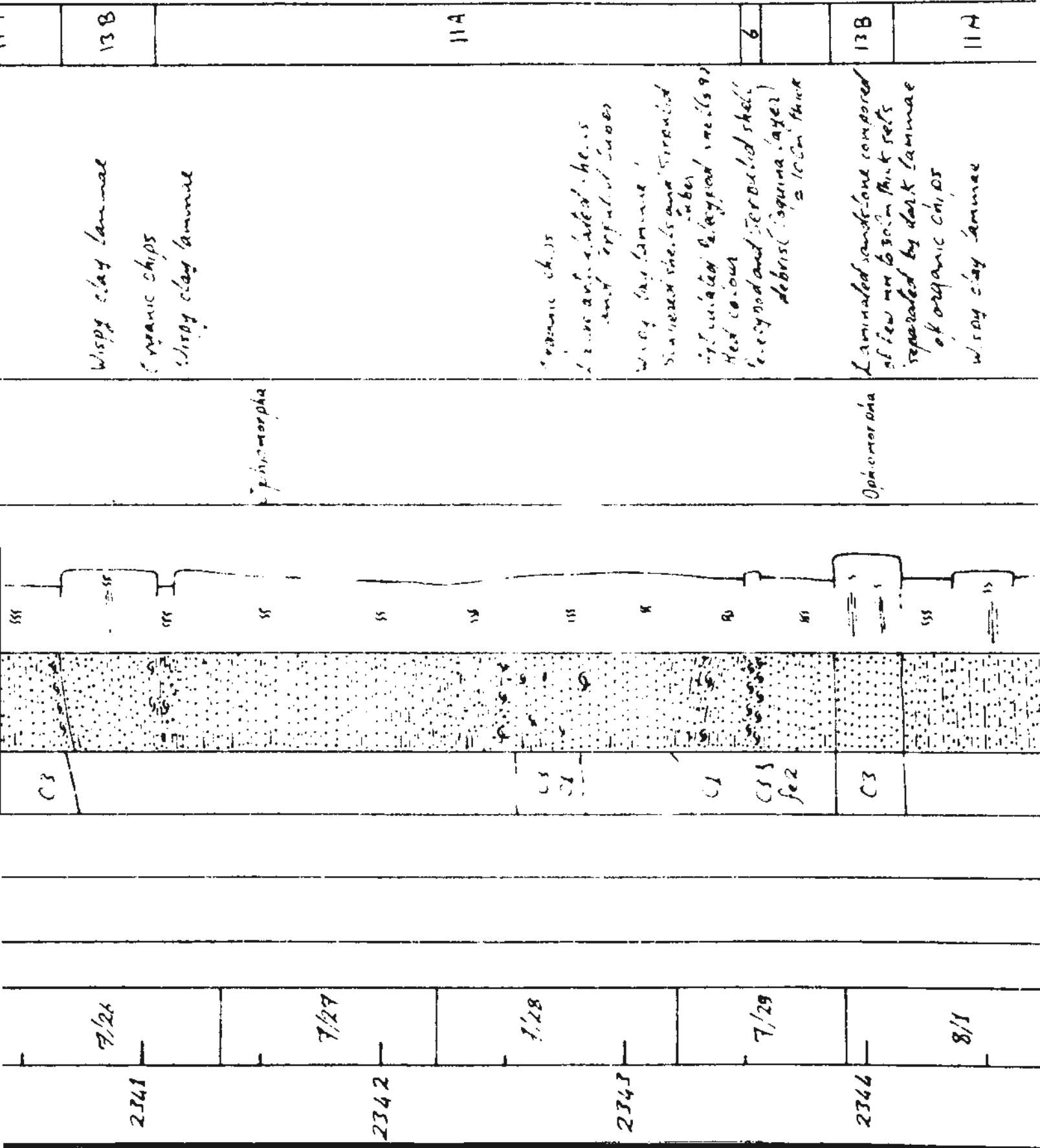
Rubble zone | II A | |
| | 7/23 | | | 01 | | ?
? | | | | |
| 2339 | 7/24 | | | C1 | | "
"
" | Cochromorpha | -

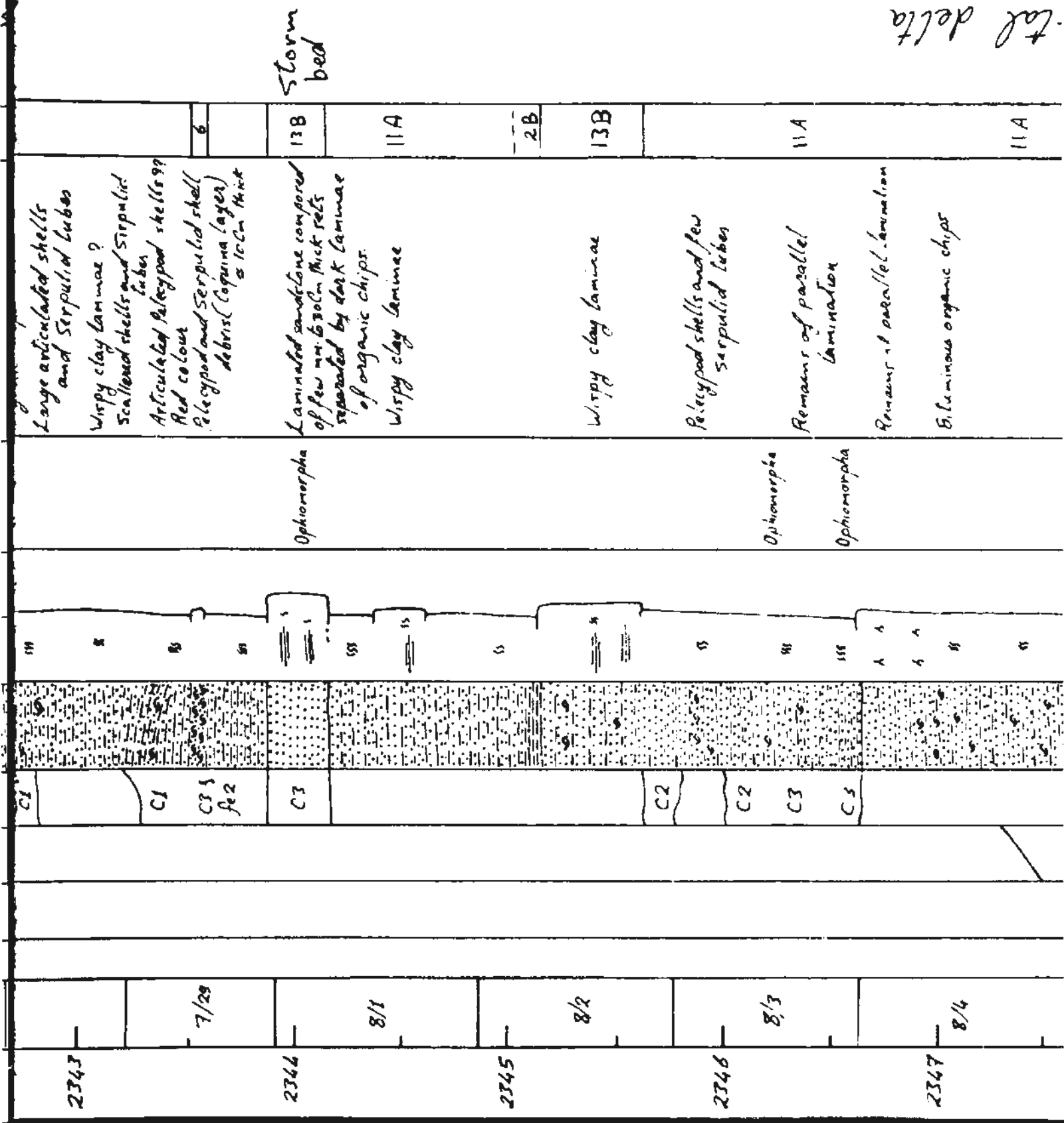
Few scattered shell debris

Silty sandstone

Thin shell debris | II A | |
| | | | | C1 | | " | | | | |
| | | | | C1 | | " | | | | |
| 2340 | 7/25 | | | C1 | | "
" | | Small and large shell debris
Some shells are bored | 6 | St. Ita |
| | | | | | | " | | | | |

Distal





tal delta

6/8

ISSI

01/15
11/81

C1 C3

23

for
c3d

63

72

13

C2

phospho

phenomena

[illegible]

119

f1A

8-11

Abundant. Alcyonoid shells
and serpulid tubes

Wisp^y clay laminae
serpulid tubes and thin
decayed shells
Bituminous organic chips

Thin eledynod shells

Few Serouid tubes

Possible root-traces
Few Serpentine tubes

0:57

| Core No. | Depth (m) | Interval | Stratigraphic Unit | Fossil Content | Remarks |
|----------|-----------|----------|--------------------|----------------|---------|
| 2349 | 8/6 | | | | IIA |
| | | C2 | | | |
| | | C3 & fel | | | |
| | | C3 | | | |
| 2350 | 8/7 | | | | IIB |
| | | C2 | | | |
| | | C1 | | | |
| | | C2 | | | |
| 2351 | 8/8 | | | | IIB |
| | | | | | |
| | | | | | |
| | | | | | |
| 2352 | 8/9 | | | | IIB |
| | | | | | |
| | | | | | |
| | | | | | |

Bay fill sediments

Organic clays and few Serpentin
clasts

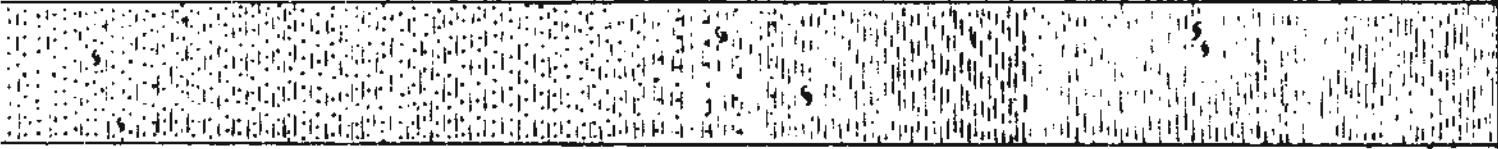
Preferential remanentation
of burrow fills.

11B

2B

2B

^ ^ ^ ^ ^ ^ ^ ^ ^ ^ ^ ^ ^ ^ ^ ^



C1

2353

2354

2355

2356

2357

8/10

8/11

8/12

8/13

8/14

96/16
57/8
3

96/16
57/6
7

Well Name: Hibernia I-46

Location: 46° 45' 40.42" N Lat. 48° 51' 17.19" W Long. Depth from: K.B.

K.B.: 33.2 m.

G.L.: - 89.4 m.

R.T.:

Logged by: Osama M. Soliman

Date:

9/9

| Core no/
Box no. | P-Prints
S=slides | Sample
no. | Fractures | cements
oil stain | Lithology | Sed. Structures
mud. <small>VF EU > 2</small> | Fossils | Remarks | Facies | Environment |
|---------------------|----------------------|---------------|-----------|----------------------|-----------|---|---------|---|--------|--------------|
| 2318 | 7/1 | | | | | " | | Few scattered Pelecypod shells | 11A | Distal delta |
| | 7/2 | | | C1 | | " | | Coal fragments | | |
| | | | | | | " | | Grey siltstone
abundant organic chips | 2B | |
| 2319 | 7/3 | | | | | " | | Abundant organic chips | | |
| | | | | | | " | | | | |
| | | | | | | " | | | | |
| 2320 | 7/4 | | | | | " | | Serpulid tubes and
Pelecypod shells | --- | |
| | | | | | | " | | Grey siltstone
Much organic chips
Convex up shell | 11B | |
| | | | | | | " | | Much organic chips | | nts |

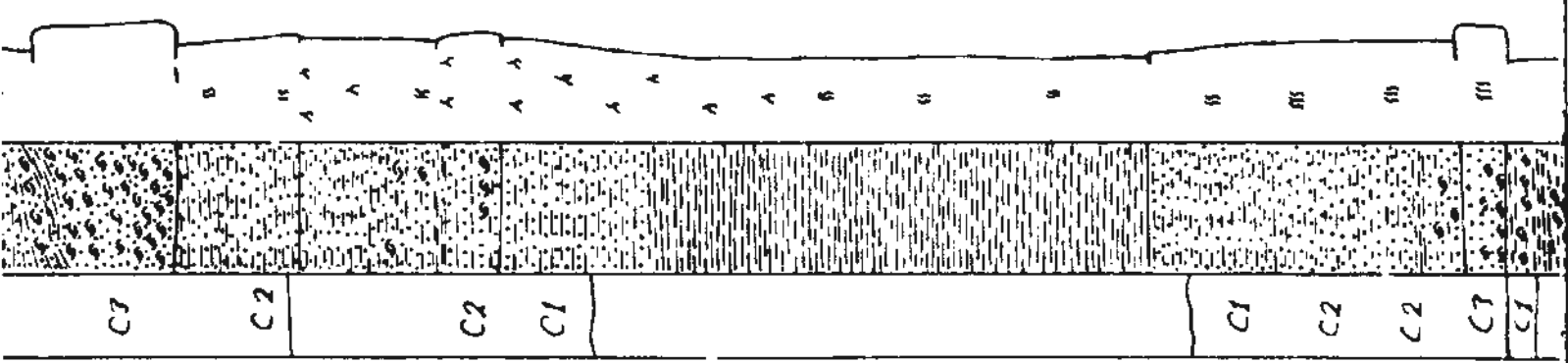
Bay mudstones

Coquina bed that grades upwards to coquinaoid sandstone

Preferential patchy calcic cementation

10 cm thick sand mud rhythmic lamination

Ophiomorpha



IS 14

PS 19
57/14
15

2328

7/13

2329

7/14

2330

7/15

2331

7/16

2332

7/17

Bay mudstones

11B

28

11A

2B

Preferential patchy calcite
cementation

10 cm thick sand-mud
rhythmic lamination

Ophiomorpha

bedded crowded with thin shells

7/13

2329

7/14

2330

7/15

2331

7/16

2332

7/17

96/19
57/14
15

C2

C2

C1

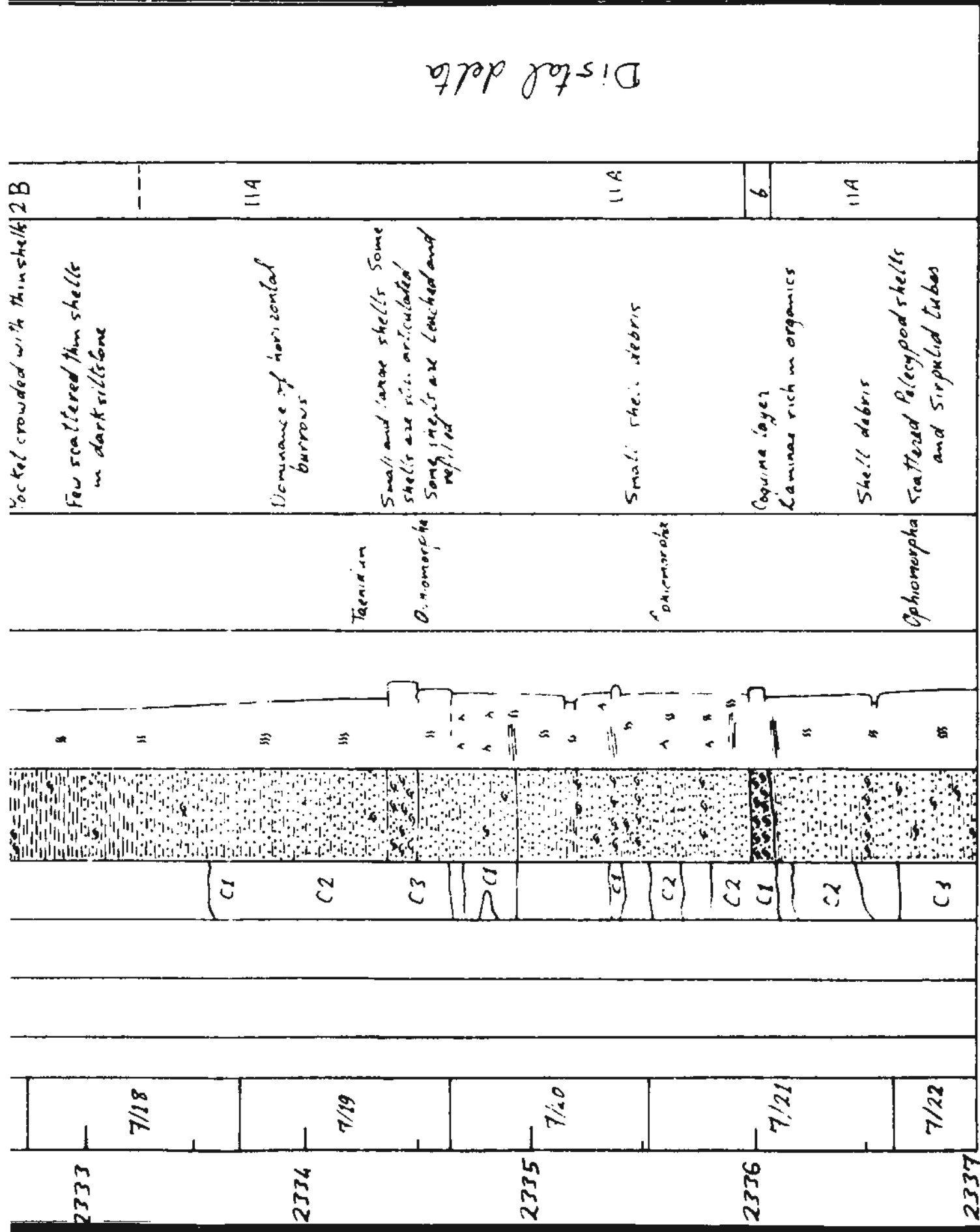
C1

C2

C2

C3

C1



Distal delta

WELL NAME: *Hibernia J-34*

LOCATION: 46° 43' 34.61" N Lat 48° 50' 11.86" W Long

K.B.: 26.7 m Depth measured from: A.T.

G.L.: - 78.3 m RT. 24.4 m

Corals: 1-13 = Log

Logged by: Osama M. Soliman

△ 2 △

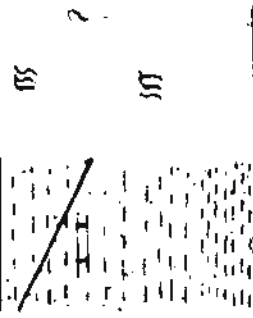
| DEPTH
(m)
Core No.
Box No. | OIL STAIN
PHOTOGRAPHS
P. Prints | LITHOLOGY
Core Sample | STRUCTURES | REMARKS | LITHO-
FACIES | ENVIRONMENT |
|-------------------------------------|---------------------------------------|--------------------------|------------|---------|------------------|-------------|
| | | | | | | |
| | | | | | | |
| | | | | | | |
| | | | | | | |
| | | | | | | |
| | | | | | | |
| | | | | | | |
| | | | | | | |
| | | | | | | |
| | | | | | | |
| | | | | | | |
| | | | | | | |
| | | | | | | |
| | | | | | | |
| | | | | | | |
| | | | | | | |
| | | | | | | |
| | | | | | | |
| | | | | | | |
| | | | | | | |
| | | | | | | |
| | | | | | | |
| | | | | | | |
| | | | | | | |
| | | | | | | |
| | | | | | | |
| | | | | | | |
| | | | | | | |
| | | | | | | |
| | | | | | | |
| | | | | | | |
| | | | | | | |
| | | | | | | |
| | | | | | | |
| | | | | | | |
| | | | | | | |
| | | | | | | |
| | | | | | | |
| | | | | | | |
| | | | | | | |
| | | | | | | |
| | | | | | | |
| | | | | | | |
| | | | | | | |
| | | | | | | |
| | | | | | | |
| | | | | | | |
| | | | | | | |
| | | | | | | |
| | | | | | | |
| | | | | | | |
| | | | | | | |
| | | | | | | |
| | | | | | | |
| | | | | | | |
| | | | | | | |
| | | | | | | |
| | | | | | | |
| | | | | | | |
| | | | | | | |
| | | | | | | |
| | | | | | | |
| | | | | | | |
| | | | | | | |
| | | | | | | |
| | | | | | | |
| | | | | | | |
| | | | | | | |
| | | | | | | |
| | | | | | | |
| | | | | | | |
| | | | | | | |
| | | | | | | |
| | | | | | | |
| | | | | | | |
| | | | | | | |
| | | | | | | |
| | | | | | | |
| | | | | | | |
| | | | | | | |
| | | | | | | |
| | | | | | | |
| | | | | | | |
| | | | | | | |
| | | | | | | |
| | | | | | | |
| | | | | | | |
| | | | | | | |
| | | | | | | |
| | | | | | | |
| | | | | | | |
| | | | | | | |
| | | | | | | |
| | | | | | | |
| | | | | | | |
| | | | | | | |
| | | | | | | |
| | | | | | | |
| | | | | | | |
| | | | | | | |
| | | | | | | |
| | | | | | | |
| | | | | | | |
| | | | | | | |
| | | | | | | |
| | | | | | | |
| | | | | | | |
| | | | | | | |
| | | | | | | |
| | | | | | | |
| | | | | | | |
| | | | | | | |
| | | | | | | |
| | | | | | | |
| | | | | | | |
| | | | | | | |
| | | | | | | |
| | | | | | | |
| | | | | | | |
| | | | | | | |
| | | | | | | |
| | | | | | | |
| | | | | | | |
| | | | | | | |
| | | | | | | |
| | | | | | | |
| | | | | | | |
| | | | | | | |
| | | | | | | |
| | | | | | | |
| | | | | | | |
| | | | | | | |
| | | | | | | |
| | | | | | | |
| | | | | | | |
| | | | | | | |
| | | | | | | |
| | | | | | | |
| | | | | | | |
| | | | | | | |
| | | | | | | |
| | | | | | | |
| | | | | | | |
| | | | | | | |
| | | | | | | |
| | | | | | | |
| | | | | | | |
| | | | | | | |
| | | | | | | |
| | | | | | | |
| | | | | | | |
| | | | | | | |
| | | | | | | |
| | | | | | | |
| | | | | | | |
| | | | | | | |
| | | | | | | |
| | | | | | | |
| | | | | | | |
| | | | | | | |
| | | | | | | |
| | | | | | | |
| | | | | | | |
| | | | | | | |
| | | | | | | |
| | | | | | | |
| | | | | | | |
| | | | | | | |
| | | | | | | |
| | | | | | | |
| | | | | | | |
| | | | | | | |
| | | | | | | |
| | | | | | | |
| | | | | | | |
| | | | | | | |

2456

917-13
517-32

2457

3
C1



9

—

26

1/3

2458

Q3



10

—

1/4

2459

C1



11

—

1/5

2460

C1



12

—

1/6

2461

C1



13

radiolaria
cementation
contact

Stickens
fractures

Muddy sand
reworked from
below

Inundation '20

Transgression

15' of delta

(2)

elta front sards (crevasse splay ?)

Transgression

Gradational
cementation
contact

Stickensided
fractures

Muddy sand
reworked from
below

Inundation lag
of mud chips
and shell hash

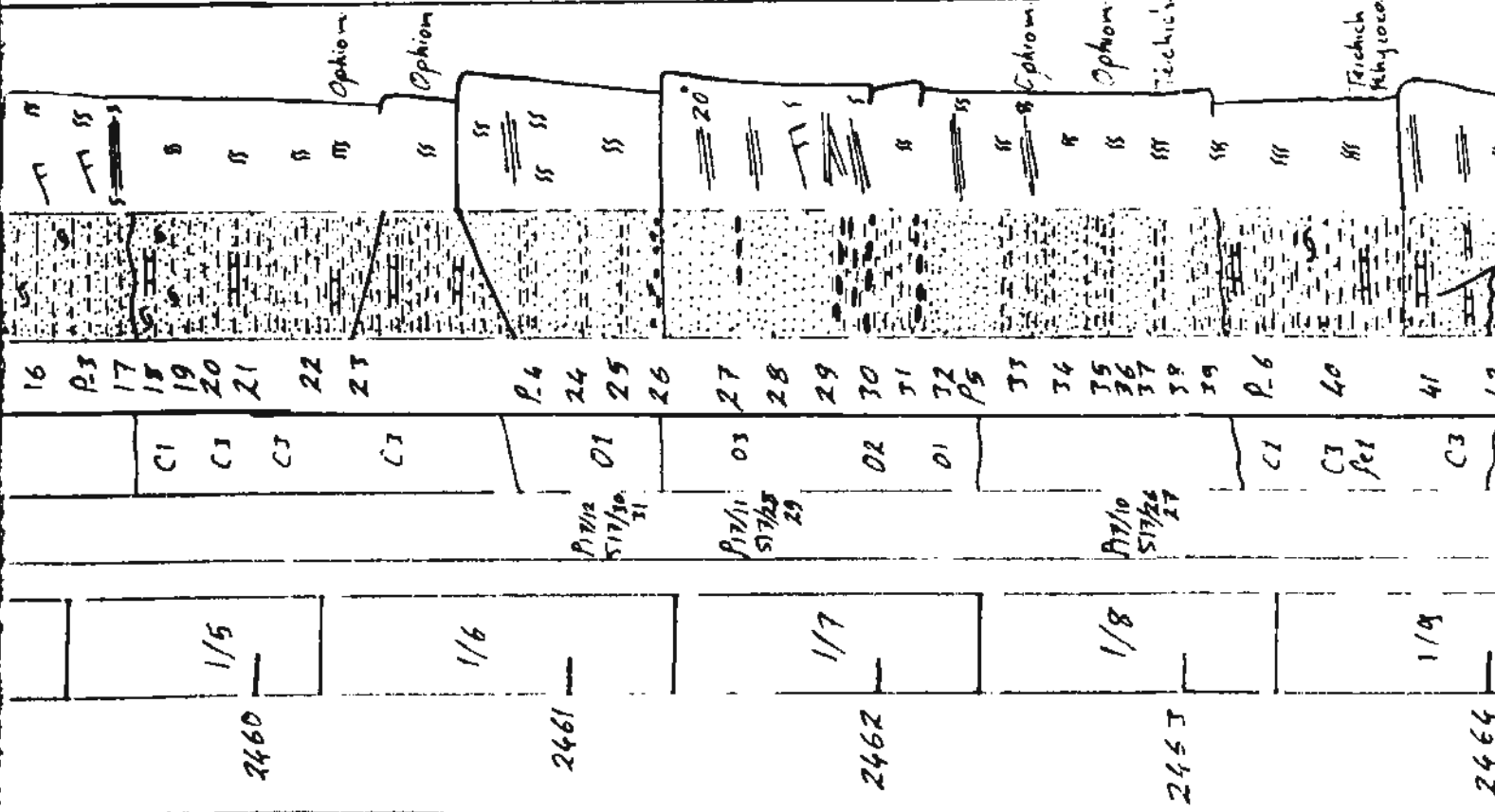
12A

12A

Red coloration

11A

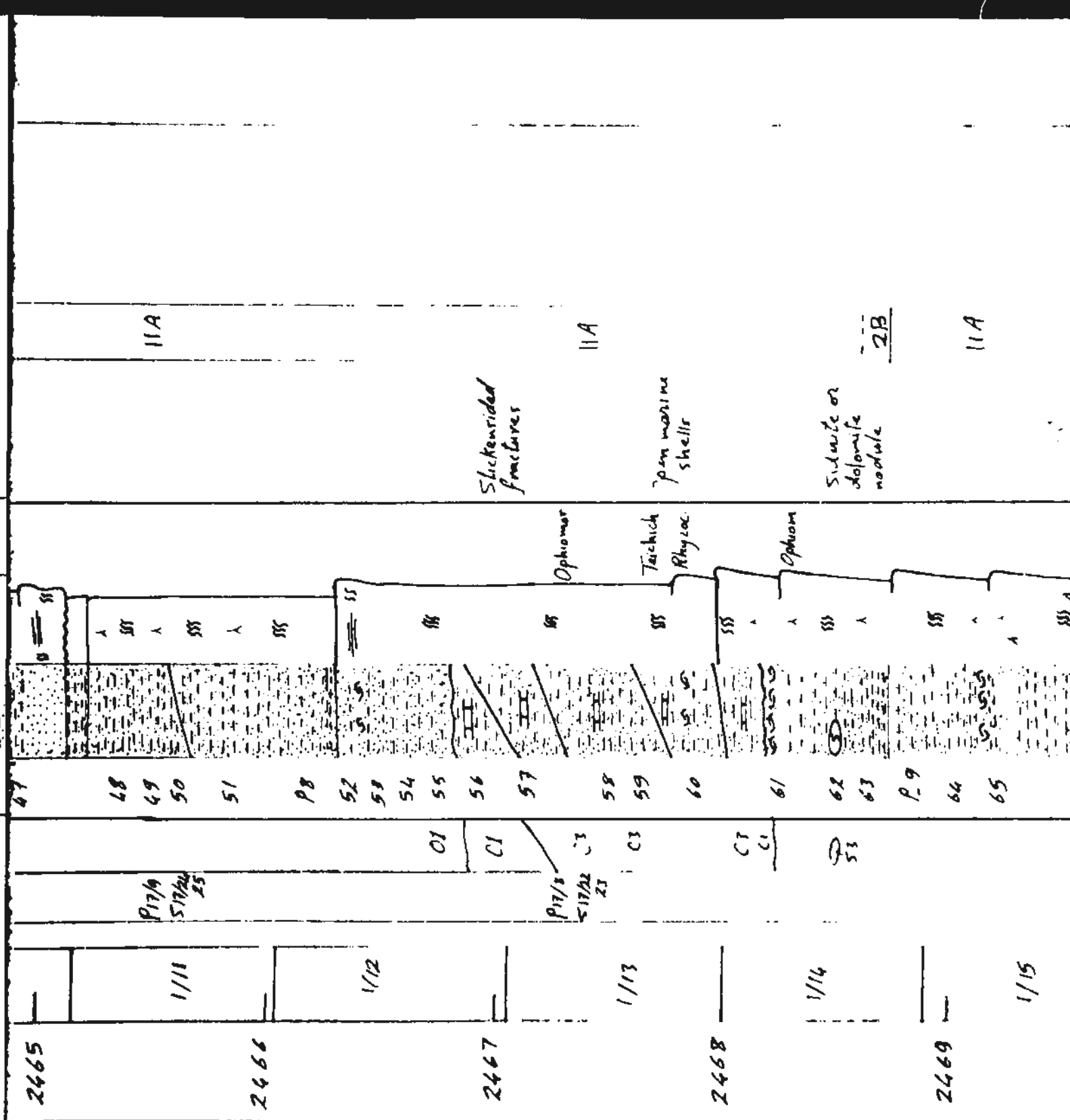
Small fractures



Geological log of well 2464. The log shows stratigraphic units and lithology from surface to 114 feet depth.

| Depth (ft) | Unit / Lithology | Notes |
|------------|------------------|-------|
| 0 - 41 | Small fractures | |
| 42 - 43 | SS | |
| 44 - 45 | SS | |
| 46 - 47 | SS | |
| 48 - 49 | SS | |
| 50 - 51 | SS | |
| 52 - 53 | SS | |
| 54 - 55 | SS | |
| 56 - 57 | SS | |
| 58 - 59 | SS | |
| 60 - 61 | SS | |
| 62 - 63 | SS | |
| 64 - 65 | SS | |
| 66 - 67 | SS | |
| 68 - 69 | SS | |
| 70 - 71 | SS | |
| 72 - 73 | SS | |
| 74 - 75 | SS | |
| 76 - 77 | SS | |
| 78 - 79 | SS | |
| 80 - 81 | SS | |
| 82 - 83 | SS | |
| 84 - 85 | SS | |
| 86 - 87 | SS | |
| 88 - 89 | SS | |
| 90 - 91 | SS | |
| 92 - 93 | SS | |
| 94 - 95 | SS | |
| 96 - 97 | SS | |
| 98 - 99 | SS | |
| 100 - 101 | SS | |
| 102 - 103 | SS | |
| 104 - 105 | SS | |
| 106 - 107 | SS | |
| 108 - 109 | SS | |
| 110 - 111 | SS | |
| 112 - 113 | SS | |
| 114 | SS | |

Notes: Small fractures, Sh. lensoided fractures, pen marine shells, Subarctic or dolomite.



1/15

2470

1/16

2471

1/17

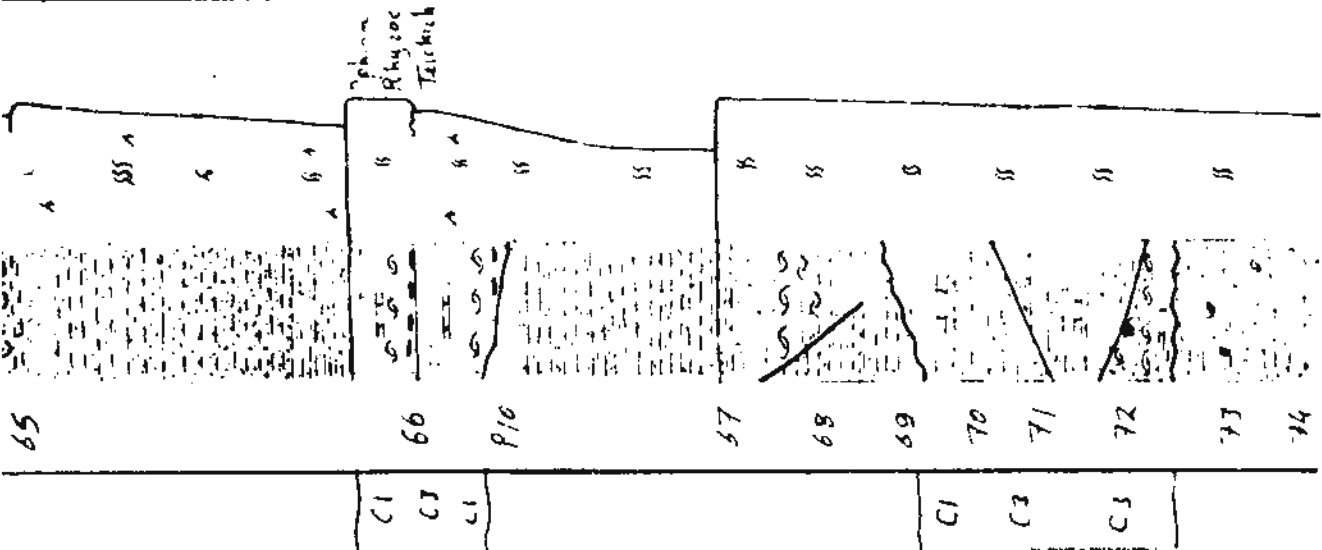
2472

1/18

121

1/19

2473



Distal delta

2B

11A

11A

Serpentinite

Larva shells

Large snails and few Serpentine tubes

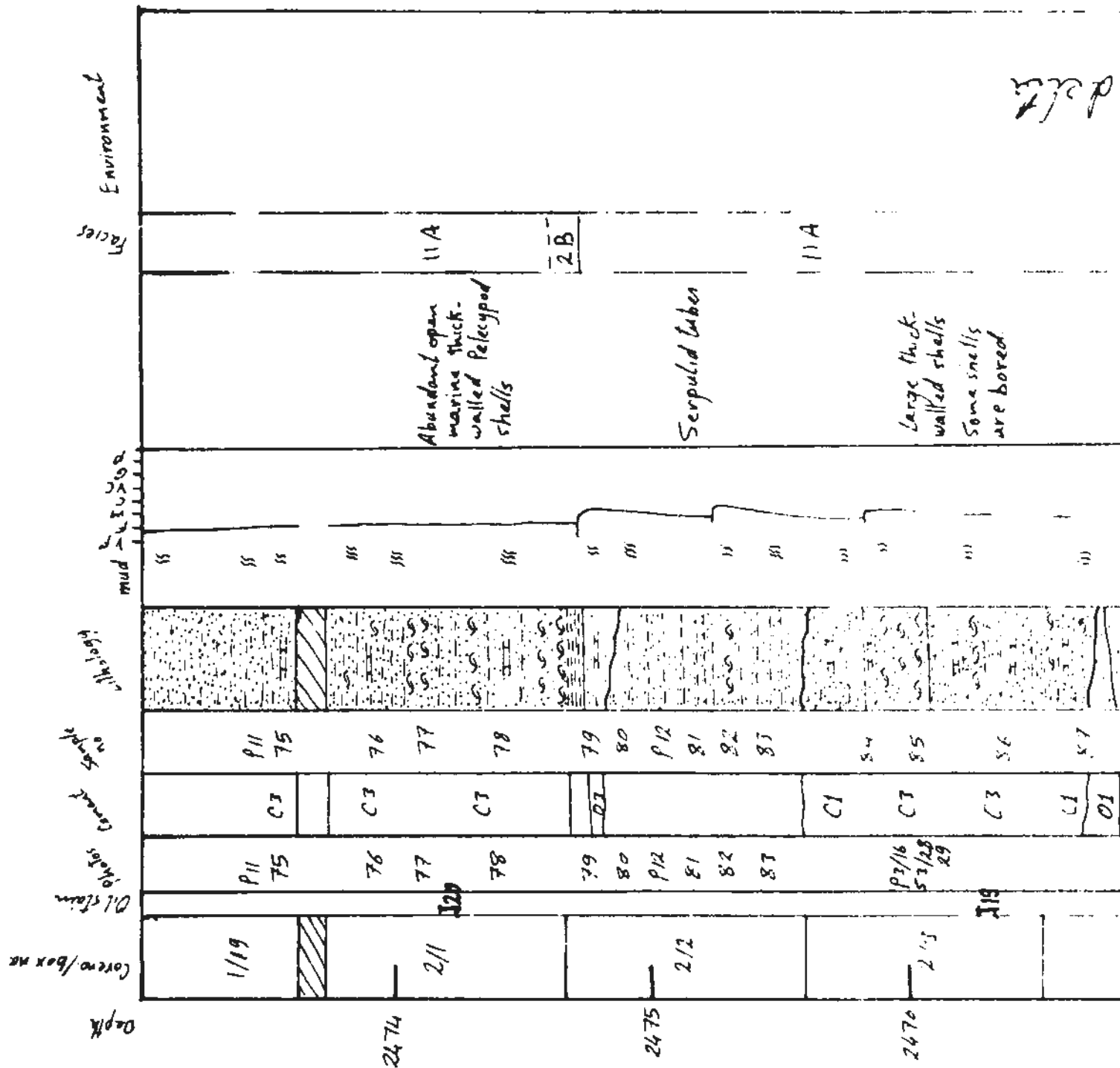
Faulting and fractured shells

Serpentine tubes

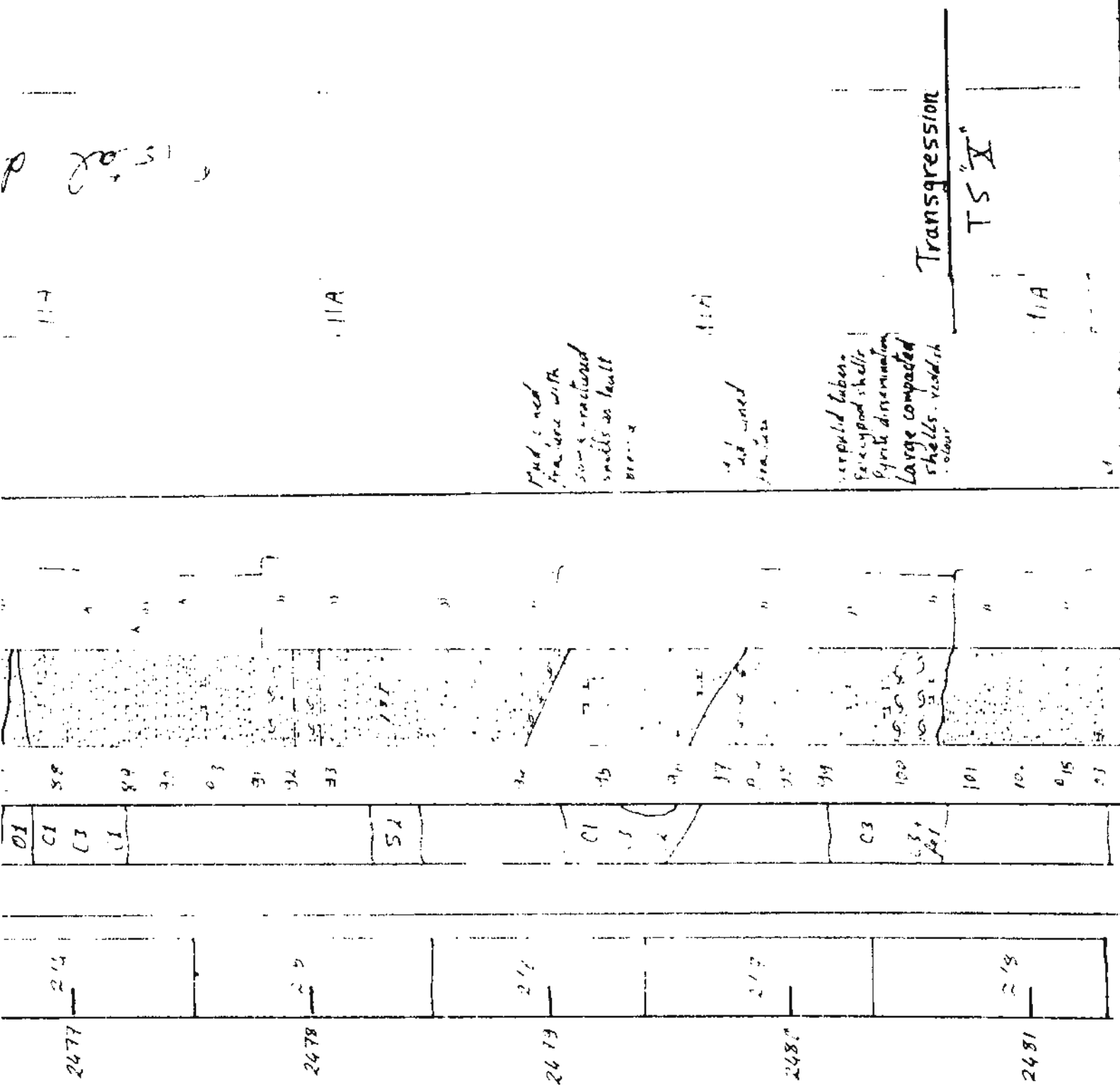
Si. Keen-sided fracture with large shells

Serpentine tubes

2/9



delta



15' 2" d

117

11A

117

11A

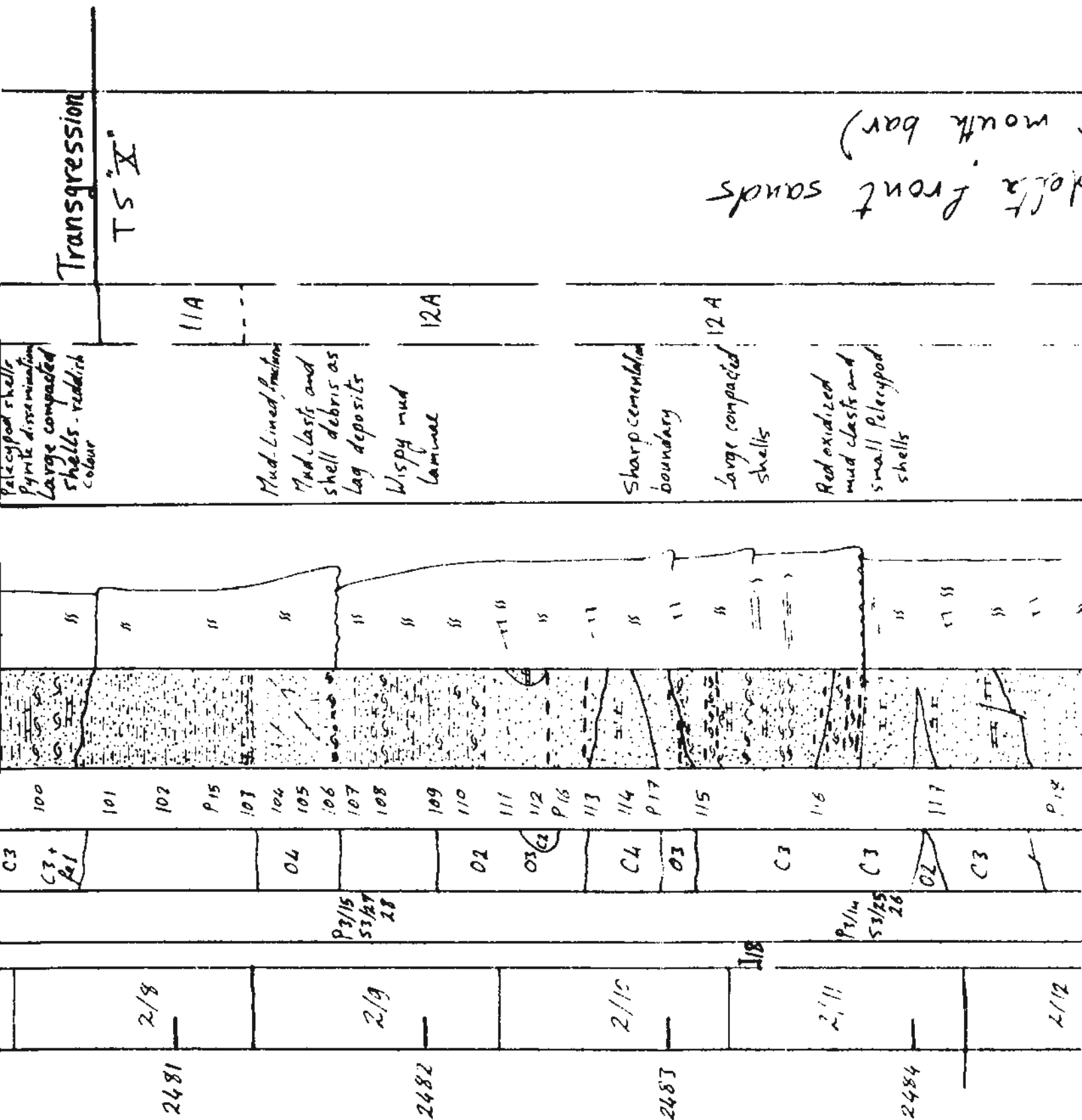
Mud & sand
fracture with
some fractured
shells on fault
surface

Mud & sand
fracture

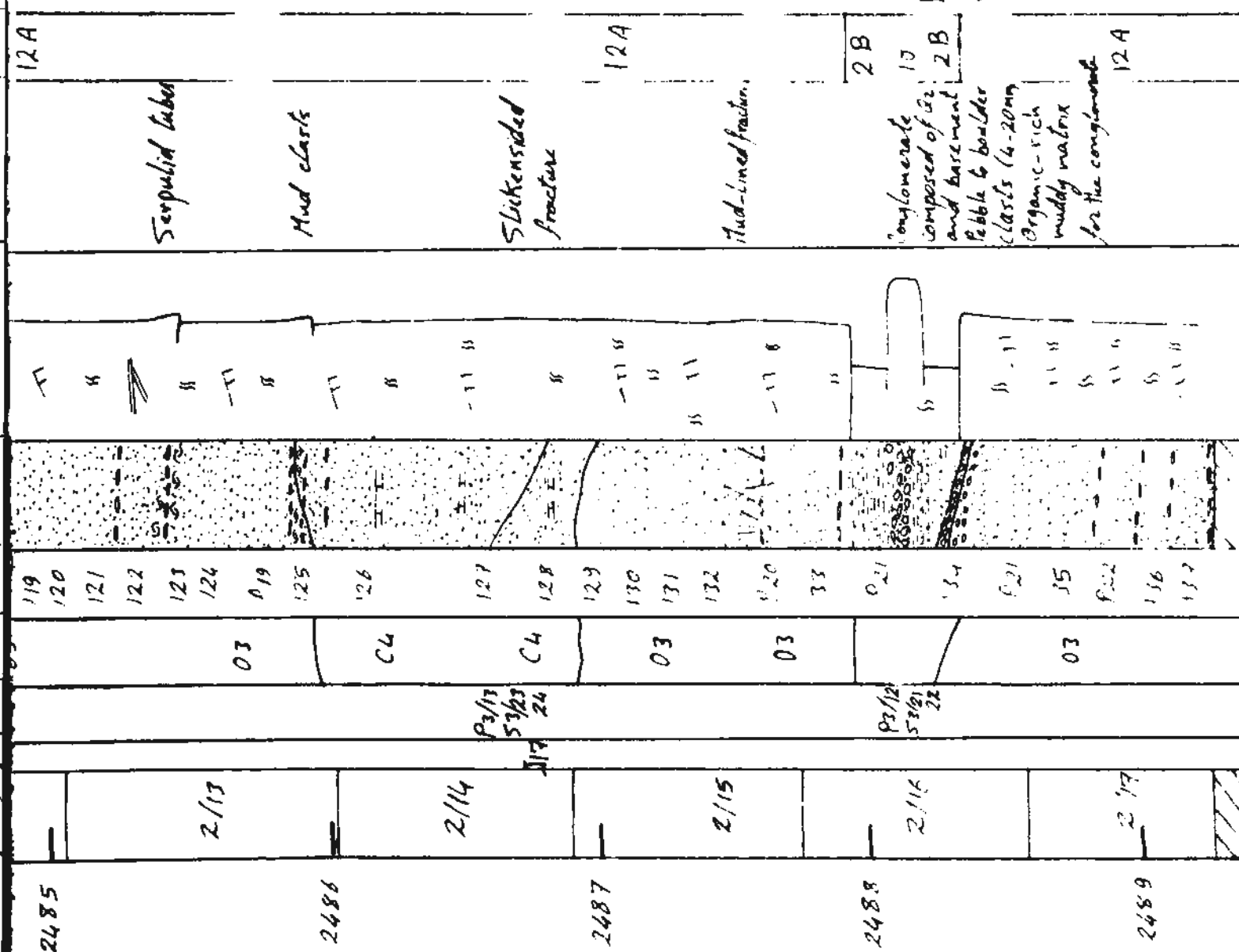
verruillid tubes
large compact
shells - veruillid
shells - veruillid

Transgression

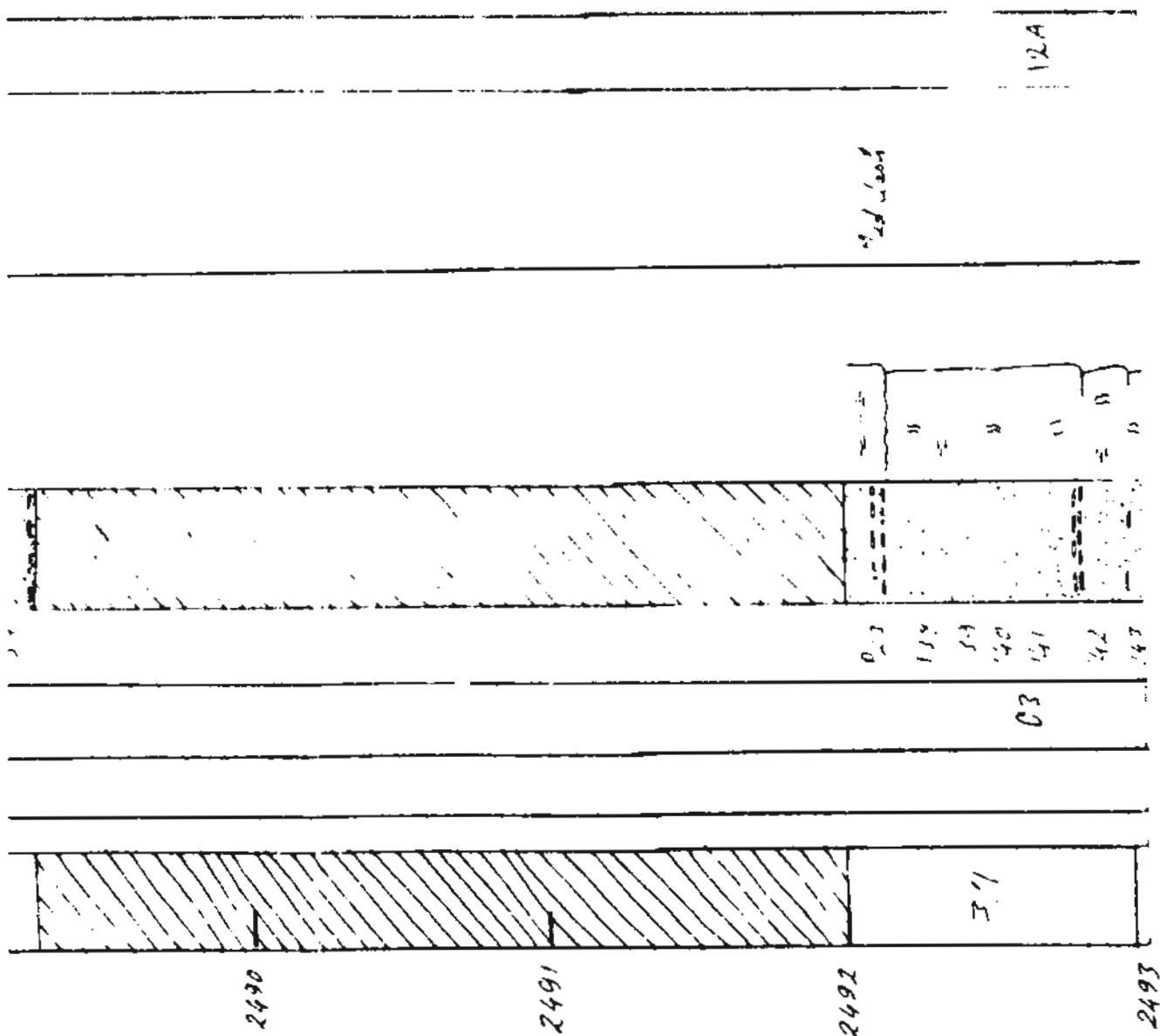
TS "X"



Proximal (R)

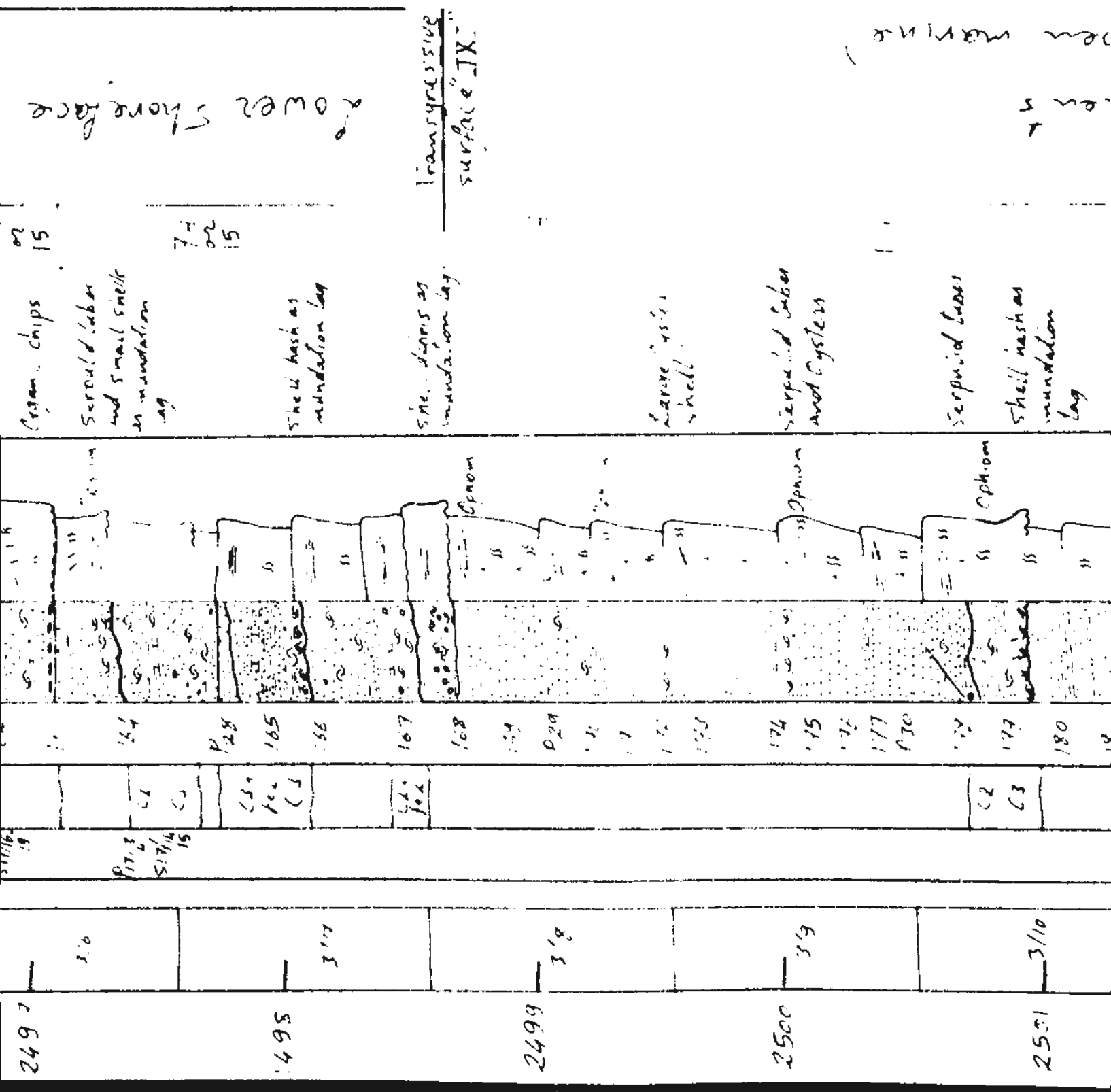


Proximal delta front sands (River mouth bar)

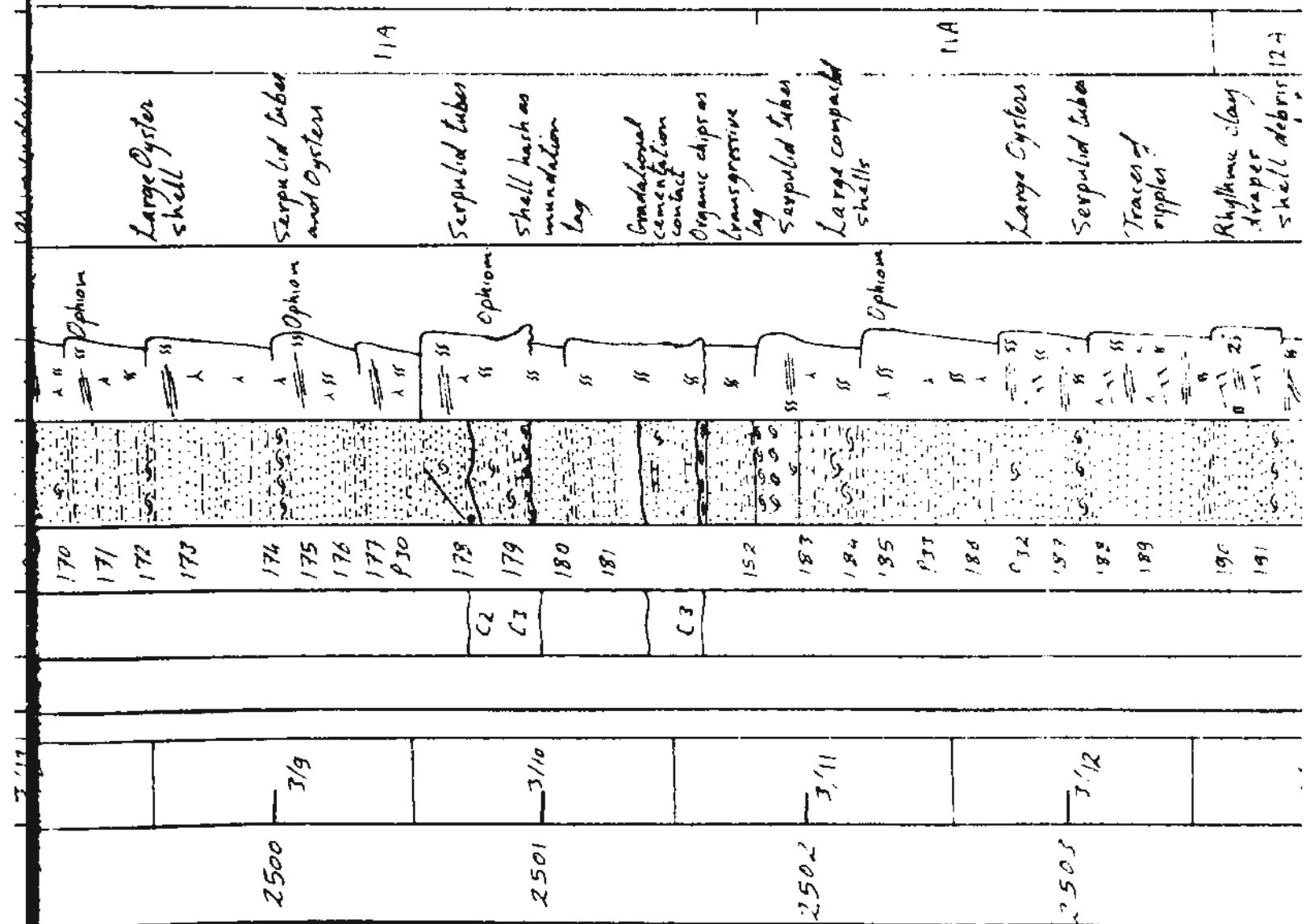


3/9

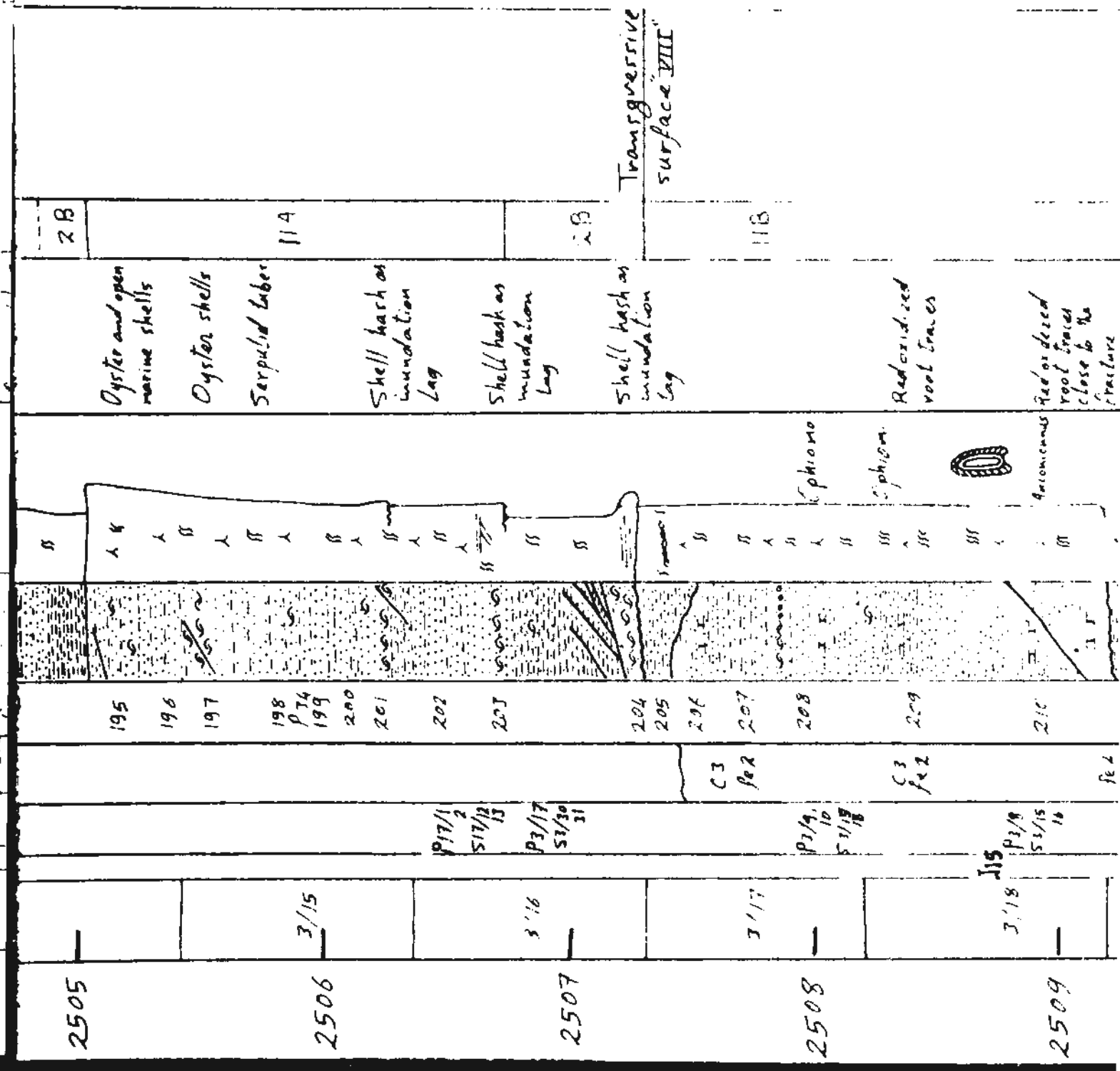
| Core no./
Box no. | Photo | Photo | Lithology | Sedimentary
Structure | Remarks | Facies | Environment |
|----------------------|-------|--------------------|---|--------------------------|--|--------|---|
| 2493 | 3/2 | | 144
145
P24
146
147
148
149
150
P25
151
152
153
154
155
156
026
157
027
158
159
160 | | Leached shells
Clay drapes
Mud clasts | 12A | Proximal delta front Sands
(River mouth bar) |
| 2494 | 3/3 | P214
5/19
20 | | | 3.5 cm thin sand
sels with basal
erosional bands
red
Mud chips | 12A | |
| 2495 | 3/4 | | | | | | |
| 2496 | 3/5 | P177
5/14
21 | | | Snail burrow
scoured tubes
and wood | 12A | |

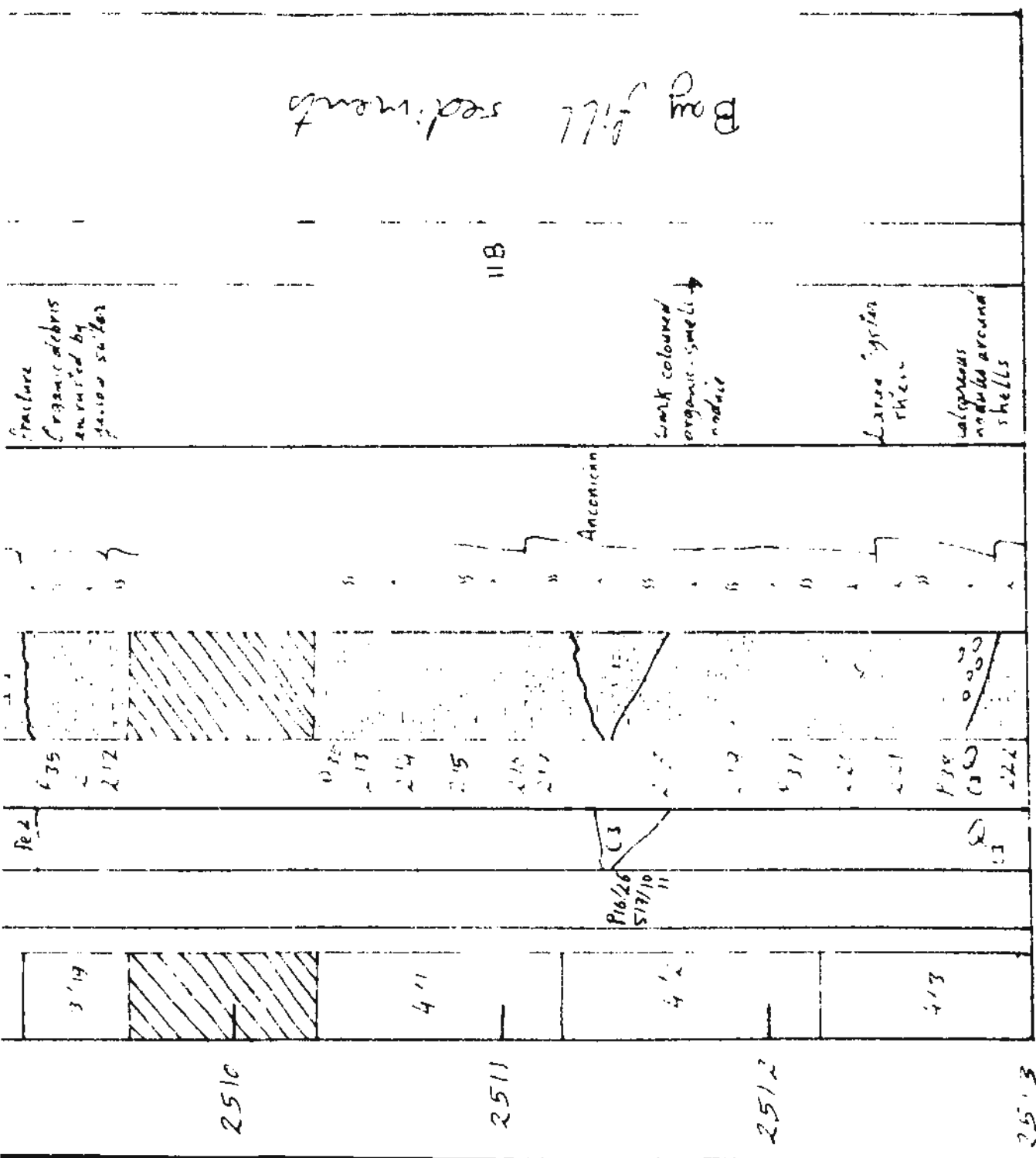


Lagoon or bay sediments (Transitional to open marine)



| | | | | | | |
|------|------|---|-----|--|-------------------------------------|------|
| 2504 | 3/13 | | 191 | | Draper shell debris as mudation lag | 12.4 |
| 2505 | 3/14 | — | 192 | | Shell hash | 2.8 |
| | | | 193 | | Oyster and open marine shells | |
| | | | 194 | | Oyster shells | |
| | | | 195 | | Serpentid tube | |
| | | | 196 | | Shell hash as mudation lag | |
| 2506 | 3/15 | — | 197 | | Shell hash as mudation lag | 2.5 |
| | | | 198 | | Shell hash as mudation lag | |
| | | | 199 | | Shell hash as mudation lag | |
| | | | 200 | | Shell hash as mudation lag | |
| | | | 201 | | Shell hash as mudation lag | |
| 2507 | 3/16 | — | 202 | | Shell hash as mudation lag | 1.8 |
| | | | 203 | | Shell hash as mudation lag | |
| | | | 204 | | Shell hash as mudation lag | |
| | | | 205 | | Shell hash as mudation lag | |
| | | | 206 | | Shell hash as mudation lag | |
| 2508 | 3/17 | — | 207 | | Shell hash as mudation lag | 1.3 |
| | | | 208 | | Shell hash as mudation lag | |
| | | | 209 | | Shell hash as mudation lag | |
| | | | 210 | | Shell hash as mudation lag | |
| | | | 211 | | Shell hash as mudation lag | |





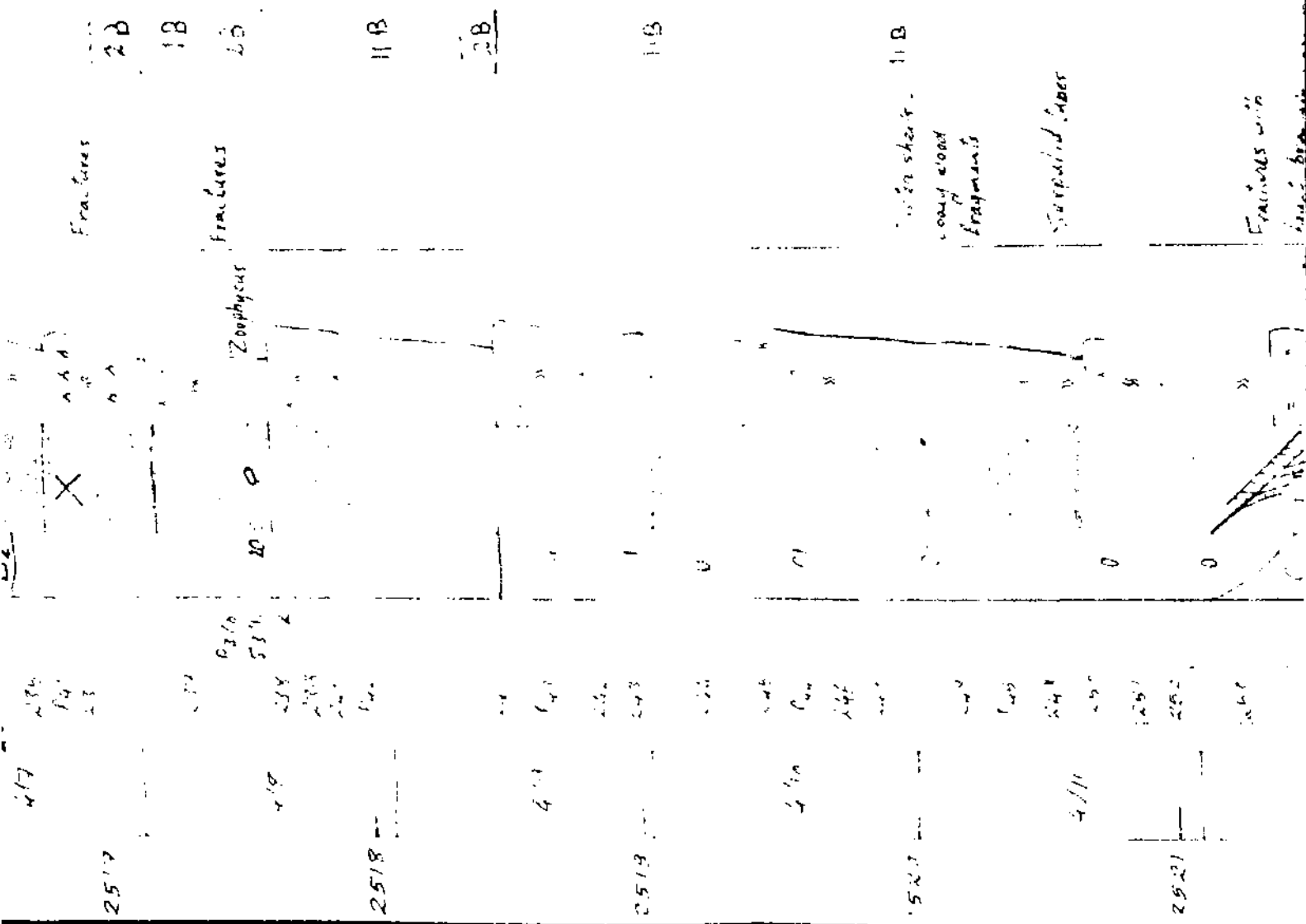
4/9

Bay fill sediments

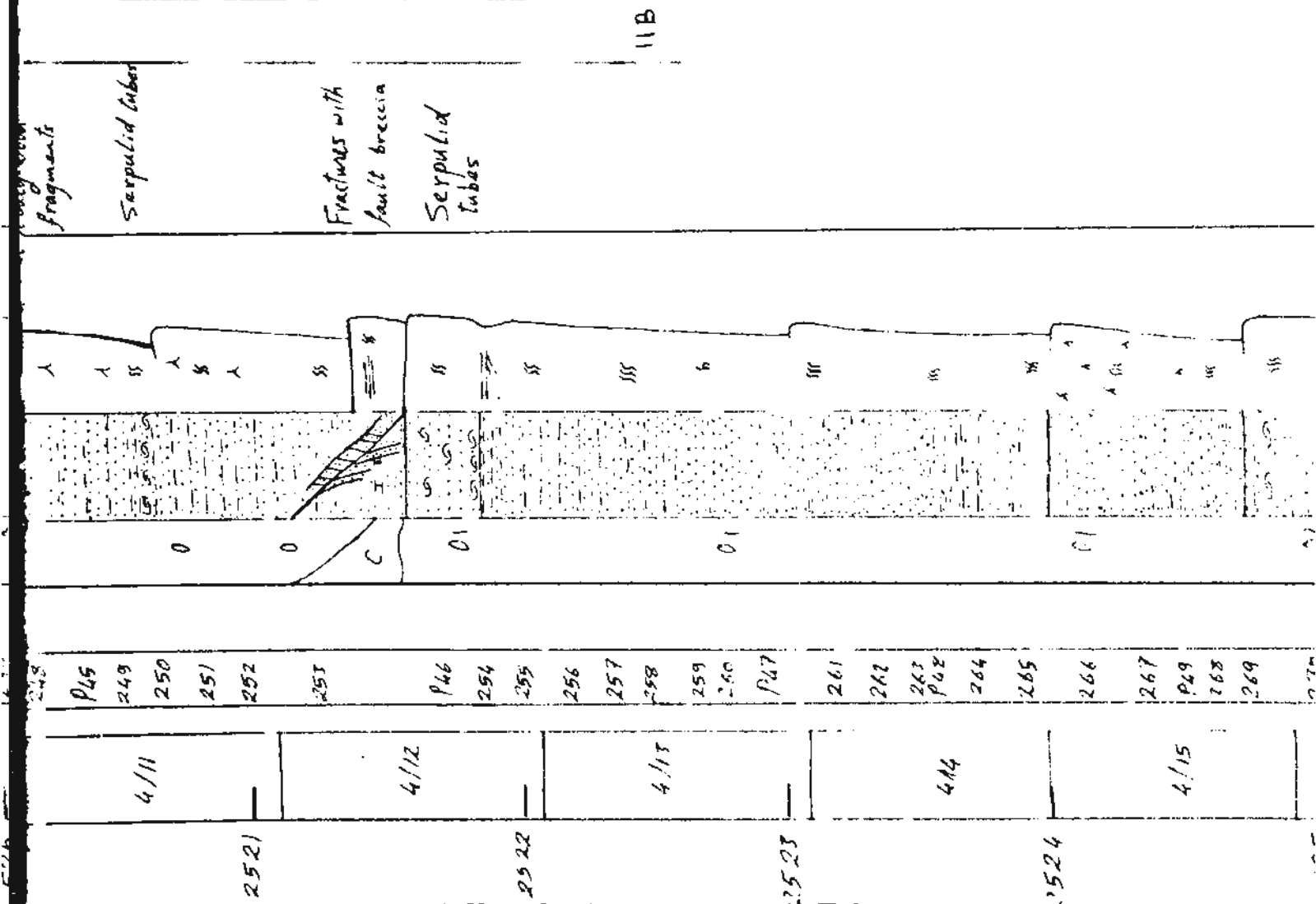
| Core no/
Box no | Sample
no | Photos
P1/P2 | Seal
+
Seal | Oil shows | Lithology | Sed structures | Remarks | Facies | Environment |
|--------------------|--------------|-----------------|-------------------|-----------|-----------|----------------|---|--------|-------------|
| 2513 | | | | | | | | | |
| | 227 | | | 0 | | | calcareous sandstone clasts | 11B | |
| | 224 | P1/P2 | | 0 | | | Siderite breccia composed of rounded clasts | | |
| | 225 | S2/P3 | | 0 | | | | | |
| | 226 | | | 0 | | | | | |
| 2514 | | | | | | | | | |
| | 227 | | | 0 | | | | | |
| | 228 | | | 0 | | | Organic-rich siderite nodule | 2B | |
| | P10 | | | 0 | | | | 2B | |
| 2515 | | | | | | | | | |
| | 229 | | | 0 | | | | 11B | |
| | 230 | | | 0 | | | Fractures with fault breccia | 2B | |
| | P48 | | | | | | | | |
| | 231 | | | | | | | | |
| 2516 | | | | | | | | | |
| | 232 | | | | | | Fractures | 11B | |
| | 233 | | | | | | | | |
| | 234 | | | | | | | | |

J13

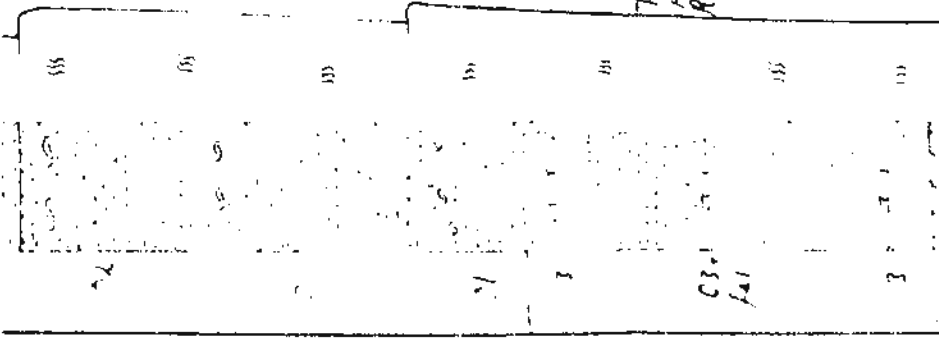
17



(Restricted marine)
(conditions)

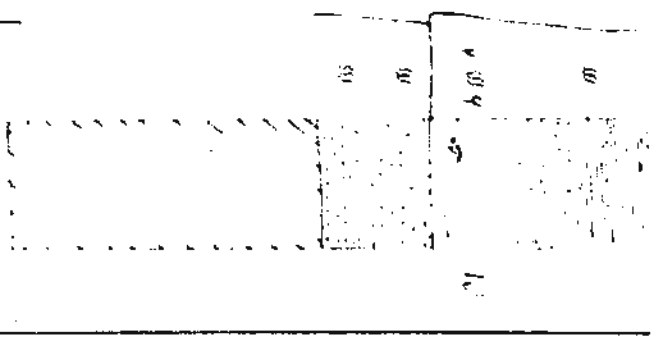


525 — 269
 — 270
 — 271
 4'16" 272
 950
 273
 274
 275
 276
 951
 277
 4'17" 278
 527 — 279
 — 280
 — 281
 — 282
 — 283



11B
 Articulated
 Oyster
 shells
 Long conical
 shells crowded
 with Anconichus
 burrows and
 large pyrite
 Rhynchonella
 crystals
 11B

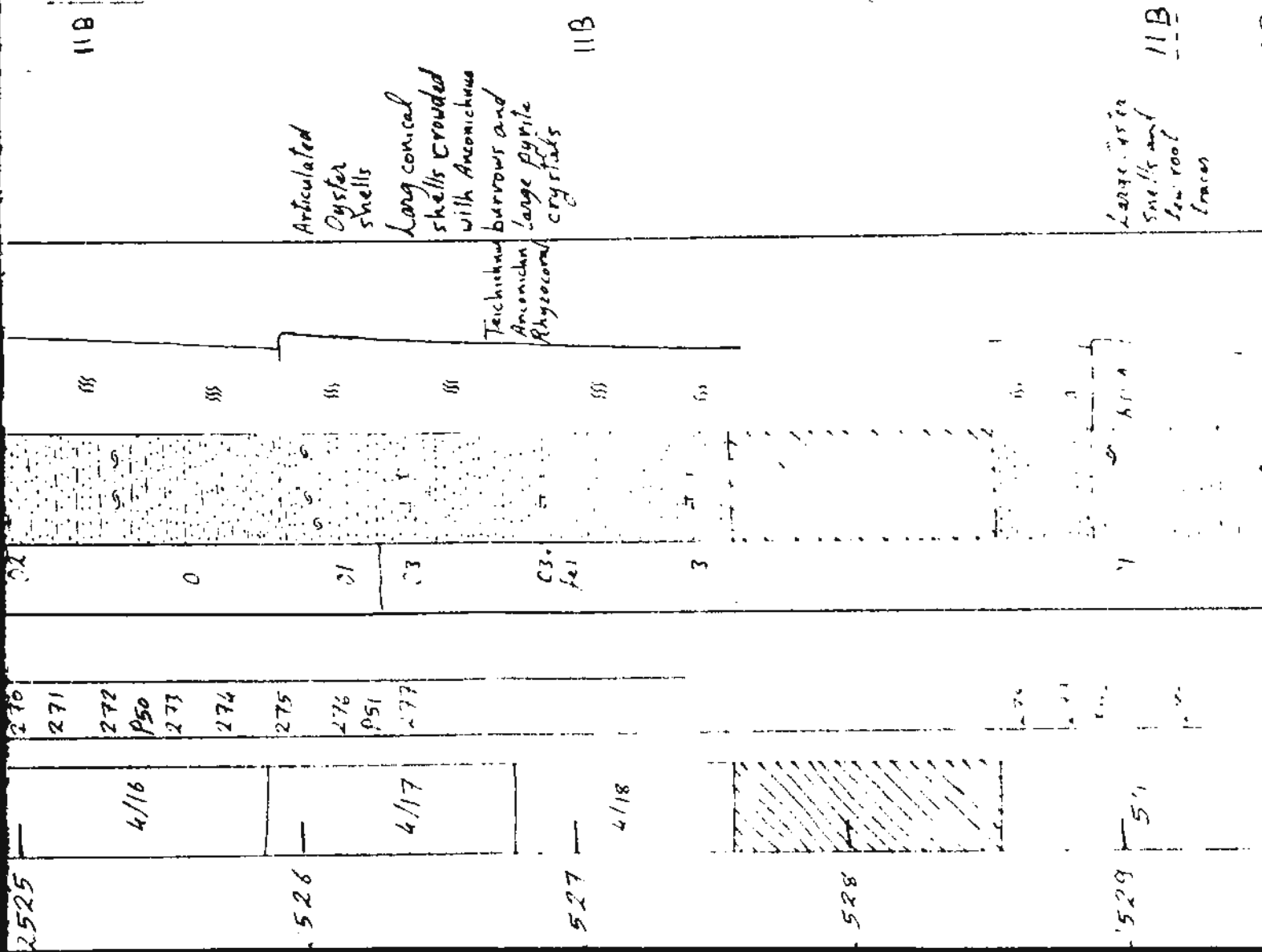
528 — 284
 — 285
 — 286
 — 287
 5'11" 288
 529 — 289
 — 290
 — 291
 — 292



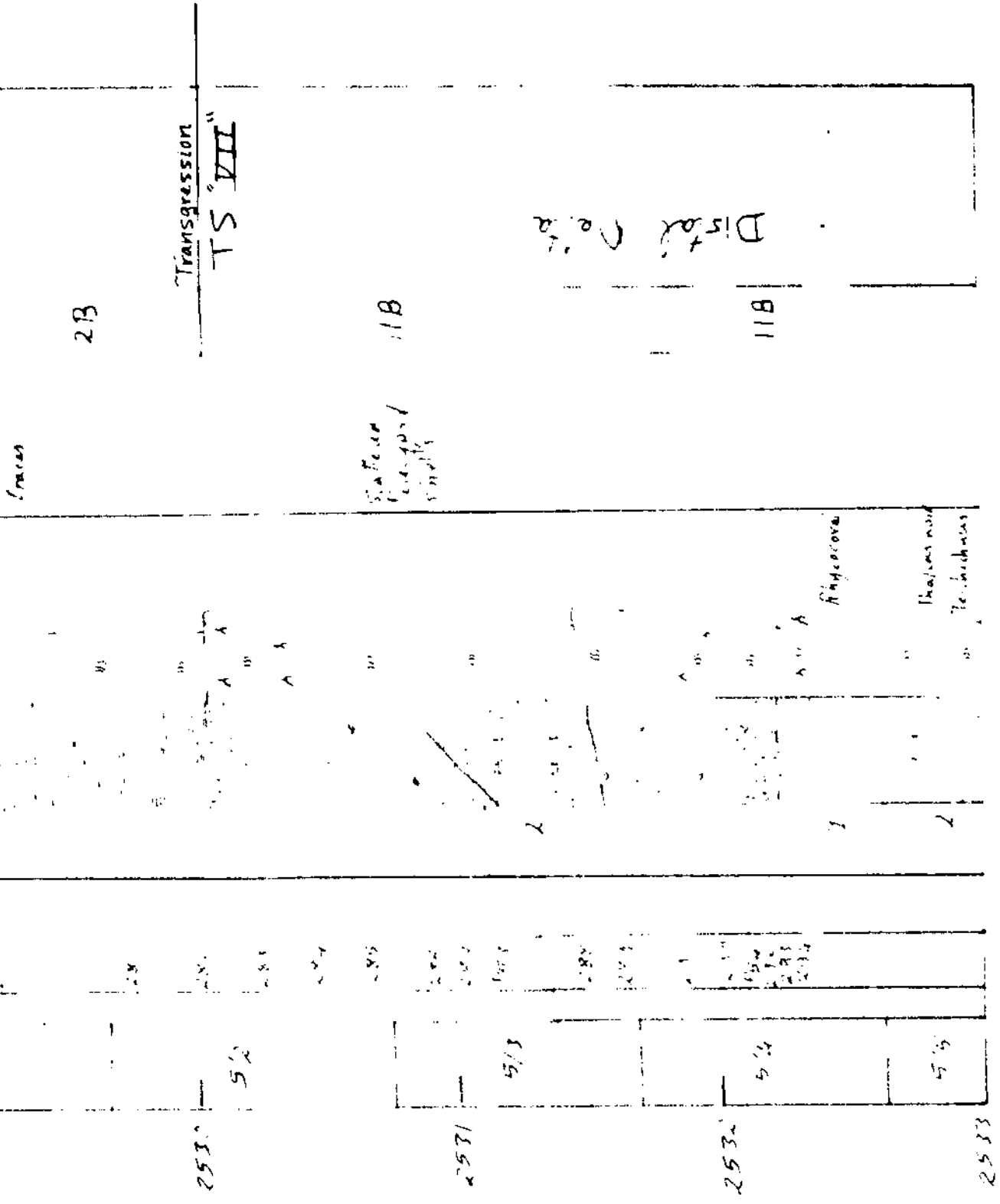
Large pyrite
 shells and
 few root
 traces
 11B

Bay fill sediments

Bay Pill sediments



train



2B

11B

5/9

| Core no/
Box no | Photos
2 | Oil show
Cement | Lithology | Sed structure
and
USDA | Remarks | Facies | Environment |
|--------------------|-------------|--------------------|----------------------|------------------------------|--|--------|-------------------|
| 2533 | 5/5 | 112 | C3
P3.4
S39.10 | SSS | Scattered
Pelecypod shells
divers trace
fossils | 11A | Distal Delta |
| | | | C3 | SSS | | | |
| | | | P3.4
S37.8 | SSS | | | |
| | | | P55 | SSS | | | |
| | | | 295 | SSS | | | |
| | | | 296 | SSS | | | |
| | | | 297 | SSS | | | |
| | | | 298 | SSS | | | |
| | | | 299 | SSS | | | |
| | | | 300 | SSS | | | |
| 2534 | 5/6 | | P56
301H
301HP | SSS | Large thick-
valled articulated
Pelecypod shells | 11B | |
| | | | 702 | SSS | | | |
| | | | 303 | SSS | | | |
| | | | 304 | SSS | | | |
| | | | 305 | SSS | | | |
| | | | P57 | SSS | | | |
| | | | 306 | SSS | | | |
| 2535 | 5/7 | | | SSS | Pelecypod shells +
serpented tubes | 11A | Distal Delta |
| | | | | SSS | | | |
| 2536 | 5/8 | | | SSS | mult contact | 28 | Distal Delta |
| | | | | SSS | | | Scattered Pelwood |

rugged
brown f's

2537

5'3

309

250

310

2538

5'10

XII

2539

5'11

312

453

313

314

450

315

2540

5'12

316

317

318

319

460

2541

5'13

320

114

Scattered
Pelecypod shells

2B

114

23

Transgressive
surface "VI"

11A

Khondriks
Rhynch

Ammonia

Ammonia
(Khondriks)

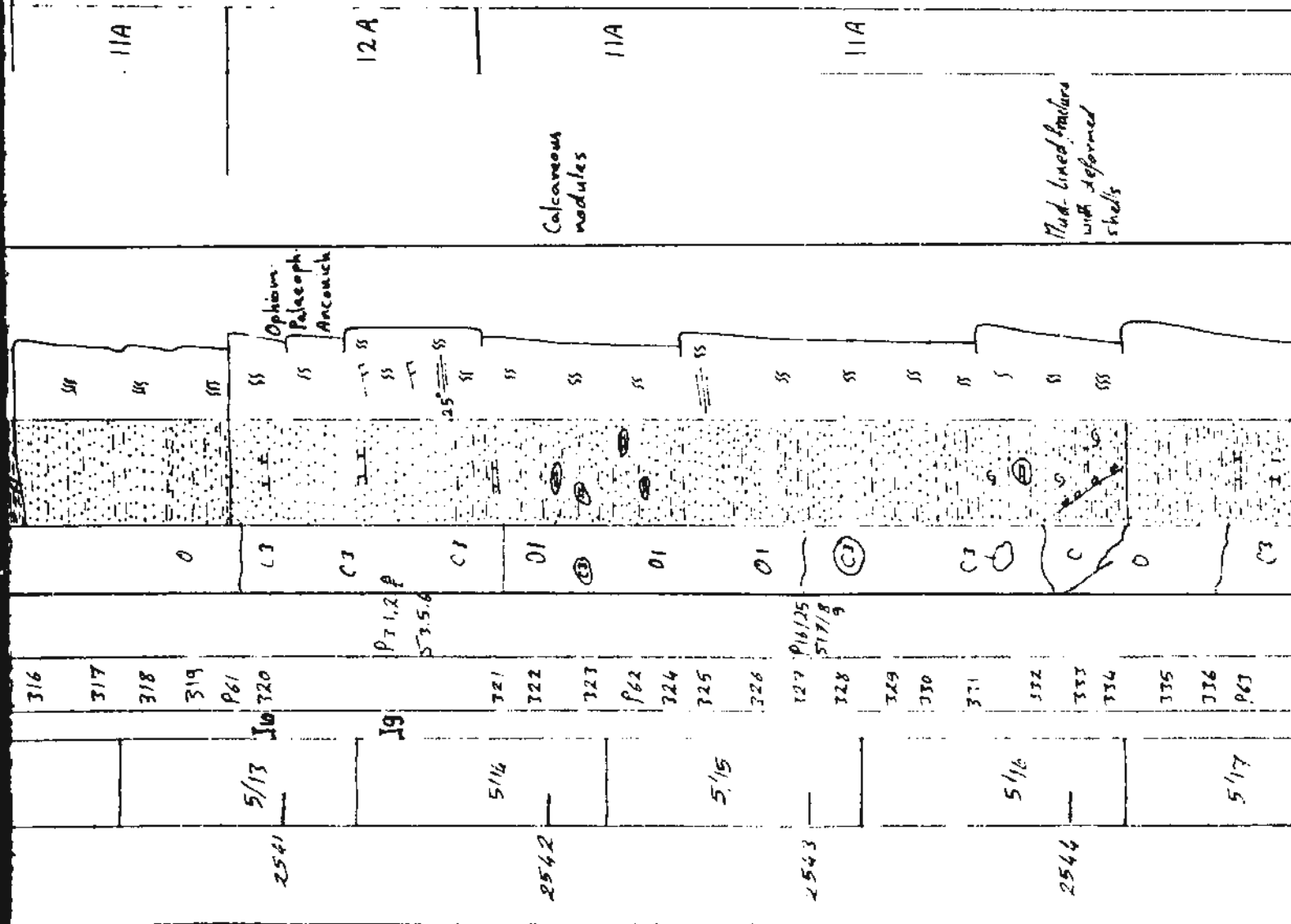
Ammonia
Rhynch

Tachina

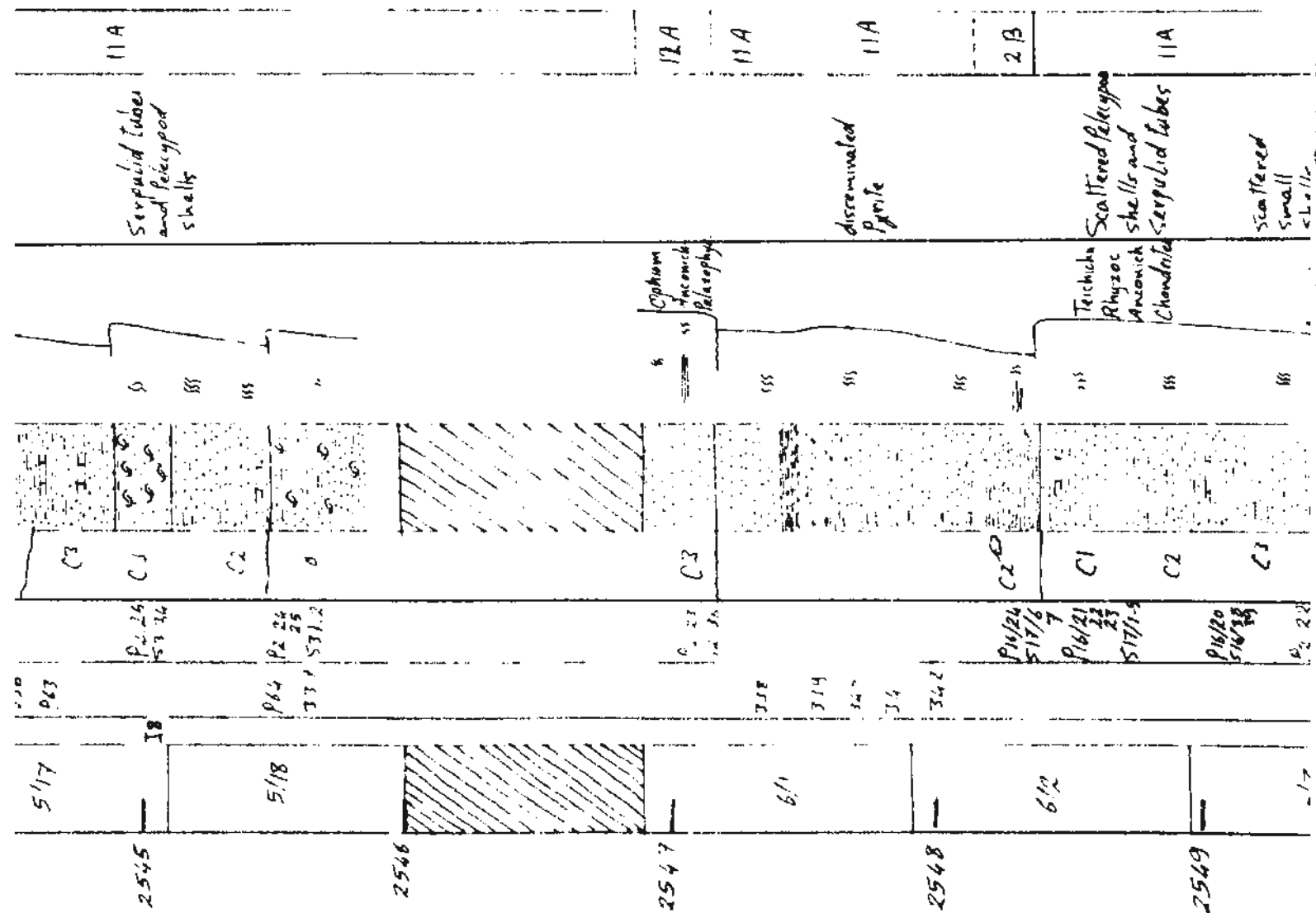
Khondriks

Optima
Palaeoph
Ammonia

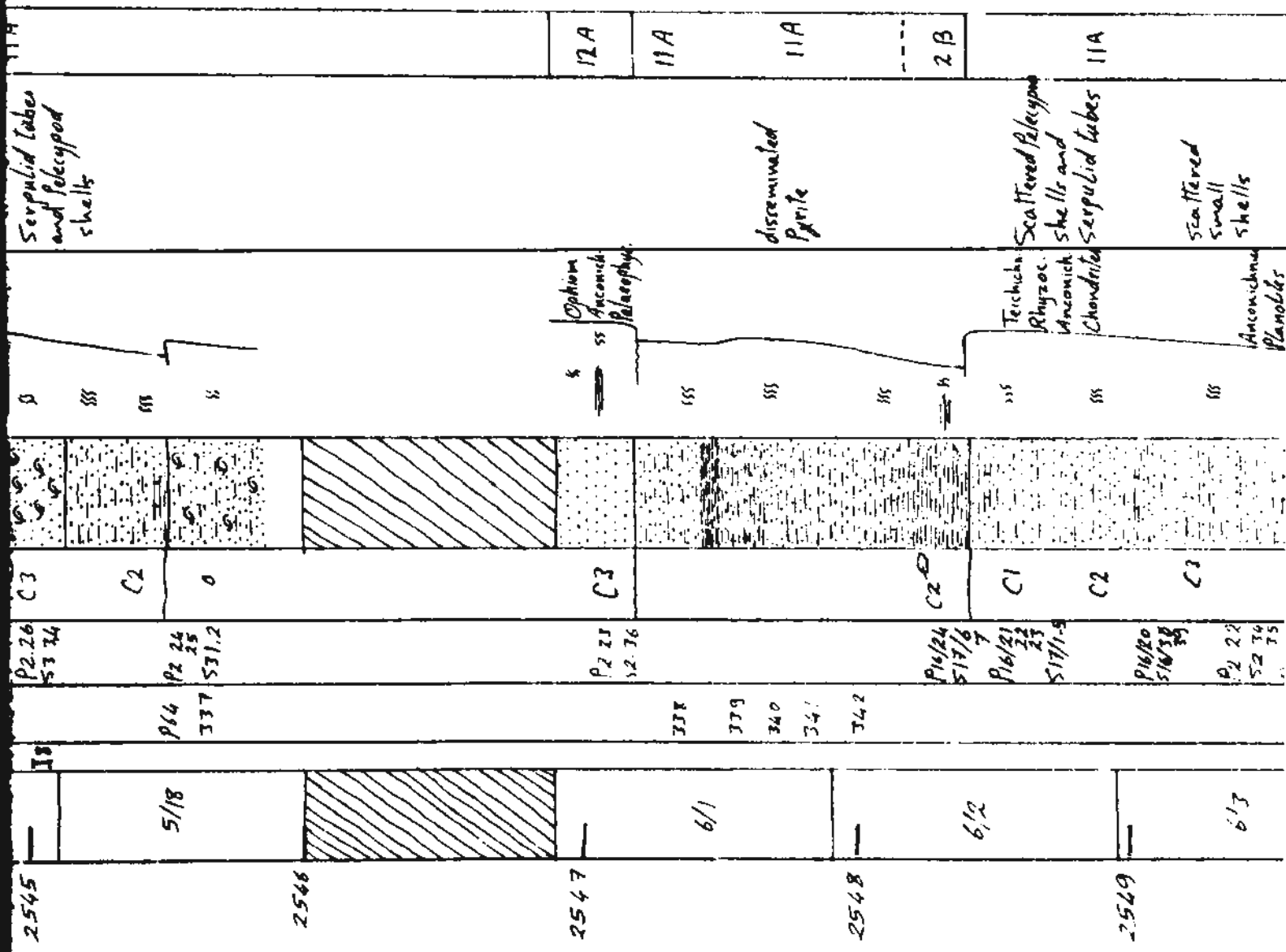
surface 'VI'

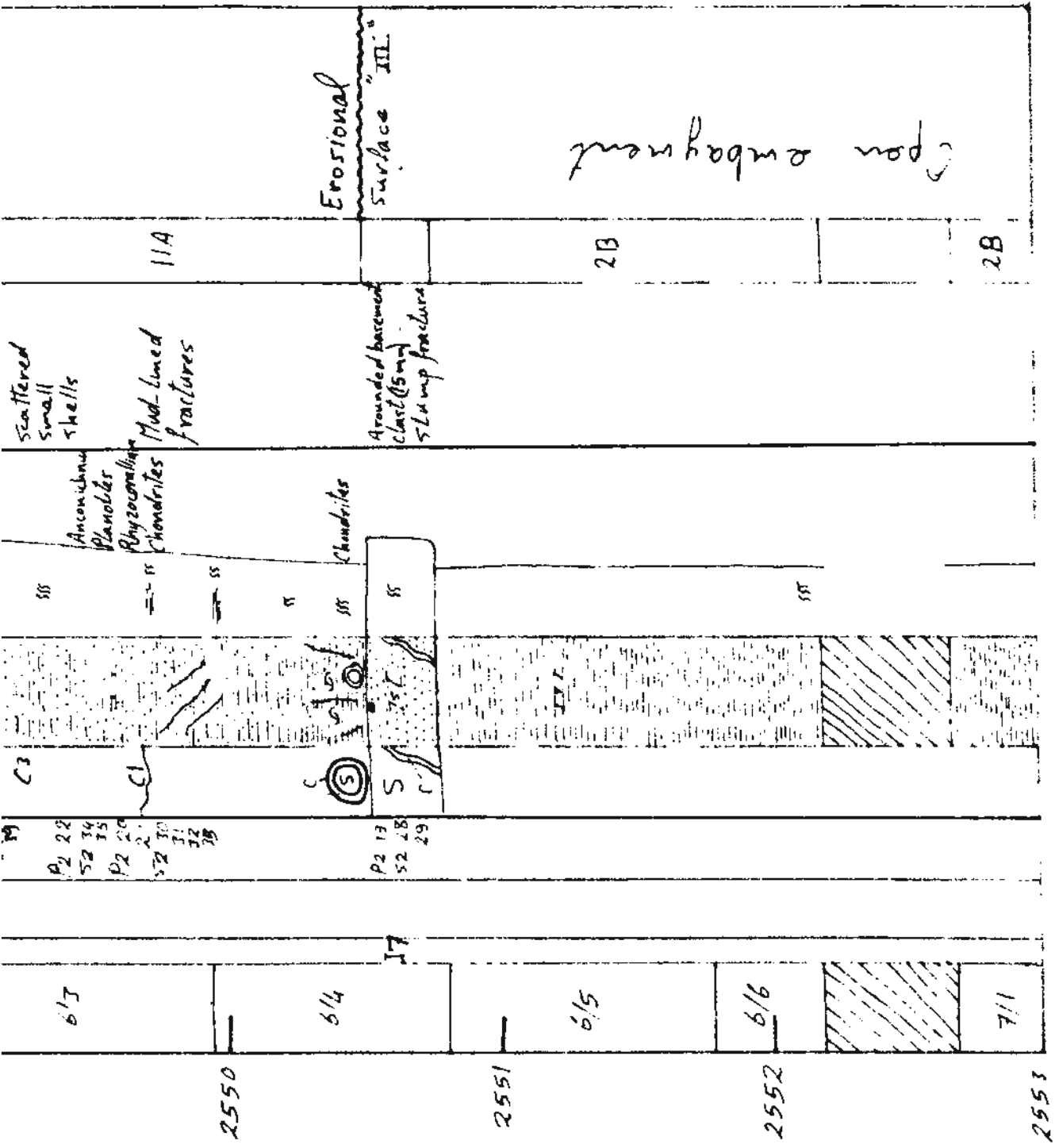


Distal Delta



Distal Delta





2B Storm
bed

Storm
13B bed

Storm
13B bed

2B

13B



P16/19
576/36
377

344

345

346

8 1/2

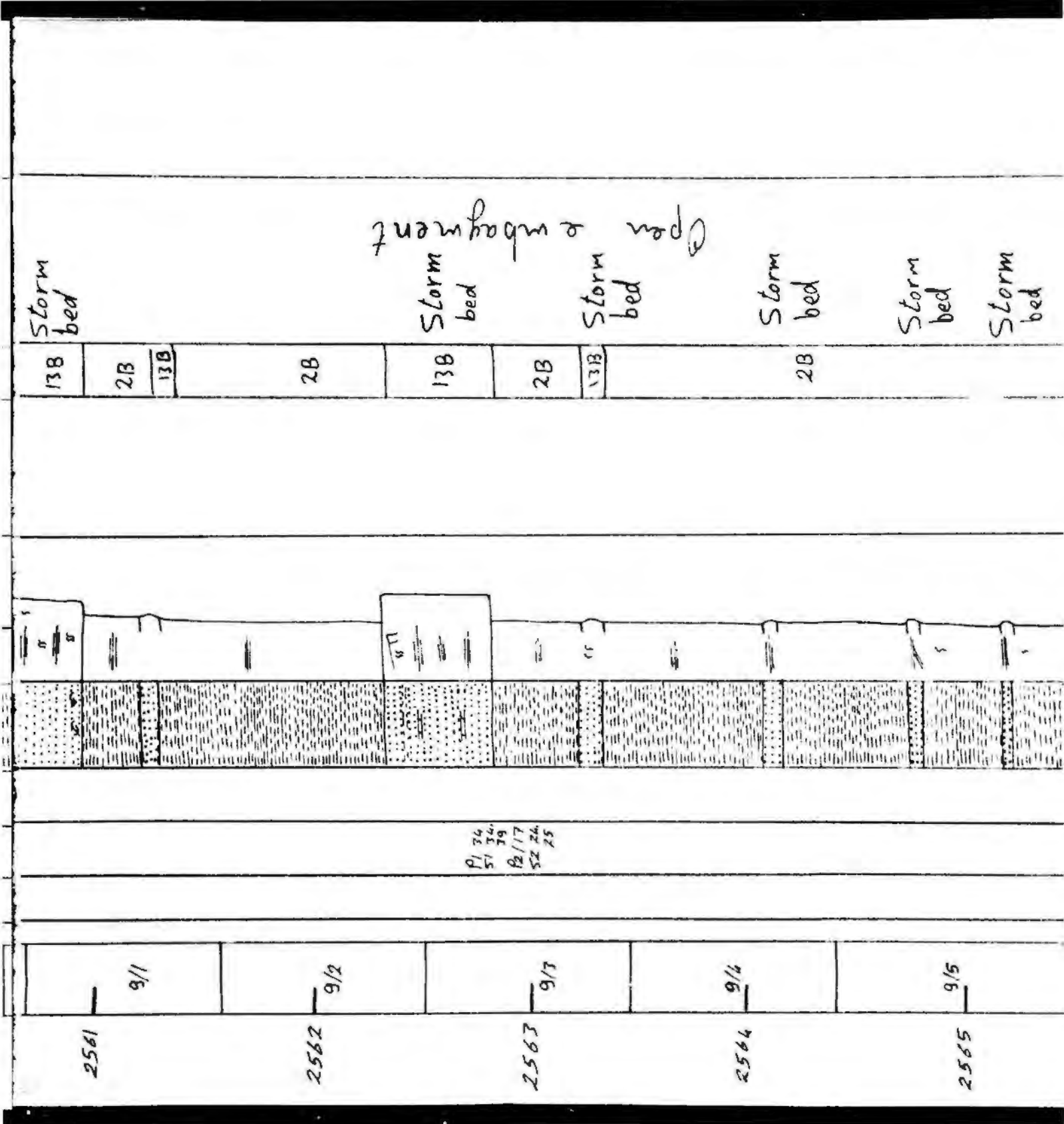
8 1/3

9 1/1

2559

2560

2561



The diagram illustrates a geological column with the following components:

- Stratigraphic Units (Left):**
 - 2B
 - 11B
 - 2B
 - 11B
 - 2B
 - 11B
 - 2B
 - 11B
- Fossil Ranges (Middle):**
 - S2, S3, S4
 - P1, P2, P3, P4, P5, P6, P7, P8, P9, P10, P11, P12, P13, P14, P15, P16, P17, P18, P19, P20, P21, P22, P23, P24, P25, P26, P27, P28, P29, P30, P31, P32, P33, P34, P35, P36, P37, P38, P39, P40, P41, P42, P43, P44, P45, P46, P47, P48, P49, P50, P51, P52, P53, P54, P55, P56, P57, P58, P59, P60, P61, P62, P63, P64, P65, P66, P67, P68, P69, P70, P71, P72, P73, P74, P75, P76, P77, P78, P79, P80, P81, P82, P83, P84, P85, P86, P87, P88, P89, P90, P91, P92, P93, P94, P95, P96, P97, P98, P99, P100
- Lithological Descriptions (Right):**
 - bed
 - Transgressive Surface "V"
 - Smooth walled Paleocypod shells
 - Crinoidal Contact

Transgressive
surface "V"

Smooth walled
Pelecypod shells

Gradational
Contact

bed

Storm
bed

Transgressive
surface 'V'

23

19

23

13

28

Smooth walled
Pelecypod shells

28

—

5/6

9/6

4/6

8/6

9/9

2565

2566

2567

2568

2569

$$\begin{array}{r} 52 \\ 15 \end{array}$$

35

41 33
 51 37

**0
02
9-5**

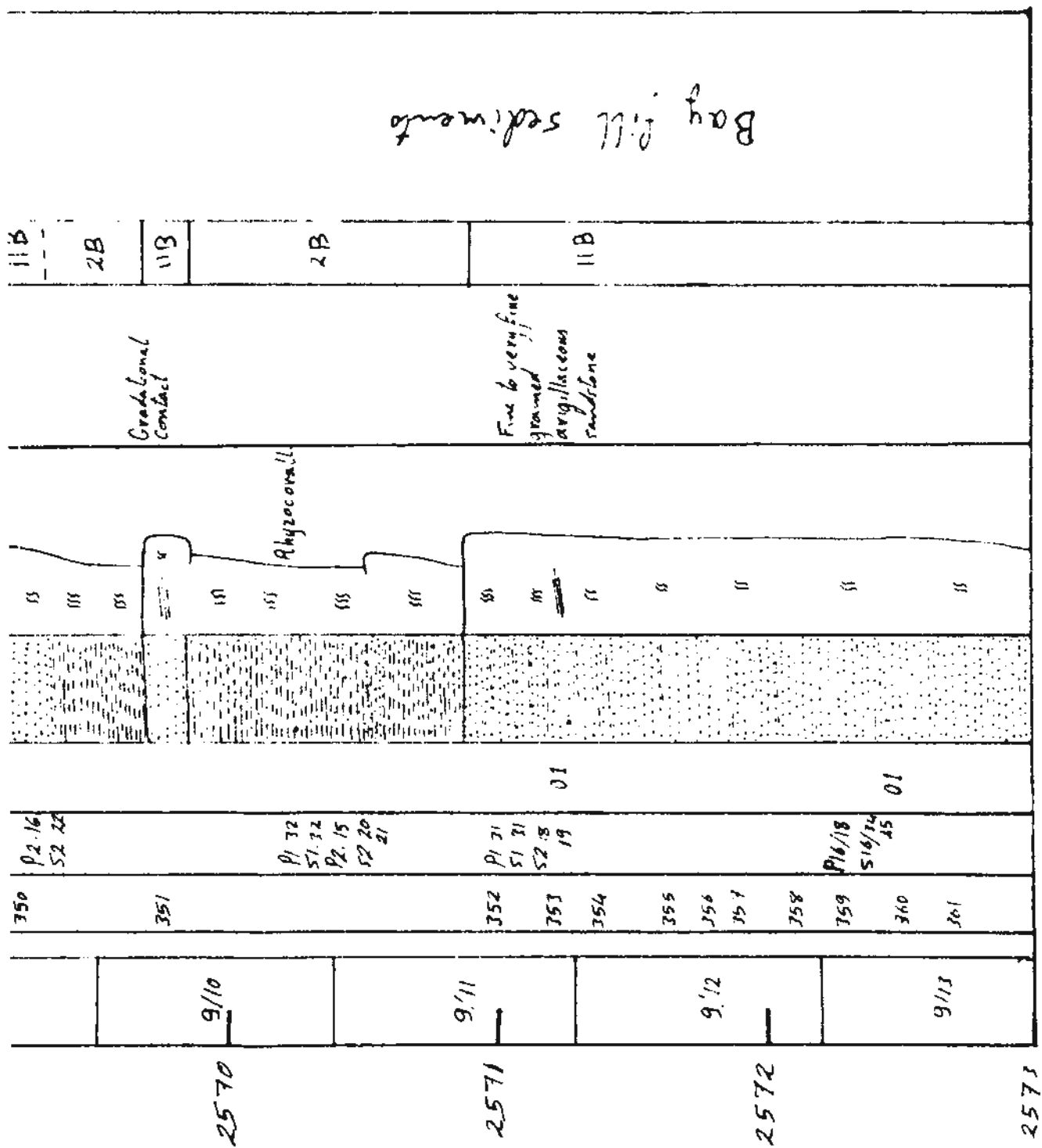
£71

348

549

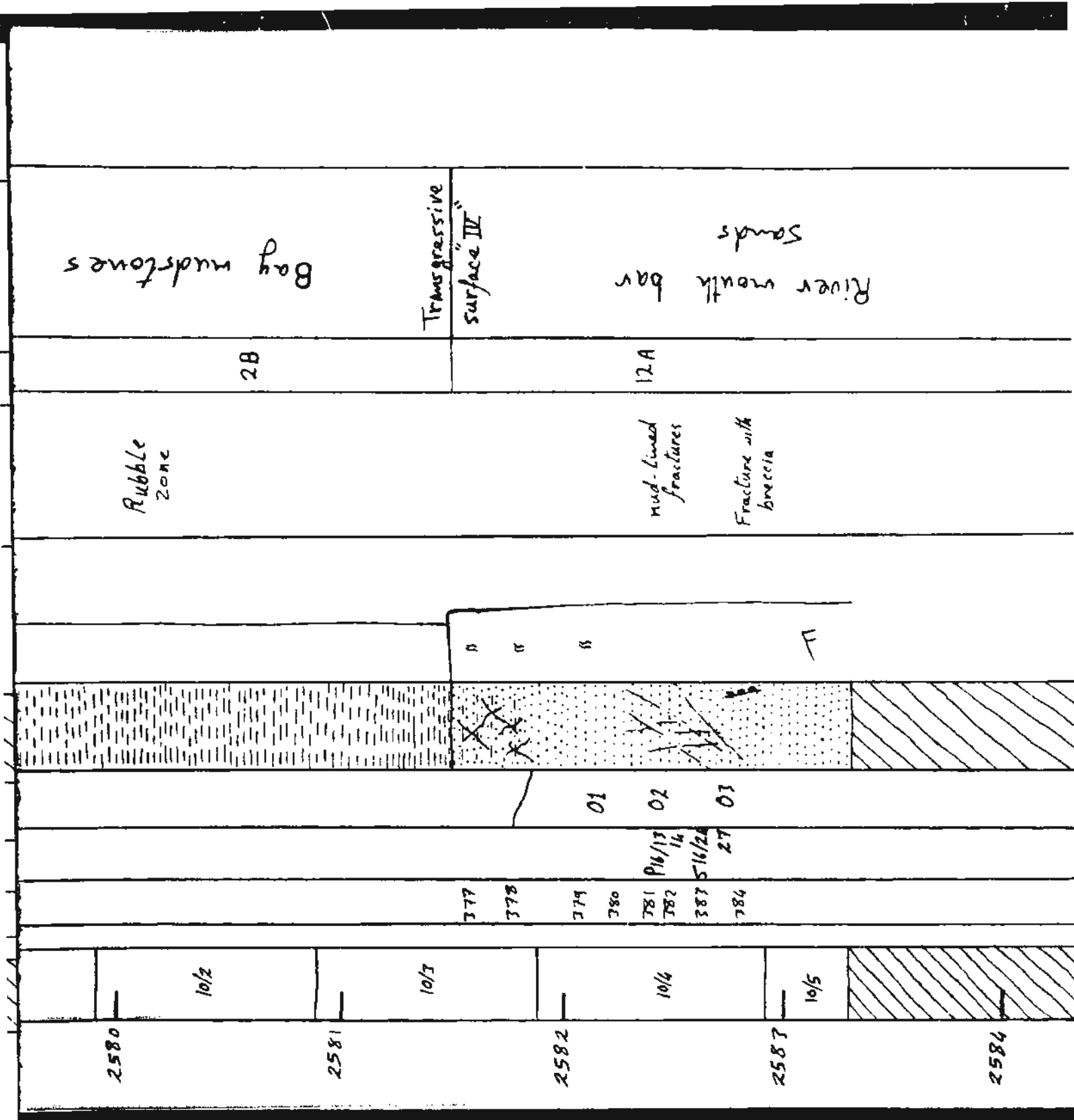
350

52 22
p2-16



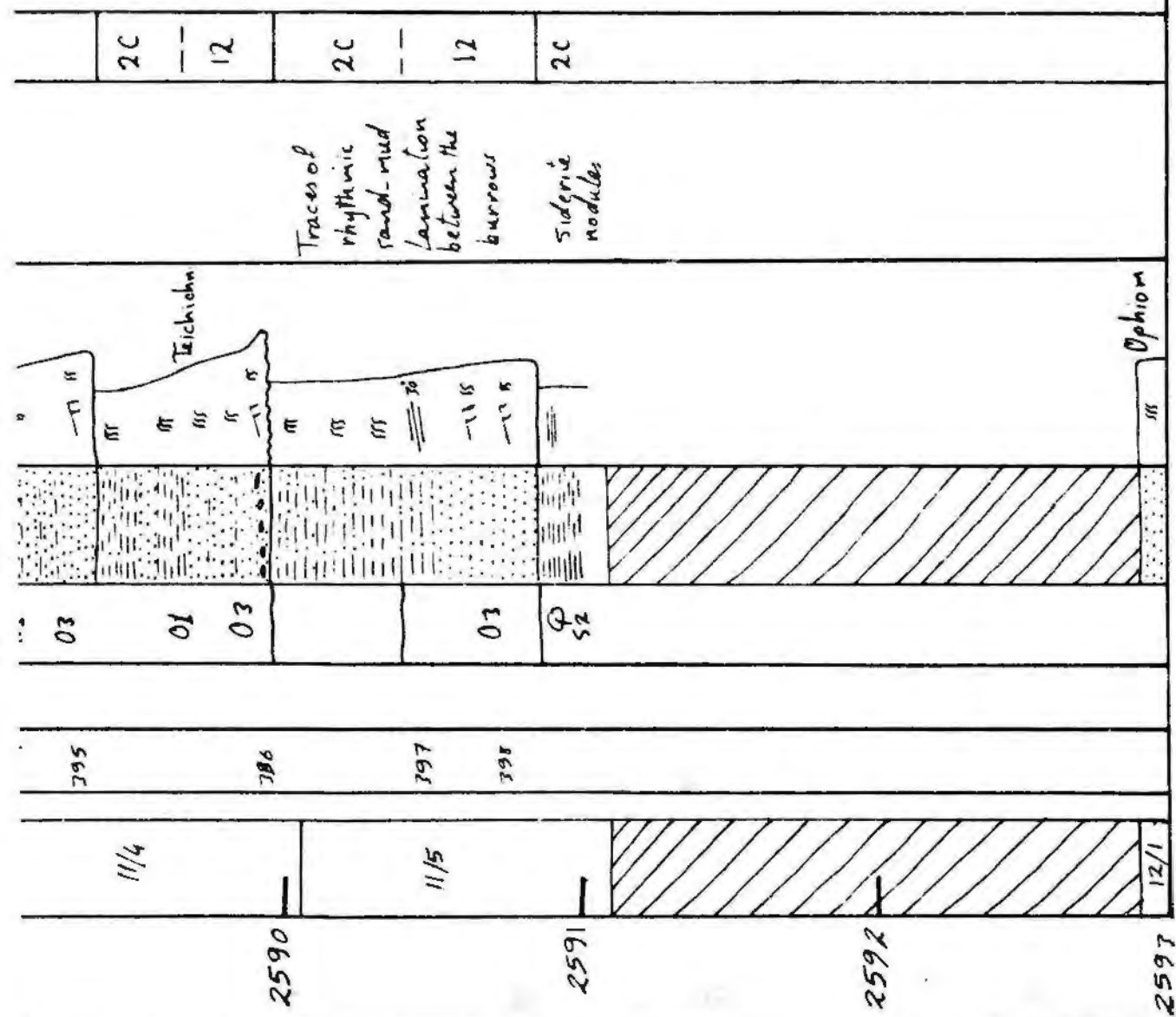
7/9

| Coring/Box no | Sample no. | Photos | Oil stains | Lithology | Sedimenting structures mud & > 500 | Remarks | Facies | Environment |
|---------------|------------|---|------------|-----------|------------------------------------|--------------------------------|--------|-------------------------------|
| 2574 | 9/14 | P51/14
P2/13
52/16
17 | | | ss | | 11B | Restricted bay fill sediments |
| | | P16/17
516/22
33 | | | ss | | 2B | |
| 2575 | 9/15 | 362
363
364
365
366 | 01 | | A ss A
s
ss
ss | | 11B | |
| | 9/16 | 367 | | | ss
Teichodon
Rhyzoc | | | |
| 2576 | 9/17 | P1 29
51 29
P2 10,
11,
12
52 14,
15
368
51 28 | 01 | | ss
Teichodon
ss | Larg convex up
Duster cl.!! | | |



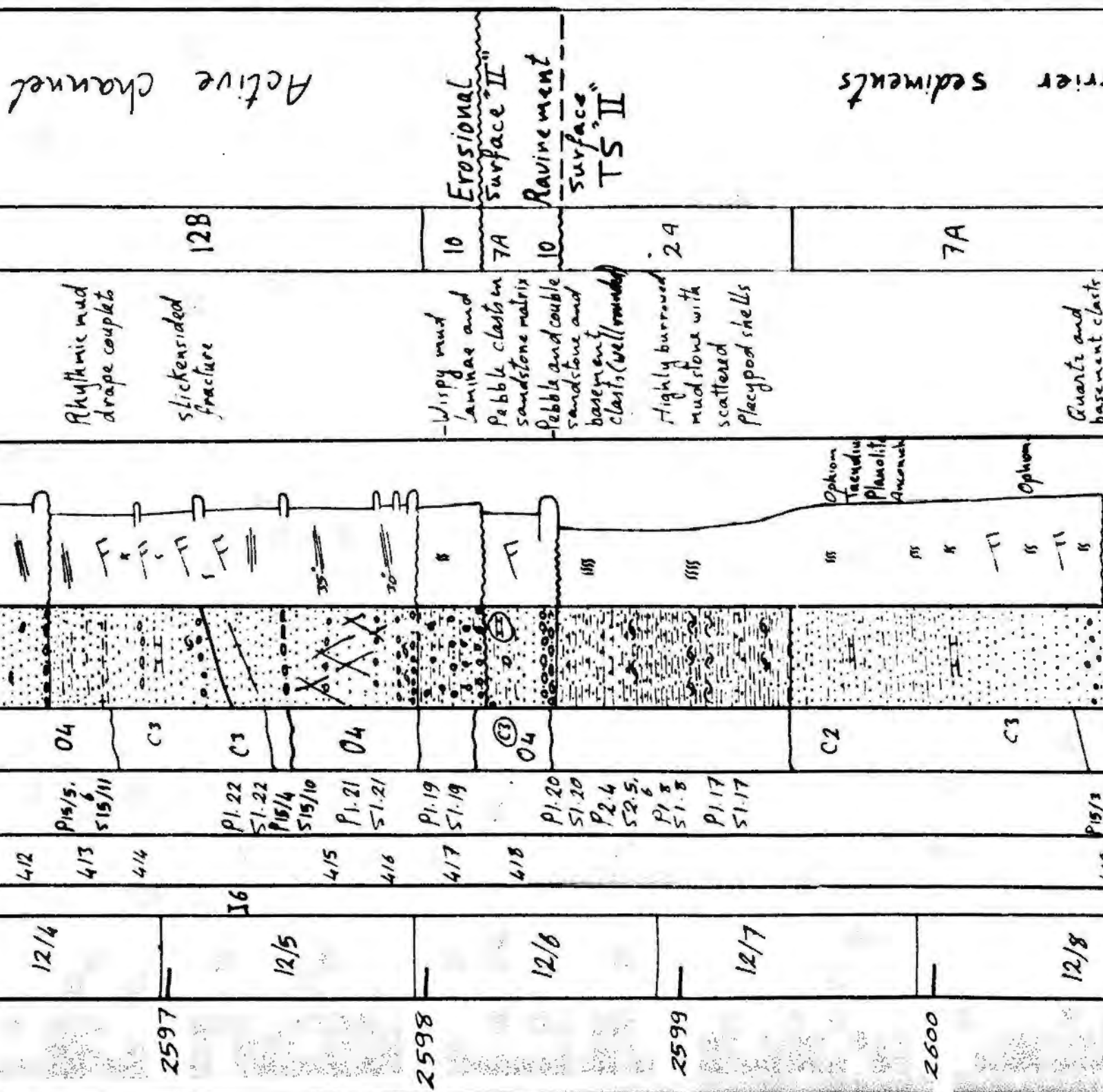
| Core Number | Interval | Depth (m) | Stratigraphic Unit | Notes | Core Number | Interval | Depth (m) | Stratigraphic Unit | Notes |
|-------------|----------|-----------|--------------------|-------|-------------|----------|-----------|--------------------|-------|
| 2585 | 11/1 | 385 | Shale | | 2586 | 11/1 | 385 | Shale | |
| | | 386 | Shale | | | | 386 | Shale | |
| | | 387 | Shale | | | | 387 | Shale | |
| | | 388 | Shale | | | | 388 | Shale | |
| 2587 | 11/2 | 389 | Shale | | 2588 | 11/2 | 389 | Shale | |
| | | 390 | Shale | | | | 390 | Shale | |
| | | 391 | Shale | | | | 391 | Shale | |
| | | 392 | Shale | | | | 392 | Shale | |
| | | 393 | Shale | | | | 393 | Shale | |

Inactive channel fill Point bar sediment



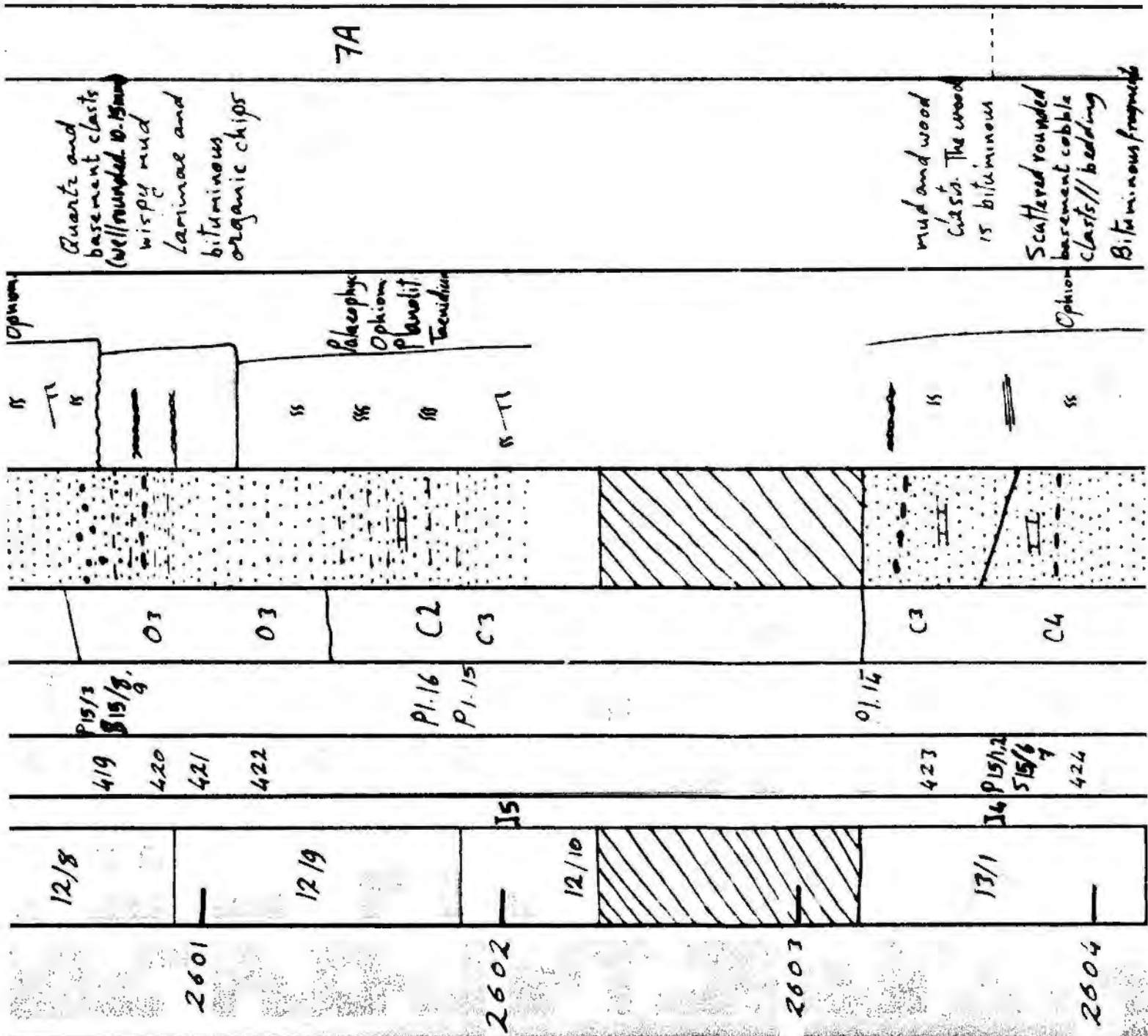
8/9

| Core no.
Box no | Sample
no | Photos | Oil stains
Cement | Lithology | Sedimentary
structures | Remarks | Facies | Environment |
|--------------------|--------------|---------|----------------------|-----------|---------------------------|---|--------|---------------------------------|
| 2594 | 399 | | | | | lag of shell debris
and mud clasts | | Transgressive
surface "III" |
| | 400 | | | | | | 2C | |
| | 401 | P1. 26 | | | | Rhythmic mud
drap couplets | 12B | Tidally-
Influenced
sands |
| | 402 | S1. 26 | 03 | | R | Fractures | | |
| 2595 | 403 | P2. 7 | | | R | | | |
| | | S2. 8. | | | | | | |
| | | 9 | | | | | | |
| | | P1. 25 | | | | | | |
| 2596 | | S1. 25 | | | | | | |
| | 404 | | | | | Traces of
rhythmic
sand-mud
lamination
between the
burrows | 2C | Inactive channel
fill |
| | 405 | P1. 24 | | | | | | |
| | | S1. 24 | | | | | | |
| 2596 | 406 | P2. 5.6 | 03 | | | Rhythmic mud
drap couplets
mud clasts | 12B | |
| | 407 | S2. 6. | | | | mud-lined slump
fractures | | |
| | 408 | 7 | | | | | | |
| | 409 | | 04 | | | mud clasts | | |
| 2596 | 410 | P1. 23 | | | | | | |
| | 411 | S1. 23 | | | | | | |
| | 412 | | | | | | | |
| | 413 | P15/5. | 04 | | | Rhythmic mud
drap couplets | | runnel fill |
| | | S15/11 | | | | | | |

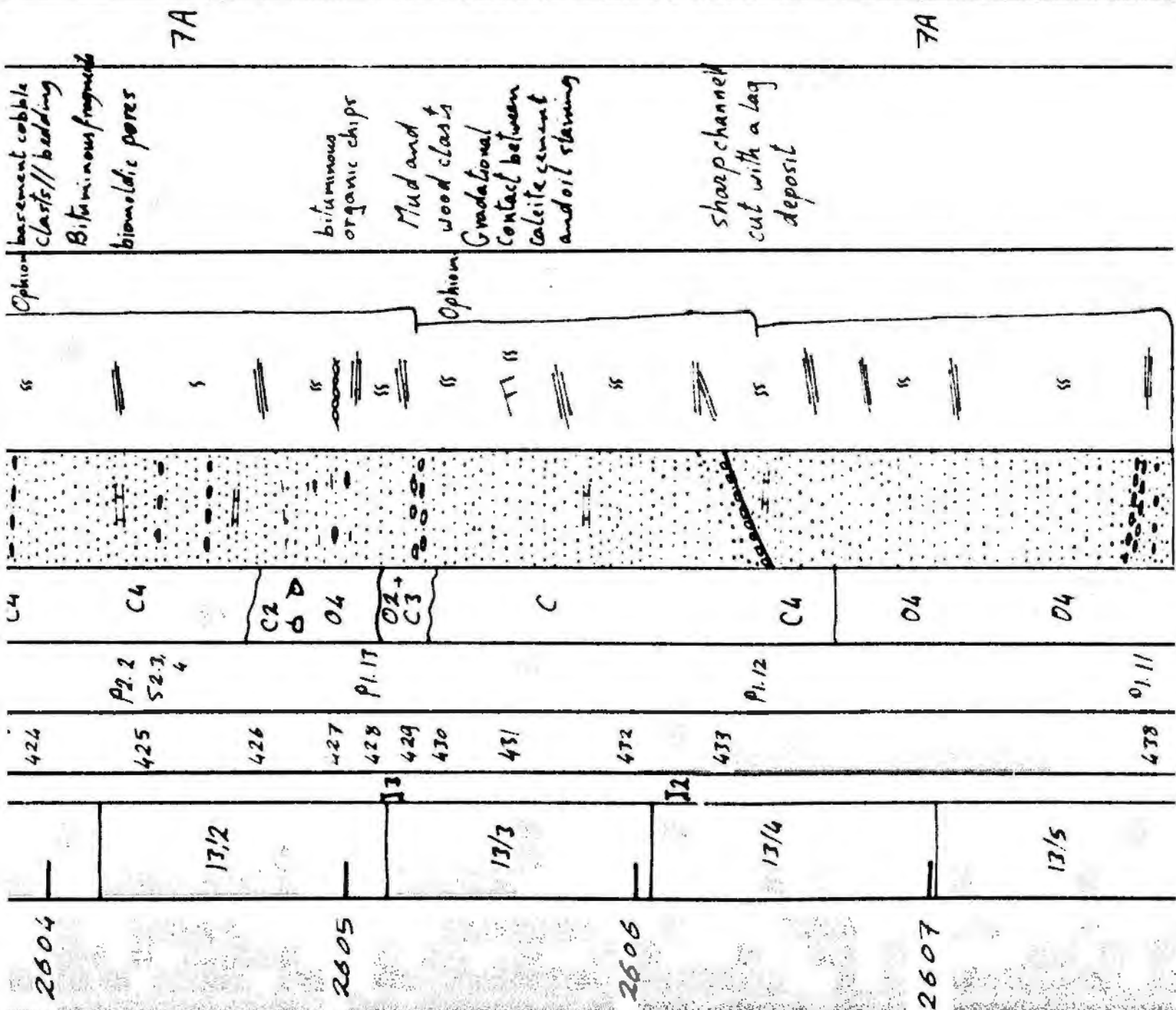


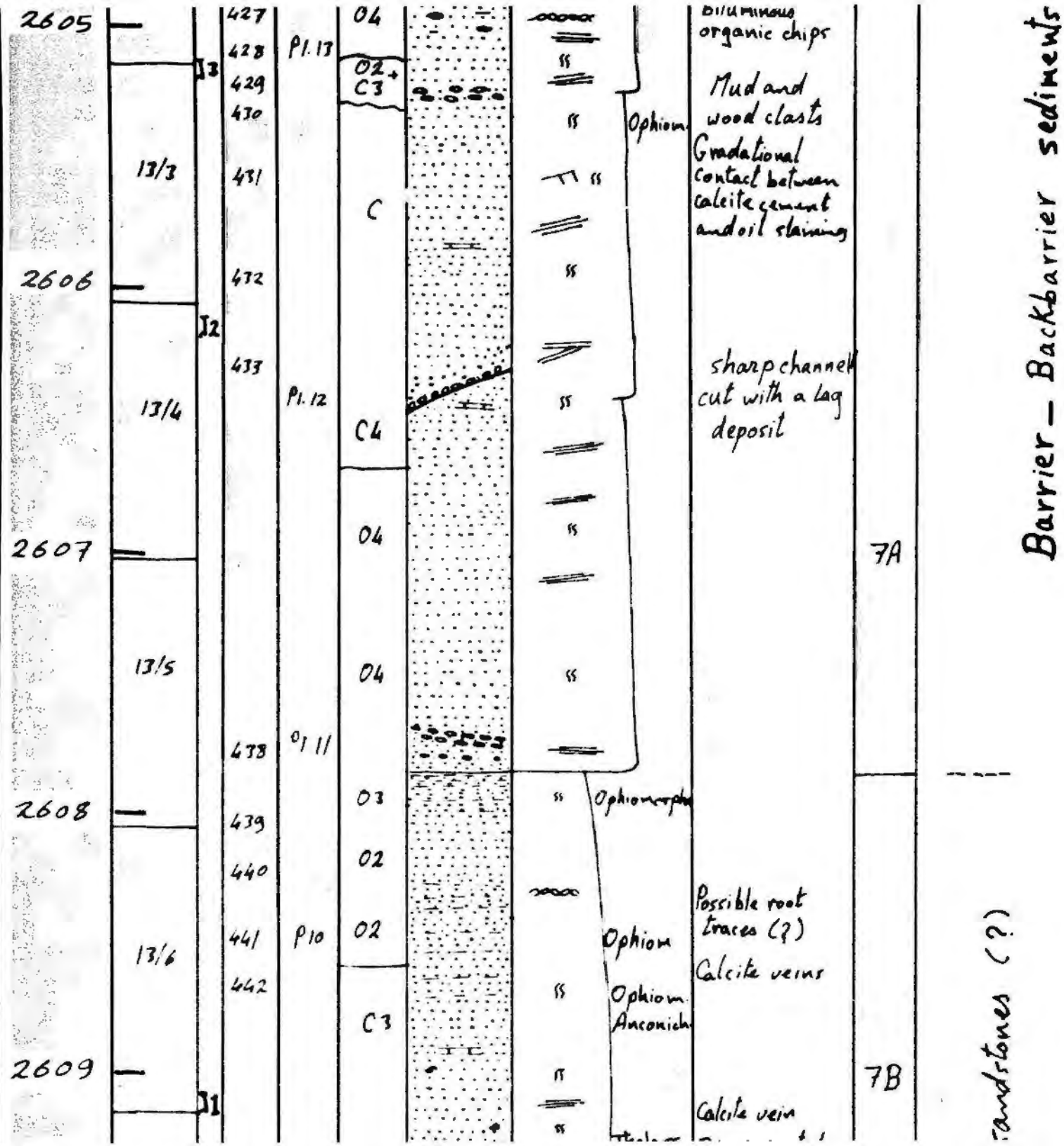
Barrier - Back-barrier

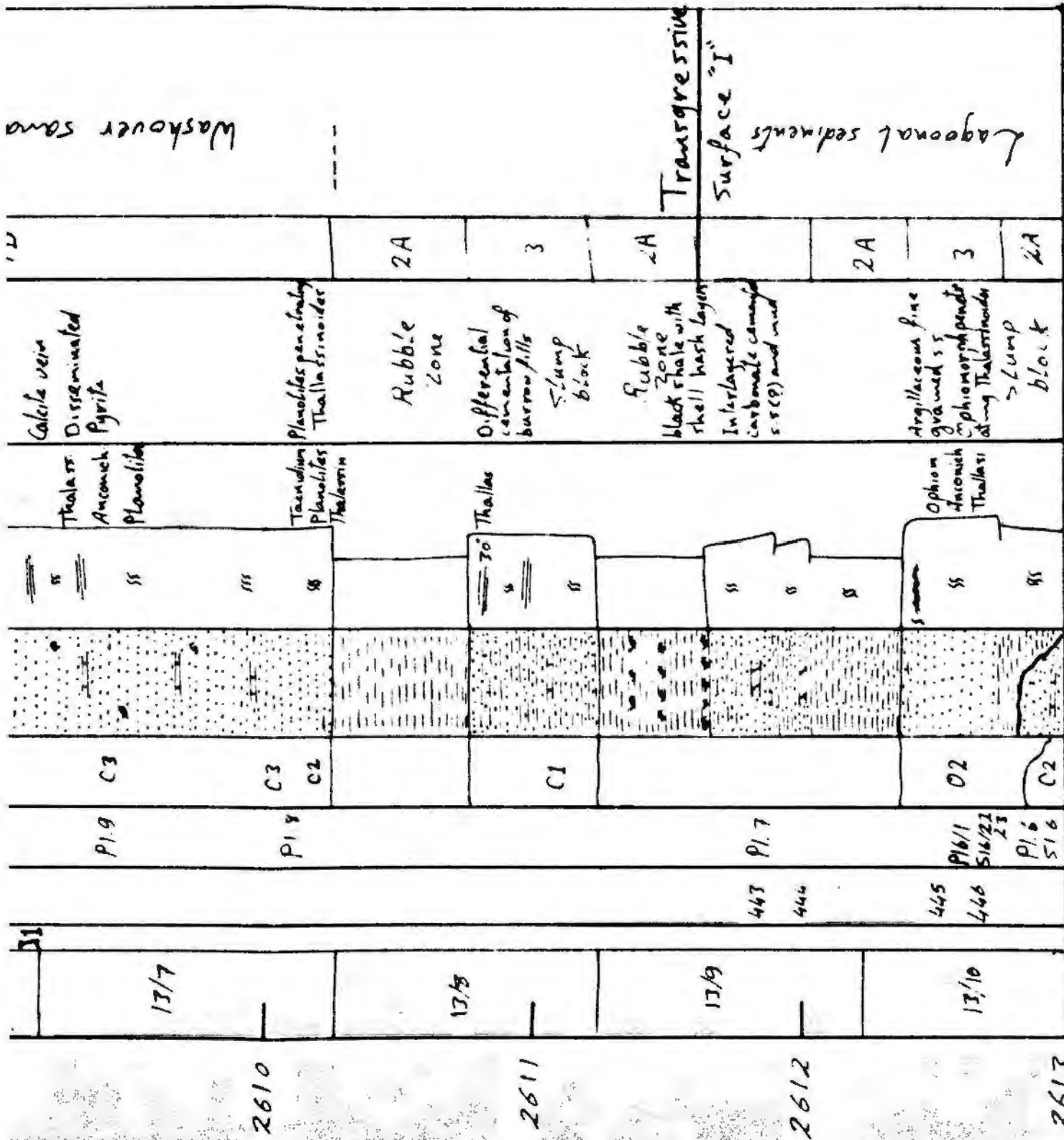
7A



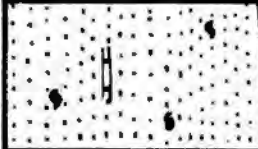
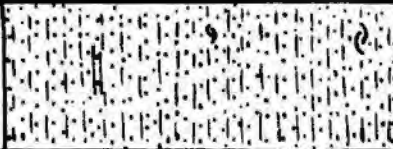
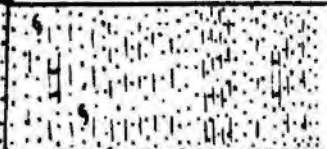

Barrier - Backbarrier sediments




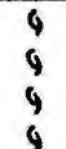















9/9

| Core no / Box no | Sample no | Photos | Oil stain / Cement | Lithology | Sedimentary structures and divisions | Remarks | Facies | Environment |
|------------------|-----------|---------------------------------------|----------------------|---|--------------------------------------|--|--------|--------------------|
| 2614 | 13/11 | P1.4, 5
S1.5
P2.1, 2
S2.1, 2 | C2
C1
C2
C1 |  | Ophiom.
Thalass.
Planolite | Few Pelecypod shells
ophiomorpha,
Thalassinoides,
and Planolites | 3 | Lagoonal sediments |
| | | P1.7, 4 | |  | Thalass.
Teichich.
Taenidium | Differential calcite
cementation of burrow
fills
abundant
carbonized
wood fragments | 2A | |
| 2615 | 13/12 | P1.2
S1.2, 3 | C1 |  | Planolite
Anconich.
Rhizoc | Abundant carbonized
wood fragments
thixotropic soft
sediment
deformation | 3 | |
| 2616 | 13/13 | P1.1
S1.1 | C3 |  | | Rubble zone | | |

| | |
|---|--|
|  | Sandstone |
|  | mudstone |
|  | argillaceous sandstone |
|  | Pelecypod shells
or
Serpulid tubes |
|  | Planar
Lamination |
|  | inclined
Lamination |
|  | current
ripples |
|  | Wave
ripples |
|  | Cross bedding |
|  | trough cross
bedding |
|  | Flaser
bedding |
|  | Lenticular
bedding |
|  | Wavy
bedding |

| | |
|------------|-----------------------------------|
| ooo | Lenticular bedding |
| ~~~~~ | Wavy bedding |
| s s | Weakly burrowed |
| ss ss | medium burrowing |
| sss | intense burrowing to bioturbation |
| ~~~~~ | Contorted bedding |
| h h h | root traces |
| C1 | weak calcite cementation |
| C2 | medium calcite cementation |
| C3 | strong calcite cementation |
| S1, S2, S3 | siderite cementation |
| D1, D2, D3 | dolomite cementation |
| O1 | weak oil |

cementation

weak oil
staining

medium oil
staining

strong oil
staining

erosional
contact

Calcite
cementation

Fractures

01

02

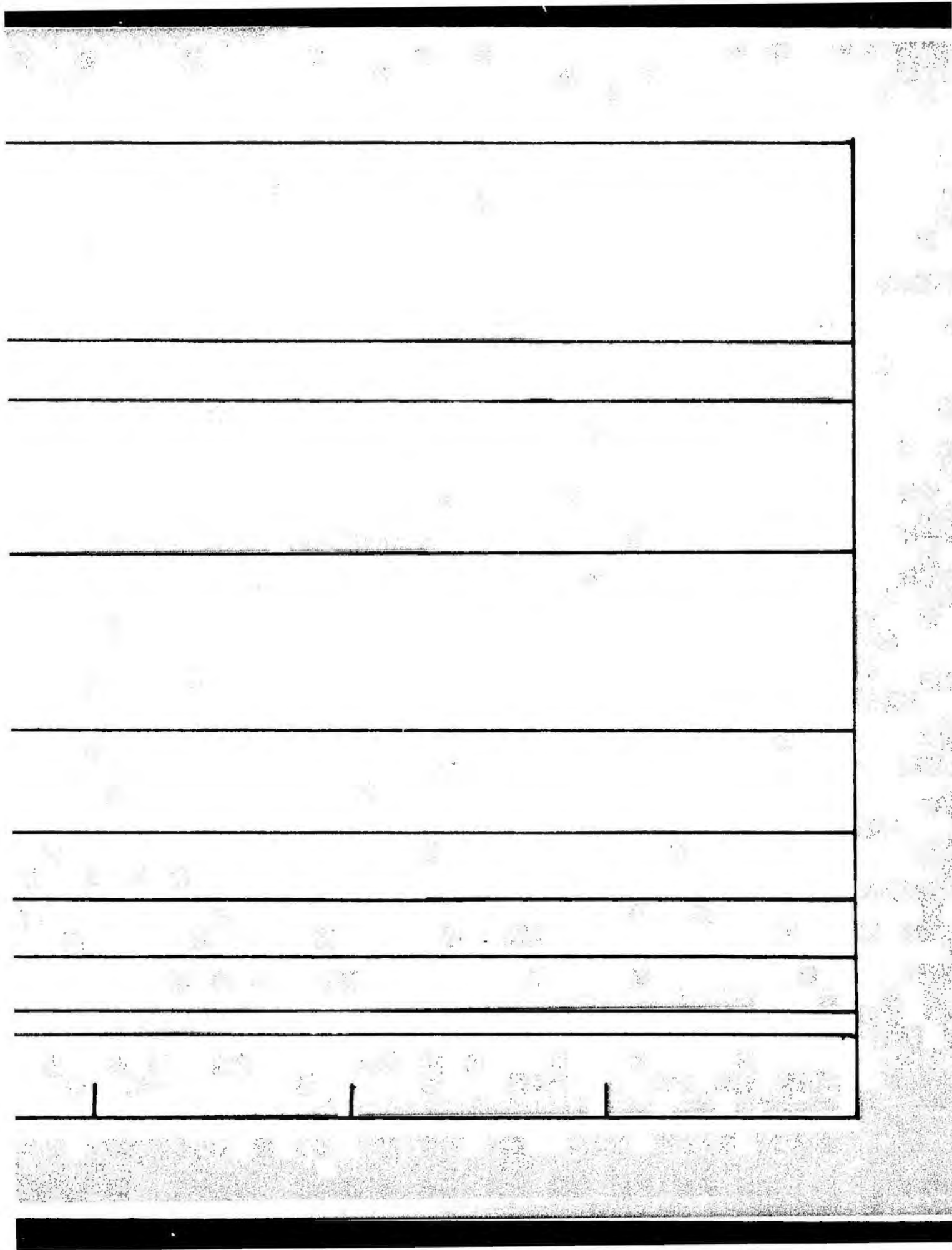
03

~

II

+/+

| | |
|------|------------------------|
| 02 | medium oil
staining |
| 03 | strong oil
staining |
| ~~~~ | erosional
contact |
| ▢ | Calcite
cementation |
| ## | Fractures |



Logged by: Osama M. Soliman

Depth from: K.B.

2/2

Date: February 8th, 1994

Long.

| Remarks | Facies | Environment |
|---------|--------|-------------|
|---------|--------|-------------|

Calcareous muddy sandstone with abundant articulated and disarticulated shells - Organic chips and disseminated pyrite

7B

to medium grained, relative in calcareous sandstone some scattered open (?) Pelicypod shells gradational boundary innivated pyrite

shale, with abundant shells and many shell fragments. The shale grades into sandstone below.

2A

Transgressive
river - Backbarrier Complex

